

## SMiRT 26

# 17<sup>th</sup> International Seminar on FIRE SAFETY IN NUCLEAR POWER PLANTS AND INSTALLATIONS

Westerburg, Huy, Germany  
October 24-25, 2022

## SMiRT 26

### 17<sup>th</sup> International Seminar on FIRE SAFETY IN NUCLEAR POWER PLANTS AND INSTALLATIONS

Westerburg, Huy, Germany  
October 24-25, 2022

Marina Röwekamp, GRS (Ed.)  
Heinz-Peter Berg (Ed.)

November 2022

#### **Remark:**

This report refers to the research project 4720R01550 which has been funded by the German Federal Ministry for Environment, Nature Conservation, Nuclear Safety and Consumer Protection (BMUV).

The work was conducted by the Gesellschaft für Anlagen- und Reaktorsicherheit (GRS) gGmbH.

The authors are responsible for the content of the report.

**Keywords**

Experimental research, fire PSA, fire simulations, future designs, human factor, nuclear fire safety, operating experience, regulation, safety assessment, standards

## **Kurzfassung**

Im Rahmen des vom Bundesministerium für Umwelt, Naturschutz, Nukleare Sicherheit und Verbraucherschutz (BMUV) beauftragten Vorhabens 4720R01550 fand im Oktober 2022 das siebzehnte internationale Seminar “Fire Safety in Nuclear Power Plants and Installations” als Post-Conference Seminar der 26<sup>th</sup> International Conference on Structural Mechanics In Reactor Technology (SMiRT 26) in Westerburg, Huy, Deutschland, statt.

Die vorliegenden Proceedings des Seminars enthalten alle Fachbeiträge des zweitägigen Seminars mit insgesamt 56 Teilnehmern aus insgesamt elf Ländern aus Europa, Asien und Nordamerika.

## **Abstract**

In the frame of the project 4720R01550 funded by the German Ministry for the Environment, Nature Conservation, Nuclear Safety and Consumers Protection (BMUV, German for: Bundesministerium für Umwelt, Naturschutz, Nukleare Sicherheit und Verbraucherschutz) the seventeenth international Seminar on "Fire Safety in Nuclear Power Plants and Installations" has been conducted as Post-Conference Seminar of the 26<sup>th</sup> International Conference on Structural Mechanics In Reactor Technology (SMiRT 26) at the Westerburg in Huy, Germany.

The following Seminar Proceedings contain the entire technical contributions to the two days Seminar with a total of 56 participants from eleven countries in Europe, Asia, and Northern America.

## Contents

|          |   |            |
|----------|---|------------|
| <b>1</b> | <b>Introduction .....</b>   | <b>1</b>   |
| <b>2</b> | <b>Seminar Agenda.....</b>  | <b>3</b>   |
| <b>3</b> | <b>Seminar Contributions .....</b>  | <b>7</b>   |
| 3.1      | Session on Recent International Developments .....                                | 8          |
| 3.2      | Session on High Energy Arcing Faults (HEAF).....                                  | 59         |
| 3.3      | Session on Fire Hazard and Risk Analyses Including Standards and Guidelines ..... | 104        |
| 3.4      | Session on Experimental Fire Research and Modelling.....                          | 148        |
| 3.5      | Session on Fire Modelling and Tools .....   | 264        |
| 3.6      | Session on Operating Experience.....  | 344        |
| <b>4</b> | <b>Seminar Conclusions and Outlook.....</b>                                       | <b>383</b> |



## 1        **Introduction**

The meanwhile 17<sup>th</sup> International Seminar on ‘Fire Safety in Nuclear Power Plants and Installations’ was held as Post-conference Seminar of the 26<sup>th</sup> International Conference on Structural Mechanics in Reactor Technology (SMiRT 26) at the Westerburg in Huy, Germany in October 2022.

In total 56 participants from Belgium, Canada, Czech Republic, France, Germany, Japan, the Netherlands, Sweden, Switzerland, the United Kingdom, and the United States of America followed the 26 presentations that were given in the different scientific sessions and participated actively in a final very short expert panel discussion at the end of the seminar.

It has to be clearly pointed out that from the first seminar of this series starting in 1987, when the safety significance of fires in nuclear reactors had just been recognized, up to today fire safety in nuclear power plants and other nuclear installations has significantly increased. This does in general concern the design of the plants and, in particular, of structures, systems and components (SSCs) important to safety. But this also considers the operation of such installations as well as all areas of assessment, inspection, and maintenance. For more than thirty-five years, methodological approaches for assessing the fire risk and the corresponding analytical tools have been evolving and are continuously being enhanced.

The two-day nuclear fire experts’ seminar started with a session on recent developments concerning fire protection at nuclear installations including regulations, standards and fire protection programs, followed by a session on the “hot” topic of high energy arcing fault induced fires. Further seminar sessions focussed on recent activities with respect to deterministic fire hazard analyses and probabilistic assessments of the fire risk in nuclear facilities. Two sessions were devoted to nuclear fire research presenting results from actual fire experiments and modelling for nuclear facilities. As usual in this seminar series, one session covered the lessons learned from nuclear installations’ specific fire and fire protection related operating experience.

The seminar topics highlighted the quite broad scope of issues and challenges related to fire safety in nuclear installations. The presentations and discussions supported the general impression that fires are still a topic to be addressed adequately in the safety assessment for various types of nuclear facilities. This topic is not limited to existing ones

designed according to former standards. However, it should also be considered in the most modern designs and operation of new built nuclear facilities.

After some years, this seminar was again organized in Germany by GRS. In addition, a technical tour of a new-built fire laboratory named ZeBra (German for Zentrum für Brandschutz) at the Institute of Building Materials, Concrete Constructions and Fire Safety (iBMB) of Braunschweig University of Technology was offered to the participants the day after the seminar itself. The organizers like to express their thanks to Prof. Dr. J. Zehfuß and his team for organizing the interesting tour as an add-on to the seminar.

Moreover, the organizers want to thank all speakers, co-authors and chairpersons as well as the entire participants for their highly active and fruitful participation and valuable, high-level contributions during this 17<sup>th</sup> International Seminar on 'Fire Safety in Nuclear Power Plants and Installations' which made this venue again a very successful one.

The next, 18<sup>th</sup> seminar of this series is intended to be held as SMiRT 27 Post-conference Seminar in France in late summer 2023.

***Dr. Marina Röwekamp and Dr. Heinz-Peter Berg***

– Scientific Chairs and Permanent Organizers –



**26<sup>th</sup> International Conference on  
Structural Mechanics in Reactor Technology (SMiRT 26)**  
**17<sup>th</sup> SMiRT Post-Conference Seminar on  
Fire Safety in Nuclear Power Plants and Installations**



Westerburg and Braunschweig, Germany; October 23 – 26, 2022

**Agenda**

**Sunday, October 23, 2022**

17:30 h      to      *Registration and SMiRT Fire Seminar Informal Welcome*  
 19:00 h

**Monday, October 24, 2022**

|         |  |  |                                   |
|---------|--|--|-----------------------------------|
| 08:30 h | <i>Registration</i>  |  |                                   |
| 09:00 h | <i>Organizers' Welcome and Introduction</i>  | H.-P. Berg,<br>M. Röwekamp                               | Germany<br>GRS, Germany           |
| 09:15 h | <i>Recent International Developments</i>   | <b>Chairperson:</b><br><b>H.-P. Berg (Germany)</b>       |                                   |
| 09:15 h | Fire Safety Regulation on Great Britain Nuclear Sites – A Comparison Between Nuclear Fire Safety and Life Fire Safety Expectations | C. Winstanley,<br>et al.                                 | ONR,<br>United Kingdom            |
| 09:45 h | ENSREG Topical Peer Review on Fire Protection – An Overview  | G. Stoppa,<br>M. Röwekamp                                | BMUV,<br>Germany,<br>GRS, Germany |
| 10:15 h | <b>Coffee Break</b>  |  |                                   |
| 10:45 h | <i>Recent International Developments (contd.)</i>  | <b>Chairperson:</b><br><b>A. Bounogui, CNSC (Canada)</b> |                                   |
| 10:45 h | Performance Objectives and Criteria for the Annual Plant Condition Inspection (API) at Nuclear Power Plants                        | A. Bounogui  | CNSC, Canada                      |
| 11:15 h | Performance of an Effective Self-Assessment to Improve Fire Safety   | P. B. Boulden Jr.  | Appendix R Solutions; USA         |
| 11:45 h | IGNIS: A New Experimental Platform Dedicated to Real Scale Fire Studies  | B. Gautier, et al.                                       | EDF, France                       |
| 12:15 h | <b>Lunch Break</b>   |  |                                   |

|         |  |   |
|---------|--|---|
| 13:45 h | <b>High Energy Arcing Faults (HEAF)</b>  | <b>Chairperson:</b><br><i>K. Shirai, CRIEPI (Japan)</i> |
| 13:45 h | Overview of U.S. Nuclear Regulatory Commission Research Activities to Update Probabilistic Risk Treatment of High Energy Arcing Faults         | K. Coyne, et al.;<br>presented by<br>K. Hamburger       |
| 14:15 h | Experimental Studies of HEAF (High Energy Arcing Fault) Phenomena for Non-Segregated Bus Ducts   | K. Tasaka, et al.                                       |
| 14:45 h | Development of Improved High Energy Arcing Fault (HEAF) Target Damage Thresholds and Zone of Influence (ZOI) Models                            | K. Coyne, et al.;<br>presented by<br>K. Hamburger       |
| 15:15 h | <b>Coffee Break</b>  |   |
| 15:45 h | <b>Fire Hazard and Risk Analyses, Including Standards and Guidelines</b>   | <b>Chairperson:</b><br><i>B. Gautier, EDF (France)</i>  |
| 15:45 h | Using An Integrated Risk-Informed Decision-Making Process to Address High Energy Arc Faults (HEAF) Issue at United States Nuclear Power Plants | S. Weerakkody;<br>presented by<br>K. Hamburger          |
| 16:15 h | Fire Modelling Automation and Visualization in the Context of Fire Probabilistic Risk Analysis for Nuclear Plants                              | R. Sampath,<br>S. Prescott                              |
| 16:45 h | Requirements in Standards and Fire Qualification of Smoke Control Dampers  | N. Ytournel, et al.                                     |
| 17:15 h | Guideline for Installation of Valves in Composite and Plastic Materials in Nuclear Power Plants  | J. Larsson, et al.                                      |
| 17:45 h | <b>Photo and Adjourn First Seminar Day</b>   |   |
| 19:00 h | <b>SMiRT Fire Seminar Aperitif and Dinner</b>  |   |

## Tuesday, October 25, 2022

|         |   |  |
|---------|---|--|
| 09:00 h | <b>Experimental Fire Research and Modelling</b>   | <b>Chairperson:</b><br><i>H.-P. Berg (Germany)</i> |
| 09:00 h | Fire Test with A Pressure Differential of 5 kPa for the ITER Nuclear Fusion Experimental Facility | R. Buffard, et al.                                 |
| 09:30 h | Experimental Study of the Behaviour of Horizontal and Vertical Cable Tray Fires                   | A. Amokrane, et al.                                |
| 10:00 h | Overview of the OECD PRISME 3 Project – Experimental Campaign Description and Main Results        | S. Suard, et al.                                   |
| 10:30 h | <b>Coffee Break</b>   |  |

|                |   |   |                                       |
|----------------|---|---|---------------------------------------|
| <b>10:50 h</b> | <b>Experimental Fire Research and Modelling (contd.)</b>  | <b>Chairperson:<br/>S. Suard, IRSN (France)</b>           |                                       |
| <b>10:50 h</b> | Experimental Investigations of the Influence of Cable Arrangement and Ventilation on Cable Tray Fires in Confined Spaces  | J. Spille   | iBMB of TU Braunschweig, Germany      |
| <b>11:20 h</b> | Investigating A Cable Tray Fire Event in the Frame of An International Benchmark Exercise   | W. Plumecocq, et al.                                      | IRSN, France                          |
| <b>11:50 h</b> | FAIR: A New OECD/NEA Fire Risk Research Project Under Development as A Follow-Up to PRISME 3  | P. March, et al.  | IRSN, France                          |
| <b>12:15 h</b> | Implementation of An Extended FLASH-CAT Model in COCOSYS  | W. Klein-Heßling  | GRS, Germany                          |
| <b>12:40 h</b> | <b>Lunch Break</b>  |   |                                       |
| <b>14:00 h</b> | <b>Fire Modelling and Tools</b>   | <b>Chairperson:<br/>D. Lisbona, ONR, (United Kingdom)</b> |                                       |
| <b>14:00 h</b> | Development of A Base Case for Modelling of A Complex Fire Scenario Through Sensitivity Analysis  | D. Bagshaw, et al.  | Atkins, United Kingdom                |
| <b>14:30 h</b> | Quality Judgement of Surrogate Models Used for Uncertainty Consideration in Fire Safety CFD Models  | K. Wothe, et al.  | Otto-von-Guericke University, Germany |
| <b>15:00 h</b> | Modelling Fire Scenarios in Complex Building Structures: A Project Presentation   | F. Köhler, et al.   | Otto-von-Guericke University, Germany |
| <b>15:30 h</b> | Implementation and Further Development of An Assessment Tool for Fire Analysis in Confined and Mechanically Ventilated Compartments Using a Well-Stirred Reactor Approach | F. Bonte, et al.  | FLEX-A, Belgium                       |
| <b>16:00 h</b> | <b>Coffee Break</b>   |   |                                       |
| <b>16:20 h</b> | <b>Operating Experience, etc.</b>   | <b>Chairperson:<br/>M. Röwekamp, GRS (Germany)</b>        |                                       |
| <b>16:20 h</b> | Sellafield Ltd. Recent Fires and Learning   | A. Seward   | Sellafield, United Kingdom            |
| <b>16:50 h</b> | Small Fire Event During Dismantling of A Steam Generator  | A. Artz, K. Borowski                                      | RWE Nuclear, Germany                  |
| <b>17:20 h</b> | Release Fractions of Radioactive Waste Packages in Case of Fire   | B. Forell, C. Richter                                     | GRS, Germany                          |

|         |                                     |   |  |
|---------|-------------------------------------|---|--|
| 17:50 h | <b>Round Table Panel Discussion</b> | <b>Chairperson:</b><br><b>M. Röwekamp</b>                               | <b>GRS, Germany</b>                                      |
|         |                                     | <b>Panelists:</b><br>A. Bounagui<br>D. Lisbona<br>K. Shirai<br>S. Suard | CNSC, Canada<br>ONR, UK<br>CRIEPI, Japan<br>IRSN, France |
| 18:15 h | <b>Adjourn Second Seminar Day</b>   |   |  |
| 19:30 h | <b>Dinner at hotel</b>              |   |  |

### Wednesday, October 26, 2022

|         |  |                                   |                                  |
|---------|--|-----------------------------------|----------------------------------|
| 09:30 h | <b>Travel/Transport to iBMB of Braunschweig University of Technology ZeBra Fire Laboratory</b> |                                   |                                  |
| 10:30 h | <b>Welcome Coffee at iBMB 15 minutes</b>   |                                   |                                  |
| 10:45 h | Welcome and Introduction   | J. Zehfuß                         | iBMB of TU Braunschweig, Germany |
| 11:15 h | ZeBra Fire Laboratory Technical Visit  | Group guided by J. Zehfuß, et al. | iBMB of TU Braunschweig, Germany |
| 13:00 h | <b>Lunch</b>   |                                   |                                  |
| 13:30 h | Final Discussion   |                                   |                                  |
| 13:45 h | <b>Adjourn of SMiRT Post-Conference Fire Seminar Technical Visit</b>                           |                                   |                                  |

### **3 Seminar Contributions**

In the following, the seminar contributions prepared for the 17<sup>th</sup> International Seminar on 'Fire Safety in Nuclear Power Plants and Installations' held as Post-conference Seminar of the 26<sup>th</sup> International Conference on Structural Mechanics in Reactor Technology (SMiRT 26) are provided in the order of their presentation in the seminar.

### 3.1 Session on Recent International Developments

The technical seminar sessions started with a session on recent international developments and activities concerning nuclear fire safety regulations and the self-assessment on fire protection of nuclear facilities by member states of the European Union (EU) chaired by Heinz-Peter Berg (Germany) as one of the technical organisers of the seminar and Abderrazaq Bounagui, regulator from the Canadian Nuclear Safety Commission (CNSC).

Two different regulators – the Office for Nuclear Regulation (ONR) in the United Kingdom and the CNSC from Canada – presented actual issues with respect to fire protection in nuclear reactor and non-reactor installations. This included a comparison of regulatory requirements for nuclear safety and life safety related to fire, demonstrating that approaches for the protection concepts applied in nuclear installations need to cover both aspects. The other presentation highlighted the requirements for annual fire related plant inspections as part of the regulatory oversight.

Another presentation provided a short overview on the already started ‘Topical Peer Review (TPR) on Fire Protection’ for nuclear installations by ENSREG (*European Nuclear Safety Regulators Group*). All countries in the European Union (EU) with nuclear installations participate in this ongoing TPR. Major goal of this activity is – according to the Technical Specification of the TPR – to compare the extent of and results from fire safety analyses and the implementation of the fire protection concepts between nuclear installations of the same types and different types from the participating countries and draw conclusions for potential improvements. Besides this regulatory self-assessment in Europe, an approach from the United States (U.S.) for an effective fire related self-assessment for nuclear power plants (NPPs) was presented aiming on continuously improving fire safety at NPPs.

Last not least, a new experimental platform named IGNIS developed by Electricité de France (EDF) was shown. This platform will enable analysts to perform fire tests in different (real) scales for nuclear installations in order to systematically support fire safety assessment. Moreover, it can serve for experiments to be performed not only on a national but also an international basis.

The corresponding five seminar contributions are provided hereafter.

# **Fire Safety Regulation on Great Britain Nuclear Sites – A Comparison Between Nuclear Fire Safety and Life Fire Safety Expectations**

Caroline Winstanley\*, Stephen Taylor, Joseph Nithsdale, Diego Lisbona

Office for Nuclear Regulation (ONR), Bootle, L20 7HS, United Kingdom

## **ABSTRACT**

This paper provides an overview of ONR regulatory expectations and experience in regulating nuclear fire safety in the context of Great Britain's (GB) goal-setting regulatory framework. ONR expectations for nuclear fire safety are documented in ONR's Safety Assessment Principles (SAPs) and Technical Assessment Guide (TAG) on Internal Hazards (NS-TAST-GD-014). ONR also regulates life fire safety across GB licensed sites in accordance with the Regulatory Reform (Fire Safety) Order 2005 in England and Wales, and the Fire (Scotland) Act 2005 in Scotland, respectively. Regulatory expectations in this area are further explained in ONR's Technical Inspection Guide on life fire safety.

The paper principally covers nuclear fire safety and presents expectations and experience in the regulation of design, operation, and decommissioning of nuclear power plants in that area. This includes consideration of fire protection and segregation of cables, other key safety systems, structures, and components, as well as other passive and active protection and mitigation measures. Ageing management considerations relating to fire safety through the installation's lifecycle is also covered. Life fire safety considerations can have synergistic but also competing requirements with nuclear fire safety. Regulatory expectations on the management of these potential conflicts are also discussed.

## **GREAT BRITAIN REGULATORY CONTEXT**

The Office for Nuclear Regulation (ONR) is Great Britain's (GB's) independent regulator of nuclear safety, security, site health and safety, transport, and safeguards. A key principle of GB law and ONR's regulatory approach is the requirement that licensees build, operate, and decommission nuclear sites in a way that ensures that risks are kept as low as reasonably practicable. This is referred to as the ALARP principle. Demonstration that risks are ALARP (as low as reasonably practicable) may include numerical risk assessments – including potential risks from hazards, optineering studies, but also includes a comparison with "relevant good practice" (RGP).

The GB regulatory framework is goal-setting in nature. To ensure an effective and efficient regulatory approach, ONR sets out its regulatory expectations in line with the ALARP principle and expects licensees to determine and justify how best to achieve them. ONR's regulatory expectations for nuclear safety are outlined within the Safety Assessment Principles (SAPs) [1] and associated Technical Assessment Guides (TAGs) – all of which are published and are freely available on the internet.

ONR's goal-setting approach enables licensees to be innovative and achieve the required high levels of nuclear safety by adopting practices that meet its particular circumstances.

Great Britain's approach is benchmarked against international standards, and international standards are generally considered as relevant good practice in many technical areas. We also take account of national standards from other countries as potential good practices. This allows us to look at designs which may have come from a variety of different countries and be open to the underlying design approaches that protect against hazards, so far that it is demonstrated that the legal duty to reduce risks to ALARP has been achieved. Relevant standards may include IAEA standards [2], [3], [4], [5], [6], but the flexibility of our approach also allows us to consider safety cases which relate to U.S. Nuclear Regulatory Commission Regulation (e.g. NUREG Reports), European Utility Requirements (EURs) and national standards (e.g. French or German ones).

## MANAGING THE RISK FROM FIRE

### Nuclear Fire Safety

In alignment with the SAPs, ONR expects a fire hazard analysis to be carried out for a plant in design, operation, or decommissioning to determine the potential for fire initiation and growth, and the consequences for structures, systems, and components (SSCs) relevant to nuclear safety. A basic requirement which is both included in ONR SAPs (EKP.3), and IAEA safety standards (SSR-2/1) [6], is to provide defence in depth. In the case of fire, this means:

- Preventing fires from starting.
- Limiting the severity of fires that start.
- Limiting the consequences of fires that start and are severe.

Preventing fire from starting by elimination or minimisation of combustible inventories is high up in the hierarchy of measures. Whilst total elimination is desirable, in many cases it is virtually impossible and, therefore, in alignment with international RGP, ONR's expectation is for the design, the high-level claims, and the fire analysis to be developed on the basis that segregation by fire compartment barriers designed to withstand full burnout is provided if practicable (the "fire containment" approach). This also stems from the expectation that SSCs relevant to safety and their components should be protected against a fire, e.g., by barriers, or qualified to withstand the effect of a fire. Extensive SSC qualification requirements will place onerous requirements on the design and manufacture of numerous SSCs across the plant. On the other hand, segregation by passive fire barrier designs substantiated against the most onerous fire conditions in the compartment, e.g., total burnout, is, therefore, the favoured and expected primary claim unless segregation is not reasonably practicable. For any severe fires that do arise, the consequences on nuclear safety relevant SSCs should be limited by design (such as by provision of redundant safety measures in segregated fire compartments).

Given the goal-setting nature of Great Britain's regulatory regime there is, however, no prescriptive requirement to provide full compartmentation by barriers, or to do so for specific systems or locations. However, implementation of full fire compartmentation provision is expected, subject to reasonable practicability.

Needless to say, for areas where segregation is not reasonably practicable, other measures, usually a combination of measures, can be proposed by a Generic Design Assessment (GDA) Requesting Party (RP) or licensee to underpin the fire safety case. They are typically:

- Elimination of combustible materials / Combustible load minimisation;
- Partial barriers;

- Separation of fire sources and/or SSCs by distance;
- Restricting the area of the fire by engineered or other means;
- Inert atmospheres;
- Provision of fire detection, alarm, and extinguishing systems (automatic or manual); or
- A combination of these.

Measures such as the above are also typically provided as defence in depth measures even where segregation by fire barriers is provided. This is because the provision of a measure does not “per se” demonstrate that further measures would be grossly disproportionate. In making regulatory judgements in this area, ONR looks for hazard robustness and defence in depth because of the inherent uncertainties associated with hazard initiation, progression, and severity.

In the subsequent sections of this paper, the degree of variability in hazard identification and characterisation techniques are discussed, together with typical points of attention during nuclear and life fire safety regulation.

## **Life Fire Safety**

The fire safety measures and arrangements provided to protect occupants of a building from fire are regularly referred to as ‘conventional fire safety’ or ‘life fire safety’. In Great Britain, the legal basis of these requirements is distinct from those relevant for nuclear fire safety. Life fire safety is regulated, but in contrast with nuclear fire safety, is not subject to a permissioning regime.

The primary legislation covering occupational health and safety (and therefore life fire safety) in Great Britain is the Health and Safety at Work etc. Act 1974 (HSWA) [7]. The HSWA requires consideration of the direct and indirect effects of fire on people but, is non-prescriptive in terms of the specific duties placed on an individual or an organisation.

The Regulatory Reform (Fire Safety) Order 2005 (FSO) [8] and the Fire Scotland Act 2005 (FSA) [9] are the secondary, Great Britain fire specific, legislation and cover general fire precautions and other fire safety duties. The legislation is, again, goal-setting rather than prescriptive and places duties on the ‘responsible person’. The FSO/FSA require fire precautions to be applied ‘where necessary’ and this therefore includes both the design and occupation of buildings. For the purposes of nuclear licensed sites in GB ONR is the enforcing body of the HSWA.

Compliance with the FSO/FSA is a legal duty and with respect to the design and construction of buildings the detailed expectations for meeting the provisions outlined in the legislation are provided by The Building Regulations [10]. These provide design requirements-level detail to designers, architects, fire engineers and other personnel with a responsibility for fire safety in the design of buildings. For buildings covered under a nuclear site licence, an exemption from absolute compliance with The Building Regulations is usually applied via the Nuclear Installations Act 1965 (as amended) (NIA) [11], although this does not apply to any buildings on the licensed site which may contain a dwelling, canteen, or offices. In practice, the legal requirement to comply with the FSO/FSA drives nuclear licensed sites to demonstrate compliance with the functional requirements of The Building Regulations where possible. This is usually achieved through benchmarking against suitable, recognised codes and standards. Where broad compliance is expected based on function and novelty of a building design, British Standard 9999 2017 (BS9999) [12] is commonly used. Where a building is bespoke in nature, a full fire engineered

approach with recognised fire analysis techniques such as the British Standard 7974 (BS7974) [13] suite of documents, may be used.

In the case of occupied buildings, compliance with the FSO/FSA is assessed against the production of a suitable and adequate Fire Risk Assessment (FRA). For nuclear licensed sites, the interface with nuclear fire requirements would be expected to be captured within the FRA. Regarding inspection, ONR's approach is documented in the Technical Inspection Guide (TIG) on The Regulation of Life Fire Safety on Nuclear Licensed Sites (NS-INSP-GD-073) [14].

In addition to the fire specific legislation outlined above, several complimentary sets of regulations overlap with life fire safety requirements. These include:

- Dangerous Substances & Explosive Atmospheres Regulations (DSEAR) [15] - the Great Britain implementation of the ATEX 99/92/EC directive. Clauses within DSEAR related to the production of risk assessments and provision of control and mitigation measures to prevent harm to personnel from fire, also form part of the FSO.
- Control of Major Accident Hazards (COMAH) Regulations 2015 [16]. COMAH places additional requirements on sites which store or use large quantities of defined dangerous substances (including flammables). The extent of the requirements depends on specific substances and the quantities held.
- The Construction (Design and Management) (CDM) Regulations 2015 [17]. CDM places legal duties on dutyholders involved in construction activities. This can include principal contractors, principal designers, and other workers. A more dynamic FRA requiring more regular scrutiny would be expected throughout construction works to ensure compliance with the FSO/FSA and the fire specific clauses of CDM.

Life fire safety is primarily concerned with ensuring occupants are able to quickly and safely escape from a building in the event of a fire and that first responders are able to safely enter the building and reach the fire in relative safety. This is reflected in the functional requirements of The Building Regulations (Approved Document B, Vol. 2) [18] (B1 – means of warning and escape, B2 – internal fire spread (linings), B3 – internal fire spread (structure), B4 – external fire spread, B5 – access and facilities for the fire service).

Safe and rapid evacuation from a building can be aided by several measures which can be both complimentary and at odds with the broad goals of nuclear fire safety.

Fire resistant construction to protect escape routes and stair cores is a key expectation of life fire safety design and is used to avoid or limit excessive escape travel distances for occupants. This generally aligns well with the segregation approach to fire safety often adopted within nuclear safety cases. Similarly, fire prevention is a key component of life fire safety including the use of fire sterile areas along escape routes. Since fire is regularly assessed as one of the most common initiating events within nuclear safety analysis, the reduction/removal of fire loading benefits both life and nuclear safety goals.

In contrast, the introduction of additional doors, to reduce escape travel distances, is often counter to nuclear safety goals such as minimising the number and size of penetrations in nuclear safety barriers and the control of contamination. A judgement on the adequacy of escape provision is thus a nuanced question and requires knowledge of all drivers for safety. For larger, more complex buildings it is the expectation of the ONR that comparison against RGP sources and analysis of a variety of options, is undertaken to demonstrate that risks have been reduced so far as is reasonably practicable.

## SYNERGIES AND CONFLICTS

### Barriers / Penetrations

For nuclear fire safety the primary means of preventing the spread of fire is through the principle of fire containment. The provision of fire barriers within a design or a facility prevents spread of fires between divisions of a reactor or beyond one fire compartment to another. However, the provision and layout of such barriers can conflict with the need for personnel to access areas of plant and also to exit from those areas in the event of a fire. The most common conflict this raises is that the lack of openings/doors often extends the travel distances to a point of safety beyond the maximum distances recommended by BS7974 [13] and the routes of travel become less direct. Therefore, additional assessment of the fire growth and spread parameters specific to those areas and possible mitigation arrangements may need to be considered.

An additional issue which can arise is that providing doors within a fire barrier which meet the same fire resistance as, for example, a three-hour fire barrier, can be challenging. This conflict has often been resolved by the provision of lobby areas between two sets of fire doors which maintains the overall fire resistance of the barrier but still allows the personnel the required egress to an area of relative safety. The provision of this lobby does introduce the potential for personnel to have to access to an area which could be designated a safe area, but it needs to be designed (with the necessary ventilation requirements) such that it cannot allow the build-up of noxious gases. It is also important that these lobbies do not attract the storage of combustible materials, even for a temporary period, or the routing of services, if this can be avoided, to remain a sterile zone that minimises the potential for fire spread.

### Combustible Loading

Both nuclear fire safety and life fire safety seek the elimination and minimisation of combustible inventories within nuclear facilities as a key measure for the prevention of fire. In both the nuclear and life fire safety areas it is acknowledged that it is virtually impossible to eliminate all combustible materials. Both require RPs and licensees to identify how they will prevent and control the build-up of combustible materials, as well as controlling ignition sources and hazardous substances. In the case of life fire safety, the controls employed would be summarized in a Fire Risk Assessment specific to the facility, whereas for nuclear fire safety key operational safety measures would be identified through the hazard analysis, attracting designations in accordance with their nuclear safety significance, and captured within the safety case. In both instances, it would be expected that the operational requirements would be communicated to the workforce through training.

The control of temporary laydown areas can be particularly challenging in terms of finding areas which are suitable to meet both life fire safety and nuclear fire safety expectations. Locations selected must neither block emergency egress routes for personnel, nor be positioned in locations where they may affect the ability of SSCs to perform their safety functional requirements from a nuclear safety perspective if a fire were to occur. Therefore, the selection of temporary laydown areas in particular must be carefully controlled. Of course, plant state is another factor to consider as the operating state of the plant may also affect the choice of laydown areas i.e., some areas requiring access by personnel may only need to be accessed during shutdown periods so some normal combustible laydown areas may need to be suspended during certain operating states.

With regard to nuclear fire safety, an area which has frequently attracted regulatory attention has been whether an RP or licensee has identified and considered all possible

combustible materials and their potential effects on fire development in the fire modelling undertaken to underpin the safety case. This is particularly important in the context of local fire effects where the direct result of either flame impingement or hot smoke may result in significant damage to key SSCs or fire barriers.

Regarding life fire safety, one area of attention has been the frequency of fire initiation and small fires arising during hot works. Whilst in themselves these may be perceived as not presenting an immediate threat to life, they indicate issues with the rigor applied to the control of combustible material and the checks carried out prior to commencement and completion of hot working activities. Depending on location and circumstances, failure to apply such controls and checks adequately could result in more significant fires. ONR has in these instances engaged with the licensees to understand the root causes and seek changes in the licensees' controls.

### **Fire Detection and Alarm**

In a nuclear safety context, fire detection and alarm systems are generally implemented as a defence in depth measure with compartmentation being the typical primary means of ensuring nuclear safety in the event of a fire. For life fire safety, the provision of appropriate fire detectors and alarms, where deemed necessary, are a legal requirement of the Regulatory Reform (Fire Safety) Order 2005 in England and Wales [8]. Ageing and obsolescence of fire detection and alarm systems are important considerations in the context of legacy facilities, facilities undergoing decommissioning or nearing the end of their operational life.

Typical issues affecting ageing fire detection and alarm systems can be the inability to repair faults and failures due to unavailability of replacement parts. This is generally linked to the age of the system, new parts are rarely compatible with older systems, and depending on the age of the system, it may no longer be compliant with the current British Standards (BS5839 [19]) requirements for detector type, location, and coverage. For short term failures limited to single devices or small local areas, mitigatory measures can include temporary suspension of operations, staffed fire watches or patrols, or provision of mobile wi-fi detectors whilst repairs are undertaken. Longer term issues, or where there are more significant issues, ONR expects assessments and plans for remedial action including replacement programs as appropriate to remain compliant with statutory duties. ONR inspectors have actively engaged with licensees so that ageing and obsolescence issues in fire detection and alarm provision are resolved in a timely manner, and these are featured in the ONR Chief Nuclear Inspector's annual report 2020 [20].

### **Fire Suppression**

To ensure the tenability of escape routes and access routes for fire firefighting, various engineered systems may also be considered and provided, as specified through codes and standards. This can include the use of fire suppression systems (sprinklers, foam, water spray, gaseous etc.), primarily to control the growth and resultant spread of fire and smoke in order to create sufficient time for the means of escape to be accessed, or smoke control systems to either extract or control the flow of smoke within a given space. There may be instances where safety case requirements include the provision of an active fire suppression system to prevent the spread of fire for either nuclear fire safety reasons in areas of high fire load [2], should fire doors fail or be left open, or where a fire could continue burning for an extended period, which would go outside the resistance rating for elements of the fire containment boundaries [21] or for asset protection reasons. For nuclear fire safety the need for such provision may form part of the dutyholder's

overall ALARP argument which ONR routinely assesses when making regulatory judgements.

The use of fire suppression systems can introduce additional hazards (dependent on the agent used) which also need to be considered. Sprinklers or water spray deluge systems often require large quantities of water which are routed into plant areas introducing internal flooding risks during intended or unintended activation. From an operations perspective, fire suppression systems are often connected to some of the largest water supplies on a site, and within the British Standards framework are intended to continuously operate until manually stopped or until the water supply is exhausted. Where fire water pipework is not seismically qualified, wet or pre-charged systems should be assumed to fail, and therefore discharge water, following a seismic event. These types of events would generally be considered under the internal and external hazards topic areas.

However, there are aspects of the provision of suppression systems which are relevant to life fire safety if they are located in areas in which personnel access is required for emergency egress. In such cases such systems, if activated, should not present a risk of injury to any personnel by, for example, asphyxiation. Where there is the potential for such risk to life, alternative fire protection methods are expected to be considered and these may involve intumescent coatings, ablative paints or similar.

## **Ventilation**

As per WENRA Safety Reference Levels (SRLs) [22], for the purposes of protecting a facility against the spread of internal fires, “*ventilation systems shall be arranged such that each fire compartment fulfils its segregation purpose in case of fire. In addition, if parts of the ventilation systems (such as connecting ducts, fan rooms and filters) are located outside fire compartments they shall have a fire resistance consistent with the fire hazard analyses or be capable of isolation from fire effects by appropriately rated fire dampers*”.

Ventilation systems in nuclear facilities are provided to meet a range of safety functions. These include nuclear safety functions such as contamination control and cooling. Therefore, it can be that closing or isolating dampers to prevent the spread of fire would be detrimental to the nuclear safety function of the system. Where this is the case, the ventilation system may either have provisions for redundancy built into it or provisions to ensure safety under the worst-case fire. However, the provision of any ventilation in a building can promote the spread of fire and it is important that dutyholders consider the effects of both forced and natural ventilation on the growth and potential spread of fires. This should be reflected in the licensee's fire modelling to ensure that worst case fire consequences are established, and these drive the safety classification of SSCs relied upon.

While the nuclear safety case may require the ventilation system to run continually under normal operating conditions, in the event of a fire, this may result in additional hazards to personnel, plant and nuclear safety. The very purpose of the ventilation system is to draw air from one area which may result in any smoke from the fire being spread through the building, affecting the ability of personnel to safely exit the building, and also having a detrimental effect on the function of key nuclear safety SSCs, if they are not qualified to continue to operate in a potentially hot, smoky environment or with a system which has been partially isolated or failed. This can pose challenges to confinement or indeed the containment under the evolving, dynamic scenario under consideration.

In line with ONR TAG on Containment: Chemical Plants (NS-TAST-GD-021) [23] the containment must be stable under normal and fault conditions when the physical, chemical, and radiological conditions of the nuclear materials may change. It also explicitly

expects that the “*containment should also retain its stability under both internal and external fault conditions for example fire and seismic events if the consequences are such that the primary function needs to be retained for safety reasons*”. To ensure the above requirements are met ONR SAP EQU 1 [1] (relating to equipment qualification) is applicable, and reference is made in the ONR SAPs to the ECV SAPs series covering containment and ventilation in that the safety case should amongst other considerations:

- a) include provision for making the facility safe following any fault or accident involving the release of radioactive material within or from containment, including equipment to allow decontamination and post-event re-entry to be carried out;
- b) minimize the size and number of service penetrations in the containment boundary, which should be adequately sealed to reduce the possibility of radioactive material escaping via routes installed for other purposes;
- c) justify that, where fire dampers are provided, their position and operation will not compromise either the containment function or the safety functions of the ventilation system;
- d) avoid the use of ducts that need to be sealed by isolating valves under fault conditions. Where isolating valves and devices are provided, their performance should be consistent with the required containment duties and should not prejudice adequate containment performance;
- e) provide for discharge routes, including pressure relief systems, with treatment system(s) to minimize radioactive discharges to acceptable levels. There should be appropriate treatment or containment of radioactive wastes generated by such systems. Should the pressure relief system operate, the performance of the containment should not be degraded;
- f) justify the continuing safe functioning of the containment and its discharge routes in faults or accidents involving combustible, explosive and/or toxic gases.

## CONCLUSIONS

The paper provided an overview of the regulation of fire safety in Great Britain from both nuclear safety and life fire safety perspectives, and reflections and expectations from recent safety case assessment and enforcement activities.

The paper also provided an overview of the synergies and potential conflicts encountered when considering life and nuclear safety perspectives in a nuclear installation context. Key areas of attention where joined-up regulation has played an important role ranged from the design philosophy applied to barriers and penetrations, the use of suppression systems, conflicts arising from the location of laydown areas for combustible materials and the design and operation of ventilation systems to cite some examples. Plant layout optimization from the early stages of design, taking due consideration of both nuclear and life fire safety is key in resolving potential conflicts before solutions are foreclosed by design development and build. Similarly, successful resolution of conflicting demands has required focus on understanding the balance of risks and evolving risk profile of the facilities (when in operation or under decommissioning) in both radiological risk and life risk terms, to ensure the optimum enforcement and remedial actions were pursued.

## REFERENCES

- [1] Office for Nuclear Regulation (ONR): Safety Assessment Principles for Nuclear Facilities, 2014 Edition Revision 1, January 2020, <http://www.onr.org.uk/saps/>.
- [2] International Atomic Energy Agency (IAEA): Protection against Internal Hazards in the Design of Nuclear Power Plants, Specific Safety Guide, IAEA Safety Standards Series No. SSG-64, STI/PUB/1947, ISBN 978-92-0-116121-5, Vienna, Austria, August 2021, [https://www-pub.iaea.org/MTCD/publications/PDF/Pub1947\\_web.pdf](https://www-pub.iaea.org/MTCD/publications/PDF/Pub1947_web.pdf).
- [3] International Atomic Energy Agency (IAEA): Protection Against Internal and External Hazards in the Operation of Nuclear Power Plants, Specific Safety Guide, IAEA Safety Standards Series No. SSG-77, Vienna, Austria, March 2022, [https://www-pub.iaea.org/MTCD/Publications/PDF/Pub1991\\_web.pdf](https://www-pub.iaea.org/MTCD/Publications/PDF/Pub1991_web.pdf).
- [4] International Atomic Energy Agency (IAEA): Safety of Nuclear Fuel Cycle Facilities, Specific Safety Requirements, IAEA Safety Standards Series No. SSR-4, STI/PUB/1791, ISBN 978-92-0-103917-0, Vienna, Austria, October 2017, [https://www-pub.iaea.org/MTCD/Publications/PDF/PUB1791\\_web.pdf](https://www-pub.iaea.org/MTCD/Publications/PDF/PUB1791_web.pdf).
- [5] International Atomic Energy Agency (IAEA): Safety of Nuclear Power Plants: Commissioning and Operation, Specific Safety Requirements, IAEA Safety Standards Series No. SSR-2/2 (Rev. 1), STI/PUB/1716, ISBN 978-92-0-109415-5, Vienna, Austria, February 2016, <https://www-pub.iaea.org/MTCD/Publications/PDF/Pub1716web-18398071.pdf>.
- [6] International Atomic Energy Agency (IAEA): Safety of Nuclear Power Plants: Design, Specific Safety Requirements, IAEA Safety Standards Series No. SSR-2/1, STI/PUB/1715, ISBN 978-92-0-109315-8, Vienna, Austria, February 2016, <https://www-pub.iaea.org/MTCD/publications/PDF/Pub1715web-46541668.pdf>.
- [7] United Kingdom Government, Health and Safety at Work etc. Act 1974, No. 37, 1974, <https://www.legislation.gov.uk/ukpga/1974/37>.
- [8] United Kingdom Government, The Regulatory Reform (Fire Safety) Order 2005, No. 1541, 2005, <https://www.legislation.gov.uk/uksi/2005/1541>.
- [9] United Kingdom Government, Fire Scotland Act 2005, [https://www.legislation.gov.uk/asp/2005/5/pdfs/asp\\_20050005\\_en.pdf](https://www.legislation.gov.uk/asp/2005/5/pdfs/asp_20050005_en.pdf).
- [10] United Kingdom Government, The Building Regulations 2010, No. 2214, 2010, <https://www.legislation.gov.uk/uksi/2010/2214>.
- [11] United Kingdom Government, Nuclear Installations Act 1965 (as amended), 1965, <https://www.legislation.gov.uk/ukpga/1965/57>.
- [12] British Standards Institute (BSI): British Standard (BS) 9999: Code of practice for fire safety in the design, management and use of buildings, 2017, <https://www.bsigroup.com>.
- [13] British Standards Institute (BSI): British Standard (BS) 7974: Fire Safety, 2021, <https://www.bsigroup.com>.
- [14] Office for Nuclear Regulation (ONR): NS-INSPI-GD-073, Nuclear Safety Technical Inspection Guide, The Regulation of Life Fire Safety on Nuclear Licensed Sites - Issue 1, April 2021, [https://www.onr.org.uk/operational/tech\\_insp\\_guides/ns-insp-gd-073.pdf](https://www.onr.org.uk/operational/tech_insp_guides/ns-insp-gd-073.pdf).
- [15] Health and Safety Executive (HSE): The Dangerous Substances and Explosive Atmospheres Regulations (DSEAR), 2002, <https://www.hse.gov.uk/fireandexplosion/dsear.htm>.

- [16] Health and Safety Executive (HSE): Control of Major Accident Hazards (COMAH), 2015, <https://www.hse.gov.uk/comah/>.
- [17] Health and Safety Executive (HSE): The Construction (Design and Management) (CDM) Regulations, 2015, <https://www.hse.gov.uk/construction/cdm/2015/index.htm>.
- [18] HM Government: The Building Regulations 2010, Fire safety, Approved Document B, Volume 2: Buildings other than dwellings, 2019 edition incorporating 2020 amendments – for use in England, online version 2020, <https://www.gov.uk/government/publications/fire-safety-approved-document-b>.
- [19] British Standards Institute (BSI): British Standard (BS) 5839: Fire detection and alarm systems for buildings, 2021, <https://www.bsigroup.com>.
- [20] Office for Nuclear Regulation (ONR): Chief Nuclear Inspector's annual report at Britain's nuclear industry, November 2020, <https://www.onr.org.uk/documents/2020/cni-annual-report-1920.pdf>.
- [21] Office for Nuclear Regulation (ONR): Internal Hazards, ONR Nuclear Safety Technical Assessment Guide NS-TAST-GD-014, Revision 7, October 2021, [https://www.onr.org.uk/operational/tech\\_asst\\_guides/ns-tast-gd-014.pdf](https://www.onr.org.uk/operational/tech_asst_guides/ns-tast-gd-014.pdf).
- [22] Western European Nuclear Regulators' Association (WENRA): Report WENRA Safety Reference Levels for Existing Reactors, Revision 2020, 17<sup>th</sup> February 2021, [https://www.wenra.eu/sites/default/files/publications/wenra\\_safety\\_reference\\_level\\_for\\_existing\\_reactors\\_2020.pdf](https://www.wenra.eu/sites/default/files/publications/wenra_safety_reference_level_for_existing_reactors_2020.pdf).
- [23] Office for Nuclear Regulation (ONR): Containment Chemical Plants, ONR Nuclear Safety Technical Assessment Guide NS-TAST-GD-021, Revision 6, July 2019, [https://www.onr.org.uk/operational/tech\\_asst\\_guides/ns-tast-gd-021.pdf](https://www.onr.org.uk/operational/tech_asst_guides/ns-tast-gd-021.pdf).

# ENSREG Topical Peer Review on Fire Protection – An Overview

**Gisela Stoppa (BMUV, Germany)**  
**Marina Röwekamp (GRS, Germany)**

 **26<sup>th</sup> International Conference on Structural Mechanics in Reactor Technology (SMiRT 26)**  
50 Anniversary Berlin-Potsdam  
17<sup>th</sup> International Post-Conference Seminar on  
"FIRE SAFETY IN NUCLEAR POWER PLANTS AND INSTALLATIONS"



## Introduction

### Background of the Topical Peer Review on Fire Protection

- EU's Nuclear Safety Directive 2014/87/EURATOM (NSD) requires member states to undertake **Topical Peer Reviews** (TPRs) on a coordinated basis at least every 6 years
- The NSD requires for the review
  - A national assessment by each MS based on a specific topic
  - All member states and the EC as observer invited to peer review the national assessment
  - Appropriate follow-up measures to be taken of relevant findings
  - Publication of its main outcome
- After the first TPR on "Ageing Management", now a second TPR is being conducted on "Fire Protection"



## TPR2 Process

<https://www.ensreg.eu/tpr-2-background>

17<sup>th</sup> International SMIRT Post-conference Fire Seminar - October 24 – 25, 2022

3



## TPR2 Objectives and Scope

### Objectives of the TPR2 Process

- Review fire protection provisions to identify strengths and weaknesses
- Share operating experience and identify findings: common issues or challenges, good practices, areas of good performance and areas for improvement
- Develop appropriate follow-up measures for addressing areas for improvement

### Scope of the TPR2

- All installations under the NSD
- All stages in the installations' lifecycle (construction, operation, decommissioning)
- Focus on installations presenting significant radiological risks in case of fire

17<sup>th</sup> International SMIRT Post-conference Fire Seminar - October 24 – 25, 2022

4



## Schedule

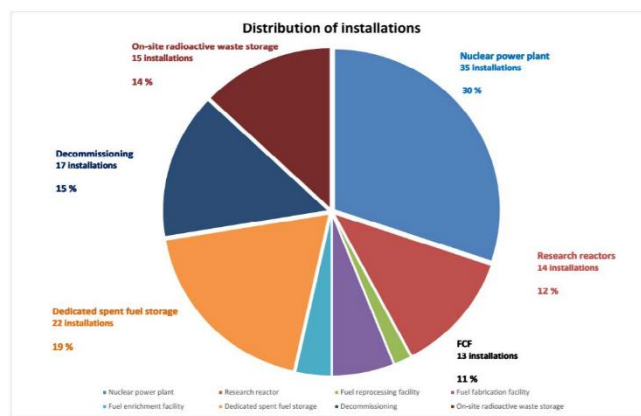


5

17<sup>th</sup> International SMIRT Post-conference Fire Seminar - October 24 – 25, 2022



## TPR2 Sampling Approach



17<sup>th</sup> International SMIRT Post-conference Fire Seminar - October 24 – 25, 2022

6



## Technical Specification (1)

### 01. TS content

| Chapter n° |  |  |
|------------|--|--|
| 00         | General requirements                           | Scope of nuclear installations to be covered in the NARs                     |
| 01         | General information                            | Description of general information about the facilities included in the NARs |
| 02         | Fire safety analyses                           |  |
| 03         | Fire protection concept and its implementation | Fire prevention and protection   |
| 04         | Overall assessment and general conclusions     | Regulator's assessment of the fire safety approach                           |

WENRA



## Technical Specification (2)

- 01 General information**
  - 01.1 Nuclear installations identification
  - 01.2 National regulatory framework
  - 01.3 Improvements in fire safety as a result of experience feedback
  - 01.4 Defence in depth principles

- 00 General Requirements**

- 02 Fire safety analysis**

- 03 Fire protection concept and implementation**
  - 03.1 Fire prevention
  - 03.2 Active fire protection
  - 03.2.1 Fire detection and alarm
  - 03.2.2 Fire suppression
  - 03.2.3 Administrative and organisational issues
  - 03.3 Passive fire protection
  - 03.3.1 Prevention of fire spreading (barriers)
  - 03.3.2 Ventilation systems

*Licensee's experience &  
Regulator's assessment  
and conclusions*



## TPR2 Technical Specification (3)

### Section 0: General requirements

- Objectives:
  - Description of overall fire safety for relevant installations in the scope of the TPR2 including
  - Identification of potential strengths
- Topic (interpretation, benefits)
- Scope of installations to be covered
- WENRA Safety Reference Levels (SRLs)
- Form and content of the NAR



## TPR2 Technical Specification (4)

### Section 1: General information

- Nuclear installations identification
- National regulatory framework
- Improvements in fire safety as a result of experience feedback
- Defence in depth principles and its application
- Contents of the NAR



## TPR2 Technical Specification (5)

### Section 2: Fire safety analyses

- Fire safety objectives
- Scope of the analysis
- Assumptions and methodologies
- Consideration of event combinations, specific plant locations and specific situations
- Consideration of on-site or off-site fire brigades
- Treatment of uncertainties
- Methods, tools and data used for the quantification of (direct and indirect) fire effects
- Consideration of fire phenomena's complexity and severity of potential consequences
- Main results of fire safety analyses regarding safety objectives, incl. for NPPs Fire PSA



## TPR2 Technical Specification (6)

### Section 3: Fire protection concept and its implementation (1)

- **Fire prevention**
  - Process in the design for minimizing likelihood of fire, with due regard to characteristics of radioactive waste in storages
  - Fire prevention means
  - Procedures for management / control of fire loads and ignition sources incl. hot work
- **Active fire protection – Fire detection and alarm**
  - Fire detection and alarm provisions in place
  - Approaches assuring systems are capable to withstand relevant conditions
  - Ensuring detection systems independence between compartments during hazards
  - Alternative arrangements for temporarily disabled fire detection systems



## TPR2 Technical Specification (7)

### Section 3: Fire protection concept and its implementation

#### ▪ Active fire protection – Fire suppression

- Approaches applied in selection, design and location of fire extinguishing systems
- Key design characteristics of the fire extinguishing provisions
- Consideration of harmful effects of inadvertent operation and assuring system reliability
- Consideration of secondary hazards from actuation or rupture of fire extinguishing systems
- Balance between fire extinguishing by fixed systems and manual firefighting in the installation



## TPR2 Technical Specification (8)

### Section 3: Fire protection concept and its implementation

#### ▪ Active fire protection – Administrative and organisational issues

- Firefighting strategies
- Written procedures in place defining responsibility and actions of staff
- Administrative measures to ensure fire protection measures' operability over installation lifetime
- Firefighting capability, responsibilities and organisation
- Safety culture and reinforcement of protection by training, drills, exercises
- Type and contents of firefighting documentation
- Specific provisions for firefighting situations with loss of access routes



## TPR2 Technical Specification (9)

### Section 3: Fire protection concept and its implementation

- **Passive fire protection – Prevention of fire spreading (barriers)**
  - Determining fire compartment barrier boundaries incl. the improvements over time
  - Ensuring that expected fire resistance and stability ratings are fulfilled
  - Description of fire barriers and other means to prevent or delay fire and by products spreading
  - Maintenance of access routes for firefighting
  - Process for justification of fire barrier efficiency over the installation's lifetime
- **Ventilation systems**
  - Specifics of ventilation systems design and operation for not compromising building compartmentation (incl. segregation of safety trains) and maintaining firefighting access routes



## TPR2 Final Outcome of the NARs

### Licensees experiences

- **Fire safety analyses**
  - Identification of strengths and weaknesses as well as actions to address them
  - Consideration of lessons learnt from events, reviews, OSART, INSARR and/or equivalent
- **Fire protection concept and its implementation**
  - Identification of strengths and weaknesses as well as actions to address them
  - Consideration of lessons learnt from events, reviews, OSART, INSARR and/or equivalent

### Regulator's assessment and conclusions

- Assessment of the licensees' reporting including experiences from regulatory oversight
- Conclusions on the adequacy of the licensee's analyses and protection concepts identifying main strengths, weaknesses and actions from overview evaluation of the self-assessment

# **Performance Objectives and Criteria for the Annual Plant Condition Inspection (APCI) at Nuclear Power Plants**

Abderrazzaq Bounagui

Canadian Nuclear Safety Commission (CNSC), Ottawa, Ontario, Canada

## **ABSTRACT**

Fire safety is important throughout the lifetime of a nuclear plant, from design to construction, commissioning, plant operation and in decommissioning. In Canada, the requirements for fire protection for a nuclear power plant (NPP) are established in CSA N293. Annual Plant Condition Inspection (APCI) is one element of the fire protection program. CSA N293 requires an APCI to be conducted by an independent third party at least once a year. The APCI is a visual inspection intended to verify that the NPP is in general compliance with the operational requirements of the CSA N293 Standard and the National Fire Code of Canada (NFCC). From a regulatory perspective, the APCI is also expected to be conclusive and to identify areas of weakness, areas containing precursors to unsafe fire conditions, as well as areas where best industry practices are implemented.

This paper presents the performance objectives and criteria for the key elements of the APCI. Given the wide range of reactor facilities – especially of advanced and small modular reactors (SMRs) – and given that reactor facilities have risk profiles that vary significantly, depending on the particular characteristics of the plant, a risk-informed approach can be applied to demonstrate that APCI's performance objectives are met.

### **Disclaimer:**

This paper represents the opinions of the author and is the product of professional research. It is not meant to represent the position or opinions of the CNSC nor the official position of any staff member. The performance objectives and criteria for the key elements of the APCI is a recommended practice. It is anticipated that sound engineering judgement will be utilized when implementing it.

## **INTRODUCTION**

Fires can start at any time and at any location which contains permanent or transient combustible inventories, providing an ignition source of sufficient energy is present. Fires generate flames, heat, smoke, and other combustion products, all of which have the potential to damage structures, systems, and components (SSCs) delivering safety functions in NPPs and to prevent normal operation and actions needed to maintain nuclear safety. Fire safety is important throughout the lifetime of a plant, from design to construction, commissioning, plant operation and into decommissioning. Therefore, operating organization for a nuclear power plant are required to implement a fire protection program to ensure adequate fire protection measures are in place to mitigate the fire risk. The general expectations regarding fire hazards from regulatory perspective is that the impact of the fire hazards on nuclear safety must be controlled and their consequences are carefully evaluated.

In Canada, the requirements for fire protection for a nuclear power plant are established in CSA N293 [1]. Annual Plan Condition Inspection (APCI) is one element of the fire protection program. CSA N293 requires an APCI to be conducted by an independent third party at least once a year. The APCI is a visual inspection of sufficient depth to

assess that the nuclear power plant can continue to comply with the operational requirements of the CSA N293 Standard and the National Fire Code of Canada (NFCC) [2].

The following thirteen key elements of an APCI have been formulated, based on the fire protection operational requirements of NFCC [2] and CSA N293 [1]:

1. Management of transient and combustibles materials;
2. Control of flammable liquids and combustible liquids;
3. Control of dangerous good;
4. Handling, use, and storage of radioactive materials;
5. Control of hot works and ignition sources;
6. Means of egress;
7. Passive fire protection features;
8. Portable extinguishers;
9. Fire alarm systems;
10. Water-based fire suppression systems;
11. Fire hoses;
12. Special fire suppression systems;
13. Impairment of fire protection systems.

The objective of the APCI is to determine whether the 13 elements of the ACFI meet the operational requirements of the N293 and NFCC and to ensure the measures in place are adequate to preclude or mitigate the consequences of a fire at a NPP.

This paper presents the performance objectives and criteria for the thirteen key elements of the APCI. These elements are considered to be the foundation for the fire protection operational requirements for a broad range of nuclear reactor designs (such as light water reactors and heavy water reactors, gas cooled reactors, and other types). The performance criteria formulated are not considered all-inclusive and in practice different criteria may be more or less important in relation to particular circumstances. Given the wide range of reactor facilities – especially of advanced and small modular reactors (SMRs) – and given that reactor facilities have risk profiles that vary significantly, depending on the particular characteristics of the activity or plan, a risk-informed approach can be applied to demonstrate that the ACFI's performance objectives are met.

## **FIRE PROTECTION PROGRAM GOALS**

The fire protection goals as defined in CSA N293 [1] are to:

- minimize the risk of radiological releases to the public that are a result of fire,
- protect nuclear power plant occupants from death or injury due to fire, and
- minimize the impact of radioactive and hazardous materials on the environment as a result of fire.

From a fire protection perspective, and to ensure that NPP are operated, and activities conducted so as to achieve the highest standards of safety that can reasonably be achieved, measures have to be taken to:

- Prevent fires from starting;
- Detect rapidly, control and promptly extinguish fires that do occur;

- Minimize the consequences of fires;
- Control severe nuclear plan conditions and mitigate the consequences of severe accidents; and
- Mitigate radiological consequences of significant releases of radioactive substances.

These objectives are achieved through a combination of design (e.g., physical barriers, spatial separation, fire detection and suppression systems), management of fire protection (e.g., operational procedures), quality assurance and emergency arrangements.

## **PERFORMANCE OBJECTIVES AND CRITERIA FOR THE ANNUAL PLAN CONDITION INSPECTION**

The following section presents the performance objectives and criteria for the key element of the APCI. The performance criteria formulated are not considered all-inclusive and in practice different criteria may be more or less important in relation to particular circumstances.

### **1. Management of transient and combustibles materials**

#### **Performance objective:**

Combustible materials are controlled throughout the plant so that they do not pose a hazard beyond the capabilities of existing fire protection measures and to limit the severity and effects of fire.

#### **Performance criteria:**

- Combustible materials, other than those for which the location, room or space is designed, are not permitted to accumulate in and around buildings in quantities or locations that constitute an undue fire hazard.
- Temporary panels, tarpaulins, and screens are of non-combustible or fire retardant material in accordance with CSA N293.
- Wood is only used where there is no reasonable alternative and where wood is used, it is treated with a fire retardant coating in accordance with CSA N293.
- Transient combustibles are eliminated from in any part of an elevator shaft, ventilation shaft, means of egress, service room, service space, areas where hot work is being conducted, areas where work with radioactive material is being conducted; areas where fissile material may be present; in the vicinity of safety system equipment and cables and areas designated as sensitive by the fire protection assessment unless under a transient material control process.
- Transient materials are governed by the fire protection program (FPP) in the form of a permit or other documentation that accompanies the material until it is removed from the plant.
- Placement of transient materials is properly assessed, analysed by a person knowledgeable in fire protection and authorized through the FPP before being implemented in the field.
- Approved locations for transient materials are based on an evaluation of the fire protection assessment (FPA) or the site review for the plan, location of nearby plant equipment and safety-related SSCs, and the presence and proximity of fixed fire protection equipment

- Areas where storage is prohibited are documented, inspected and non-compliances identified and remediated.
- Transient (i.e., non-permanent) combustible materials, particularly packaging materials, in areas identified as important to safety, are removed as soon as the activity is completed (or at regular intervals) or are temporarily stored in approved containers or storage areas.
- Combustible materials are stored in designated areas so that contact with ignition sources and obstruction of means of egress is avoided.
- Proper waste receptacles are of non-combustible construction, equipped with close-fitting, self-closing metal lid or smoke eater lid.
- Materials subject to spontaneous ignition, such as oily rags, are deposited in a receptacle.

## 2. Flammable liquids and combustible liquids

### ***Performance objective:***

Flammable liquids and combustibles liquid are controlled to minimize the risk of release of hazardous substances and to limit the severity and effects of fire.

### ***Performance criteria:***

- Flammable liquids and combustible liquids are not stored in the containment structure.
- The handling and storage of dangerous goods are not located near the control room or other areas that contain safety related systems.
- Equipment and machinery are provided with suitable protective coverings or drip guards to prevent them from absorbing flammable or combustible liquids.
- Flammable liquid cabinets are well maintained, doors closing properly, and combustible materials are not stored on or adjacent to cabinets.
- Containers constructed of electrically conducting material, for the dispensing of Class I flammable liquids are grounded / bonded against static electrical charge in accordance with the NFCC.
- Flammable liquids and combustible liquids are excluded from exits (includes stairwells), principal routes that provide access to exits (includes corridors and aisles), elevators and other areas as defined by the FPA.
- Flammable and combustible liquids are not stored in areas where temperature extremes or atmospheric pressure that could cause their containers to become deformed or rupture, or physical impact or temperature extremes that could cause a chemical reaction or chemical instability such that a fire could occur.
- Flammable or combustible liquids are not kept in a lab/area in quantities that exceed the supply necessary for normal operations.
- Flammable liquids and combustible liquids are not stored with other non-compatible dangerous goods classified as radioactive materials in quantities or in a manner that would constitute an undue risk in the event of a fire.
- Spill absorbents / neutralizers compatible with the dangerous goods present are provided at an easily accessible location.
- Flammable and combustible liquids are stored in specially designed storage areas in accordance with the FPA and NFCC.

- Room designed for the purpose of flammable and combustible liquids and compressed gas storage is:
  - located on an exterior wall,
  - accessible directly from the exterior,
  - equipped with gas-tight, self-closing and latching doors,
  - designed to prevent critical structural damage resulting from internal explosions,
  - equipped with natural or mechanical ventilation
  - free of fuel-fired appliances or high-temperature heating elements,
  - used for no other purpose.

### 3. Control of dangerous goods

***Performance objective:***

Dangerous good are controlled to limit the severity and effects of fire or explosions.

***Performance criteria:***

- Dangerous good are handled, stored, used in a manner that complies with applicable codes and standards adequate capacity, in appropriate location with adequate fire protection features for storage and laydown areas.
- Transient compressed gases and cryogenic fluids are not handled, used, located, or stored near safety-related equipment unless analysed under the FPA and governed by the FPP.
- Compressed gas cylinders are provided with protective valve caps, stored, and secured (using a non-combustible restraining straps or chains) in the upright position, and protected against mechanical damage,
- Compressed gas cylinders are not stored in any exit or corridor providing access to exits, under any fire escape, outside exit stairs, passage, or ramp, or within 1 m distance to any exit.
- Areas where dangerous goods are stored are maintained free of waste packaging material, debris of any kind, or any spilled product.
- Quantities of dangerous goods located outside of appropriately designed storage rooms and those required are limited for immediate use and assessed for potential consequences.
- Dangerous goods are not stored with other non-compatible dangerous goods and dangerous goods classified as radioactive materials in quantities or in a manner that would constitute an undue risk in the event of a fire.
- The amount of transient compressed gas or cryogenic fluids located in portable containers, cylinders, or tanks are minimized
- Compressed gas cylinders stored outdoors are supported on raised concrete or other non-combustible platforms and located in an enclosed fenced.

#### **4. Hot works and ignition sources**

##### ***Performance objective:***

Ignition sources and hot works are governed by FPP via a permit system and controlled to minimize the risk of accidental ignition.

##### ***Performance criteria:***

- Electrical installations are used and maintained so as not to constitute an undue fire hazard.
- Electrical cables do not show any damage or wearing.
- Placement of temporary ignition sources (including but not limited to hot works, heaters, grinding, the use of extension cords) is analysed by a qualified person and authorized before being implemented in the field.
- Building and machinery surfaces are kept clean of accumulations of combustible dusts using cleaning equipment that is made of materials that will not create electrostatic charges or sparks.
- Heat-generating equipment or equipment with hot surfaces is properly cooled or separated from combustible materials.
- Smoking only takes place in designated smoking areas.
- Work involving ignition sources such as welding and flame cutting are carried out under closely controlled conditions and through FPP permit system.
- Work involving hot work are authorized, verified and close out by appropriate staff.
- Persons performing hot work are trained and equipped to prevent and combat fires.
- Fire watches are implemented where welding, cutting, grinding, or open flame activity is carried out.
- All valves are closed and gas lines bled when dangerous goods are not in use.
- A fire extinguisher is placed in the immediate hot work area.
- Combustible and flammable material within 15 m distance from the hot work are protected.
- Areas designated for hot works are free of combustible and flammable contents and have walls, floors and ceilings of non-combustible construction or lined with non-combustible material.

#### **5. Handling, use, and storage of radioactive materials**

##### ***Performance objective:***

The storage, handling and use of hazardous substances are controlled in a manner that minimizes fire risk as low as reasonably achievable.

##### ***Performance criteria:***

- Radioactive Material Storage Areas (RMSA) are inspected controlled and maintained.
- Combustible materials are not to be stored in the same fire compartment as radioactive materials unless permitted by FPA and governed by the FPP.

- Radioactive materials are stored such that they are protected from fires and fire-fighting activities.
- Provisions are in place to minimize substance quantity, protect substances from fire and avoid any reactions due to substance incompatibility.

## 6. Safety to life: means of egress

### ***Performance objective:***

Means of egress are maintained to facilitate the timely movement of persons to a safe place in an emergency.

### ***Performance criteria:***

- Means of egress including aisles, corridors, stairwells and exit doors are maintained in good repair and free of obstructions.
- Exterior passageways and exterior exit stairs serving buildings are maintained free of snow and ice accumulations.
- Doors forming part of a means of access or egress are operable.
- Exit lighting and exit signs are visible and illuminated.
- Emergency lightings are maintained in operating condition.

## 7. Passive fire protection features

### ***Performance objective:***

Passive fire protection features are maintained in good condition to limit the spread of fire and to retard the effects of fire on areas beyond its point of origin.

### ***Performance criteria:***

- Fire separations are not damaged (no sign of damage that affect their integrity).
- Fire doors are equipped with a mechanism, which will hold the door in the closed position and to return the door to the closed position after each use.
- Fire doors are not damaged, not obstructed or wedged open.
- Fire doors close without gapping and door latching hardware functions securely.
- Performance barriers, radiant heat shields and local cable protection are undamaged and securely attached.
- Fire dampers, smoke dampers, combination smoke/fire dampers and fire stop flaps are in place and not obviously damaged or obstructed or altered in any way that would prevent the intended operation.
- Structural steel fire proofing is undamaged or deteriorating and structural steel is uniformly covered.
- Fire barriers and electrical and piping penetration seals are not missing from locations in which they appear to be required to complete a fire barriers wall, floor, or ceiling and seals appear to be properly installed and in good condition.

## 8. Portable extinguishers

### ***Performance objective:***

Portable extinguishers are maintained in operating condition and kept readily accessible to minimize the risk of malfunction or damage.

***Performance criteria:***

- Fire extinguishers are conspicuously located where they are readily accessible and immediately available in the event of fire.
- Fire extinguishers are not obstructed by plant equipment or other work related activities.
- Fire extinguishers are not missing from their designated locations.
- Fire extinguishers are improperly removed from their secure position or otherwise subject to corrosive damage or showing corrosion, leakage, or a clogged nozzle.
- Fire extinguishers charged, with the pressure gauge in the acceptable range.
- In large rooms and in certain locations where visual obstructions cannot be completely avoided, means are provided to indicate the extinguisher location.
- Portable fire extinguishers other than wheeled extinguishers are installed using any of the following means:
  - securely on a hanger intended for the extinguisher, in the bracket supplied by the extinguisher manufacturer,
  - in a listed bracket approved for such purpose,
  - in cabinets or wall recesses.
- Wheeled fire extinguishers are located in designated locations. The condition of tires, wheels, carriage, hose, and nozzle are acceptable for wheeled extinguishers.
- Attached monthly inspection records are current or where a bar code system is used the inspection database is updated.

**9. Fire alarm systems**

***Performance objective:***

Fire alarm systems are maintained in good operating condition to minimize the risk of malfunction, absence of alerts, and improper timely notification in an emergency.

***Performance criteria:***

- Fire alarm and detection system components are accessible for purposes of inspection or maintenance.
- The physical condition of the fire alarm and detection devices does not show physical damage, blockage, or potential interference with functionality (not painted, corroded, covered, etc.).
- Manual fire alarm activation devices are visible and readily accessible without reaching over or relocating other objects.
- There are no trouble signals on the fire alarm panel, or where there are trouble signals, appropriate staff are aware of the signal, its cause, and its scope.
- Manual fire alarm activation devices are visible and readily accessible without reaching over or relocating other objects.

## 10. Water-based fire suppression systems

### ***Performance objective:***

Automatic sprinklers are maintained in a good condition and kept readily accessible to minimize the risk of malfunction, damage, and the risk of inadequate performance.

### ***Performance criteria:***

- Sprinkler heads are installed in the correct orientation (e.g., upright, pendent, or sidewall) and are in good condition and free of obstructions.
- Valves are supervised manually or automatically.
- Pressure gauges are within the expected range for the system.
- Sprinkler piping is not used to suspend objects not associated with the sprinkler system.
- Sprinklers do not show signs of leakage; corrosion detrimental to performance or physical damage or otherwise incorrectly painted.
- A clear working space of not less than 1 metre is available around sprinkler control valves.
- Access to manual actuators for fixed suppression systems (e.g., dry water systems) is unobstructed by plant equipment or work-related activities.
- Fire department connections' location is clearly marked and readable under all weather conditions.
- Fire department connections are protected with caps and their access is free of obstructions.
- Fire hydrants are kept readily accessible, and their locations are clearly identified.
- Standpipes are unobstructed.

## 11. Fire hoses

### ***Performance objective:***

Fire hoses are in their designated locations, unobstructed and are in good condition to minimize the risk of malfunction, damage, and the risk of inadequate performance.

### ***Performance criteria:***

- Fire hoses and hose stations are in their designated locations, in good conditions, and are not damaged nor and not obstructed.
- The hose is connected to the standpipe hose connection and is properly placed on the hose rack.
- The shutoff valve is closed, hand wheel is in place, and valve is not leaking.
- Fire hoses are connected to hose rack nipple or valve and properly rolled and racked.
- Fire hose nozzles and gasket are not missing or deteriorated/damaged.
- Hose rack, hose station piping, and supports in the general area have no excessive rust and corrosion.
- Hose stations are visible, and their access are unobstructed by plant equipment or work-related activities.
- Water supply main control valves to the standpipe system are open.

## **12. Special fire suppression systems**

### ***Performance objective:***

Special fire suppression systems are in their designated locations and are in good condition to minimize the risk of malfunction, damage, and the risk of inadequate performance.

### ***Performance criteria:***

- Gaseous suppression system nozzles are not obstructed or blocked by plant equipment such that gas dispersal would be significantly impeded.
- Suppression agent charge pressure is within the normal band, extinguishing agent supply valves are in their proper orientation and the system is in the appropriate mode.
- Access to manual actuators for special fire suppression systems is unobstructed by plant equipment or work-related activities.

## **13. Impairment of fire protection systems**

### ***Performance objective:***

The impairment of fire protection systems is managed through impairment plans and procedures and impairments are corrected in reasonable time.

### ***Performance criteria:***

- Impairment of fire protection system is governed under the FPP.
- When any portion of a fire protection system is impaired, an impairment form/plan is issued and governed under the FPP.
- Impaired fire equipment and fire systems are identified, tagged, and locked out.
- Compensatory measures are put in place for out-of-service, degraded or inoperable fire protection equipment, and related supporting systems (e.g., detection and suppression systems and equipment, passive fire barrier features, etc.) to ensure that protection is maintained.
- Compensatory measures are appropriate for the level of impairment.
- Personnel, including plant staff, off-site monitoring companies, in-plant and off-site emergency responders, and others affected by the impairment are notified.
- Corrective actions are adequate to return the equipment to service in a reasonable period of time.
- Impairments are monitored and delays in return to service are reported to management.

## **LESSONS LEARNED**

Fire can be a significant risk contributor to a reactor. In many cases, the risk posed by fires is comparable to or exceeds the risk from internal events. Operating organizations are expected to take reasonable actions to mitigate postulated events that could potentially cause loss of large areas of power reactor facilities due to explosions or fires. Operating organizations are required to develop and implement a fire protection program to ensure all the activities related to fire protection are conducted in a coordinated manner and managed adequately to minimize the probability and consequences of fires.

APCI is one of the elements of the fire protection program and one of the many tools such as plant self-assessment and fire protection triennial audit that the operating organizations and the regulators use to assess the adequacy of the implementation of the fire protection program. In the last 10 years the APCI has been successful in identifying areas of weakness and opportunity for improvement associated with the various APCI elements. There is evidence the APCI's findings are being addressed in a timely manner by the stations. However, the APCI findings suggest that the following will continue to assist the operating organization in maintaining the plant in a safe condition.

- The findings of APCI's are to be assigned the appropriate level of priority in order to avoid finding spanning for long periods;
- Medium, high risk, and repeated findings to be reported to an authority capable of addressing the nature of the finding in an expedited time frame;
- Fire prevention training and enhancement to the adherence of the FP program administrative controls to be continually provided;
- Escalation program to be implemented to provide notification to upper levels of management for repeated and outstanding observations of non-compliance practices and to assist in the plants implementing corrective actions in a more timely manner;
- Enhancing the interaction between various groups within the operating organization involved with the fire protection activities.
- Performing an adequate APCI is considered to be one of the cornerstones in ensuring that the station is continually maintained in a fire safe condition.

## CONCLUSIONS

In Canada, NPPs are required to develop and implement a fire protection program in CSA N293 [1]. FPP aim to minimize both the probability of occurrence and the consequences of fire. The FPP at NPPs provides reasonable assurance, through defence in depth, that a fire will not prevent the necessary safe-shutdown functions from being performed. APCI is one element of the fire protection program that need to be of sufficient depth to assess that the nuclear power plant fire prevention and protection activities comply with the applicable codes and standards.

The performance objectives and criteria for the key elements of the APCI have been formulated, based on the fire protection operational requirements of NFCC and CSA N293. They are considered to be the foundation in determining whether fire prevention and fire protection activities meet the applicable codes and standards. The performance criteria formulated are not considered all-inclusive and in practice different criteria may be more or less important in relation to particular circumstances, and a risk-informed approach can be applied to demonstrate that APCI's performance objectives are met.

The APCI has been successful in identifying areas of weakness and opportunity for improvement associated with the various APCI elements.

## REFERENCES

- [1] Canadian Standard Association (CSA): Fire protection for nuclear power plants, CSA N293-12 (R 2017), Toronto, ONT, Canada, 2012.
- [2] National Research Council Canada: National Fire Code of Canada (NFCC) 2020, Toronto, ONT, Canada, 2020.

# Performance of an Effective Self-Assessment to Improve Fire Safety

Paul B. Boulden Jr

Appendix R Solutions, Inc., Hanover, VA 23069, United States of America

## ABSTRACT

Meeting the basic (required) separation criteria of various regulations such as United States Nuclear Regulatory Commission (U.S. NRC) 10 CFR 50, Appendix R [1] is an important first step to managing fire risk. Implementation of these requirements is challenged by availability of standards and guidance documents, qualification of personnel as well as well as the difficulty related to back fit of these new requirements to existing plants. Self-assessments are a critical element of an effective continuous improvement program to fully implement the program and to eliminate “blind spots” that result in high core damage frequency (CDF) values related to fire.

One challenge utilities often face is how to effectively perform a periodic self-assessment of their fire protection programs, and who to involve. This has a tendency to leave unidentified gaps in utility fire protection and safety programs.

Fire protection for nuclear power plants uses the concept of defence in depth to achieve the required degree of reactor safety, but also is dependent on the management of such concept. This concept entails the use of echelons of administrative controls, fire protection systems and equipment, and safe shutdown capability to achieve the following goals:

- Prevent fires from starting;
- Detect rapidly, control, and extinguish promptly those fires that do occur;
- Protect structures, systems, and components (SSCs) important to safety, so that a fire that is not promptly extinguished by the fire suppression activities will not prevent the safe shutdown of the plant.

The intent of a utility fire protection program should be to maintain a robust program that exceeds safety standards. A well-managed fire protection program should be reviewed internally by periodic self-assessment (or assessment by peers), in order to continuously improve safety.

This paper provides an overview of how a well-coordinated fire protection program may implement a periodic self-assessment as part of a continuous improvement program. This paper does not propose the concept that self-assessments can replace nor negate the need for independent regulatory oversight or inspection.

## INTRODUCTION

As identified in the IAEA-TECDOC-1125 [2], “*Experience has shown that when organizations objectively assess their own performance against standards of excellence, the understanding and need for improvements is increased and the feeling of ownership for achieving them is significantly enhanced*”. This certainly applies to the fire protection program, and a strong fire protection program will be enhanced by the utility taking ownership of their processes, and objectively assessing their own performance.

As illustrated by Figure 1, the individuals typically responsible for the performance of self-assessment (Level 1 and Level 2) are the individuals most familiar with the information. As levels are increased, there is a higher degree of separation between the subsequent levels, and the subject information being reviewed.

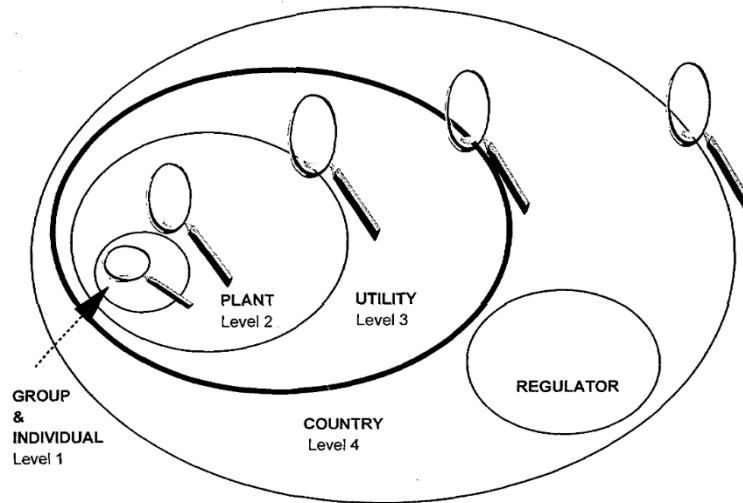


FIG. 1. Self-assessment depending on the position of the viewer.

**Figure 1** Self-assessment depending on the position of the viewer, from IAEA-TECDOC-1125 [2]

Fires can be a major contributor to both CDF and large early release frequency (LERF). In comparison to other internal and external events, many of which are limited to a single component or system failure, fire can affect multiple components or systems. When a fire occurs, it has the potential to grow, spread very quickly, affect many components, and cascade through multiple systems. As stated in (U.S. NRC RG 1.189 [3], “*the primary objectives of fire protection programs (FPPs) at U.S. nuclear power plants are to minimize both the probability of occurrence and the consequences of fire.*”

An effective fire protection program minimizes the potential of fire ignition and growth will lower the probabilistic risk of fire damage within the plant; and limit the deterministic threshold level of damage should a fire initiate.

Under “Fire Protection Program Goals and Objectives” U.S. NRC RG 1.189 [3] includes:

- “*Defense-in-Depth*

*Fire protection for nuclear power plants uses the concept of defense in depth to achieve the required degree of reactor safety. This concept entails the use of echelons of administrative controls, fire protection systems and features, and safe-shutdown capability to achieve the following objectives:*

- *Prevent fires from starting.*
- *Detect rapidly, control, and extinguish promptly those fires that do occur.*
- *Protect SSCs important to safety, so that a fire that is not promptly extinguished by the fire suppression activities will not prevent the safe shutdown of the plant.”*

Other goals cited by RG 1.189 [3] include:

- Fire protection program performance goals to protect SSCs important to safety from the effects of fire;

- Post-fire safe shutdown performance objectives related to safe shutdown after a fire;
- Prevention of radiological releases.

Beyond the regulatory goals listed in RG 1.189 [3], other goals of an effective fire protection program include life safety goals and the protection of the business unit and assets.

The primary goals of an effective and strong fire protection program are the following:

- Recognize the risk and potential consequence of a fire in any location of the power plant;
- Minimize the potential of occurrences and consequences of a fire;
- Minimize the migration of a fire and its effects from the fire area or fire compartment of origin;
- Rapidly detect a fire initiation and ensure the capability to rapidly deploy effective suppression strategies;
- Ensure plant safety, reliability, and continued electrical generation;
- Ensure that operations have the capability to effectively shut down the reactor and maintain it in a safe and stable mode for a single fire occurring in any fire area or fire compartment by maintaining at least one train free of fire damage;
- Support and exceed the local, regional, and national regulatory expectations;
- Identify the various positions of responsibilities and authority within the organization to implement an effective program;
- Verify that the firefighting systems and equipment are designed to assure their rupture or inadvertent operation does not significantly impair the safety capability of SSCs;
- Minimize the potential that a fire will release radiological particles and contaminants outside of the plant boundary.

One of the key insights from the many Fire PRAs (*Probabilistic Risk Assessments*) (also named PSAs (*Probabilistic Safety Assessments*)) performed in recent years is that fires are responsible for a significant fraction of the core damage frequency for a typical nuclear power plant. The same Fire PRAs demonstrate that if a power plant has deficiencies in the basic elements of defence in depth, fire risk could be significantly increased.

In the United States, it took many years to fully implement the requirements of 10 CFR 50, Appendix R due to issues related to availability of standards, guidance documents, qualification of personnel, as well as well as the difficulty related to back fit of new requirements to existing plants. The use of self-assessments has evolved over the last three decades since being introduced to the U.S. Nuclear Market in the 1990s.

In U.S. plants, a high level of fire safety and compliance with regulatory fire protection requirements has been achieved through a combination of regulatory focus on the significance of fire risk and utility self-assessments that allowed effective communication of best practices throughout the industry. Through a process of self-assessments and continuous improvement US plants continue to drive down the risk of fire.

This paper provides the background for how the performance of effective self-assessments can improve fire safety through periodic reviews of plant fire protection programs.

The performance of an effective self-assessment should start with the development of an Assessment Plan.

- Assessment Plan: The Assessment Plan should identify the following
  - Purpose;
  - Scope and depth of the review;
  - Assessment team;
  - Preparation;
  - Period of performance;
  - Location:
    - Determination if the self-assessment will include physical plant walkdowns and observation, or be limited to the review of documents;
    - Determination if there are specific areas within that plant that should be included / excluded from self-assessment;
  - Findings and observations.

## **WHERE TO START WITH A SELF-ASSESSMENT OF THE PLANT FIRE PROTECTION PROGRAM**

It is imperative that an Assessment Plan be developed prior to the performance of a self-assessment. An Assessment Plan is a vital tool in preparing for an efficient and effective self-assessment.

The Assessment Plan, should identify the following

- Purpose: The purpose of an annual review is to assess the plant fire protection equipment and program implementation to verify that a level of safety consistent with NRC guidelines continues to be improved, cf. RG 1.189 [3].
- Scope and depth of the review:
  - Will this assessment be performed globally for the entire facility, or for select areas/ compartments of the plant?
  - Will the assessment be limited to specific subject matters (e.g., quality assurance, periodic review, specific topical area, focus-scope review, pre-assessment in preparation for regulatory review, etc.)?
  - Will the assessment be done in conjunction with regulatory required audit?
  - Some SMEs (subject *matter* experts) have found it helpful to keep a catalog of typical questions as part of an Audit / Assessment Guide as an aid to their utility customers.
  - Note: It is also important to define an expectation for how extensive a review is required. This should be agreed and understood prior to the assessment. This will help to keep resources focused on the review of items deemed in-scope. It is generally not the goal of an assessment to solve problems.
- Assessment team: Identification of stakeholders and key personnel
  - The identification of stakeholders and key personnel will be driven by identification of the goals and objectives, as well as the identification of the scope and depth of review.

- This may include regulatory authority, program sponsor(s), fire protection program owners, site fire marshals, and may require the use of external subject matter experts.
- In U.S. plants it is required that an outside SME be included in the triennial/quadrennial audit, this may sometimes occur in tandem with annual self-assessments:

*“The triennial audit is basically the same as the annual audit; the difference lies in the source of the auditors. Qualified utility personnel who are not directly responsible for the site FPP, or an outside independent fire protection consultant, may perform the annual audit. However, only an outside independent fire protection consultant should perform the triennial audit. The outside consultant should not be an employee of the licensee of the plant being audited.” RG 1.189 [3].*

- Preparation

Once the scope has been defined, expected documents that will likely be requested as part of the assessment may be compiled. This may include plant drawings, regulatory compliance reviews, inspection / testing / maintenance logs, condition reports, reports, etc.

- Timing

- The performance of the self-assessment should be completed in a timeframe that is sufficient to facilitate the completion of the defined scope and depth, and regulatory commitments as required by U.S. NRC Administrative Letter 94-03 [5].
- Duplicate audits are not required (i.e., the 3-year replaces the annual audit for the year in which it is performed) by RG 1.189 [3].

- Location

- A review of the scope will define whether physical presence in the plant is required as part of the assessment, or if the assessment is limited to a review of available documentation.
- Physical plant walkthroughs are an excellent tool to gain insights that may not be obvious by document reviews alone.

- Findings and Observations

A determination as to how findings and observations will be documented should be included in the Assessment Plan. This may include written reports, inclusion in the plant corrective actions program or some hybrid of the two approaches. It is also worth noting that it may be beneficial to document good practices and, if possible, what the positive impact on the organization/ facility has been.

## **HOW TO PERFORM A REVIEW OF ITEMS IDENTIFIED AS ‘IN-SCOPE’ FOR A SELF-ASSESSMENT**

The nature of this question is rooted in revisiting the defined purpose, as well as a review of the scope. What type of assessment is this? Is the assessment limited in scope to particular areas and/or compartments, or subject matter? Is this assessment to prepare for a regulatory review of the fire protection program?

The nature of the assessment will drive what elements of the fire protection program are reviewed.

A good fire protection program with effective self-assessment implementation will be demonstrated by improved performance. Some of the key indicators are as follows:

- Improved engagement by plant staff;
- Reduction of reported fires / repeated events;
- Reduction in call-outs of fire brigade or fire department;
- No loss of life due to fire;
- Reduction in audit / inspection non-conformances for deviations to the program implementation processes or to license bases adherence;
- Reductions in the maintenance work backlog;
- Improved insight into plant upgrade and management of plant processes;
- Continuity of electrical production;
- The PRA continues to demonstrate the fire event analysis results maintain stable or reduced CDF and LERF;
- Competency of the fire brigade during drills;
- The activities associated with “hot work” do not result in a fire;
- The activities of plant personnel do not violate the staging of combustible or flammables materials beyond that approved for the location;
- Manual fire suppression equipment remains readily available;
- Automatic suppression and detection systems avoid multiple maintenance outages and continue to demonstrate functionality;
- Operations continues demonstrate competency in drill execution of safe shutdown procedures and emergency notifications;
- Fire impairments for maintenance and testing are kept to a minimum;
- Reduced costs.

As stated above an effective self-assessment of the plant fire protection program has the potential to reduce costs, by facilitating a healthy program, where items are identified and addressed by performing periodic review of various elements of the program. This allows for more focus being applied to the elements that require improvement.

## **CONCLUSION**

Similar to the U.S. NRC Inspections, today’s fire protection assessments not only need to verify regulatory compliance but also need to maintain risk-significant equipment consistent with assumptions in probabilistic risk models in U.S. NRC Letter SECY-22-0053 [4]. As new tools and methods are developed to manage plant fire risk, so too must the approach to fire protection assessments evolve to incorporate these new approaches.

An effective self-assessment of the fire protection program provides a periodic review of the strengths and weaknesses of a facility when compared to its licensing basis, and the general industry. Fire protection self-assessments are an integral element of an effective continuous improvement program.

As the individuals charged with this responsibility, fire protection program owners and subject matter experts are best equipped to perform this. This periodic review has the

potential to identify areas for improvement and is one of the most powerful tactics a plant can utilize to reduce its overall fire risk and improve its overall level of safety.

## REFERENCES

- [1] United States Nuclear Regulatory Commission (U.S. NRC): Fire Protection Program for Nuclear Power Facilities Operating Prior to January 1, 197910 CFR 50 Appendix R, Washington, DC, USA, March 2021, <https://www.nrc.gov/reading-rm/doc-collections/cfr/part050>.
- [2] International Atomic Energy Agency (IAEA): Self-Assessment of Operational Safety for Nuclear Power Plants, IAEA-TECDOC-1125, Vienna, Austria, 1999, [https://www-pub.iaea.org/MTCD/Publications/PDF/te\\_1125\\_prn.pdf](https://www-pub.iaea.org/MTCD/Publications/PDF/te_1125_prn.pdf).
- [3] United States Nuclear Regulatory Commission (U.S. NRC) Office of Nuclear Regulatory Research: Regulatory Guide 1.189: Fire Protection for Nuclear Power Plants, Revision 2, Washington, DC, USA, October 2009, <https://www.nrc.gov/docs/ML0925/ML092580550.pdf>.
- [4] United States Nuclear Regulatory Commission (U.S. NRC): Letter SECY-22-0053: Recommendation for Modifying the Periodicity of Reactor Oversight Process Engineering Inspections, Washington, DC, USA, June 2022, <https://www.nrc.gov/docs/ML2208/ML22080A253.html>.
- [5] United States Nuclear Regulatory Commission (U.S. NRC): Administrative Letter 94-03, Announcing an NRC Inspection Procedure on Licensee Self-assessment Programs for NRC Area-of-emphasis Inspections, Washington, DC, USA, March 1994.

# IGNIS: A New Experimental Platform Dedicated to Real Scale Fire Studies

Sébastien Thion<sup>1</sup>, Sylvère Mongruel<sup>1</sup>, Nasser Nimanbeg<sup>1</sup>, Rémi Lang<sup>1</sup>, Romain Millerot<sup>1</sup>, Benjamin Beloucif<sup>1</sup>, Inoussa Bongoro<sup>1</sup> and Bernard Gautier<sup>2\*</sup>

<sup>1</sup> Electricité de France (EDF) R&D, Chatou, France

<sup>2</sup> Electricité de France (EDF) DIPNN, Lyon, France

## ABSTRACT

IGNIS is a new experimental platform built by Electricité de France (EDF) to study real scale fire scenarios under nuclear power plant (NPP) conditions. It consists in four different fully instrumented facilities corresponding to graded configurations, one in open atmosphere and three small to large, ventilated rooms. The platform can manage fire sources up to 5 MW, and measured parameters include fuel mass loss rate, heat release rate (mechanical and calorimetric methods), temperature (inside the walls, in the compartments and in the flame), heat flux, gas concentrations, pressure inside the compartments, inlet and outlet flowrates and gas temperatures. This paper presents the platform's characteristics and capabilities as well as some of the first results obtained during the platform's starting and verification campaign. This campaign was designed with a step-by-step approach: a heptane pool fire was first characterized in the open configuration facility (ME4) and in the 20 m<sup>3</sup> compartment with natural ventilation (ME3). It was thereafter installed in the 90 m<sup>3</sup> mechanically ventilated concrete gallery (ME2) and in the 712 m<sup>3</sup> mechanically ventilated concrete compartment (ME1). The results obtained provide a relevant set of validation cases for fire codes.

## INTRODUCTION

Confined mechanically ventilated compartments are typical configurations found in the nuclear industry. Fire events in these configurations generate complex interactions between the flame and the ventilation system as well as potential impacts related to soot, heat fluxes, or temperature on various types of targets (cables, electronic equipment, or fire barriers, etc.). These issues need to be addressed in safety demonstrations, using numerical simulations or relevant experiments.

To reach this objective, EDF has been developing codes and conducting experimental studies at small scale for years on its MILONGA platform. In a recent effort to further develop our experimental capabilities, a new platform was built at Chatou, France with the aim of being able to conduct fire experiments in real scale and in configurations relevant to the nuclear industry. This paper describes the capabilities of this new installation started in February 2021 and illustrates some results obtained during the qualification campaign.

## THE IGNIS FIRE SAFETY PLATFORM

IGNIS is an experimental platform designed to study fire related phenomena in confined environment at real scale. Such configurations are typical to nuclear power plants, that imply mechanically ventilated rooms. The philosophy behind this platform is to be able

to simulate real site configurations and to study different fire scenario in controlled conditions. IGNIS is run by EDF at Chatou, France and includes four different facilities (cf. Figure 1), corresponding to graded configurations that are described thereafter.

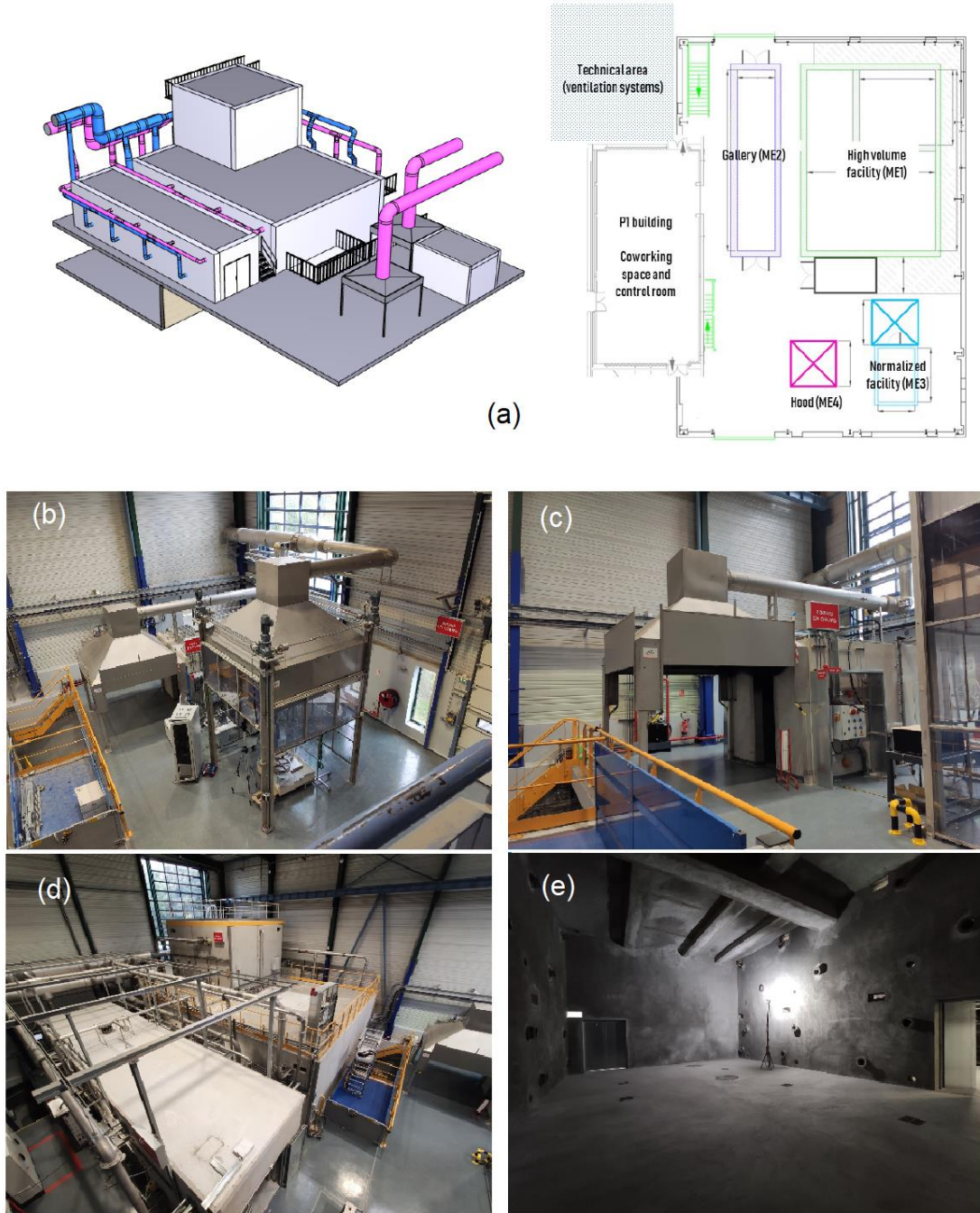


**Figure 1** Illustration of the IGNIS platform: (a) overview, (b) calorimetric hood, (c) normalized room, (d) gallery and large volume facility, (e) inside the large volume facility

### Large Volume Facility (ME1)

This facility consists in a 12 m long by 8.5 m wide building with a 6 m ceiling, and a 5 m x 5 m tower on one of the corners (cf. Figure 1). The ceiling in this corner reaches 10 m, which enables to study shaft configurations. The walls are made of two concrete layers

for a total thickness of 40 cm. The first layer (30 cm) is the perennial structure while the second one is a 10 cm sacrificial shotcrete layer. This layer's role is to protect the structure, and as such, can be removed and replaced during maintenance, which is expected after a few years. This facility is designed to withstand a 5 MW fire and a temperature of 500 °C on the walls for 2 hours. Two openings can be found at the bottom of the structure, on which doors can be adapted.

The building is completely empty, and the philosophy is to build rooms inside the 712 m<sup>3</sup> of the facility, to create each scenario to be studied. The compartment can be split up to 13 rooms distributed over three floors. The facility is connected to the ventilation network through 13 fresh air inlets and 13 exhaust outlets controlled independently.

### **Gallery (ME2)**

The gallery facility consists of a 12 m long and 2.5 m wide building with a 3 m ceiling and is designed for fire studies in gallery configurations (cf. Figure 1). Two 160 cm x 210 cm openings can be found at both sides of the facility. The walls are made of two concrete layers for a total thickness of 40 cm. The first layer (30 cm) is the perennial structure while the second one is a 10 cm sacrificial shotcrete layer. This layer's role is to protect the structure, and as such, can be removed and replaced during maintenance if necessary. This facility can be split into several rooms (up to 4 with identical volume) which can be independently ventilated. The maximum air renewal rate is 21 vol per hour, and this setting is obtained through control valves on the 8 fresh air inlets and 8 exhausts distributed all along the facility. This facility is designed to withstand a temperature of 500 °C on the walls for 2 h.

### **Normalized Room (ME3)**

This facility is inspired from the ISO 9705 norm [1] and consists of a 3.6 min by 2.4 m room with a 0.8 m wide and 2 m high opening on one of the 2.4 m walls (cf. Figure 1). The ceiling's height is 2.4 m for this facility. A 3 m x 3 m steel hood is located at the exit of the room, with a maximum intake flowrate of 7000 m<sup>3</sup>/h. Various mechanical systems (guide plates) are implemented into the exhaust pipe to produce a homogeneous flow and enhance the reliability of measurements that can be done in the exhaust stream (e.g., gas or aerosol concentration).

### **Calorimetric Hood (ME4)**

This facility consists of a 3 m x 3 m steel hood built at a 4 m height, which is used to study open fires and prepare experiments for the ME1 and ME2 facilities (see Figure 1). The maximum exhaust flow rate is 12000 m<sup>3</sup>/h. The exhaust pipe is designed in the ME3 fashion to increase the measurements' reliability. This pipe can be equipped with various measuring systems to study the HRR, soot, temperatures, or gases. The facility is also equipped with motor-driven Lexan screens on each side of the hood that can be controlled independently. These screens can be switched to wire meshes or removed to adapt to various situations.

### **Ventilation System**

The ventilation system enables to inject fresh air into the ME1 and ME2 with a controlled flowrate by modulating the fans' engine frequency and the opening of the control valves of the system. The obtained flowrate is determined based on the reading of Pitot Tubes installed at each inlet port of the two facilities. The maximum inlet flow rate is 12000 m<sup>3</sup>/h.

The combustion gases are also extracted by the ventilation system through outlets on the ME1 and ME2 and through hoods for the ME3 and ME4. Similar to the fresh air injection, Pitot tubes are used to control flowrates in each section of the ventilation network. The extracted gases are cooled by a heat exchanger and filtered by high efficiency filters to remove the soot particles. The maximum outlet flow rate is 20000 m<sup>3</sup>/h. This system is very flexible as it is possible to control every valve (inlet and/or outlet) independently to obtain the desired conditions within the facilities.

## Instrumentation and Acquisition System

### ***Acquisition System***

A specific acquisition system was developed based on LabVIEW and National Instrument Ni-cRIO hardware, which was chosen for its robustness. The architecture that was implemented includes acquisition bays that can be moved around the facilities and that provides all the necessary hardware for acquisition, and a supervision located inside the control room. During an experiment, measurements are recorded locally and regularly transmitted to the control room through an internal network. If the supervision was to crash, the data would still be available on the acquisition bays which secures the result of potentially expensive and time consuming experiments.

The acquisition bays are plugged to an internal Ethernet network, and they include various modules on which sensors can be plugged. Each bay includes 192 thermocouple slots, 32 analogue input ( $\pm 10$  V) slots, 32 analogue input (0 – 20 mA) slots and 8 free slots for evolutions. These acquisition bays can be plugged to various “acquisition stations” distributed on the platform that include network plugs for a connection with the internal network and the supervision, and power outlets. These stations are also fed with compressed air, nitrogen, water, osmosed water, propane and connected to a gas mixing system for gas measurement system calibration.

### ***Instrumentation***

The philosophy behind the conception of the platform is flexibility, that applies also on measurement systems, which means that the instrumentation is adapted to each configuration and associated needs.

Temperature measurements are carried out locally for all facilities using 1 mm Inconel sheathed thermocouples. Temperature inside the walls and roof of the gallery and large volume facilities is also measured through an optical fibre mesh installed inside the shotcrete layer. This optical measurement relies on Raman scattering and enables to monitor temperature inside the walls with a 25 cm spatial resolution and a 0.1 Hz time resolution. The total heat flux is also measured either by water cooled Gardon gauges or by thin-film heat flux sensors that can be installed on surfaces (walls or targets).

Gas concentrations inside the ventilation system or inside the facilities are measured online either by specific analysers (CO<sub>2</sub>, CO, O<sub>2</sub> and total unburned hydrocarbons) or by Fourier Transform Infrared (FTIR) spectrometers to measure 18 gases from aldehydes to inorganic acids.

Fuel mass is monitored using high precision scales. The resulting burning rate is used to compute the heat release rate (HRR) of the flame. The HRR is also computed by calorimetric methods (carbon dioxide generation or oxygen consumption) using methods developed in the literature [2].

Pressure inside the facilities is measured by pressure transducers while differential pressure sensors are used for inlet and outlet flowrates measurements. This type of sensor

is also used in conjunction with McCaffrey probes [3] to characterize flow velocities at openings.

Finally, soot mass concentration and granulometry can be measured online using Electric Low Pressure Impactors (ELPI) coupled to fine particle samplers to dilute the samples [4], [5].

## QUALIFICATION CAMPAIGN

The first experimental campaign on the IGNIS platform was designed following a step-by-step approach which consisted in setting the same sources under grated configurations. Heptane pool fires were selected as the source and were used in all the facilities to investigate various scenarios and configurations. The HRR of the resulting flames went from roughly 270 kW to 4 MW and air renewal rates varied from 0 to 10 vol/h in the closed configurations. The full campaign includes 25 tests, and an illustration of the result is provided here, with a single source (a 50 cm diameter heptane pool fire) studied in the four facilities of the platform.

The source was first characterized under the calorimetric hood, before being used in the other facilities to study naturally ventilated compartment fire, and mechanically ventilated compartment fire scenarios. Some results obtained from these experiments are presented and discussed thereafter as an illustration.

### Calorimetric Hood Results: ME4 – Hept50 Test

For these experiments, a 50 cm stainless steel burner filled with 10 l of heptane was set on a scale in the center of the hood, and the Lexan shields were lifted enough to let a 40 cm high opening. Preliminary tests were carried out to define the exhaust flow rate, to avoid strong perturbations on the flame structure. The exhaust flowrate for this test was therefore set to 4500 m<sup>3</sup>/h, which is a good compromise between efficient smoke exhaust and flame stability. The resulting flame is illustrated by Figure 2. Measurements include temperatures inside the flame, heat flux at 120 cm of the burner center (z = 50 to 250 cm), CO<sub>2</sub>, CO and O<sub>2</sub> concentrations inside the exhaust pipe, exhaust flow rate and gas temperature, and fuel mass loss rate. (MLR)

Figure 3 illustrates some results obtained during this experiment. The HRR profile (a) is consistent with the trend generally reported for such fires with three different phases: (i) flame propagation, during which the HRR sharply increases, followed by (ii) a stationary phase for which the HRR establishes at 270 kW, and (iii) a pre-extinction phase. During phase (iii), the HRR sharply increases, which is due to ebullition of the fuel when the liquid level becomes very low [6]. The HRR is lower than values from the literature, but the available data are scattered, as this parameter depends a lot on the test conditions (constant level burner or not, cooled or uncooled burner, lip height, rim conduction, depth of liquid) [7]. However, the HRR computation using carbon dioxide generation (CDG) and oxygen consumption calorimetry (OC) [2] are in very good agreement with the data obtained from the MLR (“mechanical method”), which supports the validity of the measurement. The enthalpies values used for the mechanical method (44.6 kJ/g), the OC method (12.7 kJ/g), and the CDG method (14.5 kJ/g) were taken from [8].

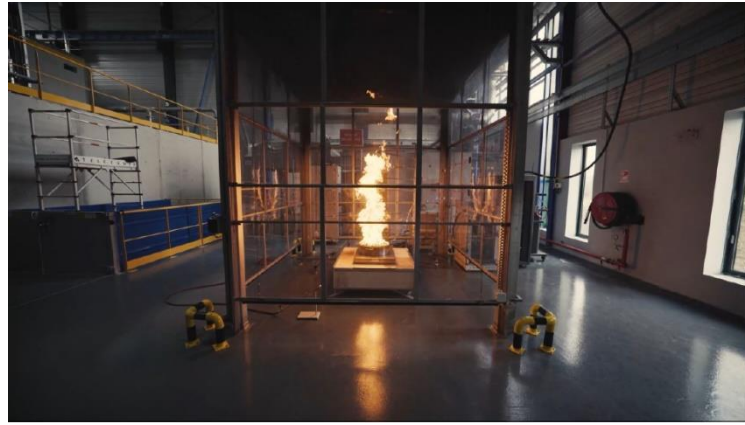


**Figure 2** View of the test in the calorimetric hood ME4

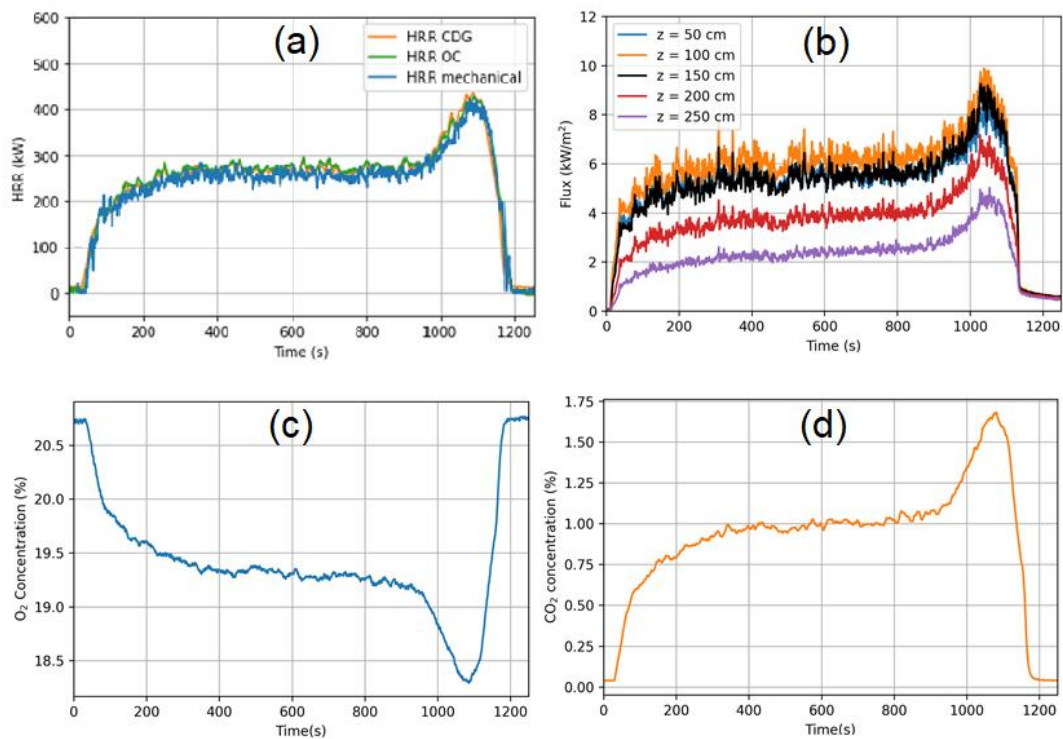


**Figure 3** Illustration of some results for the test under the calorimetric hood: (a) development of the HRR over time, (b) development of the heat flux over time emitted at 120 cm from the burner center, (c) development of the oxygen concentration over time inside the exhaust pipe, (d) development of the carbon dioxide concentration over time inside the exhaust pipe

The heat flux measured at 120 cm from the source centerline is nearly identical from  $z = 50$  cm to 150 cm and decreases for higher heights. The trend observed follows the development of the HRR over time, and the maximum heat flux during the stationary state is close to  $6 \text{ kW/m}^2$ . The trend observed on the  $O_2$  and  $CO_2$  development over time follows the HRR and the concentrations measured during the stationary state are 19.3 % and 1 % for  $O_2$  and  $CO_2$ , respectively.

## Normalized Room Scenario: ME3 – Hept50 Test

In this configuration, the source (a 50 cm diameter burner filled with 7.5 l of heptane) is set in the middle of the room. The exhaust flowrate in front of the opening of the room is set to 6000 m<sup>3</sup>/h. Instrumentation includes MLR, temperature inside the room, heat flux on the walls, heat flux at 180 cm from the burner centerline, O<sub>2</sub>, CO and CO<sub>2</sub> concentrations inside the room and in the exhaust pipe and gas velocity, and temperature along the height of the opening. This configuration and the flames obtained are illustrated by Figure 4.

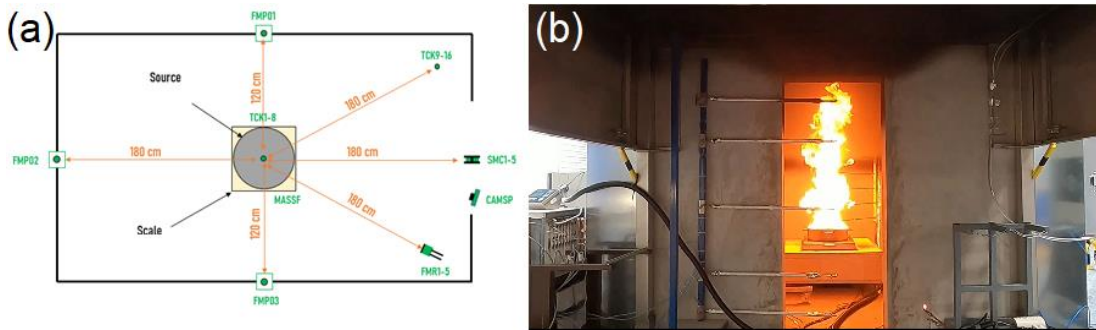


**Figure 4** ME3 – Hept50 Test: (a) configuration for the test inside the normalized room, TCK: temperature measurement, FMP: thin film heat flux sensor, FMR: cooled heat flux sensor and SMC: McCaffrey probe, and (b) view of the test in the normalized room ME3

Figure 5 illustrates some results obtained in this case. The development of the HRR over time is different from the experiment in open atmosphere as no steady state is observed. The HRR increases sharply during the ignition phase, then steadily increases during the whole experiment, until ebullition occurs at  $t = 900$  s, followed by the extinction phase. The HRR computed from the CDG method follows the exact trend of the HRR obtained through the mechanical method, which confirm the dynamic observed, but tends to give higher values. This method depends on the evaluation of the mass flowrate exiting the compartment, which is here evaluated using a limited number of sensors at the door, resulting in more uncertainties in the final HRR values.

O<sub>2</sub> and CO<sub>2</sub> concentrations measured inside the room at  $z = 210$  cm follow the trend observed on the HRR profile: the O<sub>2</sub> concentration sharply decreases during the ignition phase, then slowly drops down until the extinction phase and CO<sub>2</sub> concentration follows an opposite trend. The CO<sub>2</sub> concentrations obtained are higher than in the open atmosphere case, and the O<sub>2</sub> concentration are much lower which is expected as the sampling is performed inside the layer of hot gases that accumulates inside the room [9]. The temperature stratification is very clear (cf. Figure 5(e)): the temperature stays almost constant at 50 °C from the floor until  $z = 130$  cm. A sharp increase (+ 125 °C) is then observed at  $z = 150$  cm, which is the indicator of the hot gas layer.

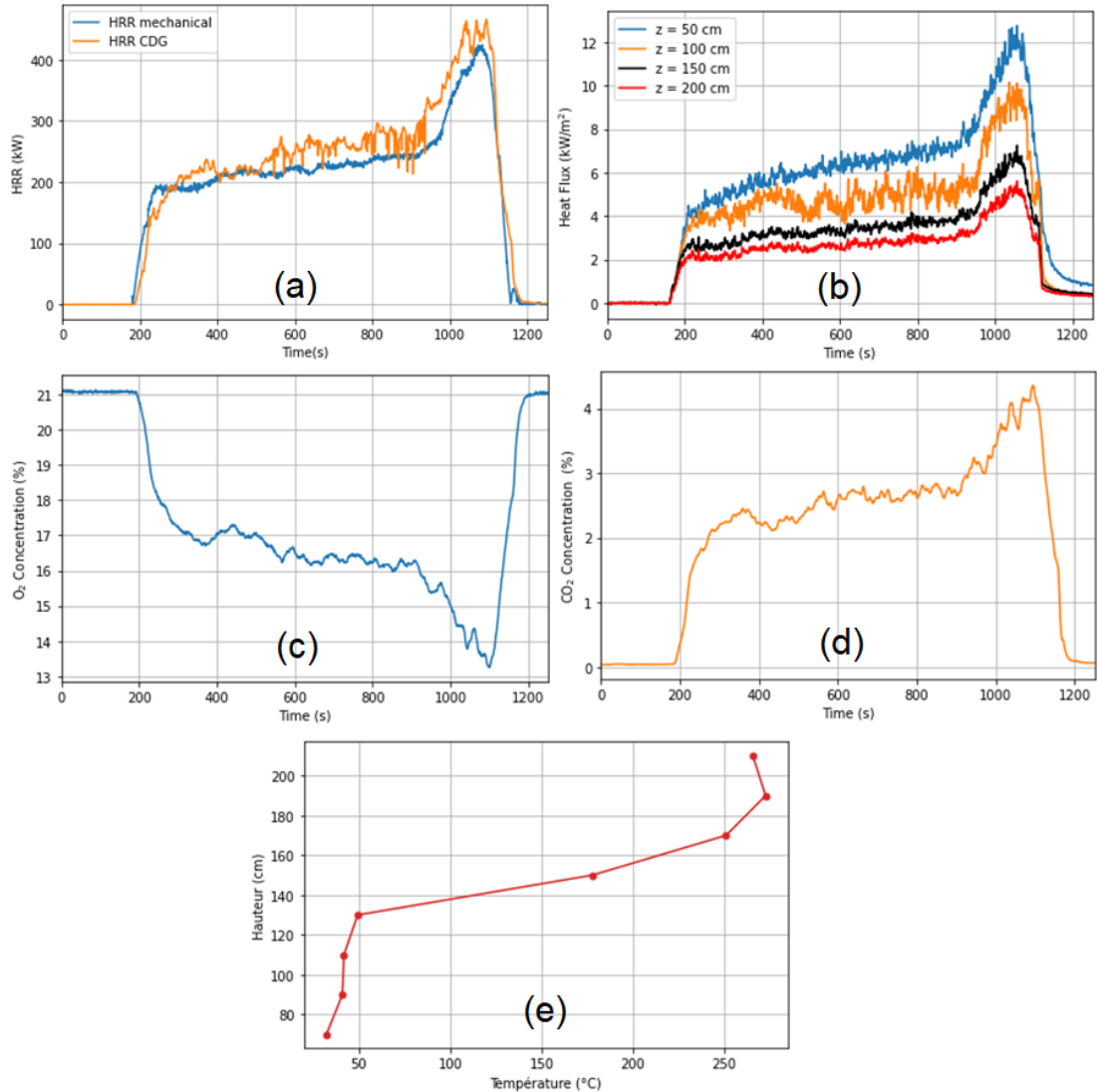


**Figure 5** Illustration of some results for the test inside the normalized room: (a) development of the HRR over time, (b) development of the heat flux over time emitted at 180 cm from the burner center, (c) development of the oxygen concentration over time inside the exhaust pipe, (d) development of the carbon dioxide concentration over time inside the exhaust pipe, (e) temperature profile inside the compartment at  $t = 900$  s

#### Gallery Configuration: ME2 – Hept50 Test

The experiment was carried out with the source (a 50 cm diameter burner filled with 10 l of heptane) in the center of the compartment, and an air renewal rate of 10 vol/h corresponding to a total flowrate of 900  $\text{m}^3/\text{h}$ . The air admission is split equally between the 8 inlets distributed on the whole length of the gallery at  $z = 0$  cm. The same strategy is applied for the exhaust flow rate, with outlets located at  $z = 240$  cm. The temperature inside the room from  $z = 35$  cm to 290 cm is measured by thermocouple trees located at three different positions. Another set of thermocouples is used to measure temperature inside the flame. Heat flux emitted by the flame is also monitored at  $z = 50$ , 100 and 150 cm at 150, 250 and 400 cm from the flame centerline. The heat flux received by the walls as well as their surface temperature are measured by thin sensors.  $\text{O}_2$ ,  $\text{CO}$ , and  $\text{CO}_2$  concentrations are measured at two heights inside the compartment ( $z = 125$  and

275 cm) and in the exhaust pipe. Inlet and outlet flowrates and gas temperature are measured at each inlet and outlet of the facility. Pressure inside the room is also monitored during the whole test. Finally, the optical fibre network is used to monitor temperature inside the walls. This whole configuration and the resulting flame are described by Figure 7.

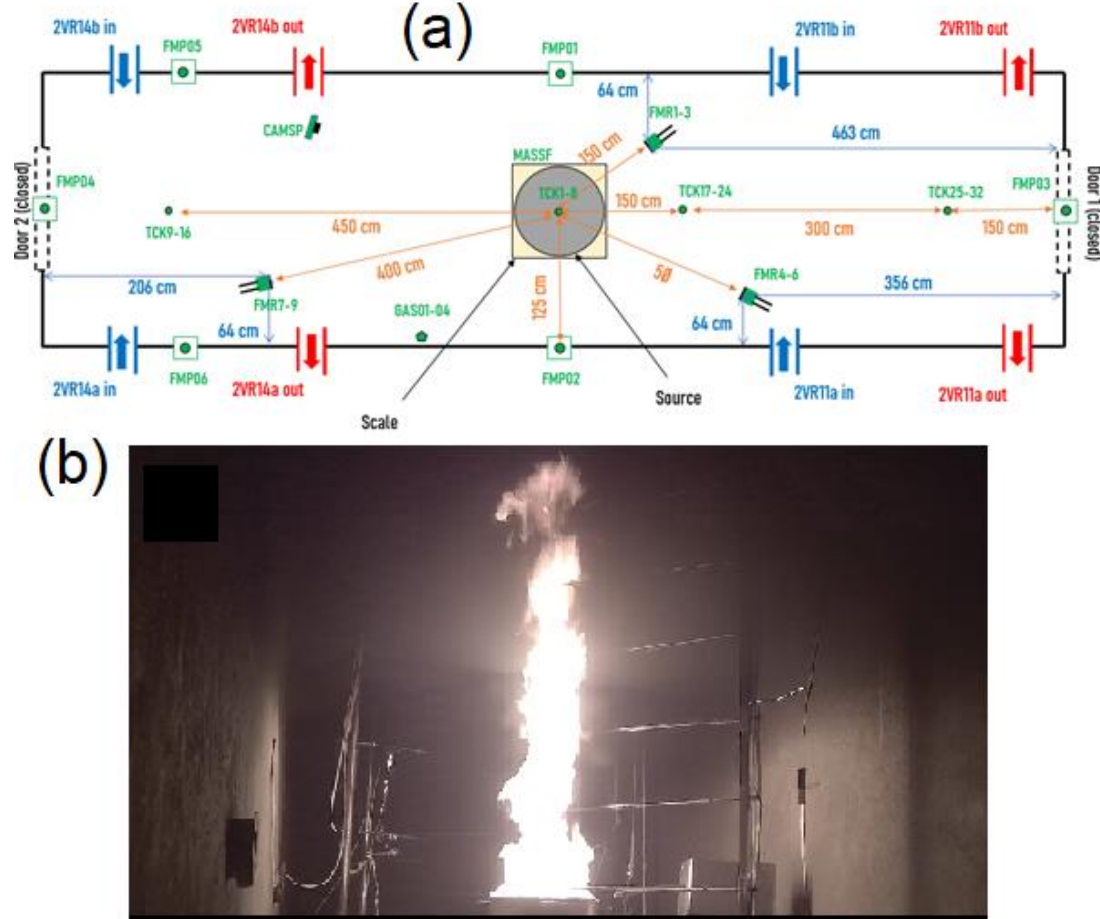


**Figure 6** ME2 – Hept50 Test: (a) configuration for the test inside the gallery, TCK: thermocouples, FMP: thin film heat flux sensor, FMR: cooled heat flux sensor, GAS: gas sampling, MASSF: scale, 2VR in/out: inlet/outlet flowrate and temperature, and (b) view of the test in the gallery (ME2)

Figure 7 illustrates some of the results obtained in this configuration. The HRR follows the same trend as in the previous configurations. The two methods used give slightly different results from  $t = 0$  to 800 s, where the HRR obtained by calorimetry is lower. The values obtained during the steady state (200 kW) are also much lower than those in open atmosphere (250 kW), illustrating the effect of the confinement and ventilation on the HRR [10]. The heat flux measurements at  $d = 150$  cm from the flame centerline show a clear steady state that correlates with the trend observed on the HRR computed by the mechanical method. The amplitude observed on these signals is lower than in the open atmosphere case which is expected regarding the combination of the higher distance to the flame and the lower HRR for this configuration.

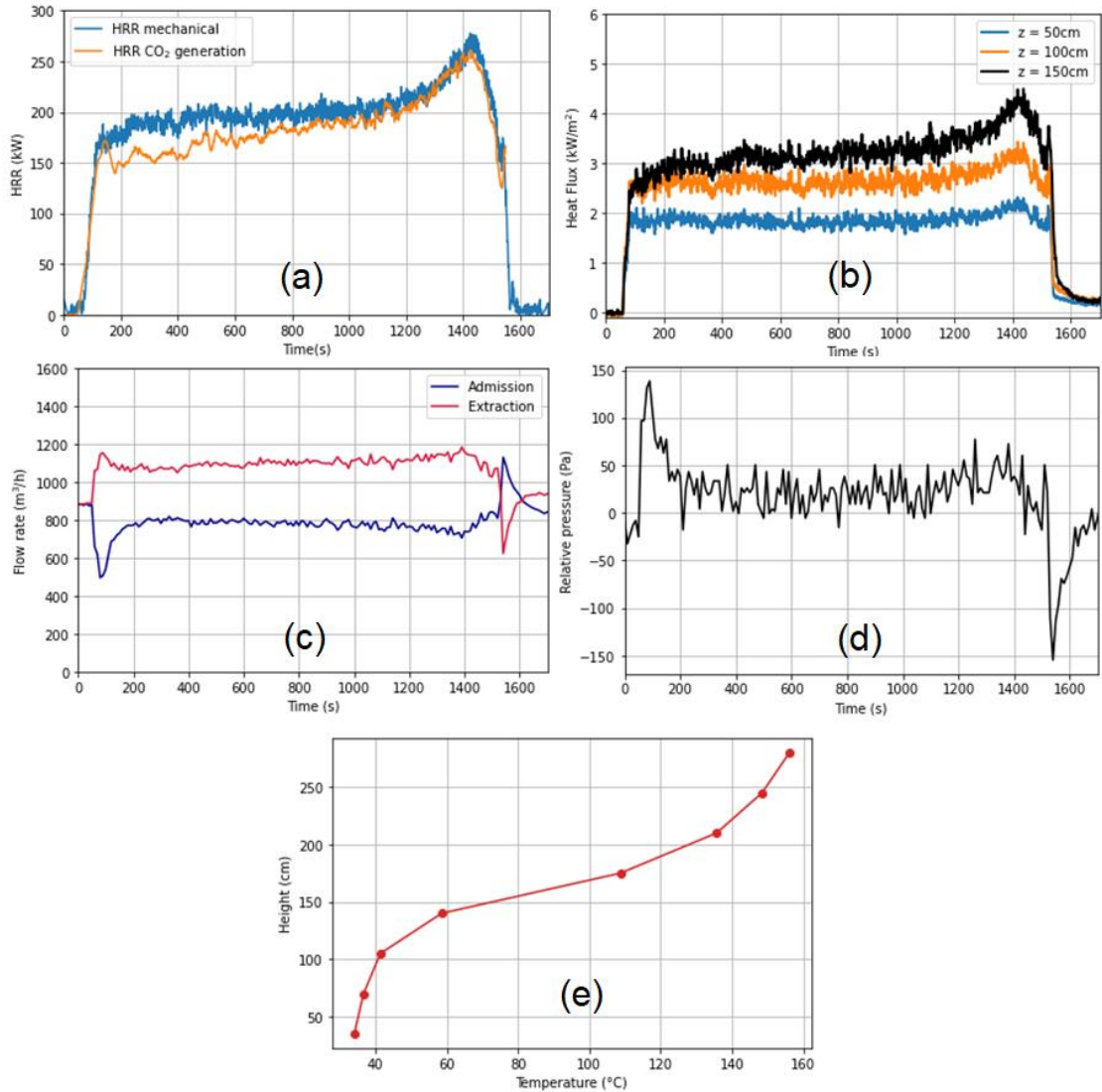


**Figure 7**

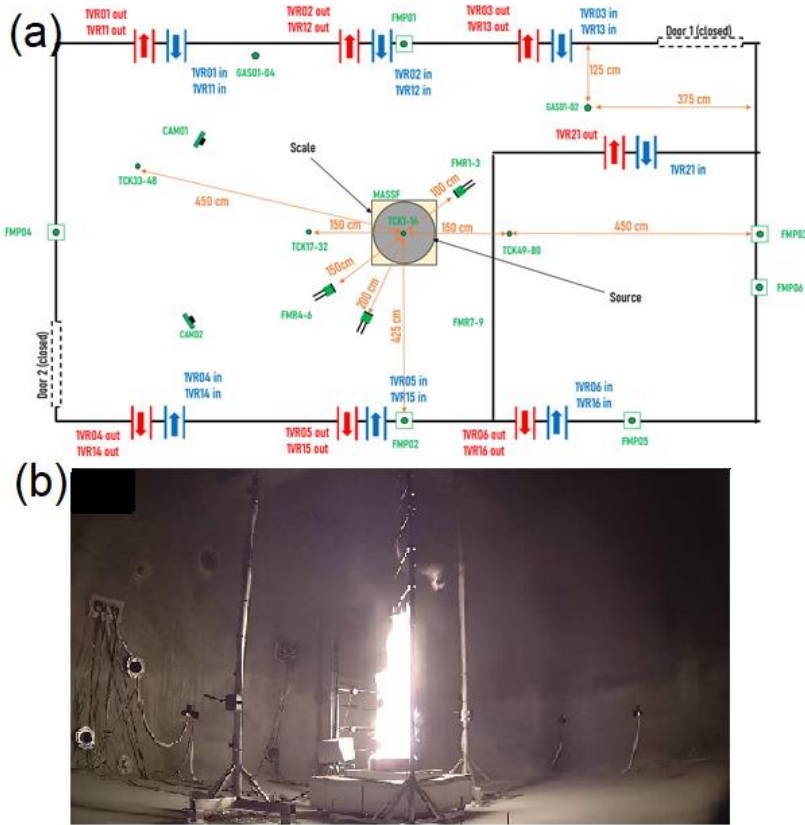
Illustration of some results for the test inside the gallery: (a) development of the HRR over time, (b) development of the heat flux over time emitted at 150 cm from the burner center, (c) development of the total admission and exhaust flow rates over time, (d) development of the relative pressure over time inside the compartment, (e) temperature profile inside the compartment averaged between  $t = 700$  and  $1200$  s

Figure 7(c) to (e) show the time evolution of flow rates and pressure, as well as the temperature profile inside the compartment at the steady state. The results obtained are coherent with the trend described in the literature [11], [12], [13]. The inlet flowrate sharply decreases at the ignition, going from  $900 \text{ m}^3/\text{h}$  to  $500 \text{ m}^3/\text{h}$ . An opposite development is observed with respect to the exhaust flow rate that increases from  $900$  to  $1150 \text{ m}^3/\text{h}$ . A steady state is then observed, with admission and exhaust flowrates respectively at  $800 \text{ m}^3/\text{h}$  and  $1100 \text{ m}^3/\text{h}$ . The pressure also increases sharply at the ignition going from  $-25 \text{ Pa}$  to almost  $+150 \text{ Pa}$  and drops by  $175 \text{ Pa}$  at the extinction. Finally, the temperature profile during the steady state clearly illustrates a stratification, with a cold layer on the bottom of the room, and a hot layer near the ceiling. This stratification is also emphasized by the ventilation configuration, where air admission is performed at the lower parts of the building, while exhaust is set the top part of the compartment.

## Large Volume Facility Configuration: ME1 – Hept50 Test

The experiment was carried out with the source (a 50 cm diameter burner filled with 10 l of heptane) in the center of the compartment, and an air renewal rate of 10 vol/h corresponding to a total of 7120 m<sup>3</sup>/h. The air admission is split equally between the 13 inlets distributed at z = 50, 380 and 685 cm. The same strategy is applied for the exhaust with outlets altitudes at z = 70, 550 and 935 cm.

Temperatures inside the compartment are measured by 4 thermocouples trees spread inside the volume. Temperature is measured from z = 0 cm to 560 cm in two different locations and from z = 0 cm to 980 cm in the tower part of the compartment. Another tree is set inside the flame and is used to record temperature from z = 70 cm to 560 cm. Heat flux sensors are used to measure total heat flux emitted by the fire at d = 100, 150 and 200 cm from the flame centerline, and z = 50, 100 and 150 cm. Similar to the gallery configuration, the O<sub>2</sub>, CO, and CO<sub>2</sub> concentrations are measured at two heights inside the compartment (z = 125 cm and 450 cm) and in the exhaust pipe. Inlet and outlet flowrates and gas temperature are measured at each inlet and outlet of the facility. The pressure inside the room is also monitored during the whole test. A total of nearly 240 parameters were recorded during this test, and the configuration as well as the resulting flame are illustrated by Figure 8.



**Figure 8** ME1 – Hept50 Test: (a) configuration for the test inside the large volume facility, TCK: thermocouple, FMP: thin film heat flux sensor, FMR: cooled heat flux sensor, GAS: gas sampling, MASSF: scale, 1VR in/out: inlet/outlet flowrate and temperature, CAM: camera, and (b) view of the test in the large volume facility (ME1)

A sample of the results obtained during this test is provided in Figure 10. The HRR measured during this test is almost identical to the HRR in open atmosphere configuration. This shows that the large volume available combined with a high air renewal rate makes

it possible to study sources with modest HRRs in open atmosphere configuration inside the large volume facility of the IGNIS platform. The heat flux emitted by the flame at  $d = 100$  cm (b) is consistent with the measurements in open atmosphere: the measured flux during the stationary state at  $z = 100$  cm and  $150$  cm ( $8.7$  kW/m $^2$ ) are higher than those measure at a distance of  $120$  cm under the calorimetric hood ( $5.7$  kW/m $^2$ ). This observation is not true for  $z = 50$  cm, but at this altitude, the sensor is set below the burner which rim is located at  $z = 60$  cm. This results in increasing blocking effect from the insulated box set under the burner when distance is reduced between the burner and the sensor.

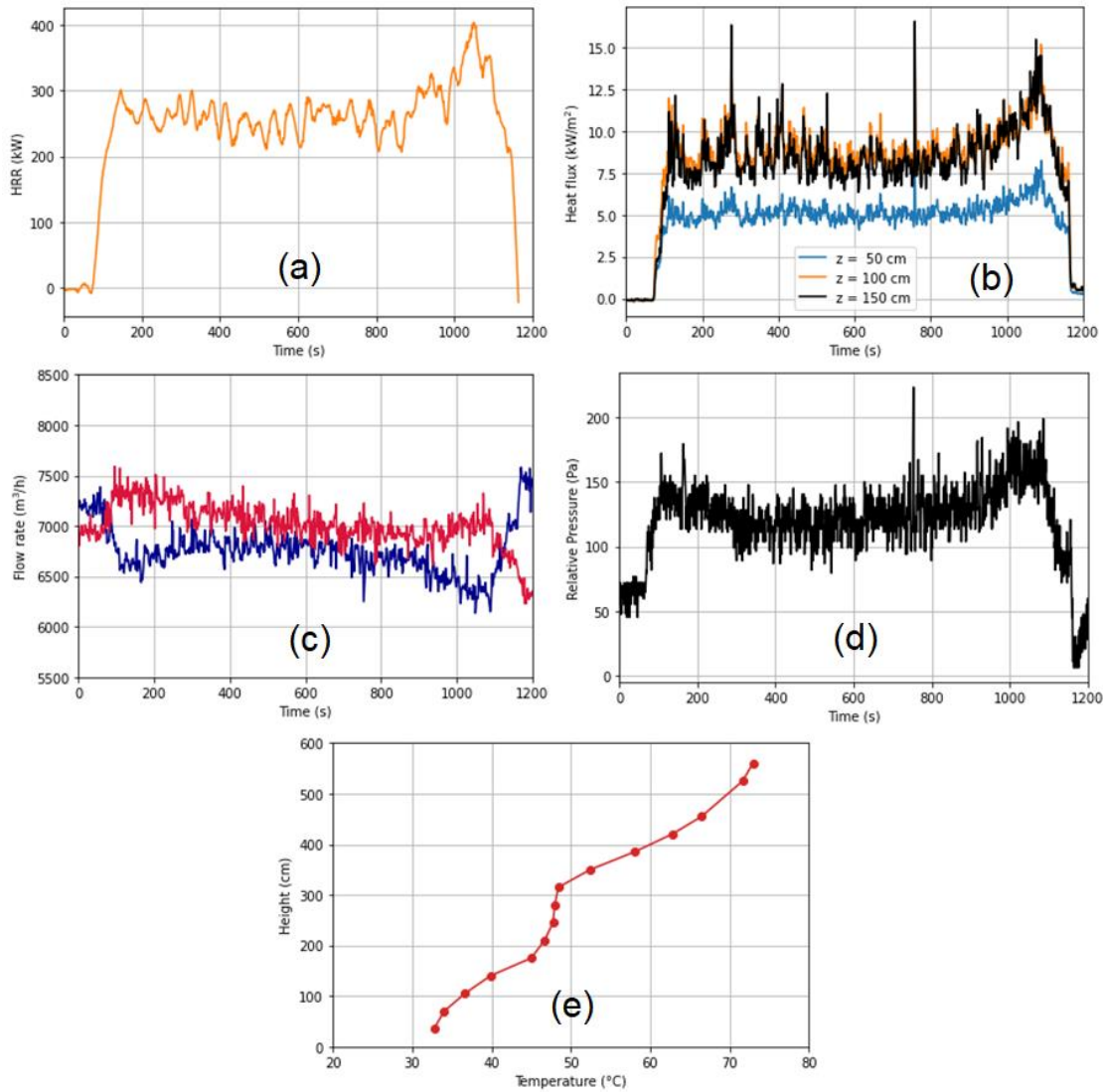


**Figure 9** Illustration of some results for the test inside the large volume facility: (a) development of the HRR over time, (b) development of the heat flux over time emitted at 150 cm from the burner center, (c) development of the total admission and exhaust flow rates over time, (d) development of the relative pressure over time inside the compartment, (e) temperature profile inside the compartment averaged between  $t = 500$  and  $600$  s

Figure 9(c) illustrates the time evolution of admission and exhaust flow rates during the experiment. The trend is similar to what was observed in the gallery configuration: the admission decreases by  $700$  m $^3$ /h at the ignition and the exhaust flow rate increases by

400 m<sup>3</sup>/h. The opposite trend is observed during the extinction phase. The pressure signal (see Figure 9(d)) is also consistent with the expected trend but with a lower amplitude variation than in the gallery case.

A temperature stratification is observed inside the compartment as illustrated by the profile obtained at the stationary state (cf. Figure 9(e)), which is more complex than in the gallery configuration. The temperature rises with height until  $z = 175$  cm, then stabilizes until  $z = 310$  cm before increasing again until the ceiling. The overall temperatures are relatively low, due to the large volume and high air renewal rate.

## CONCLUSIONS

The IGNIS platform is a new installation dedicated to real scale fire experiments recently built by EDF in Chatou, France. It consists in four facilities designed to represent four complementary configurations, from open atmosphere experiments to large volume mechanically ventilated compartment experiment. This platform will be used for improving fire phenomena understanding and further developing fire codes by studying realistic scenarios relevant to the nuclear industry.

The first campaign performed on IGNIS consisted of 25 experiments involving 270 kW to 4000 kW liquid pool fires set in various and complementary configurations to test the capabilities of the facilities. The results and phenomena observed are consistent with the literature.

## REFERENCES

- [1] AFNOR Éditions: ISO/TR 9705-2:2001: Reaction to fire tests. Full scale room tests for surface products – Part 2: Technical background and guidance (Essais de réaction au feu – Essais dans une pièces en vraie grandeur pour les matériaux de revêtement intérieur – Partie 2: données techniques et lignes directrices), June 2001, <https://www.boutique.afnor.org/en-gb/>.
- [2] Prétrel, H., W. Le Saux, and L. Audouin: Experimental determination of fire heat release rate with OC and CDG calorimetry for ventilated compartments fire scenario, *Fire Mater.*, Vol. 38, pp.474-506, 2014.
- [3] McCaffrey, B. J., and G. Heskestad: A Robust Bidirectional Low-Velocity Probe for Flame and Fire Application, *Comb. Flame*, Vol. 26, pp. 125-127, 1976.
- [4] Marjamäki, M., et al.: Performance evaluation of the electrical low pressure impactor (ELPI), *Journal of Aerosol Science*, Vol. 31, pp 249-261, 2000.
- [5] Järvinen, A., et al.: Calibration of the new electrical low pressure impactor (ELPI+), *Journal of Aerosol Science*, Vol. 69, pp. 150-159, 2014.
- [6] Babrauskas, V.: Estimating large pool fire burning rates, *Fire Technology*, Vol. 19, pp. 251-261, 1983.
- [7] Ditch, B. D., et al.: Pool fires – An empirical correlation, *Comb. Flame*, Vol. 160, pp. 2964-2974, 2013.
- [8] DiNenno, P.J. (Ed.): Society of Fire Protection Engineers (SFPE) Handbook of Fire Protection Engineering, 3<sup>rd</sup> Ed., ISBN 978-0877654513, National Fire Protection Association (NFPA), Quincy, MA, USA; 2002.
- [9] Karlsson, B., and J. Quintiere: *Enclosure Fire Dynamics*, CRC Press, Boca Raton, FL, USA, 2000.

- [10] Melis, S., .and L. Audouin: Effects of vitiation on the heat release rate in mechanically-ventilated compartment fires, *Fire Safety Science* Vol. 9, pp. 931-942, 2008.
- [11] Audouin, L., et al.: OECD PRISME project: Fires in confined and ventilated nuclear-type multi-compartments – Overview and main experimental results, *Fire Safety Journal*, 62, pp.80-101, 2013, <https://doi.org/10.1016/j.firesaf.2013.07.008>.
- [12] Prétrel, H., and J. M. Such: Effect of ventilation procedures on the behaviour of a fire compartment scenario, *Nuclear Engineering and Design*, Vol. 23, pp. 2155-2169, 2005.
- [13] Prétrel, H., W. Le Saux, and L. Audouin: Pressure variations induced by a pool fire in a well-confined and force-ventilated, *Fire Safety Journal*, 52, pp. 11-24, 2012.

### **3.2 Session on High Energy Arcing Faults (HEAF)**

The second seminar session addressed the ongoing fire risk significant specific topic of high energy arcing faults (HEAFs) which has been observed in nuclear installations and, in particular in NPPs during operation, but which could also occur during decommissioning. The risk significance of HEAFs which may cause non-negligible damage to the plant and induce ensuing fires and by this increase the contribution of fires (mainly at electrical components) to the overall plant risk. This session was chaired by Koji Shirai from CRIEPI, Japan, being also the Chair of international project on HEAF, Phase 2 (HEAF 2) by the OECD Nuclear Energy Agency (NEA).

The three presentations were focussed on recent regulatory activities in the U.S. for updating the probabilistic risk treatment in the regulation, the recently performed experimental studies of the Japanese nuclear industry on HEAF phenomena in non-segregated electrical bus ducts, and the development of approaches for determining target damage thresholds and the corresponding zones of influence (ZOI) of HEAF.

The contributions of the second seminar session are provided hereafter.

# Overview of U.S. Nuclear Regulatory Commission Research Activities to Update Probabilistic Risk Treatment of High Energy Arcing Faults

Kevin Coyne\*, Nicholas Melly, Kenneth Hamburger, Gabriel Taylor, Mark Henry Salley

United States Nuclear Regulatory Commission, Washington, DC, 20555-0001,  
United States of America

## ABSTRACT

International nuclear power plant (NPP) operating experience has demonstrated that High Energy Arcing Faults (HEAFs), which result from electrical system failures, can cause a sustained arc that leads to the rapid release of energy in the form of heat, vaporized metal, and mechanical force. Because of their hazard and potential risk significance, the U.S. Nuclear Regulatory Commission (NRC) has implemented a multi-year research plan to develop more realistic models and methods to assess HEAF hazards. This paper summarizes, and provides a status update on, the research objectives and key tasks, including: (1) model development and survey of plant electrical applications and configurations; (2) physical testing needed to inform and validate the HEAF hazard model and assess component fragility; and (3) updates to Probabilistic Risk Assessment data and methods to improve the realism and fidelity of the HEAF hazard model. This work also supports the ongoing international Organisation for Economic Cooperation and Development (OECD) Nuclear Energy Agency (NEA) HEAF 2 Project.

## INTRODUCTION

Electrical system failure HEAF events are energetic electrical arcing faults that can lead to the rapid release of energy. This energy release can result in high heat fluxes in the vicinity of the HEAF, vaporization of metal, release of ionized gas and smoke, and mechanical shocks to nearby equipment. The characteristics of HEAF events result in faster development of the fire and associated damage compared to more traditional fire events that include delay time related to the fire ignition and growth stages [1]. As a result, HEAF initiated fire events can rapidly propagate to other equipment and result in unexpected challenges associated with the rapid onset of fire related damage and impacts from smoke and ionized gases.

Because of their potential to induce an initiating event (e.g., loss of feedwater, reactor trip) and lead to failure of adjacent mitigating equipment, HEAF events can have risk-significant impacts. The NRC's Accident Sequence Precursor (ASP) program systematically evaluates U.S. NPP operating experience to identify potential severe accident precursors [2]. An ASP precursor is defined as an initiating event with a conditional core damage probability (CCDP) greater than or equal to  $1 \times 10^{-6}$  (one in a million) or a degraded plant condition resulting in an increase in core damage probability ( $\Delta$ CDP) greater than or equal to  $1 \times 10^{-6}$ . The ASP program identified nine HEAF related precursor events since 1989. Seven of the nine ASP HEAF precursors were analysed as an initiating event and quantified using CCDP, with results ranging from  $\sim 2 \times 10^{-6}$  to  $\sim 4 \times 10^{-4}$ . For these events, the HEAF events resulted in plant transients, loss of electrical busses, and losses of offsite power. Two of the ASP HEAF events were assessed as a degraded condition due to the nature of the specific condition and were quantified

by  $\Delta$ CDP, with results ranging from  $\sim 4 \times 10^{-6}$  to  $\sim 4 \times 10^{-4}$ . Key insights derived from these assessments are the risk significance associated plant transients, loss of electrical busses, and loss of offsite power for HEAF events. Further, design and quality control deficiencies that lead to high resistance breaker connections increase the potential for initiation of HEAF events. The insights from the U.S. experience are consistent with international operating experience for HEAF events [3].

Given the potential risk importance of HEAF events, the NRC has undertaken substantial work over the last two decades, in collaboration with the Electric Power Research Institute (EPRI) and the OECD/NEA, to develop methods and models to support the risk assessment of HEAFs. Specific activities include: (1) model development and survey of plant electrical applications and configurations; (2) physical testing needed to inform and validate the HEAF hazard model and assess component fragility; and (3) updates to Probabilistic Risk Assessment (PRA) data and methods to improve the realism and fidelity of the HEAF hazard model. The results of this program are expected to improve the realism of HEAF models in fire probabilistic risk assessment (Fire PRAs).

## Regulatory Context

The NRC's fire protection requirements are contained in Title 10 to the U.S. Code of Federal Regulations (CFR) Part 50.48, "Fire protection". These regulations require a NPP to implement a fire protection plan that meets the requirements of 10 CFR 50, Appendix A, General Design Criterion (GDC) 3, "Fire protection". GDC 3 specifies, in part, that NPP systems, structures, and components (SSCs) important to safety be designed and located to minimize the probability and effect of fires and explosions. The NRC's regulations provide two options for meeting this requirement: (1) a deterministic option described under 10 CFR 50.48(b) that references the requirements contained in 10 CFR 50, Appendix R, "Fire Protection Program for Nuclear Power Facilities Operating Prior to January 1, 1979," and generally applicable to NPPs licensed before 1979 or as specified in license conditions for later plants; or (2) a risk-informed, performance-based option provided under 10 CFR 50.48(c) which allows use of the National Fire Protection Association (NFPA) Standard NFPA 805, 2001 Edition [4], with some exceptions. The approach described in Appendix R provides deterministic requirements, such as limiting the damage from a fire to ensure that one train of equipment necessary to achieve hot shutdown is free from fire related damage. These criteria generally are supported by prescriptive requirements covering specific fire protection features such as the use of 1-hour or 3-hour fire barriers, installed automatic fire detection and suppression, 20 ft (6.1 m) of horizontal separation with no intervening combustibles, or use of alternate shutdown capability. Conversely, NFPA 805 specifies high level goals, performance objectives, and performance criteria for nuclear safety and radioactive release. The licensee may use engineering analysis, probabilistic risk assessment, or fire modelling calculation to demonstrate that the performance goals, objectives, and criteria are satisfied. As described in the Statements of Consideration for the final rulemaking approving use of NFPA 805 [5], the methodology incorporates a number of attributes consistent with a performance-based approach, notably:

- measurable or calculable parameters exist to monitor the system, including facility performance,
- objective criteria to assess performance are established based on risk insights, deterministic analyses, and/or performance history,
- flexibility to determine how to meet established performance criteria in ways that will encourage and reward improved outcomes, and

- a framework exists to assess the failure to meet performance criterion and to ensure that such failures, while undesirable, will not constitute or result in an immediate safety concern.

The NRC provides guidance for implementing the NFPA-805 option in Regulatory Guide (RG) 1.205, “Risk-Informed, Performance-Based Fire Protection for Existing Light-Water Nuclear Power Plants” [6]. Although a Fire PRA is not mandatory to transition to NFPA 805, RG 1.205 notes that a plant-specific Fire PRA enables a licensee to fully realize the safety and cost benefits of making a transition to NFPA 805, particularly by supporting risk-informed changes to the fire protection program that can be made without prior NRC approval. To the extent that a Fire PRA is used to support NFPA 805 implementation, the NRC must find the PRA approach, methods, and data acceptable. The NRC endorsed NUREG/CR-6850/EPRI 1011989, “EPRI/NRC-RES Fire PRA Methodology for Nuclear Power Facilities, Final Report” [7] and its Supplement 1 [8], as one acceptable method for conducting a Fire PRA. For the purposes of assessing HEAF events, NUREG/CR-6850 and its supplement define a zone of influence (ZOI) surrounding the initiation point of a HEAF event within which certain equipment is assumed to be damaged. For example, the following ZOI guidelines are provided for HEAF events in NUREG/CR-6850:

- For HEAF events within an electrical cabinet, any unprotected cables in the first overhead cable tray within 1.5 m (5 ft) vertical distance of the top of the cabinet and 0.3 m (1 ft) horizontally from the cabinet face will be within the ZOI and assumed to be damaged. Additionally, any equipment within 0.9 m (3 ft) horizontal distance from the cabinet front or rear panel and at or below the top of the cabinet will be within the ZOI (NUREG/CR-6850, Volume 2, Appendix M).
- For HEAF events within an iso-phase bus ducts, the ZOI is assumed to be a sphere centred on the fault point and measuring 1.5 m (5 ft) feet in radius (NUREG/CR-6850, Supplement 1).
- For HEAF events within non-iso phase bus ducts, the ZOI includes: (1) a downward expanding cone from the point of arcing enclosing a total solid angle of 30° to a maximum diameter of 6.0 m (20'); (2) a sphere with a radius of 0.45 m (1.5 ft) from the point of arcing (assumed to be the center of the bus duct) (NUREG/CR-6850, Supplement 1).

## Motivation for HEAF Research

In 2013 the OECD/NEA FIRE (Fire Incidents Records Exchange) Database Project published an analysis of HEAF events that occurred up to mid-2012 [3], which recommended:

*“...to perform experiments for obtaining comprehensive scientific fire data on the HEAF phenomena known to occur in nuclear power plants through carefully designed experiments, to be able to develop more realistic models to account for failure modes and consequences of HEAF, to advance the state of knowledge and provide better characterization of HEAF in fire PRA, and, in particular, to answer key questions, which cannot yet be answered from analyzing the HEAF events in the OECD FIRE Database. Such key questions can be how to prevent and to detect HEAF or what would be the best way for limiting pressure phenomena and minimizing fire barrier element failures.”*

In response to this recommendation, during the period of 2014 through 2016, twenty-six full-scale HEAF experiments were conducted under an OECD/NEA HEAF Project testing program [9]. These experiments used equipment typically found in NPP applications and controlled for four primary parameters: (1) location of arcing within the electrical enclo-

sure; (2) arcing fault current; (3) voltage; and (4) arc duration. Key findings included the potential for increased severity of a HEAF event when aluminum was present and the increased likelihood of a HEAF event leading to ensuing fires for longer duration arcing events (i.e., greater than 2 seconds). As a result of the insights developed from this testing campaign, in addition to other relevant U.S. HEAF operating experience, the NRC issued Information Notice (IN) 2017-04, “High Energy Arcing Faults in Electrical Equipment Containing Aluminum Components” [10]. IN 2017-04 noted that the equipment with copper components exhibited similar damage states as those postulated in NUREG/CR-6850; however, results obtained for equipment containing aluminum components exhibited damage states beyond NUREG/CR-6850 predictions. This observation was a key motivation for additional HEAF research activities.

## OVERVIEW OF HEAF RESEARCH PROJECT PLAN

The NRC’s HEAF research project plan [11] is built upon earlier operating and experimental experience, including the results of the OECD/NEA HEAF Project testing program. This test program also provided valuable insights for measuring HEAF phenomena, including the sensor design requirements for measurement of heat release rates and total incident energy. In addition, the NRC developed an International Phenomena Identification and Ranking Table (PIRT) expert elicitation in 2017 [12] to prioritize research and regulatory needs.

The project plan consists of five main tasks:

1. Development and validation of a computational fluid dynamics (CFD) model capable of predicting HEAF hazards for a wide variety of electrical (e.g., system voltage, available current, fault duration) and equipment configurations (e.g., geometry and materials). The development of a verified and validated predictive model will reduce the amount of testing required to provide representative HEAF results applicable to a broad range of nuclear power plants. However, as discussed below, the development of the CFD (computational fluid dynamics) model required additional physical testing to assess HEAF phenomena and configuration information regarding operating plant electrical distribution systems.
2. Survey of the U.S. nuclear fleet to ensure that full-scale HEAF experiments are representative of plant configurations, and to better understand the location, configuration, and material composition of equipment to support PRA method development. The survey provides information on equipment manufacturers, models, voltages, insulation, and the materials (e.g., aluminum, copper, steel).
3. Physical testing to support the development and validation of the CFD model. This includes a limited set of experiments that span the range of critical parameters to ensure that the development and validation of the model provide acceptable results. Three scales of experiments are included: small, medium (or “open-box”), and full-scale tests, with each series designed to investigate aspects of the HEAF phenomena that are best observed at these different length scales. As noted in the research project plan:
  - Small-scale experiments characterize the morphology and oxidation states of aluminum and copper particles generated by a HEAF event,
  - Medium-scale “open box” experiments characterize the electrical arc to support prediction of arc energy emitted during a HEAF event and provide information on enclosure and electrode mass loss data for both copper and aluminum electrodes, and

- Full-scale experiments provide prototypical nuclear power plant data on enclosure breach, pressure effects, and serve as the representative scenarios for CFD models validated.

4. Fragility testing to assess target damage considering the shorter, higher energy source term associated with HEAF events and support development of a fragility model. The fragility model supports the development of the PRA method for assessing HEAF risk.
5. PRA method development to improve the realism and fidelity of the HEAF hazard model. This task includes an evaluation of U.S. operating experience, updated fire ignition frequencies, updated target fragility thresholds, and updated non-suppression probabilities.

Figure 1 provides an overview of the HEAF research project plan activities. These activities are grouped into three main areas: analytical tasks shown in blue (e.g., tasks 1, 2, and 5), experimental tasks shown in red (e.g., tasks 3 and 4), and outputs from this work shown in green (tools, methods, and data).

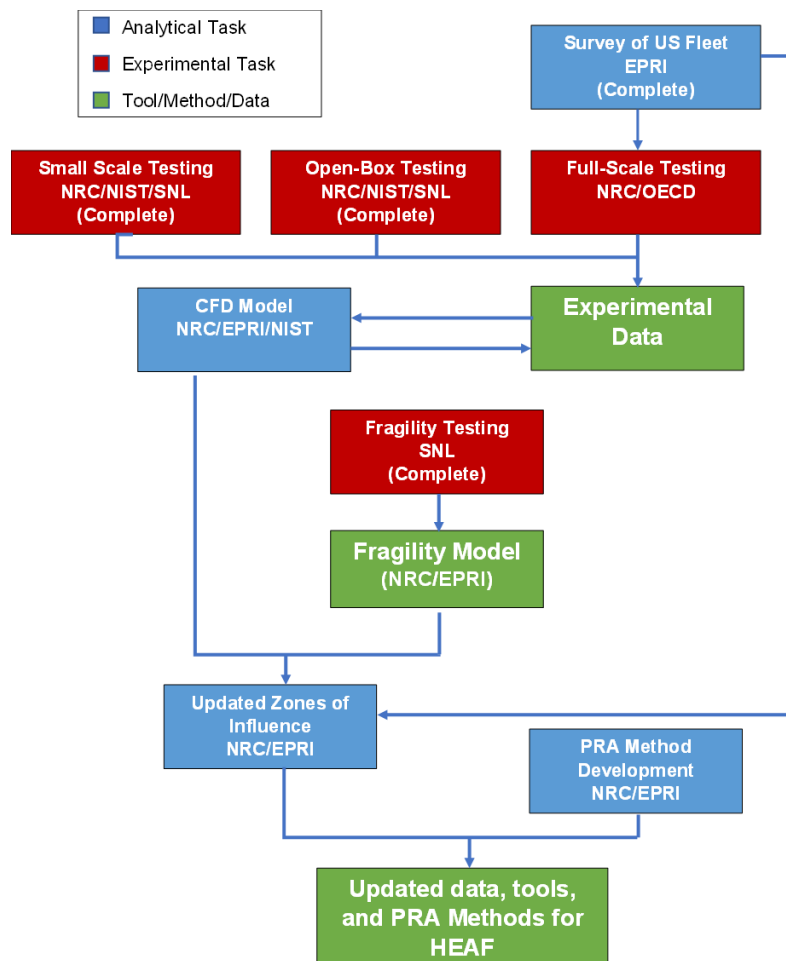


**Figure 1** Overview of HEAF research project activities

A significant portion of the research project plan is being performed under the auspices of the NRC / EPRI Memorandum of Understanding (MOU). This arrangement allows the research activity to better leverage the knowledge and expertise to support the objectives of this work.

Each of the tasks is discussed in more detail in the following sections.

## DEVELOPMENT AND VALIDATION OF A HEAF CFD MODEL

This activity focused on the development of a CFD model of HEAF events capable of calculating the incident energy for a variety of equipment configurations and materials. The predicted incident energy at various distances from the modelled electrical enclosure is subsequently used to determine the ZOIs for specific equipment. The objective of this work was the development of a tool that could leverage experimental data but provide information for configurations that were not subject to full-scale testing. This provided a more cost-effective and flexible approach considering the high costs associated with conducting full-scale HEAF experiments. The Fire Dynamics Simulator (FDS) was used to support this effort. FDS was initially released in 2000, has undergone extensive verification and validation, and provides significant capabilities to study fire dynamics and combustion. FDS includes a hydrodynamic model capable of solving the low-speed, thermally driven flow using a large eddy simulation turbulence model [13]. FDS includes a combustion model and a radiative heat transport model, in addition to capabilities for accommodating a wide variety of geometric configurations. A calculation matrix for FDS simulation runs was built on information gathered from surveying the U.S. nuclear fleet (e.g., switchgear manufacturer, bus bar materials, potential fault locations), operating experience, and previous testing. Over 130 simulation runs were identified, covering the following characteristics:

- Low voltage switchgear – bus bar material (aluminum, copper), arc duration, arc location, arc energy (34 FDS simulations);
- Medium voltage switchgear - bus bar material (aluminum, copper), arc duration, arc location, arc energy (42 FDS simulations);
- Non-segregated bus ducts – duct and bus bar material (aluminum, copper), arc duration, arc location, and arc energy (57 FDS simulations).

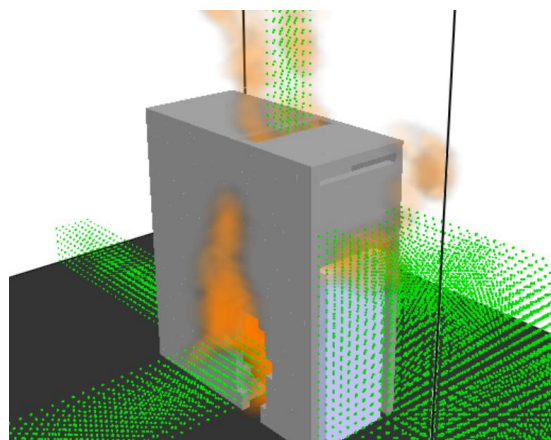


**Figure 2** FDS calculated thermal plume for a 226 MJ HEAF (medium voltage switchgear cabinet)

An overview of the preliminary results of this work was published for public comment in May 2022 [14].

To provide additional confidence in the ZOIs calculated using FDS, the NRC staff also developed a modified model based on IEEE 1584-2018, “IEEE Guide for Performing Arc-Flash Hazard Calculations” [15]. This standard was developed to estimate incident energy at various distances from an arc flash event for the purpose of electrical safety. The NRC effort modified the IEEE arc flash model and its application in several ways, including fault current input (arc current rather than bolted fault current), inclusion of an enclo-

sure breaching time, and solving for incident energy to determine a ZOI based on plant specific target fragilities [16]. Results obtained from the modified arc-flash confirmatory calculations are consistent with the more detailed FDS analysis for orientation experience of the more severe exposure conditions, thereby providing additional confidence in the CFD-derived ZOIs.

## SURVEY OF THE U.S. NUCLEAR FLEET

EPRI developed and implemented a survey of U.S. nuclear power plants to obtain information about electrical distribution systems, including materials used, fault clearing times, electrical distribution configurations, switchgear manufacturer, and switchgear configuration. The results of this survey are summarized in an EPRI technical report [17].

### Physical Testing to Characterize HEAF Phenomena

The physical testing portion of the research project plan was focused on obtaining information needed to develop and validate the FDS CFD model. Three types of experiments were performed:

- Small-scale experiments were conducted to better characterize aluminum and copper particle size distribution, rates of particle production, and particle morphology produced during electrical arc faults. Additionally, these tests provided accurate current measurements from which other electrical characteristics (e.g., arc impedance, energy, and power) could be determined. Thirty-six experiments were conducted, using variations in voltage, arc current, arc duration, arc gap size, and bus bar materials. The results from these small-scale experiments inform the energy balance model used in the FDS CFD model to predict additional energy release from particle involvement in the arc fault. The results of these experiments are documented in a Sandia National Laboratories (SNL) report [18].

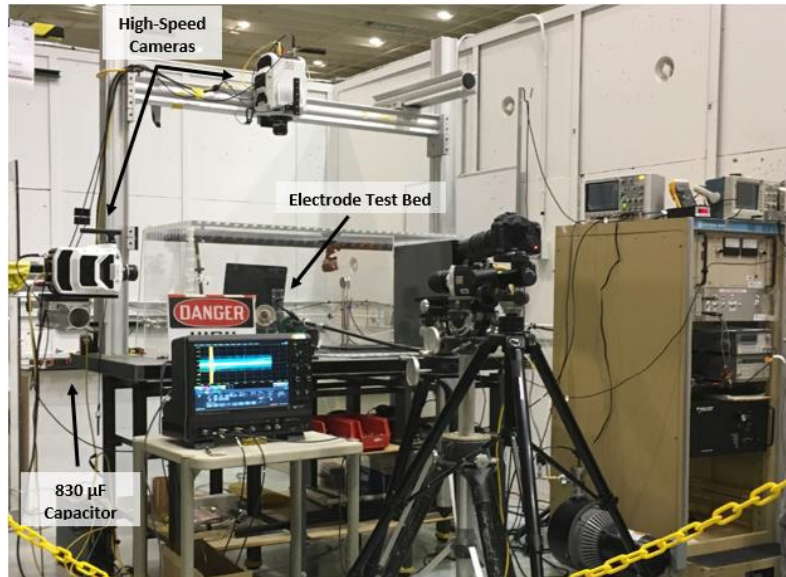


**Figure 3** Small-scale arc fault test system

- Medium-scale “open box” experiments were similar to the small-scale experiments but conducted at a larger scale. The “open box” allowed for more direct observation of the arc, enclosure breach, material loss, and electrical properties. The experiments were conducted in steel cubic metal boxes with one open face and a three-

phase arcing fault located in the center of the box. Low- and medium-voltage experiments were run with both aluminum and copper electrodes. The experiments varied arc current and arc duration. Eleven low voltage (~ 1000 V) and six medium voltage (~ 6900 V) experiments were conducted to obtain mass loss information from the enclosure and electrodes. The results are summarized in an NRC Research Information Letter [19].



**Figure 4** Open box experiment OB2 (copper electrode, 1000 V, 15 kA)

- Full-scale experiments were conducted in 2018 for nearly identical medium-voltage (~ 6900 V) switchgear with aluminum bus bars. These experiments used two different current and arc durations for a total of four full-scale tests. Insights from the experimental series included timing information related to enclosure breach, event progression, mass loss measurements for electrodes and steel enclosures, peak pressure rise, particle analysis, along with visual and thermal imaging data to better understand and characterize the hazard [20]. These experiments were run by the NRC to evaluate the aluminum HEAF hazard and are identified in the test matrix for the broader OECD/NEA HEAF 2 Project, an international joint project conducted under the auspices of the NEA [21].



**Figure 5** Medium voltage switchgear testing, Test 2-19 (6.9 kV, 25.8 kA rms)

Collectively, these experimental campaigns enhanced the state-of-knowledge about HEAF phenomena, enabled more realistic modelling of HEAF events, and provided numerous lessons learned for experimental and sensor design to capture key HEAF phenomena.

## EQUIPMENT FRAGILITY TESTING AND MODELLING

The objective of this portion of the research project plan was to establish the target fragilities for equipment that might be present within the HEAF ZOI. HEAF events generate short duration, extremely high heat fluxes and have different characteristics than traditional combustion fires. Therefore, the existing fragility for equipment exposed to a longer duration thermal fire, particularly cables, may not be applicable to the shorter duration higher heat flux expected from HEAF exposures. The fragility testing was conducted at the Solar Furnace at Sandia National Laboratories [22]. This facility is capable of concentrating sunlight to generate a heat flux of up to  $6 \text{ MW/m}^2$  within a circle that is approximately 5 cm in diameter. Several different failure modes were evaluated, including ignition, damage as a function of total energy, electrical failure of cables, and sub-jacket temperature.



**Figure 6** Parabolic dish at the Solar Furnace



**Figure 7** Solar Furnace Test 1-34 (3 cable bundle,  $\sim 25 \text{ MJ/m}^2$ )

Results from this testing, along with the full- and medium-scale data was used to develop a fragility model by the joint NRC/EPRI working group. The fragility model was based on experimental data, operating experience, and the current state of HEAF knowledge [23]. The working group focused on electrical cables; the most common target assessed for Fire PRA. Damage thresholds for both thermoplastic and thermoset cables were devel-

oped as a function of total incident energy. In addition, the working group developed damage criteria for electrical bus ducts and provided guidance for crediting electric race-way fire barrier systems. These damage criteria are used in conjunction with the hazard modelling results to determine the ZOI.

## HEAF PRA METHOD DEVELOPMENT

The previously described HEAF research activities supported the development of new methods and data to assess HEAF events more realistically within a nuclear plant PRA. In addition to providing updated ZOI limits based on operating experience and experimental testing, the research also led to updated HEAF ignition frequency and non-suppression probabilities [24]. While NUREG/CR-6850 and its supplement provided only one ZOI for each equipment type (switchgear, bus ducts, and isophase bus ducts), the new method provides a more realistic ZOI estimates based mainly on fault clearing time and arc energy. The new ZOIs were determined based on FDS simulations for load centers, switchgear, and non-segregated bus ducts. Based on the current state of knowledge, the working group could not make any distinction in the ZOIs based on the type of conductor material (copper or aluminum) in the PRA method. Future testing as part of the OECD/NEA HEAF Phase 2 Project, is expected to provide confirmatory evidence regarding this modelling conclusion.

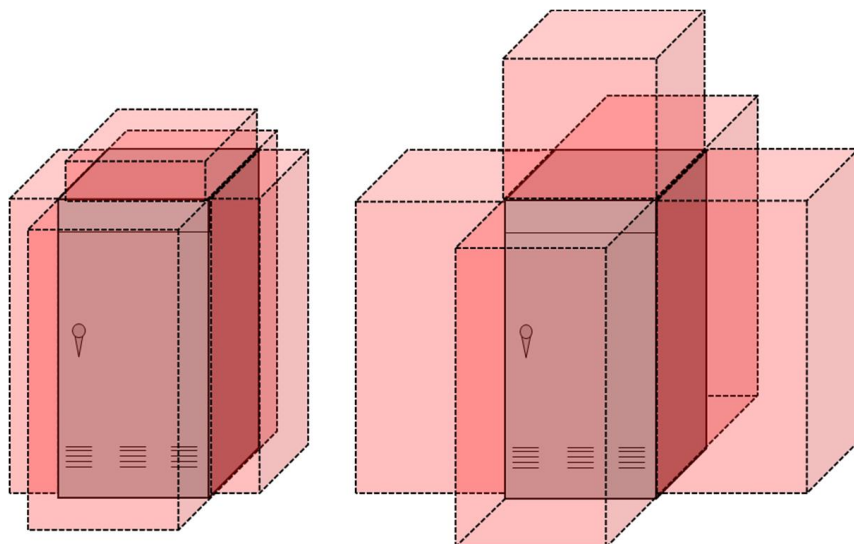


**Figure 8** Representative changes in ZOI based on fault clearing time (left figure has shorter time)

The final PRA method report is expected to be issued in final form in late calendar year 2022 or early 2023, following the public comment period.

## CONCLUSIONS

The NRC's fire research program has an overarching objective to improve the realism of fire modelling based on operating experience, experimental data, and analysis. The HEAF research project plan has effectively leveraged U.S. and international experience, in addition to a productive collaborative relationship between the USNRC and EPRI, to improve the modelling of this important phenomenon and guidance on its application.

## ACKNOWLEDGEMENTS

This work would not have been possible without the collaboration of staff from the Electrical Power Research Institute, Sandia National Laboratories, KEMA Labs, Brandon Stanton Inc., and the U.S. National Institute of Standards and Technology. The NRC gratefully acknowledges the support from the following individuals:

- U.S. Nuclear Regulatory Commission Working Group members, including Thinh Dinh, J. S. Hyslop, Kenn Miller, Charles Moulton, Reinaldo Rodriguez, David Stroup, Sunil Weerakkody, Jen Whitman, and Antonios Zoulis;
- Electric Power Research Institute: Ashley Lindeman, Marko Randelovic, Tom Short, and Fernando Ferrante. In addition, the following individuals provided substantial support to EPRI during this project: Jason Floyd, Dane Lovelace, Sean Hunt, Ken Fleischer, P. Shannon Lovvorn, and Victor Ontiveros;
- U.S. National Institute of Standards and Technology: Kevin McGrattan, Anthony D. Putorti, Scott Bareham, Edward Hnetkovsky, Christopher Brown, Wai Cheong Tam, Erik Link, Michael Selepak, Philip Deardorff, and Andre Thompson;
- Sandia National Laboratories: Chris LaFluer, Paul Clem, Byron Demosthenous, Austin Glover, Raymond Martinez, Anthony Tambakuchi, Kenneth Armijo, Alvaro Augusto Cruz-Cabrera, James Taylor, Rana Weaver, and Caroline Winters;
- OECD/NEA High Energy Arcing Fault Project participants, including the project Secretariat Markus Beilmann and participating countries including Belgium, Canada, France, Germany, Japan, Korea, the Netherlands, Republic of Korea, and Spain;
- KEMA Labs: Frank Cielo and the staff at KEMA Labs;
- Brandon Stanton, Inc.: Rob Taylor and the staff at BSI.

## REFERENCES

- [1] United States Nuclear Regulatory Commission (U.S. NRC) Office of Nuclear Regulatory Research (RES): Proceedings of the Information-Sharing Workshop on High Energy Arcing Faults (HEAFs), NUREG/CP-0311, Washington, DC, USA, 2019, <https://www.nrc.gov/docs/ML1921/ML1921A150.pdf>.
- [2] United States Nuclear Regulatory Commission (U.S. NRC): Accident Sequence Precursor (ASP) Program, 2022, online, <https://www.nrc.gov/about-nrc/regulatory/research/asp.html>, [accessed 18 July 2022].
- [3] Organisation for Economic Co-operation and Development (OECD) Nuclear Energy Agency (NEA), Committee on the Safety of Nuclear Installations (CSNI): OECD FIRE Project – Topical Report No. 1, Analysis of High Energy Arcing Fault (HEAF) Fire Events, NEA/CSNI/R(2013)6, Paris, France, June 2013, <http://www.oecd-nea.org/documents/2013/sin/csni-r2013-6.pdf>.
- [4] National Fire Protection Association (NFRA): NFPA 805, Performance-Based Standard for Fire Protection for Light Water Reactor Electric Generating Plants, 2001 Edition, Quincy, MA, USA, 2001.
- [5] Office of the Federal Register: Voluntary Fire Protection Requirements for Light Water Reactors; Adoption of NFPA 805 as a Risk-Informed, Performance-Based Alternative, 69 FR 33536, June 16, 2004, <https://www.federalregister.gov/d/04-13522>.

- [6] United States Nuclear Regulatory Commission (U.S. NRC): Regulatory Guide 1.205, Risk-Informed, Performance-Based Fire Protection for Existing Light-Water Nuclear Power Plants, Revision 2, 2021,  
<https://www.nrc.gov/docs/ML0611/ML061100174.pdf>.
- [7] United States Nuclear Regulatory Commission (U.S. NRC) Office of Nuclear Regulatory Research (RES) and Electric Power Research Institute (EPRI): Fire PRA Methodology for Nuclear Power Facilities, Final Report, EPRI/NRC-RES, NUREG/CR-6850 (EPRI 10191989), Washington, DC, and Palo Alto, CA, USA, 2005,  
<https://www.nrc.gov/reading-rm/doc-collections/nuregs/contract/cr6850/index.html>.
- [8] United States Nuclear Regulatory Commission (U.S. NRC) Office of Nuclear Regulatory Research (RES) and Electric Power Research Institute (EPRI): Fire PRA Methodology for Nuclear Power Facilities, Supplement 1: Fire Probabilistic Risk Assessment Methods Enhancements, EPRI/NRC-RES, NUREG/CR-6850 (EPRI 10191989), Washington, DC, and Palo Alto, CA, USA, 2010,  
<https://www.nrc.gov/reading-rm/doc-collections/nuregs/contract/cr6850/s1/index.html>.
- [9] Organisation for Economic Co-operation and Development (OECD) Nuclear Energy Agency (NEA), Committee on the Safety of Nuclear Installations (CSNI): Experimental Results from the International High Energy Arcing Fault (HEAF) Research Program Testing Phase 2014 to 2016, NEA/CSNI/R(2017)7, Paris, France, 2017,  
<http://www.oecd-nea.org/documents/2016/sin/csni-r2017-7.pdf>.
- [10] United States Nuclear Regulatory Commission (U.S. NRC): High Energy Arcing Faults in Electrical Equipment Containing Aluminum Components, Information Notice 2017-04, Washington, DC, USA, August 21, 2017,  
<https://www.nrc.gov/docs/ML1705/ML17058A343.pdf>.
- [11] Hamburger, K.: NRC High Energy Arc Fault (HEAF) Research, online, 2022,  
<https://www.nrc.gov/about-nrc/regulatory/research/fire-research/heaf-research.html>, [accessed 20 July 2022].
- [12] United States Nuclear Regulatory Commission (U.S. NRC) Office of Nuclear Regulatory Research (RES): An International Phenomena Identification and Ranking Table (PIRT) Expert Elicitation Exercise for High Energy Arcing Faults (HEAFs), NUREG-2218, Washington, DC, USA, January 2018,  
<https://www.nrc.gov/docs/ML1803/ML18032A318.pdf>.
- [13] McGrattan, K., et al.: Fire Dynamics Simulator User's Guide, NIST Special Publication 1019, National Institute of Standards and Technology (NIST), Gaithersburg, MD, USA, 2022.
- [14] United States Nuclear Regulatory Commission (U.S. NRC) Office of Nuclear Regulatory Research (RES) and Electric Power Research Institute (EPRI): Determining the Zone of Influence for High Energy Arcing Faults Using Fire Dynamics Simulator, Draft Research Information Letter for Public Comment, (ML22095A237), 2022,  
<https://www.nrc.gov/docs/ML2209/ML22095A237.pdf>.
- [15] Institute of Electrical and Electronics Engineers (IEEE): IEEE Guide for Performing Arc-Flash Hazard Calculations, IEEE 1584-2018, ISBN:978-1-5044-5262-5, November 2018, <https://doi.org/10.1109/IEEESTD.2018.8563139>.

- [16] United States Nuclear Regulatory Commission (U.S. NRC): Predicting High Energy Arcing Fault Zones of Influence for Aluminum Using a Modified Arc Flash Model, Draft Research Information Letter, (ML22095A236), May 2022, <https://www.nrc.gov/docs/ML2209/ML22095A236.pdf>.
- [17] Electric Power Research Institute (EPRI): Survey and Analysis of U.S. Nuclear Industry Relative to High Energy Arcing Faults in the Presence of Aluminum, Report EPRI 3002020692, Palo Alto, CA, USA, May 2021, <https://www.epri.com/research/programs/061177/results/3002020692>.
- [18] Armijo, K. M., et al.: P , Electrical Arc Fault Particle Size Characterization, Sandia Report SAND2019-11145, Sandia National Laboratories (SNL), Albuquerque, NM and Livermore, CA, USA, September 2019, <https://www.osti.gov/servlets/purl/1592574>.
- [19] United States Nuclear Regulatory Commission (U.S. NRC): Report on High Energy Arcing Fault Experiments - Experimental Results from Open Box Enclosures, Research Information Letter (RIL) 2021-18, (NIST TN 2198, SAND2021-16075 R), Washington, DC, USA, December 2021, <https://www.nrc.gov/docs/ML2136/ML21361A176.pdf>.
- [20] United States Nuclear Regulatory Commission (U.S. NRC): Report on High Energy Arcing Fault Experiments - Experimental Results from Medium Voltage Electrical Enclosures, Research Information Letter (RIL) 2021-10, (NIST TN 2188, SAND2021-12049 R), Washington, DC, USA, December 2021, <https://www.nrc.gov/docs/ML2133/ML21334A196.pdf>.
- [21] Organisation for Economic Co-operation and Development (OECD) Nuclear Energy Agency (NEA): High Energy Arcing Fault Events (HEAF) Project, Paris, France, Limited to Project Members only, [https://www.oecd-nea.org/jcms/pl\\_24977](https://www.oecd-nea.org/jcms/pl_24977) [accessed 24 July 2022].
- [22] United States Nuclear Regulatory Commission (U.S. NRC): HEAF Cable Fragility Testing at the Solar Furnace at the National Solar Thermal Test Facility, Research Information Letter (RIL) 2021-09, (SAND2021-11327), Washington, DC, USA, September 2021, <https://www.nrc.gov/docs/ML2125/ML21259A256.pdf>.
- [23] United States Nuclear Regulatory Commission (U.S. NRC) and Electric Power Research Institute (EPRI): Target Fragilities for Equipment Vulnerable to High Energy Arcing Faults, Research Information Letter (RIL) 2022-01, (EPRI 3002023400), Washington, DC, and Palo Alto, CA, USA, May 2022, <https://www.nrc.gov/docs/ML2213/ML22131A339.pdf>.
- [24] United States Nuclear Regulatory Commission (U.S. NRC) and Electric Power Research Institute (EPRI): High Energy Arcing Fault Frequency and Consequence Modeling, Draft Report for Comment, Draft NUREG-2262, Washington, DC, and Palo Alto, CA, USA, July 2022, <https://www.nrc.gov/docs/ML2215/ML22158A071.pdf>.

# Experimental Studies of HEAF (High Energy Arcing Fault) Phenomena for Non-Segregated Bus Ducts

Koji Tasaka<sup>1\*</sup>, Tsukasa Miyagi<sup>2</sup>, Koji Shirai<sup>1</sup>, Mikimasa Iwata<sup>2</sup>, and Junghoon Ji<sup>1</sup>

Central Research Institute of Electric Power Industry (CRIEPI)

<sup>1</sup> Nuclear Risk Research Center, Chiba, 270-1194, Japan

<sup>2</sup> High Power Testing Laboratory, Kanagawa-ken, 240-0196, Japan

## ABSTRACT

HEAF (High Energy Arcing Fault) events have occurred world-wide in nuclear power plants. HEAF has a potential to cause extensive damage to distribution systems and electrical components nearby an initial arcing location.

This paper presents full-scale experimental results to investigate HEAF phenomena for non-segregated (non-isolated phase) bus ducts (NSBD) containing copper or aluminum bus bars. This paper covers six internal arc tests performed on NSBD units with each unit consisted of three horizontal conductors in a parallel configuration and covered in a steel duct. These tests used a nominal voltage of 6.9 kV (AC). The HEAF consequences such as arcing current, voltage, internal pressure, total incident energy, etc. were measured.

In case of copper bus bars, the arcing energy where was discharged in 1.28 s using a three-phase short-circuit current with 18.9 kA reached to 12.8 MJ. In contrary, the arcing energy with aluminum bus bars reached up to 16.5 MJ under the same test conditions. The difference suggested the possibility that HEAF events involving aluminum induce more severe HEAF consequences to the surrounding equipment damage. In this test series, there was no catastrophic damage like secondary ignition to equipment, such as a cable, a solid bottom cable tray, or an energized electrical cabinet. Moreover, control signals on the electrical cabinet were monitored during one of the tests, there was no effect of electromagnetic noise. According to the test results, a simplified empirical model to predict the HEAF zone of influence (ZOI) for NSBD was proposed.

## INTRODUCTION

Large electrical discharges, referred to as HEAF (*High Energy Arcing Fault*) events, have occurred in electrical components of nuclear power plants (NPPs) throughout the world [1]. In general, HEAF events are initiated in one of three ways: poor physical connection between the switchgear/breaker and the metal enclosure, environmental conditions, or the introduction of a conductive foreign object [2]. Since the arc releases energy in form of heat, vaporized or molten material, and mechanical force, it leads to instant extensive damage to electrical distribution systems and components nearby an initial arcing location and a potentially ensuing fire that can damage electrical cables and components important to safety. Recently, there are many HEAF fire research activities ongoing worldwide. For example, according to the draft report NUREG-2262 [3] issued by the United States Nuclear Regulatory Commission (U.S. NRC), a new methodology for modelling to evaluate the hazards resulting from HEAF and the ensuing fire has developed [3]. As one of the insights from two pilot plant applications of the new methodology for use in Fire PRA (*Probabilistic Risk Assessment*), the total HEAF risk as CDF (core dam-

age frequency) of HEAF scenarios has been increased or decreased response to the plant specific conditions. Because the ZOI, which is the distance where a HEAF can cause damage, seems to be enlarged contrast to the previous methodology (NUREG/CR-6850, Supplement 1, etc.) especially in non-segregated (non-isolated phase) bus ducts (NSBDs), the increased risk is dominated by a potential for additional targets [4].

On the other hand, several HEAF events associated with a switchgear, a bus duct and a transformer have been experienced in Japanese NPPs. In particular, the 2011 off the Pacific coast of Tohoku Earthquake which occurred on March 11, 2011, caused HEAF in two of ten sectors of the non-emergency high or medium voltage metal-clad switchgear banks and resulted in a seismically induced HEAF fire event in the Onagawa NPP. In response, in August 2017, the NRA (Nuclear Regulation Authority) of Japan partially amended the safety requirement concerning technical standards for practical power generation nuclear reactors and their attached facilities, especially for the power supply to consider the influence of HEAF fire events [5].

In parallel, the Nuclear Risk Research Center (NRRC) of CRIEPI (Central Research Institute of Electric Power Industry) performed three phase HEAF tests using full-scale high or medium (6.9 kV) and low (420 – 480 V) voltage electrical cabinets. Based on the test results, the HEAF fire prevention evaluation method was established by clarifying the upper limit values of the arc energy leading to a HEAF fire depending on power supply conditions, such as the type of electrical cabinets and whether a diesel generator is connected to the electrical cabinet. Table 1 summarizes the design criteria for use in Japanese nuclear industry to prevent HEAF fire events [6]. However, the HEAF ZOI of the energetic phase have not been yet fully understood so far. Therefore, it is urgently necessary to establish a model for the HEAF ZOI to evaluate the potential range of collateral damage and enhance the experimental data of the HEAF events.

**Table 1** Design criteria based on the arc energy to prevent HEAF fire events [6]

| Cabinet Type   | Current Intensity                                 | Design Criteria |
|--|---|-----------------|
| High or medium voltage electrical cabinets<br>(metal-clad switchgears) | High current                                      | 25 MJ           |
|  | Low current<br>(scenario of diesel generator fed) | 16 MJ           |
| Low voltage electrical cabinets<br>(power centers)                     | —   | 18 MJ           |
| Low voltage electrical cabinets<br>(motor control centers)             | —   | 4.4 MJ          |

For developing a simplified modelling to evaluate the hazards resulting from HEAF events, the open arc tests presented in this paper were conducted under atmospheric conditions and the internal arc tests by using a full-scale high or medium voltage segmented bus duct. Based on the test results, an empirical formula was proposed to evaluate the total incident energy response within a direct distance from the initial arc location and a methodology to predict the HEAF ZOI for NSBDs.

## HEAF TESTS

### Test Facility

The High Voltage Power Laboratory (previous organization) of CRIEPI, located about 65 km in the south from the center of Tokyo, was established in 1963 to make an important contribution to the progress of power transportation technology and conducted research and tests on the short circuit performance of power equipment and materials at its high power test facilities.

The High Power Testing Laboratory as shown in Figure 1 was established in 2001, and laboratory accreditation was granted by the Japan Accreditation Board (JAB) for Conformity Assessment in compliance with ISO/IEC 17025 [7]. As a laboratory that meets international standards, we are involved in a variety of test activities that include publishing test reports and issuing certificates. In this test facility, short-time withstand current, and peak withstand current tests for circuit breakers, disconnectors, earthing switches, load break switches, metal-enclosed switchgears and gas insulated switchgears can be conducted with the test capacity of currents up to 60 kA and durations up to 2 s.

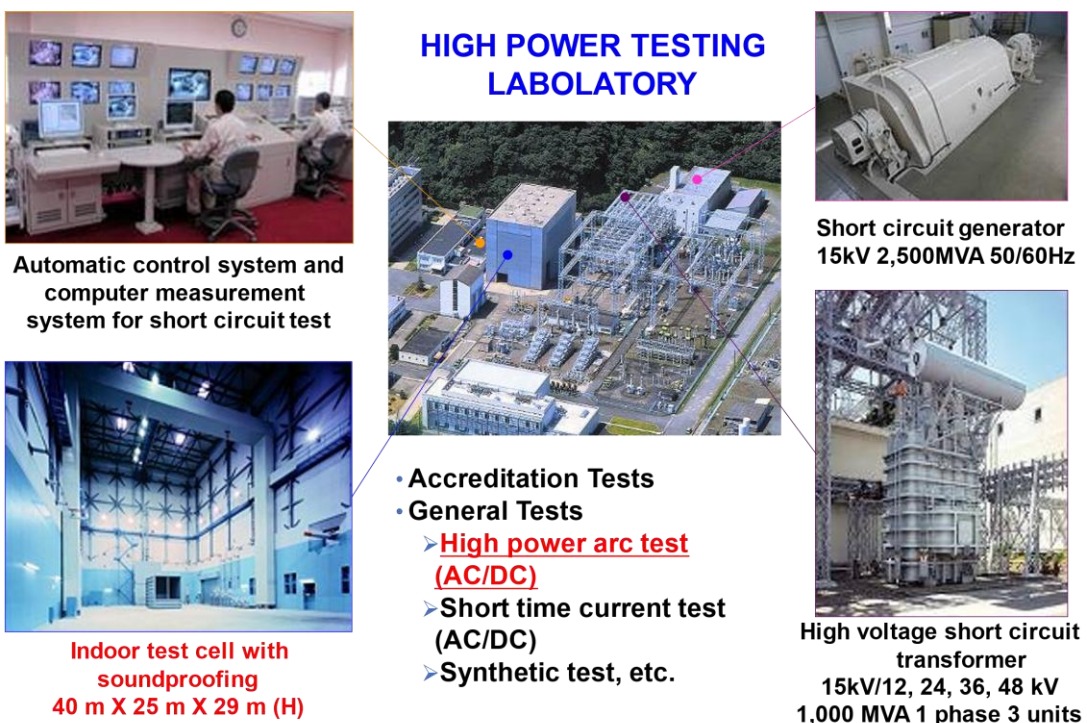


**Figure 1** High Power Testing Laboratory (Yokosuka-shi, Kanagawa-ken, Japan) [8]

### Test Program for Characterizing the HEAF ZOI

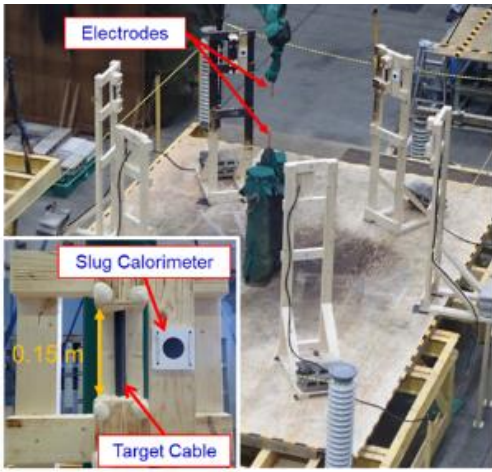
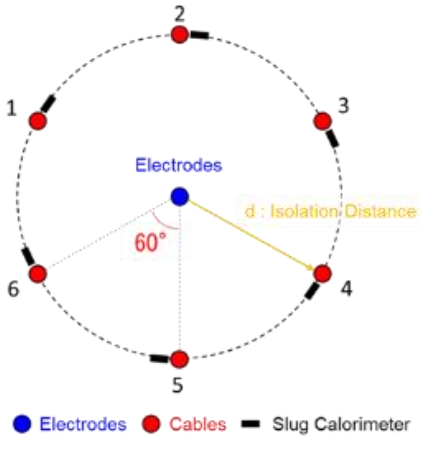
In order to define the HEAF ZOI, the HEAF tests using copper electrodes and 6.9 kV class segmented bus ducts were conducted at the High Power Testing Laboratory of CRIEPI [9]. The HEAF test program consisted of two phases for characterizing HEAF ZOI as follows.

- Phase 1: Single-phase open arc tests under atmospheric conditions using copper electrodes;
- Phase 2: Three-phase HEAF tests using high or medium voltage segmented bus ducts.

## Open Arc Test Matrix and Measurements

The objectives of test phase 1 were planned as a characterization of cable damage subjected to hot arc ejected gas and a development of an empirical formula to estimate the total incident energy generated by atmospheric arcing to the surroundings. The total number of the open arc tests was 23, varying the experimental conditions such as nominal voltage, current, arc duration, and target isolation distance. The overview of the test apparatus and the experimental conditions are summarized in Table 2.

**Table 2** Open arc test program for characterizing the HEAF ZOI [9]

| Open Arc Tests in Atmospheric Condition  |  |
|--|--|
|  |                                   |
| Total number of tests  | 23   |
| Electrode equipment  | Vertical arrangement of two opposed rod electrodes   |
| Rod Electrode  | Copper with 20 mm diameter and 300 mm gap length   |
| Phase number   | Single-phase   |
| Frequency  | 50 Hz  |
| Voltage  | 6.9 kV (up to 30 kA), 9.2 kV (35 kA)   |
| Current  | 10, 20, 30, 35 kA  |
| Duration   | 0.05, 0.1, 0.2, 0.25, 0.5, 0.7, 1.0 s  |
| Arc exposure target  | Slug calorimeters [10] and 600 V flame retardant CV cables (3 conductors and 22 mm <sup>2</sup> ) with 0.15 m length |
| Target isolation distance  | 0.6, 0.9, 1.5 m from the center of vertical rod electrodes   |

A short circuit generator (50 Hz, 15 kV, 2500 MVA) as shown in Figure 1 was used as power source. The single-phase arcing under atmospheric condition was ignited by fusing of a fine copper wire of 0.5 mm diameter which connected two rod electrodes. The copper electrodes were 20 mm in diameter with a flat tip. The arcing current was set to 10 – 35 kA. The arc duration was set to the range from 0.05 s to 1.0 s. The total arc energy (from 1 MJ to 20 MJ) was estimated by integrating the product of measured arc current and arc voltage over time. As a target, the flame-retardant cable specimen with 0.15 m length was used, and the isolation distance was set to 0.60 m, 0.90 m, and

1.50 m. After the exposure test, each cable specimen was subjected to a withstand voltage test to detect the thermal damage to the dielectric strength of the cable specimen.

### Segmented Bus Duct Test Matrix and Measurements

The objectives of test phase 2 were planned as characterization of HEAF consequences such as behaviour of hot arc ejected gas and molten metal particles and development of an evaluation method for the HEAF ZOI in case of segmented bus ducts. The total number of internal arc tests for segmented bus ducts was 6, varying the busbars material, arc duration, and the type of arc exposure targets as shown in Table 3 and Table 4. A short circuit generator (50 Hz, 15 kV, 2500 MVA) as shown in Figure 1 was used as power source. The test matrix as shown in Table 5 was set up referring the previous test program by CRIEPI to develop the HEAF fire prevention evaluation method for electrical cabinets [6], [11]. The arcing current and arc duration was set to 18.9 kA and 1.1 s, respectively. Moreover, from the safety point of view, a longer arc duration of 1.6 s was also considered.

**Table 3** Segmented bus duct HEAF test program for characterizing the HEAF ZOI [9]

| Segmented (Non-isolated Phase) Bus Duct Tests |   |          |        |
|---|---|----------|--------|
| Straight bus duct                             |   |          |        |
| Total number of tests                         | 6   |          |        |
| Test ID                                       | BD-1, BD-2, BD-5, BD-6                        | BD-3     | BD-4   |
| Phase number / Frequency                      | Three-phase / 50 Hz                           |          |        |
| Voltage / Current                             | 6.9 kV / 18.9 kA                              |          |        |
| Busbar material                               | Copper  | Aluminum | Copper |
| Duct enclosure material                       | Steel   |          |        |
| Duration                                      | 1.1 s   |          | 1.6 s  |
| Initial arc location                          | Center of three-phase busbars located in NSBD |          |        |

**Table 4** Exposure targets and locations subjected to segmented bus duct HEAF tests

| Tests BD-1, 2, 3, 4  | Test BD-5   | Test BD-6   |
|--|---|---|
|                                     |                                      |  |
| Slug calorimeters [10] and 600 V flame retardant CV cables (3 conductors and 22 mm <sup>2</sup> ) with 0.15 m length | A solid cable tray included 600 V flame retardant CV cables (3 conductors and 22 mm <sup>2</sup> ) with 1.40 m length | An energized electrical cabinet   |
| Minimum distance from the targets to the bottom of bus ducts was 0.70 m  | Minimum distance from the targets to the bottom of bus ducts was 0.055 m  | Minimum distance from the target to the bottom of bus ducts was 0.73 m              |

**Table 5** HEAF test matrix and test results for segmented bus ducts

| Test ID | Voltage [kV] | Current [kA] | Duration [s] | Arc Energy [MJ] | Loss of Essential Function of Arc Exposure Target |
|---------|--------------|--------------|--------------|-----------------|---|
| BD-1    | 6.9          | 18.9         | 1.28         | 12.6            | No*   |
| BD-2    |              |              | 1.28         | 12.8            | No*   |
| BD-3    |              |              | 1.29         | 16.5            | No*   |
| BD-4    |              |              | 1.74         | 15.4            | No*   |
| BD-5    |              |              | 1.28         | 11.9            | No*   |
| BD-6    |              |              | 1.28         | 11.7            | No**  |

\* Resulting from a withstand voltage test of cables to detect a loss of the dielectric strength  
\*\* Resulting from a monitoring test of electrical cabinet to detect a loss of the output signals

Figure 2 shows the overviews of each test setup configuration. The full-scale segmented bus ducts were procured from a Japanese electric power company for the purpose of performing our HEAF tests. The bus ducts consisted of three conductors enclosed in a steel duct. Each bus duct was set to 4.00 m height from the ground level. In addition, the bus duct was set an opening of 0.15 m in diameter on the center part to eject the products such as metallic vapours and molten metal particles resulting from HEAF. The three-phase arcing was ignited by fusing of a fine copper wire of 0.5 mm diameter which connected three busbars (see Figure 3). The purpose of tests BD-1 to BD-4 was to determine the arc ejecta characterization during the arcing.

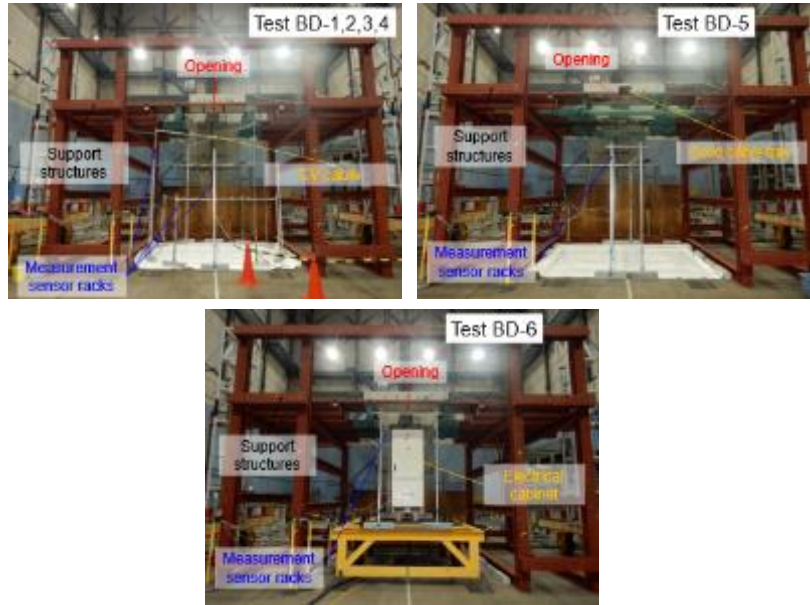


**Figure 2** HEAF test setup configurations for segmented bus ducts [9]

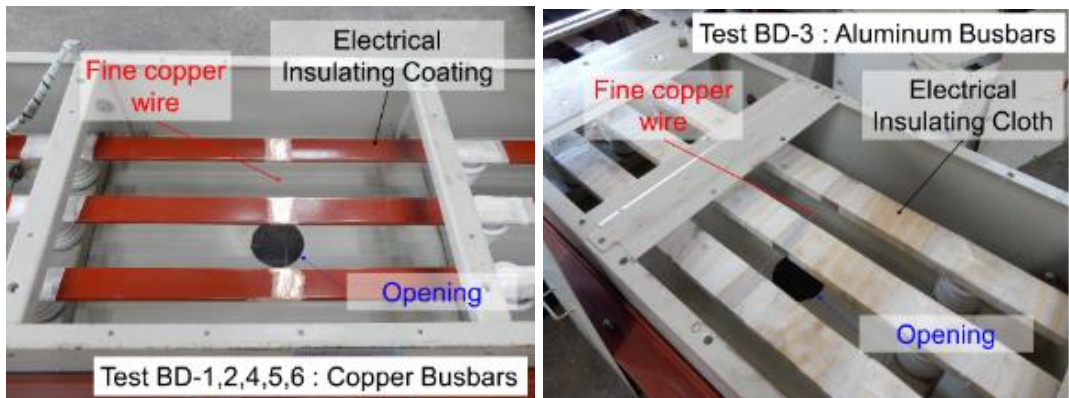


**Figure 3** Initial arc location and 0.15 m diameter opening at the center of bus duct [9]

The tests BD-5 and BD-6 were planned to investigate the impact from arc ejecta to a surrounding target such as a solid cable tray and an energized electrical cabinet. During the tests, rated current and voltage, arc duration, inner pressure inside the bus duct by pressure sensors, surface temperature of the bus ducts by thermography and total incident energy within ZOI were measured. The total arc energy is estimated by integrating the product of measured arc current and arc voltage over time. The total incident energy was estimated using slug calorimeters [10] that covered the horizontal distance  $R$  0.25 m, 0.50 m, 0.75 m, and 1.00 m from the initial arc location set on the racks which located at 0.70 m, 1.50 m, and 2.50 m in vertical distance  $H$  from the bottom of bus ducts. Additional instrumentation included the high-speed video images, and electrical cabinet monitoring system that can record the output signals from the cabinets [12] to detect a potential malfunction of the electrical or electronic components, etc.

## OPEN ARC TEST RESULTS

### Total Incident Energy

As reported in the literature [11], the thermal damage to the dielectric strength of the exposure target cables even under the total incident energy of over 2 MJ/m<sup>2</sup> was not detected. In this subchapter, we addressed to report an empirical formula associated with the total incident energy in response each direct distance from the arcing location. Referring to a technical guide [13], one of the simplified approaches is found that it regards the power source of arcing as a point source. In this case, the theoretical equation for energy in heat resulting from arcing is given as following.

$$E_{total,IE} = k_h \times \frac{E_{arc}}{4\pi r^2} \quad (1),$$

where:  $E_{total,IE}$  the total incident energy [MJ/m<sup>2</sup>],  $E_{arc}$  the arc energy [MJ],  $r$  the direct distance from an arc location [m],  $k_h$  the fraction of arcing energy leading to total incident energy in its air surroundings.

Indeed, the shape of energy release such as hot arc ejected gases observed that it seems to radiate spherically in all directions as shown in Figure 4. However, the initial arc location  $O$  that the center part of gaps between copper rod electrodes does not seem to be appropriate for the location of point source because the arc location keeps moving under influence of electromagnetic forces during arcing. Therefore, we analysed the representative value of  $k_h$  using each direct distance  $r$  from the effective arc location  $P$  to each sensor (see Figure 4). Accordingly, the range of  $k_h$  was analysed from 0.35 to 0.50 and the mean value was 0.43.

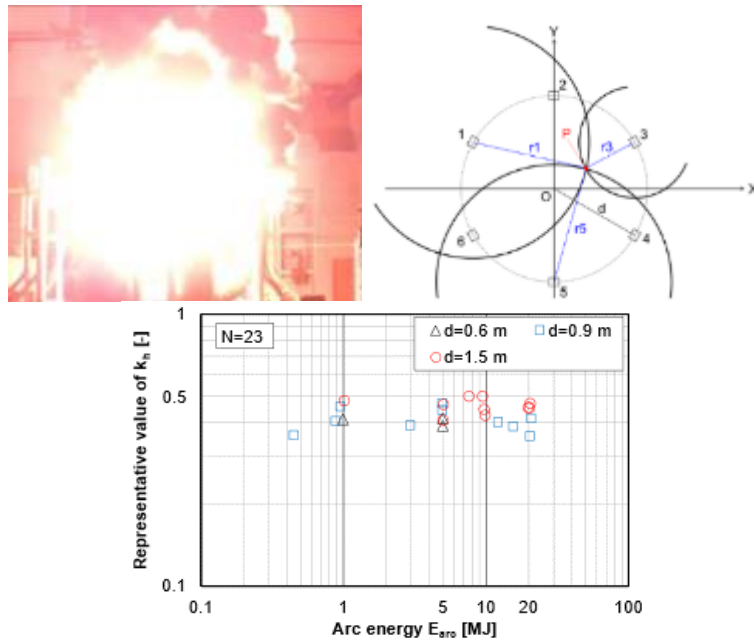
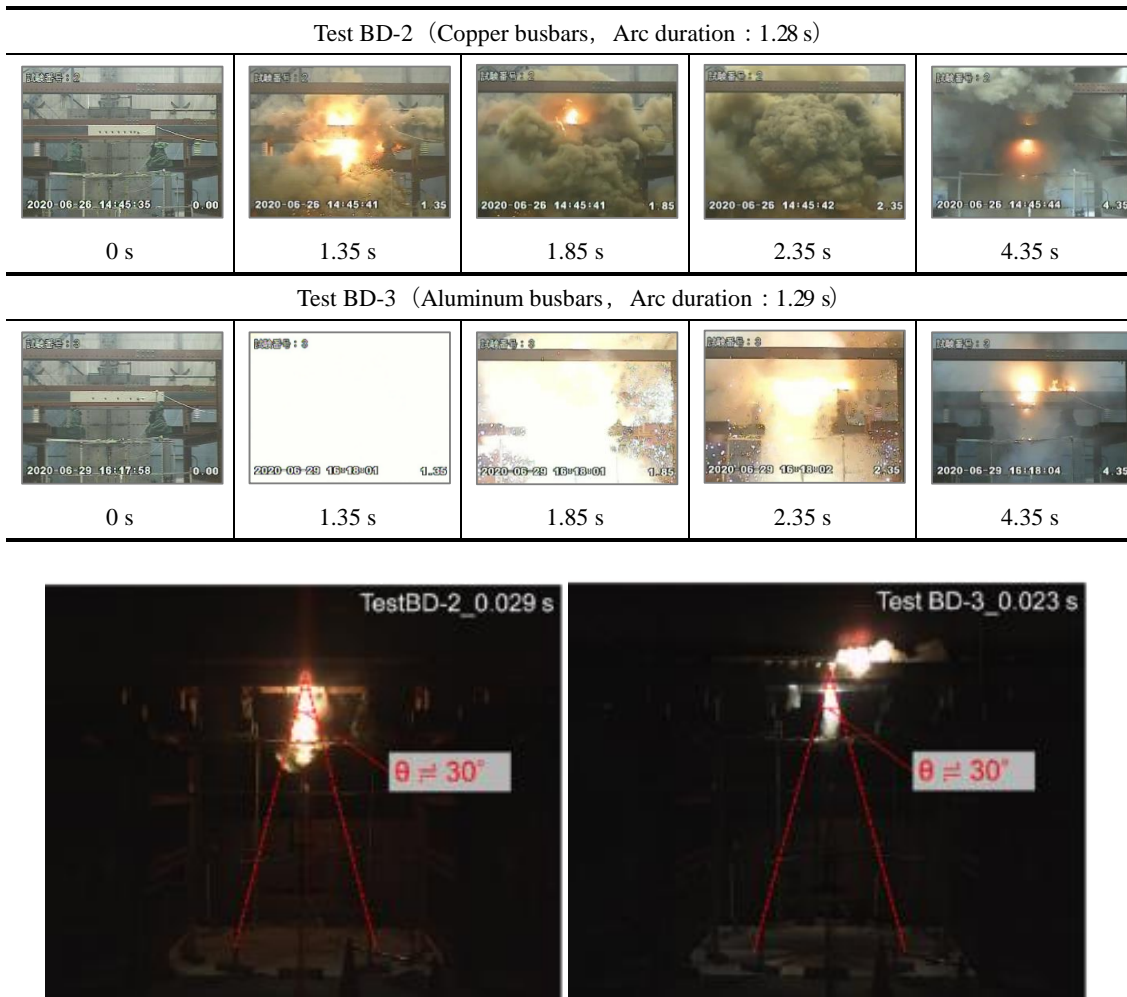


**Figure 4** Occurrence of the arc flash with arc energy 10 MJ class (left), top view of conceptual diagram for the effective arc location  $P$  (center), and analysis results of  $k_h$  using open arc test data (right) [9]

## SEGMENTED BUS DUCT HEAF TEST RESULTS

### Arc Flash and Damage of Surrounding Targets

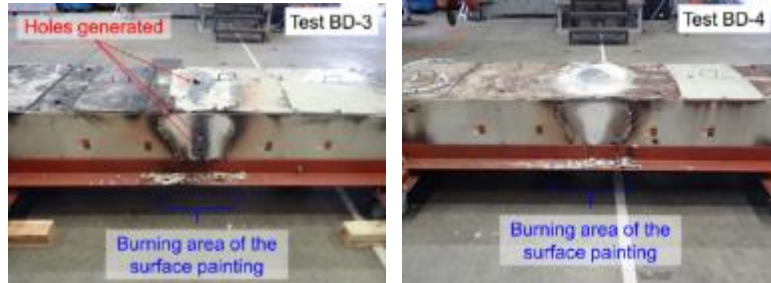
Figure 5 shows the generation of hot arc ejected gases associated with arcing in test BD-2 ( $E_{arc}$ : 12.8 MJ) and test BD-3 ( $E_{arc}$ : 16.5 MJ), as captured by a high-resolution video and a high-speed video. The hot arc ejected gases after the arcing seemed to include metal vapor and molten metal particles generated from busbar material. On the other hand, in test BD-3 which used aluminum busbars, the light emitted of gases continued until about 2.35 s after the arcing. This is because the vapourised metal vapour of the aluminum busbars chemically combined with oxygen in the atmosphere to generate energy, and the oxidation reaction energy is greater than that of the copper ones [14]. The zone of influence to the below of bus duct seems to be concentrated within around 30° apex angle from the initial arc location as given in the literature [15].



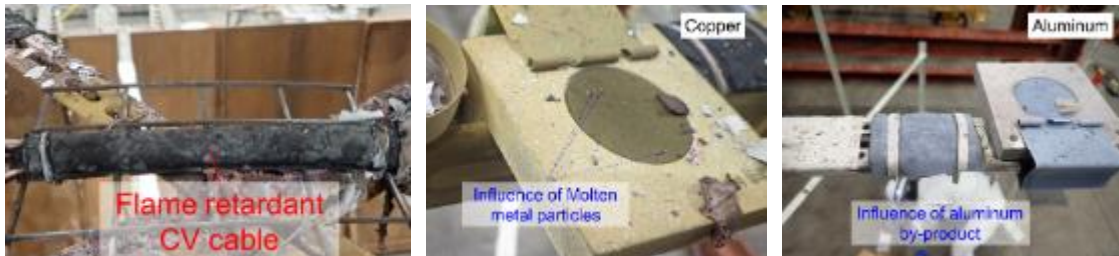
**Figure 5** Video images for the arc flash and arc ejecta from test BD-2 and test BD-3 [9]

Figure 6 summarizes the HEAF consequences to the duct enclosures (housings) and the surrounding targets. The surface of the duct enclosure in test BD-3 was observed several holes but no hole of the surface observed in test BD-4 ( $E_{arc}$ : 15.4 MJ). These holes might be generated by contact with the surface of the duct enclosure and arc in the test BD-3. An additional finding observed was the burning area of surface painting nearby the initial arc location. And some parts of targets below the bus duct were at-

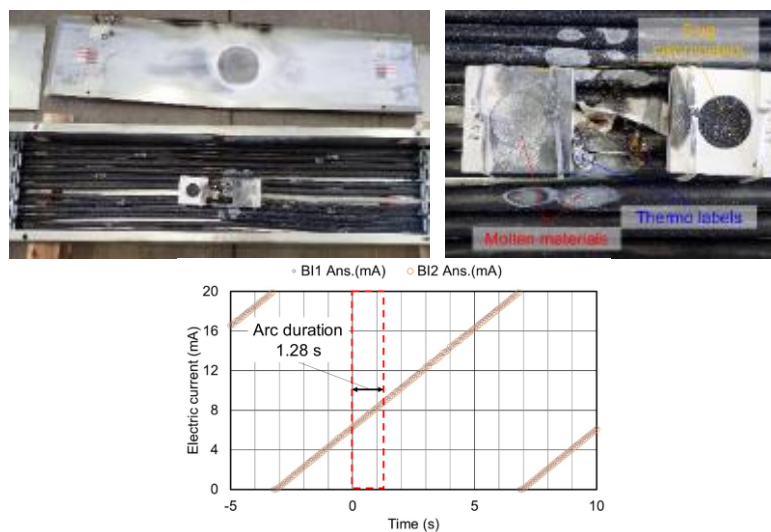
tached to copper and aluminum by-products to the surface. For cables located at 0.70 m below from the bottom of bus ducts exposed to arc ejected gases in the tests BD-1 to BD-4 the carbonization of the cable jacket was observed. In test BD-5, the cables in a solid cable tray located at 0.055 m below from the bottom of the bus duct were observed that they were fouled with the by-products generated by melting of the metallic skin for the top plate of the tray. According to the withstand voltage test results for the exposed cables, damage from the thermal impact to the dielectric strength was not detected. Moreover, according to the output signals of the monitored cabinet located at 0.73 m below from the bottom of bus duct during the test BD-6, no change and no spurious signal in the electrical outputs by electromagnetic noise generated by arcing was observed as shown in Figure 6.



comparison of the surface of segmented bus duct enclosure after the tests BD-3 and BD-4



carbonization of the cable jacket (left), influence of copper and aluminum by-products



surface fouling of cables in the solid cable tray (left), output signal from the cabinet (right)

**Figure 6** HEAF consequences of the bus duct enclosures and the surrounding targets [9]

## Arc Energy

The arc energy  $E_{arc}$  for three-phase inner arc occurrence can be calculated by equation (2) as in the literature [6], [9], [12].

$$E_{arc} = V_{arc} \times (I_{rms} \times 0.9) \times t_{arc} \quad (2),$$

with:  $E_{arc}$  the three-phase arc energy [MJ],  $V_{arc}$  the arc voltage adding up the arc voltages for the R-phase, the S-phase, and the T-phase [kV],  $I_{rms}$  the current effective value [kA] and  $t_{arc}$  the arc duration.

Figure 7 shows the measured arc voltage and the measured arc energy for the segmented bus ducts. It is found that the measured arc voltage seems to be almost constant regardless of the arc duration. In addition, their mean value for segmented bus ducts included copper busbars and the measured value for the aluminum busbars were 0.576 kV and 0.781 kV, respectively. The difference of the arc voltage seems to be depending on the difference of the busbar material. Indeed, the measured arc energy in case of aluminum busbars was higher than that of copper busbars due to the difference of the arc voltage, and a difference in the consequences to the duct enclosure was observed as shown in Figure 6. Accordingly, applying the measured arc voltage values to equation (2), the estimation formula for the arc energy can be proposed as follows.

$$E_{arc,NSBD\ Copper\ Busbars} = 0.576\ kV \times (I_{rms} \times 0.9) \times t_{arc} \quad (3),$$

$$E_{arc,NSBD\ Aluminum\ Busbars} = 0.781\ kV \times (I_{rms} \times 0.9) \times t_{arc} \quad (4).$$

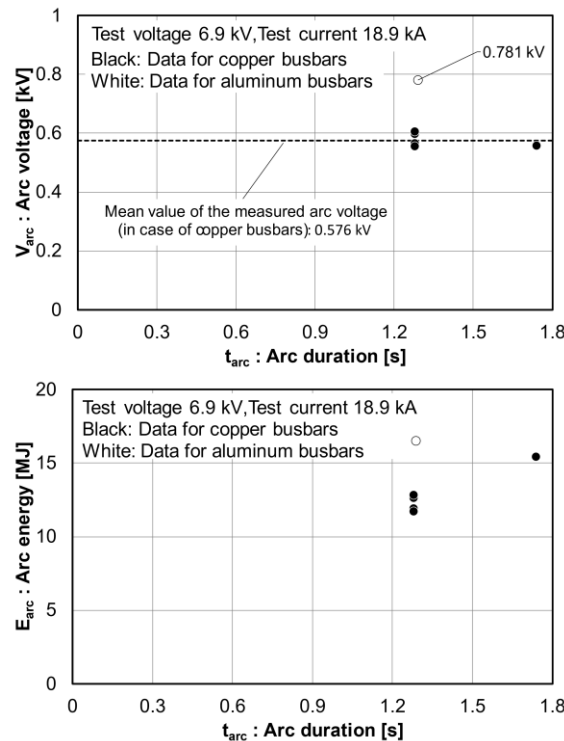
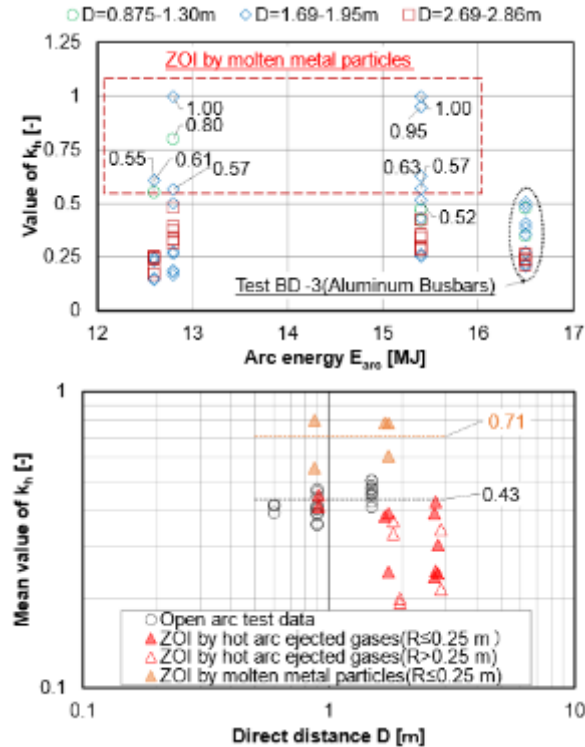


**Figure 7** Measured arc voltage and measured arc energy for segmented bus ducts [9]

## Zone of Influence Focused on Thermal Impact

The HEAF consequences to the surrounding targets focused on thermal impact seems to be characterized by each zone for hot arc ejected gases and the molten metal particles. In this subchapter, we address the analysis of the values of  $k_h$  by equation (1)

using measured total incident energy by each slug calorimeter and each direct distance from the initial arc location that was the center part of busbars in duct enclosures. Figure 8 shows the analysis results of values of  $k_h$  are associated with each direct distance. For copper busbars, the values of  $k_h$  were the range from 0.15 to 1.00. Meanwhile, the values of  $k_h$  for aluminum busbars range from 0.20 to 0.50 regardless of the attachments of aluminum by-products. According to the values of  $k_h$  and the observation of the surface of slug calorimeters after the tests, the minimum value of  $k_h$  from the slug calorimeters that attached copper by-products such as molten metal particles to the surface as shown in Figure 6 was analysed to be 0.55.



value for each sensor and the direct distance (left),  
mean value for the direct distance (right)

**Figure 8** Analysis results of  $k_h$  using segmented bus ducts HEAF test data [9]

Accordingly, in order to define the representative value for each zone, the values that were higher than or equal to 0.55 were defined as the ZOI by molten metal particles and the values that were lower than 0.55 were defined as the ZOI by hot arc ejected gases. In the definition of representative values, the mean value for each zone using the direct distance  $D$  (calculated with each distance of  $R$  and  $H$ ) from the initial arc location was analysed. The insights from the results found that the maximum representative value of  $k_h$  for the ZOI by hot arc ejected gases seems to be almost equal to the mean value 0.43 analysed by open arc test data. In addition, the ZOI by molten metal particles seems to be concentrated within the horizontal distance  $R$  of 0.25 m, and the range of representative value of  $k_h$  for the ZOI by molten metal particles was from 0.55 to 0.80 and their mean value was 0.71.

Accordingly, applying the representative values for each zone to equation (1) and a cable fragility  $E_{damage} [\text{MJ/m}^2]$ , the estimation formula for the allowable direct distance  $D_{allowable}$  [m] from an initial arc location can be proposed as follows.

$$D_{allowable} = \sqrt{(k_h \cdot E_{arc}) / (4\pi \cdot E_{damage})} \quad (5),$$

with:  $k_h = 0.43$  for the ZOI by hot arc ejected gases and  $k_h = 0.71$  for the ZOI by molten metal particles in case of segmented bus duct using copper busbars. For aluminum busbars,  $k_h$  can be regarded the same values as for copper busbars in this experimental study.

Here, they are applied such that the arc energy  $E_{arc} = 135$  MJ and the cable fragility  $E_{damage} = 15$  MJ/m<sup>2</sup> to equation (5),  $D_{allowable}$  such as  $r_{gas}$  for the ZOI by hot arc ejected gases and  $h_{molten}$  for the ZOI by molten metal particles are estimated as shown in Figure 9 referring to the report NUREG/CR-6850, Supplement 1 [15]. Accordingly, the 135 MJ class HEAF ZOI for NSBDs can be estimated around 1.8 – 2.3 ft such that  $r_{gas} = 0.55$  m and  $h_{molten} = 0.71$  m. In this simplified modelling, the ZOI by hot arc ejected gases and the ZOI by molten metal particles can be regarded as the spherical zone, and the conical zone with a 30° apex angle, respectively. This zoning approach is based on the assumptions and the interpretations as follows:

The heat energy generated by the HEAF is ejected to all directions from the initial arc location as a point source. In other words, the shield effect of the duct enclosure is neglected.

The droplets such as molten metal particles tend to concentrate mainly within the conical zone with a 30° apex angle to below the bus duct because of the impact from gravity.

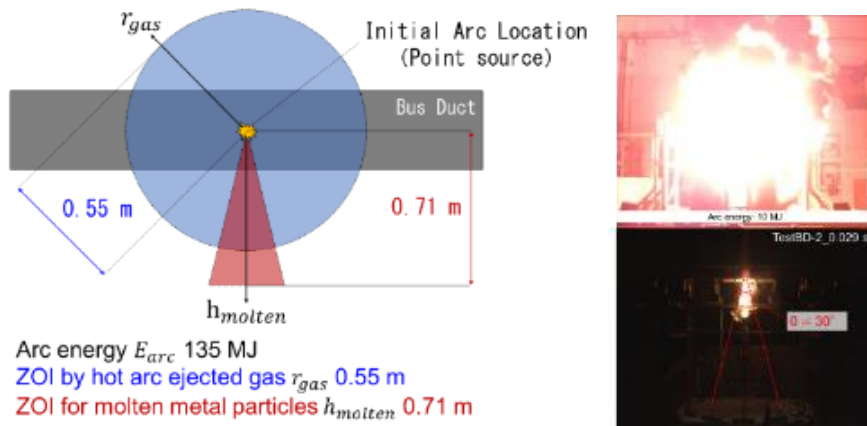


**Figure 9** Estimation and experimental observations of the HEAF ZOI for NSBDs

## CONCLUSIONS

Experimental investigations of the HEAF phenomena for 6.9 kV segmented bus ducts that have steel duct enclosures and copper, or aluminum busbars were conducted. According to the results, hot arc ejected gases and molten metal particles generated due to the arc flash were emitted out of the duct enclosure to the surroundings. In addition, for the targets such as thermoplastic cables and electrical cabinet impacts resulting from the HEAF to a dielectric strength of cables and a potential malfunction of components in the cabinet were not observed.

As a result, we propose an empirical formula to estimate the total incident energy resulting from HEAF. We also propose a representative value for the fraction of arcing energy leading to total incident energy due to hot arc ejected gases and molten metal particles and a simplified modelling approach to predict the HEAF ZOI for NSBDs.

## ACKNOWLEDGEMENTS

These experimental research activities have been supported by the Federation of Electric Power Companies and the Japanese utilities (Tokyo, Hokkaido, Tohoku, Hokuriku, Chubu, Kansai, Shikoku, Chugoku, Kyushu, JAPC, J-Power).

## REFERENCES

- [1] United States Nuclear Regulatory Commission (U.S. NRC) Office of Nuclear Regulatory Research: Joint Analysis of Arc Faults (Joan of ARC) – OECD International Testing Program for High Energy Arc Faults (HEAF), NEI Fire Protection Information Forum, Austin, TX, USA, September 2012.
- [2] Roewekamp, M., et al.: Experiences from the OECD FIRE Database and Intended Future Extensions, Paper in: Proceedings of 13<sup>th</sup> International Probabilistic Safety Assessment and Management Conference (PSAM13), Seoul, Republic of Korea, October 2016, <https://publons.com/journal/325745/proceedings-of-the-international-conference-on-pro>.
- [3] United States Nuclear Regulatory Commission (U.S. NRC): High Energy Arcing Fault Frequency and Consequence Modeling, Draft Report for Comment, NUREG-2262, Washington, DC, USA, July 2022, <https://www.nrc.gov/docs/ML2215/ML22158A071.pdf>.
- [4] United States Nuclear Regulatory Commission (U.S. NRC): NRC High Energy Arcing Faults LIC-504 Team Recommendations, (Memorandum: ADAMS Accession No. ML22201A000, Enclosure 1: ADAMS Accession No. ML22201A001, Enclosure 2: ADAMS Accession No ML22201A002, Enclosure 3: ADAMS Accession No. ML22201A003), Washington, DC, USA, July 27, 2022, <https://www.nrc.gov/docs/ML2220/ML22200A272.html>.
- [5] Cabinet Office, Government of Japan: Quoted from volume 7077 of the Japanese government newsletter, Tokyo, Japan, August 8, 2017 (in Japanese).
- [6] Shirai, K., et al.: Evaluation of Thermal Impact of High Energy Arcing Fault (HEAF) on Power Supply Facilities, CRIEPI Report, O20009, Central Research Institute of Electric Power Industry (CRIEPI), Chiba, Japan, 2021 (in Japanese).
- [7] International Standards Organisation (ISO): ISO/IEC 17025 General requirements for the competence of testing and calibration laboratories, 3<sup>rd</sup> Edition, corrected version, March 2018, <https://www.iso.org/standard/66912.html>.
- [8] Central Research Institute of Electric Power Industry (CRIEPI): Brochure of High Power Testing Laboratory, Kanagawa, Japan, October 2017.
- [9] Tasaka, K., et al.: Experimental Studies of HEAF (High Energy Arcing Fault) Event for segmented High Voltage Bus Ducts, CRIEPI Report, O20008 2021 (in Japanese).
- [10] International Electrical Commission (IEC): Protective clothing against the thermal hazards of an electric arc, Part 1-1: Test methods - method 1: Determination of the arc rating (ATPV or EBT50) of flame resistant materials for clothing, IEC 61482-1-1, 2009, <https://webstore.iec.ch/publication/5497>.

- [11] Shirai, K., et al.: Proposal of an Evaluation Method for Prevention of High Energy Arcing Fault (HEAF) Induced Fires at Low and High Voltage Electrical Cabinets, in: Roewekamp, M., H.-P. Berg (Eds.): Proceedings of SMiRT 25, 16<sup>th</sup> International Seminar on Fire Safety in Nuclear Power Plants and Installations, October 28-30, 2019, Ottawa, ONT, Canada, GRS-A-3963, Gesellschaft für Anlagen- und Reaktorsicherheit (GRS) gGmbH, Köln, Germany, December 2019, <https://www.grs.de/en/publication/grs-3963>.
- [12] Tasaka, K., et al.: Experimental study of smoke effects on energized electrical cabinets located nearby a lubricant oil pool fire, *Fire and Materials*, Volume 43, Issue 5, pp. 561-578, August/September 2019, <https://doi/10.1002/fam.2718>.
- [13] Phillips, J.: Complete Guide to Arc Flash Hazard Calculation Studies, A step-by-step approach packed with examples, tips, and calculation worksheets, ISBN 10-0615486916, brainfiller, January 2011, <https://brainfiller.com>.
- [14] Miyagi, T., et al.: Influence of Arc Current on Energy Balance due to High Current Arc in a Closed Chamber", *IEEJ Trans. PE*, Vol.130, No.2, 2010 (in Japanese).
- [15] United States Nuclear Regulatory Commission (U.S. NRC) Office of Nuclear Regulatory Research (RES) and Electric Power Research Institute (EPRI): Fire PRA Methodology for Nuclear Power Facilities, Supplement 1: Fire Probabilistic Risk Assessment Methods Enhancements, EPRI/NRC-RES, NUREG/CR-6850 (EPRI 10191989), Washington, DC, and Palo Alto, CA, USA, 2010, <https://www.nrc.gov/reading-rm/doc-collections/nuregs/contract/cr6850/s1/ind>.

# Development of Improved High Energy Arcing Fault (HEAF) Target Damage Thresholds and Zone of Influence (ZOI) Models

Kevin Coyne<sup>1\*</sup>, Gabriel Taylor<sup>1</sup>, Kenneth Hamburger<sup>1</sup>, Nicholas Melly<sup>1</sup>,  
Kevin McGrattan<sup>2</sup>, and Mark Henry Salley<sup>1</sup>

<sup>1</sup> United States Nuclear Regulatory Commission, Washington, DC, 20555-0001,  
United States of America

<sup>2</sup> U.S. Department of Commerce, National Institute of Standards and  
Technology, Gaithersburg, MD, 20899, United States of America

## ABSTRACT

In order to improve the realism of High Energy Arcing Fault (HEAF) hazard modelling, the U.S. Nuclear Regulatory Commission (NRC), in cooperation with the Electric Power Research Institute (EPRI), has developed improved HEAF target fragility estimates and a zone of influence (ZOI) model. In the context of this project, the target damage threshold (i.e., target fragility) is determined by assessing the damage threshold at which the target of interest can no longer perform its function. The ZOI defines the region in which the hazard exceeds this damage threshold. This work, being performed under the NRC's HEAF research project plan, advances the understanding of the early HEAF models contained in NUREG/CR-6850 / EPRI 1011989, "EPRI/NRC-RES Fire PRA Methodology for Nuclear Power Facilities, to better reflect arc characteristics (such as duration, power, and location); enclosure configuration; and electrical cable target fragilities. Updated fragility data was obtained from physical testing that assessed the performance of common targets to very short duration, high energy exposures expected during a HEAF. This testing information, along with relevant operating experience and the current state-of-knowledge, was evaluated by a joint NRC-EPRI Working Group to reach consensus positions on the fragility of various electrical cable configurations exposed to a HEAF. To develop the improved ZOI model, the joint NRC-EPRI Working Group relied on computational fluid dynamics simulations using the National Institute of Standards and Technology (NIST) Fire Dynamics Simulator (FDS) to calculate the thermal exposure levels in the vicinity of a HEAF. The ZOI was determined based on where thermal exposure exceeds the fragility limits for targets exposed to the HEAF. This method was applied to a large matrix of simulations that varied the fault duration, power, location, electrode composition, and type of equipment. This approach allowed the NRC-EPRI Working Group to construct a detailed tabulation of ZOIs for each simulation in the matrix and improves the realism of the ZOIs. To provide independent corroborating evidence for the model, the NRC performed additional confirmatory analysis using a modified IEEE 1584 Arc Flash model. The confirmatory NRC calculations showed good agreement with the results of the FDS simulations and provided further confidence in the new ZOI results developed by the joint NRC-EPRI Working Group.

## INTRODUCTION

Electrical system failure HEAF events are energetic electrical arcing faults that can lead to the rapid release of energy. This energy release can result in high heat fluxes in the vicinity of the HEAF failure, vaporization of metal, release of ionized gas and smoke, and mechanical shocks to nearby equipment. These effects can result in the loss of function-

ability of safety critical components in the vicinity of the HEAF, which in combination with the associated electrical system perturbations, can initiate a plant shutdown (e.g., a reactor or turbine trip) and degrade accident mitigation capability. Operating experience has shown that HEAF can be a significant contributor to plant risk [1], [2], [3].

In the United States, the fire protection regulations contained 10 CFR 50.48, "Fire Protection," require a nuclear power plant to implement a fire protection plan that meets the requirements of 10 CFR 50, Appendix A, General Design Criterion (GDC) 3, "Fire protection". GDC 3 specifies, in part, that nuclear power plant systems, structures, and components important to safety be designed and located to minimize the probability and effect of fires and explosions. The NRC's regulations provide two options for meeting this requirement: (1) a deterministic option described under 10 CFR 50.48(b) that references the requirements contained in 10 CFR 50, Appendix R, "Fire Protection Program for Nuclear Power Facilities Operating Prior to January 1, 1979", or (2) a risk-informed, performance-based, option described under 10 CFR 50.48(c) that allows use of National Fire Protection Association Standard NFPA 805, "Performance-Based Standard for Fire Protection for Light Water Reactor Electric Generating Plants, 2001 Edition" [4], with some exceptions. As described in the Statements of Consideration for the final rulemaking approving use of NFPA 805 [5], the NFPA 805 methodology incorporates a number of performance-based attributes, including identification of objective performance criteria and flexibility in the means by which a licensee determines how these criteria are met. The NRC provides guidance for implementing the NFPA 805 option in Regulatory Guide (RG) 1.205, "Risk-Informed, Performance-Based Fire Protection for Existing Light-Water Nuclear Power Plants [6]". Further, the NRC endorsed NUREG/CR-6850/EPRI 1011989, "EPRI/NRC-RES Fire PRA Methodology for Nuclear Power Facilities, Final Report" [7] and its Supplement 1 [8], as one acceptable method for conducting a Fire PRA (Probabilistic Risk Assessment). Guidance for HEAF events is provided in both NUREG/CR-6850 and its supplement. For example, the following guidelines are provided in establishing a zone of influence (ZOI), within which equipment is assumed to be damaged for the purposes of the probabilistic risk assessment (PRA) during a HEAF event:

- For HEAF events within an electrical cabinet, any unprotected cables in the first overhead cable tray within 1.5 m (5 ft) vertical distance of the top of the cabinet and 0.3 m (1 ft) horizontally from the cabinet face will be within the ZOI and assumed to be damaged. Additionally, any equipment within 0.9 m (3 ft) horizontal distance from the cabinet front or rear panel and at or below the top of the cabinet will be within the ZOI (NUREG/CR-6850, Volume 2, Appendix M [7]).
- For HEAF events within an iso-phase bus duct, the ZOI is assumed to be a sphere centred on the fault point and measuring 1.5 m (5 ft) feet in radius (NUREG/CR-6850, Supplement 1 [8]).
- For HEAF events within non-iso phase bus ducts, the ZOI includes: (1) a downward expanding cone from the point of arcing enclosing a total solid angle of 30° to a maximum diameter of 6.0 m (20 ft); (2) a sphere with a radius of 0.45 m (1.5 ft) from the point of arcing (assumed to be the center of the bus duct) (NUREG/CR-6850, Supplement 1 [8]).

A limitation of the NUREG/CR-6850 ZOI approach is that it is insensitive to a number of factors which influence the potential of hazard of a HEAF, including target equipment fragility, voltage level, amperage, and duration of the arcing event (which is related to the time needed for clear an electrical fault). In addition, recent operating experience [9], has suggested that materials used to construct conductors (e.g., copper or aluminum) and electrical enclosures (e.g., steel or aluminum) may also influence the magnitude of the HEAF hazard. These factors may either increase or decrease the ZOI size, depending on the specific HEAF conditions. To address this issue, the U.S. NRC, in collaboration with the NIST and the EPRI, implemented a research plan to improve the realism of

HEAF modelling. This research plan leveraged physical testing, computational tools, and improved fragility data to update the HEAF methods described in NUREG/CR-6850 and its supplement. Three specific activities are described in this paper:

- **Updated fragility modelling:** A joint NRC and EPRI Working Group used updated fragility data, obtained from physical testing, and operating experience insights to reach consensus positions on the fragility of various electrical cable configurations exposed to a HEAF.
- **Computational fluid dynamics simulation to update ZOIs:** The joint NRC-EPRI Working Group relied on computational fluid dynamics simulations using the NIST Fire Dynamics Simulator (FDS) to calculate the thermal exposure levels in the vicinity of a HEAF. The ZOI was determined based on where thermal exposure exceeds the fragility limits for targets exposed to the HEAF. This method was applied to a large matrix of simulations that varied the fault duration, power, location, electrode composition, and type of equipment. This approach allowed the NRC-EPRI Working Group to construct a detailed tabulation of ZOIs for each simulation in the matrix and to improve the realism of the ZOIs.
- **Confirmatory ZOI analysis:** To provide independent corroborating evidence for the model, the NRC performed additional confirmatory analysis using a modified IEEE 1584 arc flash model. The confirmatory NRC calculations showed good agreement with the results of the FDS simulations and provided further confidence in the new ZOI results developed by the joint NRC-EPRI Working Group.

These research activities are described in more detail in the following sections.

## UPDATED FRAGILITY MODELLING

The objective of this portion of the research project plan was to establish the target fragilities for equipment that might be present within the HEAF ZOI. HEAF events, which generate short duration high heat fluxes, have different characteristics than traditional combustion fires which have longer duration but lower heat fluxes. Therefore, the fragility for equipment, particularly cables, was examined under the higher heat fluxes from HEAF exposures.

### Cable Fragility Experiments

In support of this work, fragility testing was conducted at the Solar Furnace at Sandia National Laboratories (SNL) [10]. The Solar Furnace facility consists of a heliostat containing a total reflective surface of 55 m<sup>2</sup> (cf. Figure 1) which directs sunlight to a parabolic reflector. This facility is capable of concentrating sunlight to generate a heat flux of up to 6 MW/m<sup>2</sup> within a circle that is approximately 5 cm in diameter.



**Figure 1** Solar Furnace at Sandia National Laboratories

Both thermoplastic (TP) and thermoset (TS) cables were evaluated. The distinction between these cable types is that thermoplastic materials soften, flow, or distort when subjected to sufficient heat and pressure while thermoset cables do not. The failure threshold for thermoplastic cables is generally lower than thermoset cables; for example, Appendix H of NUREG/CR-6850 [7], provides generic screening non-HEAF fire scenario fragilities for TP cables of  $> 6 \text{ kW/m}^2$  and  $> 205^\circ\text{C}$  and fragilities of  $> 11 \text{ kW/m}^2$  and  $330^\circ\text{C}$  for TS cables. However, the underlying physics of failure used to determine cable fragilities for non-HEAF events, may not accurately capture the HEAF phenomena such as high heat fluxes for a short duration. The Solar Furnace testing varied the heat flux, cable material (thermoplastic and thermoset), and exposure duration. In addition, the heat flux profile was dynamically adjusted during some of the tests to better represent secondary heat fluxes to the target representing combustion of surrounding materials and thermal radiation from heated surfaces following the initial HEAF event.

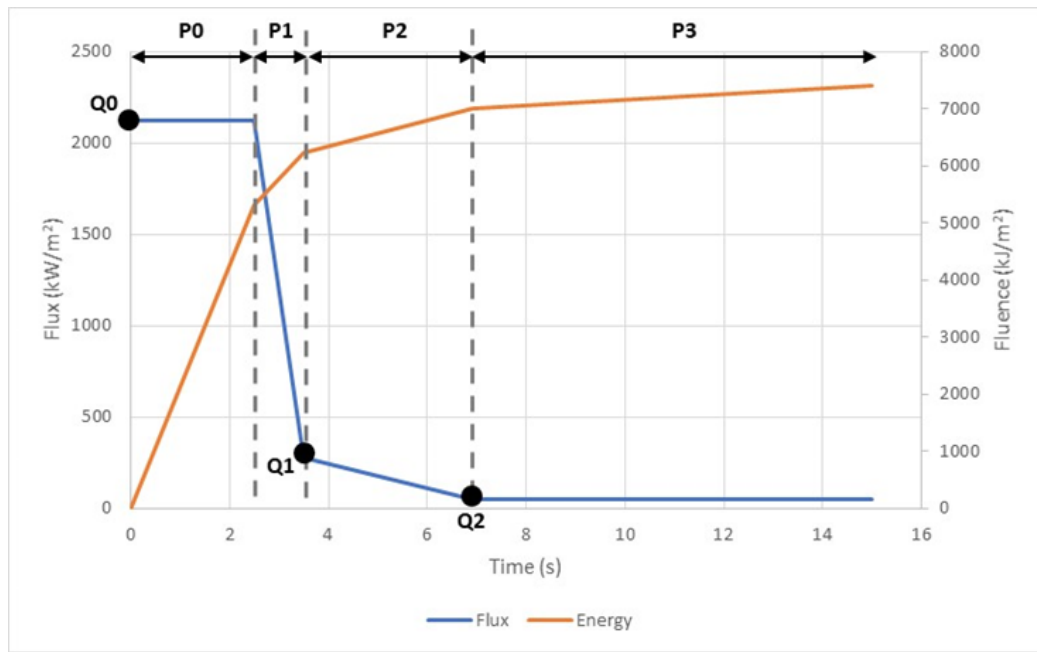


**Figure 2** Typical Solar Furnace testing heat flux profile

Several different cable failure criteria were evaluated during the testing such as cable ignition, damage as a function of total energy, electrical failure of cables, and temperature. However, some criteria did not provide repeatable results at small scale (e.g., sustained ignition) and others were not reliable indicators of failure during the time scale of

a HEAF event (e.g., electrical failure and sub-jacket temperature). Based on the testing results, it was determined that cable jacket damage resulting in exposure of the insulated cable wiring was a reliable metric for cable failure and provided repeatable data for tests conducted with different levels of heat flux. Because the cable jacket material tends to be black and the conductor insulation is multi-coloured, it is relatively easy to visually determine that the jacket is breached. Example test results for a thermoplastic cable exposed to an incident energy level of approximately 7 MJ/m<sup>2</sup> (Test 1-22, showing jacket damage), 24 MJ/m<sup>2</sup> (test 1-32, showing wiring insulation exposure), and 206 MJ/m<sup>2</sup> (test 1-09, showing wire conductor exposure) are shown in Figure 3.



**Figure 3** Post-test thermoplastic cable following incident energy exposure to 7 MJ/m<sup>2</sup> (test 1-22), 24 MJ/m<sup>2</sup> (1-32), and 206 MJ/m<sup>2</sup> (test 1-09)

A total of 38 solar furnace cable tests were conducted, and the data was analysed to categorize the results into jacket damage, insulation exposure, and conducting wire exposure. Figure 4 provides plots of the thermoplastic and thermoset cable test results for initial heat fluxes higher than 1 MW/m<sup>2</sup>, which were considered to be more representative of an actual HEAF event. These plots show the incident energy at which jacket damage, insulation exposure, and wire exposure were found.

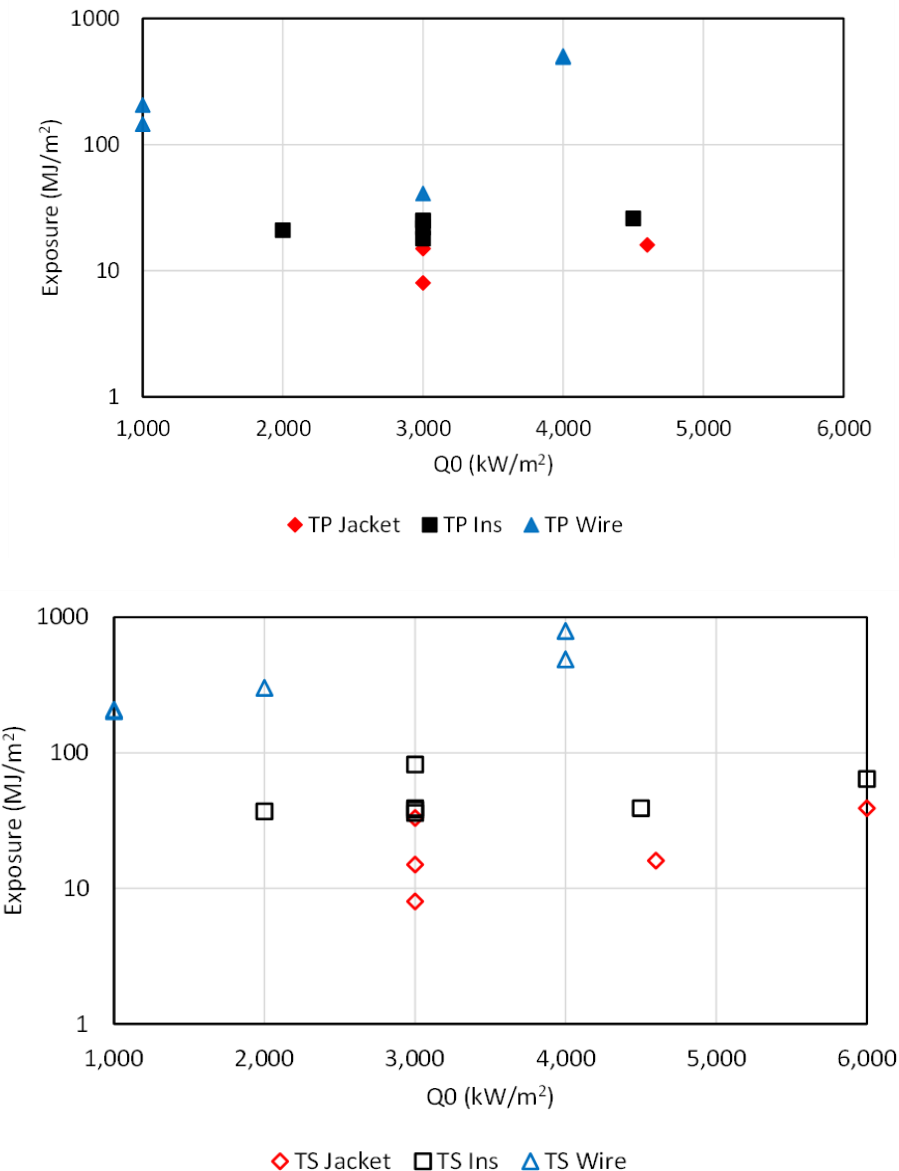


**Figure 4** Results for thermoplastic (TP, top) and thermoset (TS, bottom) cables plotting incident energy for jack damage, insulation exposure, and wire exposure

### Fragility Working Group

A joint NRC and EPRI Working Group evaluated the results of the solar furnace testing, in addition to operating experience (e.g., [1], [2], [3], and [9], HEAF related testing (e.g., [11], [12], and [13]), and the current state of knowledge to develop a consensus model for HEAF target fragilities. Results from this testing, along with the full- and medium-scale data were then used to develop a fragility model by the joint NRC/EPRI Working Group [14]. The Working Group evaluated damage by considering both the cable electrical functionality and potential for fire ignition. Further, the Working Group focused on electrical cable (control, power, and instrumentation) fragilities since these were considered to be the most common target assessed for Fire PRA. In addition, the Working Group developed fragilities for electrical bus ducts and provided guidance for crediting electric raceway fire barrier systems.

The Working Group team members were assigned specific roles supporting the expert elicitation process, but some flexibility in the process was retained to expedite determinations when consensus could be reached quickly. The Working Group roles included the following specific activities:

- Proponents: technical experts who developed, presented, and defended a proposal to the Working Group members. The proponents were organized into two different teams, each tasked with developing a proposal for each area requiring consensus
- Technical evaluators and integrators: technical experts without a vested interest in the development of any proposal and therefore were able to objectively evaluate the proposals, views, and available data to inform their decision. The technical evaluators and integrators were also responsible for developing a Working Group consensus.
- Resource experts: Subject matter experts with detailed knowledge of the data sets, experimentation, instrumentation, physics, modelling, or other discipline related to target fragility of specific devices, HEAF testing, or phenomena.

The Working Group approach consisted of the following key steps:

- Proposal development: Each of the proponent teams developed a proposal to address a specific technical issue
- Weekly meetings: The proposals were presented to the full Working Group during weekly meetings, which allowed Working Group members to ask questions and provide feedback on the proposals
- Consensus: The technical evaluators and integrators caucused to reach agreement on the path forward on each issue. The path forward involved selection of one of the proposals, combining the proposals to use key attributes of each, or requesting specific revisions to a proposal. There were no cases where the Working Group was unable to eventually reach a consensus position.

It is important to note that the Working Group focused on fragilities associated with the initial HEAF event. However, a full assessment of HEAF risk requires a two-step process which considers the immediate failures caused by the HEAF followed by an assessment of subsequent impacts from induced thermal fires. The HEAF fragility work considered the potential for a HEAF event to lead to sustained ignition of electrical cable fire and any ensuing thermal fires are addressed by the HEAF PRA method.

## Fragility Results

Based on application of the consensus process, the NRC-EPRI Working Group reached the following conclusions on cable fragility [14]:

- The threshold for electrical failure/damage of thermoplastic jacketed cables is 15 MJ/m<sup>2</sup> and the threshold for thermoset jacketed cables is 30 MJ/m<sup>2</sup>.
- Sustained ignition is assumed for cables within the enclosure of origin (e.g., internal cables and components within switchgear and load centers).
- For cables outside of the enclosure of origin, but within the postulated HEAF ZOI, no sustained ignition is assumed.

The Working Group also evaluated protective feature capabilities including electrical raceway fire barrier systems (ERFBS, also referred to as “fire wraps”), electrical raceway protection (e.g., conduit and cable tray covers) and bus duct damage limits.

In evaluating ERFBS, the Working Group considered the thermal protective properties of the barrier system (i.e., its ability to limit temperature rise on the protected side of the barrier during a fire) and the mechanical response during a HEAF event. The Working Group concluded that a 1 hour rated ERFBS is capable of protecting enclosed cables located within the HEAF zone of influence (but outside the enclosure where the HEAF originated) such that the protected cables are not damaged, ignited, or contribute to the fire load. Cables within a rated ERFBS inside an electrical enclosure are assumed to be damaged, but not ignited.

The Working Group evaluated the thermal and mechanical protection afforded by various types of conduits and cable tray covers. With regard to thermal protection, the Working Group believed that while some conduit configurations may provide some increase in thermal protection, several factors offset this benefit. For example, the increased surface area associated with the conduit (which can increase thermal load on the protected cables) and the ability of the conduit to retain heat following the HEAF event can lead to additional heat flux exposure for the protected cables. Therefore, the Working Group concluded that there was insufficient information to credit conduit with providing any additional protection during a HEAF. The Working Group used a similar process to evaluate cable tray top and bottom covers and for similar reasons concluded that no additional credit for these covers was warranted during a HEAF event. As such, cables in conduits and cables in trays with a cover should use the thermoplastic (15 MJ/m<sup>2</sup>) and thermoset (30 MJ/m<sup>2</sup>) fragility criteria.

Evaluation for bus ducts was more complicated because there is not an existing consensus on the fragility limits for electrical bus bars. The Working Group considered the capability of bus bar insulation (e.g., Noryl, a polymer-based material developed by General Electric used as an insulating bus bar sleeving) and the impact of hot gases and aerosols on bus bars following duct breach and concluded that bus duct failure would lead to immediate bus bar failure. The Working Group then used several methods to evaluate the thermal capability of bus ducts, including simplified energy balance calculations and use of a computational fluid dynamics (CFD) thermal hydraulic computer code. The analysis methods were in general agreement and the Working Group concluded that the fragility limit for steel bus ducts was 30 MJ/m<sup>2</sup> and 15 MJ/m<sup>2</sup> for aluminum ducts.

## UPDATED ZONE OF INFLUENCE MODEL USING FDS SIMULATIONS

The objective of this work was the development of a tool that could leverage experimental data and provide ZOI information for configurations that were not subject to full-scale testing. This provided a more cost-effective and flexible approach considering the high costs associated with conducting full-scale HEAF experiments. Therefore, this activity focused on the development of a CFD model of HEAF events capable of calculating the total incident energy in the vicinity of a HEAF for a variety of equipment configurations and materials. The predicted incident energy levels were then used to determine the ZOIs for specific equipment. The Fire Dynamics Simulator (FDS) [15] was used to support this effort. The FDS computer code includes a hydrodynamic model capable of solving the low-Mach number, thermally driven flow equations using a large eddy simulation turbulence model [16]. FDS includes a combustion model and a radiative heat transport model, in addition to capabilities for accommodating a wide variety of geometric configurations. Key modelling considerations for HEAF events are discussed in [16], and include the following:

- FDS is a well-recognized and validated fire model that has been used for evaluating smoke and heat transport from fires since 2000. FDS has been subjected to extensive validation activities including comparisons to full-scale experiments, standard tests, documented fire experience, and engineering correlations. These activities

have served to validate FDS models in several areas of importance to this HEAF work, including fire plumes, fire growth, flame spread, and combustion modelling [17].

- The FDS numerical solver is generally appropriate for low speed (i.e., less than ~ 30 % of the speed of sound) thermally driven flow. Although FDS is not capable of resolving the shock waves that may accompany a HEAF event, this impact is considered to be relatively minor given that the major damage to targets is via thermal radiation and convection.
- FDS does not include physical models for electric and magnetic fields; the disassociation of molecules at high temperature; or the formation of plasma. These factors limit the ability of FDS to accurately predict temperature or account for movement of the electrical arc within the cabinet. However, the FDS model does account for total arc energy (as determined by arc voltage, amperage, and duration) and can appropriately account for the arc energy associated with the HEAF event. The other modelling limitations are believed to have a minor impact on the FDS results.
- The arc itself was modelled as a volumetric heat source. Three generic arc power profiles were used: (1) a constant current source of 30 kA used for medium voltage switchgear and non-segregated bus ducts; (2) a constant current followed by a decay curve to represent generator fed faults; and (3) a two-stage profile using a high initial current followed by a reduced second stage current. The radiative emission from the arc was based on experimental data for aluminum and copper electrodes. Combustion was modelled for metal vapor oxidation and contributed to the total energy associated with the HEAF. Electrode mass loss rate was modelled using a correlation for aluminum and copper determined based on open box testing [13] and previous medium voltage switchgear tests [12].
- In order to reduce the potential for input errors given the large number of simulations, an algorithmic approach was used to automatically generate input files.

The FDS model was validated against four medium voltage switchgear experiments [12]. Data collected from the experiments was compared to FDS simulations of the same experimental configurations. Figure 5 provides the results of this comparison for temperature rise associated with two of the instrument racks used for the medium voltage switchgear testing and shows that FDS underpredicted temperature rise values (which is directly related to incident energy). Based on consideration of factors that impact the FDS results (e.g., unmodeled enclosure leakage), a bias factor and standard deviation were determined to adjust the FDS results to better align with the experimental results. This resulted in identification of a relative standard deviation of 0.71 and a bias factor of 0.59. This information allows calculation of a 95 % confidence interval for the FDS results using the following formula (where  $M$  is the FDS prediction,  $\delta$  is the bias factor and  $\sigma$  is the relative standard deviation):

- Lower bound:  $\left(\frac{M}{\delta}\right) / (1 + 2\sigma)$
- Upper bound:  $\left(\frac{M}{\delta}\right) (1 + 2\sigma)$

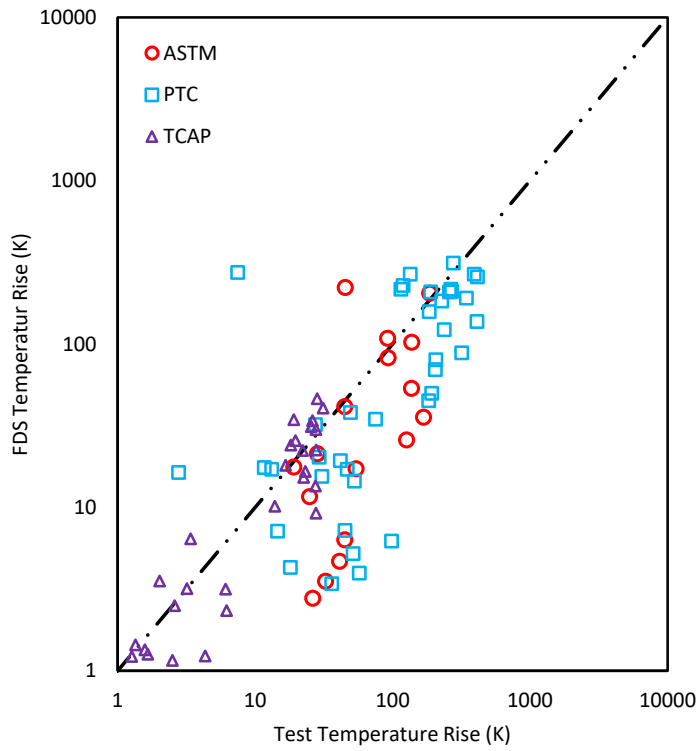


**Figure 5** Comparison between unbiased FDS predictions and experimental results for medium voltage Switchgear testing (instrument racks 1 and 4)

FDS predictions for enclosure breach were also compared to experimental results to assess the ability of FDS to predict location and extent of HEAF induced cabinet openings (see Figure 6).

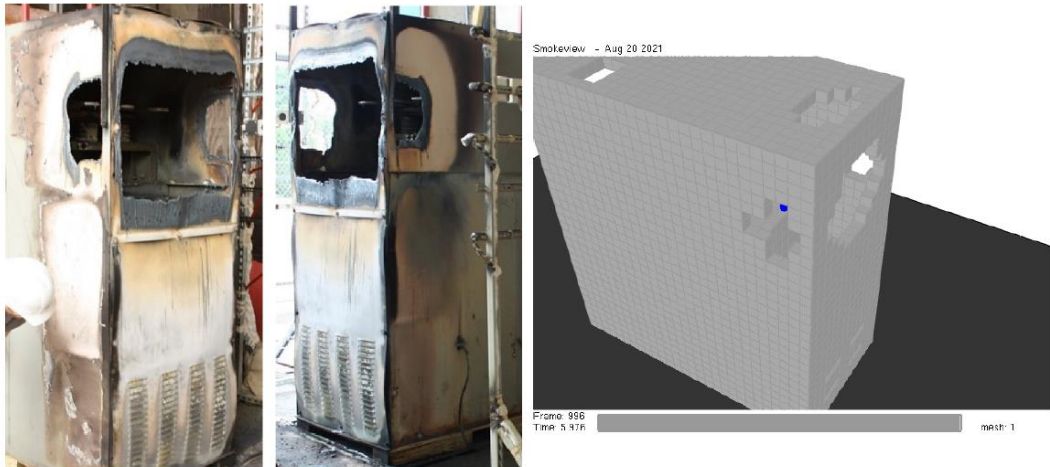


**Figure 6** Results from MV switchgear experiment 2-21 and associated FDS results

In addition to the medium voltage experiments, the FDS model was also used to evaluate several HEAF events from operating experience, in order to assess enclosure breach time and damage extent.

Following validation of the FDS model, a calculation matrix for FDS simulations was built on in-information gathered from surveying the U.S. nuclear fleet (e.g., switchgear manu-

facturer, bus bar materials, potential fault locations), operating experience, and previous testing. Over 130 simulation runs were identified, covering the following characteristics:

- Low voltage switchgear with steel enclosure – bus bar material (aluminum, copper), arc duration, arc location (mid compartment bus, circuit breaker), arc energy (34 FDS simulations);
- Medium voltage switchgear with steel enclosure - bus bar material (aluminum, copper), switchgear type (GE Magneblast, ABB/ITE HK), arc duration, arc location (main bus bars, compartment bus bars, circuit breaker), and arc energy (42 FDS simulations);
- Non-segregated bus ducts – duct material (steel, aluminum) and bus bar material (aluminum, copper), arc duration, arc location, and arc energy (57 FDS simulations).

The FDS HEAF simulations provided a significant amount of data related to particle distributions, thermal plume behaviour, heat release rates, incident energy, and temperature profiles. Figure 7 is an example of the results obtained from these simulations.

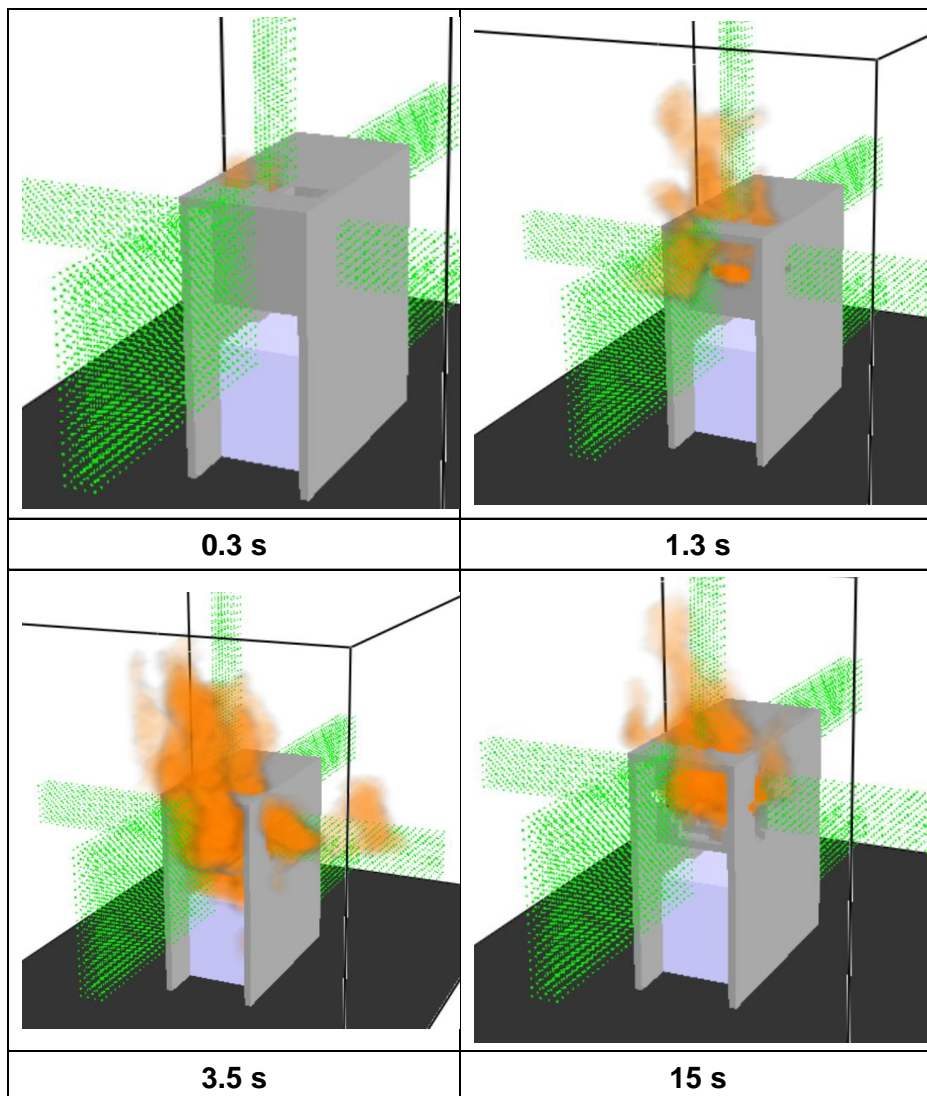


**Figure 7** FDS Results for a 226 MJ HEAF thermal plume (medium voltage switchgear cabinet)

This information allowed the determination of the distance at which the 15 MJ/m<sup>2</sup> and 30 MJ/m<sup>2</sup> target fragilities would be exceeded (which is used to determine the HEAF zone of influence). Figure 8 shows the results for medium voltage switchgear cabinet with an arc initiated at the main bus bars using a 15 MJ/m<sup>2</sup> fragility threshold.

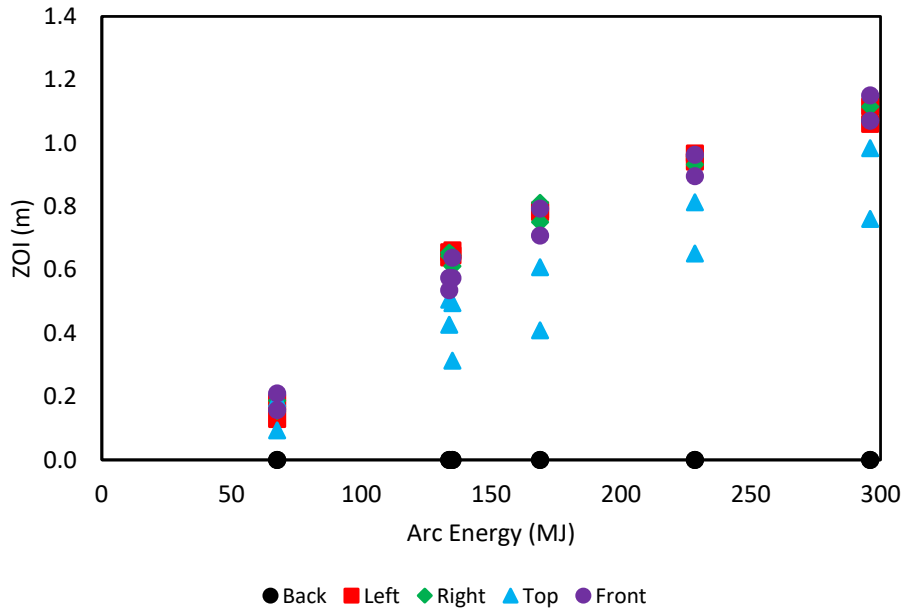


**Figure 8** Example ZOI for 15 MJ/m<sup>2</sup> fragility (medium voltage switchgear)

Zones of influence for other simulated conditions were obtained in a similar manner. Reference [16] provides a tabulation of the ZOI results for all FDS simulations. Several key insights were identified during this work:

- The dominant factor for medium voltage switchgear ZOIs was total arc energy. The results for medium and voltage switchgear were also sensitive to equipment geometry and orientation. [7], [8].
- The ZOIs for low voltage switchgear are lower than those provided in NUREG/CR-6850 and its supplement.
- The ZOIs for medium voltage switchgear are lower than the NUREG/CR-6850 guidance for some configurations, but greater for others (e.g., up to 1.24 m for a fragility threshold of 15 MJ/m<sup>2</sup>).
- The composition of non-iso phase bus duct housings (aluminum vs. steel) has a significant impact on the ZOI, with aluminum increasing the ZOI by approximately 0.15 m. The maximum ZOI is 1.41 m for a 15 MJ/m<sup>2</sup> fragility threshold. However, the ZOI results were not sensitive to electrode composition, with copper and aluminum electrode results lying within the 95 % confidence interval.

## CONFIRMATORY ZOI CALCULATIONS

To provide additional confidence in the ZOIs calculated using the FDS model, the NRC staff also developed a modified model based on IEEE guide 1584-2018, “IEEE Guide for Performing Arc-Flash Hazard Calculations” [18]. This IEEE standard was developed to estimate incident energy at various distances from an arc flash event for the purpose of electrical safety. The NRC’s model differed from the IEEE arc flash model and its application in several ways, including fault current input (arc current rather than bolted fault

current), inclusion of an enclosure breaching time, and solving for incident energy to determine a ZOI based on plant specific target fragilities [19]. Specific differences include the following:

- Arc current and voltage: The IEEE model is based on use of a bolted fault current (which is a short circuit condition that assumes zero impedance at the point of the fault). However, determining the appropriate bolted fault current requires analysis of the characteristic of the specific electrical distribution system. Since this information was not available, the staff iterated on bolted fault current to determine a value that yielded the desired arc current. Arc voltage is needed to determine total arc energy and was estimated based on use of the CIGRE-602 model [20] with a correction factor based on previous medium voltage switchgear and open box testing results [12], [13].
- Enclosure breaching time: The IEEE arc flash model is intended to address electrical safety and does assume there is a barrier (such as an electrical enclosure) between the arc and target. However, actual HEAF events that initiate within an enclosure will need to breach the enclosure before incident energy is received by the target. Therefore, a model was developed to account for the time to breach and enlarge the opening of the enclosure. The time to breach is dependent on enclosure material with aluminum enclosures breaching approximately four times faster than a steel enclosure of equivalent thickness and fault current.
- Arc energy decay due for generator fed faults – Because some faults cannot be isolated from the main generator, the arc energy was adjusted to reflect generator coast down following a turbine trip and associated energy decay.
- A spherical zone of influence, centred on the arc location, was determined by identifying the distance at which the incident energy for the simulated HEAF event is equivalent to  $15 \text{ MJ/m}^2$  and  $30 \text{ MJ/m}^2$ .

Application of the modified arc-flash model yielded the following results:

- Low-voltage switchgear: No results exceeded the 0.9 m ZOI provided in NUREG/CR-6850 and its supplement.
- Medium voltage: The maximum ZOI obtained from the modified arc flash model is slightly greater the maximum FDS calculated ZOI for both the  $15 \text{ MJ/m}^2$  fragility level (1.6 m versus 1.3 m) and the  $30 \text{ MJ/m}^2$  fragility level (1.1 m versus 0.97 m).
- Non-isophase bus ducts: The maximum ZOI obtained from the modified arc-flash model is 1.2 m, which is slightly less than the maximum FDS ZOI of 1.4 m.

The results of the modified arc-flash empirical model are consistent with the more detailed FDS analysis and appropriately reflect the influence of key factors such as arc energy, and enclosure material. Therefore, the modified arc-flash model provides additional confidence in the CFD-derived ZOIs.

## CONCLUSIONS

The development of updated fragility thresholds for thermoplastic and thermoset cabling and the use of the FDS computational fluid dynamics computer code, which allows for detailed examination of a variety of electrical equipment configuration and arc characteristics, is expected to further improve the realism of Fire PRA. The use of a joint Working Group supported by both the NRC and EPRI allowed thorough consideration of a diverse spectrum of perspectives and enabled the development of consensus positions for a number of challenging issues. Further, the NRC use of a modified arc-flash model pro-

vided additional confirmation of the results of the FDS calculations and further support NRC confidence in the results of this process.

## ACKNOWLEDGEMENTS

This work would not have been possible without the collaboration of staff from the Electrical Power Research Institute, Sandia National Laboratories, KEMA Labs, Brandon Stanton Inc., and the U.S. National Institute of Standards and Technology. The NRC gratefully acknowledges the support from the following individuals:

- U.S. Nuclear Regulatory Commission Working Group members, including Thinh Dinh, J. S. Hyslop, Kenn Miller, Charles Moulton, Reinaldo Rodriguez, David Stroup, Sunil Weerakkody, Jen Whitman, and Antonios Zoulis;
- Electric Power Research Institute: Ashley Lindeman, Marko Randelovic, Tom Short, and Fernando Ferrante. In addition, the following individuals provided substantial support to EPRI during this project: Jason Floyd, Dane Lovelace, Sean Hunt, Ken Fleischer, P. Shannon Lovvorn, and Victor Ontiveros;
- U.S. National Institute of Standards and Technology: Kevin McGrattan, Anthony D. Putorti, Scott Bareham, Edward Hnetkovsky, Christopher Brown, Wai Cheong Tam, Erik Link, Michael Selepak, Philip Deardorff, and Andre Thompson;
- Sandia National Laboratories: Chris LaFluer, Paul Clem, Byron Demosthenous, Austin Glover, Raymond Martinez, Anthony Tambakuchi, Kenneth Armijo, Alvaro Augusto Cruz-Cabrera, James Taylor, Rana Weaver, and Caroline Winters;
- OECD Nuclear Energy Agency High Energy Arcing Fault Project participants, including the project Secretariat Markus Beilmann and participating countries including Belgium, Canada, France, Germany, Japan, Korea, the Netherlands, Republic of Korea, and Spain;
- KEMA Labs: Frank Cielo and the staff at KEMA Labs;
- Brandon Stanton, Inc.: Rob Taylor and the staff at BSI.

## REFERENCES

- [1] Organisation for Economic Co-operation and Development (OECD) Nuclear Energy Agency (NEA), Committee on the Safety of Nuclear Installations (CSNI): OECD FIRE Project – Topical Report No. 1, Analysis of High Energy Arcing Fault (HEAF) Fire Events, NEA/CSNI/R(2013)6, Paris, France, June 2013, <http://www.oecd-nea.org/documents/2013/sin/csni-r2013-6.pdf>.
- [2] Raughley, W., and G. F. Lanik: Operating Experience Assessment Energetic Faults in 4.16 kV to 13.8 kV Switchgear and Bus Ducts that Caused Fires in Nuclear Power Plants 1986-2001 (ADAMS ML021290358), U.S. Nuclear Regulatory Commission, Washington, DC, USA, 2002.
- [3] Rodriguez, R., and S. Weerakkody: High Energy Arcing Faults LIC-504 Team Recommendations (ADAMS ML22200A272), U.S. Nuclear Regulatory Commission (NRC), Washington, DC, USA, 2022-
- [4] National Fire Protection Association (NFRA): NFPA 805, Performance-Based Standard for Fire Protection for Light Water Reactor Electric Generating Plants, 2001 Edition, Quincy, MA, USA, 2001.

- [5] Office of the Federal Register: Voluntary Fire Protection Requirements for Light Water Reactors; Adoption of NFPA 805 as a Risk-Informed, Performance-Based Alternative, 69 FR 33536, June 16, 2004, <https://www.federalregister.gov/d/04-13522>.
- [6] United States Nuclear Regulatory Commission (U.S. NRC): Regulatory Guide 1.205, Risk-Informed, Performance-Based Fire Protection for Existing Light-Water Nuclear Power Plants, Revision 2, Washington, DC, USA, 2021.
- [7] United States Nuclear Regulatory Commission (U.S. NRC) Office of Nuclear Regulatory Research (RES) and Electric Power Research Institute (EPRI): Fire PRA Methodology for Nuclear Power Facilities, Final Report, EPRI/NRC-RES, NUREG/CR-6850 (EPRI 10191989), Washington, DC, and Palo Alto, CA, USA, 2005, <https://www.nrc.gov/reading-rm/doc-collections/nuregs/contract/cr6850/index.html>.
- [8] United States Nuclear Regulatory Commission (U.S. NRC) Office of Nuclear Regulatory Research (RES) and Electric Power Research Institute (EPRI): Fire PRA Methodology for Nuclear Power Facilities, Supplement 1: Fire Probabilistic Risk Assessment Methods Enhancements, EPRI/NRC-RES, NUREG/CR-6850 (EPRI 10191989), Washington, DC, and Palo Alto, CA, USA, 2010, <https://www.nrc.gov/reading-rm/doc-collections/nuregs/contract/cr6850/s1/index.html>.
- [9] United States Nuclear Regulatory Commission (U.S. NRC): High Energy Arcing Faults in Electrical Equipment Containing Aluminum Components, Information Notice 2017-04, Washington, DC, USA, August 21, 2017, <https://www.nrc.gov/docs/ML1705/ML17058A343.pdf>.
- [10] United States Nuclear Regulatory Commission (U.S. NRC): HEAF Cable Fragility Testing at the Solar Furnace at the National Solar Thermal Test Facility, Research Information Letter (RIL) 2021-09, (SAND2021-11327), Washington, DC, USA, September 2021, <https://www.nrc.gov/docs/ML2125/ML21259A256.pdf>.
- [11] Organisation for Economic Co-operation and Development (OECD) Nuclear Energy Agency (NEA), Committee on the Safety of Nuclear Installations (CSNI): Experimental Results from the International High Energy Arcing Fault (HEAF) Research Program Testing Phase 2014 to 2016, NEA/CSNI/R(2017)7, Paris, France, 2017, <http://www.oecd-nea.org/documents/2016/sin/csni-r2017-7.pdf>.
- [12] United States Nuclear Regulatory Commission (U.S. NRC): Report on High Energy Arcing Fault Experiments - Experimental Results from Medium Voltage Electrical Enclosures, Research Information Letter (RIL) 2021-10, (NIST TN 2188, SAND2021-12049 R), Washington, DC, USA, December 2021, <https://www.nrc.gov/docs/ML2133/ML21334A196.pdf>.
- [13] United States Nuclear Regulatory Commission (U.S. NRC): Report on High Energy Arcing Fault Experiments - Experimental Results from Open Box Enclosures, Research Information Letter (RIL) 2021-18, (NIST TN 2198, SAND2021-16075 R), Washington, DC, USA, December 2021, <https://www.nrc.gov/docs/ML2136/ML21361A176.pdf>.
- [14] United States Nuclear Regulatory Commission (U.S. NRC) and Electric Power Research Institute (EPRI): Target Fragilities for Equipment Vulnerable to High Energy Arcing Faults, Research Information Letter (RIL) 2022-01, (EPRI 3002023400), Washington, DC, and Palo Alto, CA, USA, May 2022, <https://www.nrc.gov/docs/ML2213/ML22131A339.pdf>.

- [15] McGrattan, K., et al.: Fire Dynamics Simulator User's Guide, NIST Special Publication 1019, National Institute of Standards and Technology (NIST), Gaithersburg, MD, USA, 2022.
- [16] United States Nuclear Regulatory Commission (U.S. NRC) Office of Nuclear Regulatory Research (RES) and Electric Power Research Institute (EPRI): Determining the Zone of Influence for High Energy Arcing Faults Using Fire Dynamics Simulator, Draft Research Information Letter for Public Comment, (ML22095A237), Washington, DC, USA, 2022,  
<https://www.nrc.gov/docs/ML2209/ML22095A237.pdf>.
- [17] McGrattan, K., et al.: Fire Dynamics Simulator Technical Reference Guide Volume 3: Validation, Sixth Edition, NIST Special Publication 1018-3, U.S. Department of Commerce, National Institute of Standards and Technology (NIST), Gaithersburg, MD, USA, 2022.
- [18] Institute of Electrical and Electronics Engineers (IEEE): IEEE Guide for Performing Arc-Flash Hazard Calculations, IEEE 1584-2018, ISBN:978-1-5044-5262-5, New York, NY, USA, November 2018, <https://doi.org/10.1109/IEEESTD.2018.8563139>.
- [19] United States Nuclear Regulatory Commission (U.S. NRC): Predicting High Energy Arcing Fault Zones of Influence for Aluminum Using a Modified Arc Flash Model, Draft Research Information Letter, (ML22095A236), Washington, EC, USA, May 2022, <https://www.nrc.gov/docs/ML2209/ML22095A236.pdf>.
- [20] Conseil international des grands réseaux électriques (CIGRÉ) Comité d'études A3: Tools for the simulation of the effects of the internal arc in transmission and distribution switchgear, CIGRE 602, ISBN: 978-2-85873-303-3, 2014.

### **3.3 Session on Fire Hazard and Risk Analyses Including Standards and Guidelines**

The session on fire hazard and risk analyses, also covering the development and application of the corresponding standards and guidance available, included different new approaches for fire safety assessment and implementation of new components. This session was chaired by Marina Röwekamp (GRS, Germany) as one of the technical organisers of the seminar.

After a presentation by the U.S. Nuclear Regulatory Commission (NRC) on the use of an integrated risk-informed decision-making process for HEAF in U.S. NPPs, detailed analytical approach developed by Idaho National Laboratory (INL) and CENTROID LAB In the United States for a more automated and visualized fire modelling in the frame of Fire PSA (*Probabilistic Safety Assessment*) was presented and demonstrated by examples. A French approach for requirements regarding smoke control dampers to be applied in the qualification and implementation standards and guidelines for such components was shown by NUVIA Protection (France). In Sweden, a guideline for the implementation of valves with composite plastic materials in nuclear installations already successfully used in non-nuclear facilities has been developed by RiskPilot and was presented. This approach needs further validation and verification for application in nuclear facilities but may be an interesting alternative in the future.

The four seminar contributions prepared for this session are provided hereafter.

# Using An Integrated Risk-Informed Decision-Making Process to Address High Energy Arcing Fault (HEAF) Issues at United States Nuclear Power Plants

Sunil D. Weerakkody

United States Nuclear Regulatory Commission, Washington, DC, 20555-0001,  
United States of America

## ABSTRACT

In June 2013, the Organization for Economic Co-operation and Development (OECD) Nuclear Energy Agency (NEA) issued a report entitled “Analysis of High-Energy Arcing Fault Fire Events (HEAF)” [1], describing the international operating experience for 48 high energy arcing fault (HEAF) events occurred at nuclear power plants (NPPs). At that time, these HEAF events accounted for approximately ten percent of all fire events collected in the OECD/NEA FIRE (Fire Events Records Exchange) Database. This effort highlighted concerns about the magnitude of HEAF risk to overall risk at nuclear power plants (NPPs). The United States Nuclear Regulatory Commission (U.S. NRC) has a special interest in fire events, and particularly HEAF risks, since (a) risks associated with fires constitute a large fraction of the total core damage frequency, and (b) approximately 50 % of the U.S. NPPs have adopted NFPA 05, “Performance-Based Standard for Fire Protection for Light Water Reactor Electric Generating Plants” [2], which relies on Fire PRAs (Probabilistic Risk Assessments). In addition, testing conducted under the OECD/NEA HEAF Project identified that PRA methods may not adequately address the zones of influence (ZOIs) associated with certain HEAF events.

Therefore, NRC’s Office of Nuclear Regulatory Research (RES), in collaboration with the Electric Power Research Institute (EPRI) and the OECD/NEA embarked on an initiative to enhance the state-of-the art technology in using PRA in assessing the impacts due to HEAFs. Specifically, one objective of this initiative was to examine the validity of the PRA method documented in NUREG/CR-6850 [3] entitled “Fire Probabilistic Risk Assessment Methods”, using additional operating experience, tests, and analyses performed since the publication of that document. In parallel with this research effort, in 2021, the NRC investigated the HEAF issue using NRC’s Office of Nuclear Reactor Regulation (NRR) Office Instruction, LIC-504 entitled “Integrated Risk-Informed Decisionmaking Process for Emergent Issues” [4] to apply best available information and NRC risk assessment tools to determine whether the NRC should take prompt and/or longer-term regulatory actions to ensure that HEAF risks to the public remain at acceptable levels. This paper explains how the NRC used its Integrated Risk-Informed Decision-Making (RIDM) process via the LIC-504 process to address potential safety concerns associated with HEAF.

## INTRODUCTION

The current HEAF PRA modelling methodology accepted by the NRC as documented in NUREG/CR-6850 was first published in 2005 and addresses HEAFs associated with electrical switchgears. That method was based primarily on the evaluation of a limited number of HEAF events. Supplement 1 to NUREG/CR-6850 [3] was published in 2010 and addresses HEAFs from bus ducts. Since the publication of these HEAF methods,

the NRC, in collaboration with EPRI, has updated and issued the HEAF PRA methodology [5] for public comment using more recent operating experience, testing, and other enhancements to fire modelling. (NRC expects to issue the final report after dispositioning public comments during the fiscal year 2022). Some of the key advances to the new HEAF PRA methodology include the following:

- Changes to HEAF frequencies and non-suppression failure probabilities;
- Substantial changes to ZOIs for non-isophase bus ducts and for low and medium voltage switchgears;
- Crediting qualified electrical raceway fire barrier systems (ERFBS) in the HEAF ZOI as a means of preventing damage from HEAF effects;
- Changes to HEAF frequencies;
- More realistic HEAF damage potential that considers factors such as arc duration.

The above list constitutes significant changes to the PRA assessment methodologies of HEAF. The NRC used the updated HEAF PRA method above to examine changes to the estimated HEAF risks by comparing the current HEAF PRA methodology described in NUREG/CR-6850 [3] to the updated HEAF PRA methodology. In addition to comparing quantified risks, consistent with NRC risk-informed decision-making (RIDM) practices, the LIC-504 team's analysis also included a review of the HEAF related information to develop recommendations that could assist plant operators to maintain or reduce HEAF related risks at their facilities and to assist the NRC's inspection staff to further risk-inform HEAF related oversight activities.

This paper includes the following information:

The first section describes the motivation for and development of the NRC's LIC-504 process. The second section of this paper summarizes the approach, results, risk-informed insights, and observations obtained by comparing estimated risks for two reference U.S. NPPs) via the LIC-504 process. In the third section the NRC LIC-504 team's approach, results, risk-informed insights, and observation obtained by reviewing other HEAF related operating experience are summarized. A fourth section provides the regulatory processes that the LIC-504 team used to generate its risk-informed recommendations. The fifth section of the paper provides the recommendations developed by the LIC-504 team, and finally Conclusions are provided.

## **INCEPTION OF THE LIC-504 PROCESS**

The LIC-504 process grew out of a lesson learned initiative from a risk significant event that occurred at the Davis Besse NPP. Specifically, during an inspection of the control rod drive mechanism (CRDM) nozzles in February 2002 at the Davis Besse NPP, the licensee discovered significant degradation of the reactor pressure boundary [6]. Subsequent investigation revealed that a circumferential crack in one of the CRDM nozzles had led to leakage and boric acid corrosion that formed a cavity around the nozzle in the low-alloy steel portion of the reactor pressure vessel (RPV) head. This left only the stainless steel-clad material to maintain the reactor coolant pressure boundary over an area of approximately 16.5 square-inches.

The risk significance of this event was analysed under NRC's Accident Sequence Precursor (ASP) study program. The ASP program is described in more detail in below. The NRC staff estimated that the degraded condition that existed imposed an additional core damage probability ( $\Delta CDP$ ) of  $6 \times 10^{-3}$  during a one-year period. Since this value exceeded the ASP program "significant precursor" threshold (i.e., greater than or equal to

$1 \times 10^{-3} \Delta \text{CDP}$ ), this event was reportable in the NRC's annual Abnormal Occurrence Report [7]. Subsequently, the U.S. General Accounting Office (GAO) (now known as the Government Accountability Office), in 2004, documented its findings pertaining to the Davis Bessie event in its report GAO-04-415, entitled "Nuclear Regulation – NRC Needs to More Aggressively and Comprehensively Resolve Issues Related to the Davis-Besse Nuclear Power Plant's Shutdown" [8]. In the areas of risk evaluation, communication, and the decision-making process for determining if plant shutdown is warranted, the GAO made two recommendations:

1. Develop specific guidance and a well-defined process for deciding when to shut down a nuclear power plant. The guidance should clearly set out the process to be used, the safety related factors to be considered, the weight that should be assigned to each factor, and the standards for judging the quality of the evidence considered.
2. Improve the NRC's use of PRA estimates in decision-making by ensuring that the risk estimates, uncertainties, and assumptions made in developing the estimates are fully defined, documented, and communicated to NRC decisionmakers and provide guidance to decisionmakers on how to consider the relative importance, validity, and reliability of quantitative risk estimates in conjunction with other qualitative safety related factors.

In response to these recommendations, the NRC developed office instructions entitled "LIC-504, Integrated Risk-Informed Decision Making for Emergent Issues" [4] and "LIC-106: Issuance of Safety Orders" [9].

## **APPROACH, RESULTS, AND RISK-INFORMED INSIGHTS FROM THE ANALYSES OF TWO REFERENCE PLANTS**

This section summarizes the approach, results, and risk insights obtained from the quantitative risk analyses performed by the LIC-504 team with the assistance from the PRA practitioners at two reference plants. Details of these analyses are provided in Enclosure 1 to the NRC's LIC-504 Team Memorandum [10].

The staff secured the support of two licensees and selected two reference plants, including a Boiling Water Reactor 4 with a Mark I containment and a three-loop Pressurized Water Reactor (PWR) with a large dry containment. The use of these reference plants enabled the NRC staff to compare the estimated risks between the current NUREG/CR-6850 HEAF PRA methodology [3] and the new HEAF PRA methodology.

The staff noted that there was some variation in how each reference plant addressed HEAF modelling. For example, one reference plant credited post-Fukushima Daiichi FLEX strategies (diverse and flexible coping strategies) added to their facility in response to a NRC post-Fukushima order with regards to beyond-design-basis (BDB) external events EA-12-049 [12] in their PRA. The other reference plant did not. The reference plants also used different PRA methods and levels of refinement to develop the HEAF risk. The staff attributes this latter difference primarily to the different reference plant philosophies for evaluating fire risk; one reference plant exercised its model extensively to refine its fire risk, while the other plant concluded that a simpler level of detail was adequate to meet their intended objectives.

The LIC-504 team leveraged insights derived from the reference plants' HEAF PRA analyses to support the quantitative analysis. For example, the dominant sequences of the fire PRA HEAF scenarios were a key input that the staff used to select the areas for the plant walkdowns. The plant walkdowns enabled the LIC-504 team to determine how HEAF scenarios and associated frequencies could be modified to capture the changes related to the updated HEAF Fire PRA methodology. The walkdowns were instrumental in identifying which additional targets would be impacted and which could be eliminated.

The larger ZOIs for certain configurations associated with the updated HEAF PRA methodology expanded the number of targets in some areas. Whereas some ERFBS protected scenario targets in the HEAF ZOIs were eliminated, as they were previously assumed to fail according to the current NUREG/CR-6850 guidance.

Table 1 below summarizes the results for the two reference plants' base HEAF related risks using the current NUREG/CR-6850 guidance [3] versus the updated HEAF methodology.

**Table 1** Comparison of core damage frequency (CDF) and large early release frequency (LERF) using current versus new HEAF PRA guidance (all numbers are events/year)

| Description                  | CDF<br>(Updated<br>Method) | CDF<br>(Current<br>NUREG/CR<br>-6850<br>Method) | $\Delta$ CDF     | LERF<br>(Updated<br>method) | LERF<br>(Current<br>NUREG/CR<br>-6850<br>Method) | $\Delta$ LERF    |
|------------------------------|----------------------------|---|------------------|-----------------------------|--|------------------|
| <b>Reference Plant No. 1</b> |                            |   |                  |                             |  |                  |
| SWGR related                 | 1.7 E-06                   | 1.3E-05   | -1.1 E-05        | 3.9E-08                     | 3.5 E-07   | -3.2 E-07        |
| Bus Duct related             | 5.0 E-07                   | 4.6 E-07  | 4.5 E-08         | 3.6 E-08                    | 1.5 E-08   | 2.0 E -08        |
| <b>Total HEAF risk</b>       | <b>2.2 E-06</b>            | <b>1.4 E-05</b>                                 | <b>-1.1 E-05</b> | <b>7.5 E-08</b>             | <b>3.7 E-08</b>                                  | <b>-3.0 E 07</b> |
| <b>Reference Plant No. 2</b> |                            |   |                  |                             |  |                  |
| SWGR related                 | 8.7 E-07                   | 3.7 E-07  | 5.0 E-07         | 2.2 E-08                    | 1.2 E-08   | 9.2 E-09         |
| Bus duct related             | 3.3 E-05                   | 1.4 E-07  | 3.3 E-05         | 3.7 E-06                    | 7.4 E-09   | 3.7 E-06         |
| <b>Total HEAF risk</b>       | <b>3.4 E-05</b>            | <b>5.1 E-07</b>                                 | <b>3.4 E-05</b>  | <b>3.7 E-06</b>             | <b>1.9 E-08</b>                                  | <b>3.7 E-06</b>  |

For Reference Plant No. 1, the reduction in HEAF risk associated with the new method is largely driven by the reduction in switchgear related HEAF risks. The ability of the new method to credit protection from the ERFBS and the relatively small arc duration time for the reference plant (i.e., short electrical fault clearing time), which reduces the energy released from the HEAFs and, consequently reduces the ZOIs. For Reference Plant No. 2, the increase in HEAF risk is dominated by the estimated risk increases associated with the bus ducts due to increased ZOIs, and the potential for damaging additional targets.

To further refine the staff's perspective on the risk significance, several sensitivity studies were also performed. Details on these sensitivity studies are provided in [10], which led to risk-informed insights.

The risk-informed insights given below are based on the information obtained from the two reference plants. It is important to emphasize that since the HEAF related risks are highly plant specific, they may not be applicable to other plants. Also, as conveyed below, staff noted some increases as well as some decreases in risk when the new HEAF methodology was applied. However, it is important to note that based on the results of the overall staff's assessments, the staff concluded that there was no significant increase in total HEAF risk, warranting the need for any additional regulatory requirements.

- Application of the new methodology for bus duct HEAFs provided a significant increase in estimated risk in many, but not all, cases. The instances that showed significant increases in risk were attributed to larger ZOIs resulting from the new HEAF PRA methodology. The major difference between the new HEAF PRA methodology and the existing NUREG/CR-6850 Supplement 1 methodology is the assignment of larger ZOIs for long fault duration times. Thus, the staff concludes that those plants

with relatively long fault clearing times, and consequently larger ZOIs for bus ducts, could experience a significant increase in risk due to HEAFs.

- Application of the updated HEAF methodology for switchgear HEAFs showed an increase in estimated risk for certain configurations. The change in risk from Reference Plant No. 2 is larger than that for Reference Plant No. 1. However, the staff performed a more simplified analysis for Reference Plant No. 2 relative to Reference Plant No. 1. Furthermore, the vertical ZOI above the switchgear for the new HEAF PRA methodology is always smaller than the value from NUREG/CR-6850 [3]. Additionally, the new methodology predicts fire damage from HEAF in a region near the cabinet (just above and in front of) not covered by NUREG/CR-6850. For plant configurations with additional targets in this region, the switchgear could see a significant increase in risk with the new PRA HEAF methodology. Additionally, in a few cases the ZOI other than the vertical ZOI increased in the new methodology. Finally, longer fault clearing times lead to multiple, simultaneous switchgear HEAF fires, which may expose additional cables to fire damage.
- The updated HEAF PRA methodology credits ERFBS for preventing damage to cables within the new ZOI of the bus ducts and switchgear, unlike NUREG/CR-6850 and its Supplement 1. The staff noted that the risk decrease for the switchgear in Reference Plant No. 1 was primarily attributed to the credit given for ERFBS in the new methodology. Depending on the plant-specific configurations, fault clearing times, and risk profiles, application of the new methodology, including credit for preventing damage by ERFBS, may result in an estimated risk reduction.
- The changes in risk from the application of the updated HEAF method in Reference Plant No. 2, including the sensitivities, were generally larger than those for Reference Plant No. 1. Reference Plant No. 2 had rooms with larger amounts of cabling that were more sensitive to effects from HEAFs. Because HEAF risk, as in general for fire risk, is configuration dependent, this resulted in larger risk impacts for Reference Plant No. 2. As demonstrated by the sensitivities from Reference Plant No. 2 for the switchgear, protecting important cabling from fire damage is important to mitigate fire risk.
- A review of HEAF scenarios from the two reference plants provided additional risk-informed insights that could assist licensees in reducing their HEAF risks. Specifically, the team noted that a significant fraction of HEAF related risks were associated with only a handful of HEAF scenarios while reviewing HEAF scenarios included in their PRAs both plants. Since significant fractions of the HEAF related risk is distributed among a very small number of HEAF scenarios, it may be possible to use these scenarios to identify the subset of components that dominate the HEAF risks and focus maintenance or other related resources on that subset.

## **APPROACH, RESULTS, AND INSIGHTS FROM OTHER SOURCES OF OPERATING EXPERIENCE**

The NRC staff reviewed information from several other operating experience sources to obtain qualitative observations related to HEAF events. Each of the events reviewed provided one or more observations relating to measures that a licensee may adopt to minimize the likelihood of HEAFs or to mitigate the consequences if a HEAF were to occur. Since the staff reviewed many events, there was the potential to generate and list a large number of observations. However, a lengthy list of observations might be too unwieldy and inhibit the readers' ability to bring focus on a handful of risk-informed insights. Therefore, the staff focused on the more risk significant issues.

## Risk-Informed Insights and Observations from the ASP Event and the Maanshan NPP Station Blackout Event

The NRC's ASP program evaluates potentially risk significant events and degraded conditions that occur at NPPs. To assess the risk significance of events, the ASP uses conditional core damage probability (CCDP). To assess the risk significance of degraded conditions that exist for a specific exposure time, the ASP program uses the change in core damage probability ( $\Delta$ CDP). Events or degraded conditions for which CCDP or  $\Delta$ CDP exceed a set threshold are identified as precursors and saved in the ASP database. Irrespective of the metric used, events documented in the ASP Program provide a basis to identify the subset of risk significant HEAF events, and consequently, to generate risk-informed insights. Therefore, HEAF events or degraded conditions associated with HEAFs in the ASP database can be characterized as the subset of HEAF events that had the highest impact on safety.

Enclosure 2 of the LIC-504 memorandum [10] provides details of nine HEAF events in the ASP database as well as the 2001 Maanshan NPP HEAF event that were risk significant enough to be characterized as accident sequence precursors [11]. The staff added the 2001 Maanshan NPP event to the mix of the ASP database events because (1) the Maanshan NPP design (a power plant with two Westinghouse three loop PWRs) is similar to a number of U.S. plant designs, (2) the event constitutes the most risk significant HEAF event (highest estimated CCDP) and as such has the potential to be a rich source of risk-insights, and (3) an ASP-like analysis had been performed on the Maanshan NPP event.

Details on the HEAF event that occurred at Maanshan, Unit 1 in 2001 are provided in [11] which describes several significant HEAF events that occurred between 1986 and 2001. In summary, a fire started as the result of a fault in the safety related 4 kV switchgear supply circuit breaker. The initial fault caused explosions, arcing, smoke, and ionized gases, which propagated to adjacent safety related 4 kV switchgear and damaged six switchgear compartments. The damage resulted in the complete loss of the faulted safety bus and its emergency diesel generator (EDG) and a loss of offsite power (LOOP) to the undamaged safety bus because of faulting of its offsite electrical feeder circuit. An independent failure of the redundant EDG resulted in a loss of all alternating current (AC) power. Smoke hindered access to equipment, delaying the investigation and repair of the failures. The station blackout (SBO) was terminated after about two hours when an alternate AC EDG was started and connected to the undamaged safety bus. This event prompted the following risk-informed insight:

- HEAFs that can lead to SBOs are likely to initiate at buses or switchgear that are essential to supply AC power from both offsite power and emergency diesels (or another emergency supply). Resources focused to minimize the likelihood of HEAF occurrence at those switchgear and buses (e.g., improved preventive and predictive electrical maintenance) can reduce HEAF related risks. Measures taken to minimize the possibility of a HEAF at one emergency bus, causing failure of the redundant electrical train due to consequential failures (e.g., due to smoke, or design deficiencies), will also minimize the SBO related HEAF risks.

The plant impacts associated with the ten events identified in the Enclosure 2 of the HEAF LIC-504 memorandum [10] which documents nine ASP events and the Maanshan event included full or partial LOOP events, and the loss of a single 4 kV emergency bus. These events, in conjunction with other consequential failures have the potential to lead to SBO events such as that at Maanshan. Therefore, plant features that could mitigate SBOs can be used to further mitigate SBO related HEAF risks. In light of that, the LIC-504 team offered the following risk-informed insight:

- In general, HEAFs leading to SBOs constitute the highest HEAF related risks. Plant design and operational changes that have been adopted to enhance the mitigation of BDB accidents order [12] are likely to reduce HEAF related risks.

In addition to the risk-informed insights, based on review of the ASP events, the LIC-504 team offered the following additional observations:

- Of the nine events screened into the ASP database, eight events occurred in high- or medium-voltage equipment. The other event occurred at a 480 V load center.
- The staff investigated whether there were predominant root causes of the HEAFs that appeared in the ASP database. The root causes varied: four of the events occurred because of inadequate maintenance {two due to presence of foreign material (carbon fiber, aluminum debris), two events occurred due to other unspecified inadequate maintenance practices}; and other causes included deficient design controls, water intrusion, random failures, and faulty protective relay coordination.
- Low voltage (480 V or less) components cannot be screened out as negligibly risk significant. Particularly, HEAFs at low voltage load centers can lead to moderately risk significant events unless the systems are designed to prevent long duration arcing.
- Ingestion of dust or any other material to bus ducts creates the potential for multiple concurrent HEAFs.

To assess the risk of HEAF events in a more generic manner, the staff used a subset of the nine ASP events, and outputs of the NRC's suite of Standard Plant Analysis Risk (SPAR) models to develop a HEAF related average core damage frequency (CDF) for U.S. NPPs. The estimate is based on the frequency of risk significant ASP events multiplied by a suitably bounding CCDP. That estimate, however, is simply an approximation, and is not representative of HEAF related risks at any U.S. NPP since HEAF risks are highly plant specific. Further, as illustrated by the HEAF operating experience, the plant and operator response to the HEAF event can lead to other failures and conditions that are unrelated to the initial HEAF and are difficult to capture in a risk assessment. However, this approximation approach provides some insights regarding the relative magnitude of HEAF related risks in a general sense.

Of the nine ASP events, six occurred between 2010 and 2021. One occurred between 2000 and 2009 and two occurred before 2000. There could be a variety of possible explanations for this, including under-reporting of HEAF events before 2010 or changes in the ASP risk assessment process over time. Although the staff did not investigate the reason for this trend, the staff is confident that risk significant HEAF events occurring since 2010 have been appropriately captured in the ASP database. Therefore, to prevent inappropriate biasing of the risk significant HEAF event frequency, the staff assumed operating experience of the last twelve years is most representative of the current risk. That assumption yields 6 events over approximately 1200 reactor years (or  $\sim 5 \times 10^{-3}$  events/year).

The staff noted that the ASP HEAF events led to a variety of initiating events, including transients (reactor or turbine generator trips), LOOPS, or loss of a vital emergency AC power bus. Based on a review of SPAR model results, the most limiting CCDP for these initiating events is associated with a loss of a vital AC bus with a CCDP value of  $\sim 1 \times 10^{-3}$  (representing a 95 % upper bound value for all SPAR model results). The SPAR model CCDP results for transients and LOOPS were all below a CCDP value of  $1 \times 10^{-3}$ . Based on these estimates, the staff concluded that a reasonably bounding average HEAF NPP CDF value, based on ASP events, is approximately  $5 \times 10^{-6}$  per reactor year. This value is generally considered to be a small risk impact, compared to the NRC's safety goals [13], but constitutes a non-negligible fraction of the risk. Furthermore, on a plant-specific

basis, HEAFs may contribute to a substantial fraction of the fire risk. As mentioned earlier, the HEAF related risk is highly plant specific. For instance, for Reference Plant No. 1, the HEAF related CDF was about  $2 \times 10^{-6}$  per reactor year.

For Reference Plant No. 2, the HEAF related CDF was about  $3 \times 10^{-5}$  per reactor year. However, the Fire PRA associated with Reference Plant No. 2 included several more challenging fire scenarios and used a more simplified and bounding modelling approach compared to Plant No. 1.

### **Summary of Risk-Informed Insights from EPRI 3002015459**

In March 2019, EPRI published a report entitled “Critical Maintenance Insights on Preventing HEAFs” [14]. The Executive Summary of that report noted that HEAFs can occur, and when combined with latent protective device or switchgear issues, could escalate, and cause significant equipment damage and impact to the licensee’s capability to generate electrical power at the NPP. The Executive Summary also noted that (1) an analysis of industry data demonstrated that an effective preventive maintenance program is important in minimizing the likelihood and severity of HEAF events, (2) 64% of HEAF events were considered preventable, and (3) the most prevalent cause of failure due to HEAFs was inadequate maintenance.

The report examined four types of electrical equipment: circuit breakers/switchgear, bus ducts, protective relays, and cables. In addition to discussing the general importance of maintenance, the report provided insights on circuit breakers/switchgear. The staff characterizes two key findings of the EPRI report as “risk-informed insights” because these insights are focused on a subset of components that are likely to be of relatively high-risk significance. These two risk-informed insights from the EPRI report are provided below:

- With respect to circuit breakers, the report noted that maintenance of the Unit Auxiliary Transformer (UAT) breaker is particularly important because its failure can lead to an extended duration generator-fed fault at the first switchgear bus. Operating experience has shown this breaker to fail during automatic bus transfers. The report acknowledged the challenges that licensees confront in performing preventive maintenance due to constraints associated with outage schedules and offered risk-informed guidance so that licensees may focus their maintenance on the risk critical subset of maintenance activities.
- With respect to switchgear, the report noted that for critical switchgear, such as feeder circuit breakers that carry higher currents and switchgear that is part of a bus transfer scheme, proper maintenance of connections on both the bus duct side and the circuit breaker side is especially important.

### **Observations from the OECD/NEA HEAF Fire Events Report**

The staff reviewed the OECD/NEA report on HEAF fire events from 2013 [1] detailing 48 HEAF events, eleven of which occurred in the U.S. The definition of HEAF events used by the NRC is narrower than that used in the OECD/NEA report. For example, the OECD/NEA report includes several HEAF events that took place within large transformers installed outdoors, which are not included in the NRC HEAF definition. The large number of events included in the OECD/NEA report generated several potential observations. Based on the review of the events from this report, the LIC-504 team identified the following observations relating to HEAF event prevention and mitigation:

### Equipment Side

- Proper maintenance practices: several HEAF events were attributed to poor, or lack of maintenance.
- Aging management for electrical components: some HEAF events were caused by age related degradation of protective components, for example of bus insulation.
- Post-maintenance testing and inspection to ensure as-left conditions: the root cause of some HEAF events was identified as components not being left in the correct condition post-maintenance.

### Operations Side

- Housekeeping to prevent dust and other foreign matter accumulation: the root cause of many events was identified as the build-up and presence of dust, debris, and other foreign material inside bus ducts or breaker enclosures.
- Identification and correction of existing design issues: the severity of many of the reported events was exacerbated by long-standing design errors or problems.
- Understanding of the electrical system and event conditions to prevent incorrect operator actions: the severity of some of the reported events was increased by operators taking incorrect actions or not understanding what the correct actions were.

## **APPROACH USED TO LIC-504 TEAM RECOMMENDATIONS**

Enclosure 3 of the HEAF LIC-504 memorandum [10] provides recommendations for NRC's senior management's consideration. Some of the guidance that the LIC-504 team used to generate their recommendations are included in the LIC-504 Office Instruction itself. For instance, Section 4.2.1 of the LIC-504 Office Instruction described when the NRC should consider issuing prompt regulatory requirements such as Orders to shutdown units based on risk insights. LIC-504 also provides guidance on the nature of generic communications to licensees that NRC should consider based on risk significance. The LIC-504 team considers other NRC guidance documents also to generate its recommendations such as:

- NRC's Management Directive (MD) 8.18 entitled "Generic Communications Program" [15] to further inform on whether NRC should consider issuing a Bulletin, a Generic Letter, a Regulatory Issue Summary, or an Information Notice to address the emerging issue;
- MD 6.3 entitled "Rulemaking Process" [16] and the associated guidance document NUREG/BR-0058 entitled, "Regulatory Analysis Guidelines of the U.S. Nuclear Regulatory Commission" [17] to determine whether the issue warrants the LIC-504 team to recommend new rulemaking (or modifying an existing rule).

In addition to the above, the LIC-504 team leveraged the "Teaching Element" of the NRC's "Be RiskSMART" framework [18]. In doing so, the LIC-504 team considered various types of communication venues that the NRC will leverage to convey the actions a licensee may consider to mitigate risks associated with the HEAFs.

## **LIC 504 TEAM RECOMMENDATIONS TO NRC MANAGEMENT**

The NRC's LIC-504 team considered and investigated a full range of potential options to recommend under the NRC's licensing, rulemaking, and oversight responsibilities. As conveyed above, the team noted some increases as well as some decreases in risk when the new HEAF methodology was applied; however, team concluded that there is

no significant increase in risk warranting additional regulatory requirements. In addition, the team evaluated various communication options to share its insights with licensees so they can implement effective steps to further reduce and/or mitigate HEAF risks. The final management-endorsed recommendations are provided below:

- Issue an Information Notice (IN) to share information on (1) the operating experience and risk insights from the LIC-504 assessment, (2) regulatory framework/license conditions, and (3) the availability of the new HEAF risk assessment methodology for licensee consideration.
- Incorporate risk insights obtained from the LIC-504 assessment to inform NRR's on-going PRA configuration control initiative.
- Consider incorporating risk insights obtained from the LIC-504 assessment to inform NRR's Reactor Oversight Process.
- Communicate risk insights gleaned from the HEAF related risks / LIC-504 process with regional inspectors and senior reactor analysts.
- Share risk insights gained from the HEAF LIC-504 analysis with external stakeholders via public meetings (e.g., workshops), participation at owners group meetings, and communications at national and international forums.

## **CONCLUSIONS**

The NRC has successfully developed a process to address safety issues that emerge as a result of world-wide nuclear power plant operating experiences in an efficient and effective manner. NRR developed an Office Instruction entitled, "LIC-504, Integrated Risk-Informed Decisionmaking for Emergent Issues" that describes this process, which enables NRC staff to use best available information to assess risk (quantitative or qualitative), defence-in-depth, and safety margins. This process allows for the NRC to disposition issues in a timely manner, consistent with risk-informed decision-making principles.

## **ACKNOWLEDGEMENTS**

The significant contributions made by the following staff members of the NRC's HEAF LIC-504 team were instrumental in the author's ability to prepare this paper: Kevin Coyne, J. S. Hyslop, Nicholas Melly, Charles Moulton, Reinaldo Rodriguez, Ching Ng, Siva Lingam, and Gabriel Taylor.

## **REFERENCES**

- [1] Organisation for Economic Co-operation and Development (OECD) Nuclear Energy Agency (NEA), Committee on the Safety of Nuclear Installations (CSNI): OECD FIRE Project – Topical Report No. 1, Analysis of High Energy Arcing Fault (HEAF) Fire Events, NEA/CSNI/R(2013)6, Paris, France, June 2013, <http://www.oecd-nea.org/documents/2013/sin/csni-r2013-6.pdf>.
- [2] United States Nuclear Regulatory Commission (U.S. NRC): US Code of Federal Regulations, Part 10 CFR 50.48(c) "National Fire Protection Association Standard NFPA805", Federal Register 65 FR 38190, June 20, 2000; 69 FR 33550, June 16, 2004; 72 FR 49495, August 28, 2007.

- [3] United States Nuclear Regulatory Commission (U.S. NRC) Office of Nuclear Regulatory Research (RES) and Electric Power Research Institute (EPRI): Fire PRA Methodology for Nuclear Power Facilities, Final Report, Volume 2: Detailed Methodology, Appendix M, EPRI/NRC-RES, NUREG/CR-6850 (EPRI 10191989), Washington, DC, and Palo Alto, CA, USA, 2010, <https://www.nrc.gov/reading-rm/doc-collections/nuregs/contract/cr6850/index.html>.
- [4] United States Nuclear Regulatory Commission (U.S. NRC) Office of Nuclear Regulatory Regulation (NRR): Integrated Risk-Informed Decisionmaking for Emergent Issues, U.S. NRC's NRR Office Instruction LIC-504, Revision 5, Washington, DC, USA, March 9, 2020, <https://www.nrc.gov/docs/ML19253D401.pdf>.
- [5] United States Nuclear Regulatory Commission (U.S. NRC): High Energy Arcing Fault Frequency and Consequence Modelling, Draft Report for Comment, NUREG-2262, Washington, DC, USA, July 2022, <https://www.nrc.gov/docs/ML2215/ML22158A071.pdf>.
- [6] United States Nuclear Regulatory Commission (U.S. NRC): Reactor Coolant System Pressure Boundary Leakage Due to Primary Water Stress Corrosion Cracking of Control Rod Drive Mechanism Nozzles and Reactor Pressure Vessel Head Degradation, LER 50-346/02-002-00, Washington; DC, USA; April 29, 2002, <https://www.nrc.gov/docs/ML2011/ML20112F488.pdf>.
- [7] Federal Register (FR): Report to Congress on Abnormal Occurrences, 68 FR 19233, Fiscal Year 2002, Dissemination of Information, April 18, 2003, <https://casetext.com/federal-register/report-to-congress-on-abnormal-occurrences-fiscal-year-2002-dissemination-of-information>.
- [8] U.S. General Accounting Office (GAO): Report to Congressional Requesters, Nuclear Regulation – NRC Needs to More Aggressively and Comprehensively Resolve Issues Related to the Davis-Besse Nuclear Power Plant's Shutdown, GAO-04-415, May 2004, <http://www.gao.gov/cgi-bin/getrpt?GAO-04-415>.
- [9] United States Nuclear Regulatory Commission (U.S. NRC) Office of Nuclear Regulatory Regulation (NRR): Issuance of Safety Orders Issues, U.S. NRC's NRR Office Instruction LIC-106, Revision 1 (NRC ADAMS Accession No. ML19283B565), Washington, DC, USA, April 23, 2020.
- [10] United States Nuclear Regulatory Commission (U.S. NRC): NRC High Energy Arcing Faults LIC-504 Team Recommendations, (Memorandum: ADAMS Accession No. ML22201A000, Enclosure 1: ADAMS Accession No. ML22201A001, Enclosure 2: ADAMS Accession No ML22201A002, Enclosure 3: ADAMS Accession No. ML22201A003), Washington, DC, USA, July 27, 2022, <https://www.nrc.gov/docs/ML2220/ML22200A272.html>.
- [11] Raughley, W. S., and G. F. Lanik: Operating Experience Assessment, Energetic Faults in 4.16 kV to 13.8 kV Switchgear and Bus Ducts That Caused Fires in Nuclear Power Plants, 1986-2001, United States Nuclear Regulatory Commission (U.S. NRC), Washington, DC, USA, February 2002, <https://www.nrc.gov/docs/ML0212/ML021290358.pdf>.
- [12] United States Nuclear Regulatory Commission (U.S. NRC): Issuance of Order to Modify Licenses with Regard to Modify Licenses with Regards to Beyond-Design-Basis External Events, EA-12-049, Washington, DC, USA, March 12, 2012, <https://www.nrc.gov/docs/ML1205/ML12054A735.pdf>.
- [13] Federal Register (FR): Safety Goals for the Operation of Nuclear Power Plants; Policy Statement, 51 FR 30028, Republication, August 21, 1986, <https://www.nrc.gov/reading-rm/doc-collections/commission/policy/51fr30028.pdf>.

- [14] Electric Power Research Institute (EPRI): Critical Maintenance Insights on Preventing High-Energy Arcing Faults, EPRI 3002015459, Palo Alto, CA, USA, March 2019, <https://www.epri.com/research/products/000000003002015459>.
- [15] United States Nuclear Regulatory Commission (U.S. NRC): Generic Communication Program, U.S. Nuclear Regulatory Commission Management Directive MD 8.18, Volume 8: Licensee Oversight Programs, Washington, DC, USA, December 9, 2015, <https://www.nrc.gov/docs/ML1532/ML15327A372.pdf>.
- [16] United States Nuclear Regulatory Commission (U.S. NRC): The Rule Making Process, U.S. Nuclear Regulatory Commission Management Directive MD 6.3, Volume 6: Internal Management, Washington, DC, USA, July 3, 2019, <https://www.nrc.gov/docs/ML1921/ML19211D136.pdf>.
- [17] United States Nuclear Regulatory Commission (U.S. NRC): Regulatory Analysis Guidelines of the U.S. Nuclear Regulatory Commission, Draft Report for Comment, NUREG/BR-0058, Revision 5 (NRC ADAMS Accession No. ML171001480), Washington, DC, USA, April 2017, <https://www.nrc.gov/reading-rm/doc-collections/nuregs/brochures/br0058/index.html>.
- [18] United States Nuclear Regulatory Commission (U.S. NRC): Be riskSMART: Guidance for Integrating Risk Insights into NRC Decisions, NUREG/KM-0016, Washington, DC, USA, March 2021, <https://www.nrc.gov/reading-rm/doc-collections/nuregs/knowledge/km0016/index.html>.

# Fire Modelling Automation and Visualization in the Context of Fire Probabilistic Risk Analysis for Nuclear Plants

Ramprasad Sampath<sup>1\*</sup>, Steven Prescott<sup>2</sup>, Robby Christian<sup>2</sup>

<sup>1</sup> CENTROID LAB, Los Angeles, CA, United States of America

<sup>2</sup> Idaho National Laboratory (INL), Idaho Falls, ID, United States of America

## ABSTRACT

Internal fires are a dominant hazard contributing to the overall risk for a given nuclear power plant (NPP), potentially leading to core damage and/or a release of radioactive materials into the environment. In this respect, fire probabilistic risk assessment (PRA) has been developed to support the decision-making of NPP operators and regulators. However, in practice, conducting a fire PRA has turned into a complex, disjoint, costly, and time-consuming process requiring the use of many different data, methods, and tools (plant databases, basic and advanced fire modelling, event tree/fault tree analysis, etc.).

The Fire Risk Investigation in 3D (FRI3D) software was developed as part of the research for enhanced fire analysis under the Risk-Informed Systems Analysis Pathway of the Light Water Reactor Sustainability Program. The initial goals of this software had two parts: (1) to provide industry with a tool to simplify the process for developing and using detailed fire models and (2) to provide a backend platform for future enhanced fire analysis research. This paper focuses on the first goal and the methods used to simplify fire modelling and the benefits from visualization.

Fire models are constructed using various tools and methods. Several analytical methods are used in conjunction with fire zone models and computational fluid dynamics to calculate the various scenarios including cable and component failures. While these methods and tools have been shown to provide adequate results, they are costly to implement and are disconnected. The FRI3D software combines these tools and methods into a 3D environment with the ability to model and visualize scenarios rapidly, easily, and accurately. This integrated approach minimizes the risk of human error and reduces time by automating many of the tasks, then shows results that provide insights not easily seen in traditional processes.

The use of FRI3D by NPP operators, regulators and engineering consultancy firms is expected to lead to enhanced fire PRA, increased safety, efficient and expedient regulatory review, and reduced operating costs.

## INTRODUCTION

Fire Risk Investigation in 3D (FRI3D) software was developed over the last three years to integrate 3D spatial modelling with existing fire PRA models and fire simulation codes. The goal was to automate many of the manual tasks in fire analysis, thus reducing industry efforts in initial fire modelling and operational costs when evaluating a plant modification from the fire risk perspective. Previous research focused on coupling fire analysis codes and importing existing fire-PRA models. This work has shown success in importing existing plant data, using a fire database (FRANX by the Electric Power Research Institute (EPRI) [1]), matching the United States Nuclear Regulatory Commission (U.S. NRC) fire methods, including NUREG/CR-6850 [2] simulation results, and constructing an in-

dustry switchgear room [3], [4], [5]. The main focus of this paper is to highlight potential insights provided when directly coupling 3D simulation data and failure time results with the plant logic model.

## User Interface with Tool Integration

Detailed fire modelling of nuclear power plants (NPPs) requires many steps, tools, and calculations. By combining 3D visualization directly with the probabilistic risk assessment (PRA) data and fire calculations, FRI3D provides a single interface for developing and analysing fire models, while automating many steps. The user-friendly interface as shown in Figure 1 has five primary areas:

- Compartment/Scenario Editor (top left) – Displays all the items physically in the current compartment/scenario;
- Properties Editor (bottom left) – Shows the properties for the selected item and allows the user to edit them;
- 3D View (center) – Allows for modelling and viewing the spatial relationships, along with fire simulation results;
- FRANX or Logic View (right side) – Shows the logical mapping of raceways, cables, components, and PRA basic events;
- Timeline – Displays the timing results from fire simulation and failure calculations (i.e., when items fail).

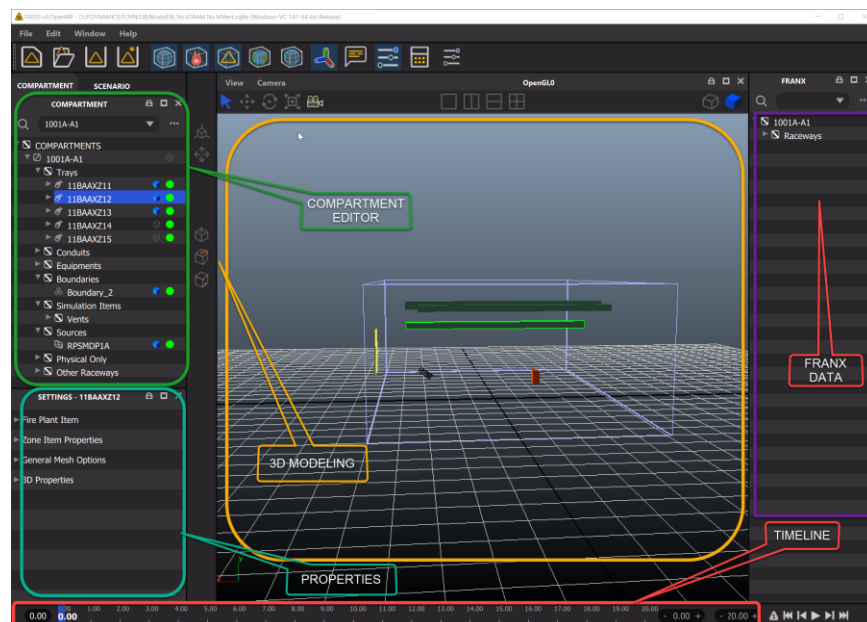


**Figure 1** FRI3D graphical user interface layout with data areas labelled

The user interface provides an easy process to find and view a compartment or specific scenario. After loading a desired compartment or scenario, items are categorized so the user can easily find items and determine their properties and location in the compartment. The 3D modelling and visualization shown in orange in Figure 1 allow the user to easily model the spatial relationships by the drag-and-drop components from the left side component list into the 3D area then correctly position it. Selecting components in one area highlights the component in the other area. The primary goals of the FRI3D interface are to make it easy to perform the following:

- Import the existing FRANX (Fire Database) [1] or PDMS (Plant Database) [6] mapping or plant logic and component models;
- Model, display, and link 3D spatial models to the imported data;
- Auto-generate fire scenarios from user-specified fire sources using industry fire simulation codes and methods;
- Visualize scenario results to show when items fail and fire progression;
- Output and calculate the scenario information using industry PRA tools.

Menu options and automated process make it easy and seamless to run the many fire tools and calculation methods currently used by industry. The following tools or calculations have been built into or coupled with FRI3D:

- Data import – FRANX [1], customized PDMS [6];
- NRC fire calculations – FLASH-CAT [7], Heat Soak [8], THIEF [9];
- National Institute of Standards and Technology (NIST) Fire simulation codes – CFAST [10], (FDS [11] in development);
- PRA tools – CAFTA [12], SAPHIRE [13], (RiskSpectrum® [14] coming soon).

## SCENARIO AUTOMATION

The key automation feature of FRI3D is auto generating scenarios. The basics of a typical detailed fire analysis are outlined below. First, each fire source in a compartment is identified with each having different heat release rates and probabilities. Then a zone of influence calculations and other NRC Fire Dynamics Tools (FDTs) [15] can be used to conservatively determine failed components. If trays are in the area for secondary combustibles, then the FLASH-CAT method [7] is used to determine if there is a fire which is spreading. If the FDTs are too conservative or secondary combustibles exist a fire simulation code is needed to provide more detail for that scenario. CFAST [10] can provide a quick two-layer heat model for the temperature in the hot gas layer. Measurement points can also be added at specific locations to include the addition of radiant heat. If CFAST is not suitable for the scenario, then a full computational fluid dynamics code such as FDS is needed. This data can then be used in a general tray calculation (Heat Soak [8]) to see if all cables in a tray fail. If failing all the cables causes a large conservative risk value, then an individual cable calculation can be made using the THIEF model [9]. Using the cable failures, a cable tracing model is used to determine specific component or PRA Basic Event failures. All failures from the fire are combined along with the ignition frequency, non-suppression probability, and severity factor to make a scenario in the PRA model. This is done for each fire source.

Performing these steps, calculations, and then manually transferring data between areas takes significant effort and is error prone without a good validation process. The automated process developed for FRI3D simplifies many of the steps and programmatically moves data between the calculations and applications. However, the user still needs to gather data, such as sources, heat release rate (HRR) info, and a cable tracing. Also, a 3D model of the compartment also needs to be created in FRI3D.

The following steps outline the automated steps FRI3D performs when generating a scenario as shown in Figure 2:

1. Construct a fire simulation model – FRI3D constructs a CFAST model creating the vents, sources, and optimal measurement points for each item. FDTs are not used because the FRI3D model can be constructed, and more accurate CFAST results

generated in less time than performing FDT calculations. (Future options will include FDS.)

2. Secondary combustibles – If using CFAST use the results from step 1 and the FLASH-CAT calculation to determine any secondary combustibles. Re-run CFAST with additional HRR information.
3. Determine failures – Use the fire simulation model results for the measurement points to determine component and cable failures. If there is no specific cable information, it uses the Heat Soak calculation; if some cables have details, it will automatically use the more accurate THIEF calculation.
4. Component or basic event failures – The cable tracing or plant logic model is used to find all components linked to the failed cables and construct a list of all failed components for the scenario.
5. New scenario – The scenario is added to the FRI3D model for the current compartment; each failed item is shown along with when it fails and fire simulation compartment temperature results. Now the user can assign the ignition frequency, non-suppression probability, and severity factor for the scenario.
6. PRA results – The user can click the calculate button and select desired scenarios; these are added to the plants PRA model and solved.

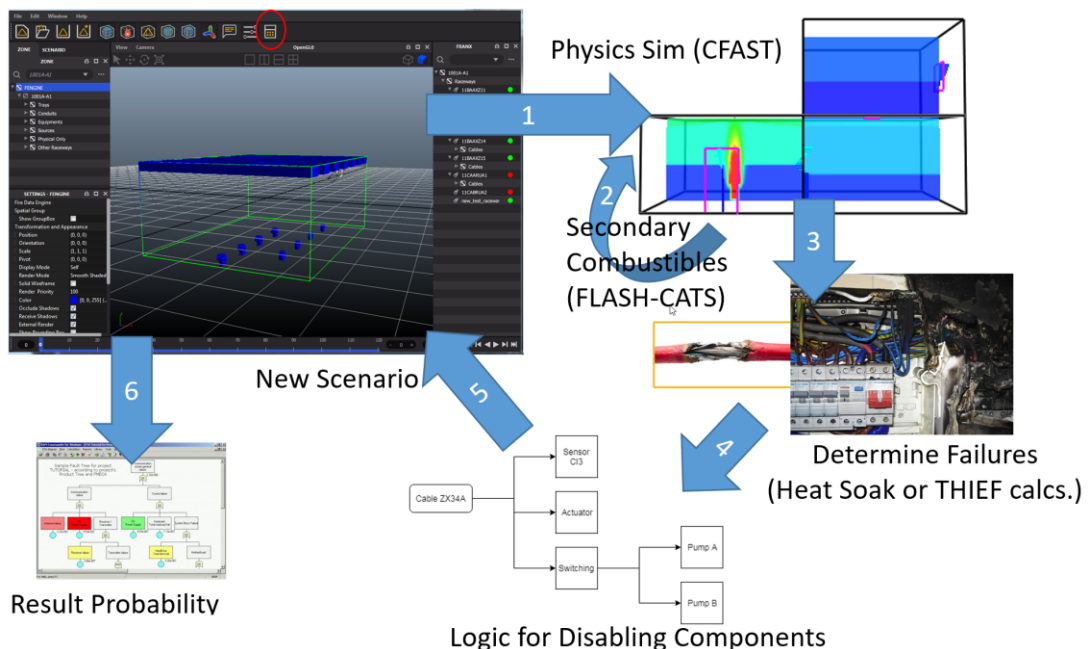


**Figure 2** Automated process for generating fire scenarios and viewing results in FRI3D

While automation requires a 3D model to be constructed for the compartment, research has shown that even with this time FRI3D can reduce time needed for detailed fire modelling scenarios by more than 50 % and significantly reduce time for regulatory fire reviews required for plant modification [9]. Testing was done using two NRC examples: Appendix A and B of NUREG-1934 [16] and an industry switchgear room (the same plant switch gear room used in this LiDAR scan research).

The 3D modelling area provides an easy way to model basic components in their correct locations. Architectural drawings or floorplans can be imported to simplify the modelling process. Even with significant time reductions, one of the major concerns by industry

was the need to make accurate 3D models of the fire compartment using architectural drawings and walkdown notes. In the further testing of FRI3D, some modelers had the LiDAR scan available as a virtual walkdown and measurement tool. This simplified some of the modelling tasks and eliminated the need for in-person inspections for those tests.

## RESULTS VISUALIZATION

Visualization of results is key to easily understanding what happens because of a fire. By being able to see temperatures, components, failures, and changes over time, analysts can see the effects of the scenario and identify importance, if there are errors, mitigation opportunities, and whether more detail is needed. Our research identified a few key areas for visualization and implemented them in FRI3D. The following sections outline those areas, and the insights they can provide.

## Scenario View Visualization

FRI3D's scenario and compartment inspectors list the various scenarios and compartments that can be viewed and simulated. While the compartment consists of all the items in the defined area, the scenario consists of the items that have failed for that specific scenario. Each scenario is associated with a certain compartment, and a compartment can have multiple scenarios.

Like the compartment inspector, the scenario inspector lists the various items appearing under the appropriate category and sub-category. *Cables* appear as a sub-category under *Trays* or *Conduits*. *Boundaries* and *Physical Only* items do not appear in the scenario inspector, as they do not affect the PRA logic. The default scenario or a manually created scenario view starts as full room burnup scenario in which all the items in the compartment have failed.

When in compartment view, all items in the compartment list as shown in Figure 3 (left). Green and red markers indicate items in the current scenario. By switching to the scenario tab as shown in Figure 3 (right), only the items for the scenario are shown in the list. In the 3D area, the failed scenario items are indicated with a red outline, and their temperatures are colour coded. The items which do not fail are outlined in white. When there are multiple fire scenarios for a compartment, they are listed in the interface dropdown, and the user can easily switch between them and the inspector which simultaneously updates the 3D area to reflect that scenario.

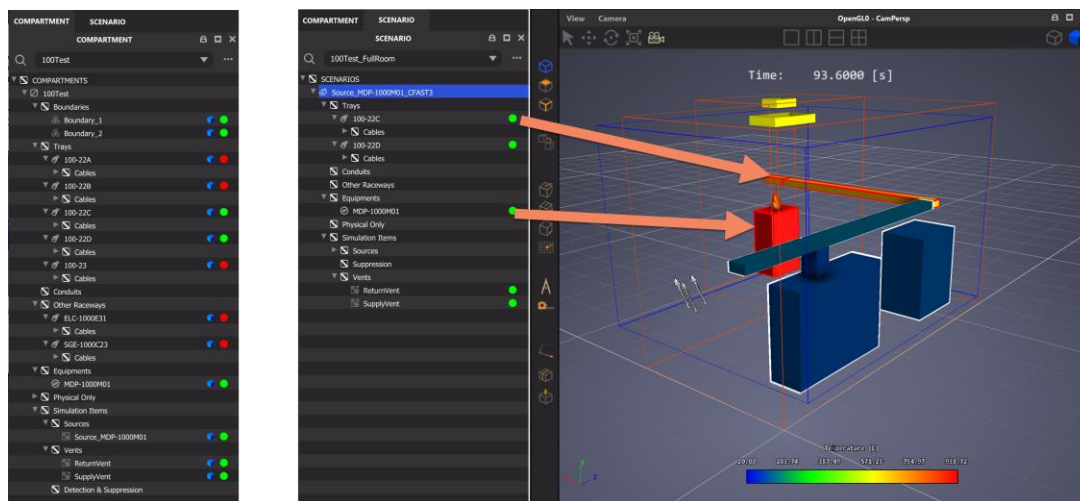


**Figure 3** *Compartment inspector (left), Scenario inspector with 3D area (right)*

## Failure Timeline

After a successful simulation, the results are displayed with colours as visual cues as well as item failures. The following picture indicates results of a simulation with the various failures indicated in the timeline (see Figure 4 below) with their appropriate times of failure.

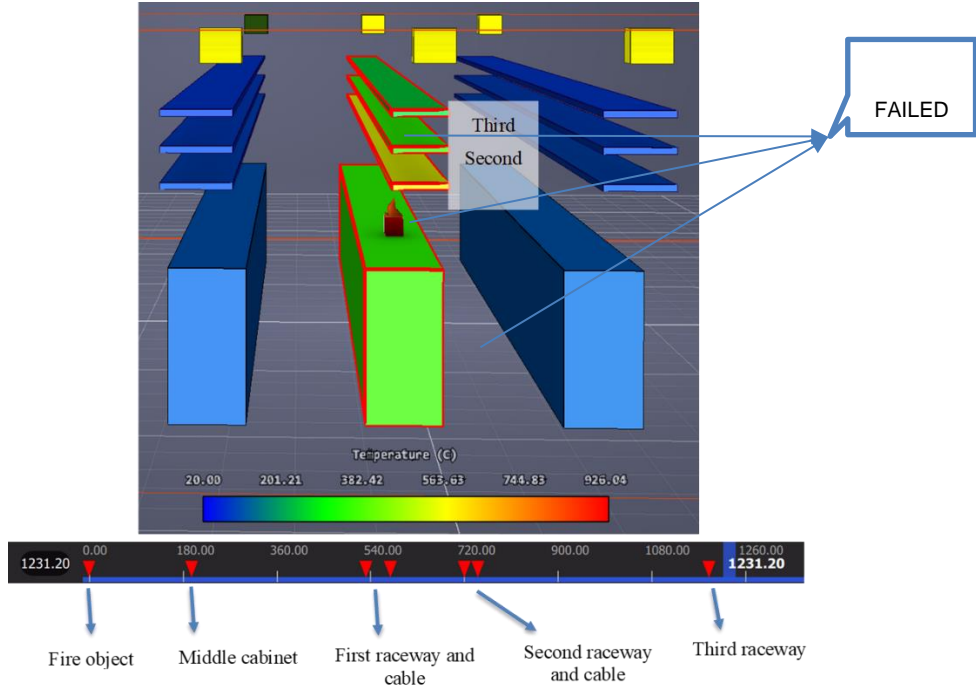


**Figure 4** Timeline indicating item failure times in the fire scenario

The failure timeline visualization can assist the fire modeler in two key areas. The first is non-suppression probability. In a typical fire PRA, fire suppression is not always credited because determining fire non-suppression probabilities requires additional analyses and advanced fire modelling. The two essential parameters required to calculate fire non-suppression probability are time for smoke detection and time to target damage. Simulations in FRI3D provide the necessary timing parameters, and these time values are linked to the visualization module of fire scenario progressing. This, for example, allows the user to quickly identify potential benefits of refining fire scenarios to take advantage of decreased non-suppression probability associated with given target sets and assign that value in the scenario instead of using 1.0.

The second key benefit from the timeline is it helps with visualizing how to break up scenarios according to the HRR severity factor bins. To explain the process, the HRR peak and distribution rates from NUREG/CR-6850 [1] are used (cf. Table 1), as severity factors are readily available from the tables in Appendix E. In practice, for fire scenarios where an electrical cabinet is an ignition source, a fire engineer would use HRR peak and distribution rates from NUREG/CR-2178, Tables 4-1 and 4-2 [8] to calculate severity factors. The fire scenario guidance did not change from NUREG/CR-6850 to the later NUREG/CR-2178. NUREG/CR-2178 provides refined (i.e., more realistic and less conservative) HRR peak and distribution rates for selecting ignition sources.

Let us assume that no components fail with a HRR from bin 1, but the first component fails using the HRR from bin 2. A conservative, time-saving approach would be for the fire analyst to just find the first bin where a component fails then use the most significant fire HRR; the severity would be 0.494 SF2, a sum of bin 2 through 15 severity factors.

However, let us assume that the same component fails for bins 2 to 11, but it is not as safety significant. Ideally you would want to make two scenarios: one with a severity factor of 0.489 SFR2 with the one component failure and the second with a severity factor of 0.005. This would greatly reduce the core damage contribution.

**Table 1** NUREG/CR-6850, Table E-3 from [1]

**Table E-3**  
Discretized Distribution for Case 2 Heat Release Rate (Vertical Cabinets with Qualified Cable, Fire in more than One Cable Bundle)

| Bin | Heat Release Rate – kW (Btu/s) |             |             | Severity Factor (P <sub>i</sub> ) |
|-----|--------------------------------|-------------|-------------|-----------------------------------|
|     | Lower                          | Upper       | Point Value |                                   |
| 1   | 0 (0)                          | 90 (85)     | 34 (32.7)   | 0.506                             |
| 2   | 90 (85)                        | 179 (170)   | 130 (123)   | 0.202                             |
| 3   | 179 (170)                      | 269 (255)   | 221 (209)   | 0.113                             |
| 4   | 269 (255)                      | 359 (340)   | 310 (294)   | 0.067                             |
| 5   | 359 (340)                      | 448 (425)   | 400 (379)   | 0.041                             |
| 6   | 448 (425)                      | 538 (510)   | 490 (464)   | 0.026                             |
| 7   | 538 (510)                      | 628 (595)   | 579 (549)   | 0.016                             |
| 8   | 628 (595)                      | 717 (680)   | 669 (634)   | 0.010                             |
| 9   | 717 (680)                      | 807 (765)   | 759 (719)   | 0.006                             |
| 10  | 807 (765)                      | 897 (850)   | 848 (804)   | 0.004                             |
| 11  | 897 (850)                      | 986 (935)   | 938 (889)   | 0.003                             |
| 12  | 986 (935)                      | 1076 (1020) | 1028 (974)  | 0.002                             |
| 13  | 1076 (1020)                    | 1166 (1105) | 1118 (1060) | 0.001                             |
| 14  | 1166 (1105)                    | 1255 (1190) | 1208 (1145) | 0.001                             |
| 15  | 1255 (1190)                    | Infinity    | 1462 (1386) | 0.001                             |

Using FRI3D, the user can assign the most significant HRR and see which components fail and how quickly. This would allow them to visualize the best binning groups and know if further detail is needed. For example, in Figure 5 we can see that two or three groupings (orange or yellow) could be used as the user can easily select less severe HRRs, run the scenario, and find the tipping points. Future versions of FRI3D could include an automated method to find optimal grouping points.



**Figure 5** Example item failure timeline showing possible two or three severity factor binning options

## Fire Simulation

FRI3D initially supports simulation by a zone model (CFAST [10]) with a fully 3D computational fluid dynamics (CFD) model, FDS simulation, in progress. In a two-zone model, the lower gas layer and the upper gas layer temperatures are colour coded in the 3D visualization window as soon as the simulation completes (see Figure 6). An on-screen display is also shown, indicating the mapping between the colours and the temperatures. A fully 3D CFD simulation showing the resulting temperatures over the whole 3D domain is also in progress.

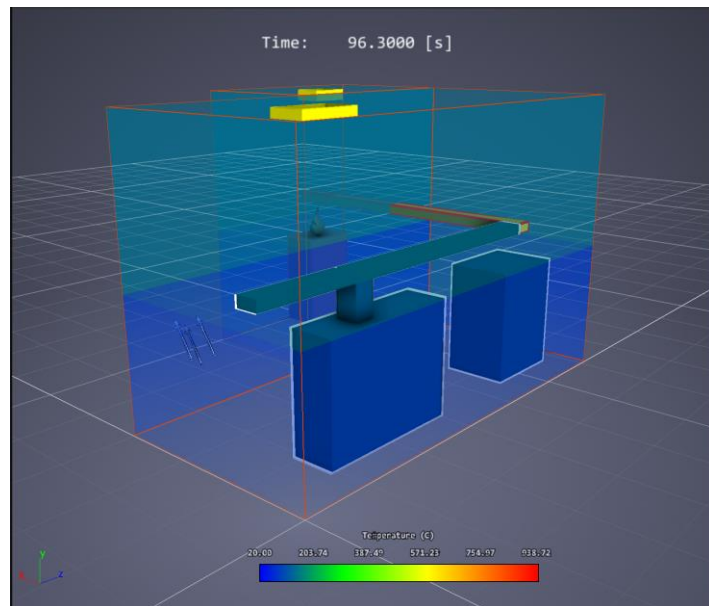


**Figure 6** Fire heat layers and temperatures

The progression of temperatures on the various components which take part in the simulation is also displayed. As the user adjusts the time, the temperatures of each component, shown by the colour, adjusts according to the heat scale, as shown in Figure 7.

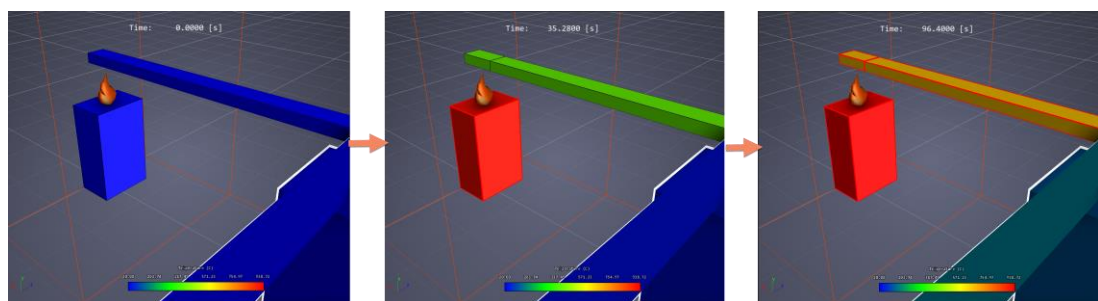


**Figure 7** Progression of component temperature

There are many benefits to visualizing the fire simulation results in FRI3D. A key one is being able to see the fire progression and qualitatively verify that it is as expected. Errors in the model such as venting issues or other incorrect simulation parameters can often be identified. By showing component failures and temperatures over time, the modeler can visualize and identify key items to add shielding or other simple modifications that could eliminate large risk contributions. Additionally, when making plant modifications, the user can easily determine good locations for equipment and cables.

## CONCLUSIONS

The Idaho National Laboratory in collaboration with CENTROID LAB has successfully developed a platform to simplify and automate many aspects of detailed fire modelling. This automation significantly reduces the time needed to develop fire models. Visualization features such as item temperature over time, heat layers, and failure times on a timeline can significantly help the user understand the fire scenario and reduce modelling errors. The timeline of failures and the ease of generating scenarios enables modelers to split scenarios into bins and reduce unnecessary conservatism. By including 3D visualization and software automation for generating scenarios in fire PRA, nuclear power facilities can make detailed fire modelling more cost effective.

## REFERENCES

- [1] Electric Power Research Institute (EPRI): FRANX v4.3, software, Product ID 3002002729, Palo Alto, CA, USA, November 6, 2015, <https://www.epri.com/research/products/3002000098>.
- [2] Nowlen, S. P., et al.: EPRI/NRC-RES Fire PRA Methodology for Nuclear Power Facilities, Volume 2: Detailed Methodology, NUREG/CR-6850, EPRI 1011989, Electric Power Research Institute (EPRI), Palo Alto, CA, USA, and United States Nuclear Regulatory Commission (U.S. NRC) Office of Nuclear Regulatory Research, Washington, DC, USA, September 2005, <https://www.nrc.gov/reading-rm/doc-collections/nuregs/contract/cr6850/v2/cr6850v2.pdf>.
- [3] Prescott, S., et al.: Fire Risk Investigation in 3D (FRI3D) Software and Process for Integrated Fire Modeling, INL/EXT-20-59506, Idaho National Laboratory (INL), Idaho Falls, ID, USA, 2020, [https://lwns.inl.gov/RiskInformedSafetyMarginCharacterization/FRI3D\\_Tools\\_Methods\\_Demo.pdf](https://lwns.inl.gov/RiskInformedSafetyMarginCharacterization/FRI3D_Tools_Methods_Demo.pdf).
- [4] Prescott, S., et al.: Industry Level Integrated Fire Modeling Using Fire Risk Investigation in 3D (FRI3D), INL/EXT-21-604079, Idaho National Laboratory, Idaho Falls, ID, USA, 2021, <https://lwns.inl.gov/RiskInformedSafetyMarginCharacterization/IndustryLevelIntegratedFireModelingUsingFRI3D.pdf>.
- [5] Prescott, S., et al.: Visualization and Automation of Fire Modeling Using Fire Risk Investigation in 3D (FRI3D), in: Proceedings of ANS PSA 2021 International Topical Meeting on Probabilistic Safety Assessment and Analysis, Columbus, OH, USA, November 7 – 11, 2021, on CD-ROM, American Nuclear Society, LaGrange Park, IL, USA, November 2021.
- [6] Gryphon Investors: JENSEN HUGHES Acquires Cygna Energy Services, Baltimore, MD, USA, November 1, 2017, <https://www.gryphon-inv.com/news-article/jensen-hughes-acquires-cygna-energy-services/>.

- [7] McGrattan, K., et al.: Cable Heat Release, Ignition, and Spread in Tray Installations During Fire (CHRISTIFIRE) Phase 1: Horizontal Trays, NUREG/CR-7010, Volume 1, United States Nuclear Regulatory Commission (U.S. NRC) Office of Nuclear Regulatory Research, Washington, DC, USA, July 2012, <https://www.nrc.gov/reading-rm/doc-collections/nuregs/contract/cr7010/v1/index.html>.
- [8] Salley, M. H., and A. Lindeman: Refining and Characterizing Heat Release Rates from Electrical Enclosures During Fire, Volume 2: Fire Modeling Guidance for Electrical Cabinets, Electric Motors, Indoor Dry Transformers, and the Main Control Board, NUREG-2178, Vol. 2, and EPRI 3002016052, United States Nuclear Regulatory Commission (U.S. NRC) Office of Nuclear Regulatory Research, Washington, DC, USA, 2020, <https://www.nrc.gov/docs/ML2016/ML20168A655.pdf>.
- [9] McGrattan, K. B.: Cable Response to Live Fire (CAROLFIRE) Volume 3: Thermally-Induced Electrical Failure (THIEF) Model, NUREG/CR-6931, Vol. 3 and NISTIR 7472, United States Nuclear Regulatory Commission (U.S. NRC) Office of Nuclear Regulatory Research, Washington, DC, USA, and National Institute of Standards and Technology (NIST), Gaithersburg, MD; USA, April 2008, <https://www.nrc.gov/docs/ML0811/ML081190261.pdf>.
- [10] National Institute of Standards and Technology (NIST): CFAST, Fire Growth and Smoke Transport Modeling, Engineering Laboratory Fire Research Division, Gaithersburg, MD, USA, updated October 16, 2019, <https://www.nist.gov/el/fire-research-division-73300/product-services/consolidated-fire-and-smoke-transport-model-cfast>.
- [11] National Institute of Standards and Technology (NIST): FDS-SMV: Fire Dynamics Simulator (FDS) and Smokeview (SMV), Gaithersburg, MD, USA, accessed September 2022, <https://pages.nist.gov/fds-smv/>.
- [12] Electric Power Research Institute (EPRI): “Computer Aided Fault Tree Analysis System (CAFTA), Version 6.0b, software, Product ID 3002004316, Palo Alto, CA, USA, August 26, 2014, <https://www.epri.com/research/products/000000003002004316>.
- [13] Idaho National Laboratory (INL): SAPHIRE – Risk and Reliability Assessment Tools for the 21<sup>st</sup> Century, Idaho Falls, ID, USA, accessed September 2022, <https://saphire.inl.gov/>.
- [14] Lloyd’s Register (LR): RiskSpectrum®: Risk and Reliability Software, Sundbyberg, Sweden, accessed September 2022, <https://www.lr.org/en/riskspectrum/>.
- [15] Stroup, D., G. Taylor, and G. Hausman: Fire Dynamics Tools (FDT<sup>s</sup>) Quantitative Fire Hazard Analysis Methods for the U.S. Nuclear Regulatory Commission Fire Protection Inspection Program, NUREG-1805, Supplement 1, Vol. 1, United States Nuclear Regulatory Commission (U.S. NRC) Office of Nuclear Regulatory Research, Washington, DC, USA, Office, Washington, DC, USA, December 2004, <https://www.nrc.gov/docs/ML1321/ML13211A097.pdf>.
- [16] Salley, M. H., and R. Wachowiak: Nuclear Power Plant Fire Modeling Analysis Guidelines (NPP FIRE MAG), Final Report, NUREG-1934, and EPRI 1023259, United States Nuclear Regulatory Commission (U.S. NRC) Office of Nuclear Regulatory Research, Washington, DC, USA, November 2012, <https://www.nrc.gov/docs/ML1231/ML12314A165.pdf>.

# Requirements in Standards and Fire Qualification for Smoke Control Dampers

Nicolas Ytournel\*, Vincent Raillard and Emilie Levet

NUVIA PROTECTION, Morestel, France

## ABSTRACT

In case of fire accidents, installations for the supply of fresh air or the removal of exhaust air from rooms must be designed to prevent the propagation of fire and fire by-products (e.g., hot smoke gases) to any room other than that where the fire originated. The ventilation system consists of ducts and in-line equipment such as dampers (fire dampers, smoke control dampers, etc.), valves, bellows, sensors, etc. The operation of ventilation and smoke extraction equipment is essential to allow air exhaust.

Designs of nuclear power plants (NPPs) with pressurized water reactor (PWR) in France and the United Kingdom are compliant with the nuclear standard RCC-F [1] code to manage fire safety issues. According to this code, smoke management is a significant issue for fire safety, smoke being a potential hazard for personnel, environment, and equipment. In parallel, the smoke dampers must be qualified according to the non-nuclear standards EN 12101-8 [2], EN 1366-8 [3] and EN 1366-10 [4] and associated with fire resistant smoke exhaust ducts EN 1366-8 [5] which for a large spectrum of applications are not concerned by nuclear cases. Smoke control dampers must perform as required by [2] with the major objective to meet requirements for fire resistance rating of fire barriers and their elements. A suitable fire resistance rating is demonstrated by fire tests according to the EN 1366-10 [3] standard.

In order to meet the new project, standard and code requirements, NUVIA has developed and qualified a new range (NuSDA-220) of multi-compartment smoke control dampers during the last months.

This contribution is related to the operational experiences and feedback issued from the equipment qualification step. It provides an overview of the standards to comply with and outlines their singularities and the difficulties to adapt the nuclear configurations to the standards regarding the fire resistance of fire barriers.

## INTRODUCTION

In case of fire hazards, installations for the supply of fresh air or the removal of exhaust air from rooms must be designed to prevent the propagation of fire and fire by-products (e.g., hot smoke gases) to any room other than that where the fire originated.

EPRs (European Pressurized Reactors) in France and the United Kingdom are designed according to the RCC-F code (EPR Technical Code for Fire Protection) [1] which provides recommendations issued from French and United Kingdom's regulations regarding fire protection including the exhaust of fumes in NPPs, with respect to the industrial risk, the life safety, and the environment.

NUVIA Protection has conducted extensive research and a variety of tests to develop a new range of multi-compartment smoke control damper (NuSDA-220 products) in order

to respond to the RCC-F code [1] and to comply with the requirements of non-nuclear fire protection standards such as EN 1366-8 [3] and EN 1366-10 [4].

Specialised qualification relates to our customers specific reference system (HPC/ENGIE) not only dealing with fire but also waterproofing, displacements (e.g. by earthquake) and any other requirements from sensitive industrial plants.

## STANDARDS AND DEFINITIONS

### **Smoke Protection, Control and Exhaust Systems for Nuclear Applications**

The RCC-F code [1] provides requirements regarding the plant internal fire protection for the technical buildings of a PWR type NPP (rules for the design, manufacturing, and installation of fire protection systems and equipment). According to this code, smoke management is a significant issue for fire safety, smoke being a potential hazard for personnel, environment, and equipment.

Different principles, potentially combined, can be applied to ensure smoke management in different situations:

- **Smoke protection** to keep clear protected access and escape routes, and muster zones used for evacuation and emergency interventions,
- **Smoke control** associated with fire partitioning, to limit the spreading of fire and smoke, in particular with the objective of radioactive or toxic materials confinement or functional separation,
- **Smoke exhaust** in areas where air scavenging is required and possible, for personnel or asset protection purposes.

In fire compartments with nuclear safety separation requirements, automatic smoke exhaust systems must be avoided (to control the nature of discharge and so to release neither toxic nor radioactive materials to the environment) [1].

### **Smoke Control Dampers and Their Performance**

The NuSDA-220 smoke damper (cf. Figure 1) is a mechanical equipment whose running is based on the rotation of the blade from the close position to the opened position (90° rotation) in case of:

- fire events (on request),
- functional tests,
- maintenance activities.

To reclose the blade, the rotation is reversed.

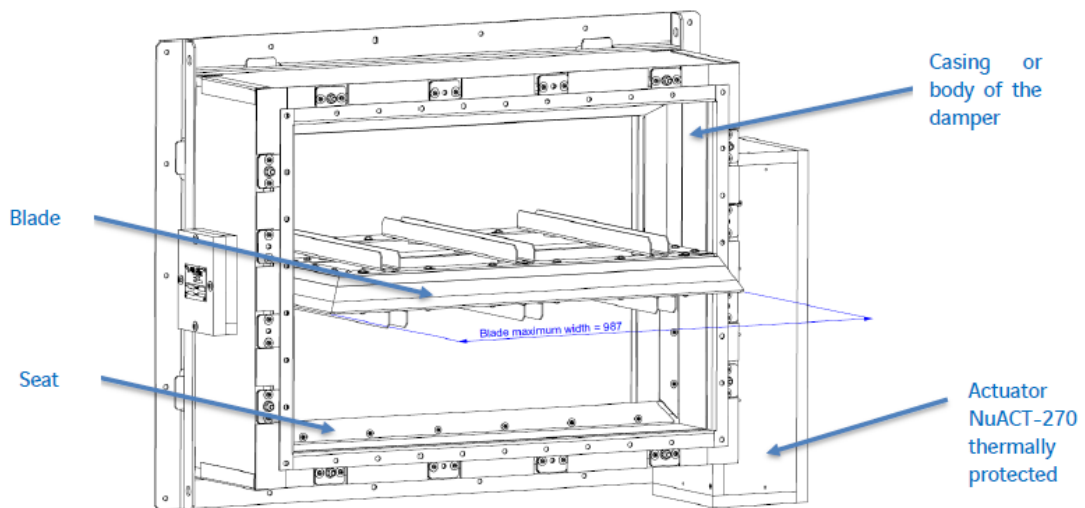


**Figure 1** NuSDA-220 smoke control damper

A smoke control damper is a device automatically or manually actuated which can be opened or closed in its operational position, in order to control the flow of smoke and hot gases into, from or within a ventilation duct.

- In "open" position, it directly contributes to the confinement of smoke in the room affected by enabling a vacuum to be drawn after the system fans have been put into operation.
- In "closed" position, it contributes to the fire resistance of the smoke control duct of the sleeve in each fire-free area.

Smoke control dampers must meet the performances requirements of EN 12101-8, where the main feature is to satisfy the required fire resistance. The fire resistance is demonstrated by fire tests according to the standard EN 1366-10 [4]. The smoke control dampers shall be tested according to their end-use application to enable the classification to be made. They are broadly split into the two main groups of single and multi-compartment applications described as follows:

- Smoke extraction of a unique fire compartment to the outdoor of building (single compartment system, cf. Figure 2)

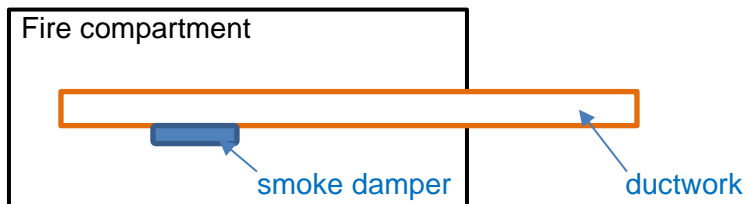


**Figure 2** Single compartment smoke damper illustration

- Smoke extraction of two or more fire compartments in a building (multi-compartment system, cf. Figure 3)

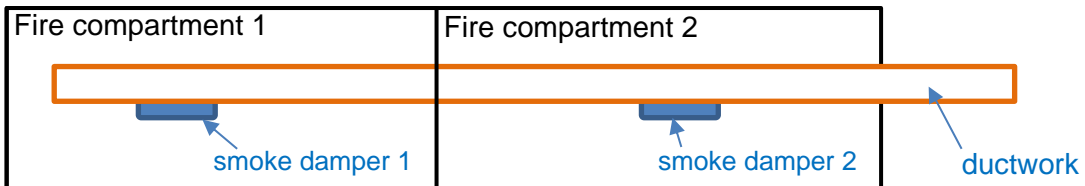


**Figure 3** Multi-compartment smoke damper illustration

The designed smoke control dampers NuSDA-220 have a multi-compartment application. Within this application there are further tests as for example the ignition regime and cycling test depending also on the end-use of the dampers and the location where they are installed on the smoke extraction circuit (either mounted within or on the face of a compartment structure, or mounted on the surface of a duct, vertically or horizontally). Therefore, many fire test configurations have to be tested. For a multi-compartment configuration, the qualification according to [4] is divided into three parts (ambient leakage, cycling tests, fire tests) using several smoke control damper prototypes (cf. Figure 3):

- Small size: height 300 mm x width 300 mm:  
one smoke control dampers to be used for ambient leakage and cycling tests (horizontal or vertical):
- Large size: height 700mm x width 850 mm:  
four smoke control dampers to be used for ambient leakage, cycling tests, and fire tests (horizontal and vertical).

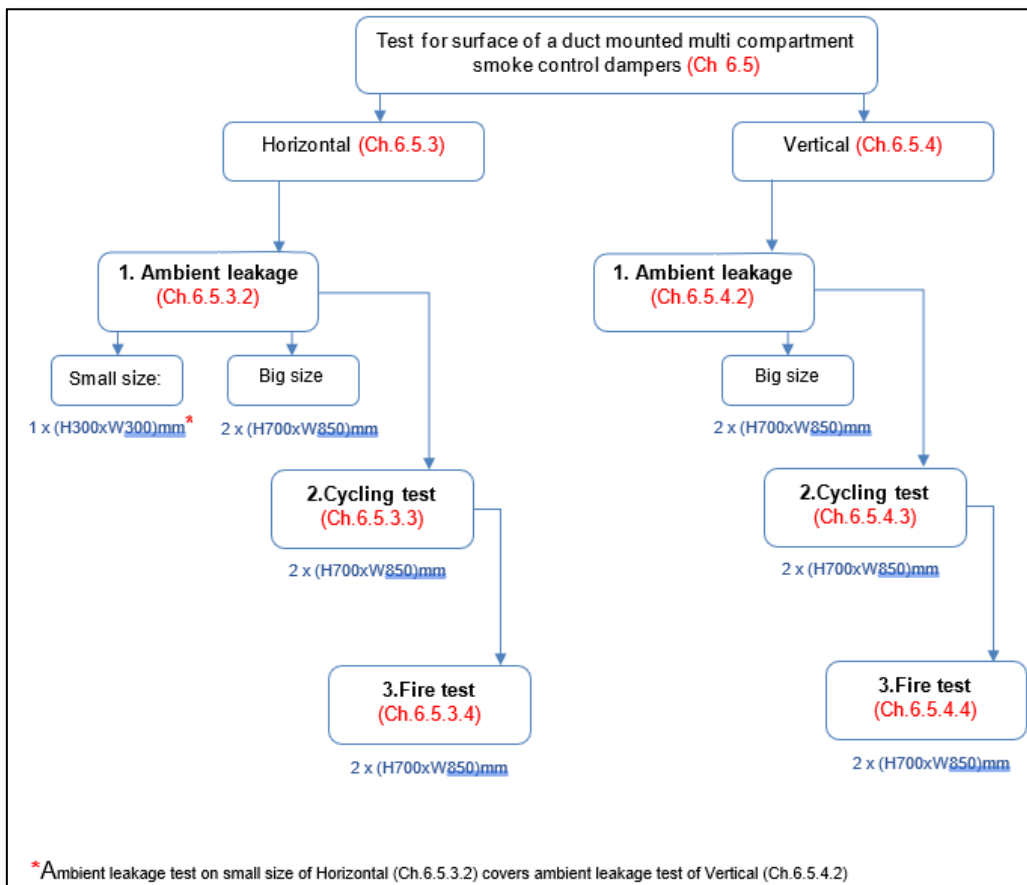


**Figure 4** Test sequence program

Using the data from the fire resistance tests according to EN 1366-10 [4], NuSDA-220 smoke control dampers, with an indifferent fire side for mounting on a smoke extraction duct, vertical orientation of dampers, and a section of 300 mm x 300 mm up to 850 mm x 700 mm, obtained the following European class according to EN 13501, Part 4 [5]:

**EI 120 (Ved i <-> o) S 1500 C300 MA multi,**

with:

- “E” as for hot gases sealing,
- “I” as for thermal insulation,
- “120” as for time (fire resistance duration) in minutes,
- “Vedw” / “Hodw” as for vertical/ horizontal orientation in a duct (d = duct) and/or on a wall (w = wall),
- “i <-> o” as for the direction of fire propagation, inside to outside and/or outside to inside,
- “S” as for the leakage rate,
- “1500” as for the operating pressure in Pa,
- “C300” as for use only in dedicated smoke control systems, operated only in the case of emergency,
- “MA” as for manual intervention,
- “multi” as for multi-compartment.

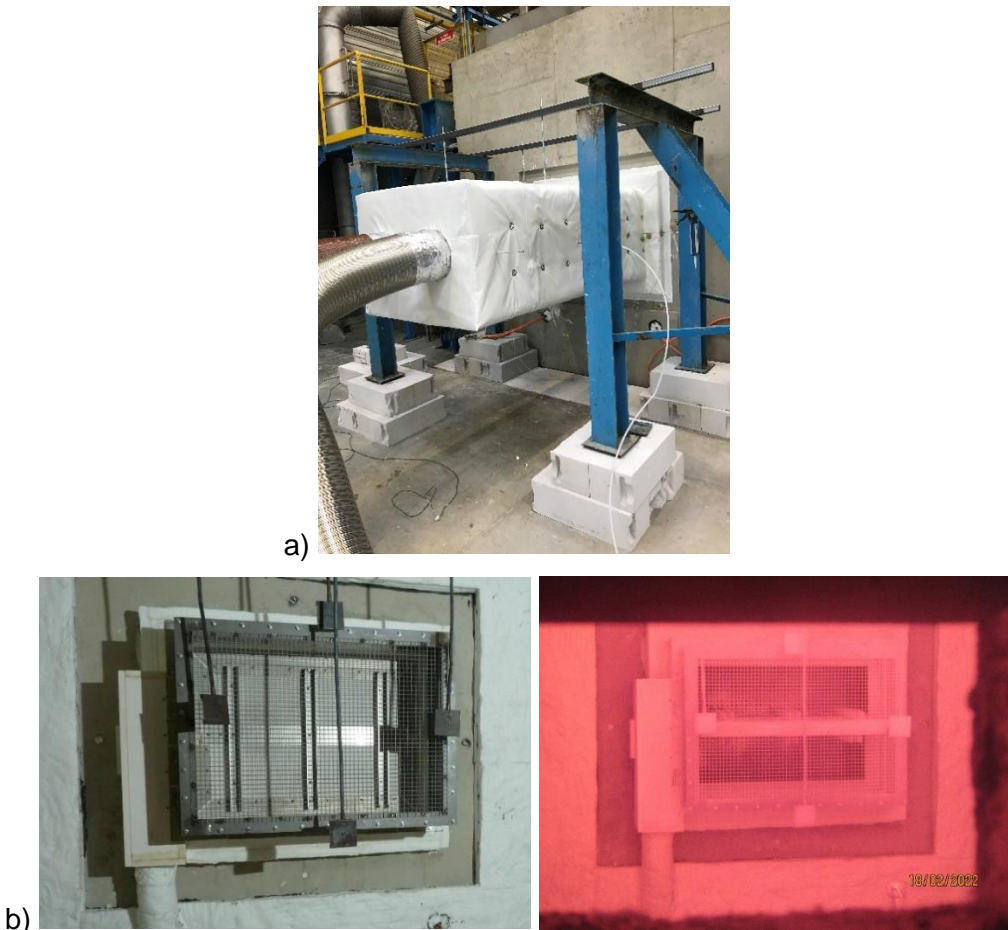
## FIRE TESTS

If we consider the requirements one by one separately, more than twelve fire tests would have to be performed according to the EN1366-10 standard [4]. Thanks to technical discussions with the accredited French laboratory Efectis, we succeeded to optimize the number of fire tests. Therefore, seven fire resistance test configurations had to be tested to cover all our requirements for the United Kingdom project.

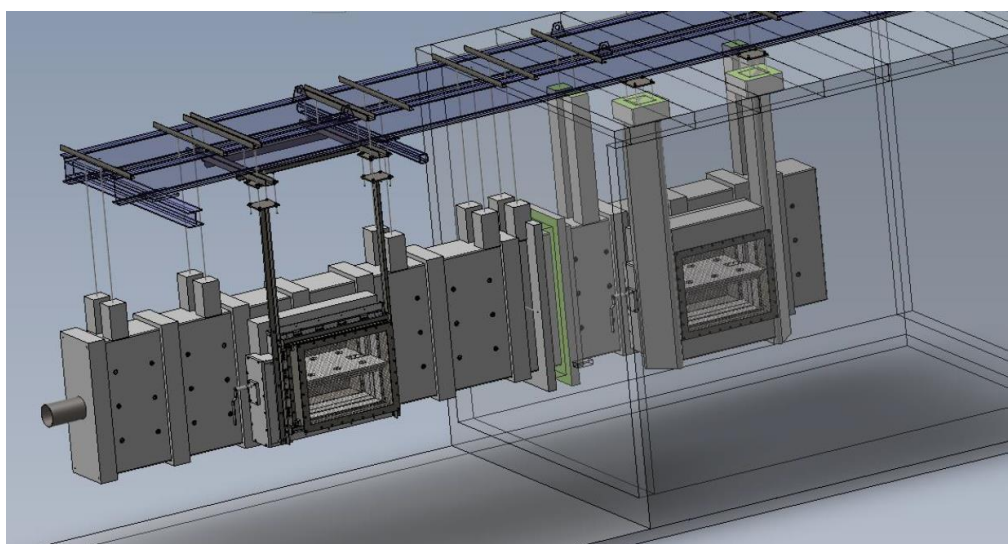
Five fire tests were performed with smoke dampers mounted on the face of a compartment structure (one of them tested with a grille) and two fire tests with smoke dampers mounted on the surface of a duct.

Figure 5 illustrates a fire test with a grille fixed on the smoke control damper. According to EN 1366-10 [4], the NuSDA-220 smoke control damper is in closed position at the beginning of the test. After 25 minutes, the damper opened (MA criteria) and remained open for hot gases extraction until the 120<sup>th</sup> minute of the fire test.

In case a test is performed with smoke control dampers fixed on the surface of the duct (see Figure 6), two dampers are fixed on a duct, one is on the exposed face (exposed to outside fire), the other one is on the non-exposed face (subjected to inside fire).



**Figure 5** Fire test of NuSDA-220 fixed on the wall, with grille; a) non-exposed face view: fire protected duct, b) exposed face view: before the fire (left), during the fire test (right)



**Figure 6** 3D view of a fire test with NuSDA-220 mounted on a surface of a duct

The smoke damper fixed on the exposed face is in closed position at the beginning of the test. After 25 minutes, this smoke control damper was opened (MA criteria) and remained opened for hot gases extraction until the 120<sup>th</sup> minute of the fire test. The smoke

control damper fixed on the non-exposed face shall always remained in closed position, so that the fire could not propagate from the inside duct to the outside duct. The strains applied to these smoke control dampers are completely different during the fire test.

It is important to notice that fire resistant ducts on which the smoke control dampers are fixed had been previously tested and met the requirement of EN 1366-8 [3] for use in multi-compartment applications.

## **SINGULARITIES / DEVIATION OF NUCLEAR CONFIGURATIONS TO THE FIRE RESISTANCE STANDARDS**

Due to the high level of stress (high depressurization of the duct, SC1 seismic level, etc.), the smoke control dampers must be supported, whereas the EN 1366-10 standard [4] does not consider any hanging system.

This aspect needs to be considered and studied before the test to determine the worst configurations to be tested during the qualification, in order to be sure that the qualification is the most representative regarding the plant specific configuration, and compliant with the standard.

### **Cycling Test**

Before performing the fire test, the damper has to be aged by means of 300 cycles. The standard [4] provides details on the procedure and the parameters to be respected for this ageing test.

One of the parameters deals with a counter-weight to be mounted on the blade. The mass and positioning of the counter-weight are defined by the following torque formula:

$$T = 34,4 \times \left( \frac{BW}{1000} \right) \times \left( \frac{BH}{1000} \right)^2$$

with: BW = width of the blade, BH = height of the blade, and 34.4 = constant value.

This formula is defined for one dedicated design and one air speed, i.e., 10 m/s.

There are three paradoxical aspects on this requirement:

- Nuclear applications require a higher level of air speed. Consequently, the standard should be less restrictive regarding the final use on-site.
- The constant value (34.4) defined in the standard is linked to the shape of the blade. However, the NuSDA-220 smoke control damper has a specifically sloped shape. As a result, the maximum torque (T) value does not appear for the same opening angle as the one considered in the standard due to the change of the air flow around the blade (cf. Figure 7).
- In order to respect the standard torque to be applied, the mass of the counterweight needs to be increased and the distance between the blade and the counterweight needs to be reduced. In this case, the weight creates a stress which can be largely negative for the design (flexion on the blade axis) in comparison to the maximum design airflow, whatever the position of the blade is.

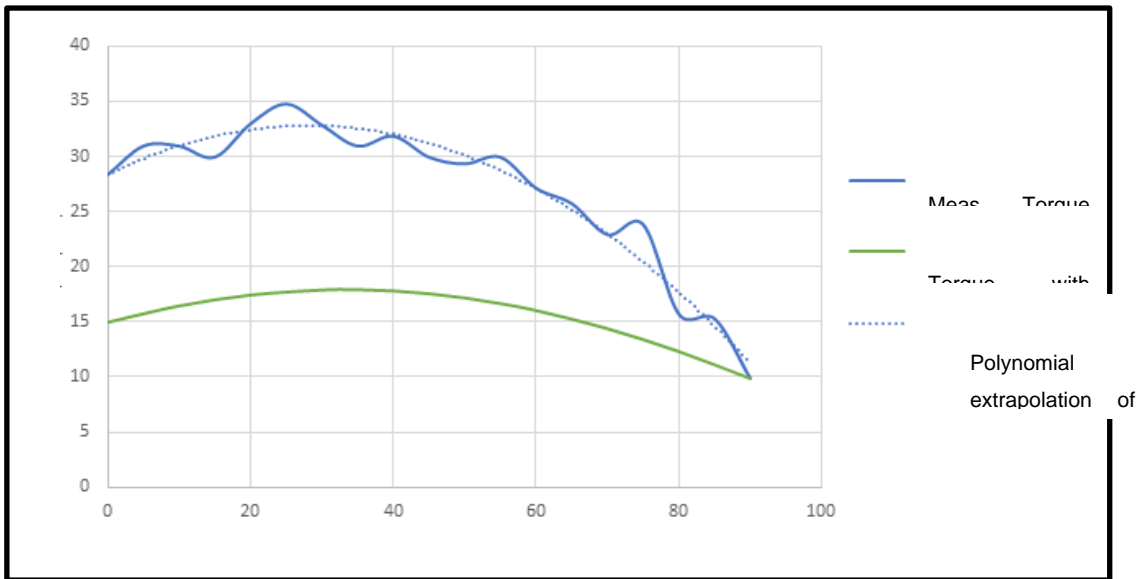


**Figure 7** Air torque depending on the opening angle ( $0^\circ$  = closed position)

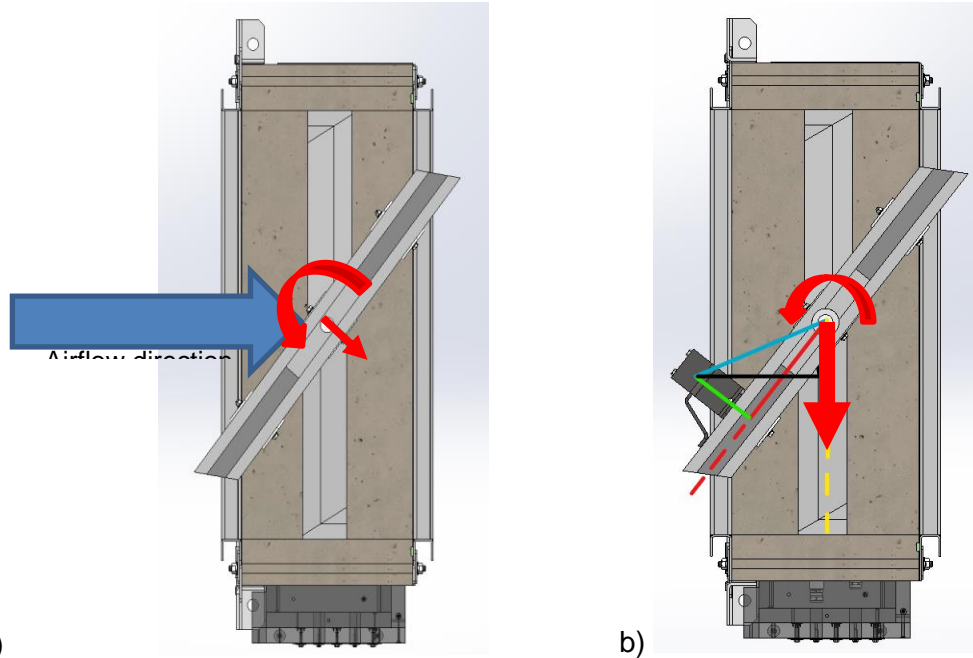


**Figure 8** 3D cross-sectional views of the NuSDA-220 smoke control damper for each case of use (nominal and test); a) nominal condition of functioning and force resulting, b) test condition with mass and force resulting

### Grille

Smoke control dampers are used to ensure the capability of exhausting the fumes in case of a fire hazard. The standard EN 1366-10 [4] defines the minimum efficiency ratio of the exhausting to be 75 %. This ratio is calculated considering that the reference section is the section of the duct.

This efficiency ratio usually decreases along the fire test due to

- the smoke damper design in opened position creating a first reduction of the passage section at ambient temperature; this can be reduced along the fire test due to the damage of the damper.
- the reduction of the duct section, which is linked to the temperature development over time.

When the damper is placed at the end or side of the duct, an (anti-intrusion) grille should be installed. Regarding this aspect, the standard precisely requires that for the grille placed in less than 200 mm, the fire tests shall be performed with the grille. If the distance is larger the test does not have to be performed with the grille.

However, the design of the grille directly affects the result of the test regarding the efficiency ratio of the exhaust fumes. It has consequently to be carefully chosen. In order to provide an idea of the influence, an example of the exhausting ratio decrease is given below, at initial temperature for a smoke control damper placed on the side of a duct:

$S_{duct}$  0 duct section = 1000 x 250 mm<sup>2</sup>,

$S_{SCD}$  = smoke damper Section = 850 x 700 mm<sup>2</sup>,

$\eta_{grille}$  = free section of the grille with a minimum ratio of X % empty,

$\eta_{SCD}$  = free section of the damper = 0.85 % of the whole section 850 x 700 mm,

$$\Rightarrow S_{SCD} \times \eta_{SCD} \times \eta_{grille} \geq 0.75 \times S_{duct},$$

$$\Rightarrow \eta_{grille} \geq (0.75 \times S_{duct}) / (S_{scd} \times \eta_{SCD}),$$

$$\Rightarrow \eta_{grille} \geq (0.75 \times 1000 \times 250) / (850 \times 700 \times 0.85),$$

$$\Rightarrow \eta_{grille} \geq 0.37.$$

In conclusion, the void ratio of a grille has to be carefully fitted with the damper characteristics and must take into account a safety margin.

## CONCLUSIONS

NUVIA Protection has conducted extensive research activities and tests in order to develop a new range of multi-compartment smoke control dampers (NuSDA-220 products) according to the RCC-F code [1], and to comply with the requirements of the European non-nuclear fire protection standards such as EN 1366-8 [3] and EN 1366-10 [4]. Encountered challenges were to adapt the fire test configurations considering specific nuclear requirements.

This experience feedback of NuSDA-220 development highlighted ways of improving to be considered for the next studies for nuclear markets.

## REFERENCES

- [1] AFCEN: RCC-F: Design and construction rules for fire protection of PWR nuclear plants, First Edition, Courbevoie, France, 2017, <https://www.afcen.com/en/>.
- [2] AFNOR Éditions: NF EN 12101-8: Smoke and heat control systems – Part 8: Smoke control dampers, July 2011, <https://www.boutique.afnor.org/en-gb/>.
- [3] AFNOR Éditions: NF EN 1366-8: Fire resistance tests for service installations – Part 8: Smoke extraction ducts, January 2005, <https://www.boutique.afnor.org/en-gb/>.

- [4] AFNOR Éditions: NF EN 1366-10: Fire resistance tests for service installations – Part 10: Smoke control dampers, June 2017,  
<https://www.boutique.afnor.org/en-gb/>.
- [5] AFNOR Éditions: NF EN 13501-4: Fire classification of construction products and building elements – Part 4: Classification using data from fire resistance tests on components of smoke control systems using data from fire resistance tests on components of smoke control systems, July 2016,  
<https://www.boutique.afnor.org/en-gb/>.

# **Guideline for Installation of Valves in Composite and Plastic Materials in Nuclear Power Plants**

Jacob Larsson<sup>1\*</sup>, Elin Fahrman<sup>2</sup>, Alexander Nilsson<sup>2</sup>, Fredrik Necander<sup>2</sup>,  
Mattias Håkansson<sup>3</sup>, Jenny Leckborn<sup>2</sup>

<sup>1</sup> Risk Pilot AB, Malmö, Sweden

<sup>2</sup> Risk Pilot AB, Göteborg, Sweden

<sup>3</sup> Risk Pilot AB, Stockholm, Sweden

## **ABSTRACT**

To solve the problem of corrosion and its consequences on metal valves in seawater systems they can be replaced by valves made of plastics and composites. This, however, introduces new challenges in the form of fire risks. On behalf of the National Fire Safety Group in Sweden (NBSG) Risk Pilot has developed practical guidelines with the purpose to assist process engineers responsible for decisions about installation of plastic and composite valves at nuclear power plants (NPPs), focusing specifically on fire related issues. The intended use of the guidelines is as a tool in decision-making, and to contribute with understanding of plastics and composites, as well as how they are affected by a fire and the potential consequences for both people and systems.

The risks and preventive measures that have been identified are presented with a theoretical background and summarised as a series of guidelines that underline the most important aspects from each area. The study also includes topics of discussion to handle in collaboration with suppliers of plastic or composite valves, with the aim of adapting the material based on use, system, and resistance to fire.

The guidelines should be viewed as a work in progress, to be supplemented with additional information and details, such as recommendations for specific materials and a more detailed fire classification procedure.

## **INTRODUCTION**

To remove residual heat at NPPs, seawater is commonly used. The seawater systems are essential to safe operation of the plants and thus have high demands on availability. Saltwater is however highly corrosive to metals, and these piping systems are therefore associated with frequent replacements of damaged equipment, such as valves, and high maintenance costs. To resolve the problem of corrosion and its consequences on metal valves in seawater systems they can be replaced by valves made of plastics and composites. However, this introduces new challenges in the form of fire risks and consequently a loss of system integrity. There are also other risks associated with burning composites and plastics such as increased fire propagation and development of soot and gases, which may be harmful to both humans and the surrounding systems. Furthermore, as metal valves are generally considered unaffected by a fire incident, the effect on process systems caused by fire is commonly not considered in safety analyses.

An opportunity for improvement has been identified at the Swedish NPPs concerning the risks associated with fires in composite and plastic valves. Therefore, on behalf of the National Fires Safety Group in Sweden (NBSG) Risk Pilot has developed practical

guidelines with the purpose to assist process engineers responsible for decisions about installation of plastic and composite valves at NPPs, focusing specifically on fire related issues. The intended use of the guidelines is as a tool in decision-making, and to contribute to the understanding of plastics and composites as well as how they are affected by a fire and the potential consequences for both people and systems.

Only risks related to composite valves and fire have been considered in this work. Other aspects concerning the installation of composites and plastics at NPPs, such as ageing due to radiation, have not been considered. The guideline is therefore to be viewed as a complement to be applied together with other technical standards used at each plant.

## METHOD

The work consists of two major parts, each described in a separate subchapter:

- the development of the guideline, and
- a benchmark, with the purpose to compare the findings from the development of the guideline to actual installations of composite valves at NPPs.

### Guideline

The guideline was developed in collaboration with an expert group, consisting of experts with experience in systems engineering, fire engineering, as well as representatives from the Swedish nuclear facilities interested in utilizing the guideline. Information was collected through a literature study as well as through interviews with employees at the NPPs.

The guideline contains theoretical parts, intended to give the reader some background and basic understanding of the topic as well as a set of practical guidelines.

### Benchmark

Each area discussed in the guideline form a subject of comparison for real installations of plastic or composite valves at Swedish nuclear facilities. Information about the installations is collected from various installation reports with the purpose to research what the responsible process engineers have taken into consideration. The findings are presented in a spreadsheet with the different areas from the guideline as columns and the installed valves as lines. If no information about a certain area is presented the cell is filled with "not assessed", otherwise the cell is filled with a short description of the available information.

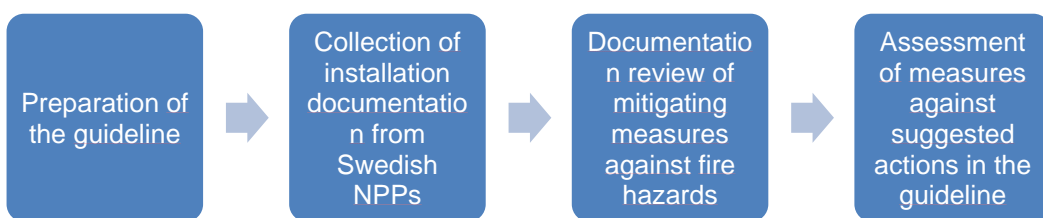


**Figure 1** Flowchart showing the work process for the benchmark

## RESULTS

The guideline consists of the following parts:

- An introduction to plastic and composite materials, pros and cons, and utilization areas;
- Types of fire;
- Aspects to consider when using valves made from plastics and polymers, including a short theoretical background, associated risks, and general guidance;
- Fire protection and preventive measures;
- Guidance to evaluate potential suppliers, including suggestions of relevant discussion points.

### Plastics and Composites

Plastics in this work it refers to synthetic polymeric materials. There is a wide range of plastics of different qualities and uses. The properties of a plastic material are determined by its chemical composition. These properties include the behaviour of a plastic material when exposed to elevated temperatures, such as melting point, and the substances released during combustion of the material [1].

Composites are a combination of two or more materials. The properties of a composite can be a combination of, or different from the properties of the separate materials. In this work, a composite refers to a combination of a porous plastic matrix, combined with a strong fibre, such as carbon or glass fibre. This is the type of composite which is commonly used in valves.

#### *Advantages and Disadvantages of Plastics and Composites*

In general, the properties of composites and plastics differ; however, they are the same with respect to some aspects. Both types of materials are light compared to metals such as steel, and resistant to corrosion.

Plastics are generally cheaper than steel. However, composites can be quite expensive depending on the complexity of the material.

The main disadvantage of plastics and composites compared to metal piping is the structural integrity of the material. Plastics and composites are more easily deformed when exposed to e.g., fire or mechanical impact, which may cause the system - where a plastic or composite valve is installed - to lose its function, or a leakage to occur. The materials cannot be welded, and valves are most often installed with flanges, or in some cases glued to the piping. Valves in plastics and composites are therefore in general not suitable for high pressure systems or systems with requirements on integrity. Specifically related to nuclear power, the radiation resistance of polymeric materials is in general poor.

### Fire Specific Aspects and Risks Related to Plastics and Composite Materials

The risks associated with fire in plastics or composites were identified based on the following areas, each shortly described in the following subchapters:

- Function and integrity of the system;

- Fire load in the compartment;
- Spread of fire;
- Reactions with other media;
- Spread of soot and gases.

### ***Function and Integrity of the System***

A fire in a plastic or composite valve may cause a system to lose its function or integrity. This, however, does not necessarily mean that a valve should not be installed in an area solely based on the risk of fire exposure. Different systems have different demands on system integrity and function after a fire incident. For example, the requirements may be formulated such that a system should be able to maintain its integrity for a specific duration of time. If the advantages of using a plastic or composite valve in a specific system outweighs the disadvantages, and the requirements for the systems are met, plastics or composites may still be a viable option.

The properties of a composite material can also be modified to a higher degree than those of plastics. There are for example composite materials that have been developed specifically for improved fire resistance.

### **Guidelines for Function and Integrity of a System**

The following guidelines are suggested with respect to system integrity and function:

- A general evaluation of the consequences should be made if the system were to lose its integrity or function.
- The demands on the system in terms of integrity and function after a fire incident should be carefully checked and serve as a basis for the choice of material.
- Composite materials can be modified for better fire resistance and may be a better option than plastic materials.

### ***Fire Load***

Since plastics and composites are in general composed of combustible materials, the fire load in the compartment where the valve is installed will be affected. It is therefore important to assess the effect on the fire load and to evaluate the consequences.

In summary, the fire load density is a measure on the amount of energy that can be released during complete combustion of combustible materials in a specific compartment. Usually, it is stated as energy per square meter. The area may refer to the compartment floor area or the total area of the walls, floor, and ceiling. For each compartment, there are requirements on the maximum fire load. When a new combustible object is implemented in the compartment (permanently or temporarily), the effect on the fire load density needs to be assessed.

It is however important to keep in mind that there are several factors which the fire load density does not take into account, such as the way the fire propagates through ventilation ducts, etc., and how easily a material is ignited. In this context, it must be distinguished between combustible or hardly combustible materials.

### Guidelines for Fire Load

The following guidelines are suggested with respect to the fire load (and fire load density):

- Evaluate the fire load added to a compartment when a plastic and composite valve is installed. The acceptable fire load may differ depending on the type of compartment and its safety significance.
- If the existing fire load of a compartment is close to its maximum acceptable value, the heat of combustion of the new combustible component to be installed must be determined. A general value is 40 MJ/kg [2], but the exact value should be provided by the vendor of the product.

### ***Fire Propagation***

When installing a plastic or composite valve, increased risk for fire propagation must be evaluated. Additionally, the safety (deterministic and probabilistic) analyses may have to be re-evaluated. A new verification of the compartment may also be needed.

### Guidelines for Fire Propagation

The following guidelines are suggested with respect to fire propagation:

- Verify, through safety analyses and through physical inspection of the area, that the risk of fire propagation is not unacceptably high, i.e., that it does not exceed the requirements.

### ***Reactions with Media Inside and Outside the System During Combustion***

The polymers of a plastic material are organic substances and consist of a carbon chain with hydrogen. To obtain different plastics, some of the hydrogen atoms are replaced by other chemical components. Common substitutes are halogens, such as chloride and fluoride. When plastics are combusted, these chemical components are released. These components can in themselves be harmful; however, there is also a risk of reaction with other media such as air and water. For example, chloride and water form hydrochloric acid which can cause severe damage, in particular to metal equipment [3]. Stainless steel is particularly sensitive, as a phenomenon called pitting may occur which causes the steel to become porous and brittle.

### Guidelines for a Reaction with Media

The following guidelines are suggested with respect to a reaction with other media:

- Identify what chemical components may be released during combustion from the specific material, and if there is a risk for reaction with other media inside or outside of the system where the valve is installed.

### ***Combustion Gases and Soot***

The combustion gases from burning plastics and composites are both harmful to humans and to surrounding equipment [4]. The gases can also carry harmful soot that settles on equipment and causes damage. Sanitation after such an incident can be very expensive.

Apart from the gases that occur from combustion itself, the products of reaction with surrounding media must also be considered.

The gases from burning plastics mostly consist of carbon dioxide and carbon monoxide. In a small compartment, the oxygen in the air may be consumed faster by a fire, causing incomplete combustion, which means that the share of carbon monoxide and soot in the smoke increases.

Composite materials are, apart from a plastic matrix, composed of some type of strong fibre, commonly carbon fibres. Carbon fibres are relatively inert and require temperatures of about 800° C to degrade to harmful particles. These temperatures can be reached, e.g., during a petroleum fire, or during flashover. Breathing fragments of carbon fibre can be dangerous as they can get stuck in the respiratory system. The symptoms and effects are similar to those of asbestos and pose a cancer risk.

Additionally, carbon fibres are excellent electrical conductors and can severely damage electrical equipment [5]. Sensitive electrical equipment should therefore be placed such that there is no risk of contact with carbon fibre particles in case of a fire incident.

### Guidelines for Combustion Gases and Soot

The following guidelines are suggested with to combustion gases and soot:

- Mitigate the spreading of soot and smoke by, e.g., encasing the valve in protective cladding.
- If protective cladding cannot be used to completely prevent the spreading of combustion gases and soot the composition of the smoke in case of fire must be determined. The potential effect on the surrounding systems and on humans, as well as on escape and access (rescue) routes must be determined.
- Avoid installing plastics and composites in cramped compartments with limited access to oxygen. Ensure there are clearly marked emergency exits.

### **Fire Safety and Preventative Measures for Plastic and Composite Valves**

Based on the identified risks associated with fire in plastics or composites, several preventive measures are suggested, each described in a separate subchapter.

- Testing and classification;
- Valve location in the fire compartment;
- Maintenance;
- Protective cladding.

### ***Testing and Classification***

As mentioned before a system may be required to remain functional or keep its integrity for a certain time period during a fire incident, e.g., systems with the purpose to prevent releases of radioactive substances [6].

Similar requirements do exist for construction and maintenance of building parts regarding the load bearing capacity (R), integrity (E), and insulation (I) during a certain amount of time [7]. For example, REI 60 means that a component must maintain its load-

bearing capacity, its integrity, and its insulating properties for 60 minutes in the event of fire. Similar requirements can conceivably be set on pipe fittings inside the compartment as these can contribute to the propagation of fire.

Surface layers are also classified based on how resistant they are to fire. The classification system for construction products' fire-technical properties varies from A, which is completely non-combustible, to F, which means that the object does not meet any fire requirements or that it has not been tested [8]. NPPs belong to a building class with a very high need for protection, which means that the classification of surface layers and components is not determined based on standards but must be analysed based on location and function of the system in the NPP. An untested composite valve will receive class F according to the classification system. This means careful consideration before installation as the valve does not meet the same requirements as other surface layers in the compartment.

If a new installation or replacement of a component is planned with different requirements on the REI or the surface layer compared to the previous configuration it should be demonstrated that all parts of the entire fire protection features in the area can be replaced by other (compensatory) measures. These measures can e.g. consist of spot insulation in the form of protective cladding or of automatically actuated fixed fire extinguishing systems.

### Guidelines for Testing and Classification

The following guidelines are suggested with respect to testing and classification:

- Determine the resistance time requirements that a valve may need to meet for load bearing capacity, integrity, and insulation in order not to risk the system's function being lost.
- With support by a fire officer or a fire engineer, assess the risk of a plastic or composite material catching fire as well as the suitability of the intended compartment based on that.

### ***Fire Testing***

It is of high importance to check if a valve still maintains its function and does not have any leakage during a given time period after fire occurrence. Usually there are fire requirements on building parts in the vicinity of the valve and therefore, the valve would have to meet the same requirements. Since for most plastic and composite valves it is not documented in how far they meet the fire safety requirements on load bearing capacity, integrity, and insulation it can be wise to perform fire tests. Each time a new model of the valve is to be installed, tests should be performed to ensure that the component meets requirements both regarding itself and regarding the plant as a whole.

In a furnace it is possible to program a fire curve, based on temperature and time of the surroundings and on the possible sources of a fire that can occur in the system in which the equipment is to be installed [6]. The test requirements are decided according to the situation, type of valve, and the conditions in the system where it is to be installed. The effectiveness of the insulation and a fire protection paint can also be tested in the furnace.

### Guidelines for Fire Testing

The following guidelines are suggested with respect to fire testing:

- Verify through testing in a furnace if the valve has the same fire resistance rating as the structural elements in the vicinity.
- Contact can also be made to the supplier of the valve and checked if they have performed any fire testing.

### ***Valve Location and Implementation***

An initial control of the system, area and surrounding regarding fire load and potential propagation of fire should be performed before installation of a new plastic or composite valve. The purpose of fire protection for individual components is to meet the requirements for personnel safety, material losses, and to protect the safety systems so that a fire does not endanger radiological safety [6]. To ensure that these requirements are met when installing a new plastic or composite valve the following should be considered:

- Plastic (or composite) parts must not be implemented in such a way that they pose a risk of exposure to fire. Implementing valves in rooms that do not have any safety related and/or supporting functions is preferable as a fire would not affect nuclear safety.
- As the integrity of a composite valve is more likely to be affected by fire than a steel valve there is also a higher risk of leakage. It is therefore important to consider the potential consequences of a leakage and its spread to adjacent rooms.
- Process engineers should coordinate with fire protection requirements for the compartment before installation.

### **Guidelines for Valve Placement**

The following guidelines are suggested with respect to valve location and implementation:

- Verify that the intended location and implementation is feasible for the installation of a composite valve instead of a traditional one, without drastically increasing the fire load in the room.
- Verify that the medium in the system does not pose more serious consequences because of fire in the plastic or composite valve.

### ***Protective Cladding and Insulation***

To reduce the risk that a plastic or composite valve is exposed to fire it should be provided with a kind of protective cladding, especially if placed in systems with higher safety requirements. This measure both protects the valve and reduces the risk of fire propagation. The reduction of the risk of fire spreading could be a reason to install protective cladding in systems with lower safety requirements as well. When installing the cladding it is important to ensure that the function and manoeuvrability of the valve is not inadmissibly impacted. An assessment should be performed together with a fire protection engineer to ensure that the purpose of protecting the valve from fire is properly fulfilled.

Insulations installed to reduce the risk of fire should consist of non-combustible materials [9], e.g., of non-combustible building materials. To protect the insulation material itself from the flames it can be covered with metal sheets. Another purpose with this casing is

to protect the insulation material from leakage of oil or other types of fuels to penetrate the material and, in this way, to reduce the insulating properties.

### Guidelines for Protective Cladding and Insulation

The following guidelines are suggested with respect to protective cladding and insulation:

To increase the fire protection of plastic or composite valves with high safety classification they can be supplied with protective cladding, consisting of non-combustible materials.

A metal sheet plating can be added to reduce the risk of fire starting inside the insulating material.

### **Maintenance**

Valves installed should periodically be examined to ensure that the fire protection function is maintained [6], and that no new fire risks have been added. It is also important to ensure that the maintenance procedures are included in the instructions during the installation of the valves. For locations with fire protective paint, it should be noted how the paint ages over time and if it is compatible with the surface it covers.

### Guidelines for Maintenance

The following guideline is suggested with respect to maintenance:

- Check the fire protection periodically to ensure that the required fire protection function is maintained, and no new risks have been added.

### **Evaluation of Vendors**

When purchasing equipment, many alternatives and vendors are usually evaluated. To make an informed decision it is important to ask the vendors for guidance regarding the different properties of different materials and their suitability for installation in a NPP. The following topics should be considered and discussed when choosing a valve:

- What plastics and composite materials are available?
- Is it possible to select composite materials that are resistant to fire, and how does this affect the material properties?
- Does the material contain substances that could be released in the event of fire and that could be harmful to surrounding process equipment?
- Does the material contain substances that can form harmful smoke gases?
- Are the valves fire tested or do they have a fire classification?
- What is the contribution of a composite valve to the fire load?

### **Benchmark**

A benchmark has examined ten different systems in Swedish NPPs. The valves all have been installed in seawater systems where the previous installation of metal valves suffered from corrosion issues. The level of consideration to different fire aspects in the installation documentation varies from non-existent to covering some of the above-discussed areas. For example, safety demonstration regarding the fire load (and fire load

density), reactions with media and the location and implementation of valves were mentioned during an installation of one type of plastic valve. Composite valves placed in systems with a high degree of safety classification have been provided with protective cladding.

No fire testing has been carried out prior to the installation of these valves; however, several of the models installed have been tested afterwards. There was no account of what type of maintenance is carried out on the fire protection or what requirements were discussed with the suppliers before the valves were purchased. However, this is not uncommon for the different areas to be described from a more general point rather from a fire perspective, e.g., a description of the system and the medium inside the system which can be used in an assessment of the fire risks.

## CONCLUSIONS

The project has identified a set of risks associated with installation of plastic and composite valves. Based on the risks, a set of guidelines and actions to reduce the risks have been suggested to help mechanical construction engineers when plastic or composite valves are considered for a system. The guidelines can help engineers making relevant decisions regarding the fire risks associated with the installation of plastic and composite valves and provide knowledge on how to prevent or reduce the effects of a potential fire near to or in a valve.

Furthermore, the project concludes that installations of composite and plastic valves in NPPs is a rather unexplored topic of research, although useful. The guideline should therefore be viewed as a work in progress to be supplemented by further information. Examples of topics which can be further explored are comparing different types of composites and gaining more detailed information on fire cladding.

During discussions with the expert group from Swedish NPPs, a common database for classification and fire tests of plastic and composite valves has been suggested. The database would be a platform for NPPs to share their knowledge and to help each other choosing suitable valves from a fire safety perspective.

## ACKNOWLEDGEMENTS

The authors would like to express their thanks to the members of the expert group from Forsmark, Ringhals, SKB, and Oskarshamn for sharing their knowledge with the project. The authors would also like to thank the members of staff at the nuclear facilities who participated in interviews.

## REFERENCES

- [1] Nordic Plastic Group, Allt om plaster, Sweden, 2022, <https://www.npgroup.se/om-plast/> (in Swedish).
- [2] DiNenno, P. J. (Ed.): Society of Fire Protection Engineers (SFPE) Handbook of Fire Protection Engineering, 5<sup>th</sup> Ed., ISBN 978-1-4939-2564-3, National Fire Protection Association (NFPA), Quincy, MA, USA, 2016.
- [3] PVC Forum: PVC och brand, <https://swe.sika.com/dms/getdocument.get/701d5e46-a205-3876-853f-a75f49b930a8/PVC%20och%20brand.pdf> (in Swedish).

- [4] Myndigheten för Samhällsskydd och Beredskap (MSB): Hantering av kolfiberkomposit vid olyckor, MSB1747 ISBN: 978-91-7927-136-7, Karlstad, Sweden, December 2021 (in Swedish).
- [5] Hertzberg, T.: Risker med kolfiberlaminat vid brand. Sveriges Provnings- och Forskningsinstitut. SP-Rapport 2003:31, ISBN 91-7848-969-5, Borås, Sweden, 2003 (in Swedish).
- [6] Isaksson, S.: Litteraturstudie angående brandskydd i kärnkraftverk, Del 1: Brandteknisk separation, Statens Kärnkraftsinspektion (SKI), SKI-Rapport 95:28, Borås, Sweden, 1995 (in Swedish).
- [7] Boverket: Boverkets byggregler, BBR, BSS 2011:6 med ändringar till och med BFS 2020:4, p. 43, ISBN: 978-9-7563-985-7, September 2020 (in Swedish).
- [8] Boverket: regler om byggande, Brandklasser för golv, väggar tak, rörisolering och kablar, Sweden, 2019, <https://www.boverket.se/sv/PBL-kunskapsbanken/regler-om-byggande/boverkets-byggregler/brandskydd/brandklasserd-for-ytskikt/> (in Swedish).
- [9] Nuclear Safety Standards Commission (KTA, German for Kerntechnischer Ausschuss): Safety Standards of the Nuclear Safety Standards Commission (KTA): KTA 2101.3 (2015-11), Fire Protection in Nuclear Power Plants, Part 3: Fire Protection of Mechanical and Electrical Plant Components, November 2015, [http://www.kta-gs.de/e/standards/2100/210\\_1\\_3\\_engl\\_2015\\_11.pdf](http://www.kta-gs.de/e/standards/2100/210_1_3_engl_2015_11.pdf).

### **3.4 Session on Experimental Fire Research and Modelling**

Experimental fire research with respect to nuclear fire safety and the corresponding analysis by fire modelling was one of the major topics of the seminar. The respective session of the seminar, chaired by Sylvain Suard (IRSN, France) covered seven expert presentations.

The speakers of this session presented actual research activities and their results such as fire tests with high pressure differences, the fire behaviour of horizontally and vertically arranged cable trays, the effects of cable arrangements and boundary conditions on fires of electrical cables on trays, the analytical investigations of cable fires within a Benchmark Exercise comparing analyses (fire simulation results) of a cable fire observed in a NPP with the results from a representative real scale cable fire experiment. In addition, calculations by GRS with the lumped parameter code COCOSYS of a cable fire experiment based on a model extension were presented.

Moreover, IRSN presented the planned experimental fire project by the OECD/NEA which will start as a follow-on of the PRISME Projects in 2023. The major goals of this international research project are to investigate the propagation and stratification of smoke gases, propagation of fires on cables with a higher length than analysed before, the effects of cable ageing on the fire behaviour, and fire scenarios with propagation between different fire sources.

The seminar contributions of this session are provided hereafter.

# Fire Test with A Pressure Differential of 5 kPa for the ITER Nuclear Fusion Experimental Facility

Rémi Buffard<sup>1</sup>\*, Nolwenn Le Duff<sup>1</sup>, Léo Kremer<sup>2</sup>, Roman Chiva<sup>2</sup>, Sébastien Diaz<sup>1</sup>,  
Vincent Raillard<sup>1</sup>

<sup>1</sup> NUVIA PROTECTION, Morestel, France

<sup>2</sup> Efectis France, Maizières-lès-Metz, France

## ABSTRACT

ITER is a scientific project that aims to design a nuclear fusion power plant under construction on the Cadarache<sup>1</sup> site.

In order to ensure the fire safety in the plant, our product must answer to an EI120 fire qualification. This EI120 requirement means that for these products and equipment a fire resistance rate of 120 minutes must be ensured. On the ITER site, this requirement must be met with a pressure factor of 5 kPa.

Qualification standards as the NF EN 1366-3 [1] for seals do not take in consideration the application of such a differential of pressure during the test. The NF EN 1366-2 [2] standard for fire dampers requires a minimum of 300 Pa differential pressure. As a result of this deviation new test methods had to be implemented in collaboration with the test laboratory Efectis France. These tests were able to highlight the impact of pressure on the tested equipment which required design improvements to meet the requirements.

## INTRODUCTION

One of the main safety risks in nuclear power plants is the fire risk. NUVIA PROTECTION, a specialist in passive fire protection, designs, qualifies and installs equipment and products mainly on nuclear sites. For installation in nuclear power plants, the equipment must be qualified according to EDF specifications and must meet the RCC-F [3] code and the CRT 62C00802 [4] for seals. The RCC-F code defines the rules for the design, construction and installation of fire protection systems used to manage the occurrence of plant internal fire hazards with respect to the nuclear risk involved, and therefore to the control of fundamental nuclear functions.

The requirements that must be met are the integrity, the insulation, and the leakage.

Unlike power plants, ITER is designed to harness the energy of fusion. This project is governed by the ITER Organization. Usual specifications and guidelines for EDF cannot be used for this qualification project. Because of its specific requirements, the usual qualification tests for power plants must be updated, especially for the EI120 fire requirement with 5 kPa. This requirement comes from the pressure increase during fire in a confined area.

---

<sup>1</sup> Cadarache is the biggest Research and Development center for low carbon energies, located at 13108 Saint-Paul-lez-Durance, France.

This paper presents the fire qualification campaign specific to ITER that has been conducted for the caulking systems of mechanical penetrations as well as for fire dampers.

## DEFINITIONS

### Penetration

In the following, the main terminology regarding penetration seal qualification according to the standard NF EN 1366-3 [1] and NF EN 1363-1 [5] is provided:

- **Penetration:** aperture in a separating element for the passage of one or more services;
- **Penetration seal:** system used to maintain the fire resistance of a separating element at the position where services pass through or where there is provision for services to pass through a separating element;
- **Service:** system such as a cable, conduit, pipe (with or without insulation), or trunking;
- **Construction support:** form of construction of known fire resistance used to support the penetration seal being evaluated;
- **Integrity E:** This is the time period in full minutes that the test element continues to maintain its separation function during the test without;
  - a) causing ignition of a cotton swab applied as specified, or
  - b) allowing penetration of an opening gauge as specified, or
  - c) lead to sustained ignition.

The time of failure is the end of the measurement, i.e., when the observation has been made.

- **Insulation I:** This is the time period in full minutes that the test element continues to maintain its separation function during the test without its unexposed surface exhibiting temperatures that exceed at any point the initial average temperature by more than 180 K.

Sealing systems tested to be qualified for the ITER project are composed (cf. Figure 1) of several parts:

- Backfilling: concrete used to reduce the dimensions of the penetration to be sealed;
- Infilling: sealing product that can be mortar or elastomer according to systems;
- Shell: soft part around the service composed of mineral wool or elastomer. This part allows service displacements;
- Coating: tight elastomer or fabric used for the tightness of the penetration and the ability to be decontaminated;
- Sleeves: parts composed of wool used on pipes to reduce the thermal conductivity.

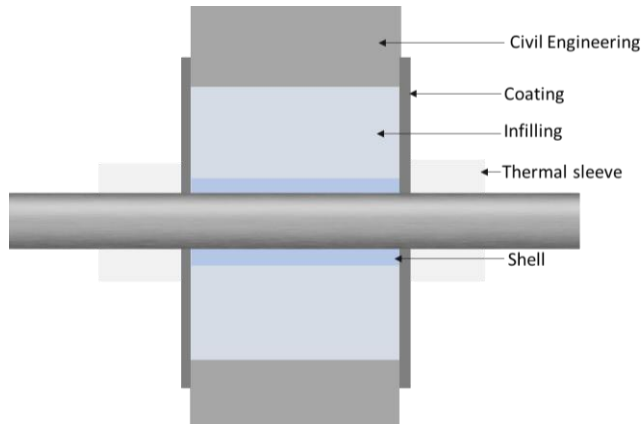


**Figure 1** Scheme of a sealing system

### Fire Damper

In the following, the main terminology regarding fire damper qualification according to the standard NF EN 1366-2 [2] is provided:

- **Fire damper:** device for use in heating, ventilation, and air-conditioning (HVAC) systems at fire boundaries in order to maintain compartmentation and to protect means of access and escape in case of fire;
- **Connecting duct:** duct section between the fire damper or supporting construction and the measuring station;
- **Test construction:** complete assembly of the test specimen, the connecting duct, and the supporting construction;
- **Measuring station:** equipment installed between the connecting duct and the exhaust equipment to determine the volume flow rate of gases passing through the fire damper under test;
- **Integrity E:** From 5 min after the start of the fire test the leakage through the fire damper shall not exceed  $360 \text{ m}^3 / (\text{h m}^2)$  (corrected to  $20^\circ\text{C}$ ).

The integrity around the perimeter of the fire damper shall be judged in accordance with the criteria given in NF EN 1363-1 [5].

The  $360 \text{ m}^3 / (\text{h m}^2)$  (corrected to  $20^\circ\text{C}$ ) is a fixed value, correspondingly, if the test was to be undertaken at a different pressure difference (e.g., 500 Pa), this value of  $360 \text{ m}^3 / (\text{h m}^2)$  (corrected to  $20^\circ\text{C}$  as ambient temperature), shall remain and shall not be increased in proportion to the pressure difference.

- **Insulation I:** The temperature criteria shall be as defined in NF EN 1363-1 [5]. The maximum temperature shall be taken from the thermocouples T<sub>1</sub>, T<sub>3</sub>, T<sub>5</sub>, T<sub>s</sub>, T<sub>sA</sub>, etc. as shown in Figure 2 and the roving thermocouple. The average temperature shall be determined from the thermocouples T<sub>2</sub>, T<sub>4</sub>, T<sub>6</sub>, etc. as also shown in Figure 2.

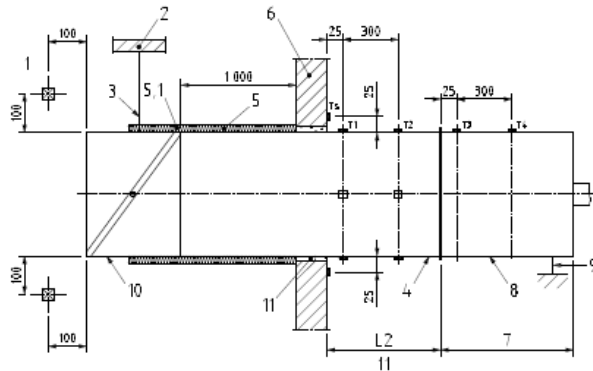


**Figure 2** Damper mounted remote from the standard supporting and inside the furnace

The temperature shall not exceed at any point

- the initial average temperature by more than of 180 K for local thermocouple positions;
- the initial average temperature by more than of 140 K for the average;
- **Leakage S:** Before the test, a leakage through the fire damper shall not exceed  $200 \text{ m}^3 / (\text{h m}^2)$  at ambient temperature (corrected to  $20^\circ\text{C}$ ).

From 5 min after the start of the fire test the leakage through the fire damper shall not exceed  $200 \text{ m}^3 / (\text{h m}^2)$  (corrected to  $20^\circ\text{C}$ ).

To gain a S classification according to EN 13501-3 [6], the damper shall not exceed  $200 \text{ m}^3 / (\text{h m}^2)$  at ambient temperature (corrected to  $20^\circ\text{C}$ ), even not for the smallest damper size.

## TEST METHODS

### Fire Dampers

Fire resistance tests are conducted for fire dampers according to the European non-nuclear standard EN 1366-2 [2] with a minimum under-pressure of  $300 \pm 15 \text{ Pa}$  applied to the equipment depending on the ventilation inside the buildings. For our applications, fire resistance tests for fire dampers are usually conducted with an under-pressure of  $1500 \pm 75 \text{ Pa}$ , as required by the specifications of customers.

For ITER, the required under-pressure is  $-5000 \text{ Pa}$ , having an impact on the test method and on the equipment tested. The main impact is on the exhaust fan which must be powerful enough to maintain the under-pressure of  $-5000 \text{ Pa}$  during all the tests.

The fire damper is installed on a supporting construction on the wall or remote from the supporting construction (cf. Figure 3), inside or outside the furnace. A connecting duct is fixed to the system in order to create the under-pressure to the fire damper and to measure the leakage of the fire damper.



**Figure 3** Picture of the installation outside the furnace

### Penetration Seals

Penetration seals for fire resistance tests are defined by the standard NF EN 1366-3 [1]. This standard presents the test method for a fire qualification of cable penetration seals, pipe penetration seals, modular systems, and mixed penetrations seals. This includes the test specimen configuration, the test procedure, and the evaluation performance criteria with the position of thermocouples.

However, no differential pressure is applied during the fire resistance test. Therefore, a specific method was studied in collaboration with the French Efectis laboratory, to implement a pressure vessel at the test specimen to apply the under-pressure on the unexposed side.

Several components were added to the usual test procedure (cf. Figure 4 and Figure 5):

- A metal pressure vessel fixed to the test specimen, composed of an oculus and some ventilation hatch that allows adjustable air circulation to avoid artificial confinement of the unexposed side;
- A diaphragm between the pressure vessel and the fan, allowing to control the air flow and the measure of the pressure;
- A fan allowing the air intake.

A CO<sub>2</sub> control at the fan outlet was carried out to indicate the possible passage of hot gas through the test specimen.

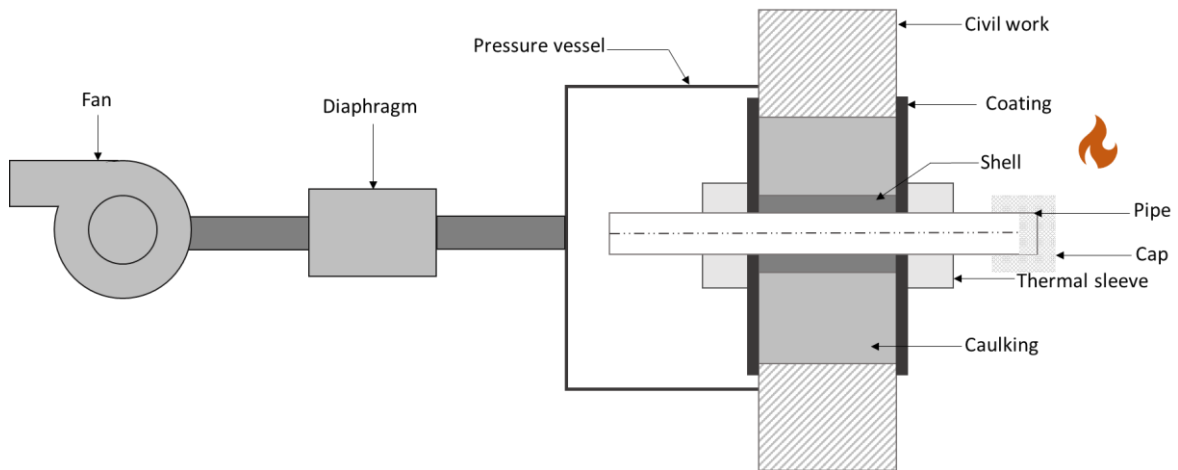


**Figure 4** Schema of the fire test implementation with the 5 kPa requirement



**Figure 5** Pressure vessel implemented on the test mock-up in the wall

To validate this test method, some risk elimination tests have been performed before the qualification tests to demonstrate the validity and robustness of the test method and their suitability for use in our qualification tests.

### **Deviation from the Standard**

The fire resistance criteria are evaluated and judged according to the standard NF EN 1663-1 [5]. As detailed in § 1.1 of [5] the criteria of integrity E and insulation I must be verified for each stage (60, and 120 minutes). However, due to the presence of the pressure vessel, the tightness criteria cannot be checked with the cotton pad. Only the presence of flames may be observed through an oculus on the pressure vessel depending on the amount of steam.

The only possibility to check the specimen is to stop the depression and to remove the pressure vessel. In order to limit the pressure variations on the unexposed side, only two major observations are made, after 1 hour testing and at the end. For this purpose, the pressure must be stopped, and the pressure vessel partially removed to have some visibility on the unexposed face of the test specimen. Once observations are made, pressure vessel and pressure are fixed to the test specimen. This manipulation must be done as quick as possible to limit the temperature increase in the pressure vessel due to the stop of the ventilation.

At the end of the test, once the pressure is removed, the test is continued to verify the possible effects of the pressure variation on the test specimen.

## **TEST PRESENTATION**

### **Fire Dampers**

For fire dampers, the test is the same as for a standard under-pressure. Different configurations of fire dampers have been tested (see Figure 6):

- one 300 mm x 300 mm section fire damper on the side exposed to fire,
- one 300 mm x 300 mm section fire damper on the side not exposed to fire,
- two serial 600 mm x 600 mm section fire dampers; one on the side exposed to fire and the other one on the side not exposed to fire, and
- one 600 mm diameter fire damper on the side exposed to fire.

All fire dampers tested were equipped with pneumatic actuators.



**Figure 6** Picture of damper tested; 300 mm x 300 mm (left), and 600 mm section and 300 mm x 300 mm (right)

## Penetration Seals

In order to qualify our systems for the entire scope of penetrations concerned, several mock-ups were tested (example see Figure 7). The dimensions of the penetrations, the size and thickness of pipes as well as their disposition follow the NF EN 1366-3 [1] standard. According to the largest dimension to qualify, blank penetrations have been tested if dimensions were too large to be tested with service.

Stainless steel pipes have been tested with the cap/uncapped configuration with the cap on the side exposed to fire. In order to protect the welding from fire and to ensure the tightness of the mock-up regarding the under-pressure, mineral wool plugs have been inserted in pipes and around the welding.

Each system has been tested in wall and floor position of 200 mm thick penetrations to validate all larger thicknesses of the wall and floor.



**Figure 7** Example of the mock-up for the fire tests of penetration seals

## IMPACT ON THE RESULTS

For the fire damper tests, there was no major consequence of increasing the under-pressure from the typical value of 1500 Pa to 5000 Pa. Otherwise, for sealing, it was noted that the application of a depressurization on the unexposed side of the mock-up implied adverse effects on the seal behaviour. For each elastomer shell systems, the increased heat conduction within the services involved a partial melting of the shell around the bushing which may have allowed the passage of hot gases and/or flames and therefore resulted in the downgrading of the pipes.

## CONCLUSIONS

The request of a fire resistance requirement combined with a pressure for ITER applications allowed to set up new test methods and opening to other possibilities.

Thanks to this, the fire dampers and sealing systems are being qualified in collaboration with the Efectis laboratory.

For seals, the qualification is ongoing with downgraded systems with some design modifications such as thermal sleeves lengths and thicknesses of construction support.

A main aspect of improvement would be to anticipate this temperature increase within the pressure vessel which can be the source of an anticipated downgrading of the thermocouples.

## ACKNOWLEDGEMENTS

The authors want to thank the entire NUVIA PROTECTION team participating in that development project. Moreover, we thank Efectis France helping us in the fire qualification of the sealing systems. Last not least we want to express our thanks to the attention of the SMiRT Post-conference Fire Seminar Technical Committee given to this contribution and to permit us to present our work.

## REFERENCES

- [1] AFNOR Éditions: NF EN 1366-3: Fire resistance tests for service installations – Part 3: penetration seals (Essais de résistance au feu des installations techniques – Partie 3: Calfeutrement des trémies), December 2021, <https://www.boutique.afnor.org/en-gb/>.
- [2] AFNOR Éditions: NF EN 1366-2: Fire resistance tests for service installations – Part 2: fire dampers (Essais de résistance au feu des installations techniques – Partie 2: Clapets résistants au feu), August 2015, <https://www.boutique.afnor.org/en-gb/>.
- [3] AFCEN: RCC-F: Design and construction rules for fire protection of PWR nuclear plants, First Edition, Courbevoie, France, 2017, <https://www.afcen.com/en/>.
- [4] Cahier de Règles Techniques (CRT 62C00802): Traversées coupe-feu et écrans isolants, France, 2004 (in French).
- [5] AFNOR Éditions: NF EN 1363-1: Fire resistance tests – Part 1: General requirements (Essais de résistance au feu – Partie 1: Exigences générales), February 2020, <https://www.boutique.afnor.org/en-gb/>.
- [6] AFNOR Éditions: NF EN 13501-3: Fire classification of construction products and building elements – Part 3: Classification using data from fire resistance tests on products and elements used in building service installations: fire resisting ducts and fire dampers, (Classement au feu des produits et éléments de construction – Partie 3: classement utilisant des données d'essais de résistance au feu de produits et éléments utilisés dans des installations d'entretien : conduits et clapets résistants au feu), 2012, <https://www.boutique.afnor.org/en-gb/>.

# Experimental Study of the Behaviour of Horizontal and Vertical Cable Tray Fires

Abdenour Amokrane<sup>1\*</sup>, Bernard Gautier<sup>2</sup>

<sup>1</sup> Electricité de France (EDF) R&D Lab. Chatou, Chatou, France

<sup>2</sup> Electricité de France (EDF) DIPNN DT, Lyon, France

## ABSTRACT

Cables are one of the most important fire loads in nuclear power plants (NPPs). They may be present in hundreds of kilometres and thus constitute the highest fire heat load [1]. In 1975, a fire involving several electrical cables occurred at the Browns Ferry NPP [2]. Following this operating experience, Electricité de France (EDF) has performed a series of real-scale cable tray fire experiments. These tests included horizontal and vertical cables tray configurations and were performed on two types of cables, namely PVC insulated cables and halogen free (HF) ones. Relevant measuring systems were used. The objectives of these tests were multiple, including the study of the fire propagation and behaviour, assessment of fire detection and extinguishing approaches, model development and validation, etc. These data and knowledge are EDF property which had not been published before. This paper corrects this situation by presenting the tests carried out and discussing some of the main lessons learnt.

**Keywords:** horizontal cable tray fire, vertical cable tray fire, real scale experimental measurements, fire modelling

## INTRODUCTION

### Operating Experience and General Issues

Electrical Cables are one of the most important fire loads in NPPs. They may be present in hundreds of kilometres and thus constitute the highest fire load. The Organisation for Economic Co-operation and Development (OECD) Nuclear Energy Agency (NEA) FIRE (*Fire Incidents Records Exchange*) Database reported about 80 fire events involving electrical cables between the late 1980s and 2014 [1]. As a result, this risk is accounted for and highly considered by power plant manufacturers and operators, to ensure the safety of people and installations. Reaction to fire of cables became an important issue in nuclear regulations and standards.

In NPPs, cables are typically arranged as trays, a majority of them routed horizontally, but some also vertically. These trays are filled with cables without exceeding loading limits fixed by the standards [3]. The trays are supported by tablets whose number is also regulated. Other aspects of the cable trays such as the spacing between the trays, their size, etc. are also regulated. The cable disposal in trays complicates the understanding and modelling of cable tray fires. In addition, understanding and modelling the behaviour of cable combustion in fire is a tough task due to the variable nature of the materials employed, some of them being intumescence. A single cable is constituted of several materials, giving birth to complex phenomena inside the cable itself. Interactions between the cables themselves, between the trays, and the whole tray with the surrounding environment, etc. must also be taken into account.

## Short Survey of Experimental Studies on Cable Fire

To understand the behaviour of cables tray fires, the fire community conducted several experimental activities in the past. Some of these were performed at a reduced scale, mainly under cone calorimeter [4] to [17]. The idea here was to reduce the scale to ease the study of such complex configurations and to try to find correlations between the behaviour of the cables at reduced and real scales. However, even though these studies have allowed to acquire valuable knowledge, experiments at a real scale were necessary. Indeed, the complexity of the problem and the multitude of interactions involved render full scale experiments unavoidable. Early full-scale tests found in the literature were carried out at Sandia National Laboratories (SNL) or the U.S. NRC [18], [19]. The primary objective of these tests was to answer regulatory concerns, but some general insights on the behaviour of such fires as well as on the modelling attempts were gained as well. Since that, several full-scale tests have been conducted, involving both horizontal and vertical cable configurations [17], [20] to [26].

The most important measurement campaign during these last decades was performed by the National Institute of Standards and Technology (NIST) on behalf of the U.S. NRC in the frame of the CHRISTIFIRE project [6], [27]. During this project, several horizontal tests were performed in open atmosphere, using thermoset and thermoplastic type cables. The effect of smoke radiation feedback on cable trays was also studied. Vertical configuration measurements were conducted as well. The experimental findings of this project served as a basis for the development of the FLASH-CAT model [6].

In the frame of the OECD/NEA PRISME (French: *Propagation d'un Incendie pour des Scenarios Multi-locaux Élémentaires*) experimental project, eight real-scale tests have been performed in horizontal configuration [28], [29]. These tests covered four tests in open atmosphere and another four in mechanically ventilated compartments (two compartments connected by a door).

## EDF Large Scale Tests

Going back a few years ago, following the Browns Ferry fire event [2], EDF conducted its own real-scale cable tray fire experimental program. These tests were performed in the early 1980s, and the experimental data remained undisclosed. The objectives of those tests were multiple:

- studying cable tray fire propagation,
- ventilation and confinement effect,
- assessment of detection techniques and their effectiveness,
- assessment of extinction methods,
- assessment of passive fire protection means,
- smoke extraction study,
- behaviour of different cable types, etc.

Several tests were performed under different configurations. They included tests of horizontal cable trays in a ventilated compartment as well as vertical cable trays in open atmosphere (in a hall which considered to represent an open atmosphere). The shaft effect was also studied for the vertical configuration. Different cable types were studied separately, namely PVC and HF type cables, as well as a mix of them. The effect of smoke radiation feedback was studied in terms of ceiling vicinity to the upper cable tray. Different detection methods as well as extinction systems were assessed, including their efficiency. Regarding the instrumentation used on these tests, several measurements

were performed, including the mass loss of the combustible, gas temperatures using thermocouples and heat fluxes using radiometers, gas species concentration using sensors. Original and very useful measurements of targets temperatures were also done on several points and positions. This type of measurements is highly important from the safety assessment point of view. The measurement points were distributed in the whole compartment as well as in the vicinity of the fire source or on top of it. This allowed a good overview of the spatial distribution of the different physical quantities. Thermocouples installed on the cable trays for some tests allowed to determine the fire spread velocity as well as the burning length. In addition to these quantitative measurements, ocular observations were performed during the tests was as far as possible (e.g., for the vertical cable tray fire).

The EDF tests were designed to be at par with industrial practice, adopting the standards applied and configurations implemented in existing NPPs. They adopted real cable trays arrangements and loadings. The cable loading is of particular importance since it greatly affects the fire behaviour through the quantity of combustible available for combustion, oxygen diffusion inside the tray as along with cable interactions. Hence, the findings from the EDF tests are worthy to be shared to the fire community knowledge. The data could also be useful to validate numerical models. These tests are the basis to the development of a cable tray fire model used by EDF in its cable fire assessment studies [30] to [32]. Last not least, for target temperature measurements being very scarce in literature, the present measurements could provide interesting knowledge on the behaviour of targets subjected to cable tray fires.

### **Objective of the Paper**

The objective of this paper is to share EDF's feedback gained from cable tray fire experiments performed, starting with a comprehensive description of the experiments. Only the main features of the experiments will be presented followed by a discussion of the principal findings.

## **EXPERIMENTS CONDUCTED**

Several real scale experimental campaigns have been carried on by EDF between 1979 and 1986. These included cable tray fire experiments both in horizontal and vertical configuration. The cables that have been used to perform the experiments are of two types: PVC (polyvinyl chloride) insulated cables and HF ones. Certain real scale tests included one type of these cables; some tests included a mix of them. Indeed, studying the cable types separately allows to understand and compare their corresponding behaviour. Studying the mix of cable allows to represent a situation where new types of cables, namely the HF ones, are added on existing installed PVC ones.

### **Horizontal Cable Tray Fire Experiments**

Figure 1 and Figure 2 below present the cellular concrete room that has been used to perform the experiments, including the fire source, the ventilation system, and the measurement points. The room is 4 m wide, 8.10 m long and 2.15 m high. Air is supplied through a vent located on a wall side, while extraction is performed using a duct in the upper part of the compartment connected to a fan through ventilation circuit. The air volume renewal rate is obtained through the outlet volume flow rate and gas temperature. Thus, the ventilation effect was studied by varying this parameter between different tests and during certain tests.

The fire source made of five trays of 5 m length and 0.45 m width spaced by 0.25 m from each other is located in the middle of the room. The upper tray is located 0.45 m below the ceiling. Some tests involved five cable trays filled with cables, while the others involved only three filled cable trays. The ceiling effect (heating by hot smoke gases) was captured this way. In these configurations, the last tray is plunged inside the smoke layer. Table 1 illustrates the different tests that have been performed and their mean features. The loading is expressed in mass of combustible per meter. "Combustible mass" means the combustible material, excluding *de facto* the conductors. The loading adopted for the present tests is equal or more than 80 kg of cables per tray, consistent with the loading given by the standards. The combustible loading provided in Table 1 is calculated depending on the characteristics of the cable (its size and the combustible material fraction). Considering those features, the present tests are consequently representative for industrial configurations.

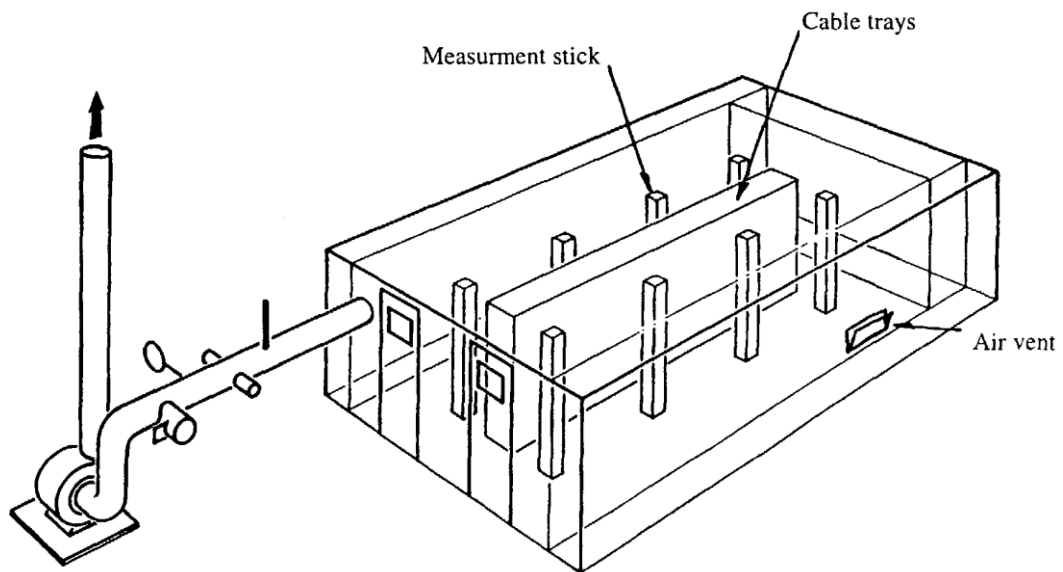


**Figure 1** Horizontal real scale test room, cable tray fire source, ventilation system and some measurements

**Table 1** Horizontal cable trays tests configuration and characteristics

| Test        | Cable Type | Cable Length [m] | No. of Trays | Combustible Mass / Length [kg/m] | Ceiling Vicinity (< 50 cm) |
|-------------|------------|------------------|--------------|----------------------------------|----------------------------|
| F1-A & F1-B | PVC        | 5.00             | 3            | 20.6 / 26.3                      | No                         |
| F2-A & F2-B | PVC        | 5.00             | 5            | 20.6 / 26.3                      | Yes                        |
| SH1         | HF         | 5.00             | 5            | 15.8                             | Yes                        |
| SH2         | HF         | 5.00             | 5            | 15.8                             | Yes                        |
| SH3         | PVC        | 5.00             | 5            | 26.4                             | Yes                        |
| ES1         | HF         | 5.00             | 3            | 15.8                             | No                         |
| ES2         | HF/PVC     | 5.00             | 3            | 21.2                             | No                         |
| ES3         | HF/ADR     | 5.00             | 3            | 20.0                             | No                         |

The fire is ignited using a gas burner of 40 kW, located under the lowest tray (at one third of its length). The burner is maintained until the fire is sustained by itself. This duration and the burner heat release rate (HRR) were negligible compared to the total fire duration and the fire source HRR, respectively.

The measurement locations are illustrated in Figure 2. The cable trays are equipped with a weighing system with lever arms leaning on strain gauges. Each tray is weighted separately, and a global system is installed on the other extremity to weight the whole five trays together. This allowed to compare the relative contribution of the mass loss of the individual tray compared to the global one, giving valuable information on fire propagation and combustible consumption.

Measurement columns were installed at 8 locations as illustrated in Figure 1 and Figure 2 (locations 1, 2, 3, 4, 6, 7 and 8 surrounded by a square in Figure 2). These columns were made of steel and were 5 cm by 5 cm. Each column supported four thermocouples, spaced by 50 cm (the first one is located 50 cm above the floor). 4 thermocouples were installed just below the ceiling at the locations indicated by circles in Figure 2. Nine thermocouples were installed above each cable tray. The thermocouples were placed on the cables and were spaced by 50 cm from each other. Temperature of extracted air extraction was also measured using a thermocouple placed in the ventilation duct. Another thermocouple was used to measure the temperature of the water used to cool heat flux gauges. The total number of thermocouples reached 86 during the experiments.

Two cooled heat flux gauges were installed at each of the measurement columns, at the 1 m and 2 m height. Smoke opacity was measured at seven different locations, while the pressure was also recorded using an inclined tube manometer.

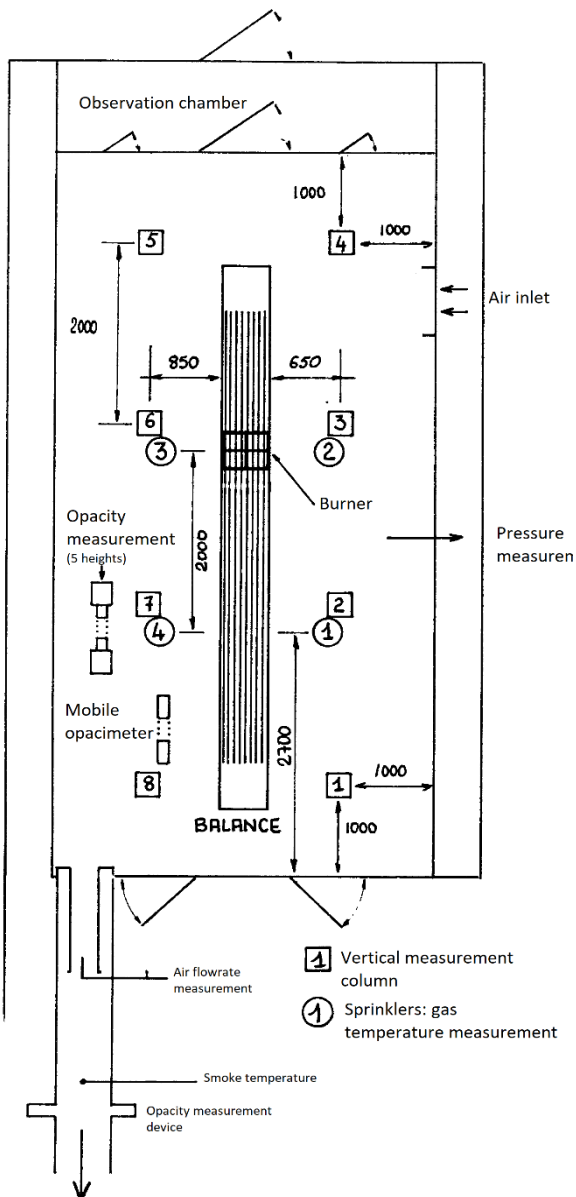


**Figure 2** Top view of the fire room illustrating air admission and ventilation system and measurement locations (measurement types are given in Table 2)

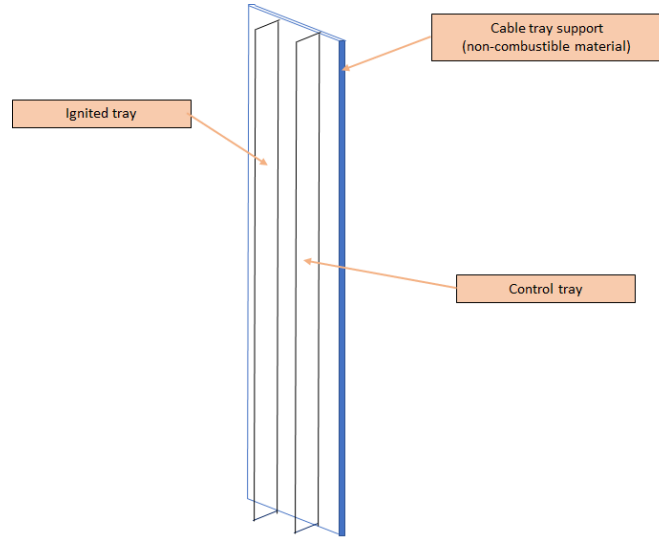
**Table 2** Measurement types and location (see Figure 2)

| Measurement Symbol | Measurement Type  |
|--------------------|---|
| [1]                | Gas temperature at heights 0.5 m, 1.0 m, 1.5 m, and 2.0 m |
| [1]                | Heat flux at heights 1.0 m and 2.0 m                      |
| (1)                | Gas temperature below the ceiling                         |

### Vertical Cable Tray Fire Experiments

The objective of the vertical cable tray fire campaign was to assess the propagation of fire in a vertical configuration. PVC type cables were used and mounted on a 5 m high shelf.

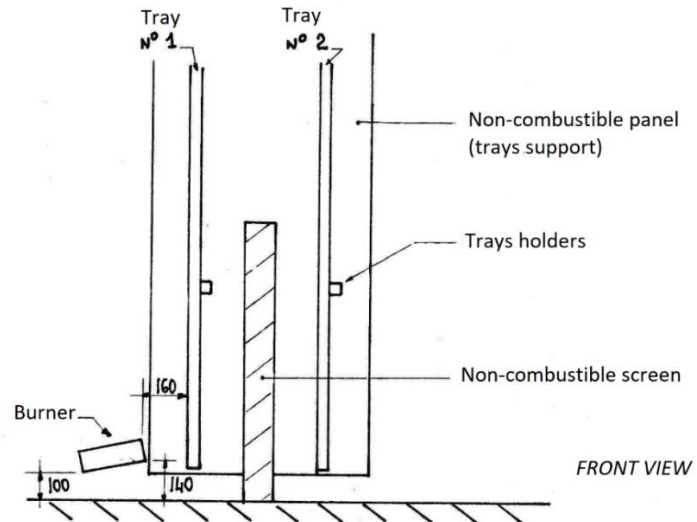
Figure 3 illustrates the experimental setup. A panel of non-combustible material supports two cable trays: the first one is ignited (using a burner) and serves as primary fire source, while the second one is a control cable tray. The latter is not ignited by the burner, it assesses the eventual propagation of fire from the first to the second tray. The whole assembly is weighed by a bending beam balance.



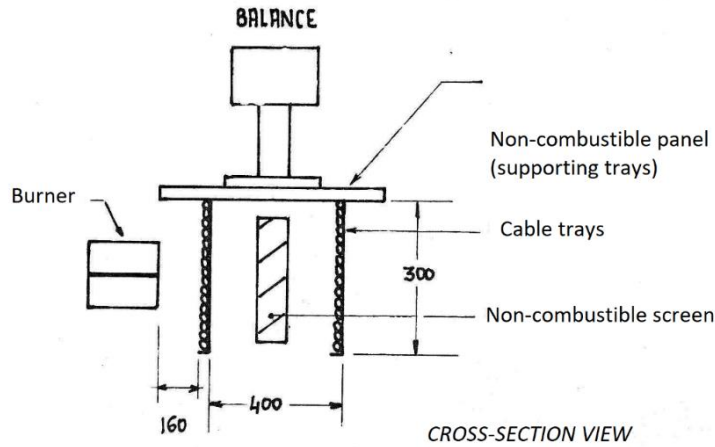
**Figure 3** Vertical cable tray setup. Two cable trays were used: the first one constitutes the primary fire source and the second one the secondary fire source

Figure 4 and Figure 5 show a front view and a cross-section view of the device. In particular, the propane burner is shown in brick form, with a power of 55 kW. A non-combustible screen is placed between the burning tray and the control one to protect the latter from the burner. The distance between the two trays is 40 cm. Their width is 30 cm.

The tests were carried out in a 14 m high hall which was naturally ventilated with openings to ensure smoke clearance and avoid ceiling effects (no smoke layer in the top part of the hall).



**Figure 4** Front view of the vertical cable tray experimental setup



**Figure 5** Cross-section view of the vertical cable tray experimental setup

The cables used for the tests have the characteristics given in Table 3. There were 16 cables per layer, with a length of 5 m. In all tests, the control tray accommodates a single layer of cables, while the ignited one may accommodate one or two layers depending on the test. If two layers of cables are used, they are fixed back-to-back around the support, leaving a gap between them.

**Table 3** Characteristics of the cables used for the vertical cable tray experiments

| Cables Characteristics   |                         |
|--------------------------|-------------------------|
| Type                     | 3 x 2.5 mm <sup>2</sup> |
| Nature                   | PVC                     |
| Diameter [mm]            | 15                      |
| Weight [kg/m]            | 0.416                   |
| Combustible fraction [%] | 60                      |
| No. of cables            | 16                      |
| Width [cm]               | 30                      |

The measurements were performed at different heights, as given in the following Table 4.

**Table 4** The different levels at which the measurements were performed and their corresponding heights

| Level | Height [m] |
|-------|------------|
| 1     | 0.5        |
| 2     | 1.5        |
| 3     | 2.5        |
| 4     | 3.5        |
| 5     | 4.5        |

Instrumentation devices on these different levels are as follows:

- The burning tray:
  - Gas temperature at each level;
- The control tray:
  - Gas temperature at each level;
- A target control cable fixed on a mast located at 40 cm from the burning tray:
  - Surface temperature of the cable at each level;
  - Surface temperature of a copper disc at each level (thermocouple soldered on), with the copper disc placed right next to and at the level of the cable;
  - Radiation heat flux received at the surface of the cable at each level (the flux meter being placed at the cable);
- A target control cable fixed on a mast located at 80 cm from the burning tray:
  - Surface temperature of the cable at each level;
  - Radiation heat flux received at the surface of the cable at each level.

Figure 6 and Figure 7 illustrate the positioning of the two masts.

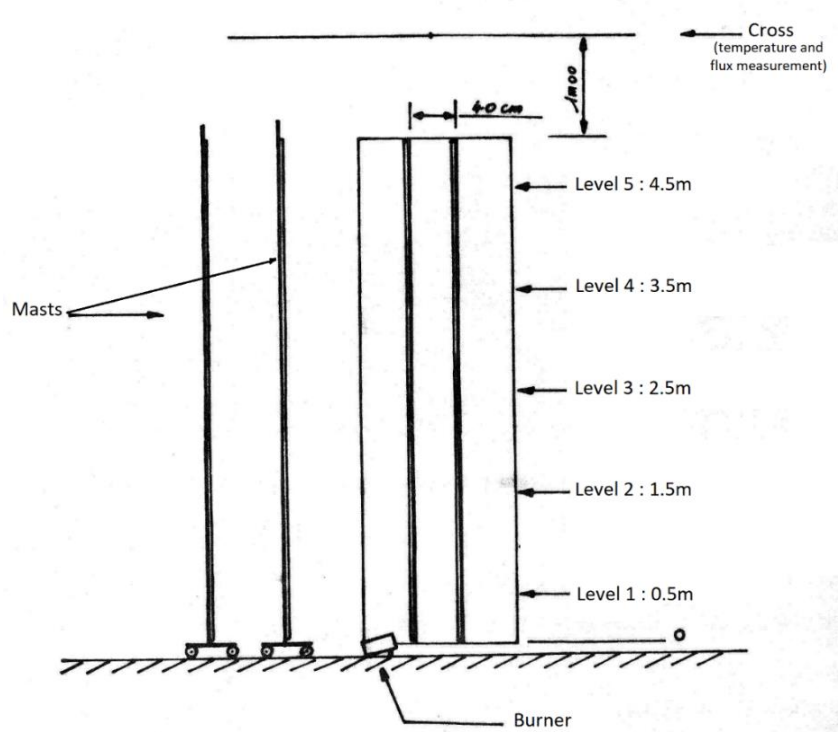


**Figure 6** Location of the measurement levels and the masts; the masts support a control cable used as a target (measurement of surface temperature and heat flux)

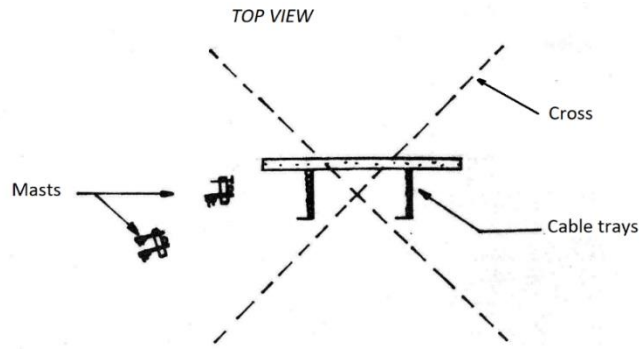


**Figure 7** Top view of the setup with the masts shown in the figure and a cross is placed above the setup at 6 m above the ground supporting 17 thermocouples and 2 heat flux gauges

In addition, a steel cross is suspended at a height of 6 m above the experimental setup (cf. Figure 6 and Figure 7). This cross holds 17 thermocouples measuring gas temperature, as well as 2 flux meters. Figure 8 shows the positioning of these thermocouples on the cross.

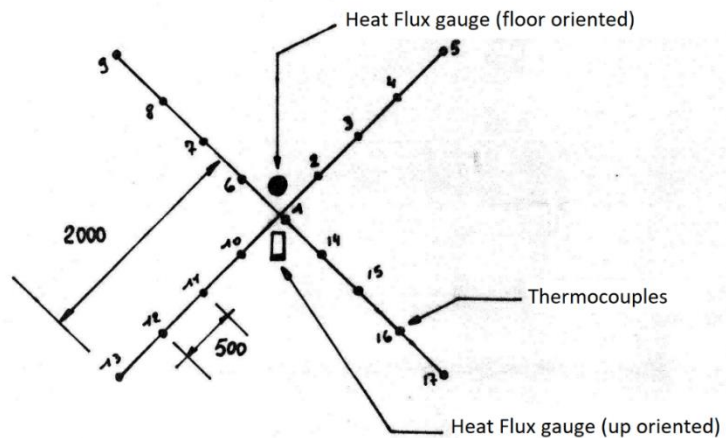


**Figure 8** Location of the thermocouples and the heat flux gauges on the cross fixed above the setup

The mass loss is measured by a scale. The mass loss rate (MLR) by pyrolysis is calculated by the first derivative. However, it should be noted that this mass loss represents the mass loss of the complete system, i.e., the ignited tray and the controlled one.

Several tests have been performed during this campaign. The tests were carried out in different configurations to determine the conditions to be met in order to achieve fire propagation. Thus, a test is often similar to the previous one with the modification of one element. Only three tests amongst the nine ones performed experienced fire spread to the top of the cables. In all other tests, the fire stopped just after the burner had been switched off and did not spread any more. Details will be presented below in the discussion section.

## RESULTS AND DISCUSSION

The following paragraphs are dedicated to the discussion of the results of the horizontal and vertical cable tray fire tests. Due to the number of tests and results, this paper will discuss only some limited aspects.

### Horizontal Cable Tray Fire

It is interesting to analyse the behaviour of the horizontal cable tray fire to understand its development. Since a lot of data has been acquired, only few of the above introduced tests will be analysed here.

Figure 9 illustrates the mass loss observed in the tests F1-A, F1-B, F2-A and F2-B. The general behaviour observed during the development of the cable tray fire corresponds to different phases. The fire started with an incubation period. This corresponds to a period where the first tray directly impacted by the burner burns while the other trays are only heated up. This incubation phase is more linked to the ventilation rate than to the number of trays: the ventilation feeds the fire source with fresh air, which allows the pyrolyzed gases to be cooled. It should be noted that the ventilation rate was changed during these four tests to ensure a constant depression of 20 Pa. The goal being to assess the ability to ensure smoke confinement. Table 5 illustrates the ventilation renewal rates for these tests. It should also be noted that the test F1-B for which the renewal rate was kept to 20 V/h provided the shortest period of incubation, while the other tests (F1-A, F2-A and F2-B) for which the renewal rate was increased to 60 V/h showed similar incubation periods.

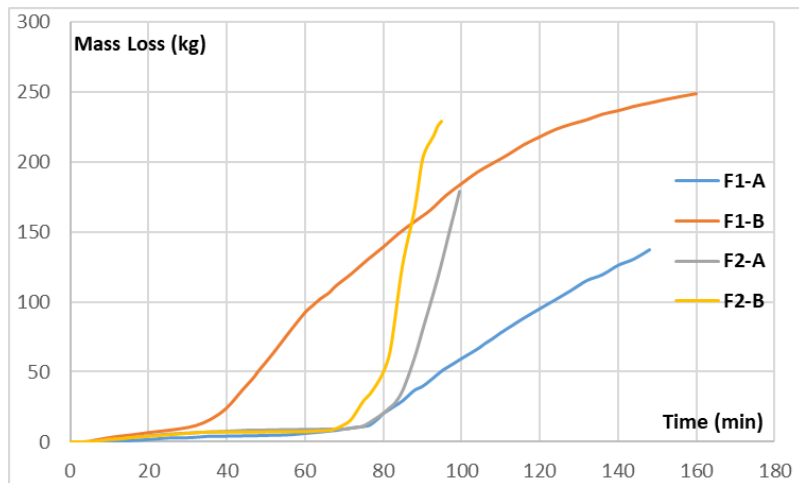


**Figure 9** Mass loss in the tests F1-A, F1-B, F2-A and F2-B

**Table 5** Ventilation renewal rates and their duration for each one of the tests

| Test        | 8 V/h  | 20 V/h  | 60 V/h        |
|-------------|--------|---------|---------------|
| <b>F1-A</b> | 9 min  | 28 min  | until the end |
| <b>F1-B</b> | 9 min  | 141 min | until the end |
| <b>F2-A</b> | 11 min | 35 min  | until the end |
| <b>F2-B</b> | 14 min | 22 min  | until the end |

The second phase corresponds to the growth phase. The beginning of this phase corresponds to the inflammation of the second and third tray. The inflammation accelerates the fire propagation due to the supplementary HRR. This phase regime depends on the ventilation rate but seems to be also linked to the number of trays. It could be observed from Figure 9 that once the inflammation of the gases is initiated, the rate of fire spread is more intense in the case of tests involving five trays. This can be observed through the slopes of the mass loss curves: mass loss is quicker for the tests F2-A and F2-B compared to F1-A and F1-B. The presence of five trays combines two affects: the first one is the quantity of pyrolyzing gases being more important for the cases presenting more quantity of combustible (five trays), the second is linked to ceiling effect. In configuration with five trays, the last tray is drowned in smoke very quickly. Hence, this tray is quickly ignited and contributes to the acceleration of the fire spread.

The third phase is the stabilized phase during which the HRR is quasi constant. This phase is not observed for all the tests since the present tests were extinguished using sprinklers at the end. The sprinklers assessment was one of the objectives of this campaign. Finally, the decay phase corresponds to the decrease of the fire (either natural or after sprinkling).

### ***Fire Propagation***

Figure 10 and Figure 11 present the distribution of the mass loss over the trays in the tests F1-A and F2-A. These two tests were chosen because the ventilation and the incubation time are similar. These figures allow to compare the distribution of the mass loss between the different trays. This information is rarely available in the literature. It was noted that whatever the number of trays constituting the fire source, the mass loss increased from the bottom to the upper tray. The MLR also increased. Indeed, this is attributed to the heating up of the upper trays by the trays below. Propagation is achieved from the lower tray to the upper one and so on until the last tray is reached. Once a tray is ignited; horizontal spreading is observed. The vertical propagation is quicker for the tests with five trays compared to the ones with three trays. This is due to the hotter conditions in the room and the abundance of smoke for the case with five trays compared to the one with three. The smoke contributed to heat up the trays by radiation feedback. This is especially exacerbated for the upper last tray.

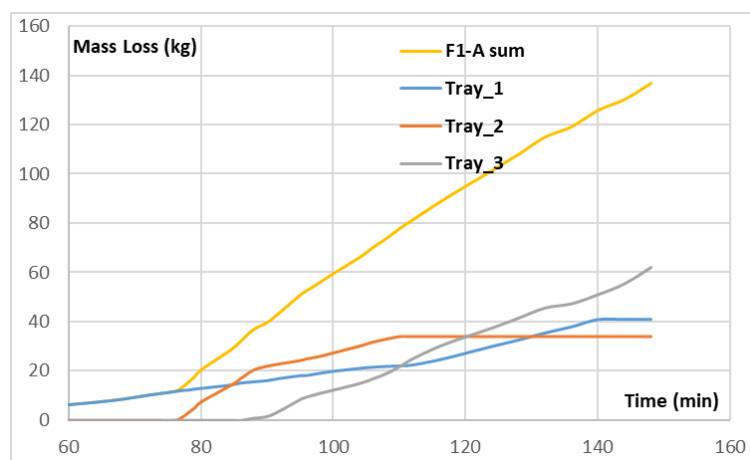


**Figure 10** Mass loss distribution over the three trays in test F1-A

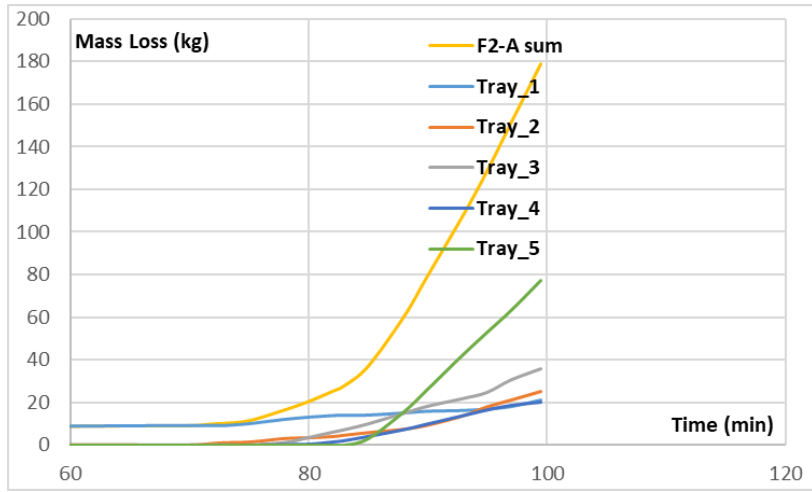


**Figure 11** Mass loss distribution over the five trays in test F2-A

The above discussed fire propagation mechanism seems to validate the well-known V-shape fire propagation scheme discussed in the literature [6], [19]. However, it should be noted that this pattern was not clearly observed for all tests. Figure 12 to Figure 15 illustrate the status of the cables at the end of the tests F1-A, F1-B, F2-A and F2-B, respectively. It should be noted that the V-shape is present for the tests F2-A and F2-B, while this shape is not present for the test F1-A. This latter provided a relatively homogenous propagation on the three trays. Regarding the test F1-B, the pattern resembles to a V-shape, but the orientation is inversed. It should be noted that a careful analysis of the CHRISTIFRE tests [6] leads to the same conclusion. At least half of the horizontal tests in that report did not show the V-shape. However, this is not necessarily an issue from the modelling point of view and the use of a FLASH-CAT model [6] or a similar model since the model could be adapted by adopting e.g. a 0-degree inclination for the flame front.

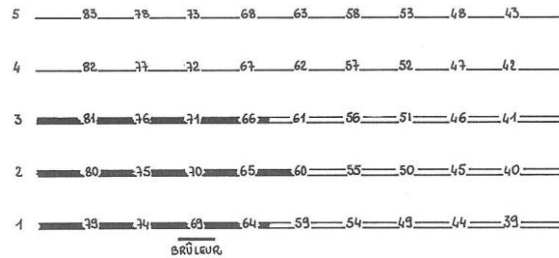


**Figure 12** Illustration of the consumption/degradation status of the cables at the end of test F1-A; numbers correspond to the thermocouples: cables are consumed/destroyed, cables are degraded/damaged, cables are like in their initial state

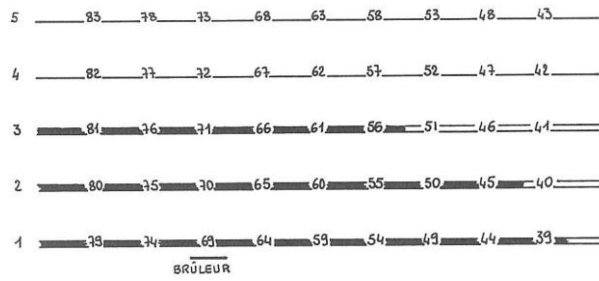


**Figure 13** Illustration of the consumption/degredation status of the cables at the end of test F1-B; numbers correspond to the thermocouples: ——— cables are consumed/destroyed; - - - cables are degraded/damaged, ——— cables are like in their initial state

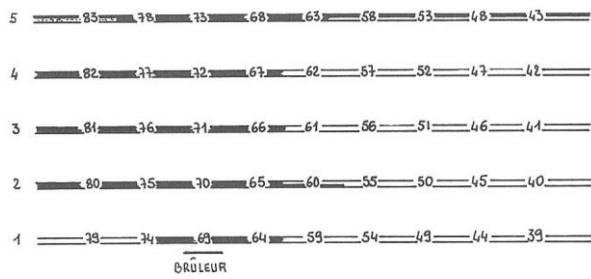


**Figure 14** Illustration of the consumption/degredation status of the cables at the end of test F2-A. The numbers correspond to the thermocouples. ——— the cables are consumed/destroyed; - - - the cables are degraded/damaged; ——— the cables are like in their initial state

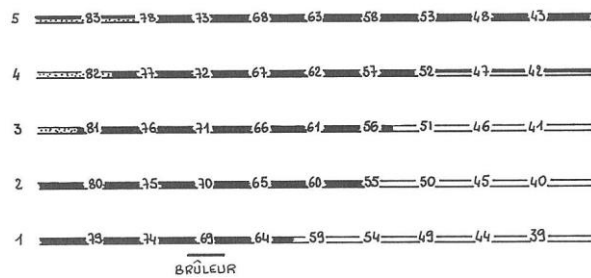


**Figure 15** Illustration of the consumption/degredation status of the cables at the end of test F2-B. The numbers correspond to the thermocouples. ——— the cables are consumed/destroyed; - - - the cables are degraded/damaged; ——— the cables are like in their initial state

### Fire Growth

The fire growth provides important information on the development of a fire and its dynamics. During the different phases of fire progression, the burning rate could be measured. This rate is given in the following Table 6 and Table 7.

**Table 6** Mean burning rates for tests with 5 trays (F2-A and F2-B)

|                                      | Burning Rate [kg/s] | Duration             |
|--------------------------------------|---------------------|----------------------|
| <b>Incubation (initiation) phase</b> | 0.0025              | from 0 to 4200 s     |
| <b>Inflammation phase</b>            | 0.0750              | from 4200s to 4800 s |
| <b>Flashover phase</b>               | 0.2500              | Beyond               |

**Table 7** Mean burning rates for tests with 3 trays (F1-A and F1-B)

|                                      | Burning Rate [kg/s] | Duration              |
|--------------------------------------|---------------------|-----------------------|
|                                      | 0.0067              | from 0 to 1800 s      |
| <b>Incubation (initiation) phase</b> | 0.0500              | from 1800 s to 3600 s |
| <b>Inflammation phase</b>            | 0.0300              | Beyond                |

The burning rates given in the previous tables are “mean burning rates”. It can be observed that they are a function of the number of trays. Indeed, tests with five trays showed a more intense progression of fire due to the ceiling affect but also to a more important quantity of combustibles. Compared to the literature [33], the growth rate for the three trays case corresponds to a fast growth rate, while the five trays case is closer to an ultra-fast behaviour.

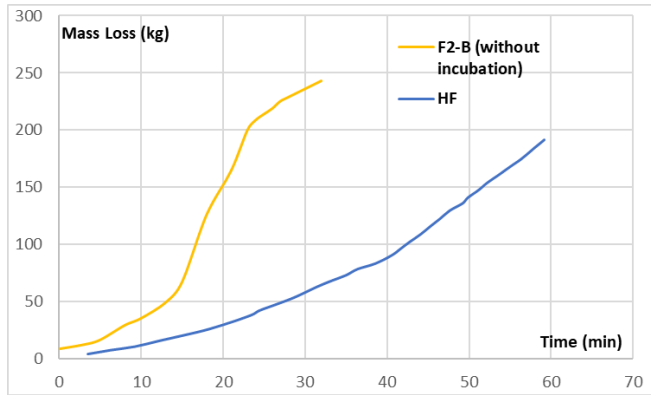
The burning rate is not the same for the different trays. For the first tray (exposed to the burner) it varies between initiation phase and the inflammation phase from 0.0025 kg/s to 0.0150 kg/s. This value is linked to the burner. In fact, similar values were recorded for the other tests for this phase. The burning rate for the trays 2, 3 and 4 starts with the inflammation and is between 0.010 kg/s and 0.0230 kg/s, and could be averaged to 0.017 kg/s. Regarding the fifth tray whose mass loss starts with the flashover phase, the burning rate is more important and corresponds to a mean value of 0.083 kg/s. As discussed above, the latter is affected by the ceiling vicinity through smoke radiation feedback.

### **Cable Type Effect**

The study of different types of cables allowed to compare their behaviour in case of fire. The general behaviour of the HF cables (tests SH1, SH2 and SH3) was found to be similar to that of the PVC cables. Hence, the HF cables presented the same stages than for the PVC cables described above. The main difference observed during the HF tests is the absence of the incubation phase. However, even though the general behaviour was the same, the time scale was different, meaning that the different fire stages were longer for the HF cables. Indeed, HF cables are found to burn slowly compared to PVC cables.

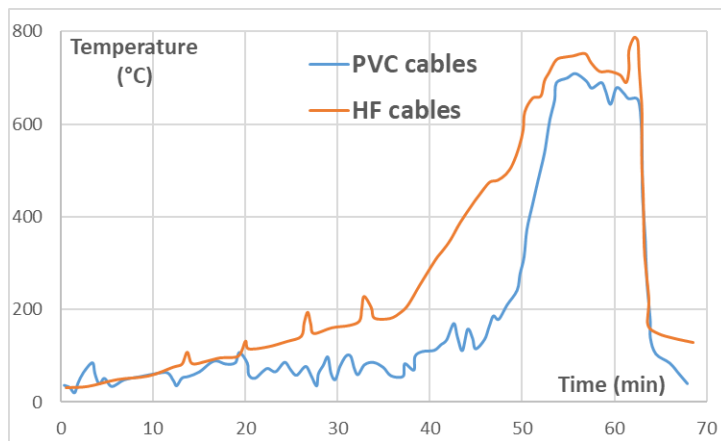
Figure 16 provides a comparison of the mass loss in the F2-B cable tray fire compared to a case with HF cables. The compared HF case is similar in terms of ventilation. The F2-B test curve is shown without the incubation phase to ease dynamics comparison. It is obvious that the dynamics of the PVC cables is much higher than the one of the HF cables. Compared to PVC cables, an increase of the ventilation rate has different consequences on HF cable fire. The time period for increasing the ventilation enhanced the feeding of the combustibles with oxygen allowing an increase of the mass loss. Hence, the competitive effect of pyrolysis gases cooling and fire source feeding with

oxygen acts differently depending on the type of cables. For PVC cables, the cooling of pyrolysis gases is dominant, while it is the reverse for the HF cables.



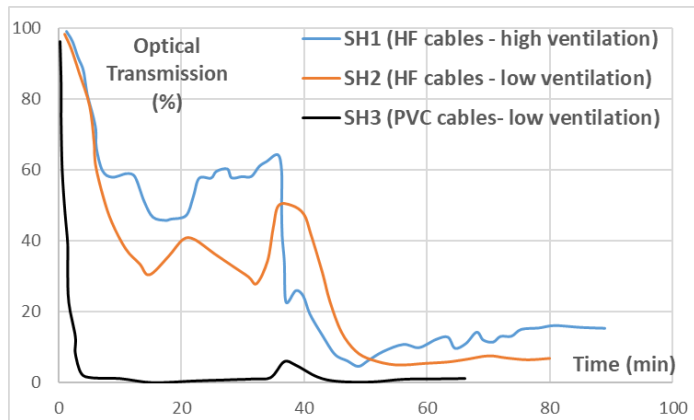
**Figure 16** Mass loss of HF cables compared to the F2-B PVC cables

Figure 17 illustrates the gas temperatures measured below the ceiling for two cases: the first one is the F2-B PVC test, while the second one is a HF test (similar in terms of ventilation and test procedure). It is interesting to note that the temperature environment of both tests is close in the beginning of the curve. Discrepancies start to appear at approx. 20 min, with hotter environment for the case with HF cables. However, the discrepancies are drastically reduced in the stabilized phase when the gas temperatures become comparable. It should be noted that even though the HF cables showed a slower dynamic, these cables produce more energy for the same quantity of burnt combustible material (in other words, the heat of combustion is higher for HF cables compared to PVC ones, which may explain the above-mentioned observation. However, it is interesting that for the well-developed phase, the temperatures become comparable.



**Figure 17** Gas temperature below the ceiling: comparison of two similar cases, one with PVC cables and the other with HF cables

Other advantages of the HF type cables were highlighted during these experiments, among them, the visibility. During these experiments, the HF cables-based cases showed a better visibility with a lower production of smoke. This is expressed by a better optical transmittivity for HF cables as shown in Figure 18. In addition, the smoke produced by HF cables is not corrosive. Of course, these are expected results.



**Figure 18** Optical transmission for the tests SH1 (HF cables), SH2 (HF cables) and SH3 (PVC cables)

### Vertical Cable Tray Fire

The aim of vertical cable tray tests was to determine the conditions to be met for a fire to propagate on a vertical cable tray. Different configurations were tested, including the ignition type, the ignition position, the installation of the cables on the tray, the number of layers on the cable tray and the cable tray configuration, etc. Nine tests were performed and are summarized in the following Table 8.

**Table 8** Vertical cable tests configuration and observations

|                | <b>Test Configuration and Observations</b>   |
|----------------|--|
| <b>Test #1</b> | Blank tests to test the ignition   |
| <b>Test #2</b> | Test with only one layer of cables on the ignited tray. No propagation.  |
| <b>Test #3</b> | The same thing as Test #2 but this time by changing burner's arrangement by tilting it. No propagation is observed. The burner power is considered insufficient.   |
| <b>Test #4</b> | Similar to Test #3 but this time ignition was achieved using a petrol pan. The flames reached the 4 <sup>th</sup> level, however, as soon as the petrol pan was extinguished, the fire went out.   |
| <b>Test #5</b> | Two layers of cables were laid over the ignited tray and the gas burner is used again. Flames reached the 2 <sup>nd</sup> level. At 12 min, there is no flame on the cables. The little that remains is blocked at 80cm from the ground, blocked by a cable tray holder. The test was stopped as the situation was not improving.  |
| <b>Test #6</b> | Similar to Test #5 but with the burner raised at a certain height ( $h = 1.2$ m). This time, the propagation took place over the whole height.   |
| <b>Test #7</b> | In Test #6, it was observed that propagation was hindered by the presence of the cable tray holders and the wires holding the cables. Test #7 is a solution to these problems by removing the obstacles and reducing the number of fixings. The burner is returned to its original position at ground level. Propagation took place over the entire height and more quickly than in test B6. |
| <b>Test #8</b> | The device was modified by positioning a single cable tray parallel to the non-combustible panel at a distance of 10 cm. No propagation was observed in this test.   |
| <b>Test #9</b> | Similar to the previous Test #8, with the burner positioned high up. The fire spread well this time.   |

The analysis of these tests shows that two factors have a significant effect on the propagation of fire in vertical cable trays: the source of ignition (power and location) and the presence of obstacles, even if they are small. It was noticed that two conditions should be met in order to achieve propagation: first, the presence of a critical mass allowing the heat up the neighbouring cables leading to the sustenance of the pyrolysis process resulting in propagation, and second, the chimney or wall effect that allows to channel hot gases towards the cables to be burnt allowing them to heat up. For those tests involving one layer no propagation was observed, while a complete propagation was achieved for the case with two cable layers (spaced by 5 cm) without obstacles. The same conclusion could be drawn for the test with one layer parallel to the non-combustible panel.

The chimney effect (or wall effect) was particularly visible in the last test (one cable layer parallel to the panel). Fire propagation was observed to be more pronounced in the wall side since the flame front in the wall side preceded the opposite one by at least 0.5 m. This chimney effect could also explain the absence of propagation for tests where small obstacles were present (trays holder or even wires fixing the cables). The chimney effect is normally taking place also between the cables; however, in such a situation, it is neutralized by the obstacles.

Figure 19 and Figure 20 show the surface temperatures at the first mast cable, at the first mast copper discs, and at the second mast cable, respectively, for the five measurement levels.

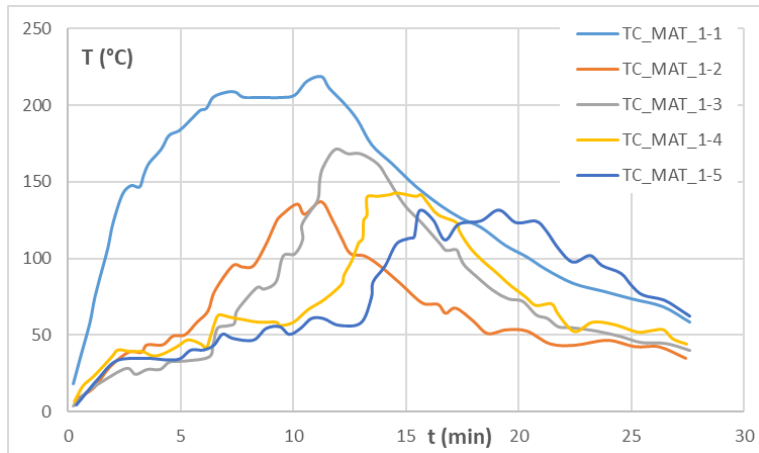


**Figure 19** Surface temperature: first mast target cable (Test #7 for illustration)

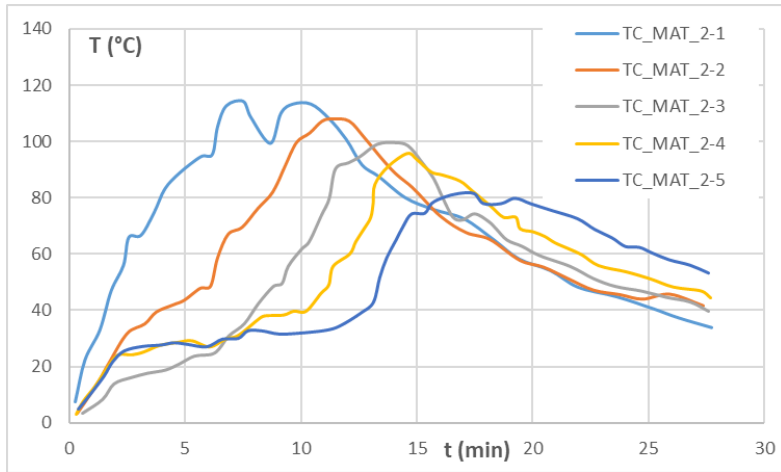


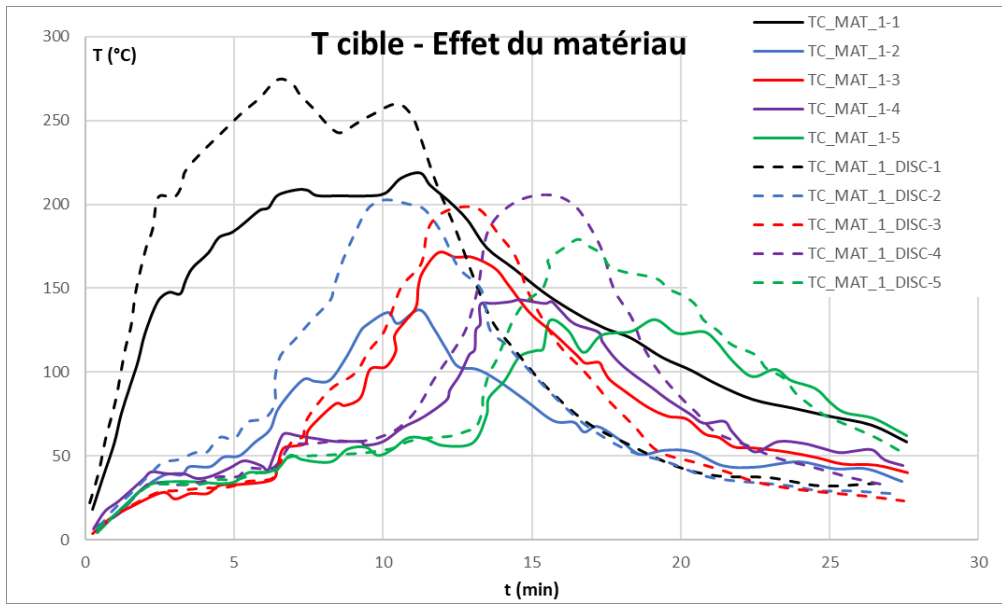
**Figure 20** Surface temperature: second mast target cable (Test #7 for illustration)

First, the shift in the peak temperature of the different thermocouples indicates the flame propagation. The temperature levels reached are almost similar, particularly for the targets of the first mast, except for the first target. This can be interpreted by the presence of a propagating flame zone, which would mean that an equivalent level of power would attack the target when it is in front of it and then progress towards the next target. Only the first target on the first mast deviates from this behaviour. This target is also exposed to the radiation of the burner. Thus, taking the burner into account seems important for reproducing the behaviour of the close targets in case of modelling.

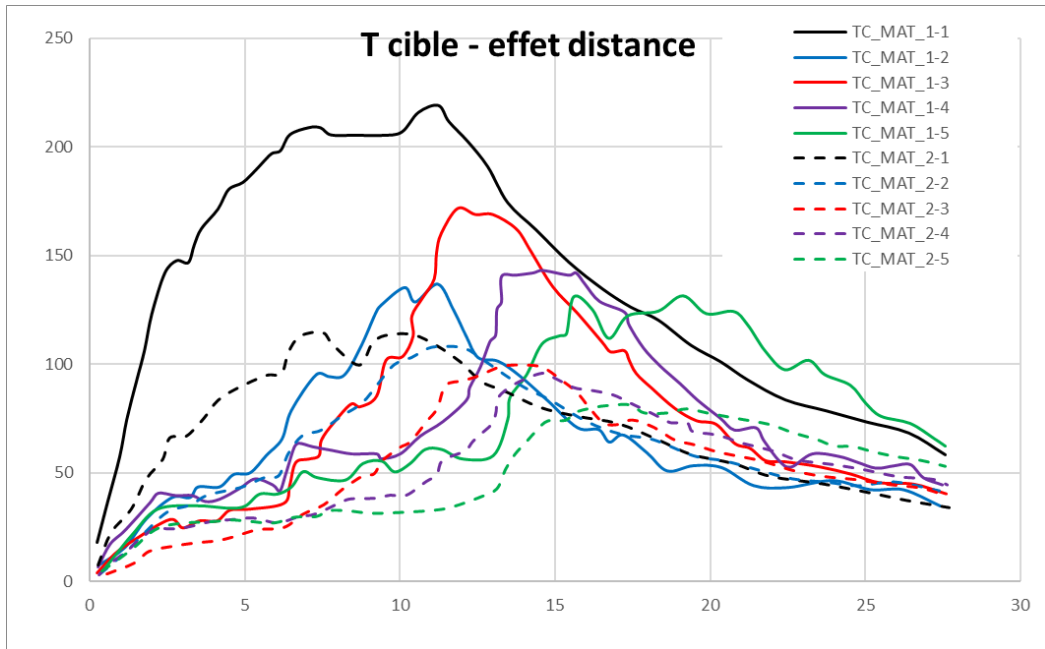
The targets of the second mast show a slightly different behaviour. Similarly, the shift of the temperature peaks can be seen. But this time, the value of this peak decreases as the flame spreads. This is due to a view factor effect becoming more important for the second mast. On the other hand, the first target of the second mast seems to be little affected by the presence of the burner.

Figure 21 illustrates the effect of the nature of the material on the target temperatures on mast 1. During the growth phase, the targets show similar dynamics, with a slight difference resulting from the higher thermal conductivity of the copper discs. The temperature peaks are in the same places, with higher values for the copper discs, again due to a higher conductivity. However, during the decay phase, this higher conductivity leads the copper discs to discharge their energy more quickly. Thus, the thermal inertia are larger for the electric cables than for the copper discs. This is reflected in the crossing of the temperature curves in the decay phase.

In addition to the nature of the material, there is also an effect related to the thickness of the target. As the thickness of the copper disc is not exactly known (a few millimetres), the given diagrams indicate that it is much smaller than the cable. This effect will tend to further reduce the thermal inertia of the copper discs.



**Figure 21** Effect of material type on target temperatures for cable targets and copper discs on the first mast (Test #7 for illustration)



**Figure 22** Distance effect: comparison of surface temperatures of mast 1 and mast 2 cables (Test #7 for illustration)

Using similar targets at different distances illustrates the effect of distance on target temperatures. This effect is illustrated in Figure 22 showing a comparison of the surface temperatures of the cables placed on the two masts. As expected, the distance strongly reduces the aggression of the targets, despite the relatively small distance between the two masts. It is interesting to note that the temperature difference is not constant. Indeed, it is likely that two factors play a role in reducing the target temperature, namely the view factor and the power.

## Spread Velocity

The spread velocity is an important quantity, particularly for estimating the exposure time of targets. It is also important for predicting the HRR curve using models (e.g., FLASH-CAT).

Flame propagation was achieved through the progression of a burning area estimated to be about 1 m. The flame circulation is also visible in the temperature curves. Again, the passage of the flame can be linked to the peak observed in the curves. Two methods have been used to determine the spread velocity. The first one is based on observation of the burning area progression during the experiments (observation made by the experimentalists in the test report). The second one uses temperature curves. Figure 23 shows the temperatures measured on the burning tray at different levels for Test #7. The temperature peaks may correspond to the passage of flames and were used to estimate the flame spread velocity. The estimated velocities by the two methods are given in Table 9.

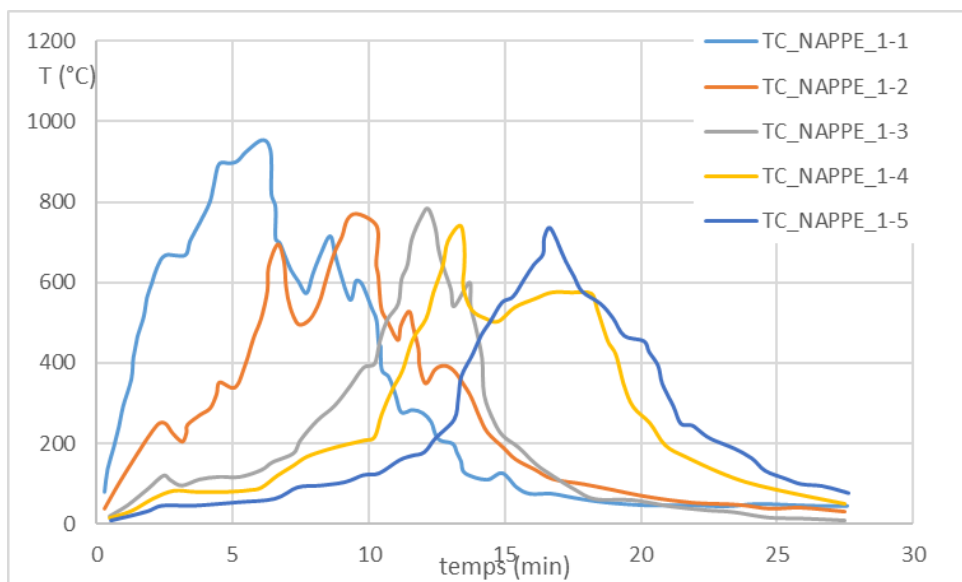


**Figure 23** Gas temperature on the burning tray (Test #7 for illustration)

**Table 9** Spread velocity measured by observation and using the gas temperature curves

|                | Spread Velocity by Observation [m/s] | Spread Velocity Using Gas Temperature Curves [m/s] |
|----------------|--------------------------------------|--|
| <b>Test #6</b> | –                                    | 0.0025   |
| <b>Test #7</b> | 0.0058                               | 0.0066   |
| <b>Test #9</b> | 0.0052                               | 0.0045   |

We note that these speeds obtained by the two methods are consistent. However, it looks more relevant to rely on the velocities obtained from the temperature profiles, which are less subject to the assumptions and uncertainties of the observations. It should also be noted that the orders of magnitude are nevertheless similar. In conclusion, the spread velocity varies between 0.0025 and 0.0066 m/s.

It is interesting to compare the velocities estimated here with those available in the literature, including those reported by NIST in NUREG/CR-7010 v2 [27]. In their test campaign, they devoted the second part of the report to the study of cable tray fires in vertical

configuration. Only five of the 17 experiments experienced the fire propagate to the top of the cables. Two values were given for the spread velocity: 0.007 and 0.014 m/s.

Compared to the present EDF test results, literature shows higher velocities. Different factors may justify this discrepancy. First, it should be noted that the velocities given in NUREG/CR-7010 v2 [27] have not been actually measured, but only based on the total duration of the test and the distance travelled. Furthermore, both spread velocities in [27] seem to be rounded and correspond to an order of magnitude. In addition, the cables that have been studied were different, as well as the tests configuration (cables loading, cables arrangement, etc). The EDF tests also presented longer cables compared to the experiments in [27] (5.0 m vs 3.6 m). Hence, the flames velocity in the tests presented in [27] probably had not stabilized yet and were in the acceleration phase, explaining the higher velocities. Moreover, it should be noted that for the calculation of the HRR with FLASH-CAT, the NIST retained the highest speed for all the tests (50 m/h).

Comparisons, which will not be detailed here, showed that the FLASH-CAT model [6] and the EDF vertical cable tray model (see ISO 18195 [31], [32]) obtained comparable conservative results on the MLR when applied to these experimental tests (EDF tests and NIST tests).

### **Burning Area**

The burning area could be estimated from the observation that have been made during the experiments. The position of the base and the top of the burning area were recorded at some time intervals. However, the information we have is the instant when a given level in reached by the top of the flaming region, and the instant when the base is reaching the same level. Hence at a given instant, we do not know the position of the base and the top. In order to make the estimation, the following method has been adopted: for example, in Test #9, at the time 6 min the top of the flame is at level 3. Using the spread velocity of the flaming region base (determined from observations), the location of the base of the ignited zone at that time can be estimated (here we know the instant, e.g., where it was at level 1 or 2). In this way, the size of the burnt area is determined. We do this for the different levels.

Table 10 and Table 11 provide the results of the estimated burning area size for Test #7 and Test #9. We note that the burning area is not constant and increases for Test #7. For Test #9, it increases and then decreases. This variation in the burning area is linked to the local behaviour of the fire. It is interesting to note that even though the test configuration is different, the same order of magnitude is obtained. For both tests combined, the size of the burnt area varies between 0.4 and 1.4 m. If we look for an average value, we can say that it is about 1 m.

**Table 10** Burning area for Test #7 (based on observation of the position of top and base of the burning area)

| Test #7   |                         |                          |                         |
|-----------|-------------------------|--------------------------|-------------------------|
| Instant   | Top of Burning Area [m] | Base of Burning Area [m] | Burning Area Length [m] |
| 14 min 30 | 4.50                    | 2.90                     | 1.60                    |
| 12 min    | 3.50                    | 2.40                     | 1.1000                  |
| 10 min 30 | 2.50                    | 2.10                     | 0.4                     |
| 6 min     | 1.50                    | 1.20                     | 0.3                     |

**Table 11** Burning area for Test #9 (based on observation of the position of top and base of the burning area)

| Test #9  |                         |                          |                         |
|----------|-------------------------|--------------------------|-------------------------|
| Instant  | Top of Burning Area [m] | Base of Burning Area [m] | Burning Area Length [m] |
| 13 min   | 4.50                    | 3.66                     | 0.84                    |
| 7 min 30 | 3.50                    | 2.12                     | 1.38                    |
| 6 min    | 2.50                    | 1.69                     | 0.81                    |

### **Flame Height**

From the above information, it is possible to deduce the flame height. It can be estimated as the distance between the base of the burning area and the flame tips. However, as the times of the observation do not necessarily correspond, one is forced to use the estimated speed of propagation to match them. It is therefore an order of magnitude.

Table 12 and Table 13 below provide an estimation of the flame height. Here the flame height is greater in Test #9. This is mainly due to the higher propagation speed, especially of the flame tips. In other words, the differences are linked to the flame tips velocities more than to the size of the ignited area. The behaviour of the two tests is different since for Test #7 the flame height seems to be quite constant, while it is increasing for Test #9, even though the order of magnitude is similar. It should be noted that Test #9 includes the effect of the wall which may explain higher flame heights favoured by a chimney effect.

**Table 12** Flame height estimation for Test #7 (based on observation – includes the burning area)

| Test #7 |                 |                       |                  |
|---------|-----------------|-----------------------|------------------|
| Instant | Flames Tips [m] | Burning Area Base [m] | Flame Height [m] |
| 12 min  | 4.50            | 2.50                  | 2.00             |
| 8 min   | 3.50            | 1.56                  | 1.91             |

**Table 13** Flame height estimation for Test #9 (based on observation – includes the burning area)

| Test #9 |                 |                       |                  |
|---------|-----------------|-----------------------|------------------|
| Instant | Flames Tips [m] | Burning Area Base [m] | Flame Height [m] |
| 5 min   | 4.50            | 1.41                  | 3.09             |
| 3 min   | 3.50            | 0.85                  | 2.65             |

## **CONCLUSION**

The objective of this paper was to share new insights from the large-scale cable tray fire experiments performed by EDF in the 1980s for horizontal and vertical cables tray fires. The discussion of the results focused on some interesting aspects of cable fire trays in

both configurations. The general behaviour of the horizontal cable trays was discussed, with a vertical and horizontal fire propagation. The well-known V-shape pattern was only observed for some of the tests. The influence of the ventilation depends on the cable type. However, for PVC cables the ventilation increase led to the cooling of the environment resulting in fire slowing down, while the feeding of the fire source with oxygen took over for HF cables. The vicinity of the ceiling was found to have an influence on the fire dynamics by an increasing burning rate. This effect is explained by the smoke radiation feedback to the combustible surface. In comparison to PVC cables, HF cables show a slower dynamic and propagation, better visibility, less and non-corrosive smoke.

Regarding the vertical cable tray fires, the fire ignition/propagation was difficult to obtain. The presence of small obstacles hindered the propagation of the fire. Reversely, the chimney effect favoured fire propagation. Fire spread velocities were measured and found to be in the same order of magnitude as those found in the literature. The burning area as well as the flame height were estimated.

Some links to recent models (FLASH-CAT [6], ISO 18195 [31], [32]) were also proposed for vertical cable trays in the present article.

Finally, this test campaign covers many aspects that are still questioned in the recent literature on cable fires. It appeared therefore interesting to share these results with the community in order to complete the experimental information with respect to the important issue of full-scale electrical cable tray fire behaviour.

It is intended to go further in comparing those experimental results to the predictions (e.g., HHR per unit area, vertical and horizontal spread velocities, etc.) by current models.

## REFERENCES

- [1] Organisation for Economic Co-operation and Development (OECD) Nuclear Energy Agency (NEA), Committee on the Safety of Nuclear Installations (CSNI): OECD/NEA FIRE Database 2019:01, Paris, France, May 2021 (limited to FIRE member countries only).
- [2] United States Nuclear Regulatory Commission (U.S. NRC): Cable Fire at Browns Ferry Nuclear Power Station, NRC Bulletin BL-75-04, Washington, DC, USA, March, 1975.
- [3] National Fire Protection Association (NFPA): NFPA-70 – National Electric Code, 2011 Edition, Quincy, MA, USA, 2008.
- [4] Wang, Z., and J. Wang: An experimental study on the fire characteristics of new and aged building wires using a cone calorimeter, Journal of Thermal Analysis and Calorimetry, Vol. 135, No. 6, pp. 3115-3122, 2019.
- [5] Martinka, J., et al.: Assessing the fire risk of electrical cables using a cone calorimeter », Journal of Thermal Analysis and Calorimetry, Vol. 135, No. 6, pp. 3069-3083, 2019.
- [6] McGrattan, K., et al.: Cable Heat Release, Ignition, and Spread in Tray Installations During Fire (CHRISTIFIRE) Phase 1: Horizontal Trays, NUREG/CR-7010, Vol. 1, prepared for United States Nuclear Regulatory Commission (U.S. NRC) Office of Nuclear Regulatory Research, Washington, DC, USA, July 2012, <https://www.nrc.gov/docs/ML1221/ML12213A056.pdf>.
- [7] Hirschler, M. M.: Electrical Cable Fire Hazard Assessment with the Cone Calorimeter, ASTM International, West Conshohocken, PA, USA, 1992.

- [8] Meinier, R., et al.: Fire behavior of halogen-free flame retardant electrical cables with the cone calorimeter, *Journal of hazardous materials*, Vol. 342, pp. 306-316, 2018.
- [9] Magalie, C., et al.: Fire behaviour of electrical cables in cone calorimeter: Influence of cables structure and layout, *Fire Safety Journal*, Vol. 99, pp. 12-21, 2018.
- [10] Murer, L.: Influence of model assumptions on charring polymer decomposition in the cone calorimeter, *Journal of Fire Sciences*, Vol. 36, No. 3, pp. 181-201, 2018.
- [11] Matala, A.: Methods and applications of pyrolysis modelling for polymeric materials, VTT Technical Research Centre of Finland, Espoo, Finland, 2013.
- [12] Al-Sayegh, W. A.: PVC cable fire toxicity using the cone calorimeter, in: *Fire Science and Technology 2015*, Springer, Berlin, Germany, pp. 175-182, 2017.
- [13] Zhang, H., et al.: Study on Combustion Characteristics of Cable Based on Cone Calorimeter, *Energies*, Vol. 15, No. 5, p. 1904, 2022.
- [14] Chatenet, S., et al.: Reaction to fire of polymethylmethacrylate and polyvinylchloride under reduced oxygen concentrations in a controlled atmosphere, *Journal of Fire Sciences*, 40(4): 2022, <https://doi.org/10.1177/07349041221092968>.
- [15] Qu, H., et al.: Using cone calorimeter to study thermal degradation of flexible PVC filled with zinc ferrite and Mg (OH) 2, *Journal of Thermal Analysis and Calorimetry*, Vol. 115, No. 2, pp. 1081-1087, 2014.
- [16] Rao, B. N., and R. Arunjothi: Assessing smoke and heat release during combustion of electric cables using cone calorimeter, in: *Proceedings of the 9th International Conference on Insulated cables — 4JICABLE*, pp. 21-24, Versailles, France, 2015,.
- [17] Grayson, S. J.: Assessing the fire performance of electric cables (FIPPEC), *Fire Mater*, Vol. 25, No. 2, pp. 49-60, March 2001, <https://doi.org/10.1002/fam.756>.
- [18] Klamerus, L. J.: Preliminary Report on Fire Protection Research Program Fire Barriers and Fire Retardant Coatings Tests, Sandia National Laboratories (SNL), Albuquerque, NM, USA, 1978.
- [19] Nowlen, S. P.: A Summary of Nuclear Power Plant Fire Safety Research at Sandia National Laboratories 1975-1987, SAND-89-1359, Sandia National Laboratories (SNL), Albuquerque, NM, USA, and NUREG/CR-5384, United States Nuclear Regulatory Commission (U.S. NRC), Washington, DC, USA., December 1989. <https://doi.org/10.2172/5227320>.
- [20] Riches, W. M.: Report on full-scale horizontal cable tray fire tests, FY 198, Fermi National Accelerator Laboratory, Batavia, IL, USA, 1988.
- [21] Mangs, J., an O. Keski-Rahkonen: Full-scale fire experiments on vertical and horizontal cable trays, VTT Technical Research Centre of Finland, Espoo, Finland, 1997.
- [22] Röwekamp, M., J. Dreisbach, S. Miles, et al.: International Collaborative Fire Modeling Project (ICFMP) - Summary of Benchmark Exercises 1 to 5; GRS-227, Gesellschaft für Anlagen- und Reaktorsicherheit (GRS) mbH, ISBN 978-3-939355-01-4, Köln, Germany, September 2008, <http://www.grs.de/content/grs-227-international-collaborative-fire-modeling-project-icfmp>.

- [23] Riese, O., D. Hosser, and M. Röwekamp: Evaluation of Fire Models for Nuclear Power Plant Applications, Benchmark Exercise No. 5: Flame Spread in Cable Tray Fires, International Panel Report, Gesellschaft für Anlagen- und Reaktorsicherheit (GRS) Report Number GRS-214, ISBN 978-3-931995-81-2, Köln, Germany, November 2006, <http://www.grs.de/en/content/grs-214-evaluation-fire-models-nuclear-power-plant-applications>.
- [24] Li, L., et al.: An enhanced fire hazard assessment model and validation experiments for vertical cable trays, Nuclear Engineering and Design, Vol. 301, pp. 32-38, 2016, <https://doi/10.1016/j.nucengdes.2015.12.034>.
- [25] Huang, X., et al.: An improved model for estimating heat release rate in horizontal cable tray fires in open space, Journal of Fire Sciences, Vol. 36, No. 3, pp. 275-290, 2018.
- [26] Huang, X., et al.: Burning behavior of cable tray located on a wall with different cable arrangements, Fire and Materials, Vol. 43, No. 1, pp. 64-73, 2019.
- [27] McGrattan K. B., and et S. D. Bareham: Cable Heat Release, Ignition, and Spread in Tray Installations During Fire (CHRISTIFIRE) Phase 2: Vertical Shafts and Corridors, NUREG/CR-7010, Vol. 2, prepared for United States Nuclear Regulatory Commission (U.S. NRC) Office of Nuclear Regulatory Research, Washington, DC, USA, December 2013, <https://www.nrc.gov/docs/ML1334/ML13346A045.pdf>.
- [28] Zavaleta, P., et al.: Multiple horizontal cable tray fire in open atmosphere, in: Thirteenth International conference of the Fire and Materials, pp. 57-68, San Francisco, CA, USA, 2013.
- [29] Zavaleta, P., and L. Audouin: Cable tray fire tests in a confined and mechanically ventilated facility, Fire and Materials, Vol. 42, No. 1, pp. 28-43, 2018.
- [30] Gautier, B., M. Mosse, and O. Eynard: EPRESSI Method–Justification of the Fire Partitioning Elements, in: Proceedings of the Sixth International Seminar on Fire & Explosion Hazards, p. 374-385, 2011.
- [31] Gautier, B., and D. Joyeux: SO/DIS 18195: A New Standard for Justification of Nuclear Power Plants Fire Barriers, in. Röwekamp, M., H.-P. Berg (Eds.): Proceedings of SMiRT 24, 15th International Seminar on Fire Safety in Nuclear Power Plants and Installations, October 4-5, 2017, Bruges, Belgium, GRS-A-3912, Gesellschaft für Anlagen- und Reaktorsicherheit (GRS) gGmbH, Köln, Germany, December 2017, <https://www.grs.de/en/publication/grs-3912>.
- [32] International Standards Organisation (ISO): Method for the justification of fire partitioning in water cooled nuclear power plants (NPP), ISO International Standard, ISO 18195:2019(E), Geneva, Switzerland, 2019.
- [33] Karlsson, B., and J. Quintiere: Enclosure Fire Dynamics. CRC Press, Boca Raton, FL, USA, 1999.

# Overview of the OECD PRISME 3 Project – Experimental Campaign Description and Main Results

Sylvain Suard\*, Hugues Prétrel, Jérémie Séguillon, Pascal Zavaleta, Philippe March,  
and Joëlle Fleurot

Institut de Radioprotection et de Sûreté Nucléaire (IRSN), PSN-RES/SA2I, Cadarache,  
St Paul-Lez-Durance, France

## ABSTRACT

This OECD/NEA PRISME 3 (French acronym for *Propagation de l'Incendie lors de Scénarios Multi-locaux Élémentaire*) research program on confined and mechanically ventilated fires, has been carried out from 2017 to 2022. During this project, three campaigns have been conducted. The first campaign, S3 for Smoke Stratification and Spread, was defined in order to propose original and complex configurations with regard to the propagation of smoke and the gas stratification. The second campaign, ECFS (Electrical Cabinet Fire Spread), implemented open and confined electrical cabinet fires to study the spread of the fire to surrounding cabinets. Finally, the last campaign, CFP (Cable Fire Propagation), was dedicated to the study of electric cable fires. The first part complements the achievements of previous PRISME experimental programs by studying new configurations related either to the fire source layout or to the installation itself. The second part was dedicated to the study of propagation over long cable trays. An original and complex configuration was implemented in order to be able to determine quantities of interest, such as the mass loss rate (MLR) or the heat release rate (HRR) throughout all the fire duration.

The objectives of the PRISME 3 Project are introduced and the experimental campaigns are briefly described. The significant and valuable results for some selected tests of each campaign, either in terms of new knowledge for fire safety studies or in terms of validation of simulation tools, are presented.

## INTRODUCTION

Fire hazard analyses and probabilistic fire safety analyses have demonstrated that fires may cause significant damages in nuclear power plants (NPPs). Fire modelling is nowadays widely applied by licensees or technical safety organisations to assess the consequences of fires to the safety of NPPs. Thereby, one important aspect is the availability of verified and validated fire models for such fire scenarios. On the other hand, certain configurations are too complex to be simulated. In this case the judgment of the experts could refer to the state-of-the-art, by using fire experiments carried out on large scales. In the frame of these issues, several member countries of the Organization for Economic Co-operation and Development (OECD) Nuclear Energy Agency (NEA) Committee on the Safety of Nuclear Installations (CSNI) expressed their interest in continuing in a joint international research project on the topic of mechanically ventilated fires. By this way, and from the experimental findings and modelling considerations of the previous PRISME Projects [1], [2], the outlines of the PRISME 3 experimental program were defined by including recommendations for addressing some specific phenomena not studied in detail in the past programs [3]. Thus, the PRISME 3 Project aimed at addressing phenomena, such as smoke stratification and spread within a mechanically ventilated

large-scale facility, fire propagation between electrical cabinets, and electrical cable tray fires, and at providing answers to various issues of interest regarding nuclear safety.

Institutions from in total eight member countries have joined the PRISME 3 Project: Belgium (Bel V and Tractebel-ENGIE), Finland (Technical Research Centre VTT), France (IRSN as Operating Agent and Électricité de France – EDF), Germany (Gesellschaft für Anlagen- und Reaktorsicherheit – GRS), Japan (Nuclear Regulation Authority – NRA and Central Research Institute of Electric Power Industry – CRIEPI), Republic of Korea (Korea Institute for Nuclear Safety – KINS and Korea Atomic Energy Research Institute – KAERI), the United Kingdom (Office for Nuclear Regulation – ONR) and the United States of America (United States Nuclear Regulatory Commission – U.S. NRC). The duration of this OECD/NEA project was six years, from 2017 to 2022.

The experimental program with the three test campaigns is described in the next section. Safety issues and scientific objectives of the campaigns have been described in [3] for the definition of the program. A total of 21 fire tests were planned at large scale, and a budget was consolidated for an extra campaign with complementary tests. In this way, two cable fire tests in open atmosphere were defined by the PRISME 3 Program Review Group (PRG) and the Management Board (MB) to be carried out as part of a joint Cable Benchmark Exercise together with the OECD/NEA FIRE (Fire Incidents Records Exchange) Database Project. More details are given in [4]. Another campaign, not described here, dedicated to studying the functioning of a network of an automatically actuated fire detection system was also defined by the members of the PRISME 3 Project.

## PROGRAM DESCRIPTION

### **Smoke Stratification and Spread (S3) Tests**

The objective of the PRS3-S3 campaign was to study new configurations regarding smoke propagation in a mechanically ventilated multi-room facility. Three topics have been identified: multiple propagation modes, multiple fire sources, and elevated fire sources. A total number of six large-scale fire tests were realized in the DIVA facility of IRSN including two tests for each of the first two topics, one test for the third topic, and one reference test. The configurations of the ventilation, the fuel type and its location are summarized in [3]. The lubricant oil DTE MOBIL Medium was selected to study the propagation of smoke inside the facility because it can be representative of a real scenario. For the tests with multiple fire sources, dodecane fuel ( $C_{12}H_{26}$ ) was used in order to ensure pool ignition of both pools at the same time. Dodecane fuel has also been used for the elevated fire test to avoid facing safety constraints regarding preheating of the fuel at an elevated position.

### ***Multiple Propagation Mode Tests (Series A)***

Two tests A1 and A2 considered the issue of “Multiple Propagation Modes” (see schematic configurations in Figure 1 hereafter). Four rooms were involved with two propagation modes, “doorway” and “vent”. The fire source was located in the room R3 which allowed the study of the two modes of propagation, “vent” and “doorway”. The first test, A1, aimed at investigating a configuration with no mechanical ventilation in the fire room (room R3). The flows entering the fire room, through the doorway and the vent were mainly governed by natural convection mode. The adjacent rooms R1 and R2 were also not ventilated. Only the upper room, R4, was ventilated to ensure the feeding of oxygen in the fire room. This configuration reproduced a real situation of the breakdown of the ventilation for an assembly of three rooms, connected to another room zone (via a vent) for which the ventilation remains in operation. The second test, A2, focused on smoke propagation in confined and non-ventilated rooms, considered here as so-called “dead

zones". This low-speed propagation mode is complex to simulate and relevant for the validation of fire models.

The fire source was positioned at the centre of the room R3. This fire room was the only mechanically ventilated room. The three other rooms were not ventilated, the inlet and outlet branches being closed. For these two tests, the opening vent between the rooms R3 and R4 was a  $1 \text{ m}^2$  section, and the doorways between the rooms R1 and R2 and R2 and R3 were  $0.79 \text{ m} \times 2.1 \text{ m}$  rectangular sections. The fire source was positioned off-centre in one corner of the room R3.

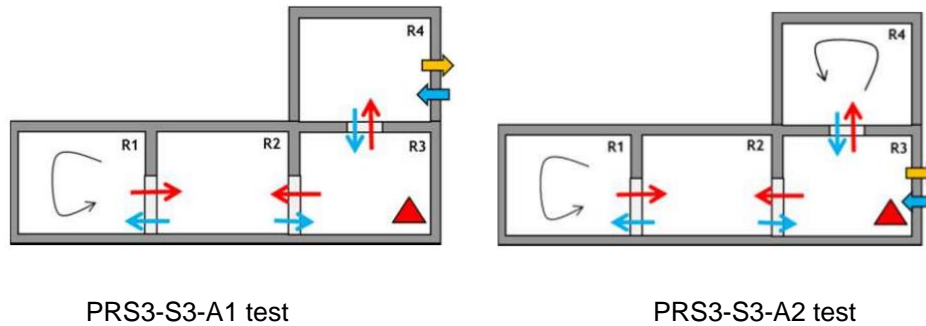


**Figure 1** Configuration of the fire tests series A in the DIVA facility

#### **Multiple Fire Source Tests (Series B)**

The second topic of interest concerned the issue of multiple fire sources, simulating for example a seismically induced fire event and its consequences on smoke propagation. The fire scenario involved two fire sources ignited simultaneously and located in two adjacent rooms or in two rooms separated by another one. The distance between the fires was a key parameter, determining different combustion regimes with or without interaction. Two tests, B1 and B2, were conducted, and three rooms were involved (R1, R2 and R3), with one propagation mode through open doorways (cf. Figure 2). The test B1 considered no interaction between the two fire sources which were centred in the rooms R1 and R3. The purpose of the second test, B2, was to study the interaction between the two fire sources and the consequence of this configuration on the doorway flow and gas stratification in the third room. For both tests, the two fire sources were  $0.56 \text{ m}^2$  dodecane liquid pools, centred in the rooms.

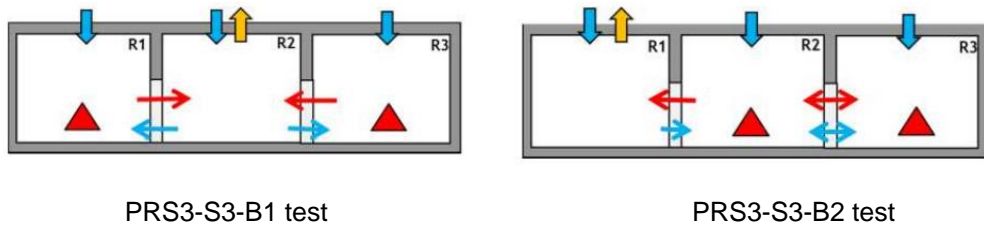


**Figure 2** Configuration of the fire tests series B with  $0.56 \text{ m}^2$  dodecane pool fires

#### **Elevated Fire Source Tests (Series C)**

The C1 test addressed the issue of elevated fire source. Three rooms (R1, R2 and R3) were involved with one propagation mode through open doorways. The fire was a  $0.56 \text{ m}^2$  dodecane pool fire located at 2 m height from the floor at the centre of room R3 (cf. Figure 3). The objective was to investigate the fuel combustion regime, the possible

flame displacement towards the adjacent room through the doorway, and the thermal stratification in the fire room. The ventilation configuration was identical to that of test B1 in order to compare these tests to the reference test that was performed as a qualification test. Thus, this qualification test (named B0) was identical to the test C1, except the fire source that was located on the floor of the room R3.

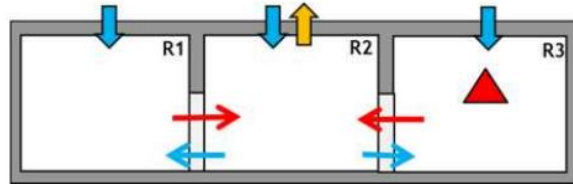


**Figure 3** Configuration of the fire test series C with an elevated pool fire of  $0.56 \text{ m}^2$

### Electrical Cabinet Fire Spread (ECFS) Tests

The main objective of the ECFS test campaign was to investigate the ability of a fire to propagate from an electrical cabinet with open doors to neighbouring cabinets with doors being closed, located next to or in front of the main cabinet (cf. Figure 4). The effects of the environment and of the cable type, located on an upper cable tray and in a false floor, on the fire propagation were also studied. To achieve this, four tests were conducted in open atmosphere in the SATURNE facility and four other tests were performed in the confined and mechanically ventilated DIVA facility. For each environment, the adjacent and opposite configurations, using two types of cables, were implemented. Each of the cable trays was filled with cable samples, arranged tightly. Both types of cables corresponded to low-qualified electric cables made of polyvinyl chloride (PVC) or to well-qualified electric cables with a halogen-free flame-retardant (FRNC) insulation. All the cable samples were 3 m long. The PVC and FRNC cables were identical to the cables G and A, used in the previous PRISME 2 Project. The main characteristics of the cables are specified in Table 1. For all tests, the open-doors cabinet identified as fire source, was ignited by a propane gas burner, located at its bottom, which provided a fire power of about 10 kW for a duration of 5 min.

In addition to this campaign, some support tests were performed in the SATURNE facility to quantify the effects of some parameters on the fire spread. The main results are provided in [5] and [6].

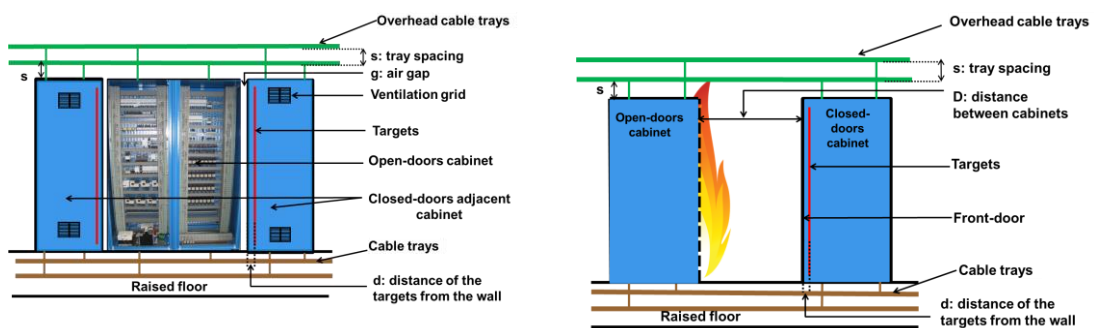


**Figure 4** Schemes of adjacent (left) and opposite (right) cabinet configurations

**Table 1** Main characteristics of the electric cables used in the ECFS campaign

| Cable Type     | ECFS Tests     | Cable Specification (Diameter, Weight)                    | Polymeric Material (Flame Retardant)                                 | Supplier Reference                  | Cable Reaction to Fire (IEC and NF Standard Tests)   |
|----------------|----------------|---|--|-------------------------------------|--|
| <b>Cable G</b> | S1, S3, D1, D3 | 5 x 25 mm <sup>2</sup> power cable (28 mm, 2000 kg/km)    | PVC <sup>2</sup> , PE (halogenated, chlorine)                        | NYM-J 5 x25 mm <sup>2</sup> RM GRAU | IEC <sup>3</sup> 60332-1 (C2)  |
| <b>Cable A</b> | S2, S4, D2, D4 | 12 x 1.5 mm <sup>2</sup> control cable (20 mm, 540 kg/km) | EVA <sup>4</sup> , PE <sup>5</sup> (halogen-free, ATH <sup>6</sup> ) | NU-SHX(ST)HX 1 kV                   | NF <sup>7</sup> C 32-070/C1, IEC 60332-1 (C2), IEC 60332-3-22, -23, -24 IEC 61034-2, IEC 60754-2 |

### Adjacent Configurations

The adjacent electrical cabinet setup was composed of an open-doors central cabinet with two adjacent closed-door cabinet modules, two overhead cable trays, and a raised floor located below the electrical enclosures and containing two cable trays. As introduced above, the main objectives of these tests were to study, in open atmosphere and in confined conditions, and for the two types of cables, the potential fire spread from the central open-door electrical cabinet to the adjacent closed-door electrical cabinets, through the three following potential fire spread paths (see Figure 5): through the double wall with an air gap of 1 cm, via the overhead cable trays and via the raised floor.

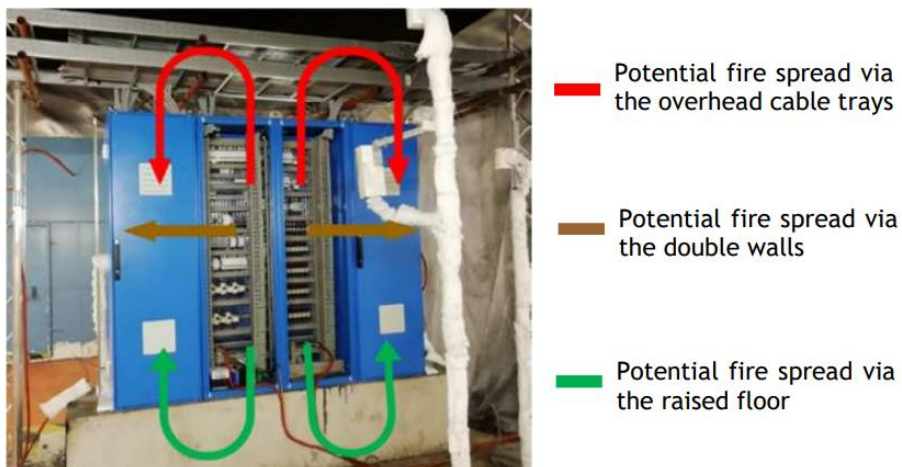


**Figure 5** Potential fire spread paths between the electrical cabinets for the adjacent configuration

<sup>2</sup> PVC: polyvinyl chloride)

<sup>3</sup> IEC: International Electrotechnical Commission

<sup>4</sup> EVA: ethylene-vinyl acetate

<sup>5</sup> PE: polyethylene

<sup>6</sup> ATH: alumina trihydrate

<sup>7</sup> NF: Norme Française

### **Opposite Configuration**

The opposite electrical cabinet configuration was composed of an open-doors central cabinet and three closed-doors cabinet modules located at the opposite, two overhead cable trays, and a raised floor positioned below the cabinets and containing two cable trays. As introduced before, the main objectives of these tests were to study, in open atmosphere and in confined conditions, and for the two types of cables, the potential fire spread from the open-door electrical central cabinet to the three opposite closed-door modules through the overhead cable trays, the closed-doors of the three opposite cabinets, and the subfloor cable trays (see Figure 6). The distance between the cabinets was 1.2 m for the test conducted with the low-qualified cables and 0.8 m for the test conducted with the well-qualified cables.

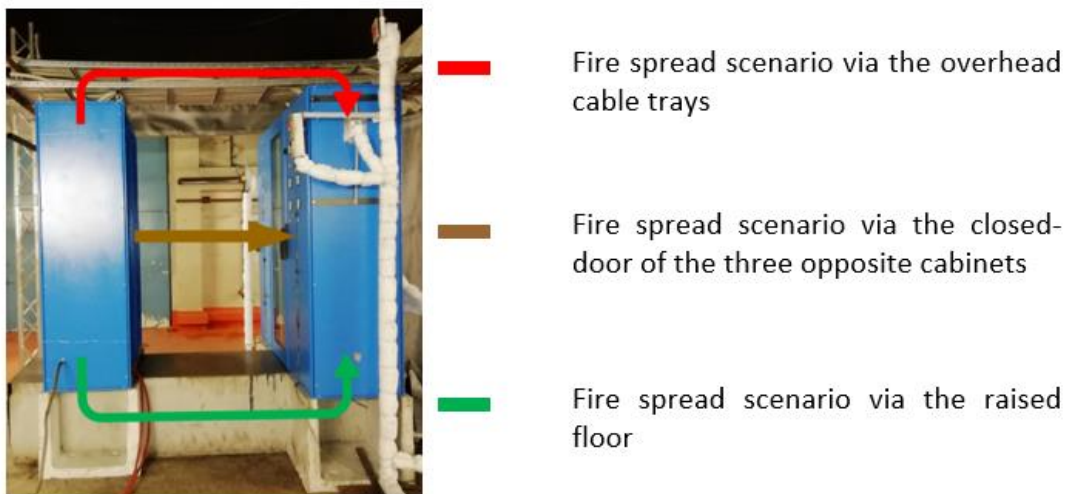


**Figure 6**      Opposite cabinet configuration; left: open-door cabinet, right: overview of the configuration

### **Confined and Mechanically Ventilated Conditions**

As mentioned above, in the introduction part, two tests of the adjacent configuration and two other tests of the opposite configuration, were conducted in the confined and mechanically-ventilated facility DIVA. The fire tests used the rooms 1, 2 and 3 of the facility, as shown in Figure 7. The cabinet setup was installed in room 2 (R2) at the centre of the north wall. The three rooms were connected by two open doorways. An inlet duct was located in the upper part of room 1 while an outlet duct was positioned in the upper part of room R2 and of room R3. The ventilation (air) renewal rate before ignition for the R1 to R3 volume (i.e.,  $330 \text{ m}^3$ ) was about  $11 \text{ h}^{-1}$ , leading to initial volume flow rates of about  $3600 \text{ m}^3/\text{h}$  at the inlet and  $1800 \text{ m}^3/\text{h}$  at each of the two outlets.

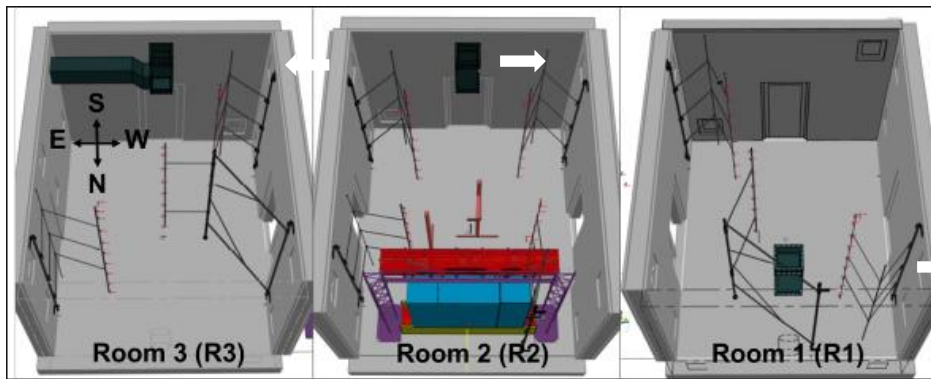


**Figure 7** Configuration of the DIVA facility for the adjacent cabinet configuration

### Cable Fire Propagation (CFP) Tests

Horizontal cable trays of 3 m length were implemented in the SATURNE and DIVA facility during the CFP (Cable Fire Propagation) test campaign. These first tests, realized both in open atmosphere and in confined environment, were defined to complete past analysis. The objective was to study the effects of certain parameters, related to the fuel itself or to the configuration of the installation, and to complete the analysis of the tests carried out in the frame of the PRISME 2 Project. The last part of the campaign was dedicated to a new cable tray configuration by implementing cable trays of 6 m length in the DIVA facility. Only the tests conducted in confined conditions are described hereafter.

### Confined Cable Fire Tests

Three fire tests were defined in order to study the effect of the ventilation on the combustion regime of a 5-ladder cable tray fire of 3 m length. The ventilation layout considered in the PRISME 2 Project consisted of two rooms connected through an open doorway, for which the admission was connected to the fire room and the exhaust to the adjacent room (cf. Figure 8, configuration B). A new configuration was proposed to maximize the exhaust flow rates of combustion products in the fire room (cf. Figure 8, configuration A). This definition also provides a new configuration of air vitiation near the fire location, which is appropriate for fire model validation. Two tests were planned with this new configuration, by using the two ventilation flow rates of the previous PRISME 2 CFS (Cable Fire Spreading) tests. This way, the air renewal rates were fixed to  $4 \text{ h}^{-1}$  and  $16 \text{ h}^{-1}$ , and the cable type was the same as used in the CFS tests, PE-EVA-HFFR (halogen free flame-retardant) cables. The third test consisted of reproducing the configuration of the PRS2-CFS-3 test by increasing the ventilation flow rate to  $6 \text{ h}^{-1}$ . One of the objectives of this test was to complete the understanding of the oscillatory behaviour reported in the PRS2-CFS-3 tests.

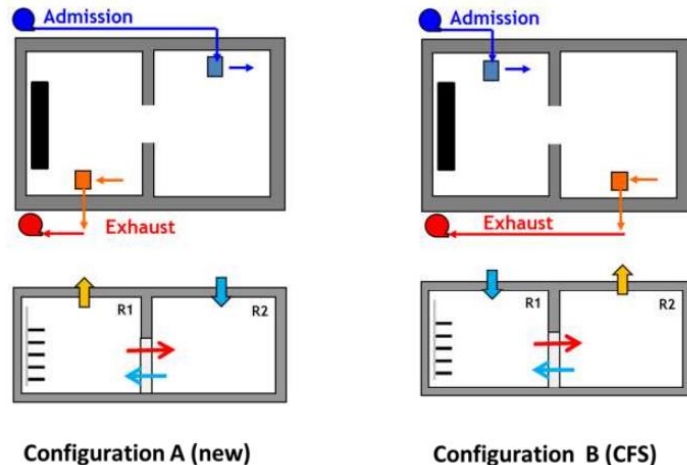


**Figure 8** Ventilation configuration for the CFP tests using 3 m long cable trays in the DIVA facility

### Long Confined Cable Fire Tests

Long horizontal cable trays represent a complex and challenging configuration for fire testing. However, the absence of fire tests, implementing long horizontal cable trays, has been noticed. Most cable tests have been carried out with a short length; therefore, the measured HRR remains limited to the tested configuration. For these cases, the predictive modelling of a quasi-steady flame propagation and consequently of the most important parameters, the HRR, are complex tasks. Therefore, there is a limited number of numerical simulations for this experimental setup and the validation of numerical tools seems questionable. This way, three tests of the PRS3-CFP campaign were defined with the aim to study a long horizontal cable fire in a confined environment.

The main objectives of these tests were to characterize a quasi-steady flame propagation on cable trays and a maximum fire HRR. As this fuel configuration in a confined environment was not studied by the fire community it was decided to first focus this campaign, on a well-ventilated combustion regime in order to avoid additional effect as vitiated environment or the production of unburned gases.

The fire source consisted of three cable trays of 6 m length, which were located in the corridor of the DIVA facility, adjacent to the three rooms. The admission flow rate in each room was set to 1,500 m<sup>3</sup>/h. The exhaust flow rate was set to 3,000 m<sup>3</sup>/h in the corridor and in the room R3 (cf. Figure 9). This configuration was defined to obtain well-ventilated conditions. Each cable tray was filled with 32 halogen-free cables for the tests D41 and D61 (well-qualified cables). For the test D51, the trays were filled with 21 halogenated PVC cables in order to study the effects of a change in the cable type (low-qualified). The two tests D41 and D51 were implemented near the floor (see Figure 10) and the last test, D61, was implemented near the ceiling at a distance of 1 m.

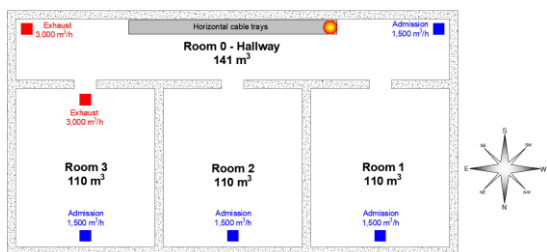


**Figure 9** Ventilation configuration

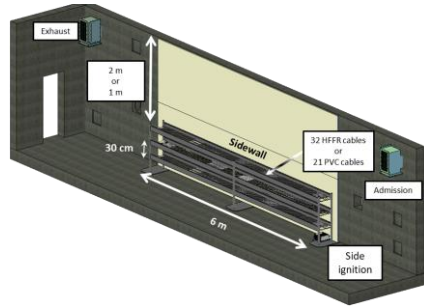


**Figure 10** Configuration of tests

## MAJOR RESULTS

### Smoke Propagation and Gas Stratification

As mentioned above, the objectives of the first experimental campaign were to evaluate the smoke propagation in the facility in the aim to predict the consequences of a fire in terms of gas stratification and smoke concentration. Knowledge of the changing of environmental conditions allows in fine to predict the functioning of electrical equipment. The academic nature of these fire tests will allow the fire modellers using the experimental data to extend their validation domain.

### Multiple Fire Sources

In the case of a configuration with multiple fires, the main experimental results highlight that the burning rates of each pool fire cannot be described accurately from the knowledge of a reference pool fire that burns alone in the same configuration. There is a global effect of smoke propagation and oxygen vitiation in the whole facility and thus feedback of the environment on the combustion process of each multiple fires. For comparison, a reference test with one centred pool fire was conducted; the different HRRs determined from the MLR, and an effective heat of combustion are given in Figure 11. As the reference test shows a HRR at a certain value during the quasi steady-state, the results of the test B1 present a HRR of about 30 % inferior, for each of the two pool fires. The same description can be done for the test B2 concerning the intensity of the two fires. However, while the test B1 shows that the two pool fires evolve in an equivalent way, the B2 test indicates a quasi-steady combustion regime for the pool fire located in room R2 and a more disturbed regime for the pool fire located in room R3. In this case, the fire is not adjacent to the room equipped with the inflow ventilation branch, and the disturbed combustion regime is the result of a strong interaction between the two pool fires. The global HRR of each fire test is also presented in Figure 12. In the case of a weak interaction between the pool fires, the global power is about 35 % superior of the reference test whereas it is very close for the second test.

In terms of fire safety analyses, a recommendation to study precisely the fire behavior and its consequences, should be to consider each of the fire sources in the scenario rather than considering the global sum of the different sources. Further experimental studies are also needed on this issue.

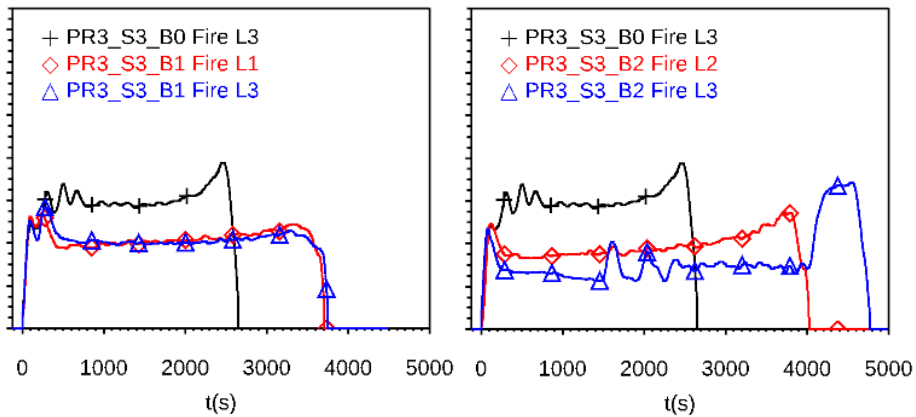


**Figure 11** Comparison of the different HHRs determined from the reference test B0 and the two multiple fires tests B1 (left) and B2 (right)

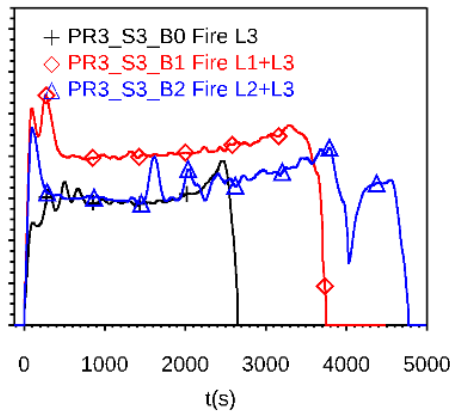


**Figure 12** Development over time of the global HRR determined for the tests B0, B1 and B2

### **Elevated Fire Source**

The third topic of interest concerns smoke propagation induced by an elevated fire. This configuration leads to complex situations for fire dynamics since the fire develops in a hot and vitiated environment. A fire test was conducted aiming at being more representative of certain situations encountered in NPPs, where a lot of systems are located high-up and usually against a wall. The reference test B0, previously described and composed of an identical pool fire located on the floor, was used for comparison. The results mainly showed that although the burning rate of the elevated fire is lower than that measured for the reference pool fire, the stratification for the elevated configuration is clearly more pronounced. For this scenario, fire dynamics and smoke flows inside the compartment tend to increase the gas temperature near the ceiling and to decrease it near the floor. More precisely, the physical analysis of this test shows a significant reduction of the HRR of around 25 %. The difference between the two fire scenarios for this quantity is fairly normal and mainly due to the presence of a vitiated environment which participates to the combustion process, in the case of the elevated fire. The oxygen concentration is reduced, resulting in a less intense combustion process. On the other hand, while the fire is less powerful, the ceiling gas temperature is a hundred degrees higher, in the elevated configuration.

This result is counter-intuitive in a global approach and remains challenging for fire modelling in case of safety studies. In fact, the use of this well-known correlation without any modification, for predictive fire simulations, significantly underestimate the MLR (and thus the HRR), by about 30 % (cf. Figure 13). This correlation is therefore not conservative with its native formulation. Certain additional terms, such as the external radiative flux, must be taken into account for a more predictive calculation.

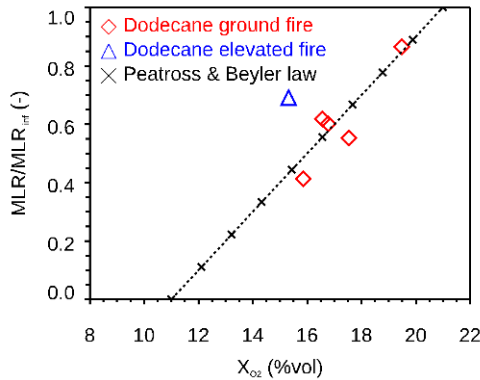


**Figure 13** Comparison of the fire MLR of dodecane pool fires with the Peatross and Beyler's correlation

### Fire Propagation Between Electrical Cabinets (ECFS) Tests

The objective of the PRS3-ECFS test campaign was to describe the different fire propagation paths between a burning electrical cabinet and neighbouring cabinets placed adjacent or opposite to the main enclosure. As explained in the section of the description of the experimental campaign, the electrical cabinets were connected by two overhead cable trays and two other subfloor ones contained in a concrete false floor. The effects of the cable type on the fire propagation and of the environment were studied during this campaign.

#### ***Adjacent Configuration***

In the adjacent configuration, the electrical cabinets were separated by an air gap of 1 cm. The three cabinets were connected between each other by two overhead and two subfloor cable trays. The PRS3-ECFS-S1 and -S2 test devices, implemented in open atmosphere, were identical, except for the type of electrical cables installed along the cable trays. This was also the case for the tests D1 and D2, conducted in the confined DIVA facility. The S1 and D1 tests used a low-qualified cable (LQ) type which was made of polyvinyl chloride while the S2 and D2 tests implemented a well-qualified (WQ) cable type which contained a halogen free flame retardant. All cables were tightly arranged over the different cable trays. It is also recalled that the central cabinet contained no doors in the aim to represent the scenario of an open-door electrical cabinet fire, ignited by a gas burner.

The two tests in open environment showed a propagation of the fire from the central cabinet to the adjacent enclosures, via the double steel panels (or walls) which were separated by an air gap of 1 cm. Indeed, several inflammations of the wall paintwork first occurred in the adjacent cabinets as soon as the side wall temperature exceeded 500 °C. This then caused the inflammation of electrical components (used as targets) also occurred in the adjacent cabinets and resulted in a fire in the adjacent cabinets. These results from open door cabinets are of primary importance as they are questioning the

recommendation found in NUREG 6850, Appendix S [7], in case of fire Probabilistic Risk Assessment (PRA). Appendix S assumes no fire propagation in case of separation of electrical cabinet by a double wall with an air gap. Concerning the effect of the cable type on the fire spread between the enclosures, the tests in open atmosphere have shown notable results. Even the two central cabinet fires were similar for both tests (HRR peak of about 1,900 kW), LQ cables have propagated the fire, whereas WQ cables extinguished by themselves after ignition. Consequently, the results showed a propagation of the fire on the two overhead cable trays and along the raised floor cable trays only for the first test which was composed by LQ cables.

The three fire spread paths have also been studied in a confined environment, using the DIVA facility. First, the fire propagated from the central cabinet to the adjacent cabinets via the double walls. Similar to the open atmosphere tests, the wall paint and the target ignited in the adjacent cabinets when their steel panels exceeded 500 and 600 °C, respectively. Identical behaviours were obtained regarding the effect of the cable type on the fire propagation in a confined environment. Flame propagations were effective on the overhead cable trays and in the false floor, but only in case of the low-LQ cables. In addition, the reduction of the HRRs for the cabinet and cable fires in the confined environment compared to those obtained in open atmosphere was not as significant as expected, given the lower oxygen concentration in the DIVA facility. This is shown in Figure 14 which provides the HRR determined for the four tests in open and confined environments. In these situations, the preheating of the overhead cable trays by the hot gas layer for the LQ cables counterbalanced the decrease of the oxygen concentration and allowed its complete burning.

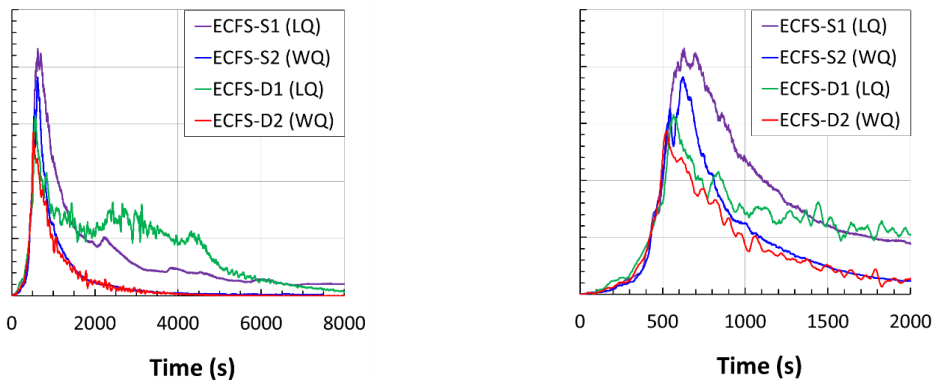


**Figure 14** HRRs of the PRS3-ECFS-S1, -S2, -D1 and -D2 tests; left:  $0 \leq t \leq 8,000$  s, right:  $0 \leq t \leq 2,000$  s

### Fire Propagation on Cable Trays

Three sets of fire tests were conducted in the frame of the last experimental campaign in open atmosphere, in the two compartments of the DIVA facility and, last not least, in the corridor of the facility. Concerning the first tests conducted in the DIVA facility, the objective was to study the effect of the configuration of the ventilation on the fire behaviour and the conditions of emergence of an oscillatory combustion regime (not described here). Finally, the tests conducted in the corridor of the DIVA facility involved three cable trays of 6 m length placed against a wall. Two tests were performed near the floor and studied the effect of the cable type on the fire propagation. A third test was realized near the ceiling allowing to quantify the effects of the environment (cable preheating, oxygen vitiation, etc.) using WQ cables for the fire propagation.

### Confined Cable Fire Tests

Two tests were conducted with a new configuration (named A) and another test was performed with an old ventilation configuration (configuration B) but with a higher ventilation renewal rate of  $6 \text{ h}^{-1}$  in comparison to the PRS2-CFS-3 test of the PRISME 2 Project which was conducted with an air renewal rate of  $4 \text{ h}^{-1}$ . All the tests consider an assembly of five cable trays placed against a side wall, filled with 32 samples of HFFR cables of 2.4 m length, using a loose cable arrangement. The first test of the configuration A was realized with a ventilation flow rate of  $3,660 \text{ m}^3/\text{h}$  whereas the second one was conducted with a ventilation of  $1,010 \text{ m}^3/\text{h}$  which stand for air renewal rates of about  $16$  and  $4 \text{ h}^{-1}$ .

It is well known that the configuration of the ventilation may significantly influence the fire scenario. The admission line in configuration A was located in the adjacent room and the exhaust located in the fire room, opposite therefore to configuration B. This setup can promote the fire development because combustion products can escape directly from the exhaust ventilation branch (same room) whereas the latter could potentially be stirred with fresh air in case of configuration B. The results have also shown that the location of the door in front of the fire allows a good channelling of fresh air.

Figure 15 presents a comparison for the two ventilation flow rates. For the most ventilated case ( $3,660 \text{ m}^3/\text{h}$ ), the HRR of the configuration A is similar to the one determined in open atmosphere, despite an air renewal rate of  $11 \text{ h}^{-1}$ . A reduction of about 30 % was obtained for configuration B where fresh air comes from the fire room. For the lower ventilation flow rate ( $1,010 \text{ m}^3/\text{h}$ ), the reduction is also significant with about 40 % difference between configurations A and B. This trend to increase the HRR with configuration A can be explained by the concentration of the oxygen flow field near the fire source, which is much higher in configuration A than in configuration B. Furthermore, gas stratification was also more pronounced in case of configuration A with a lower temperature at the ground and a higher temperature near the ceiling, in comparison to configuration B.

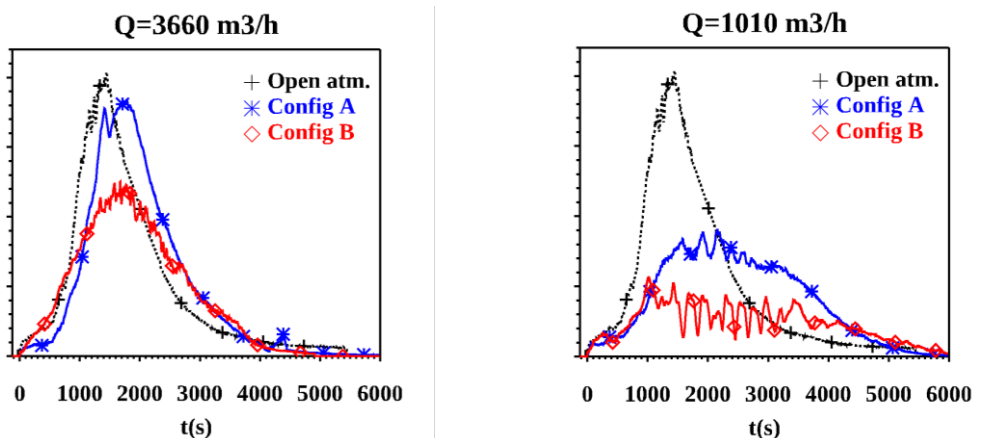


**Figure 15** Comparison of the HRRs for configurations A and B; left: ventilation flow rate of  $3,660 \text{ m}^3/\text{h}$  (air renewal rate of  $16 \text{ h}^{-1}$ ), right: ventilation flow rate of  $1,010 \text{ m}^3/\text{h}$  (air renewal rate of  $4 \text{ h}^{-1}$ )

### Long Cable Trays

The objectives of the last tests were to determine a free burning combustion length and a maximum HRR for some cable fires, and to compare them with values prescribed by

the fire safety community. The configuration was defined in order to obtain well-ventilated conditions since these tests could potentially damage the installation due to the cable length. As in the previous cable tests, the fire was ignited with a gas propane burner located below the lower tray at the first part of the setup near the air supply in the corridor. The burner was maintained to 80 kW for a period of 60 min for the tests with WQ cables and of 20 min for the test with LQ cables, ensuring a distance from the ignition flame front of 3 m from the burner. The objective was to achieve a self-propagation of the fire without interaction with the burner or the cable edges.

The fire HRR, the burning length and the fire spread velocities were determined to quantify the effects of halogenated PVC cables (test D51) and the elevation of the fire source (test D61) in comparison to the first test D41 (WQ HFFR cables located near the floor). The burning length and the fire velocity were estimated from temperature measurements along each cable tray. A quasi-steady combustion regime was also determined from the HRR variations and some videos of the fire. This regime was defined after the burner had been stopped over a period with a nearly constant HRR (changes of less than 10 % of the average value).

The most powerful fire was obtained for the second test using LQ cables, cf. Figure 16. A quasi-steady combustion regime with a nearly constant HRR was determined with a duration of 20 min. The shorter duration of this stage is explained by a flame spread velocity 2.5 times higher than that observed for the first test (around 2 mm/s). The maximum burning length was about 12.2 m.

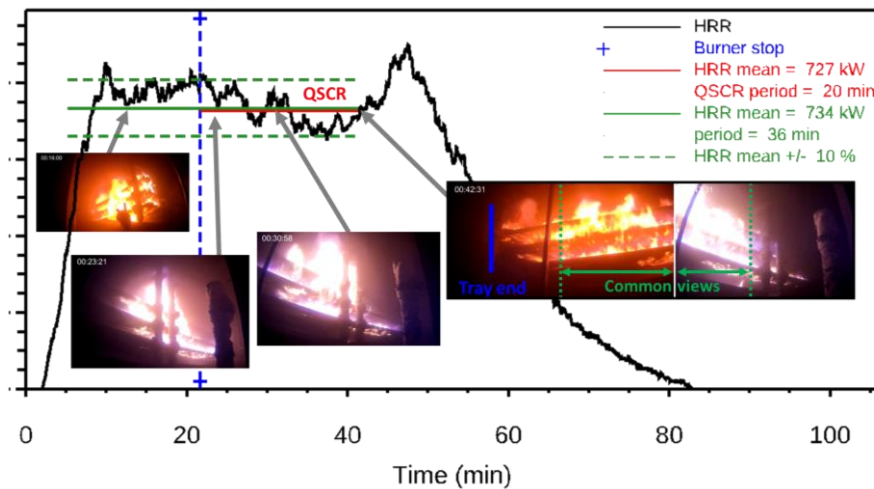


**Figure 16** Development of the HRR over time and determination of a free quasi-steady combustion regime (QSCR) for test D51 (low-qualified cables)

The originality of this part of the PRISME 3 Project was to recreate a configuration in a large-scale experimental facility where the cable fire could propagate freely. This makes it possible to extrapolate the results obtained to a real configuration encountered in safety studies. In addition, the set of the new experimental data can be used to perform a more efficient validation process of fire models. Measurements concerning the flame spread velocity indicates, for the studied configuration, values two times more important than those recommended in [7].

## CONCLUSIONS

A total of 23 large-scale fire tests has been performed either in open atmosphere or in a confined environment in the frame of the OECD/NEA PRISME 3 Project. In addition to

these contractual tests, some support tests were also conducted in order to check the reproducibility of some fire scenarios, to qualify the entire acquisition system and to design large-scale fire tests from medium-scale experiments. The experimental campaigns were conducted from 2017 to 2021 in the GALAXIE platform of IRSN at Cadarache (France).

According to the agreement of the Project, the experimental program was split into three topics (i) smoke propagation and gas stratification, (ii) fire propagation from an electrical cabinet to another one, and finally (iii) fire propagation along electrical cables on horizontal cable trays. Each experimental campaign was delivered with several documents: functional specification of the tests, test reports, and analysis reports. The rough and validated data are also delivered to allow each member of the Project to validate their own fire model. The entire Project is accessible via the OECD/NEA but is also archived on the secure IRSN GFORGE website (<https://gforge.irsn.fr/gf/project/prisme3/>).

From the main outcomes of the PRISME 3 experimental program, it is possible to mention the following.

- For multiple fires in a confined environment, the results show that modelling all fire scenarios is more accurate rather than considering an overall fire source by adding the contribution of each individual fire source. The coupling between the burning rate of several fire sources and the oxygen concentration is indeed very complex and depends on local phenomena to be considered in the model.
- The results on the elevated fire showed a lower HRR in comparison to a reference fire, located on the ground. However, the ceiling gas temperature is more important in the raised configuration. This result is thus counter-intuitive and remains a challenge for fire modelling in the frame of safety studies. It appears that standard correlations without any modification underestimate the HRR by about 30 %. This type of approach is therefore not conservative in its native formulation and some additional terms, such as the external radiative flux, must be taken into account for a more predictive calculation.
- One of the most important results obtained during the electrical cabinet fire spread campaign was the fire propagation from the central cabinet to the adjacent enclosures, via the double steel panels which were separated by an air gap of 1 cm. This result is of primary importance because it calls into question the recommendation in NUREG/CR-6850 [7] which assumes that there is no fire propagation in case of a separation of the electrical cabinets by a double wall with an air gap. Concerning the effect of the cable type on the fire spread between the enclosures, the tests have also shown notable results. For the adjacent cabinet configuration, fire spread was only observed in the tests with LQ cables.
- The reduction of the HRRs obtained in confined conditions was not as significant as expected for electrical cabinet fires. In these test configurations, the effect of the decrease of the oxygen concentration on the HRR, which is typically observed for confined conditions, is counterbalanced by the overhead cable tray preheating by the hot gas layer. The HRR is thus maintained at a fairly high level.
- The results obtained with the three tests performed in two rooms of the DIVA facility using five cable trays filled with well-qualified cables are significant both for modelers and safety issues. First, it was shown that the ventilation configuration, i.e., the location of the inlet and outlet ventilation branches, in relation to the fire source, is an important parameter for designing the fire scenario and prescribing the HRR. Depending on the configuration, the fire power can be similar to that obtained in open atmosphere or considerably reduced. These considerations should then be included in fire safety studies regardless the method used. Finally, the last test (not described here) showed that the emergence of an unsteady or oscillatory combustion regime

can be related to small variations of some parameters. The prediction of these regimes therefore requires a fairly detailed description of all the physical phenomena as well as the different couplings involved in any fires.

- One of the originalities of the PRISME 3 Project was to recreate in a large-scale experimental facility, a configuration where the cable fire can propagate freely. This allows to extrapolate the results obtained to a real configuration encountered in safety studies. In addition, the new experimental data set can be used to perform a more efficient validation process of fire models. The measurements concerning the flame spread velocity indicate, for the studied configuration, values two times higher than those recommended by the fire community. This study configuration, very complex to implement, must be continued and consolidated in future experimental programs.

The continuation of the PRISME 3 experimental program is already underway, and the main experimental campaigns have been roughly determined by potentially interested partners, through a PIRT-type process. The phenomenon of fire propagation will be again widely studied, through the implementation of complex fire sources such as vertical or horizontal cable trays of higher lengths. New topics of interest have also appeared such as the ignition of unburned gases or the effect of cable aging on combustion parameters. This new project is called FAIR (*Fire Risk Assessment through Innovative Research*) and will be conducted under the auspices of the OCDE/NEA.

## ACKNOWLEDGEMENTS

The authors would like to thank all PRISME 3 members for fruitful discussions, the Chair of the Management Board and of the Program Review Group, for managing this project and the OECD/NEA for the high-quality support during these five years.

## REFERENCES

- [1] Organisation for Economic Co-operation and Development (OECD), Nuclear Energy Agency (NEA), Committee on the Safety of Nuclear Installations (CSNI): PRISME Project Application Report, NEA/CSNI/R(2012)14, Paris, France, July 2012.
- [2] Organisation for Economic Co-operation and Development (OECD), Nuclear Energy Agency (NEA), Committee on the Safety of Nuclear Installations (CSNI): Investigating Heat and Smoke Propagation Mechanisms in Multi-Compartment Fire Scenarios, Final Report of the PRISME Project, NEA/CSNI/R(2017)14, Paris, France, January 2018.
- [3] Organisation for Economic Co-operation and Development (OECD), Nuclear Energy Agency (NEA): Agreement on the OECD/NEA PRISME 3 project to further investigate fire propagation by means of experiments and analyses relevant for nuclear power plant applications, Paris, France, revision March 26, 2018.
- [4] Plumecocq, W., et al.: Investigating A Cable Tray Fire Event in the Frame of An International Benchmark Exercise, in: Röwekamp, M., H.-P. Berg (Eds.): Proceedings of SMiRT 26, 17<sup>th</sup> International Seminar on Fire Safety in Nuclear Power Plants and Installations, Westerburg Huy, Germany, October 24-26, 2022, GRS-705, ISBN 978-3-949088-96-4, Gesellschaft für Anlagen- und Reaktorsicherheit (GRS) gGmbH, Köln, Germany, November 2022, <https://www.grs.de/publikationen/grs-705>.

- [5] Zavaleta, P., O. Bouygues, and C. Lapuerta: Electrical component ignition in a closed enclosure adjacent to a controlled fire, *Fire and Materials*; 45, pp. :331-344, 2021, <https://doi.org/10.1002/fam.2792>.
- [6] Zavaleta, P.: Experimental study at reduced-scale of fire spread between electrical cabinets located opposite each other, *Fire Safety Journal* 122, 2021, <https://doi.org/10.1016/j.firesaf.2021.103319>.
- [7] Nowlen, S. P., et al.: EPRI/NRC-RES Fire PRA Methodology for Nuclear Power Facilities, Volume 2: Detailed Methodology, NUREG/CR-6850, EPRI 1011989, Electric Power Research Institute (EPRI), Palo Alto, CA, USA, and United States Nuclear Regulatory Commission (U.S. NRC) Office of Nuclear Regulatory Research, Washington, DC, USA, September 2005, <https://www.nrc.gov/reading-rm/doc-collections/nuregs/contract/cr6850/v2/cr6850v2.pdf>.

# Experimental Investigations of the Influence of Cable Arrangement and Ventilation on Cable Tray Fires in Confined Spaces

Jens Spille

Institute of Building Materials, Concrete Constructions and Fire Safety (iBMB),  
Braunschweig University of Technology, Braunschweig, Germany

## ABSTRACT

In the frame of fire risk assessment for nuclear facilities such as nuclear power plants (NPPs) or nuclear waste storage facilities but also for non-nuclear industrial installations electrical cable tray fires are a major issue. In the past, a significant number of research studies have been conducted on cable tray fires including a large number of fire tests such as CHRISTIFIRE [1] or within the frame of the PRISME (French: *Propagation d'un incendie pour des scénarios multi-locaux élémentaires*) Projects of the Organisation for Economic Co-operation and Development (OECD) Nuclear Energy Agency (NEA). These fire tests have in common that cable trays within large rooms combined with gas burners with heat release rates (HRRs) of up to 80 kW as primary ignition source were investigated. In nuclear and other industrial facilities cable trays can also be arranged within confined spaces like supply tunnels or false ceilings. In these confined spaces the cross-section area is small compared to the length of the spaces.

To investigate the fire behaviour of cable tray fires in confined spaces, a total of 20 fire tests with PVC cables (NYM-J 5x25) were performed at the Institute of Building Materials, Concrete Constructions and Fire Safety (iBMB) of Technische Universität (TU) Braunschweig in Germany using a 10 kW gas burner for ignition. The tests were conducted under confined atmosphere with two different cable arrangements in a small compartment with a height of 1.00 m, a width of 1.20 m, and a length of 2.00 m. Two different ventilation conditions were investigated. Compared to Kawagoe's equation [2] for determining the HRR in ventilation-controlled regimes, the tests show a significant lower maximum HRR. The cable arrangement strongly influences the ignition behaviour of the cable trays as well as the flame spread and burning time of the cable trays. It can be concluded that for a loose cable arrangement it is more likely that the fire develops to flashover compared to a dense cable arrangement under the same boundary conditions.

## INTRODUCTION

An evaluation of the annual reports on reportable events in the nuclear installations of the Federal Republic of Germany reveals 16 fires from German NPPs, nuclear fuel supply and nuclear waste management facilities between 2000 and 2018. About 40 % of these fires were related to electrical installations (cables, switchgears, etc.). It can therefore be stated that electrical installations have an increased probability being involved in a fire. On the other hand, none of the above-mentioned fires related to electrical installations resulted in a significant flame spread on cable trays. However, in the case of the documented small-scale fire events, the fire led to the triggering of emergency plans in nuclear facilities in any manner (e.g. deployment of the plant fire brigade) due to smoke propagation. In the frame of the research project "Numerical and experimental investigations of polymer fire loads in nuclear facilities to improve the predictability of fire simulations" carried out at iBMB, the fire development on cable trays ignited by fires with low

heat release was investigated. One major issue was to identify boundary conditions that affect the fire development such that a fully developed fire occurs. The research project focused on confined spaces, like false ceilings or false floors, as main location of cable installations.

## FIRE TEST DESCRIPTION

### Cable Type Information

For all tests carried out PVC insulated cables with the specification NYM-J 5x25 were used. This cable type is standardized in Germany according to DIN VDE 0250-204 [3] for use in low-voltage installations (< 1,000 V). Regarding the fire behaviour, the selected cable only meets the basic requirements for insulated cables in case of fire. Flame retardancy is only based on flame poisoning of the halogens contained in PVC, further requirements regarding smoke density, etc. are not met. The market share of PVC insulated cables in the low voltage sector in Germany is approx. 90 % [5] and the selected cable type has been installed in German nuclear facilities [6]. For this reason, the selected cable type is relevant for nuclear and non-nuclear installations.

Measured mass fractions and the diameter of the selected PVC insulated cable type are shown in Table 1.

**Table 1** Mass fractions and dimension of the selected cable type

| Mass [kg/m]   | NYM-J 5x25  |       |
|---------------|---|-------|
|               | Sheath  | 0.195 |
|               | Filler  | 0.204 |
|               | Insulation  | 0.208 |
|               | Copper  | 1.003 |
|               | Inner Filler  | 0.029 |
|               | Sum   | 1.639 |
| Diameter [mm] | 26  |       |
| Picture       |  |       |

The selected cable type was also used in previous research projects at iBMB [6], [7] as well as in the OECD/NEA PRISME 2 Project [8]. Since the mass of the cables used in this research project was lower than the cables used in previous projects, cone calorimeter test were conducted. Two different batches were tested. The first one (PK1) was the batch of 2021 used in the present tests. The second one was the batch of 2014 (PK2), which was used within the OECD/NEA PRISME 2 CORE campaign carried out at the French Institut de Radioprotection et de Sûreté Nucléaire (IRSN) in Cadarache. Unless the effective heat of combustion determined in the cone calorimeter was comparable for both batches (cf. Table 2), the HRRs determined in the cone calorimeter show a different fire behaviour for PK1 and PK 2.

**Table 2** Effective heat of combustion for batch 2021 (PK1) and batch 2014 (PK2)

| Heat flux            | PK1<br>[MJ/kg] | PK2<br>[MJ/kg] |
|----------------------|----------------|----------------|
| 30 kW/m <sup>2</sup> | 23.00          | 25.93          |
| 40 kW/m <sup>2</sup> | 24.06          | 22.42          |
| 50 kW/m <sup>2</sup> | 22.37          | 15.02          |
| 60 kW/m <sup>2</sup> | 24.70          | 23.85          |
| Mean                 | 23.53          | 21.81          |
| Standard deviation   | 1.05           | 4.75           |

Figure 1 shows the measured HRRs for both batches under a heat flux of 60 kW/m<sup>2</sup>. The HRRs shown represent the mean values of three different tests. Compared to the batch of 2014 the HRR of the batch of 2021 shows a strong second peak, which almost reaches the first peak. This behaviour could be observed for all investigated heat fluxes.

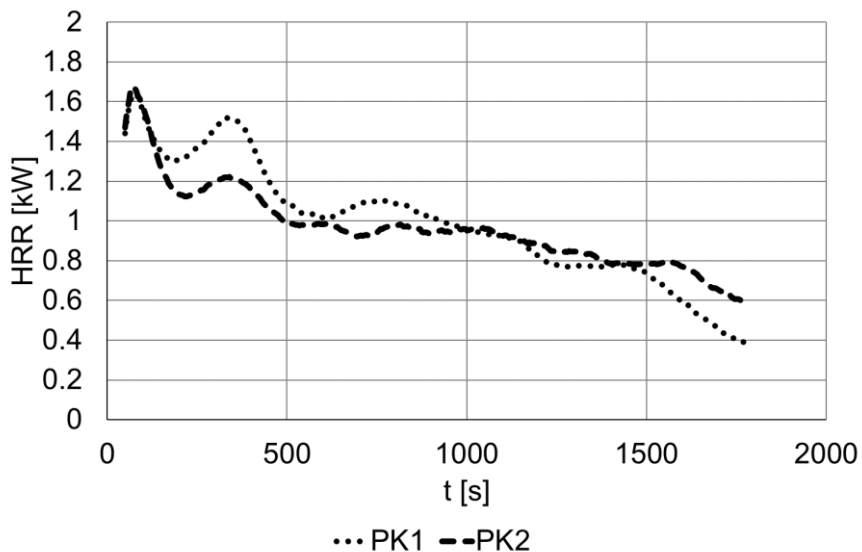


**Figure 1** HRR from the cone calorimeter (heat flux 60 kW/m<sup>2</sup>) for batch 2021 (PK1) and batch 2014 (PK2)

### Test Setup

In order to investigate the fire development of cable trays in confined space a test setup with a small room was developed, which will be described in the following. For analysing the gas concentrations in the smoke, the exhaust system of the ISO 9705 Room Corner Test [9] at iBMB was used. The small room was placed under the hood of the Room Corner Test as shown in Figure 2. The front door of the Room Corner Test was closed using a gypsum fibre board, creating an open atmosphere for the test with the restriction that the flow at one side of the hood was blocked by the room of the Room Corner Test. The small room itself was built out of light concrete. The thickness of the walls was 0.175 m and the thickness of the ceiling 0.20 m. The floor area of the room was 1.20 x 2.00 m<sup>2</sup>. The walls and the ceiling were covered with gypsum fibre boards of a

thickness of 0.0125 m, which were renewed after each test to ensure that the boundary conditions remained the same. At the transverse side of the room openings were arranged for air supply and smoke exhaust. The area of the opening was one parameters of the test design. The height of the opening was chosen in a way that at least the upper trays were located in the hot gas layer of the room.

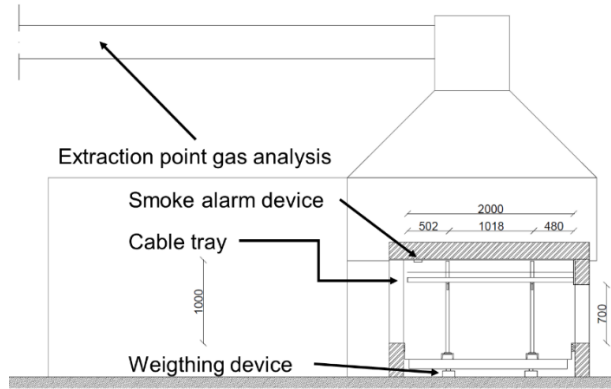


**Figure 2** Test setup in the ISO 9705 Room Corner Test [9]

Within the room a support system for cable trays was mounted on a steel pan used for pool fires with liquid fire loads. Overall, three ladder-type cable trays were placed in the room as shown in Figure 3. Each tray had a width of 0.40 m and a length of 2.00 m. The distance between the rungs was 0.30 m. The vertical distance between the trays was set to 0.30 m and the horizontal distance was set to 0.40 m. Between the gypsum fibre board cover and the cable trays there was a small gap of approximately 0.02 m.

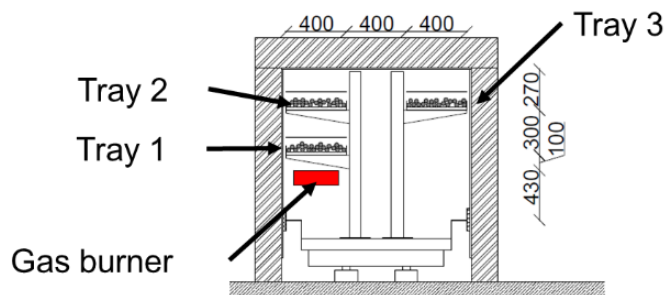


**Figure 3** Cable tray arrangement within the small room

Each cable tray was filled with 21 2.0 m long cable samples (NYM-J 5 x 25). The total mass of cables per tray was 69 kg with 27 kg of combustible material. The cable arrangement was the second parameter of the test design. Tight and loose cable arrangements were investigated. The filling height was average 0.065 m for the loose cable arrangement and 0.05 m for the tight cable arrangement as there were two layers of cables (15 cables on the lower layer and 6 cables on the upper layer).

A propane sand burner (300 x 300 mm<sup>2</sup>), located 0.10 m below the lower tray at the centre of the trays, achieved ignition of the cables. The sand burner provided a constant power of 10 kW. The operating time of the sand gas burner was a third parameter of the test design.

## Instrumentation

In total, data from 120 sensors were recorded during the tests. The O<sub>2</sub>, CO and CO<sub>2</sub> concentrations were measured in the analysis system of the room corner test. The sampling point of the smoke gas for the gas analysis was located in the horizontal pipe of the exhaust system (cf. Figure 2). To determine the flame spread velocities from the temperature data a grid with thermocouples was placed with a distance of 0.06 m above each cable tray (cf. Figure 4). The distance between the thermocouples in the direction of the width of the cable tray was 0.10 m and 0.20 m in the direction of the length of the cable tray.

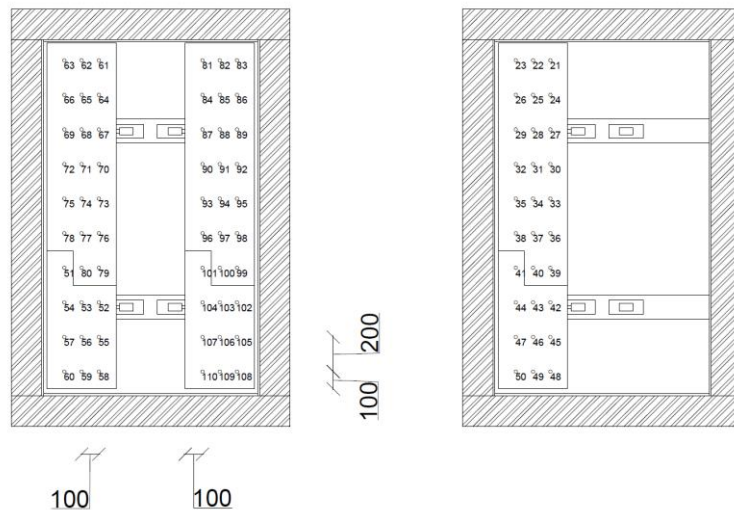


**Figure 4** Thermocouple grid 0.06 m above the cable trays

Thermocouples were also placed 0.10 m below the ceiling. A customary smoke alarm device was placed under the ceiling at the larger opening. The time interval between the data points was set at 10 s.

## Determination of the Heat Release Rate and the Effective Heat of Combustion

Gas concentrations measured in the exhaust flow were used to calculate the HRR of the fire source. The first method used is based on evaluating the oxygen consumption during the combustion reaction. According to [10], the HRR can be determined using three different equations depending on which gas analysis is used:

Oxygen concentration  $\dot{Q}_{O_2}$ ,

Carbon dioxide and oxygen concentration  $\dot{Q}_{CO_2,O_2}$ , and

Carbon monoxide, carbon dioxide, and oxygen concentration  $\dot{Q}_{CO,CO_2,O_2}$ .

Figure 5 shows the calculated HRRs using the three different equations for an open atmosphere test without walls and ceiling. The calculated HRR using only the measured oxygen concentration is significantly higher (up to 22 %) compared to the other equations. The reason for this could be the property of PVC as a fuel to form combustion products of other types than CO<sub>2</sub> and soot. The deviation between the HRR calculated with the carbon dioxide and oxygen concentration on the one side and the carbon mon-

oxide, carbon dioxide, and oxygen concentrations on the other side is much lower (less than 5 %).

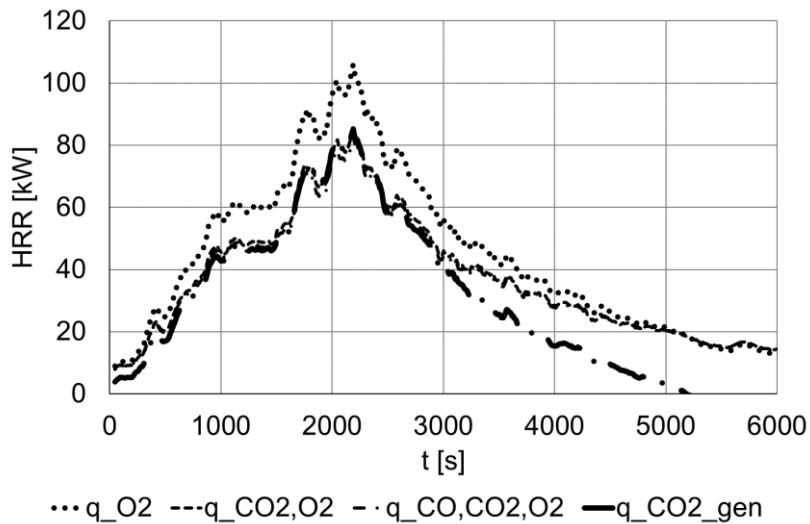


**Figure 5** Calculated HRR of the test 5 with different formulations using oxygen consumption and carbon dioxide calorimetry

Compared to the HRR ( $q_{CO2\_gen}$ ) calculated with the carbon dioxide calorimeter method, the HRRs calculated with the oxygen consumption method do not decrease to zero at the end of the combustion phase (cf. Figure 5). The reason for this behaviour, which does not agree to visual observations, was found in the recorded oxygen concentration. Therefore, the HRR calculated with the carbon dioxide calorimeter method was used.

The effective heat of combustion may change over time due to the limited oxygen concentration in the small room and flame poisoning by the halogens of PVC. Therefore, the effective heat of combustion  $\Delta h_{c,eff}$  of the fire source is determined over time:

$$\Delta h_{c,eff}(t) = \frac{\dot{Q}(t)}{\dot{m}(t)}$$

(1).

Here,  $\dot{m}$  is the mass loss rate (MLR) derived from the mass measured by the weighting device by using five-point numerical differentiation formulae as presented in [11].

### Test Matrix

Including the calibration tests and the tests on the actuation time of the smoke detector, 20 tests were carried out with the test setup described above. The following parameters were changed between the individual tests:

Tests were performed without walls and ceiling (open) and two different ventilation configurations (see Figure 2):

- V1: Left hand opening  $1.20 \times 1.00 \text{ m}^2$ ; right hand opening  $1.20 \times 0.70 \text{ m}^2$ ;
- V2: Left hand opening  $1.20 \times 0.70 \text{ m}^2$ ; right hand opening  $1.20 \times 0.30 \text{ m}^2$ .

Operating time (OT) of the gas burner: The operating time of the sand gas burner was set to 5, 10 and 20 m.

Cable arrangement: The tests were carried out with loose and tight cable arrangements as mentioned before.

The test configurations discussed below are listed in Table 3.

**Table 3** Test matrix to investigate the influence of the Cable Arrangement and Ventilation conditions

| Test | Ventilation | OT Gas Burner [min] | Cable Arrangement |
|------|-------------|---------------------|-------------------|
| 1    | Open        | 20                  | loose             |
| 2    | Open        | 20                  | loose             |
| 3    | Open        | 20                  | tight             |
| 4    | Open        | 30                  | loose             |
| 5    | Open        | 30                  | loose             |
| 6    | V1          | 5                   | loose             |
| 7    | V1          | 10                  | loose             |
| 8    | V1          | 20                  | loose             |
| 9    | V2          | 20                  | loose             |
| 10   | V1          | 5                   | tight             |
| 11   | V1          | 10                  | tight             |
| 12   | V1          | 20                  | tight             |

## EXPERIMENTAL RESULTS AND DISCUSSION

The experimental results of test No. 8 (T8) are used as reference test results to show the influence of the cable arrangement and ventilation on the fire behaviour.

Figure 6 shows the calculated HRR and MLR. The HRR increases very slow in the beginning. At  $t = 1080$  s an exponential growth of the HRR begins. The maximum value of the HRR (174 kW) is reached after 1860 s followed by a decay phase. After the maximum value of the HRR a kind of plateau phase with two more peak values is reached. The global decay phase begins 3250 s after the start of the gas burner. No more flames were observed 5940 s after the starting the gas burner. This observation fits quite well with the calculated HRR. The total heat release (THR) was calculated to 410.6 MJ.

The calculated MLR follows the calculated HRR. Between  $t = 2410$  s and  $t = 3300$  s parts of the gypsum fibre board fell down causing large deviations in the signal of the weighting device. A MLR could therefore not be determined and was set constant in Figure 6. The overall mass loss (ML) was 30.38 kg, which corresponds to only 37.5 % of the combustible mass of the cables at the starting point.

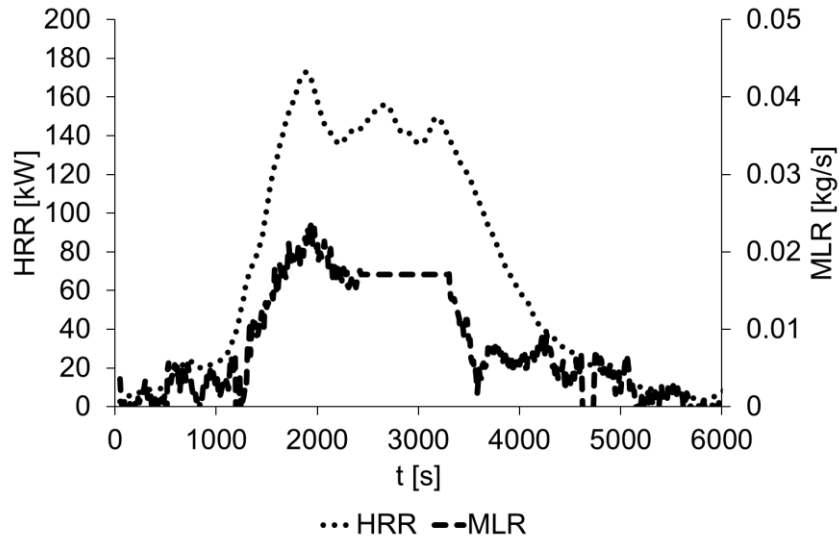


**Figure 6** Calculated HRR and mass loss rate of the test T8

As described above, the calculated HRR and MLR was used to determine the time-dependent effective heat of combustion, as shown in Figure 7. The effective heat of combustion increases constantly in the first 1800 s, followed by a plateau between 8 and 9 MJ/kg. After 2900 s the effective heat of combustion increases again. The average of the effective heat of combustion between  $t = 1000$  s and  $t = 3000$  s was calculated to 8.24 MJ/kg and the overall effective heat of combustion ( $\Delta H_{c,eff} = THR/ML$ ) was determined to 13.51 MJ/kg. Both values are significantly lower compared to the effective heat of combustion determined by cone calorimeter as shown above.

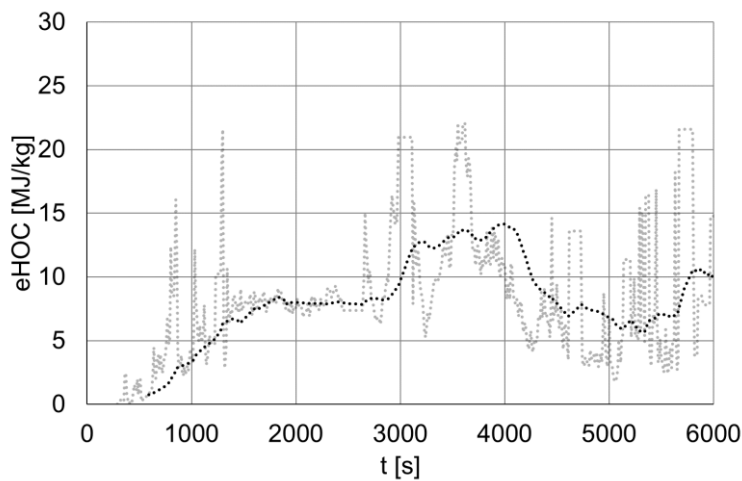


**Figure 7** Calculated effective heat of combustion T8

In order to describe the local fire behaviour on the cable trays the temperature data 0.06 m above the cable trays was used to calculate flame spread velocities and ignition times. For this 500 °C was selected as threshold temperature in accordance with [12]. It is assumed that for temperatures higher than 500 °C flaming combustion takes place at the location of the thermocouple. Using the different times combined with the distance between the thermocouple flame spread velocities can be derived. The 500 °C criterion

was also used to determine the ignition time, which is the time when one thermocouple on a cable provides temperatures higher than the threshold temperature. As a temperature criterion is selected the ignition times do not match with the start of thermal degradation of the cables which starts earlier.

1180 s after starting the gas burner the temperatures above cable tray T1 exceed 500 °C in the middle of the cable tray (above the gas burner). From this point the fire propagated horizontally in the direction of the cable tray as well as in vertical direction to cable tray T2. The flame spread velocity depends on the direction of flame spread. In direction with the air inflow, entering the room through the smaller opening, the average flame spread velocity is 1.66 mm/s and against the air inflow the average flame spread velocity is 0.83 mm/s (see Figure 8). The flame spread velocity on the last 0.30 m direct located to the smaller opening on cable tray T1 is very slow (0.15 mm/s). From the different flame spread velocities on cable tray T1 it can be assumed that there is an air flow within the small room from the smaller opening to the bigger opening as planned. Flame spread from cable tray T1 to cable tray T2 was determined by the 500 °C temperature criterion to 1.33 s. Compared to T1 no influence of the air inflow on the flame spread velocity can be observed. The flame spread velocity in the direction of the air inflow is 2.60 mm/s and 2.59 mm/s against the air inflow. 1650 seconds after ignition of the gas burner (450 s after its extinction) the flames spread over complete cable tray T2. 650 s later the flame spread from cable tray T2 to cable tray T3. For cable tray T3 no flame spread velocity could be determined since the temperatures of all thermocouples above this tray exceeded the 500 °C criterion within few seconds.

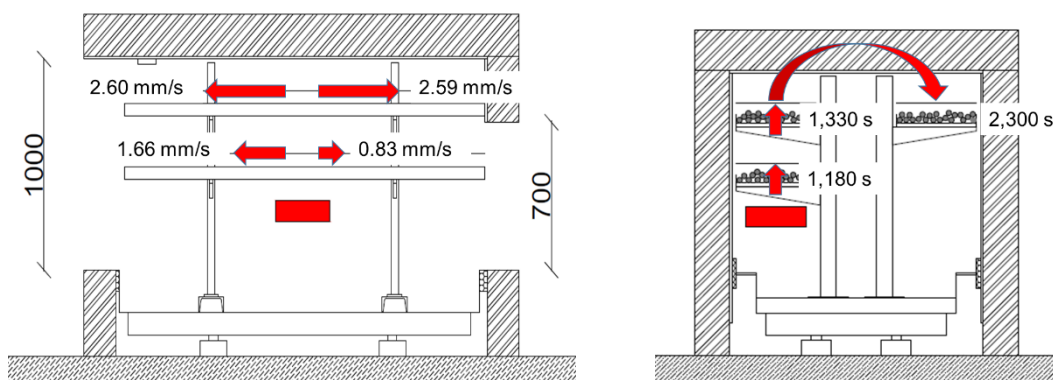


**Figure 8** Flame spread velocities (left) and ignition times (right) of cable trays T8

Figure 9 shows the average temperature 0.10 m under the ceiling. The exponential growth of the HRR results in an exponential growth of the temperature. After a short plateau phase, the temperature reached its maximum value of 694 °C (t = 2820 s). The decrease of the HRR led to a decrease of the temperature under the ceiling even though the temperature decreased slowly compared to the decrease of the HRR. 9250 s after ignition the temperature fell under 100 °C.

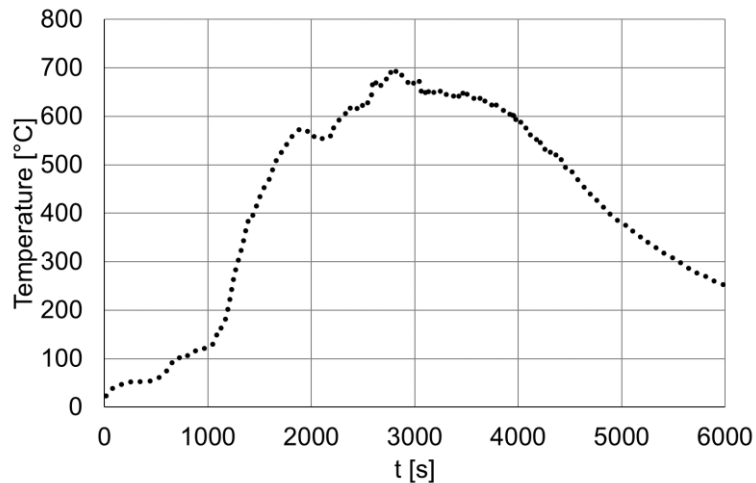


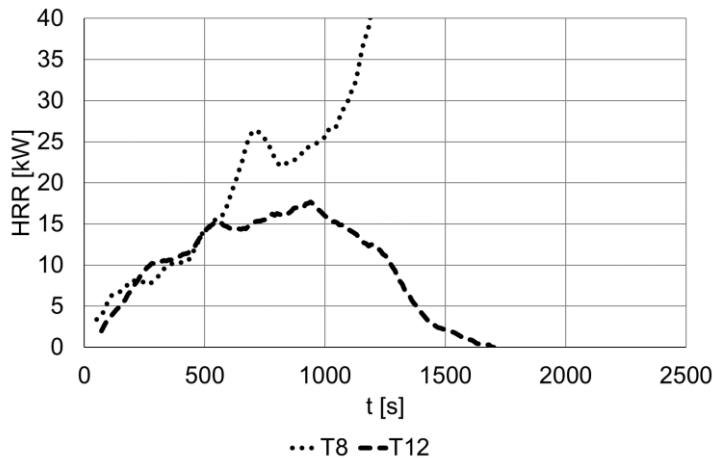
**Figure 9** Average temperature 0.10 m below the ceiling in the test T8

The temperatures in the small room itself are not sufficient to describe the fire behaviour. It is important to mention that 1410 s after ignition, flames could be observed outside the larger opening. The height of these external flames increased to about 1.00 m above the ceiling. Therefore, part of the HRR shown in Figure 6 was not released within the small room.

### Influence of the Cable Arrangement

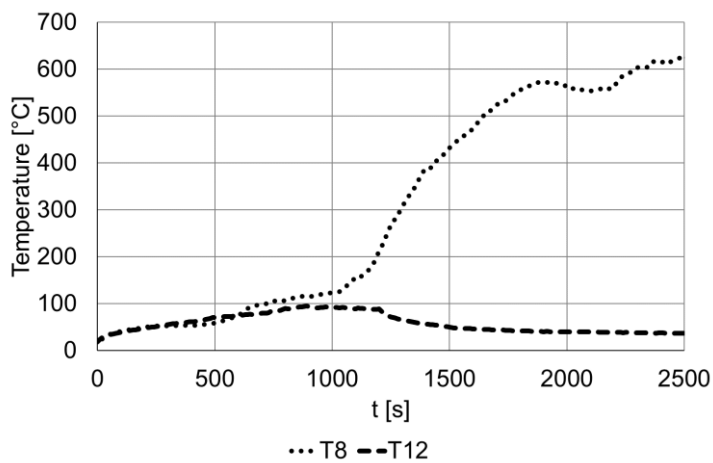
Test T12 was chosen to show the influence of the cable arrangement on the fire behaviour. In test T12 the cables were arranged tightly, which is the only changed parameter compared to test T8. The operating time of the gas burner was 20 min in each test and ventilation was set to ventilation configuration V1.

Figure 10 shows the calculated HRRs for test T8 and T12. Within the first 600 s the HRRs are quite similar. While the HRR for the loose cable arrangement continues to increase and changes into an exponential growth from  $t = 1080$  s onwards, the HRR for the tight arranged cables already reaches its maximum value of 18.5 kW at  $t = 910$  s. After this maximum the HRR decreases. After extinction of the gas burner ( $t = 1200$  s) the HRR decreases faster and reaches 0 kW at  $t = 1700$  s. The last small flames were observed at  $t = 1800$  s.



**Figure 10** Calculated HRR of a tight cable arrangement (T13) compared to the calculated HRR of the loose cable arrangement (T8)

The temperatures 0.10 m below the ceiling are significantly lower for the tight cable arrangement (see Figure 11). The maximum of 95 °C is reached after 890 s for the tight cable arrangement, while for the loose cable arrangement the temperature increases following the HRR.



**Figure 11** Average temperature 0.10 m below the ceiling for the tight cable arrangement (T13) compared to the loose cable arrangement (T8)

Regardless of the type of cable arrangement, a rapid extinguishing of the fire was observed for operating times of the gas burner shorter than 20 min (tests T6/T7 and T10/T11).

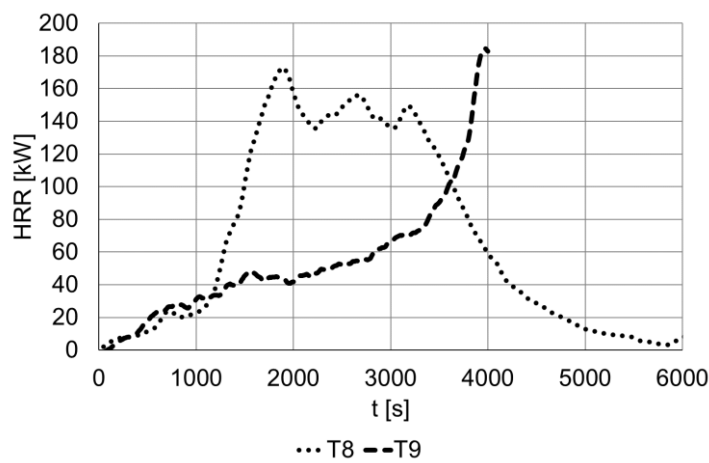
From these results, it can be stated that the cable arrangement has a significant influence on the fire behaviour in the early fire phase. Especially in the case of low power ignition sources a tight cable arrangement can effectively hinder the spread of fire and prevent a scenario, in which the fire spread over the complete fire load. From the fact that the HRRs in each test are very similar within the first 600 s, it can be deduced that the fire development in the early fire phase is mainly controlled by radiation. From a fire risk assessment's point of view it can be concluded that the risk of fire spread can be hin-

dered by using solid-bottom trays, which reduce the radiation impacting the cable surfaces.

### Influence of the Ventilation Conditions

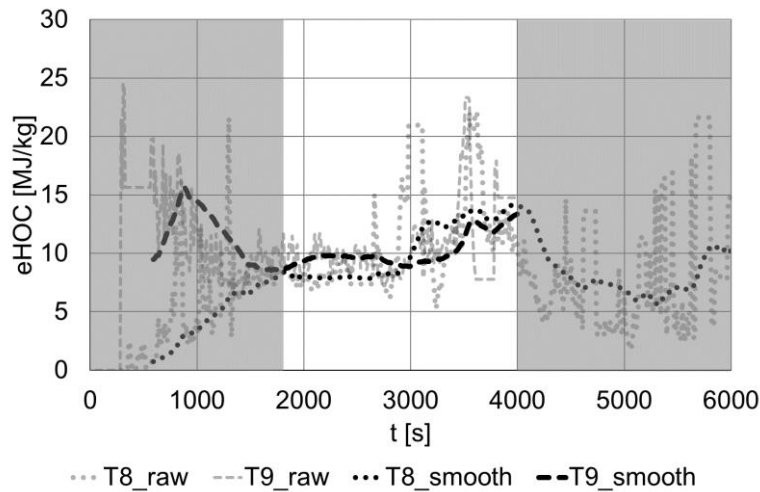
For cables in false ceilings or false floors, ventilation can be much lower than in the ventilation configuration V1 with big openings at both sides of the small room. To investigate the influence of the ventilation conditions one test with a loose cable arrangement was performed with the ventilation configuration V2. Smaller opening areas were also investigated in preliminary tests. However, it has been shown that with smaller opening areas the large release of soot from the fire load leads to early extinguishing of the gas burner by mixing soot into the flames of the gas burner.

Figure 12 shows the calculated HRRs for loose cable arrangements for both ventilation configurations V1 and V2. Due to the combination of the hot gas layer forming and the measurement of the gas concentration in the exhaust pipe of the Room Corner Test [9], a larger measurement error must be assumed for test T9. The actual HRR during the period between  $t = 1000$  s and  $t = 3000$  s may therefore be higher than shown in Figure 12. The HRRs are quite similar within the first 1100 s. While the exponential growth for ventilation configuration V1 starts at 1080 s, the exponential growth for the smaller opening area starts later at about 3000 s. The HRR increases until 180 kW before the test had to be cancelled at  $t = 4000$  s due to the fact, that the flame height outside the small room exceeded 1.50 m and combustion within the exhaust system was assumed because of high temperatures in the cooling trap of the gas analysers being observed. In addition, the exhaust system of the Room Corner Test was not able to purge the smoke gases from the fire load. At the time the test was cancelled most heat release was observed outside the small room. The first flames outside the small room were observed at  $t = 1860$  s, 450 s later compared to test T8.



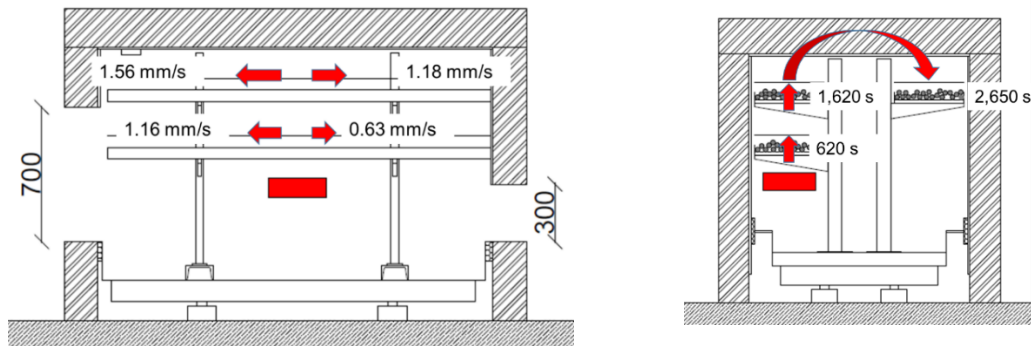
**Figure 12** Calculated HRR of the loose cable arrangement for ventilation configuration V1 (T8) and ventilation configuration V2 (T9)

Figure 13 shows the calculated effective heat of combustion of test T9 (ventilation configuration V2) compared to the effective heat of combustion of test T8. The raw calculated data were smoothed with a moving average with a step size of 60 s. The effective heat of combustion for ventilation configuration V2 reaches a maximum of 15 MJ/kg at  $t = 870$  s and decreases to a kind of plateau phase. Between  $t = 1750$  s and time  $t = 4,000$  s, the effective heat of combustion of each test is quite similar.



**Figure 13** Calculated effective heat of combustion for ventilation configuration V1 (T8) and for ventilation configuration V2 (T9)

The significantly lower HRR in the test T9 leads to significantly slower flame spread velocities, as shown in Figure 14. Compared to the test T8, the flame spread velocities are slower by factor of up to 2.2 for the flame spread velocity on tray T2 against the air inflow (2.59 mm/s vs. 1.18 mm/s). The changed ventilation configuration also leads to different flame spread velocities depending on the direction of the flame spread on the trays T1 and T2. Compared to the test T8, the ignition of the trays T2 and T3 occurs later (1620 s vs. 1330 s; 2650 s vs 300 s), but the tray T1 ignites significantly earlier (620 s vs. 1180 s).



**Figure 14** Flame spread velocities (left) and ignition times (right) of the cable tray T9

Since a hot gas layer was able to form under the ceiling in test T9, this affects the temperatures below the ceiling as shown in Figure 15. The temperatures under the ceiling for the test T9 increase earlier, starting at  $t = 300$  s. The temperature curve for test T9 is similar to the ISO standard fire curve, but the temperatures of test T9 are clearly below it. Compared to the temperature curve of test T8, there are two intersections. At  $t = 1460$  s the temperature curve of test T8 crosses the temperature curve of test T9. The second intersection occurs shortly before the termination of test T9. The temperature maximum of 650 °C of test T9 was measured at the time of the test termination.

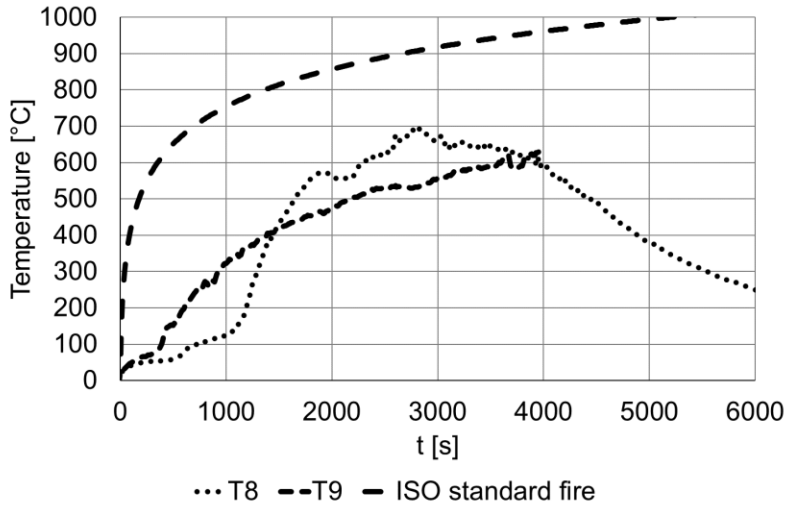


**Figure 15** Average temperature 0.10 m underneath the ceiling for the ventilation configurations V1 (T8) and V2 (T9) compared to the ISO standard fire curve

From these results, it can be concluded that the size of the openings and whether a hot gas layer can form have a significant influence on the fire development.

In test T9, a hot gas layer was able to form, which led to a faster temperature increase under the ceiling. In addition, the radiation from the hot gases within this hot gas layer led to an earlier ignition of the cable tray T1 compared to test T8.

On the other hand, the changed ventilation configuration in test T9 resulted in a larger proportion of the fire load being located within the smoke layer compared to test T8. The smoke shields the gaseous fuel from the oxygen in the ambient air necessary for combustion. This explains the significantly lower effective heat of combustion in both tests compared to the cone calorimeter tests.

According to [13], the fire in a compartment can be controlled by ventilation or by fuel. The transition between fuel-controlled and ventilation-controlled fires is described by the opening factor:

$$A_T / A_w H^{1/2} \quad (2).$$

Here,  $A_w$  is the area and  $H$  the height of the ventilation opening and  $A_T$  is the total internal area of walls and ceiling, excluding ventilation openings. Values of  $A_T / A_w H^{1/2}$  less than  $8 \text{ m}^{1/2}$  correspond to fuel-controlled fires [13], which is the case for the test setup shown here. For fuel-controlled fires the HRR can be determined by:

$$\dot{Q}_{fuel}(t) = \Delta h_{c,eff}(t) \cdot \dot{m}(t) \quad (3).$$

For the tests T8 and T9 equation (3) using the effective heat of combustion of the cone calorimeter test would result in a HRR more than twice than that measured in the tests (cf. Figure 16).

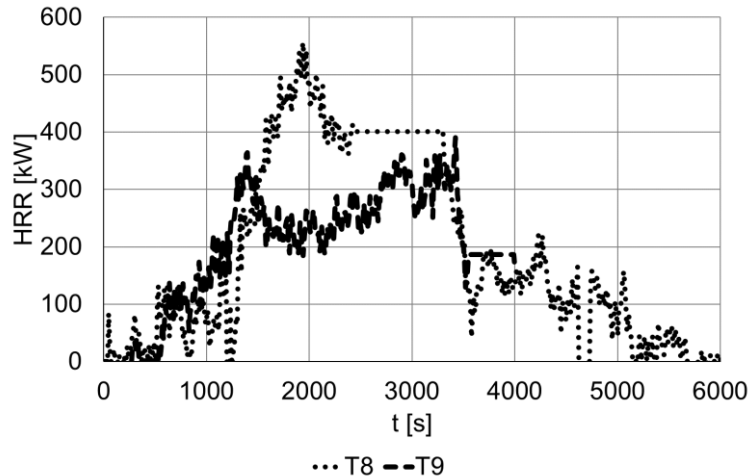


**Figure 16** Calculated HRR for the tests T8 and T9 following equation (3)

In the event of a ventilation-controlled fire, the maximum HRR can be calculated using the approach first derived by Kawagoe [2] via the air mass flow entering the room:

$$\dot{Q}_{Air} = \Delta h_{c,oxygen} \cdot \dot{m}_{air} \cdot w_{O_2} = 13100 \cdot 0,52 A_w H^{1/2} \cdot 0,23 \quad (4).$$

Using equation (4) leads to a maximum HRR of 2946 kW for the test T8 and 1,329 kW for the test T9 for those test setups presented here. It can thus be stated that the equations for compartment fires presented in [13] cannot be applied to cable tray fires in confined spaces. In the test setup presented here, the heat release is not only controlled by fuel and oxygen, but to a large extent also by the smoke gases that are released during combustion and surrounding the fire load.

## CONCLUSIONS

Based on three selected tests out of a total of 20 cable fire tests performed in a medium-scale test setup, this study has determined the influence of cable arrangement and ventilation configuration on the fire behaviour of cable trays within confined spaces. PVC-insulated cables installed in German NPPs has been chosen as fire load. The ignition was carried out by a sand gas burner with a relatively small HRR of 10 kW under the lowest tray.

The major outcomes of this study are that cable tray fires in confined spaces, in which parts of the cable fire load are located within a hot gas layer being formed, cannot be described by applying the boundary conditions of a compartment fire. In addition, it could be demonstrated that for loose cable arrangements it is more likely that the fire develops to flashover compared to a dense cable arrangement under the same boundary conditions.

Moreover, this work provides an experimental database of PVC insulated cable fires within confined atmosphere that can be used for calibration and validation of fire simulation codes.

## ACKNOWLEDGEMENTS

The research project "Numerical and experimental investigations of polymer fire loads in nuclear facilities to improve the predictability of fire simulations" has been funded by the former German Federal Ministry for Economics and Energy (BMWi) which is now the Federal Ministry of Economic Affairs and Climate Action (BMWK), and the German Federal Ministry for the Environment, Nature Conservation, Nuclear Safety and Consumer Protection (BMUV), respectively. The author wants to thank the "Gesellschaft für Anlagen- und Reaktorsicherheit (GRS) gGmbH" for supervision and supporting this work.

## REFERENCES

- [1] McGrattan, K., et. al.: Cable Heat Release, Ignition, and Spread in Tray Installations during Fire (CHRISTIFIRE): Phase 1 – Horizontal Trays, Report, NUREG/CR-7010, Vol. 1, United States Nuclear Regulatory Commission (U.S. NRC) Office of Nuclear Regulatory Research, Washington, DC, USA, July 2012, <https://www.nrc.gov/reading-rm/doc-collections/nuregs/contract/cr7010/v1/index.html>.
- [2] Kawagoe, K., T. Sekine: Estimation of Fire Temperature-Time Curves in Rooms, Occasional Report No. 11, Building Research Institute of Japan, Tokyo, Japan, 1963.
- [4] Deutsches Institut für Normung e.V. (DIN) und Verband der Elektrotechnik, Elektronik und Informationstechnik e.V. (VDE): DIN VDE 0250-204 (VDE 0250-204): Isolierte Starkstromleitungen, PVC-Installationsleitung NYM, Beuth Verlag GmbH, Berlin, Germany, December 2000 (in German).
- [5] Pohle, H.: PVC und Umwelt – Eine Bestandsaufnahme, Springer-Verlag Berlin Heidelberg, Berlin, 1997 (in German).
- [6] Hosser, D., O. Riese, and M. Schmeling: Durchführung von vergleichenden Brandversuchen mit unterschiedlichen Kabelmaterialien und Kabelschutzsystemen, Abschlussbericht, VGB-Kennziffer SA „AT“ 11/00, iBMB, TU Braunschweig, Braunschweig, Germany, 2003 (in German).
- [7] Zehfuß, J., and M. Siemon: Entwicklung, Erprobung und Validierung eines erweiterten Pyrolysemodells für Kabelbrandlasten, Kurztitel: Pyrolysemodell, Abschlussbericht -- Im Rahmen des BMWi-Vorhabens, Förderkennzeichen: 1501419, iBMB, TU Braunschweig, Braunschweig, Germany, 2017 (in German).
- [8] Zavaleta, P.: PRISME2 – Core Campaign, Analysis report of the CORE-1 to CORE-4 fire tests, Institut de Radioprotection et de Sûreté Nucléaire (IRSN), Saint Paul-Lez-Durance, France, 2016.
- [9] International Organization of Standardization (ISO): ISO 9705-1: Reaction to fire tests – Room corner test for wall and ceiling lining products – Part 1: test method for a small room configuration, First edition, Geneva, Switzerland, February 2016.
- [10] Janssens, M.: Calorimetry, in DiNenno, P.J. (Ed.): Society of Fire Protection Engineers (SFPE) Handbook of Fire Protection Engineering, 3<sup>rd</sup> Ed., ISBN 978-0877654513, National Fire Protection Association (NFPA), Quincy, MA, USA; 2002:
- [11] International Organization of Standardization (ISO): ISO 5660-1: Reaction-to-fire tests – Heat release, smoke production and mass loss rate – Part 1: Heat release rate (cone calorimeter method) and smoke production rate (dynamic measurement), Third edition, Geneva, Switzerland, March 2015.

- [12] Prétrel, H.: PRISME 3 and FIRE common benchmark exercise – Step#2\_2, Analysis Report, Institut de Radioprotection et de Sûreté Nucléaire (IRSN), Saint Paul-Lez-Durance, France, 2020.
- [13] Drysdale, D.: An Introduction to Fire Dynamics, 3<sup>rd</sup> Edition, ISBN 78-0-470-31903-1, John Wiley & Sons, Ltd., Chichester, United Kingdom, 2011.

# Investigating A Cable Tray Fire Event in the Frame of An International Benchmark Exercise

William Plumecocq<sup>1\*</sup>, Sophie Bascou<sup>1</sup>, Marina Röwekamp<sup>2</sup>, Kenneth Hamburger<sup>3</sup>

<sup>1</sup> Institut de Radioprotection et de Sûreté Nucléaire (IRSN), Cadarache, France

<sup>2</sup> Gesellschaft für Anlagen- und Reaktorsicherheit (GRS) gGmbH, Köln, Germany

<sup>3</sup> Nuclear Regulatory Commission (NRC), Washington, DC, United States of America

## ABSTRACT

Based on a request from the OECD (Organization for Economic Co-operation and Development) Nuclear Energy Agency (NEA) Fire Incidents Records Exchange (FIRE) Database Project) in 2016, the PRISME 2 (French: *Propagation d'un incendie pour des scénarios multi-locaux élémentaires*) Program Review Group recommended a common Benchmark Exercise on a realistic cable fire scenario that resembles, as closely as possible, a real cable fire event included in the FIRE Database, using information on electrical cable fires from the OECD/NEA PRISME projects. This led to the joint venture of the two OECD/NEA Projects called "Common OECD/NEA FIRE and PRISME Cable Benchmark Exercise".

The major goal of this Benchmark Exercise was to simulate a real cable fire event in order to assess the behaviour of fire models for a complex and real fire scenario with the current state of knowledge.

Since a numerical Benchmark Exercise on a real fire event is quite challenging, the following three-step methodology for conducting this Benchmark Exercise was adopted: (1) a calibration phase of the cable fire models on a PRISME 2 cable fire test, (2) a blind simulation of a PRISME 3 cable fire test, and (3) the real cable fire event simulation.

The selected fire event from the FIRE Database to be addressed during the Benchmark occurred in 2014 in a heater bay of a nuclear power plant (NPP) and involved two horizontal electrical cable trays. The characteristics of the event made it necessary to provide knowledge on the specific fire source involved in the real fire event and to re-calibrate the fire models on the event-like fire source. Consequently, an intermediate step (Step 2\_2) between Step 2 and Step 3 was introduced in the Benchmark Exercise. The methodology is based on the fact that a similar behaviour is expected between Step 1 and Step 2\_1, and between Step 2\_2 and Step 3, making it possible to transpose the error increment of quantities.

Thirteen institutions from nine NEA member countries (Belgium, Finland, France, Germany, Japan, Korea, Spain, the United Kingdom, and the United States of America) participated in this Benchmark Exercise. Simulations were performed using computational fluid dynamics codes, a lumped parameter code, and more simple zone codes. The simulations by the Benchmark participants have provided a wide range of results which reflect the difficulty for fire simulation codes to correctly predict the development over time of the fire heat release rate of a cable tray fire, even under simple, open atmosphere conditions.

This paper focuses on a real fire event selection, the difficulties this represents in terms of availability of data and further investigations necessary to perform such an international Benchmark Exercise to assess fire models on a real fire scenario.

## INTRODUCTION

Based on a request from the FIRE Database Project of the OECD/NEA in 2016, the PRISME 2 Program Review Group (PRG) recommended that there should be a common Benchmark Exercise on a realistic cable fire that resembles, as closely as possible, a real cable fire event recorded in the FIRE Database, using information on electrical cable fires from the OECD/NEA PRISME Projects. This led to the joint venture of the two OECD/NEA Projects called “Common OECD/NEA FIRE and PRISME Cable Benchmark Exercise”.

Observations from the FIRE Database [1], [2] have clearly demonstrated the significance of fire events involving cables and shown that a majority of these events were either safety related or had the potential to impair nuclear safety. On this topic, the PRISME 2 cable fire experiments [3], [4] have significantly increased the knowledge regarding cable fire behaviour and investigated various types of cables implemented in nuclear power plants (NPPs) in member states.

The major goal of this Benchmark Exercise was to simulate a real cable fire event in order to assess the behaviour of fire models for a complex real fire scenario based on the current state of knowledge.

Since a numerical Benchmark Exercise on a real fire event is quite challenging, the following three-step methodology for conducting this Benchmark Exercise was adopted: (1) a calibration phase of the cable fire models on a PRISME 2 cable fire test, (2) a blind simulation of a PRISME 3 cable fire test, and (3) the simulation of the real cable fire event from the FIRE Database.

For selection of a real NPP cable fire event recorded in the FIRE Database, the at the start of the Benchmark Exercise latest version of the Database (2017:02) [5] released in May 2019, with more than 500 fire events recorded up to the end of 2017, was used. The criteria for the cable tray fire event selection, as prescribed by the PRISME 2 PRG members, were the following:

- a cable fire scenario with flames and smoke,
- a quite recent event (from about the last ten years),
- a sufficiently well-documented event,
- the significance of being able to receive additional information on the fire event besides that recorded in the Database,
- the closeness to PRISME cable fire experimental scenarios,
- preferably only one compartment involved in the fire,
- a fire duration between 15 min and 60 min.

A shortlist of four potential candidates providing a quite detailed description of the ignition phases and the sequences of the events from the available information was established. The ability to gather enough data on the event from the licensees supporting the activity was a decisive criterion for the final event selection. Based on all prerequisites, the real fire event finally selected was an event that had occurred in 2014 in a heater bay of a NPP involving two horizontal electrical cable trays, mainly loaded with Polyvinyl Chloride (PVC) insulated cables.

The characteristics of the event made it necessary to gain knowledge on the specific fire source involved in the real fire event and to re-calibrate the fire models on the event-like fire source. Consequently, an intermediate step (Step 2\_2) between Step 2 and Step 3 was introduced in the Benchmark Exercise. The methodology was based on the fact that

a similar behaviour is expected between Step 1 and Step 2\_1, and between Step 2\_2 and Step 3, making it possible to transpose the error increment of quantities.

## THE HEATER BAY FIRE EVENT

The selected fire event occurred in the heater bay of a NPP turbine building. The fire involved two 0.90 m wide horizontal cable trays mainly loaded with PVC insulated cables. The source of the cable flaw was identified as a non-conforming cable routing of the Instrument Bus (IB, 3 cables) and Essential Service Bus cables (ESS, 3 cables), i.e., in a manner inconsistent with the current standard for minimum static bend radius for this type and size of cable, i.e., resting across rungs and exiting at a sharp angle downward into a 12-m vertical run (see Figure 1). The fire started by self-ignition of 120 V power cables due to an arc fault. It was initiated when the high humidity and condensate from a steam leak (see Figure 2) provided the environment necessary for the existing flaw in an electrical cable to short to ground.

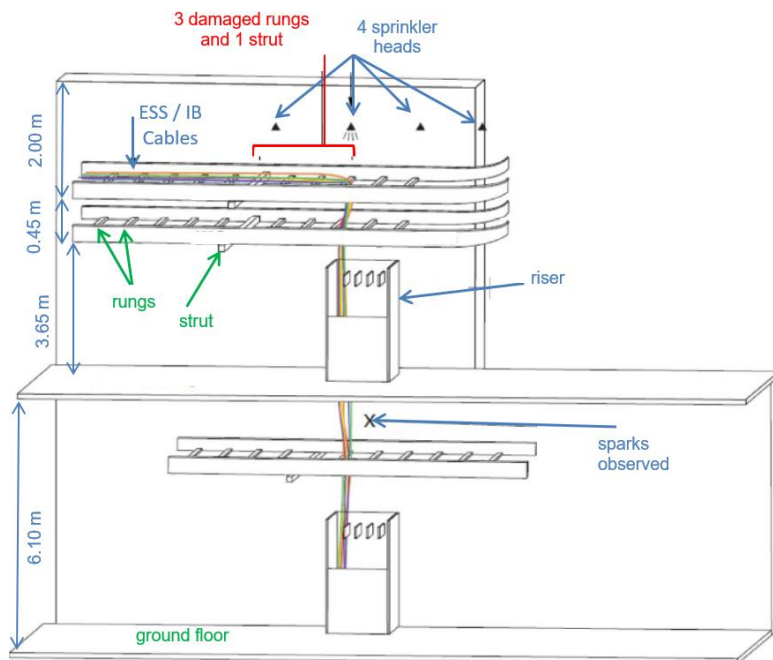


**Figure 1** Front view scheme of the cable routing in the heater bay

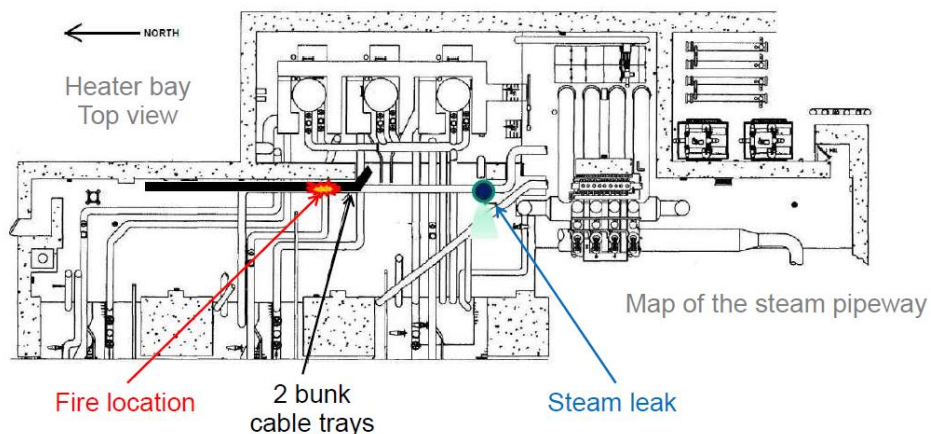


**Figure 2** Top view scheme of the heater bay

The fire duration between ignition and successful extinction by a wet pipe sprinkler was estimated to be approximately 20 min ( $\pm 2$  min). Investigations by the licensee provided a detailed description of the fire behaviour and the sequence of the event detailed hereafter.

The non-conforming cable routing concerned three instrument bus (IB) cables and three essential service system (ESS) bus cables. The arc fault from one of the six cables to the rung at the exit point damaged the insulation of nearby cables and heated the rung, leading to the severing of five (2 IB and 3 ESS) of the six cables. This conclusion is based on in-situ examination recording the remaining riser portion of each of the five cables of equal length, with severed ends at the rung, and the remaining horizontal portions of two of the ESS bus cables also aligned with the rung. When they were severed, the two-line cables for the IB feed arced together. These cables continued to arc until approximately 0.61 m of copper had melted from each of the IB line cables.

The arc fault between the IB line cables ended at a strut support, as evidenced by the ends of the IB cables being found aligning with and in the molten portion of the strut. It is likely that the breaker for the IB feed tripped at this time, as evidenced by the remaining intact copper. The total time from the initial arc fault to the IB feed breaker trip is estimated to be approximately 1 min, corresponding to the time when sparks were observed outside the heater bay, and the time of the swap of the IB from its main feed to a backup feed.

The fire on the lower tray was initiated by debris falling from the fire on the upper tray and radiative heat from the fire source of the upper tray. This is evidenced by the concentration of the damaged cable in the upper levels of the lower tray, with the lower levels undamaged or much less damaged. Additionally, there is no evidence of molten copper conductor in the lower tray. The fire in the lower tray appears to have continued to burn until extinguished by the fixed fire extinguishing system (wet sprinklers).

Four sprinkler heads were located in the vicinity of the fire, at about 1.20 m to 1.50 m above the top of the upper tray. The sprinkler heads initiate by thermal (fusible) links set to break at 100 °C with a standard response time index (about 100 to 360 m<sup>1/2</sup>s<sup>1/2</sup>) [6]. The heat generated by the fire caused flow from only one of the four sprinkler heads in the area. Laboratory testing provided the result that there was no existing flaw for the three sprinkler heads which did not actuate and that the three heads were physically capable of responding if actuation was required. The actuated sprinkler head successfully extinguished the cable tray fire.

The time sequence of the cable fire event is summarized in Table 1.

**Table 1** Time sequence of the fire event from the FIRE Database

| Time           | Event   |
|----------------|---|
| $t_0$          | The main control room (MCR) received a fire alarm for the heater bay area. The on-site fire brigade leader was sent to the area to assess the situation.  |
| $t_0 + 10$ min | Based on observations at that time, the fire brigade leader reported neither fire nor smoke, but a steam leak.  |
| $t_0 + 30$ min | The reactor unit was switched to another mode per operating procedure; the MCR was unaware at this time of the exact source of the steam leak. It was anticipated that allowing steam to the main turbine and rolling the turbine would assist in mitigating the observed steam leak. |

| Time           | Event   |
|----------------|---|
| $t_0 + 34$ min | The MCR received numerous unexpected alarms and observed other anomalous indications on the MCR panels.   |
| $t_0 + 35$ min | Based on these alarms and indications, and since there was a known steam leak, the unit was manually scammed.   |
| $t_0 + 39$ min | In response to field operator reports that sparks had been observed in the building ground floor hallway, the MCR operators actuated the plant fire siren and sent on-site fire brigade leaders.  |
| $t_0 + 44$ min | The main steam isolation valves were closed, isolating the steam leak.  |
| $t_0 + 47$ min | The MCR received a report that smoke was now observed at the hydrogen seal oil vacuum pump breaker cubicle in a motor control center.   |
| $t_0 + 53$ min | The east side of the turbine Fire Alarm System alarmed caused by the actuation of the fire extinguishing system (a sprinkler actuated by fusible link). The fire was extinguished by the automatically actuated fixed sprinkler system. |

## FIRE SIMULATION APPROACHES

Thirteen institutions from nine NEA member countries (Belgium, Finland, France, Germany, Japan, Korea, Spain, the United Kingdom, and the United States of America) participated in this Benchmark Exercise. Simulations were performed using computational fluid dynamics (CFD) codes, a lumped parameter code (LPC), and zone codes (ZC). Most of the CFD simulations (10 out of 12) were performed with the open source FDS (*Fire Dynamics Simulator*) software [7] developed by the U.S. National Institute of Standards and Technology (NIST). Details are reported in [7], Table 6.

Cable tray fire modelling remains a complex issue. Given the multitude of parameters involved in the definition of such a fire source (cable orientation, cable length, number of cable trays, spacing between trays, cables loading, flame retardant compounds, etc.), no theory has yet been put forward on how to model all the aspects of the problem, even for simple, open atmosphere conditions. Some approaches in the form of experimental studies [8], [9] and more recently [3], [4], [10] have nevertheless been carried out and an empirical model (FLASH-CAT [9]) was developed by the NIST for horizontal cable tray fires in open atmosphere. FLASH-CAT (short for *flame spread over horizontal cable trays*) is a relatively simple model for predicting the growth and spread of a fire within a vertical stack of horizontal cable trays.

Hypotheses used by the FLASH-CAT model suggest that the fire would propagate upward through the cable trays depending on an empirical timing sequence only based on the tray order in the stack model and assumes that, once ignited, the cables burn over a length that is larger than that of the tray below. The burning pattern has therefore an expanding V-shape as there is an increasing length of cable that ignites when the fire propagates upwards due to the lateral propagation of fire. As the mass of combustible material at the center of the V is consumed, a horizontal extinction front appears at the center of the trays and the V-shape becomes an open wedge until the full length of cable is burnt. The model parameters indicated in [9] have been chosen based on the observation of tests performed at Sandia National Laboratories (SNL) under very particular conditions.

During this Benchmark Exercise, most of the participants used a FLASH-CAT-like approach by adapting the original model to compartment fires. Indeed, fires in confined and

mechanically ventilated compartments often result in a significant decrease in the mass loss rate (MLR), and hence in fire heat release rate (HRR), compared to that obtained in open atmosphere.

Other participants used a macroscopic model which allows for the estimation of the HRR of a cable tray fire knowing some parameters, generally calibrated by comparing the model to real scale experiments available in the literature. From general observations of real scale cable tray fire experiments a conservative HRR curve is built. As this curve is conservative in open conditions, an oxygen limiting law is used to account for the effect of the confinement.

Whatever the simulation approach selected by the Benchmark participants, the common point is the knowledge of the fire source and the associated parameters required by their model. Due to the originality of the real fire event compared to the PRISME experiments available so far, a specific test has been planned for the Benchmark needs which is presented in the next paragraph.

## THE SPECIFIC PRISME 3 PRF-BCM-S2 TEST

### Overview of the PRF-BCM-S2 Test

The PRF-BCM-S2 test was carried out in order to gain knowledge on the specific fire source of the real cable fire event and to re-calibrate the fire models on the event-like fire source between Step 2 and Step 3 of the Benchmark.

Considering that oxygen depletion is not assumed to be an important factor in the real fire event, the PRF-BCM-S2 test was conducted under the large-scale calorimetric hood of the SATURNE experimental facility (10 m long, 10 m wide and 20 m high) of IRSN (*l*nstitut de Radioprotection et de Sûreté Nucléaire), as it provides enough air to maintain the oxygen concentration at 21 % in the vicinity of the fire source as in open atmosphere.

A simplification for the cable information for the simulation of the real fire event was proposed by the U.S. NRC so that Benchmark participants could operate with known generic properties for the testing and modelling work. The starting point was the THIEF (Thermally-Induced Electrical Failure) [11]. Thus, simulations of the real cable fire event were performed with PE/PVC (Polyethylene/Polyvinyl chloride) insulated cables, as the ones supplied by the U.S. NRC and tested in the PRF-BCM-S2 test.

The PRF-BCM-S2 test fire source consists of two horizontal cable trays, similar to the cable trays involved in the real fire event, as illustrated in Figure 3. The tray dimensions are 900 mm in width, 3000 mm in length, and 150 mm in height. The distance between trays is 450 mm. The cable trays are ladder-type cable trays, open on the bottom side. Rungs are arranged every 300 mm and measure approximately 25 mm. The two-cable-tray stack is set up against an insulated side wall. The side wall consists of a panel of insulated material (Superwool 607 HT Board, 40 mm thick) attached to a metallic frame with angle bars.

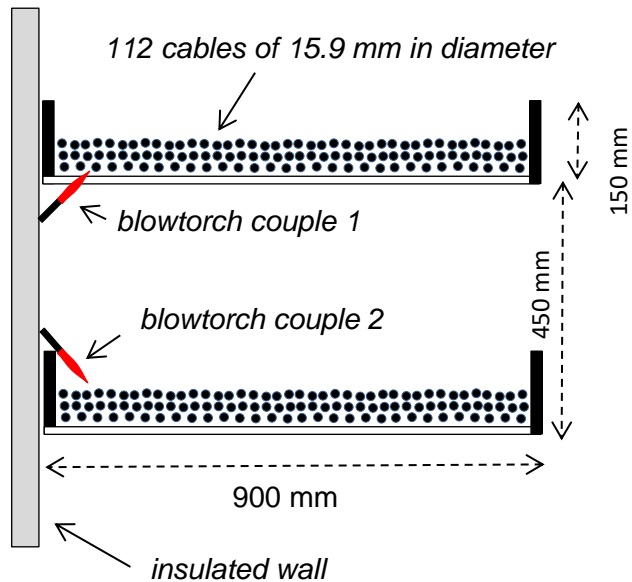


**Figure 3** Scheme of the PRF-BCM-S2 test fire source

Each tray was filled with 112 PE/PVC insulated cable samples (15.9 mm in diameter, 2.4 m long). The cables were set loosely in the trays with a height filling rate corresponding to approximately half the height of the tray and, consequently, half the cable depth of that in the real fire event.

In order to reproduce the real fire event as closely as possible, the cable ignition in the PRF-BCM-S2 test was achieved by means of two couples of blowtorches, one located below the upper cable tray and directed upwards and the other, above the lower cable tray and directed downwards, as shown in Figure 3. The blowtorches were located at the center of the trays and near the sidewall. Each blowtorch couple provides a power source of about 6.5 kW (0.15 g/s of propane) for 2 min and 30 s; then the power was increased to 9 kW (0.2 g/s) to ensure ignition.

The blowtorch flame forms a tube (1 mm in diameter, 100 mm in length) touching the cables. The temperature of the jet flame ejected from the blowtorch is about 1200 °C and is comparable to the melting temperature of copper (1085 °C) as it probably happened in the real fire event with the arc fault. The blowtorches were stopped after 760 s (12 min and 40 s).

The composition of the cables and their burning characteristics are reported in Table 2 and Table 3, respectively. For the FLASH-CAT-like modelling, the average bench-scale HRR per unit area under 50 kW/m<sup>2</sup> irradiance is 245 kW/m<sup>2</sup> and 314 kW/m<sup>2</sup> under 75 kW/m<sup>2</sup> irradiance. Since the cable's thermal inertia and ignition temperature were not available, values of 0.27 kW<sup>2</sup>s/m<sup>4</sup>K<sup>2</sup> for the thermal inertia and 218 °C for the ignition temperature were suggested according to PVC insulated cables tested in the PRISME 2 CFS-2 test [4].

**Table 2** Composition of the cables

|                     |     |
|---------------------|-----|
| Insulation material | PE  |
| Jacket material     | PVC |
| Conductors          | 7   |

|                              |      |
|------------------------------|------|
| Diameter [mm]                | 15.9 |
| Jacket thickness [mm]        | 1.85 |
| Insulator thickness [mm]     | 1.07 |
| Mass per length [kg/m]       | 0.38 |
| Copper mass fraction [-]     | 0.55 |
| Jacket mass fraction [-]     | 0.27 |
| Insulation mass fraction [-] | 0.10 |
| Filler mass fraction [-]     | 0.08 |

**Table 3** Burning characteristics of the cables

| $Y_{CO_2}$<br>[g/g] | $Y_{CO}$<br>[g/g] | $Y_{CnHm}$<br>[g/g] | $Y_{soot}$<br>[g/g] | $Y_{HCl}$<br>[g/g] | $\Delta H_c$<br>[MJ/kg] | Radiative<br>Heat Fraction<br>[-] |
|---------------------|-------------------|---------------------|---------------------|--------------------|-------------------------|-----------------------------------|
| 1.60                | 0.11              | 0.08                | 0.03                | 0.03               | 24                      | 0.35                              |

Note: The yield of a species  $i$  ( $Y_i$ ) is defined as the ratio of the total cumulative mass of species  $i$  produced up to the total mass loss of the combustible

## Results Analysis

The experimental and simulated development of the fire HRR over time is plotted in Figure 4. The experimental HRR was computed as the average of two formulations based on the oxygen consumption rate and on the carbon dioxide generation rate.

In accordance with the power delivered by the blowtorches, the incubation stage of the fire lasted for 620 s. This time corresponds to the preheating time of the cables. Then, a fast increase in the HRR was observed, with a HRR peak of 2.3 MW reached in a few minutes and corresponding to the fast-spreading stage of the fire. The two blowtorches directed towards the bottom of the upper tray induced a ceiling flame regime for approximately 10 min favouring the preheating of the cables on the lower tray. After the HRR peak, the fire HRR decreased progressively until fire extinction. During the decay stage of the fire, small increases in the HRR were observed, as shown in Figure 4. According to a video analysis, these peaks are correlated to the flame colour changes (soot effect).

The low power ignition protocol over a longer time as used in the PRF-BCM-S2 test led to a better preheating of the cables and a higher fire growth rate compared to a conventional ignition of cables with a sand burner located below the lower cable tray and delivering a power source of 80 kW as used in the PRF-BCM-S1 test, for the same type of fire source under the calorimetric hood in the SATURNE facility.

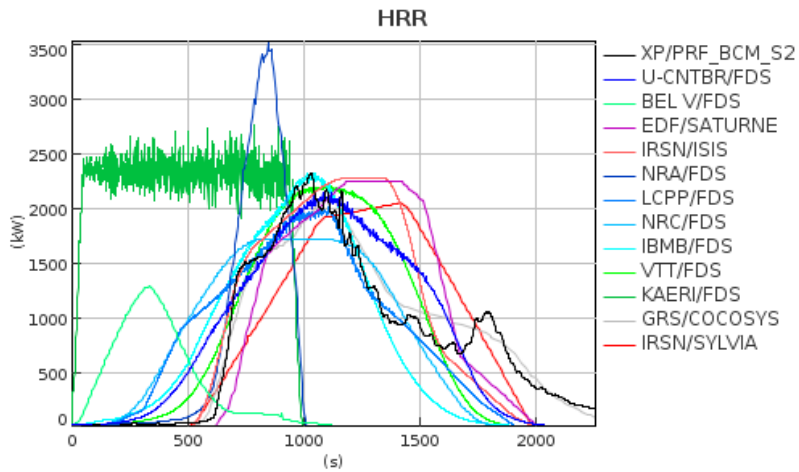


**Figure 4** Simulation results of the HRR compared to the BCM-S2 experimental results

The predicted HRR peak is captured by the models applied by most participants; however, deviations from the experimental values were observed on the duration of the incubation stage of the fire, clearly demonstrating the difficulty of correctly predicting the preheating of the cables. The lack of data on the thermal inertia and ignition temperatures of the cables contributed to these deviations when preheating was calculated since these quantities play an important role regarding the preheating time of cables. It is important to capture the incubation stage of the fire with this specific ignition power because in the real fire event the actuation of the automatic sprinkler system prevented the full development of the fire.

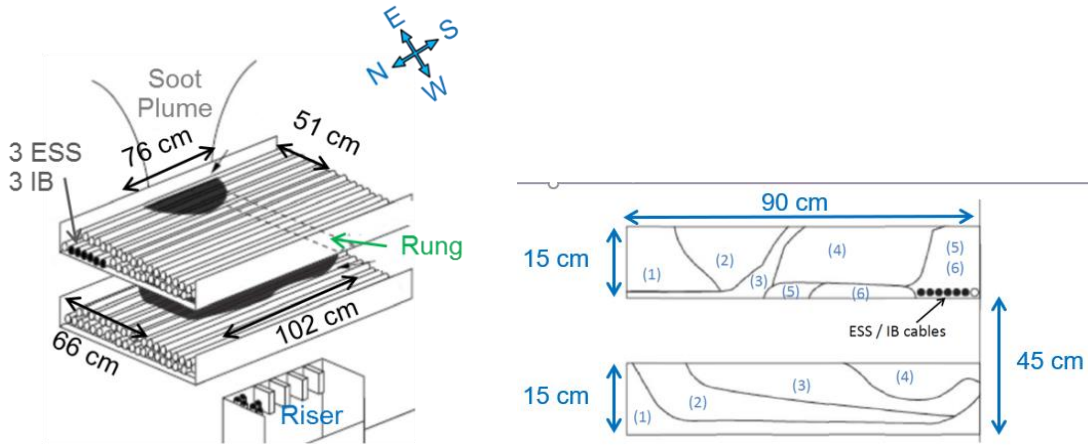
## SIMULATIONS OF THE REAL FIRE EVENT

### Assumptions and Available Data

Real fire events do not occur under laboratory conditions; therefore, the available data are limited. In the heater bay fire event, at the exit point from the upper tray (see Figure 1), cables were severed, and the jacket/insulation was removed due to excessive heat. An initial inspection showed localized fire damage in the shape of a semicircle 0.76 m long and 0.51 m wide, as illustrated in Figure 5. Charring was present throughout the entire depth of cables in that section (approximately 0.15 m deep).

The extent of cable damage in this area included cables severed, cable jacket/insulation damage, cable jacket/insulation completely removed and sections of the cables missing. The most extensive charring and damage was observed on those cables located at the bottom of the upper tray with signs of an arc flash. The initial inspection of the lower tray showed localized fire damage in the shape of a semicircle approximately 1.02 m long and 0.66 m wide (see Figure 5). Charring was present throughout the 0.10 m top of cables in that area. Molten drips could be observed on top of numerous cables on the lower tray (tests subsequently verified that cuprous oxide ( $Cu_2O$ ) was present in large quantities on the cables of the lower tray).

Signs of minor concrete spalling were observed on the diagonal concrete overhang located above the affected cable trays. The smoke damage to the wall formed a V-pattern with a wide shape that extended to the ceiling, indicating a slowly burning fire.



(1) No damage, (2) Moderate damage (partial jacket damage), (3) Medium damage (complete jacket damage), (4) Heavy damage (complete jacket damage with partial insulation wire damage), (5) Extreme damage, (6) Severed cables

**Figure 5** Damage pattern of the cable trays

A coarse estimation of the fire load involved in the real fire event was carried out. Details are reported in Table 4. This estimation is based on the assumptions that damage classes 3 to 6 on both cable trays are idealized by a half-truncated cone and that the volume of damage class 2 is located around the larger affected areas. Assuming a raw density of the combustible parts of the cables of  $230 \text{ kg/m}^3$  and combustion heat of  $24 \text{ MJ/kg}$  deduced from the PRF-BCM-S2 test results, about  $630 \text{ MJ}$  energy would have been released by the fire (excluding any electrical heat due to arcing), corresponding to a mass loss of about  $26 \text{ kg}$ .

**Table 4** Coarse estimation of the fire load

|               |                        | Upper Tray                |                |                | Lower Tray                |                |                |
|---------------|------------------------|---------------------------|----------------|----------------|---------------------------|----------------|----------------|
| Damage Class  | Pyrolyzed Fraction [%] | Volume [cm <sup>3</sup> ] | Mass Loss [kg] | Heat Loss [MJ] | Volume [cm <sup>3</sup> ] | Mass Loss [kg] | Heat Loss [MJ] |
| 2             | 15                     | 46,186                    | 1.59           | 38.1           | 60,691                    | 2.08           | 49.9           |
| 3             | 50                     | 27,489                    | 3.16           | 75.8           | 53,073                    | 6.09           | 146.1          |
| 4             | 80                     | 37,672                    | 6.92           | 166.1          | 10,866                    | 1.99           | 47.7           |
| 5             | 100                    | 4,199                     | 0.96           | 23.0           |                           |                |                |
| 6             | 100                    | 5,726                     | 1.31           | 31.4           |                           |                |                |
| 5 - 6         | 100                    | 9,558                     | 2.20           | 52.8           |                           |                |                |
| <b>Total:</b> |                        | <b>16.14</b>              | <b>387.2</b>   |                |                           | <b>10.1</b>    | <b>243.7</b>   |

The dimensions of the ground of the turbine building including the heater bay are almost the only available data regarding the building geometry as shown in Figure 6. It is a very large building of about  $1,900 \text{ m}^2$  ground surface with approximately  $600 \text{ m}^2$  ground surface for the heater bay. The heater bay is an area of the plant containing high pressure feedwater heaters, pipes, cable trays, risers, and overhangs as shown in Figure 2. A free volume of  $2,900 \text{ m}^3$  is set by default, corresponding to 80 % of the estimated physical volume of the heater bay from available data. The heater bay has a mezzanine located

at 6.1 m from the ground (see Figure 1) where the fire occurred. In addition, the heater bay is connected to the rest of the turbine building by several openings, indicated by orange lines in Figure 6. The riser also creates an opening between the mezzanine level and the ground level, just beneath the fire. The trays' routing and pictures of the event indicate a passage through a hole to the back area of the heater bay. The latter two openings have not been considered in the overall dimensions, but they potentially induced flows in the vicinity of the fire ignition.

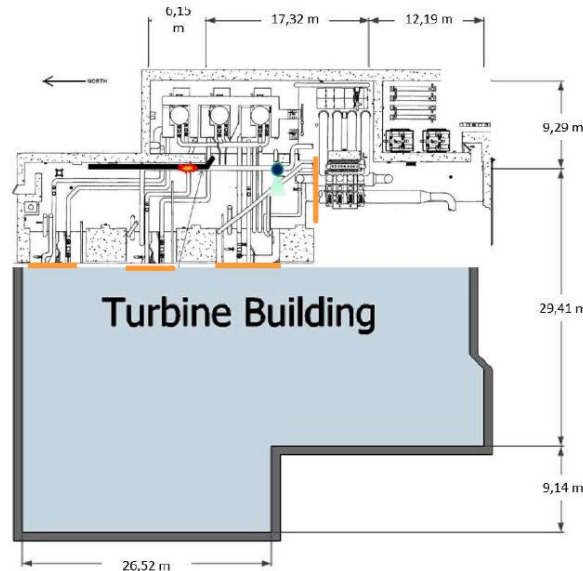


**Figure 6** Scheme of the top view of the turbine building including the heater bay

According to the fire event sequence (see Table 1) and the statement of the representative of the FIRE member country where the fire occurred, it was concluded that the fire was not affected by the mechanical ventilation since the room's ventilation was isolated by closing of the fire dampers actuated by smoke detection. Therefore, simulations were performed without mechanical ventilation. In addition, the overall pressure rise in the turbine building is likely to be negligible, even with the steam leak. This assumption is based on the small size of the steam pipe (a few centimetres in diameter) and the supposed large openings to the rest of the turbine building. Thus, the steam leak was not considered in the simulations, but its effects were nevertheless taken into account through the presupposed initial gas temperature (30 °C) and relative humidity in the compartments (90 %).

As mentioned before, a simplification for the cable information was proposed by the U.S. NRC so that Benchmark participants could operate with known generic properties for the testing and modelling work. Thus, the fire source for the simulation of the real event was equivalent to that of the PRF-BCM-S2 test (see Figure 3).

The fire ignition scenario is very far from scenarios studied in the PRISME Projects. Fire ignition due to an arc fault is typically not modelled by fire simulation tools. Therefore, it is assumed that the complete electric power of the defective cables is converted into a localized heat source. Nevertheless, simulating an arc fault by an "equivalent" heat source requires information on the power of cables and the duration of the arc fault. Since these data are not available, default values were set in the simulations. It was suggested to use a power source equivalent to that of the propane sand burner used in the PRISME 2 CFS-2 test for the ignition of PVC insulated cables. It provided a power source of 80 kW for 2 min and 26 s. It was also suggested to use thermally thick targets to ignite the cables (one in each cable tray). The ignition of cables would then be dominated by a temperature criterion.

Four sprinkler heads (manufacturer reference C-DURASPEED) were located in the vicinity of the fire, at about 1.20 m to 1.50 m above the top of the upper tray, as illustrated in Figure 7. The sprinkler heads are actuated thermally by fusible links set to break at 100 °C with a standard response time. The heat generated by the fire caused a flow from only one of the four sprinkler heads 19 min after fire detection (cf. Table 1). Since the fire source was located under an overhang below the ceiling of the heater bay, the overhang probably played an important role in the actuation time of the sprinkler.

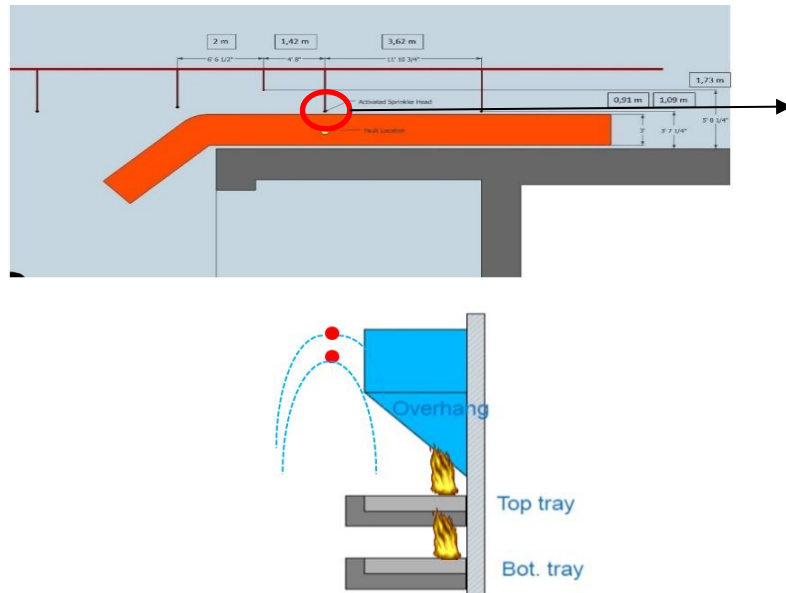


**Figure 7** Scheme of the spatial arrangement of the active sprinkler heads

## Results Analysis

According to the time sequence of the event (see Table 1), the time for starting the simulations ( $t = 0$  s) was set at the event time  $t_0 + 34$  min, because no indication of fire was reported by the fire brigade before this time.

The Benchmark participants were requested to simulate the development of the fire until the temperature criterion of 100 °C was reached at the elevation of the actuated sprinkler, considering that fire extinction will occur when the sprinkler is actuated, as in the real fire scenario.

The predicted development of the fire HRR over time is plotted in Figure 8 and is compared to the mean simulation result over the common simulated period (341 s according to the shortest simulation). Despite this short time, the mean simulation gives an indication of how the ignition of cables has been modelled by the Benchmark participants.

The fire growth rates predicted by different codes and users are very different from each other, highlighting the difficulty of predicting the ignition of cables as well as the incubation stage of the fire of such a fire source. For those simulations predicting the triggering of the sprinkler, the predicted HRR just before the actuation of the sprinkler ranges from 290 kW to 2600 kW with most of the predictions below 1000 kW.

One explanation to this observation is that Benchmark participants neither have the same models, nor the same requested input data for the simulation, nor the same approach of choosing them. Differences are also linked to the predictivity level of the simulation tools (i.e., the number of parameters defined by the user compared to the parameters fully predicted from basic data) and from the user choices. The Benchmark strategy required the use of, as far as possible, the same input data as from in the previous steps

and, in particular, similar input parameters taken from the PRF-BCM-S2 test. Even if the intention was to characterize the new configuration through the PRF-BCM-S2 test, it must be admitted that the experiment may not be sufficiently representative of the real fire event sequence characteristics (e.g., different type of ignition, time and sequence of ignition and trays loading). Therefore, an important question raised is to what extent the PRF-BCM-S2 data are suitable and sufficiently reliable in order to characterise the event.

The phenomenology and observations from the real fire event and the PRF-BCM-S2 test are different. Therefore, one open question is how it was possible to receive good results using strictly all the PRF-BCM-S2 data. This again raises the question of the user choices. Which burning surface at ignition should be considered according to the damage picture (cf. Figure 5)? In the PRF-BCM-S2 test, cables were burnt along the entire width of the cable tray, which was not the case in the real fire event. This user choice could be shown to play a key role regarding the fire development, even though the other propagation parameters in the FLASH-CAT model remained the same as for the previous steps.

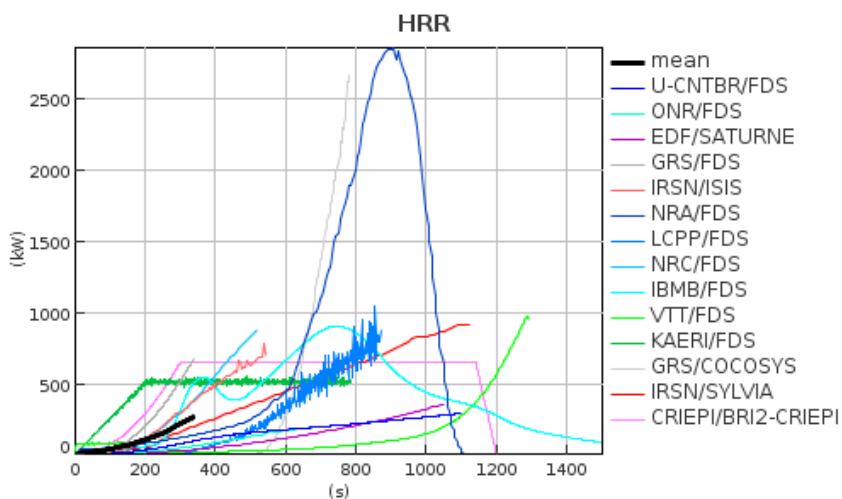


**Figure 8** Predictive simulation results of the HRR for Step 3 compared to the mean simulation result

The predictive simulation results of the gas temperature at the elevation of the actuated sprinkler head compared to the mean simulation result are plotted in Figure 9.

The simulations were performed assuming the location of the sprinklers between 1.20 m and 1.50 m above the top of the upper tray (50 cm to 80 cm below the ceiling of the heater bay). The gas temperature at the sprinkler head was the reference temperature used in the simulations for actuation of the sprinkler.

In most simulations, the critical temperature of 100 °C for the actuation of the sprinkler was reached. Only three simulations out of fourteen did not predict the actuation of the sprinkler. The maximum value of the gas temperature at the sprinkler head location predicted just before actuation ranges from 100 °C up to 215 °C. The predicted temperatures above the critical temperature of 100 °C are due to the consideration of the response time index (RTI) of the sprinkler head in the simulations. The RTI is a measure of the thermal sensitivity of the sprinkler's heat sensitive element. The exact RTI was not given by the manufacturer because of the age of the sprinklers. It is reportedly  $80 \text{ m}^{1/2}\text{s}^{1/2}$  or greater. Therefore, the RTI was set at  $100 \text{ m}^{1/2}\text{s}^{1/2}$  by default in the simulations.

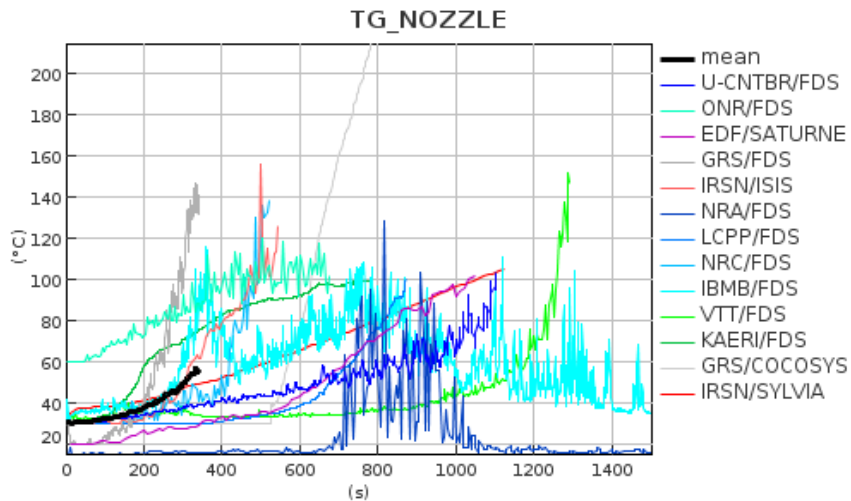


**Figure 9** Predictive simulation results of the gas temperature at the elevation of the actuated sprinkler head compared to the mean simulation result

The predicted actuation time of the sprinkler and the mass and heat losses resulting from the burning of cables are reported in Table 5. For those simulations that do not predict the sprinkler, actuation the values reported in the table are those after a fire duration of 60 min (end time of the simulation in this case).

**Table 5** Predicted actuation time of the sprinkler and mass and heat losses from the burning of cables

| Institution (Country)     | Code Type | Software                         | Sprinkler Actuation Time [min] | Upper Tray Mass Loss [kg] | Lower Tray Mass Loss [kg] | Total Heat Loss [MJ] |
|---------------------------|-----------|----------------------------------|--------------------------------|---------------------------|---------------------------|----------------------|
| VTT (Finland)             | CFD       | FDS v6.7.1/3                     | 22                             | 3.4                       | 0.5                       | 3501                 |
| EDF (France)              | CFD       | SATURNE v5.2                     | 18                             | 11.6                      | 11.6                      | 371                  |
| LCPP (France)             | CFD       | FDS v6.7.1                       | 15                             | 4.6                       | 3.7                       | 199                  |
| IRSN (France)             | CFD       | CALIF <sup>3</sup> S-ISIS v5.3.0 | 9                              | 4.4                       | 2.1                       | 154                  |
| IRSN (France)             | ZC        | SYLVIA v10.0                     | 19                             | 10.0                      | 9.8                       | 466                  |
| GRS (Germany)             | CFD       | FDS v6.7.1                       | 6                              | 1.9                       | 1.0                       | 70                   |
| iBMB (Germany)            | CFD       | FDS v6.7.1                       | –                              | 16.8                      | 11.0                      | 592                  |
| GRS (Germany)             | LPC       | COCOSYS v3.0                     | 13                             | 7.3                       | 8.0                       | 245                  |
| NRA (Japan)               | CFD       | FDS v6.7.0                       | –                              | –                         | –                         | –                    |
| CRIEPI (Japan)            | ZC        | BRI2-CRIEPI v1.0                 | –                              | 16.2                      | 10.1                      | 632                  |
| KAERI (Republic of Korea) | CFD       | FDS v6.7.1                       | 13                             | 5.3                       | 9.3                       | 350                  |

| Institution (Country)          | Code Type | Software     | Sprinkler Actuation Time [min] | Upper Tray Mass Loss [kg] | Lower Tray Mass Loss [kg] | Total Heat Loss [MJ] |
|--------------------------------|-----------|--------------|--------------------------------|---------------------------|---------------------------|----------------------|
| U-CANTABRIA (Spain)            | CFD       | FDS v6.7.0   | 18                             | 3.4                       | 3.4                       | 147                  |
| ONR (United Kingdom)           | CFD       | FDS v6.7.1/4 | 11                             | 0.9                       | 1.2                       | 51                   |
| NRC (United States of America) | CFD       | FDS v6.7.1   | 9                              | 3.6                       | 2.9                       | 155                  |

The predicted actuation time of the sprinkler ranges between 6 min and 22 min. These times are to be compared to the estimated fire duration i.e., 20 min ( $\pm 2$  min). Almost all simulations in which the sprinkler is actuated predict a shorter fire duration. The large variation in range highlights the difficulty of predicting such a fire scenario. Indeed, when considering the development of the fire in the inner part of the cable trays involving cables not directly exposed to the (open) flames but surrounded by the outer cables, the presence of an overhang with uncertain dimensions above the cable trays (see Figure 7), potential flows induced by the riser beneath the cable trays and the uncertainty related to the exact position of the actuated sprinkler head made it difficult to estimate the time of triggering the sprinkler. Short fire durations are obtained if the fire plume rapidly reaches the sprinkler head position. Longer fire durations are obtained if the sprinkler head is not located in the area of the fire plume, thus allowing time for the fire to fill the ceiling with smoke, until the smoke line reaches the sprinkler elevation.

Based on what is known from the event, none of these two situations is the right one. It is likely that, for some reasons already mentioned, the deviation of the flow in the real event from that in the experiment was sufficient to prevent the fire plume from reaching the sprinkler at the very beginning of the fire when the flame was quite weak and therefore more prone to flow disturbances. In contrast, the hypothesis of a regular smoke filling of the ceiling down to the sprinkler elevation would have resulted in the actuation of all four sprinkler heads (which was not the case in the event) in the area, unless the sprinkler head in the direct vicinity of the fire plume had become hotter due to thermal radiation from soot in the fire plume.

In the simulations predicting the sprinkler actuation, the predicted mass loss of the cables in the upper tray just before sprinkler actuation, ranges from 0.9 kg up to 11.6 kg. All predicted values are lower than the coarse estimation from the figure of the damaged areas i.e., 16 kg for the upper tray (see Table 4). However, this value must be taken with caution considering the uncertainties in this estimation. For the lower tray, the predicted mass loss of the cables just before sprinkler actuation ranges from 0.5 kg up to 11.6 kg compared to 10 kg from the coarse estimation. Most of the simulations predict a lower mass loss of the cables in the lower tray compared to that of the upper tray, as observed in the event. Finally, the total heat loss predicted just before sprinkler actuation ranges from 51 MJ up to 3501 MJ, with almost all values below 500 MJ. These values are to be compared to the coarse value of 631 MJ estimated from the figure of the damaged areas.

## CONCLUSIONS

A joint OECD/NEA FIRE and PRISME Cable Benchmark Exercise has been conducted for a realistic cable fire scenario in an electrical system of a NPP. The major goal of this Benchmark Exercise was to simulate a real cable fire event in order to assess the be-

haviour of fire models for such a complex fire scenario from the operating experience of nuclear installations with the available knowledge.

The event for the Benchmark has been selected from the OECD/NEA FIRE Database thus ensuring the reality of the scenario. Several criteria were applied to select a suitable event from all those recorded in the Database. The predominant criterion was the ability to obtain additional information on the event sequence and characteristics from the licensee. Conducting this Benchmark activity solely based on information contained in the FIRE Database turned out to be not possible, as the available data deal with operating conditions of the plant before and during the fire, the event description and interpretation, safety procedures, root causes identifications, fire detection, fire suppression, and corrective actions.

Various additional data have therefore been provided by the licensee enabling the organisers and participants of the Benchmark Exercise to use the selected cable fire event for Benchmark purposes. The time sequence of the event, the floor dimensions of the turbine building, where the event had occurred, the characteristics of the sprinkler heads close to the fire, and the diagram of the damage caused to the cable trays are almost the only available information for the participants' understanding of the fire scenario.

Nevertheless, it was necessary to carry out a specific cable fire test, named PRF-BCM-S2, under the large-scale calorimetric hood in the SATURNE facility of IRSN in order to characterize the fire source despite the knowledge already provided by the PRISME experimental programs, and to re-calibrate the fire models. Many hypotheses have been agreed among the participants to make up for the remaining unknowns or uncertainties. To some extent, the simulated scenario is, in fact, an event-based scenario from what was understood of the event and what was technically possible to achieve.

In terms of the Benchmark simulation work, Step 2\_2 of the Benchmark Exercise consisted of an open simulation of the PRF-BCM-S2 test. The lack of data on the cable thermal inertia and cable ignition temperature for the PRF-BCM-S2 test contributed to the deviations observed from the experimental data since these quantities play an important role in the preheating time of cables.

Benchmark Step 3 consisted of the simulation of the real fire event. The wide variety of results, with remarkable differences between the simulation results by different codes and code users as well as in comparison to the event data, is the expression of the difference between the real fire event, what had been understood from the real cable fire event and what had been tried to simulate with the knowledge and tools available so far.

In order to overcome this the difficulty in obtaining reliable input data on cable fires, the authors suggest collecting additional data by an expert group including modellers upon occurrence of an event in view of future research activities on simulating real fire events.

## **ACKNOWLEDGEMENTS**

The authors of this paper are grateful for the financial and technical support by the OECD/NEA member countries Belgium, Finland, France, Germany, Japan, Korea, Spain, the United Kingdom, and the United States of America participating in the joint OECD/NEA PRISME 2, PRISME 3 and FIRE Projects.

## REFERENCES

- [1] Organisation for Economic Co-operation and Development (OECD) Nuclear Energy Agency (NEA), Committee on the Safety of Nuclear Installations (CSNI), FIRE Project Report: "Collection and Analysis of Fire Events (2010-2013) – Extensions in the Database and Applications", NEA/CSNI/R(2015)14, Paris, France, August 2015, <https://www.oecd-nea.org/nsd/docs/2015/csni-r2015-14.pdf>.
- [2] Organisation for Economic Co-operation and Development (OECD) Nuclear Energy Agency (NEA), Committee on the Safety of Nuclear Installations (CSNI): Combinations of Fires and Other Events – The Fire Incidents Records Exchange Project Topical Report No. 3, NEA/CSNI/R(2016)7, Paris, France, July 2016, <http://www.oecd-nea.org/documents/2016/sin/csni-r2016-7.pdf>.
- [3] Zavaleta, P., and L. Audouin: Cable tray fire tests in a confined and mechanically ventilated facility, *Fire and Materials*, Vol. 42, Issue 1, pp. 28-43, Wiley & Sons, Hoboken, NJ, USA, 2018, <https://doi.org/10.1002/fam.2454>.
- [4] Zavaleta, P., S. Suard, and L. Audouin: Cable tray fire tests with halogenated electric cables in a confined and mechanically ventilated facility, *Fire and Materials*, Vol. 43, Issue 5, pp. 431-609, Wiley & Sons, Hoboken, NJ, USA, 2019.
- [5] Organisation for Economic Co-operation and Development (OECD) Nuclear Energy Agency (NEA), Committee on the Safety of Nuclear Installations (CSNI): OECD FIRE Database Version 2017:02, Paris, France, May 2019 (limited to FIRE member countries only).
- [6] Sze, C. K.: Response time index of sprinklers, *International Journal on Engineering Performance-Based Fire Codes*, Number 1, pp.1-6, 2009.
- [7] McGrattan, K., at al.: Fire Dynamics Simulator, Technical Reference Guide, Sixth Edition, Special Publication (NIST SP), National Institute of Standards and Technology, Gaithersburg, MD, USA, 2013, (online), <https://doi.org/10.6028/NIST.sp.1018> (accessed July 22, 2022).
- [8] Sumitra, P. S.: Categorization of Cable Flammability. Intermediate-Scale Fire Tests of Cable Tray Installations, Interim Report NP-1881, Research Project 1165-1, Factory Mutual Research Corp., Norwood, MA, USA, 1982.
- [9] McGrattan, K., et al.: Cable Heat Release, Ignition, and Spread in Tray Installations During Fire (CHRISTIFIRE) Phase 1: Horizontal Trays, NUREG/CR-7010, Vol. 1, prepared for United States Nuclear Regulatory Commission (U.S. NRC) Office of Nuclear Regulatory Research, Washington, DC, USA, July 2012, <https://www.nrc.gov/docs/ML1221/ML12213A056.pdf>.
- [10] Prétrel, H., P. Zavaleta, and S. Suard: Experimental study of the influence of the mechanical ventilation on the behavior of cable tray fires in a confined compartment, Special Issue PRISME 3, *Fire Safety Journal*, in publication, 2022.
- [11] McGrattan, K. B.: Cable Response to Live Fire (CAROLFIRE) Volume 3: Thermally-Induced Electrical Failure (THIEF) Model, NUREG/CR-6931, Vol. 3 and NISTIR 7472, United States Nuclear Regulatory Commission (U.S. NRC) Office of Nuclear Regulatory Research, Washington, DC, USA, and National Institute of Standards and Technology (NIST), Gaithersburg, MD; USA, April 2008, <https://www.nrc.gov/docs/ML0811/ML081190261.pdf>.

# FAIR: A New OECD/NEA Fire Risk Research Project Under Development as A Follow-Up to PRISME 3

Philippe March\*, Sylvain Suard, Hugues Prétrel, Pascal Zavaleta, and Joëlle Fleurot

Institut de Radioprotection et de Sûreté Nucléaire (IRSN), PSN - RES/SA2I,  
Cadarache, St Paul Lez Durance, France

## ABSTRACT

The main objective of the new OECD/NEA FAIR Project on fire risk is to obtain additional or complementary data to those of the previous three OECD/NEA PRISME Projects, by addressing new fire scenarios and new topics of interest for a better fire risk assessment in nuclear power plants and other nuclear facilities.

FAIR has been built by the partners of the previous Projects PRISME 2 and PRISME 3 and will include three main topics of study:

- Propagation along cable trays with a focus on the effects of long length cables and cable ageing;
- Fires in confined and mechanically ventilated compartments, with a focus on the effects of hot and vitiated environments on the combustion and the re-inflammation of unburned material;
- Multi-source and multi-compartment complex scenarios, with a focus on fire propagation between discrete sources and smoke propagation in complex room configurations.

The experimental campaigns of the FAIR Project will be carried out in the GALAXIE platform facilities (operated by IRSN at Cadarache) for a period of five years starting in 2023.

## INTRODUCTION

The PRISME (French: *Propagation d'un incendie pour des scénarios multi-locaux élémentaires*) Projects were conducted as Joint Projects under the auspices of the Nuclear Energy Agency (NEA) of the Organisation for Economic Co-operation and Development (OECD) from 2006 to 2022.

The first OECD/NEA PRISME Project (2006 - 2011) concerned smoke movement from a fire compartment to adjacent rooms, the effects of underventilated conditions on the fire source (mainly liquids), and the behaviour of electrical cables exposed to high thermal stress. The second OECD/NEA PRISME 2 Project (2012 - 2016) allowed the completion of studies on smoke movement from the fire compartment to adjacent rooms through a horizontal opening, fires of complex sources such as cable trays, fire spreading from an electrical cabinet to targets, such as cable trays or electrical modules, and the efficiency of water-based fire extinguishing systems for fire control. The third OECD/NEA PRISME 3 Project (2017 - 2022) investigated new scenarios of smoke propagation in a mechanically ventilated multi-room facility using multiple and elevated fire sources, the spread of fire from an open door electrical cabinet to neighbouring cabinets with closed doors, and new configurations of cable tray fires in open and confined atmosphere, including configurations involving a long corridor representative of a service gallery.

A key accomplishment of the PRISME, PRISME 2 and PRISME 3 Projects was the enhanced knowledge gained on the phenomena occurring during a fire in a confined mechanically ventilated installation. Important issues to be considered in safety analysis have been studied, and the analysis of the tests also contributed to enhancing the understanding of under ventilated fires including realistic fire sources typical for nuclear installations such as electrical cable trays or electrical cabinets.

As the PRISME 3 Project entered its final year, the Project partners conducted an activity for identifying subjects of interest with high safety concerns for which there is still a lack of knowledge and experimental research will be beneficial. As a result, a new Project FAIR (*Fire risk Assessment through Innovative Research*) has been developed, whose objective is to obtain additional or complementary data to those of the previous three OECD/NEA PRISME Projects, by addressing new fire scenarios and new topics of interest for an improved fire risk assessment in nuclear power plants (NPPs) and other nuclear facilities.

In order to achieve the above-mentioned objectives, the experimental programme FAIR is intended to be organized in the following three major topics:

- Fire propagation along cable trays with a focus on the effects of long length cables and cable ageing;
- Fires in confined and mechanically ventilated compartments, with a focus on the effects of hot and vitiated environments on the combustion and the re-inflammation of unburned material;
- Multi-source and multi-compartment complex scenarios, with a focus on fire propagation between discrete sources and smoke propagation in complex room configurations.

This paper presents the safety issues associated with each of the topics identified above and describes the outline of the experimental program planned within the FAIR Project for improving the state of our knowledge for each of them.

It should be noted that the final definition of the project content is likely to evolve from what is presented in this document according to the technical discussions that will take place throughout the Project between the partners, but without fundamentally changing the topics addressed and the main objectives of the Project.

## CABLE FIRE PROPAGATION

Nuclear installations can contain several hundreds of kilometres of electrical cables distributed along cable trays. Thus, electrical cables make up the largest amount of combustible material present in these installations. Power cables are e.g. used in NPPs in process rooms for supplying electricity to pumps, turbines, transformers, heaters, etc., or in the switchgear rooms that contain numerous electrical cabinets connected to multiple cable trays [1]. Furthermore, many cable trays filled with both instrumentation and control (I&C) cables are also found in the cable spreading rooms and in the main control room. Instrumentation cables are typically used for digital or analogue transmission for various types of transducers, while control cables can operate valves, relays, or contactors, etc.

Electrical equipment and cables are potential fire sources since they contain both combustible materials and live electrical circuits. These circuits can experience electrical failures, such as a short circuit's, overheating, or electrical arcs[1], [3] that first ignite plastic material of both electric wires and cables. A serious cable fire occurred at the Browns Ferry NPP in the United States in 1975 [4]. Over 1600 cables were damaged by the fire that caused short circuits between powered conductors, resulting in loss of the emer-

gency core cooling system of the NPP unit 1. Since then, many efforts have been made to prevent cable tray fires such as the increasingly use of flame retardant non corrosive cable insulation materials [5], flame retardant cable coatings [6] or qualified fire barriers. Nevertheless, tens of fire events involving electrical cables in NPPs were recorded in the OECD/NEA FIRE Database between the late 1980s and the end of 2019 [7]. This fire related operating experience from fourteen OECD/NEA member countries worldwide clearly demonstrates that electrical cables still significantly contribute to the fire hazard in NPPs. Fire safety analyses need to assess potential fire spread over cable trays, and the resulting heat release rate (HRR) in order to determine the damage on the functionality of various items important to safety.

### Long Vertical and Horizontal Cable Trays

Significant efforts have been made over the past 40 years to investigate the fire spread for horizontal and vertical cable tray configurations. Almost all the above investigations used cable trays with a maximum length of 4 m for both horizontal as well as vertical configurations. However, horizontal cable stacks and vertical cable trays can be significantly longer in nuclear installations.

The expected insights of the FAIR Project will allow an accurate assessment of the HRR and thus contribute to a reasonably conservative assessment of the cable fire hazard and its consequences. An additional key matter also aims at characterizing the fire spread patterns. Characterization of the flame front spread velocities is important for confirming the prediction abilities of the current cable fire models for long horizontal and vertical cable trays. In addition, specific vertical cable tray configurations such as that related to a cable tray located in a vertical shaft setup need also to be addressed for longer trays than previously studied [10]. Finally, assessing the consequences of such cable tray fires in confined compartments is also of prime importance for fire safety analyses for nuclear installations.

A first series of large-scale tests is proposed to address the full characterization of fire propagation over long horizontal cable trays in mechanically ventilated confined compartments. These tests will complement the recent OECD/NEA PRISME 3 CFP (Cable Fire Propagation) corridor test campaign that involved 6 m long horizontal cable trays in the corridor of the IRSN DIVA facility, as represented in Figure 1. These tests showed that longer cable trays are more suitable to avoid any edge effect and thus allow a more extensive validation of the analytical models. Taking into account the feedback of these tests regarding the DIVA safety criteria, tests using 8 to 10 m long cable trays will be performed in the corridor of the DIVA facility.

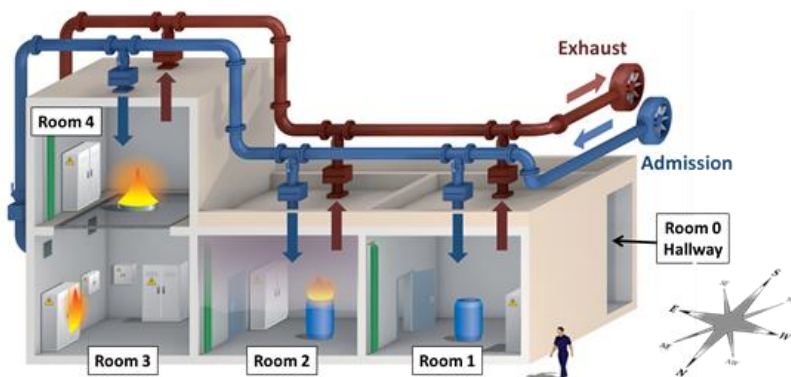


**Figure 1** DIVA Facility

A second series of large-scale tests is proposed to study both the fire spread over long vertical cable trays and the consequences of such fires in mechanically ventilated confined compartments. To this end, tests using a 6 to 7 m vertical cable tray will be considered either in the DIVA facility or in a large-scale compartment called PLUTON. This second test series will complete the previous works [8], [9], [10], [11] that all involved 2 to 4 m long vertical cable trays.

### Cable Ageing

The lifetime extension of NPPs has become one of the major concerns in the world nuclear industry. The electric cables that cannot be easily replaced, can degrade with age due to exposure to several ageing sources [12]. Consequently, life evaluation of electric cables over more than 40 years<sup>8</sup> has become a major topic for the upcoming safety of NPPs. In particular, the issue of cable ageing and its consequences on the cable fire vulnerability was chosen as focus of the previous investigations for a number of reasons [13], [14].

Six types of ageing sources have been identified as the most relevant parameters inducing the change of the fire behaviour of flame-retarded polymers: temperature, moisture, UV radiation, ionizing radiation, chemical solvent, and physical stress (such as vibration of cables connected to running machines) [15]. However, in NPP environments, safety related cables are often subjected to exposure conditions comprising a simultaneous combination of radiation dose rate and temperature [13], [14], [16]. Nevertheless, the impact of other ageing sources such as oxygen, moisture and physical stress on cable ageing cannot be excluded without a deeper examination of suitable corresponding literature [12]. Furthermore, another study [15] also points out that considering the variety of phenomena which could occur upon exposure to ionizing radiation, much work is needed to document the effects of such stimuli on the flame retardancy.

Moreover, according to the wide range of ageing conditions, polymers, and flame retardants (FR), ageing can lead to a decrease, no change or even an increase in flame retardancy [15]. Study [14] explored the effects of thermal ageing on two of the most common nuclear qualified cables that were used in the U.S. nuclear industry in the 1990s. For these two cable types, thermal ageing did affect the thermal damageability of the cables (i.e., the exposure temperature at which electrical failure was observed). However, in one case, ageing increased the susceptibility to thermal damage, while in the other case, the susceptibility was reduced. Moreover, [17] highlights that thermal ageing led to more severe combustion characteristics and gas production on the whole for a cable type with halogenated components (polychloroprene). In contrary, [15] also showed that thermal ageing-induced nanoparticles migration can generate a protecting layer during combustion.

Accordingly, for each electrical cable for which the ageing impact could be investigated, the detailed specification of the cable materials and the related exposure conditions is of prime importance. This is in accordance with the recommendation in [16] suggesting getting a better knowledge of the actual in-containment ageing environments in operating NPPs.

This brief review shows that the exposure conditions found in nuclear installations (thermal stresses, ionizing radiation, etc.) can affect the fire properties of cables. However, to

---

<sup>8</sup> Safety related equipment such as cable materials were subjected to qualification testing intended to demonstrate that the equipment would remain functional if a major accident such as a loss-of-coolant accident (LOCA) occurred at any time during the 40-years expected operation of the NPP [13].

our knowledge, there is no study that has quantified the cable ageing impact on the main cable fire properties (time to ignition, HRR, etc.) and particularly the fire spread. Therefore, the FAIR Project proposes to provide information on the effects of ageing of sheathing materials on the fire behaviour of cables and fire propagation.

A selection will be performed among the proposed cable candidates for the ageing study, paying specifically attention to the availability of information concerning the “ageing history” for all suggested cable candidates and concerning the precise composition of materials. Even if the priority of the tests is given to cables that have aged naturally in the installations, it is still possible to carry out ageing acceleration protocols on new cables. The specification of the nuclear installations’ representative exposure conditions for accelerating the ageing effects is still a key issue in the scientific community [15]. This issue will deserve a lot of attention and will take benefit of both the recommendations provided in [15], [16], [17] and the recent test protocols as implemented as part of both the ongoing European Team Cables project [19] and additional studies [20] to [23]. The ionizing radiation will not be considered in the intended FAIR test campaign because the recovered cables from nuclear installations should not be contaminated or activated by neutron flux.

Fire characterizations will concern all the cable samples of interest, whatever their origin (naturally or artificially aged) to assess the ageing impact on the cable fire behaviour. These characterizations will be conducted both in cone calorimeter and, at medium-scale, with tests using the CISCCO device (cf. Figure 2). The cone calorimeter tests will allow to evaluate the ageing impact on the time to ignition and HRR of cable samples. The CISCCO tests will allow to assess the ageing impact on the flame spread velocity along a horizontal cable tray and the related HRR.

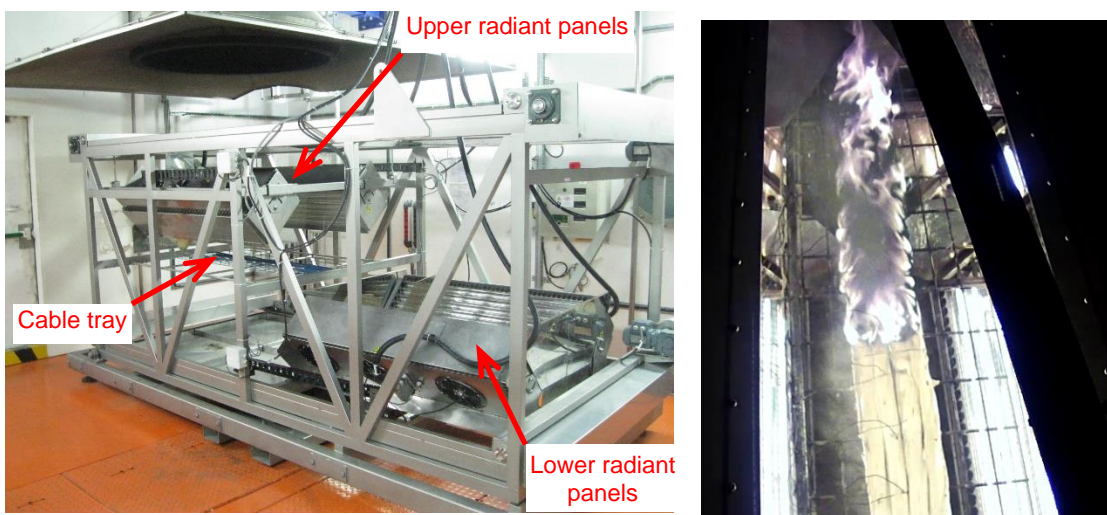


**Figure 2** CISCCO test device; left: an overview on the upper radiant panels located above the cable tray while the lower ones were moved to the relocation area, right: top view showing the flame front spread along the cable tray and the lower radiant panels

## FIRE IN CONFINED AND MECHANICALLY VENTILATED COMPARTMENTS

For fire scenarios in confined and ventilated compartments typically found in nuclear installations, the combustion process highly depends on the environmental conditions [24]. Generally, for normal operating conditions, the environment becomes rapidly oxygen depleted and the fire scenario is called “poorly ventilated” in case of fire. For such situations, the fire development does not only depend on the combustible properties but

is also strongly affected, by the oxygen concentration levels, gas temperature and heat fluxes from the fire near field environment. The analytical models considered in fire studies to predict the fire power for such situations show a satisfactory predictive capacity for simple configurations, mostly pool fires, for which the effect of oxygen depletion is dominant. However, these models fail for situations where the oxygen concentration is close to the extinction limit or if the gas temperature or external heat fluxes are significant and may compensate the effect of oxygen depletion. The antagonist effects of oxygen depletion and temperature are not well understood theoretically as well as numerically; therefore, a remarkable effort is needed to perform a realistic fire risk assessment for such fire scenarios.

Fires in confined environments, such as NPP rooms, can also lead to the production of unburned gases, either because the fire is poorly oxygenated [37] or since some materials are subjected to pyrolysis (without subsequent ignition) under the effect of a heat flux. Unburned gases can cause explosion hazards when they are mixed with air in proportions between the lower and upper flammable limits [38]. The premixed medium can ignite if either its temperature exceeds that for spontaneous ignition, or it comes across an ignition source. In both cases, this ignition can lead to a deflagration that moves through the flammable premixed gas mixture. The result can be a rapid and potentially damaging pressure increase in a confined environment that prevents the expansion of the combustion products [39]. Croft [40] specified that the related overpressures can be higher than 50 hPa. The deflagration consequences in NPPs can be the loss of fire barrier elements (fire doors, dampers, etc., induced by the pressure effects, or a sudden propagation of the fire by the ignition of nearby combustible materials. The potential ignition of unburned gases in NPPs is therefore another major fire safety issue.

## Hot and Vitiated Environments

Up to now, research on under-ventilated combustion regimes has mainly focused on the influence of the oxygen concentration on the burning rate of pool fires [25], [26]. The reduction of the oxygen concentration leads to a decrease of the burning rate and thus of the fire power. Analytical formulations have been proposed and implemented in modeling tools. These studies have shown the satisfactory predictive capability of the simulation for simple configurations [27]. The topic of poorly ventilated fire has been largely investigated during the three OECD/NEA PRISME Projects, with numerous large scale fire tests with different sources (pool fire, electrical cabinets, and cable trays) during which the decrease of oxygen in the compartment led to decrease of the fire HRR in comparison to its level in open atmosphere. The methodology developed to predict these phenomena consists of a correction (based on the oxygen concentration in the vicinity of the fire) of the behaviour in open atmosphere (usually known from fire tests or from full modelling of the fuel pyrolysis in case of simple fire sources). For simple fire sources (as liquid pool), this approach led to satisfactory predictions [28] to [32].

For more complex sources (as cable trays) or for sources rapidly engulfed by the smoke layer results are encouraging but the method needs improvements [33]. The additional effects of high temperature or external heat fluxes because of the vicinity of smoke or of walls (as corner or ceiling) favour the fuel pyrolysis and increase the fire HRR. The thermal conditions of the environment may induce an antagonist effect in comparison to the one induced by oxygen depletion. The methodology only based on the oxygen vitiation correction turns out to be insufficient. Up to now, most of the strategies adopted is to consider fire tests results (mostly the mass loss rate or the HRR) as input parameters for the simulation [34]. Although the combined contributions of oxygen depletion and external heat fluxes have been identified, no analytical methodology has been proposed to treat these fire scenarios. No predictive approach for the fire development is available. In addition, there is a lack of large-scale fire tests highlighting these situations and provid-

ing data for code development. This is the target that the presented work package will focus on.

The FAIR Project proposes to provide insights into the combined influence of oxygen depletion and gas temperature (or external heat flux) increase on the development of fire and the conditions of ignition and extinction for a fire developing in a very hot and strongly under-oxygenated atmosphere. A twofold experimental approach is proposed: one based on large-scale experiments in order to gather real scale realistic fire scenarios and a second one based on a medium-scale analytical approach in order to support both the analysis and understanding of large-scale test results and the development of a modelling methodology.

A first test series will include large-scale experiments involving one mechanically ventilated compartment of the DIVA facility. The objective is to reproduce configurations for which the external heat fluxes towards the combustibles is significant and can compensate the negative effect of the oxygen vitiation. Typical examples are cable trays or electrical cabinets under the ceiling and engulfed within the smoke layer.

A second series of medium-scale experiments will be performed in a controlled atmosphere device. The objective is to collect data for proposing a correlation that quantifies the combined effects of the oxygen concentration and the temperature on the burning rate. Simple fire sources are considered as liquid pool and homogenous solid. The intermediate experimental device that is considered is the NYX facility of IRSN [35], [36], which is a reduced-scale mechanically ventilated compartment in which advanced diagnostics are possible for a detailed description of the fire development. The design of the experiments at both large and reduced scale will be conducted in order to demonstrate the performance of scaling laws.

### **Re-Inflammation of Unburned Material**

Fleischmann et al. [41] and Rasoulipour et al. [42] identified the backdraft and smoke explosion as two distinct deflagration types. The backdraft can occur after a sudden change in the ventilation of a room where unburned gases have accumulated. This change can be caused, for example, by the opening of a door by a firefighter, the early reactivation of ventilation or the loss of a sectorization component. The same authors named a deflagration occurring while the major openings remained closed, the only air supply coming from leakages a “smoke explosion”. In these conditions, the unburned gases mix with the available oxygen within the compartment and result in a premixed atmosphere where only a small amount of oxygen is needed to lead the mixture into the flammable range. Backdrafts and smoke explosion events significantly differ by the characteristics of the pre-existing flow (high velocity gravity current for the backdraft phenomenon, and rather quiet atmosphere for smoke explosion), turbulence level, and geometry of the explosive area (possibly only a thin layer separating the fresh air inflow and the compartment atmosphere for the backdraft, thicker zones for smoke explosion).

Smoke explosions were recently observed during large-scale cable tray fire tests that were conducted in representative rooms of NPPs in the frame of the OECD/NEA PRISME 2 experiments [43]. Several deflagrations, characterized by overpressures exceeding 100 hPa, and fast flame propagation occurred while there was no sudden change in the ventilation. Smoke explosion therefore cannot be excluded from fire safety analyses performed for rooms of NPPs. In addition, this phenomenon may occur without any external triggering event, as a mere consequence of the NPPs’ usual under-ventilated conditions.

Consequently, the proposed program is dedicated to smoke explosions. The project proposes to provide insights into the conditions that promote the formation of a premixed gas mixture, and the conditions that lead to deflagrations.

It is foreseen to conduct medium-scale experiments that will be more favourable than large-scale experiments to provide a detailed characterization of both the conditions for the occurrence of deflagrations and their development. The detailed data collected at the intermediate scale will also be supplemented by simulations that will allow computational access to physical quantities too complex to be measured directly.

The reduced-scale test device should be similar to that illustrated in Figure 3 with volume of 2 m<sup>3</sup> corresponding to one-quarter scale model of one room of the DIVA facility (cf. Figure 1). The proposed reduced-scale test device will also be equipped with two ventilation ducts for simulating either air leakages or moderate ventilation flow rates that both will contribute to gradually form the premixed gas mixture as observed prior to the smoke explosion phenomenon. Several fuel types will be considered, from the simplest one (liquid hydrocarbon) to the more realistic one (electrical cable samples). The second purpose of the medium-scale experiments will be, on the one hand, to highlight the conditions that lead to deflagrations (e.g., the related temperature and concentration criteria), and, on the other hand, to characterize their development (e.g., the premixed flame propagation velocities).

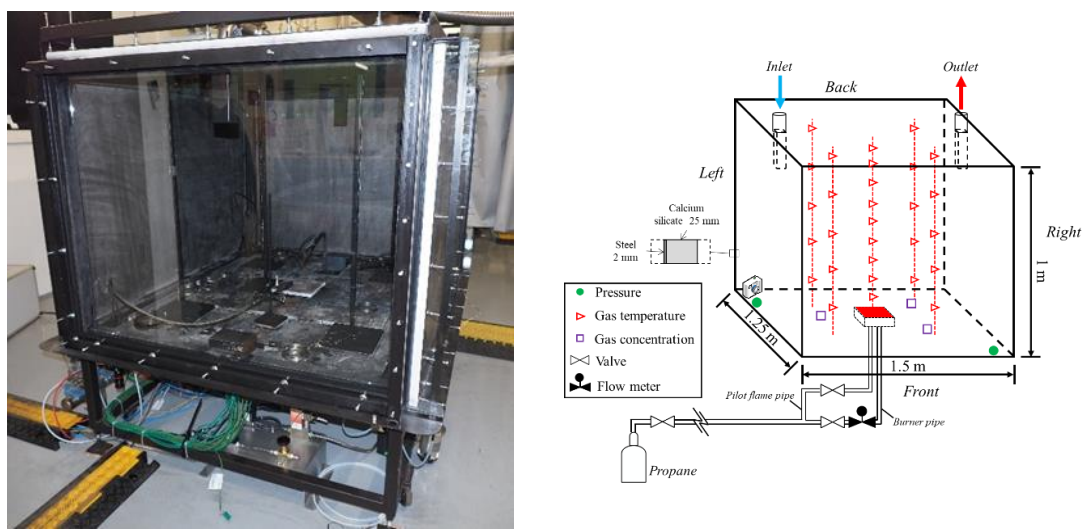


**Figure 3** Example of an experimental device illustrating the future test device used for the unburned gas combustion experiments

## MULTI-SOURCE AND MULTI-COMPARTMENT COMPLEX SCENARIOS

An important issue in assessing fire risks and in simulating fire scenarios is fire propagation from one localized fire source towards other potential discrete sources. The simultaneous involvement of several fire sources increases the severity of the fire event by increasing the fire HRR or by inducing a displacement of the fire (travelling fire). The issue of predicting fire propagation over several discrete sources is therefore a challenging topic and a major concern for fire safety assessment in nuclear installations.

The physical mechanism involved in such scenarios is the process of ignition which results from the combination of two effects: the thermal radiation emitted by the initial fire source and the convection induced by the hot environment. A first scientific issue concerns the thermal properties of the combustible and, in particular, the critical heat flux that characterizes the minimum heat flux required for ignition. A second scientific issue

concerns the assessment of the incident heat flux that includes two contributions: one emitted by the initial fire source (and then transmitted through an environment made of gas products and soot) and one convected by the hot smoke flowing toward a potential secondary target.

In the frame of fire scenarios in nuclear installations, the configuration of several discrete source in a same area is largely encountered. The capability of assessing the propagation over several discrete sources which directly affects the fire development and the fire HRR has been barely treated in the literature and remains a difficult challenge for modellers. There is definitively a need for gaining more knowledge regarding the capability of predicting these fire scenarios.

Another important issue in assessing fire risks and in simulating fire scenarios is not only due to the complexity of the fire source but also to the complexity of configurations and geometries, specific to nuclear installations. Fire scenarios mostly concern assemblies of several interconnected rooms equipped with mechanical ventilation to ensure dynamic confinement with pressure cascade. Whatever the types of fire sources, the mechanically ventilated multi-compartment characteristics of the scenario make the fire risk assessment more complex. The determination of the gas temperature, soot concentration, and size distribution as well as the prediction of the fire development are closely related to the capability of assessing the flow fields in the rooms and, in particular, the smoke propagation. The topic here is to broaden the domain of fire scenarios in investigating realistic arrangements of compartments for which the prediction remains uncertain.

Scientific issues concern the prediction of smoke flows (and in particular the gas temperature) as ceiling jet or filling process, the specific influence of compartment geometry (large volume, corridor or shaft-like compartment) and its clutter on the flow and on the fire source, the behaviour of soot (deposition on walls and clogging of High Efficiency Particulate Air (HEPA) Filters) and the effect of the ventilation characteristics (layout, position of intake/outlet, flow rate, safety operating procedure, clogging of HEPA filters) on the fire development.

### **Fire Propagation Between Discrete Sources**

In the past decades, ignition and flame propagation topics have been investigated within the scientific community. These are key phenomena that control the prediction of the fire occurrence and the flame spread over combustibles. Ignition depends on the combustible properties, the environment (incident heat flux and convective flow) as well as geometrical considerations of the combustible with respect to the direction of the gravity force (upwards, downwards, or inclined propagation direction). In the fire community, the topic of propagation between discrete fire sources is encountered for a rack storage facility [46], which led to the development of some propagation model to predict the progressive propagation of flames towards a large assembly of discrete  $1\text{ m}^3$  combustible items. This topic has also been investigated for wildland fires considering the combustible as discrete item of fuel material [47] or for multi-story apartment buildings [48] to [50]. These studies point out the effect of the combustible shape and the free space between items.

Regarding applications in nuclear installations, multi-source fire scenarios have been investigated in the PRISME 3 Project. The first topic concerned the fire development in case of two simultaneous fires. Results have pointed out the effect of the distance between fires [51]. The topic of propagation between two discrete sources in the same room has also been interrogated with different scenarios: two electrical cabinets, one electrical cabinet and cable trays, or an open-doors electrical cabinet to neighbouring targets in a confined and mechanically ventilated facility [52]. The outcomes confirm the possible fire spreading between discrete sources like electrical cabinets and the signifi-

cant influence of the material type installed inside the target and the distance between the sources. These configurations have mainly addressed fire sources close to each other and the resulting fire not “travelling” significantly within the enclosure.

In the intended FAIR test campaign, it is proposed to focus on configurations with several discrete sources in the same environment (electrical cabinets, cable trays, pumps, etc.) and on the propagation between discrete sources leading to a displacement of the fire location in the compartment or to the occurrence of two simultaneous fires. From the modelling point of view, the main issues concern the ability in assessing the thermal heat fluxes emitted by the source, transferred within the gas phase (through radiation and convective transfer) as well as the identification of the ignition criteria for different fire sources.

The program proposal will involve some large-scale experiments performed in a confined environment in the DIVA (or PLUTON) facility of IRSN focusing both on real configurations and academic scenarios, either in confined or in open atmosphere. The practical configurations will focus on two scenarios of fire spreading. The first one will focus on vertical spread, mainly induced by convection because of the smoke motion. The second one will focus on horizontal spread, mainly induced by radiation from the flame. The fire source will be a real fire source as an open electrical cabinet or cable trays.

The second approach, also at large-scale, will deal with more academic configurations in order to focus on the physical mechanisms involved and to propose academic cases for code validation. The fire source will be well-mastered as pool fire or homogenous solid for which the thermal characteristics are known (critical heat fluxes and ignition temperature). The configuration will concern simple source arrangements such as horizontally or vertically aligned sources.

### **Smoke Propagation in Complex Configurations**

The basic flows encountered in case of compartment fire scenarios are mainly the fire plume, the induced ceiling jet, and the resulting smoke filling process. According to the ventilation layout, the gas phase within the room could be either well-mixed and homogeneous or highly thermally stratified. The main modes of propagation are the buoyancy induced by the temperature difference due to the fire HRR and the forced convection induced by the mechanical ventilation. In case of multi-room arrangements, the flows propagate through the rooms towards horizontal (vent) or vertical (doorway) openings. All along the three PRISME Projects, different scenarios have been investigated from the basic configuration with one room up to four rooms interconnected by doorways or horizontal vents [53] to [55]. The effect of mechanical ventilation and specific ventilation layout (position of inlet and outlet lines) on the doorway and vent flows has been investigated. The conclusions enhance the significant effect of the compartment arrangement (rooms side by side or one above the other), opening locations, and inlet/outlet ventilations positions on the fire development (in the upper part or lower part of the room). Predictive tools with zone model or CFD (computational fluid dynamics) approaches have shown their capability to predict these flows [56] to [61].

However, there is a need for going further towards more complex arrangements often encountered in real installations which can lead to more complex flow fields. The shape of the enclosure - tall, narrow (shaft-like) or long (like corridor or gallery) configurations - may significantly affect the fire plume and the smoke filling of the room in comparison to enclosures with similar lengths (heights, widths). For instance, in a large and tall room thermally stratified, the fire plume may stop rising at a given height, being captured by the density stratification [62]. Another particular configuration is the shaft-like enclosure geometry in which the plume rise may be accelerated. Another specific scenario is the one with the presence of gratings (or grid flooring) within the enclosure that may also

add a difficult constraint in the prediction of the flows. Questions regarding the applicability of existing tools in case of grid flooring are raised, in particular for assessing e.g. the performance of detection devices.

Another subject of interest in this kind of configurations is the assessment of the conditions of malfunction of the electrical and electronic components essential for the operability of items important to safety present in the fire compartment or adjacent rooms. The question of the effect of the ventilation system is also of non-negligible importance. The topic of cluttered compartments with equipment such as ducts, pipes, or grid flooring are of interest.

The program proposal will include large-scale experiments involving various compartment arrangements and mechanically ventilated scenarios. The main topics proposed for being studied are the interaction between smoke flow and grid flooring, the effect of the room shape (tall, large, gallery, etc.) on the smoke propagation, stratification, and deposition.

## CONCLUSIONS

The intended FAIR Project will investigate three major topics:

- Fire propagation along cable trays with a focus on the effects of long length cables and cable ageing;
- Fires in confined and mechanically ventilated compartments, with a focus on the effects of hot and vitiated environments on the combustion and the re-inflammation of unburned gases;
- Multi-source and multi-compartment scenarios, with a focus on fire propagation between discrete sources and smoke propagation in complex multi-compartment configurations.

The experimental campaigns of the FAIR Project will include tests carried out in the GALAXIE platform facilities (operated by IRSN at Cadarache), either on a large scale in the DIVA, SATURNE and PLUTON facilities, or with more analytical devices on a medium scale, such as CISCCO, NYX, or still to be designed devices (as for unburned combustion). The Project is intended to last 5 years starting in 2023.

## ACKNOWLEDGEMENTS

The authors warmly thank all partners of the OECD/NEA experimental projects PRISME 2 and PRISME 3 for their active participation in the work of identification and classification of subjects of interest with high safety concerns for which there is still a lack of knowledge. The development of an approach for the OECD/NEA FAIR Project is the result of these fruitful discussions.

## REFERENCES

- [1] Salley, M. H., and R. P. Kassawara: Verification and Validation of Selected Fire Models for Nuclear Power Plant Applications: Experimental Uncertainty, NUREG-1824, Volume 2, EPRI 1011999, Final Report, prepared for:United States Nuclear Regulatory Commission (U.S. NRC), Washington, DC, USA, May 2007, <https://www.nrc.gov/docs/ML0717/ML071730305.pdf>.
- [2] Keski-Rahkonen, O., J. Mangs: Electrical ignition sources in nuclear power plants: Statistical, modelling and experimental studies, Nuclear Engineering and Design 213(2), pp. 209-221, April 2002, [https://doi.org/10.1016/S0029-5493\(01\)00510-6](https://doi.org/10.1016/S0029-5493(01)00510-6).

- [3] Novak, C., et al.: An analysis of heat flux induced arc formation in a residential electrical cable, FSJ 50, pp. 61-68, 2013, <https://doi.org/10.1016/j.firesaf.2012.10.007>.
- [4] United States Nuclear Regulatory Commission (U.S. NRC): Cable Fire at Browns Ferry Nuclear Power Station, NRC Bulletin BL-75-04, Washington, DC, USA, 1975.
- [5] Morgan, A. B., and J. W. Gilman: An overview of flame retardancy of polymeric materials: application, technology, and future directions, *Fire Mater.*, 37, pp. 259-279, 2013, <https://doi.org/10.1002/fam.2128>.
- [6] Zeng, D., Y. Wang, and D. Boardman: Effect of passive protection on fire propagation of electrical cables, *Fire and Materials*, 45, pp. 345-354, 2021, <https://doi.org/10.1002/fam.2793>.
- [7] Organisation for Economic Co-operation and Development (OECD), Nuclear Energy Agency (NEA), Committee on the Safety of Nuclear Installations (CSNI): OECD/NEA FIRE Database, Version 2019:01, Paris, France, May 2021 (limited to FIRE Database Project member countries only).
- [8] Riese, O., D. Hosser, M. Röwekamp: Evaluation of Fire Models for Nuclear Power Plant Applications, Benchmark Exercise No. 5: Flame Spread in Cable Tray Fires, International Panel Report, Gesellschaft für Anlagen- und Reaktorsicherheit (GRS) mbH, GRS-214, ISBN 978-3-931995-81-2, Köln, Germany, November 2006, <http://www.grs.de/en/content/grs-214-evaluation-fire-models-nuclear-power-plant-applications>.
- [9] McGrattan K. B., and S. D. Bareham: Cable Heat Release, Ignition, and Spread in Tray Installations During Fire (CHRISTIFIRE) Phase 2: Vertical Shafts and Corridors, NUREG/CR-7010, Vol. 2, prepared for United States Nuclear Regulatory Commission (U.S. NRC) Office of Nuclear Regulatory Research, Washington, DC, USA, December 2013, <https://www.nrc.gov/docs/ML1334/ML13346A045.pdf>.
- [10] Passalacqua, R., et al.: Experimental characterisation of ITER electric cables in postulated fire scenarios, *Fusion Engineering and Design*, 88, pp. 2650-2654, 2013, <https://doi.org/10.1016/j.fusengdes.2013.01.026>.
- [11] Audouin, L., J. L. Torero: Special issue on PRISME - Fire safety in nuclear facilities, FSJ, Volume 62, Part B, pp. 7, November 2013, <https://doi.org/10.1016/j.firesaf.2013.11.002>.
- [12] Kim, J.-S.: Evaluation of Cable Aging Degradation Based on Plant Operating Condition, *Journal of Nuclear Science and Technology*, 42:8, pp. 745-753, 2005, <https://doi.org/10.1080/18811248.2004.9726444>.
- [13] Subudhi, M., and S. K. Aggarwal: Literature Review of Environmental Safety-Related Qualification of Electric Cables, NUREG/CR-6384, BNL-NUREG-52480, Vol. 1, prepared for United States Nuclear Regulatory Commission (U.S. NRC) Office of Nuclear Regulatory Research, Washington, DC, USA, April 1996, <https://www.nrc.gov/reading-rm/doc-collections/nuregs/contract/cr6384/index.html>.
- [14] Nowlen, S. P.: An Investigation of the Effects of Thermal Aging on, the Fire Damageability of Electric Cables, NUREG/CR-5619, SAND90-2121; prepared for United States Nuclear Regulatory Commission (U.S. NRC) Office of Nuclear Regulatory Research, Washington, DC, USA, March 1991, <https://www.nrc.gov/docs/ML0625/ML062510133.pdf>.

- [15] Vahabi, H., R. Sonnier, and L. Ferry: Effects of ageing on the fire behaviour of flame-retarded polymers: a review, *Polym. Int.*, 64, pp. 313-328, 2015, <https://doi.org/10.1002/pi.4841>.
- [16] Gillen, K. T., and R. Bernstein: Review of Nuclear Power Plant Safety Cable Aging Studies with Recommendations for Improved Approaches and for Future Work, Sandia Report, SAND2010-7266, Sandia National Laboratories (SNL) Albuquerque, NM, USA, 2010, <https://doi.org/10.2172/1002106>.
- [17] Kim, M. H, et al.: Influence of Thermal Aging on the Combustion Characteristics of Cables in Nuclear Power Plants, *Energies* 2021, 14, 2003, <https://doi.org/10.3390/en14072003>.
- [18] Celina, M. C., K T. Gillen, and E. R. Lindgren: Nuclear Power Plant Cable Materials: Review of Qualification and Currently Available Aging Data for Margin Assessments in Cable performance, Sadia Report, SAND2013-2388, Sandia National Laboratories (SNL) Albuquerque, NM, USA, 2013, <https://www.nrc.gov/docs/ML1312/ML13127A088.pdf>.
- [19] Broudin, M., et al.: Team Cables project, European Tools and Methodologies for an efficient ageing management of nuclear power plant cables, Horizon 2020 Euratom Research, <https://www.team-cables.eu>.
- [20] Suraci, S. V., et al.: Ageing Assessment of XLPE LV Cables for Nuclear Applications through Physico-Chemical and Electrical Measurements, *IEEE Access*, Institute of Electrical and Electronic Engineers (IEEE), 2020, 8, pp.1-11, Piscataway Township, NJ, USA; 2020, <https://doi.org/10.1109/ACCESS.2020.2970833>.
- [21] Verardi, L., D. Fabiani, and G. C. Montanari: Electrical aging markers for EPR-based low-voltage cable insulation wiring of nuclear power plants, *Radiation Physics and Chemistry*, Volume 94, pp. 166-170, 2014, <https://doi.org/10.1016/j.radphyschem.2013.05.038>.
- [22] Liu, H., L. S. Fifield, and N. Bowler: Aging mechanisms of filled cross-linked polyethylene (XLPE) cable insulation material exposed to simultaneous thermal and gamma radiation, *Radiation Physics and Chemistry*, Volume 185, 2021, <https://doi.org/10.1016/j.radphyschem.2021.109486>.
- [23] Verardi, L., D. Fabiani, G. C. Montanari: Electrical aging markers for EPR-based low-voltage cable insulation wiring of nuclear power plants, *Radiation Physics and Chemistry*, Volume 94, pp. 166-170, 2014, <https://doi.org/10.1016/j.radphyschem.2013.05.038>.
- [24] Audouin, L., et al.: OECD PRISME project: Fires in confined and ventilated nuclear-type multi-compartments - Overview and main experimental results, *Fire Safety Journal*, Vol. 62, pp. 80-101, 2013, <https://doi.org/10.1016/j.firesaf.2013.07.008>.
- [25] Peatross, M. J., and C. L. Beyler: Ventilation Effects on Compartment Fire Characterization, *Fire Safety Science* 5, pp. 403-414, 1997, <https://doi.org/10.3801/IAFSS.FSS.5-403>.
- [26] Suard, S., et al., Analytical Approach for Predicting Effects of Vitiated Air on the Mass Loss Rate of Large Pool Fire in Confined, in *International Symposium of Fire Safety Science*, 2011, <https://doi.org/10.3801/IAFSS.FSS.10-1513>.
- [27] Nasr, A., et al.: Fuel mass-loss rate determination in a confined and mechanically ventilated compartment fire using a global approach, *Combust. Sci. Technol.*, Vol. 183, no. 12, pp. 1342–1359, 2011, <https://doi.org/10.1080/00102202.2011.596174>.

- [28] Perez Segovia, J. F., T. Beji, and B. Merci: CFD Simulations of Pool Fires in a Confined and Ventilated Enclosure Using the Peatross–Beyler Correlation to Calculate the Mass Loss Rate, *Fire Technology*, Vol. 53 (no. 4-5), April 2017, <https://doi.org/10.1007/s10694-017-0654-2>.
- [29] Sikanen, T., and S. Hostikka: Predicting the heat release rates of liquid pool fires in mechanically ventilated compartments, *Fire Safety Journal*, 2017, <https://doi.org/10.1016/j.firesaf.2017.03.060>.
- [30] Wahlqvist, J., and P. Van Hees: Validation of FDS for large-scale well-confined mechanically ventilated fire scenarios with emphasis on predicting ventilation system behavior, *Fire Safety Journal*, 2013, <https://doi.org/10.1016/j.firesaf.2013.07.007>.
- [31] Klein-Heßling, W.: Validation of the lumped parameter code COCOSYS against large-scale OECD PRISME 2 fire experiments, *Fire Materials*, Vol. 43, no. 5, pp. 591-609, 2019, <https://doi.org/10.1002/fam.2752>.
- [32] Pelzer, M., and W. Klein-Heßling: Validation of COCOSYS pyrolysis models on OECD PRISME fire experiments, *Fire Safety Journal*, Vol. 62, no. PART B, pp. 174-191, 2013, <https://doi.org/10.1016/j.firesaf.2013.01.016>.
- [33] Plumecocq, W., L. Audouin, and P. Zavaleta: Horizontal cable tray fire in a well-confined and mechanically ventilated enclosure using a two-zone model, *Fire Materials*, Vol. 43, no. 5, pp. 530-542, 2019, <https://doi.org/10.1002/fam.2698>.
- [34] Bascou, S., P. Zavaleta, and F. Babik: Cable tray fire tests simulations in open atmosphere and in confined and mechanically ventilated compartments with the CALIF3S/ISIS CFD software, *Fire Materials*, 2019, <https://doi.org/10.1002/fam.2680>.
- [35] Alibert, D., et al.: Effect of oxygen concentration on the combustion of horizontally-oriented slabs of PMMA, *Fire Safety Journal*, Vol. 91, no. , pp. 182-190, 2017, <https://doi.org/10.1016/j.firesaf.2017.03.051>.
- [36] Prétrel, H., B. Lafdal, and S. Suard: Multi-scale analysis of the under-ventilated combustion regime for the case of a fire event in a confined and mechanically ventilated compartment, *Fire Safety Journal*, 2020, <https://doi.org/10.1016/j.firesaf.2020.103069>.
- [37] Gottuk, D. T., and B. Y. Lattimer: Effect of Combustion Conditions on Species Production, in: DiNenno, P.J. (Ed.): Society of Fire Protection Engineers (SFPE) Handbook of Fire Protection Engineering, 3<sup>rd</sup> Ed., ISBN 978-0877654513, National Fire Protection Association (NFPA), Quincy, MA, USA; 2002.
- [38] Zalosh, R: Explosion Protection, in: DiNenno, P.J. (Ed.): Society of Fire Protection Engineers (SFPE) Handbook of Fire Protection Engineering, 3<sup>rd</sup> Ed., ISBN 978-0877654513, National Fire Protection Association (NFPA), Quincy, MA, USA, 2002.
- [39] Dobashi, R.: Studies on accidental gas and dust explosions, IAFSS 12<sup>th</sup> Symposium 2017, *Fire Safety Journal* 91, pp. 21-27, 2017, <http://dx.doi.org/10.1016/j.firesaf.2017.04.029>.
- [40] Croft, W. M.: Fires Involving Explosions – A literature review, *Fire Safety Journal*, 3 (1980/81) 3 p. 24, 1981.
- [41] Fleischmann, C. M., and Z. Chen: Defining the difference between backdraft and smoke explosions, The 9<sup>th</sup> Asia-Oceania Symposium on Fire Science and Technology, *Procedia Engineering* 62, pp. 324-330, 2013, <https://doi.org/10.1016/j.proeng.2013.08.071>

[42] Rasoulipour, S., et al.: Experimental investigation of underventilated fires in enclosures with two front vertical openings and occurrence of smoke explosions, *Fire Safety Journal*, Vol. 116, 2020, <https://doi.org/10.1016/j.firesaf.2020.103176>.

[43] Zavaleta, P., S. Suard, and L. Audouin: Cable tray fire tests with halogenated electric cables in a confined and mechanically ventilated facility, *Fire and Materials*, 43, pp. 543-560, 2019, <https://doi.org/10.1002/fam.2717>.

[44] Institut de Radioprotection et de Sûreté Nucléaire (IRSN): CALIF3S/ISIS software (n.d.-a), collaborative website: <https://gforge.irsn.fr/gf/project/isis>.

[45] Institut de Radioprotection et de Sûreté Nucléaire (IRSN)CALIF3S/P<sup>2</sup>REMICS software (n.d.-a), collaborative website: <https://gforge.irsn.fr/gf/project/y>.

[47] Markus, E., et al.: Application of the thermal pyrolysis model to predict flame spread over continuous and discrete fire load, *Fire Safety Journal*, Vol. 108, no. January, p. 102825, 2019, <https://doi.org/10.1016/j.firesaf.2019.102825>.

[47] He, Q., et al.: Fire spread in discrete fuels with varying packing ratios: An experimental investigation, *Fire Safety Journal*, Vol. 126, no. May, p. 103470, 2021, <https://doi.org/10.1016/j.firesaf.2021.103470>.

[48] Zhou, B., et al., Influence of air-gap and thickness on the upward flame spread over discrete wood chips, *Therm. Sci. Eng. Prog.*, Vol. 26, p. 101106, September 2021, <https://doi.org/10.1016/j.tsep.2021.101106>.

[49] Cui, W., and Y. T. T. Liao: Experimental study of upward flame spread over discrete thin fuels, *Fire Safety Journal*, Vol. 110, no. May, p. 102907, 2019, <https://doi.org/10.1016/j.firesaf.2019.102907>.

[50] Park, J. H., et al.: Concurrent flame spread over discrete thin fuels, *Combust. Flame*, vol. 191, pp. 11-125, 2018, <https://doi.org/10.1016/j.combustflame.2018.01.008>.

[51] Prétrel, H., and W. Plumecocq: Experimental and numerical study of fire event involving two simultaneous fire sources in confined and ventilated compartments, in: *Interflam 2019 Conference Proceedings*, pp. 477-489, Interscience Communications, 2019.

[52] Zavaleta, P., S. Suard, and L. Audouin: Fire spread from an open-doors electrical cabinet to neighboring targets in a confined and mechanically ventilated facility, *Fire Materials*, Vol. 43, no. 5, pp. 466-485, 2019, <https://doi.org/10.1002/fam.2685>.

[53] Audouin, L., et al.: PRISME project: Fires in confined and ventilated nuclear-type multi-compartments - Overview and main experimental results, *Fire Safety Journal*, Vol. 62, pp. 80-101, 2013, <https://doi.org/10.1016/j.firesaf.2013.07.008>.

[54] Suard, S., et al.: Fire development in multi-compartment facilities: PRISME 2 project. *Fire and Materials*, 43, pp. 433-435, <https://doi.org/10.1002/fam.2754>.

[55] Prétrel, H., A. Koché, and L. Audouin: Doorway Flows Induced by the Combined Effects of Natural and Forced Ventilation in Case of Multi-compartments Large-Scale Fire Experiments, *Fire Technol.*, vol. 52, no. 2, pp. 489-514, 2016, <https://doi.org/10.1007/s10694-015-0524-8>.

[56] Bonte, F., N. Noterman, and B. Merci: Computer simulations to study interaction between burning rates and pressure variations in confined enclosure fires, *Fire Safety Journal*, Vol. 62, PART B, pp. 125-143, 2013, <https://doi.org/10.1016/j.firesaf.2013.01.030>.

- [57] Gay, L., B. Sapa, and F. Nmira: MAGIC and Code-Saturne developments and simulations for mechanically ventilated compartment fires, *Fire Safety Journal*, Vol. 62, PART B, pp. 161-173, 2013, <https://doi.org/10.1016/j.firesaf.2013.01.017>.
- [58] Vaux, S., and H. Prétrel: Relative effects of inertia and buoyancy on smoke propagation in confined and forced ventilated enclosure fire scenarios, *Fire Safety Journal*, Vol. 62, pp. 206-220, 2013, <https://doi.org/10.1016/j.firesaf.2013.01.013>.
- [59] Prétrel, H., and S. Vaux: Experimental and numerical analysis of fire scenarios involving two mechanically ventilated compartments connected together with a horizontal vent, *Fire Mater.*, vol. 43, no. 5, pp. 514-529, 2019, <https://doi.org/10.1002/fam.2695>.
- [60] Le, D., et al.: Assessment of the capabilities of FireFOAM to model large-scale fires in a well-confined and mechanically ventilated multi-compartment structure, *J. Fire Sci.*, vol. 36, no. 1, pp. 3-29, 2018, <https://doi.org/10.1177/0734904117733427>.
- [61] Wahlqvist, J., and P. Van Hees: Validation of FDS for large-scale well-confined mechanically ventilated fire scenarios with emphasis on predicting ventilation system behavior, *Fire Safety Journal*, 2013, <https://doi.org/10.1016/j.firesaf.2013.07.007>.
- [62] Vaux, S., et al.: Fire Plume in a Sharply Stratified Ambient Fluid, *Fire Technol.*, Vol. 57, no. 4, pp. 1969-1986, 2021, <https://doi.org/10.1007/s10694-021-01100-6>.

# Implementation of an Extended FLASH-CAT Model in COCOSYS

Walter Klein-Heßling

Gesellschaft für Anlagen- und Reaktorsicherheit (GRS) gGmbH,  
Köln, Germany

## ABSTRACT

Fire simulations and analytical validation approaches have gained more and more relevance, in particular with respect to fire safety assessment of operating nuclear power plants (NPPs). For providing an added value to the regulatory authorities and the technical safety experts authorized by them suitability and applicability of the analytical tools applied such as fire simulation codes need be known and demonstrated.

The COCOSYS (Containment Code System) code developed by the Gesellschaft für Anlagen- und Reaktorsicherheit (GRS) gGmbH contains i.e. models for simulating cable as well as liquid fuel fires. In an NPP, cables represent a non-negligible fire load as initial fire source or contributor to fire spreading.

To overcome some generic deficiencies of the existing so-called simple cable fire model in COCOSYS the model has been improved based on an extended FLASH-CAT model. The extended model has a flexible mass loss rate (MLR) profile, can consider composite materials to regard the increase of heat of combustion at later phase of fire and is able to consider under-ventilated conditions.

The model was validated on three Organisation for Economic Cooperation and Development (OECD) Nuclear Energy Agency (NEA) PRISME 2 experiments in the SATURNE and DIVA facility of the French Institut de Radioprotection et de Sûreté Nucléaire (IRSN). One main objective is to provide one single set of input parameters for all three experiments. The paper presents capabilities and limitations of the new model.

## INTRODUCTION

Fires can jeopardize the entire safety of an NPP. Hence, much effort is spent on the enhancement of fire simulation tools. Nowadays, these tools have gained more and more relevance, in particular with respect to fire safety assessment of operating nuclear installations. For providing an added value to the regulatory authorities and the technical safety experts authorized by them suitability and applicability of the analytical tools applied such as fire simulation codes need be known and demonstrated. This is realized via validation on conducted experiments, such as in the OECD/NEA PRISME Projects.

Major objective of the international PRISME (French: *Propagation d'un incendie pour des scénarios multi-locaux élémentaires*) Project launched by the OECD/NEA was to study amongst others the effects of under-ventilated and confined conditions on cable fires and the propagation of heat and soot in a multi-compartment configuration. Before, corresponding cable fire experiments were conducted inside the SATURNE facility of the French IRSN in Cadarache.

A crucial point for simulation of fires in a confined compartment is the estimation of the pyrolysis rate (i. e. the rate of vaporized fuel mass) respectively the burning rate and its development over time. For computer code validation on available experimental data,

the experimentally obtained pyrolysis rate is usually entered into the code as user input. It is evaluated whether the code is capable to manage the combustion product generation and distribution as well as the thermodynamics of the fire compartment and its surrounding area in a suitable manner.

Especially for blind pre-test calculations or real applications, it is important to predict pyrolysis rates. Since, related to a wide range of uncertainty due to the complexity of the processes taking place during combustion, at least a prediction of pyrolysis and heat release rate within some uncertainty boundaries is desired.

Cable fires represent quite complex fire scenarios and are due to the high fire load highly relevant for many installations, hence they are widely used for fire experiment, e.g. during the experimental PRISME 2 Project [1] of the OECD/NEA.

The existing so-called simple cable fire model in COCOSYS [2] shows some major deviations. One major deviation is the long-lasting pyrolysis of cables, which cannot be simulated with the simple cable fire model using constant specific MLRs with a given heat of combustion. In general, the decrease of the MLR and heat release rate (HRR) was too strong in the long-lasting phase, leading to shorter fire durations. Second, the consideration of oxygen depletion could be considered by means of a switch to a different set of coefficients only. This led to a somehow stepwise behaviour in the calculated results. Therefore, it was decided to extend the simple cable fire model in order to resolve the above-mentioned problems. The extended model is based on a FLASH-CAT model [3], with some extensions.

In this paper, the model implemented into COCOSYS is described. It has been validated on three selected OECD/NEA PRISME 2 experiments, using the same set of input parameters.

## OUTLINE OF THE MODEL

In general, it is difficult to specify or even calculate the pyrolysis rate for complex cable fire scenarios. Therefore, a simplified concept has been developed in COCOSYS to consider partially the feedback from the thermal hydraulic boundary conditions. Each cable tray is represented in the model and segmented according to the nodalisation (grid of control volumes) in the input file (cf. Figure 1). To be able to simulate an increasing effective heat of combustion the new model uses several (here two) different cable materials  $k$ . This allows to apply different values for the heat of combustion and also different chemical compositions. The extended model based on FLASH-CAT assumes a user provided specific local MLR history profile  $r_k(t)$  [1/s] for each material  $k$ , comparing to the trapezoid characteristic of the heat loss rate in the original FLASH-CAT model.

The flame propagation (point of ignition) maybe be asymmetric, and the propagation velocity maybe be different for both directions (e.g., downward, and upward flame propagation). Then, the resulting equation is as follows:

$$R_i(t) = b f(c_{O_2}) \sum_k D_k \int_0^l r_k(t' - t_{ign,i}(x)) dx \quad (1),$$

with the user-defined and time dependent mass loss profiles  $r_k$  [1/s] for each material. These profiles have to be normalized, so that  $\int r_k dt = 1$ . Other variables are the width  $b$  and length  $l$  of the tray, and the cable mass density  $D_k$  [kg/m<sup>2</sup>] of the material  $k$  without the residual mass fraction. The time of ignition at location  $x$  considers two different propagation velocities  $v_+$  and  $v_-$ .

$$t_{ign,i} = t_{ign,i,0} + \begin{cases} \frac{x_{l,0}-x}{v_-} & x < x_{l,0} \\ 0 & x_{l,0} \leq x \leq x_{r,0} \\ \frac{x-x_{r,0}}{v_+} & x > x_{r,0} \end{cases} \quad (2).$$

To consider the dependency on the oxygen concentration  $c_{O_2}$  it is assumed that a reduced amount of oxygen will lead to a slowdown of burning process and resulting in a somehow time delay  $t'$

$$t' = \int_0^t f(c_{O_2}) \quad (3).$$

This time  $t'$  is used as argument of  $r_k$  in equation (1).

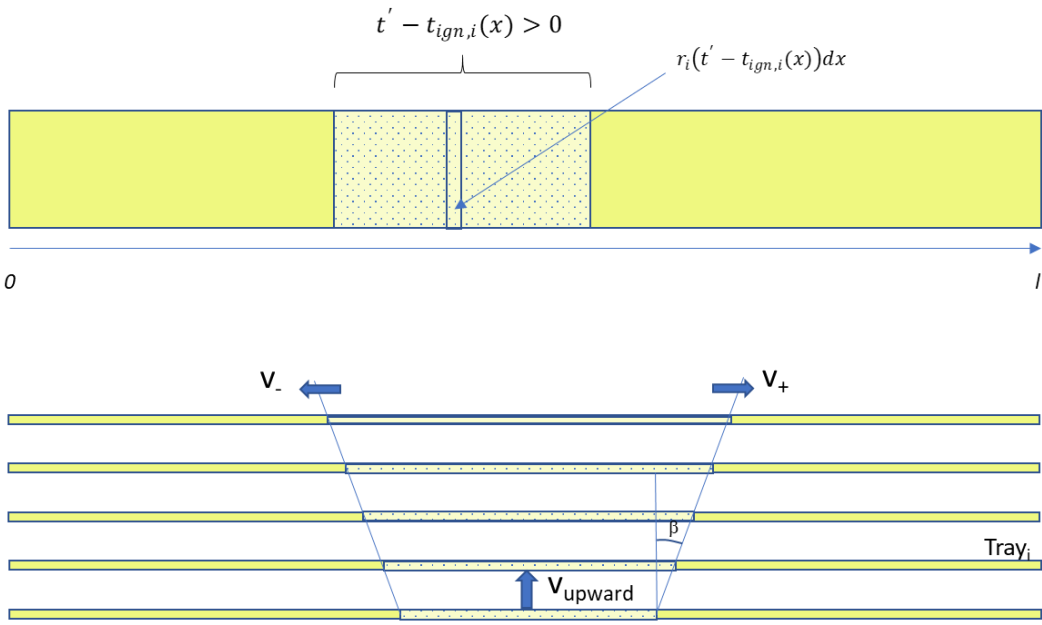


**Figure 1** Concept of the extended simple cable pyrolysis model in COCOSYS

In summary, the user must provide the following data:

- Cable geometry (width  $b$ , length  $l$ ),
- Cable material density  $D_0$  [kg/m<sup>2</sup>], residual mass fraction  $f_{rest}$ , and mass fractions of materials,
- Time dependent profile  $R_k$  for each cable material,
- Oxygen dependency factor  $f(c_{O_2})$ ,
- Initial ignition conditions  $t_{ign,i,0}$ ,  $x_{l,0}$  and  $x_{r,0}$ ,
- Horizontal propagation velocity  $v_{horizontal}$ ,
- Vertical propagation velocity  $v_{upward}$  and vertical propagation angle  $\beta$ .

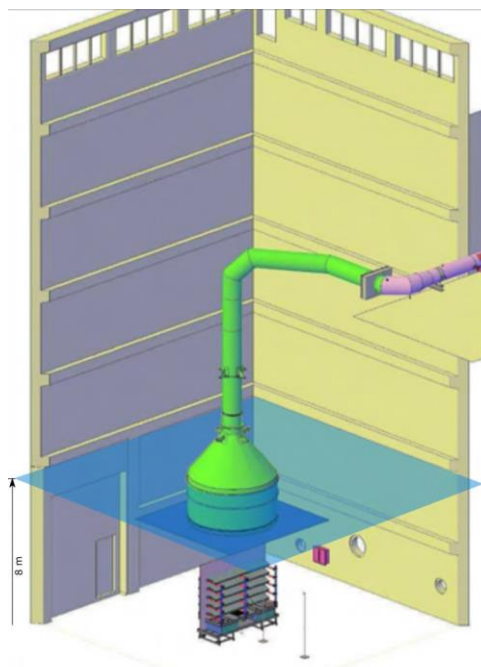
## VALIDATION OF THE NEW MODEL ON PRISME EXPERIMENTS

In order to qualify the new cable fire model, the model has been validated on the OECD-NEA PRISME 2 experiments PRS2-CFSS-2, PRS2-CFS-3, and PRS2-CFS-4 [4], [5], [6]. The first one is a test in the SATURNE facility under open atmosphere conditions. PRS2-

CFS-3 and PRS2-CFS-4 are tests inside the DIVA facility with different ventilation rates ( $4 \text{ h}^{-1}$  and  $15 \text{ h}^{-1}$ ). All tests used the same FRNC (fire retardant non-corrosive) cable types provided by GDF-SUEZ (Belgium) and the same cable tray configuration. The objective of this test was to investigate fire spreading over five horizontal cable trays under different boundary conditions. The trays were 2.4 m long, 0.45 m wide, and their horizontal distance was 0.3 m. The cables were ignited by a gas burner underneath the trays. The area of the gas burner was 0.4 m x 0.4 m and was operated with an ignition power of 80 kW. The gas burner was stopped as soon as the HRR measured by the calorimeter exceeded 400 kW. Each tray was loaded with 32 cables.

### PRS2-CFSS-2 Experiment in the SATURE Facility

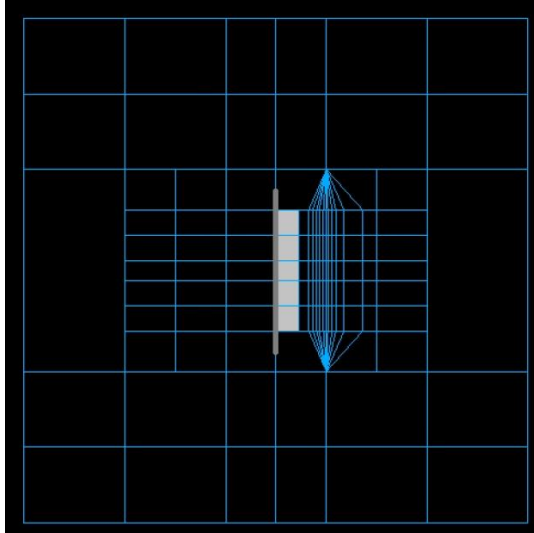
In order to investigate differences between open and confined cable fires the PRISME 2 CFSS (cable fire spreading support) tests have been conducted in conjunction with the PRISME 2 CFS (cable fire spreading) fire tests. These fire tests were performed in the SATURNE facility of IRSN (cf. Figure 2). A large-scale calorimeter was installed in the 2000 m<sup>3</sup> SATURNE enclosure (10 m long, 10 m wide and 20 m high). The hood with a diameter of 3 m was connected to an exhaust duct linked to a ventilation network. The initial flowrate at the outlet duct was 20,000 m<sup>3</sup>/h. The exhaust duct collects the entire combustion products. Openings in the upper part of the fire compartment allow fresh air to flow in.



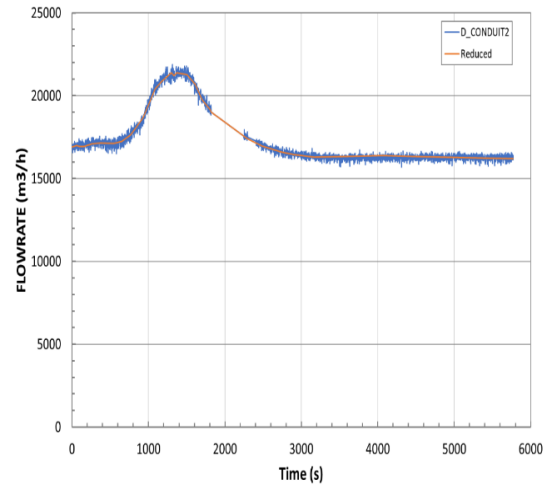
**Figure 2** Scheme of SATURNE facility including five cable trays device, hood and exhaust duct, transparent intersecting plane indicate the upper limit of the volume considered in the COCOSYS nodalisation [4], [6]

Figure 3 shows the top view on the nodalisation of the fire compartment. The position of the cable trays is marked in light grey. At the front side of the trays plume zones are applied to simulate a realistic upward flow of the hot gases. A thin wall installed in the back of the trays in the experiment is considered in the input deck. To calculate thermal stratification a subdivision into layers is necessary (up to 8 m as shown in Figure 4). The volume flow rate of the hood shows a strong variation, partly caused by the clogging of filters leading to higher pressure losses. The correct consideration of the volume flow

rate inside the hood is quite important. Applying the experimental data, it should be ensured that the entire fire gases are exhausted.



**Figure 3** Fire compartment nodalisation in COCOSYS (top view) for the experiments inside the SATURNE facility



**Figure 4** Volume flow rate measured in the PRS2-CFSS-2 experiment

One main extension of the new model is the splitting of cable material into two ‘different’ materials with different heat of combustion (24 MJ/kg and 38 MJ/kg, instead of 28 MJ/kg). The propagation velocity used is higher compared to the previous calculation. The new model can consider a flame shape in upper direction. The value of 35° is taken from the FLASH-CAT model [3]. For all three experiments the same input data, presented in Table 1, have been used, except the residual mass, which had to be adjusted for each experiment, due to a missing model.

Figure 5 presents the comparison of mass loss profiles used. These are normalized according to the mass density. The new model can consider a smooth increase of the rate and particularly a slow decrease of the MLR. Using the original model, different values for open and confined fires have to be used. Concerning the oxygen dependency, the original model was only able to switch between two modes (normal reaction rate and reduced reaction rate) and considering a hysteresis between these modes. However, it was not possible to calculate the PRS2-CFS-3 and PRS2-CFS-4 tests with the same input data. For PRS2-CFS-4 the factor is always one. In the new model a continuous factor can be defined (cf. Figure 6). However, this factor is quite difficult to estimate, because although the MLRs in the tests PRS2-CFS-3 and PRS2-CFS-4 are quite different the resulting oxygen concentrations in the fire compartment are quite similar.

**Table 1** Cable input data used

| Property                              | Original   | New   |
|---------------------------------------|--|---|
| Material density [kg/m <sup>2</sup> ] | 29.51  | 28.33 <sup>9</sup>  |
| Residual mass fraction                | PRS2-CFSS-2: 0.46<br>PRS2-CFS-3: 0.45<br>PRS2-CFS-4: 0.40    | PRS2-CFSS-2: 0.43<br>PRS2-CFS-3: 0.46<br>PRS2-CFS-4: 0.36 |
| Heat of combustion [kJ/kg]            | PRS2-CFSS-2: 28000<br>PRS2-CFS-3: 24640<br>PRS2-CFS-4: 28000 | Material 1: 24000<br>Material 2: 38000                    |
| Mass fraction                         |  | Material 1: 0.62<br>Material 2: 0.38                      |
| Horizontal propagation velocity [m/s] | 0.0015   | 0.003   |
| Vertical propagation velocity [m/s]   | 0.0020   | 0.008   |
| Propagation angle                     |  | 35°   |

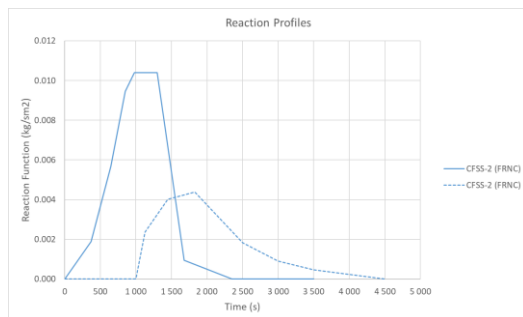


**Figure 5** Reaction profile used for GDF-SUEZ FRNC cable

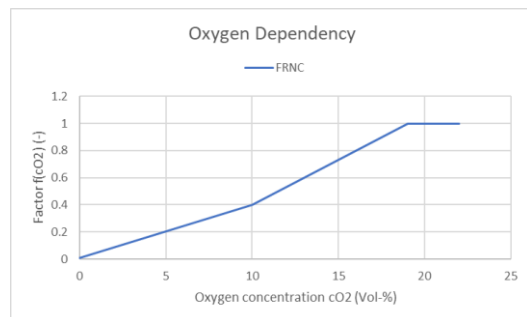
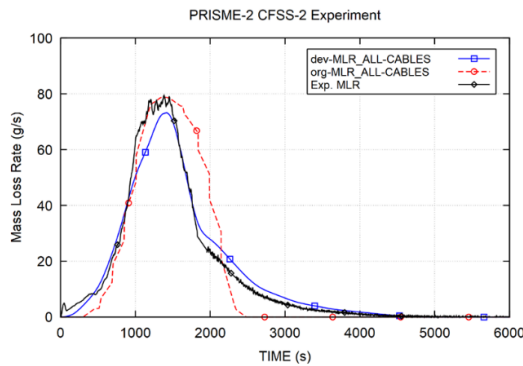


**Figure 6** Oxygen dependency function  $f(CO_2)$  used for GDF-SUEZ FRNC cables

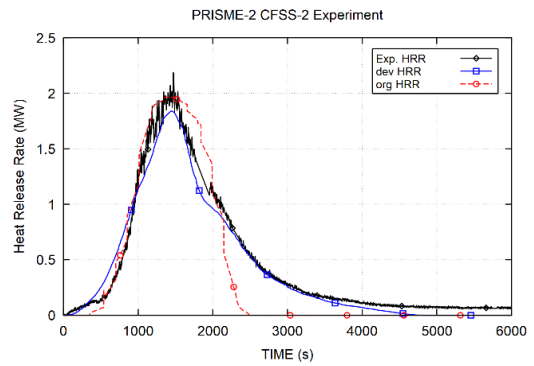
In the following figures the experimental results are presented in black (grey) colour, those of the original calculation (named 'org') in red and those of the new calculation ('dev') using the COCOSYS developer version in blue colour.

Figure 7 provides the comparison of the MLR for all cable trays. The new model provides better results, particularly for the long-lasting phase. Therefore, the issue of constant specific reaction rates leading to a stepwise behaviour has been successfully resolved. The maximum MLR is slightly underestimated. The HRRs are compared in Figure 8. In the original calculation the value for the heat of combustion was 28 MJ/kg. In the new model the cable mass is subdivided into two fractions of 24 MJ/kg and 38 MJ/kg. This allows to simulate the quite high HRR in the long-lasting phase, leading to much better results.

<sup>9</sup> In the input the length of cable is 2.5 m instead of 2.4 m. Therefore, the mass density has been reduced to get the correct total cable mass. The residual mass must be adjusted as well.



**Figure 7** Comparison of measured and calculated MLR in the PRS2-CFSS-2 test



**Figure 8** Comparison of measured and calculated HRR in the PRS2-CFSS-2 test

In the following, some data inside the hood are compared. The comparison of gas temperatures is presented in Figure 9. The calculated temperature in the new calculation is overestimated by about 80 K and somewhat lower compared to the previous calculation. The overestimation might result from the heat losses neglected inside the ducts. The prediction of the long-lasting phase is much better. Figure 10 provides the oxygen concentration, with a deviation at the time of maximum MLR of approximately 0.6 Vol.-%. This is somewhat larger compared to the previous calculation and caused by the underestimation of the maximum MLR.

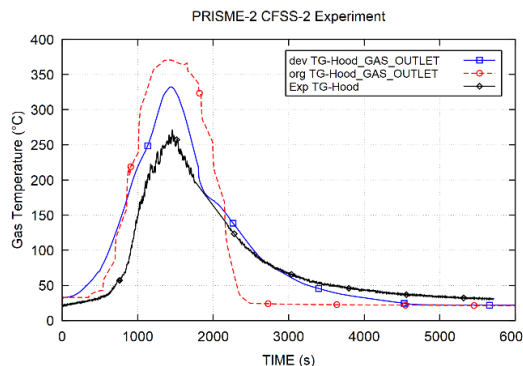


**Figure 9** Comparison of measured and calculated gas temperatures inside the hood of the PRS2-CFSS-test

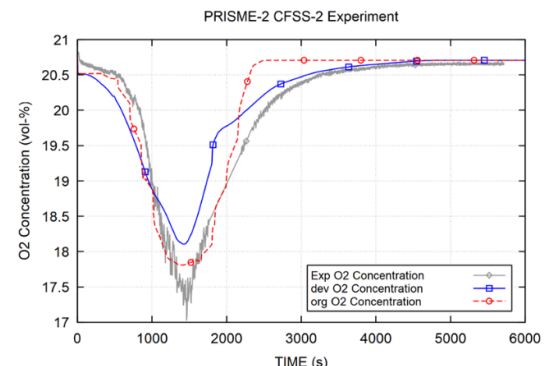


**Figure 10** Comparison of measured and calculated oxygen concentrations inside the hood of the PRS2-CFSS-2 test

## PRS2-CFS-3 and PRS2-CFS-4 Experiments

The PRISME 2 Project focused on fire scenarios of interest in NPPs, particularly with regard to - as far as realistic - possible fire sources such as cable fires. The main objective of the PRS2-CFS tests was to investigate the fire spreading over five horizontal cable trays in a confined geometry. The fire tests PRS2-CFS-3 and PRS2-CFS-4 were carried out in the DIVA facility of IRSN in Cadarache. The two used rooms were connected by an open doorway and ventilated by a fan system. The inlet of the fan system was in the

fire compartment and the outlet in the adjacent room. The ventilation rate was  $4 \text{ h}^{-1}$  ( $960 \text{ m}^3/\text{h}$ ) in the PRS2-CFS-3 tests and  $15 \text{ h}^{-1}$  ( $3600 \text{ m}^3/\text{h}$ ) in the PRS2-CFS-4 test. A top view on the room configuration is given in Figure 11.

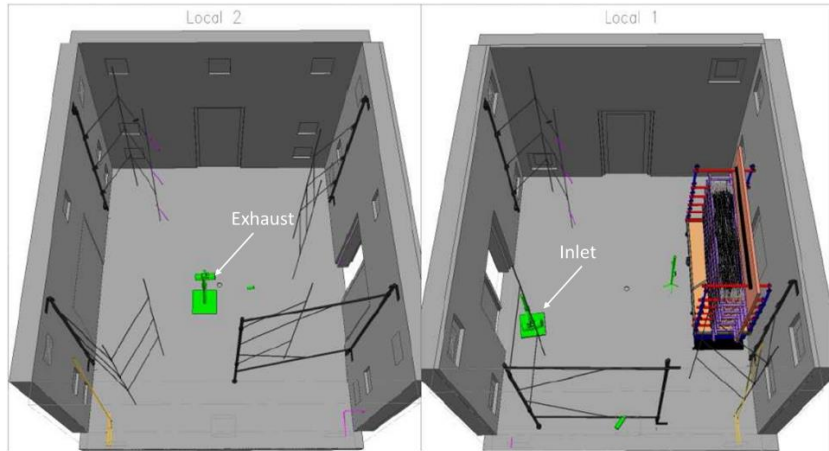


**Figure 11** Top view on the rooms of the DIVA facility used for the PRS2-CFS tests [5]

In Figure 12 and Figure 13 the nodalisation of the rooms used for the PRS2-CFS tests in the DIVA facility are shown. The position of the cable trays is marked in grey. At the front side of the trays plume zones are applied in order to simulate a realistic upward flow of hot gases. A thin wall, which is installed at the back of the trays in the experiment, is considered in the input deck. A second plume is applied in room L2 above the doorway. The ventilation system is represented by zones and junctions. The loss coefficients have been adjusted to the provided initial conditions.

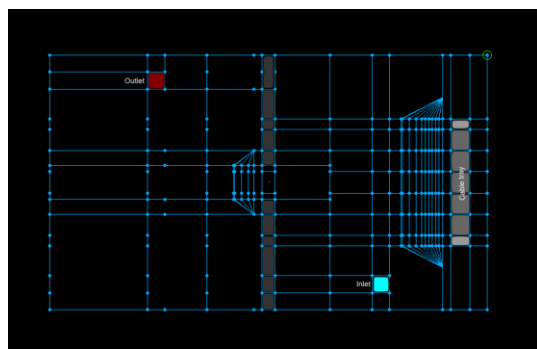


**Figure 12** Top view on the nodalisation of the rooms used by COCOSYS for the PRS2-CFS tests

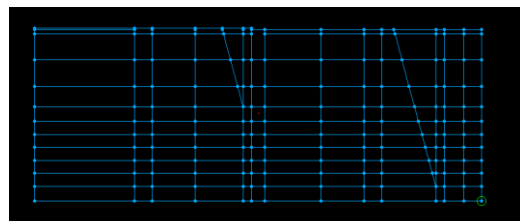
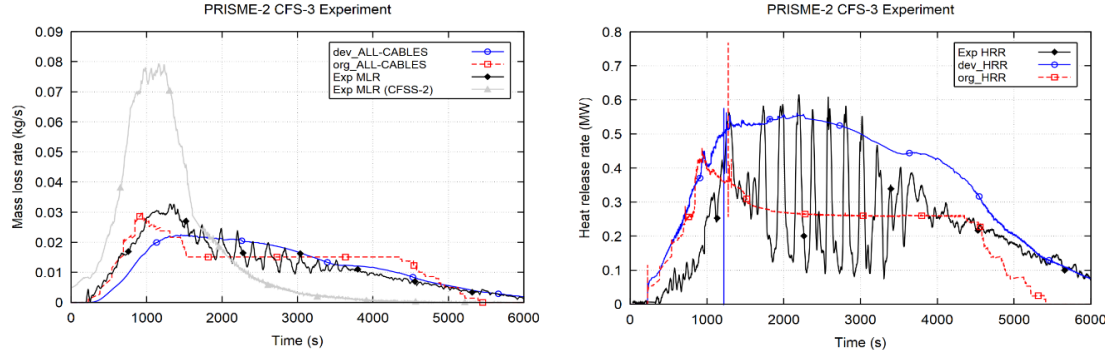


**Figure 13** Side view on the nodalisation of the rooms used by COCOSYS for the PRS2-CFS tests

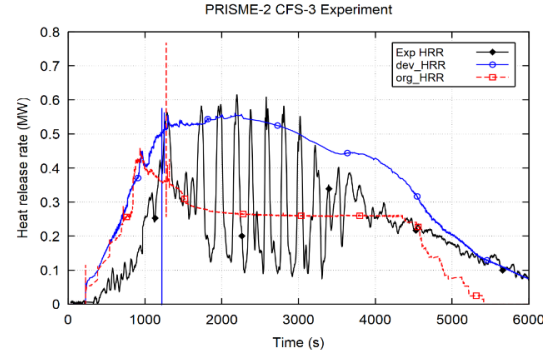
### COCOSYS Simulation Results for the PRS2-CFS-3 Experiment

Figure 14 presents the comparison of the total MLR of all cable trays. The MLR results of the new model show a too slow increase but a much better behaviour for the long-lasting phase. As already observed for PRS2-CFSS-2, the characteristic is much smoother. There is no more stepwise behaviour. The oscillations observed in the experiment could not be reproduced by this cable fire model. The HRR results are compared

in Figure 15. In both calculations, the increase of the calculated HRRs occurs somewhat too early. Such as for the MLRs, the strong oscillations are not simulated. Furthermore, in the original calculation the decrease of the HRR is calculated too strong and too early. The new results are somewhat higher and show the correct decrease of the HRR. Due to the higher average HRR higher gas temperatures are expected.



**Figure 14** Comparison of measured and calculated MLR in the PRS2-CFS-3 test



**Figure 15** Comparison of measured and calculated HRR in the PRS2-CFS-3 test

In Figure 16 the temperatures above tray 4 are shown, looking quite reasonable. Although the MLR and the HRR are both quite low, the measured gas temperatures above the cables are still quite high. In Figure 17 the room temperatures measured in the north-west corner of the fire compartment are presented. During the period of combustion, the calculated room temperatures of the new calculation ('dev') are consistent to the experiment, although the temperature increase starts somewhat too early. The strong temperature oscillations are not simulated, but the temperature level is simulated quite well. Compared to previous simulations the temperature decrease is simulated correctly. Temperatures at the lower elevation are underestimated.

Compared to the original calculation the time characteristic of the results regarding oxygen concentration (see Figure 18) compared to the experimental data is significantly better. This is valid for the initial as well as for the long-lasting phase. Differences could be observed for the concentration stratification. Here, the spread is larger in the experiment.

The velocity distribution in the doorway is presented in Figure 19 showing quite reasonable results.

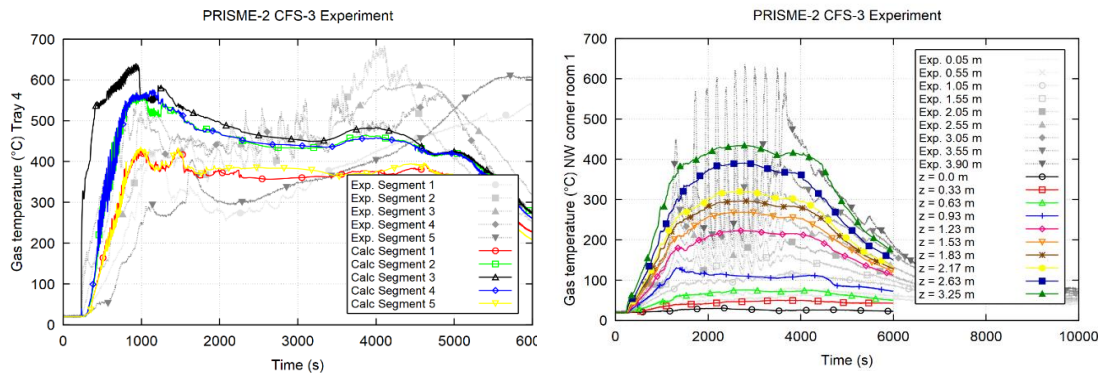


**Figure 16** Comparison of measured and calculated gas temperatures along cable tray 4 in the PRS2-CFS-3 test

**Figure 17** Comparison of measured and calculated gas temperatures in the north-west corner of the fire compartment (room L1) in the PRS2-CFS-3 test

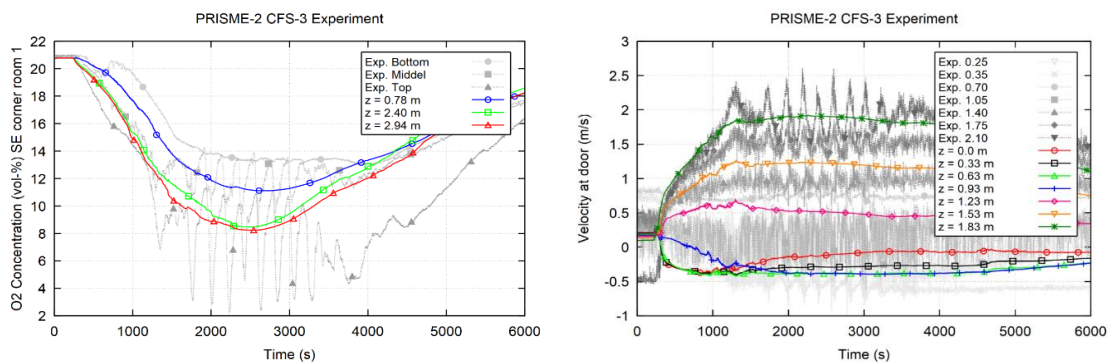


**Figure 18** Comparison of experimental and simulated  $O_2$  concentrations in the fire compartment (room L1) in the PRS2-CFS-3 test

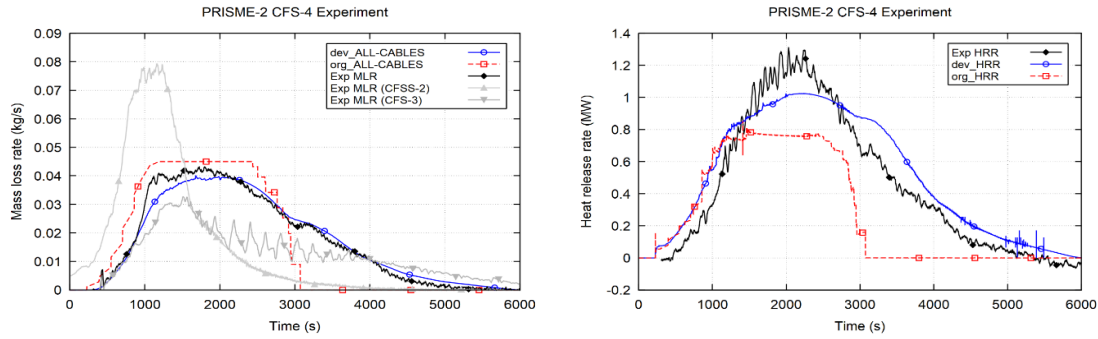
**Figure 19** Comparison of measured and calculated gas velocities in the doorway in the PRS2-CFS-3 test

### COCOSYS Simulation Results for the PRS2-CFS-4 Experiment

The configuration of the PRS2-CFS-4 experiment is the same as for PRS2-CFS-3, only the ventilation rate has been increased to  $15 \text{ h}^{-1}$ . Figure 20 compares the MLR of the original and the improved COCOSYS model. The original calculation shows the typical problems with this model. The decrease of the MLR occurs much too early and is too strong. Using the variable MLR profiles the MLR results are significantly better. At around 1000 s there is a slight underestimation of the MLR. The grey curves show the experimental MLRs of the corresponding open fire test PRS2-CFSS-2 and the confined test PRS2-CFS-3 with a lower ventilation rate of  $4 \text{ h}^{-1}$ . Except the residual mass fraction all input data are the same. The HRR is presented in Figure 21. The results of both calculations are quite similar during the initial phase. They show a slight overestimation of the HRR, although the MLR is underestimated. In the new model the long-lasting phase is pre-

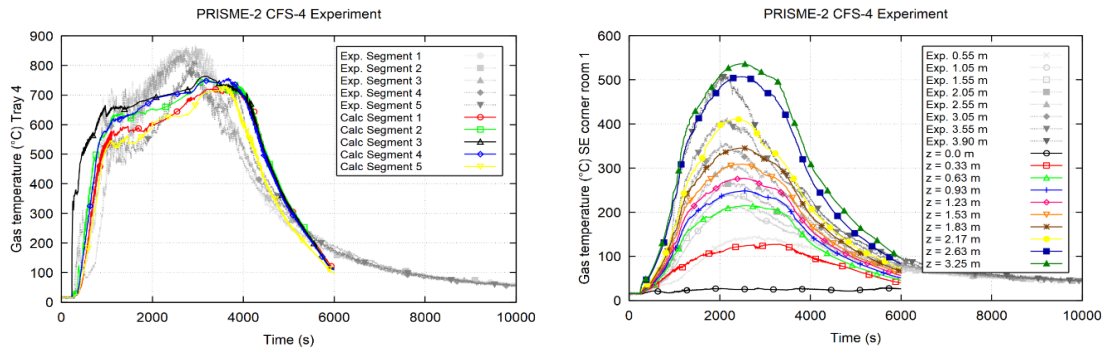
dicted much better due to the use of two separate values for the heat of combustion. However, the peak HRR is somewhat underestimated.

Figure 22 compares the gas temperature above the tray 4. The time characteristic of the calculated temperatures compared to experimental data looks quite reasonable. Figure 23 shows the comparison of gas temperatures in the southeast corner of fire compartment (room L1). The increase of the temperatures in the upper part is simulated quite well. The decrease occurs somehow too late. In the lower part of fire compartment, the temperatures are underestimated.



**Figure 20** Comparison of measured and calculated MLR in the PRS2-CFS-4 test

**Figure 21** Comparison of measured and calculated HRRs in the PRS2-CFS-4 test



**Figure 22** Comparison of measured and calculated gas temperatures along cable tray 4 in the PRS2-CFS-4 test

**Figure 23** Comparison of gas temperatures in the SE corner of the fire compartment L1 in the PRS2-CFS-4 test

The oxygen concentrations in the fire compartment and in the adjacent room L2 are compared in Figure 24 and Figure 25, respectively. The oxygen concentrations at lower and middle location show good results. At the upper location the oxygen concentration is overestimated. The strong change in the experimental data at about 1800 s is caused by falling down of measurement instrumentation. At this time, the deviation is about 4 Vol.-%. The oxygen concentrations in the adjacent room L2 are compared in Figure 25. Again, the oxygen concentration is overestimated in the middle and upper part. The maximum deviation is about 2 Vol.-%.

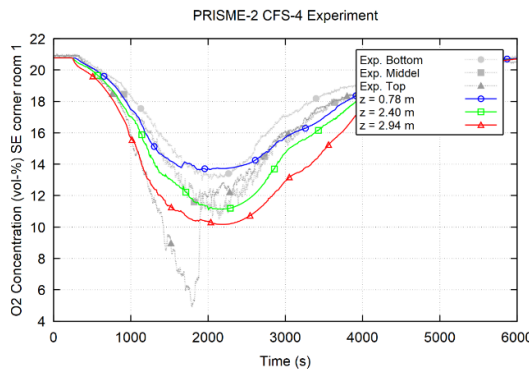


**Figure 24** Comparison of experimental and simulated  $O_2$  concentrations in the fire compartment (room L1) in the PRS2-CFS-4 test

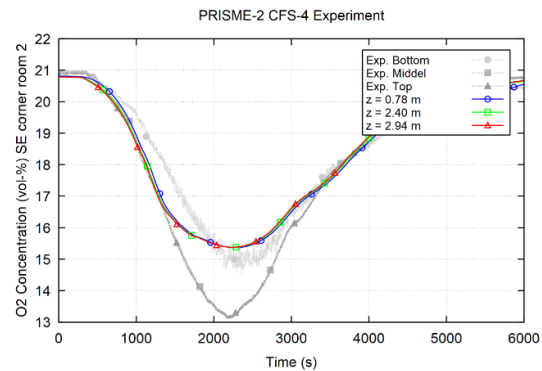


**Figure 25** Comparison of experimental and simulated  $O_2$  concentrations in the adjacent compartment (room L2) of the PRS2-CFS-4 test

## CONCLUSIONS

With the implementation of an extended FLASH-CAT model in COCOSYS certain modelling deficiencies have been successfully resolved. Major aspects are:

- The originally simulated MLR shows a somehow stepwise behaviour due to the constant specific MLR. Furthermore, the decrease of the MLR is too strong in the simulation and occurs too early. Using profile tables for the MLR and a concept based on a FLASH-CAT model in the new version the MLRs are smooth and show the correct behaviour for the long-lasting phase.
- Splitting the cable mass into several fractions allows the use of different heat of combustion values. So, the new model is able to simulate the increase of the effective heat of combustion.
- As in the original model, the residual mass has to be specified by user input, because the fire itself is not modelled.
- Compared to the simulations with the original model version the results gained with the new version are significantly better. In this context, it is important that for all three tests with different ventilation conditions the same input related to cable properties and combustion process has been used.

The MLR and HRR show in general good results. However, the temperatures seem to be somewhat overestimated. Compared to the original model version, particularly the gas temperatures in the adjacent room L2 are too high. As the  $CO_2$  concentrations are somehow underestimated it can be concluded that the heat of combustion may be too high.

## ACKNOWLEDGEMENTS

The author wants to acknowledge the support by the experts from IRSN and all members from the Analytical Working Group of the PRISME Projects.

The activity presented in this paper activity has been carried out within the research and development projects RS1579 and 4720R01550 funded by the German Federal Ministry for Economics and Energy (BMWi) and Federal Ministry for the Environment, Nature Conservation and Nuclear Safety (BMU), respectively. The current project 4722R01410 is funded by the German Federal Ministry for the Environment, Nature Conservation, Nuclear Safety and Consumer Protection (BMUV). The participation of Germany in the OECD/NEA PRISME Projects is granted by the former German Federal Ministry for Economics and Energy (BMWi), now the German Federal Ministry of Economic Affairs and Climate Action (BMWK).

## REFERENCES

- [1] Suard, S., et al.: Special Issue: Fire Development in Multi-Compartment Facilities: PRISME 2 Project, *Fire and Materials*, Volume 43, Issue 5, 2019.
- [2] Klein-Heßling, W.: Status of the pyrolysis models in COCOSYS, in: Proceedings of SMiRT 17 Post Conference Seminar Nr. 21 on Fire Safety in Nuclear Power Plants and Installations, NPP Jaslovske Bohunice, Slovak Republic, August 25 - 28, 2003, 2003.
- [3] McGrattan, K., et al.: Cable Heat Release, Ignition, and Spread in Tray Installations During Fire (CHRISTIFIRE) Phase 1: Horizontal Trays, NUREG/CR-7010, Vol. 1, prepared for United States Nuclear Regulatory Commission (U.S. NRC) Office of Nuclear Regulatory Research, Washington, DC, USA, July 2012, <https://www.nrc.gov/docs/ML1221/ML12213A056.pdf>.
- [4] Zavaleta, P.: PRISME-2 Cable Fire Spreading Support Tests, Analysis Report, Report PSN-RES/SA2I-2013-074, Institut de Radioprotection et de Sûreté Nucléaire (IRSN), Cadarache, France, June 2013.
- [5] Zavaleta, P.: PRISME-2 CFS – phase 2 Analysis report of the CFS-1 to CFS-4 fire tests, Analysis Report, Report PSN-RES/SA2I/2015-028, Institut de Radioprotection et de Sûreté Nucléaire (IRSN), Cadarache, France, July 2015.
- [6] Klein-Heßling, W.: Improvement of Cable Fire Simulations with COCOSYS and Blind Simulation of the PRS3-CFP-D1 Fire Test, GRS-V-RS 1579 – 2/2021, Technical Note, Gesellschaft für Anlagen- und Reaktorsicherheit GRS gGmbH, Köln, Germany, August 2021.

### 3.5 Session on Fire Modelling and Tools

In the frame of the expert session on fire modelling and tools chaired by Diego Lisbona (ONR, United Kingdom) researchers and analysts (e.g., German scientists from Braunschweig University of Technology and Otto-von-Guericke University Magdeburg, but also from the French Institut de Radioprotection et de Sûreté Nucléaire (IRSN)) were the main presenters. The session mainly focussed on analytical tools for fire safety assessment, their enhancements, and applications for various purposes.

In the United Kingdom, Atkins has developed together with ONR a base case for modelling a complex fire scenario derived from the international PRISME experimental series and conducted a detailed sensitivity analysis in order to validate the model against this scenario. The results of this activity were presented and discussed within the expert community.

Two presentations were focussed on a German research and development project, in the frame of which the computational fluid dynamics (CFD) model FDS (*Fire Dynamics Simulator*) had been applied and surrogates been used in order to better consider uncertainties in fire modelling, in particular for the complex building geometries, e.g., of nuclear installations.

Another newly developed analytical effort was presented by Flex-A (Belgium) for analysing fires under complex boundary conditions (e.g., building geometries and ventilation conditions) in nuclear power plants.

The four contributions of this seminar session are provided hereafter.

# Development of a Base Case for Modelling of a Complex Fire Scenario Through Sensitivity Analysis

David Bagshaw<sup>1\*</sup>, Peter Rew<sup>1</sup>, Leslie Nyokeri<sup>2</sup>, Jacob Plummer<sup>2</sup>, Joshua Peacock<sup>1</sup>

<sup>1</sup> Atkins, Epsom, United Kingdom

<sup>2</sup> Office for Nuclear Regulation, Cheltenham, United Kingdom

## ABSTRACT

This paper presents an approach for developing a base case model of a real fire event (from the OECD/NEA FIRE Database using the NIST Fire Dynamics Simulator (FDS) CFD tool. The paper describes the applied methodology utilising sensitivity analysis to define the parameters that have the greatest influence on the simulation. The fire event occurred within a turbine hall of an operating nuclear power plant. The fire was ignited by an electrical arc fault in the upper of two stacked cable trays, subsequently spreading to the lower tray. The fire duration was estimated at 19 minutes, terminating at activation of a sprinkler located close to the fire. The presented modelling is relevant to unconfined, non-ventilation-controlled cable tray fires and is treated as a blind simulation due to the limited information available.

A geometrically representative model was developed in FDS. To inform an appropriate base case development, a sensitivity analysis was performed to determine the impact of key variables on simulated conditions local to the fire suppression heads. Of the variables studied, the time to sprinkler activation was found to be primarily determined by the specified fire spread rate. Other variables impacted the temperature at the sprinkler head, including: the combustion reaction stoichiometry, the tray obstruction representation, the concrete overhang position, the initial ambient temperature, and the fire heat release rate per unit area.

## INTRODUCTION

The PRISME 3 Project is an Organisation for Economic Cooperation and Development (OECD) Nuclear Energy Agency (NEA) experimental research programme designed to investigate multi-compartment fires in under-ventilated conditions with ventilation systems and real fire sources representative of nuclear operational facilities.

Alongside the experimental programme a Benchmark Exercise was initiated by the PRISME 3 Analytical Working Group (AWG) and undertaken by a specific PRISME Benchmark Group (PBG) to further develop and validate fire modelling methods through utilisation of the PRISME Project experimental data.

The Benchmark Exercise comprised three steps, as devised by the AWG: Step 1, an open calculation, based on a cable fire experiment from the PRISME 2 Project (PRS2-CFS-2 test); Step 2, a blind calculation, based on a cable fire experiment from PRISME 3; Step 3, a blind calculation simulating a real cable tray fire event from the OECD/NEA FIRE Database [1].

This paper presents the United Kingdom (UK) contribution to the PRISME 3 Benchmark Exercise for Step 3, the real cable tray fire event. Engagement across the United Kingdom nuclear industry was held throughout the PRISME 3 programme, with the modelling

approach influenced through discussions at industry workshops and questionnaires. The UK's contribution to PRISME 3 was funded by the ONR research project ONR-RRR-071. Further details can be found in the ONR research register and status reports available at <https://www.onr.org.uk/research/regulatory-research-register.htm>.

## FIRE EVENT DESCRIPTION

The fire event occurred within a heater bay of the turbine building at an operating nuclear power plant. The heater bay is connected to the turbine building via several openings and has a mezzanine 6.1 m from the ground where the fire occurred. In addition to two 0.9 m-wide cable trays loaded with polyethylene (PE) / polyvinyl chloride (PVC) insulated cables (where the fire initiated), the heater bay contains high pressure water heaters and piping. The cable fire was ignited by electrical arc-fault as a product of both non-conforming routing (tight bending) of the power cables and a steam leak. The high humidity and condensate from the leak provided the environment necessary for the existing flaws in the electrical cables to short to ground. Figure 1 presents a plan view of the area where the event occurred.

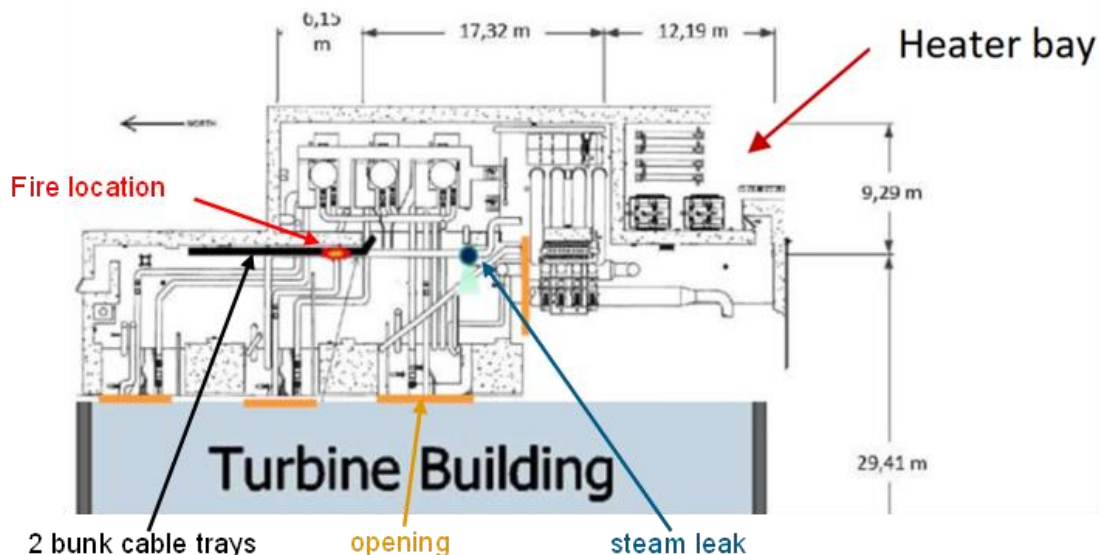


**Figure 1** Plan view of heater bay with relative dimensions [2]

Four sprinkler heads were in the vicinity of the fire, estimated to be between 1.2 and 1.5 m above the upper tray. The sprinkler heads initiate by thermal (fusible) links set to break at 100 °C. Figure 2 (left) shows a plan view of the sprinkler positions relative to the trays (red) and wall (grey). Figure 2 (right) shows a section view, including the trays (grey), sprinklers (red) and the overhang (blue) that sits directly above the fire area, thus likely to interact with and influence the fire plume.

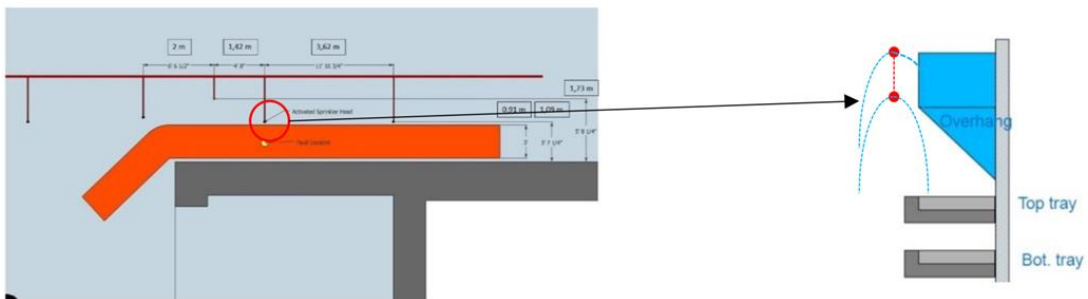


**Figure 2** Spatial arrangement of sprinkler heads

According to the fire event sequence, summarised in Table 1, the fire began at  $t_0 + 34$  min, after which heat from the fire caused the closest sprinkler to activate at  $t_0 + 53$  min, successfully extinguishing the fire. The total fire duration from ignition to extinguishing is thus estimated to be approximately 19 minutes.

**Table 1** Key assumptions of the trialled reaction scenarios

| Time           | Event   |
|----------------|---|
| $t_0$          | The main control room (MCR) received a fire alarm for the heater bay area. The on-site fire brigade leader was sent to the area to assess the situation.  |
| $t_0 + 10$ min | Based on observations at that time, the fire brigade leader reported no fire or smoke, but a steam leak.  |
| $t_0 + 30$ min | The unit was switched to another mode per operating procedure; the MCR was unaware at this time of the exact source of the steam leak. It was anticipated that allowing steam to the main turbine and rolling the turbine would assist in mitigating the observed steam leak. |
| $t_0 + 34$ min | The MCR received numerous unexpected alarms and observed other anomalous indications on the MCR panels.   |
| $t_0 + 35$ min | Based on these alarms and indications, and since there was a known steam leak, the unit was manually scammed.   |
| $t_0 + 39$ min | In response to field operator reports that sparks had been observed in the building ground floor hallway, the MCR operators actuated the plant fire siren and sent on-site fire brigade leaders.  |
| $t_0 + 44$ min | The main steam isolation valves were closed, isolating the steam leak.  |
| $t_0 + 47$ min | The MCR received a report that smoke was now observed at the hydrogen seal oil vacuum pump breaker cubicle in a motor control center.   |
| $t_0 + 53$ min | The east side of the turbine fire alarm system alarmed caused by the actuation of the fire suppression system (a fusible link sprinkler). The fire was extinguished by the automatic sprinkler system.  |

The arc fault, from one of six power cables, damaged the insulation of nearby cables and heated the cable ladder rung, leading to the severing of five of the six cables. The heat from this arc fault is considered [2] to have ignited the cable insulation in the upper tray. The fire on the lower tray was considered to have been initiated by debris falling from the upper tray fire and radiative heat from the upper tray. Much lower levels of damage were observed in the lower tray. Post event fire damage is presented in Figure 3. The

description and illustrations of post-event fire damage are presented in Figure 4 and Figure 5.

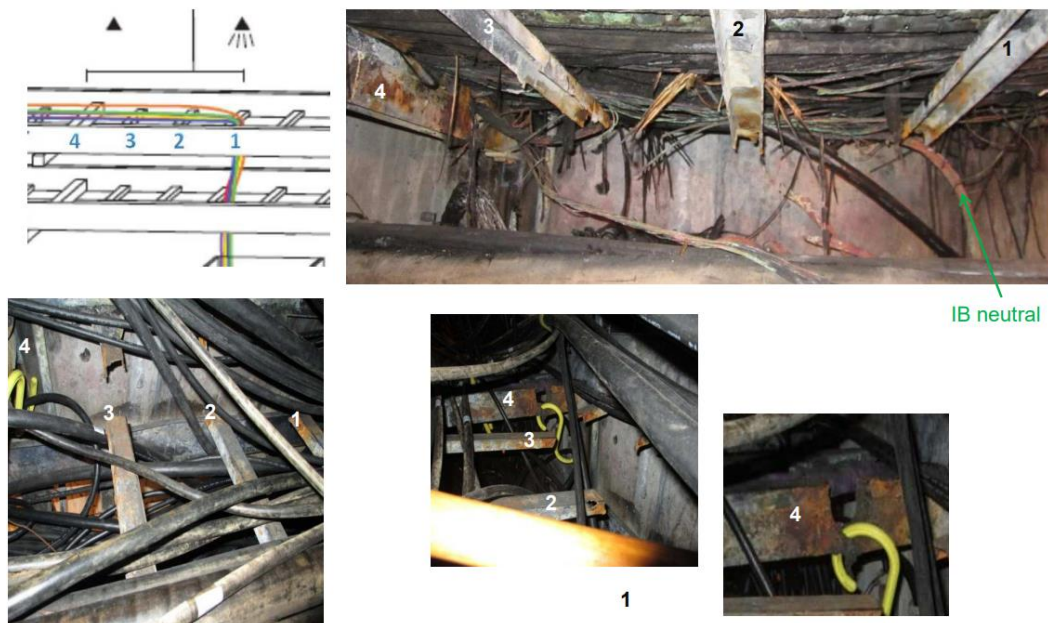


**Figure 3** Cable trays damage evidence [3]

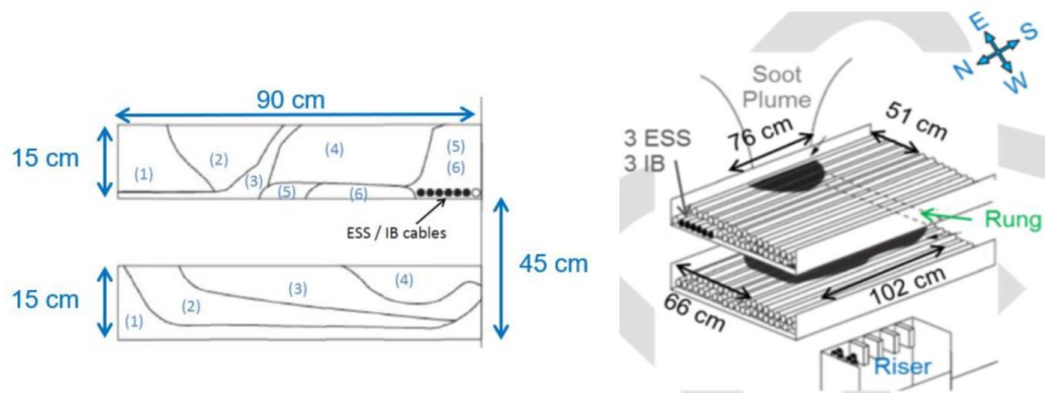


**Figure 4** Cable trays damage pattern (left) and isometric view of damaged area (right) [3]



**Figure 5** Cable trays damage evidence, top tray, and overhang (eft) and top tray (right) [3]

**Disclaimer:** Where possible information has been provided, however, due to publication constraints, a summary is provided of the key input parameters. Full detail of the scenario is contained within [2] and [4].

## MODELLING APPROACH

The fire scenario, as identified in the previous section, was predominantly a localised event which caused local damage to trays and adjacent concrete and did not involve other fuel inventory or develop into a global fire within the compartment. The local nature of the fire does not lend itself to zonal fire models such as CFAST by the National Institute of Standards and Technology (NIST) nor is the problem sufficiently simple for a correlation-based fire dynamics tool (plume temperature or radiative heating) to be used.

Based on the limitations of the scenario, it was determined that the most appropriate tool to be used was a computational fluid dynamics (CFD) code. CFD tools are capable of solving the fundamental physics involved in the fluid dynamic, heat transfer and combustion processes of a fire. Fire Dynamics Simulator (FDS) was selected as it is a “*computational fluid dynamics code developed specifically for the simulation of fire driven flows and heat transfer processes*” [5], and therefore judged an appropriate tool.

However, it should be recognised that a CFD based fire modelling tool is highly dependent on the selection of data for the multitude of variables required to define each scenario. Each variable can have a wide range of values associated, increasing the potential for modeller decisions to have a direct influence on the modelling output, therefore it is essential that modelers are aware of the importance of the sensitivities of their assumptions and the impact of data selection.

## UNCERTAIN INPUTS AND THEIR LIKELY IMPACT

As noted previously, with the increased number of variables in CFD based modelling, the fire modeller needs to be aware of their potential influence, in order to make appropriate modelling decisions. For this modelling activity a number of parameters have been identified which may influence the result, they are:

Suppression head performance – The fire event is considered to end abruptly when the temperature of the suppression head reaches its trigger value. Detail on the individual head, its actual performance and condition at the time is not known. The Response Time Index (RTI) and the trigger temperature are assumed [2], the impact of the RTI can be determined by using multiple suppression head sensors in the fire modelling tool.

Ambient temperature – The event occurred in the heater bay adjacent to the turbine hall. The event was preceded by a steam leak. The normal ambient conditions and impact of steam leak on temperatures of the equipment, including the suppression heads, is unknown. In the present scenario, due to the low temperatures involved in trigger and therefore small difference in temperature between the ambient and trigger, any uncertainty in ambient temperature is expected to have a measurable impact.

Event timing – The timing of the sequence of events that has been made available to the AWG [2] is based on observations and the assumed impacts of fire on power plant systems/instrumentation. The timings provided are a best estimate and are not certain. The timing affects all predictive post event modelling because it is used to gauge the fire development.

Fire development – Information on the nature of the fire, the ignition mechanism, the spread of fire within a tray and the spread to the tray below are all based on post event photographs of the cable tray damage, consumption of cable insulation and (to a limited extent) observations made by power station staff [2]. The fire specification provided to AWG and PBG participants [2] stated that the fire was ignited by an arcing fault. The quantity of energy released from, and duration of, the arcing fault is not given. The energy release from such a fault may preheat a volume of cable insulation/cable tray (if the faulting cable is buried) thereby giving potential for rapid growth but also unignited release of pyrolysis products. The total inventory consumed has been estimated [6] based on damage levels observed post event. The estimate provides an upper bound on the fuel release from the insulation but does not guide on the proportion of the fuel that is involved in the fire. These uncertainties feed into the Heat Release Rate Per Unit Area (HRRPUA) and spread rate assumptions.

Cable tray porosity / location of burning – Whilst we expect that, globally, the fire is well ventilated (with large almost full height openings of the compartment on one side), locally (on the lower tray and on buried cables) the fuel is effectively released into a confined space between the two trays. The fuel release from the lower tray could exit vertically, through gaps in the cabling of the upper tray or laterally / horizontally to the edges of the tray if the cabling in the upper tray is filled. The path of the lower tray pyrolysis products impacts the location of burning by either adding to the intensity of the upper tray fire (through gaps) or by pushing the fire further out into the compartment and altering the trajectory of the plume.

Local geometry – The position of the suppression heads relative to the cable tray is documented [2], but detail of the local geometry between the cable tray and the suppression head is not fully described. A concrete overhang structure above the upper cable tray has dimensions [2] but no elevation information. The location of the overhang, between the fire source and the target (suppression head) is likely to impact the conditions seen at the target.

Global geometry – The overall dimensions of the (heater bay) compartment are well documented [2]; however, information on the ventilation openings between the compartment and the adjacent space has incomplete definition, with the soffit depth not specified. The size (and elevation) of ventilation openings will impact the depth of the hot gas layer and, for objects close to the ceiling, their temperatures. As noted previously, due to the relatively small difference in temperature between the ambient and the trigger temperature of the suppression head, global geometric changes which alter the depth of the hot gas layer, such as the elevation of vent opening soffit, are likely to impact the activation of the suppression.

Fuel and combustion reaction – To gain an understanding of the cable insulation fuel involved in the fire, a representative sample was made available with similar properties

to the cables in the real event and has been tested [7] providing information on the production rates of heat and reaction products, e.g. chlorine compounds.

The nature of the fuel and the manner of its combustion are not expected to impact global conditions but may impact the local fire conditions.

To gain the greatest understanding of the local fire scenario, it was decided to assess as many of the uncertainties as possible through sensitivity analysis. In order to ensure an efficient analysis, all parameters of the sensitivity assessment were bounded by a credible range, e.g., bulk temperatures unlikely to be higher than 60 °C, minimising analysis overheads.

For sensitivities of discrete (not continuously variable) parameters, such as combustion reaction definition, previous modelling experience and judgement on the available information was used to select the sensitivity cases. Of all of the uncertainties listed, only the event timing was not considered as a sensitivity – this is because the parameter is an output of the modelling, that is influenced by all the other inputs.

## MODELLING IN THE FIRE DYNAMICS SIMULATOR

### Approach

Due to the limited amount of information and the complexity of the scenario, it was decided to undertake a sensitivity analysis to determine the most appropriate model choices and identify the parameters with the greatest influence on the local fire conditions. Using the data provided [2], a geometrically representative model of the event has been built in FDS and known parameters have been set.

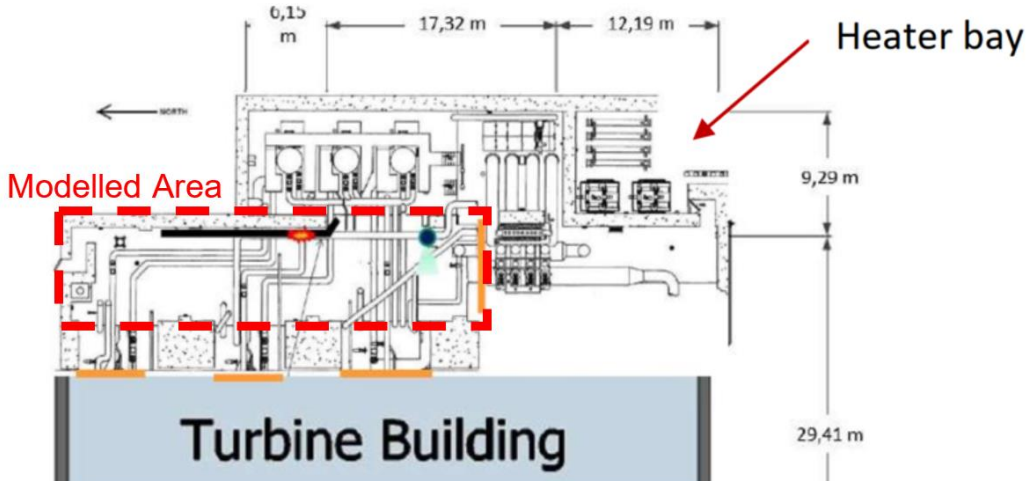
There remains significant uncertainty in the behaviour of the fire, in particular the transient HRR (fire power curve), due to the ignition by an arc fault of unknown power and duration.

The inventory data is not certain and therefore the inventory consumption has not been used as the metric for assessing the validity of the simulation against the real fire event. Instead, the validity of the simulation is assessed against fire event data by comparison of time for the sprinkler head to reach activation temperature.

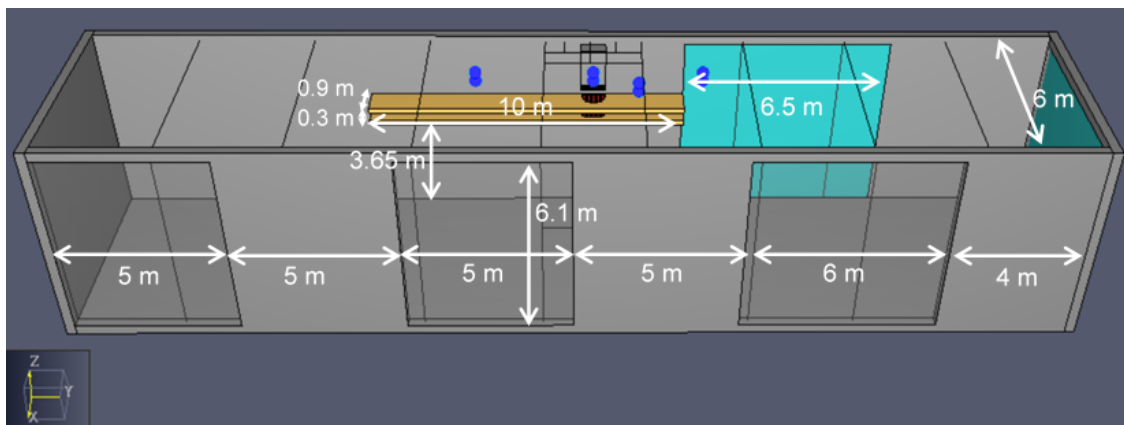
### Compartment and Obstructions

Figure 6 indicates (by red dashed line) the boundaries of the CFD model, relative to the surrounding building. Only the immediate heater bay area is considered as the model domain.

Based on the data available [2], the geometry of the modelled compartment and trays have been approximated on a conservative basis to ensure that the volume and geometry enable the required localised modelling, priority was given to ensure the local areas of interest were as representative as possible due to their impact on resolution of fire plume and interaction with local geometry, as illustrated in Figure 7 (without ceiling shown).



**Figure 6** Plan view of the modelled heater bay area



**Figure 7** Representative FDS model geometry (ceiling not shown)

Other key modelling decisions related to the compartment and tray geometries are described below. Each of these decisions was made by the modeller.

Five large openings have been included, initially assumed equal to the room height. Vents at the openings are set to 'Open', assuming that the surrounding bay and turbine building are of sufficient size to enable a non-ventilation-controlled fire.

Concrete wall thickness has been set to 0.3 m as default because no information was given on this element of the geometry, and heat loss into the concrete wall is not expected to significantly influence local fire conditions at sprinkler head within 19 minutes.

The floor/ceiling material and thickness have been assumed identical to the walls. These values impact global conditions more than local conditions, and heat loss into concrete floor and ceiling is not expected to significantly influence local fire conditions.

- Backing of all concrete boundaries has been set to 'insulated', where no heat loss occurs to the outside. This is because the rate of heat loss from the back of the concrete to adjacent rooms is expected to be minor within the 19-minute timeframe of the scenario.
- Only obstructions with potential impact on local fire conditions have been modelled because local fire conditions are predominantly influenced by plume trajectory – ad-

ditional piping etc is disregarded as plume and hot gases 'see' this after passing the sprinkler head.

- Trays are initially assumed as inert, non-permeable obstructions because the level of tray loading indicated in some pictures suggests limited gas path through the trays.
- Trays have been placed flush to the wall.

In summary, the modelling detail for the compartment and obstructions was concentrated around the area of interest, local to fire and target sprinkler providing appropriate idealisation of the scenario and analysis of the fire dynamics within that region. Other areas are approximated, and detailed representation is not considered of benefit to the calculation.

## Sprinklers

Suitable representation of the location and physical properties of the target is required in order to capture the target thermal response. Based on the provided data, the sprinkler positions are set as shown in Figure 8.

Specification data estimates that the sprinkler height is 1.2 – 1.5 m above the upper tray. Sprinklers are thus implemented at both heights to capture potential differences in recorded temperatures.

Sprinkler water droplets are not active in the model since the time to activation is the primary metric of interest.

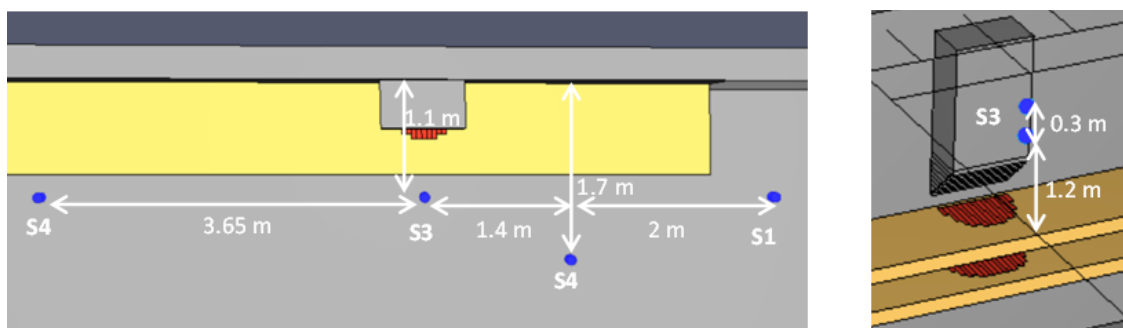


**Figure 8** Top view (left) and isometric view (right) of labelled sprinkler positions

The sprinkler activation temperature was set to 100 °C, based on data supplied. The exact Response Time Index (RTI) of the sprinklers present during the fire has not been given by the manufacturer. An RTI value above  $80 \sqrt{m/s}$  was assumed for the purposes of this analysis.

To determine the significance of the RTI parameter on the results, a sensitivity analysis was undertaken based on three typical RTI values. Figure 9 shows variation of the RTI value has a small impact on temperatures initially, with no difference seen once temperatures stabilise.

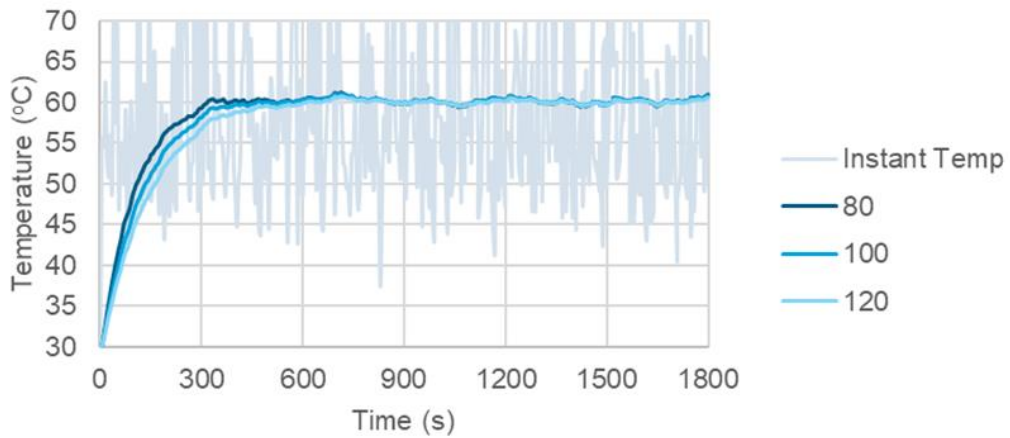


**Figure 9** Instant temperature vs sprinkler temperature at 80, 100 and 120  $\sqrt{m/s}$  RTI

Figure 9 also provides the instantaneous temperature measurement at the same location in order to understand the sprinkler response relative to the instantaneous gas temperatures. The presented results are for an instantaneous full power fire, i.e., no fire growth profile. The observed growth (delay) in sprinkler temperature is due to the time taken for the sprinkler to heat up, in line with its response time index and is not attributable to actual fire growth. This temperature increase behaviour can be assumed for all sensitivities presented in this work except where the scenario is defined as a spreading fire.

The RTI of all sprinklers was assumed as 100  $\sqrt{m/s}$  for all subsequent calculations, as suggested in the specification [2], but is noted to have insignificant impact for this scenario.

### Fire Source

Accurate representation of the heat input into the model is critical, particularly for small, enclosed volumes (which are impacted by transient heating) and where time sensitive parameters are under investigation, e.g., time to sprinkler activation.

The definition of the fire source (the maximum fire base size and fire duration) was based upon available information [2]. The representation of the fire within the CFD model, as determined by the modeller, is shown in Figure 10, with the fire base dimensions, tray spacing, and arrangement identified. Key assumptions relating to the model representation of the fire are listed below.

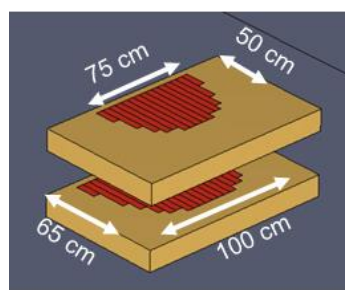


**Figure 10** Representation of the fire

The fire shape was assumed to be semi-circular. This was chosen following review of the damaged cable photographs and applying dimensions that matched the damage areas, in order to limit the spread to the areas that were observed to have been damaged.

It was decided that for the sensitivity cases applying instantaneous full power fires, the upper and lower tray fires would be set to ignite at the same time with a nominal 1 s ramp-up to full heat release rate.

For the sensitivity cases using spreading fires, the ignition point was positioned at the centre of the edge of the vent closest to the wall in line with the location of the cables that are observed to have arc-faulted. The approach ensures that the fire spreads radially from the arch point at the specified rate.

Using a representative PRISME cable fire test (PRF-BCM-S2 test [7]), the reaction heat of combustion was defined as 24 MJ/kg throughout. Further sensitivity analysis was undertaken on combustion reaction influences and is reported in the relevant section of this paper.

The HRRPUA and spread rate are two key variables that complete the definition of the fire. These variables have been studied as part of the sensitivity analysis in defining the base case model for this fire scenario.

## MODEL SENSITIVITIES

This section describes the sensitivity analysis work undertaken using the FDS model described above. Each of the modelling parameters of interest was assessed in a limited sensitivity analysis and each sensitivity was considered in isolation.

Following the learning from the previous Benchmark Exercise work, the following parameters were identified as important as being appropriate for sensitivity analysis:

1. Mesh size
2. Reaction
3. Tray representation
4. Global geometry
5. Local geometry
6. Ambient temperature
7. Fire intensity
8. Fire spread rate

### Mesh Size

Mesh size, resolution and grid definition all have a potential influence on how the physical elements (fluid dynamics) of the model is resolved.

Based on the objectives of the modelling exercise it was recognised that a more refined mesh would provide increased resolution and therefore accuracy. A nominal cell size of 0.05 m was implemented local to the fire and sprinkler. A lower resolution (0.20 m cell size) was implemented across the wider compartment in order to keep cell count at a reasonable level.

This mesh arrangement therefore had two different cell sizes interfacing with each other. A sensitivity study was undertaken to understand the effect of the mesh interface position (mesh partition between the fine and coarse meshes). The temperatures recorded by the

sprinkler were studied using four different mesh arrangements, as presented in Figure 11. Each of the meshes have progressively larger regions of refined cells with the interface position moving from coincidence to enveloping one then both sprinkler locations.

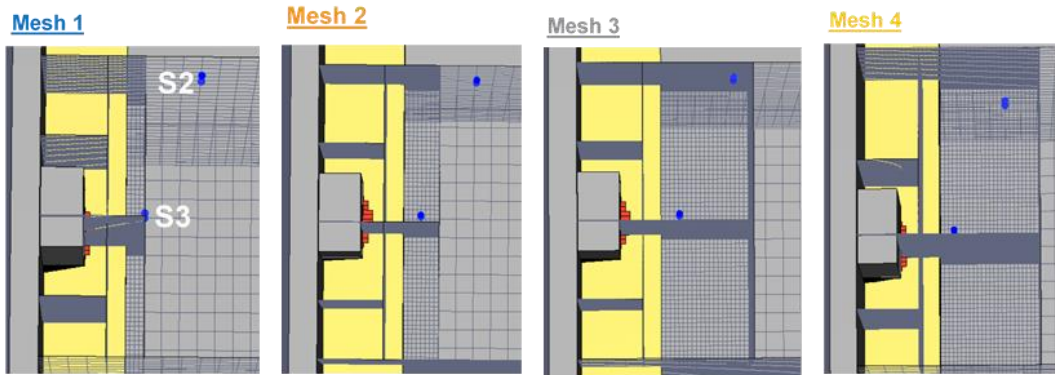


**Figure 11** Plan view of mesh set-ups studied

The key observation from the sensitivity analysis, as illustrated in Figure 12, is that the recorded temperature at sprinkler 3 is significantly higher when the device is on the mesh interface in 'Mesh 1'. As the interface is moved away, and sprinkler 3 is incorporated further into the fine mesh in 'Mesh 2', the recorded temperature is much lower. Subsequent impact from positioning the mesh interface even further away again in 'Mesh 3' and 'Mesh 4' is negligible.

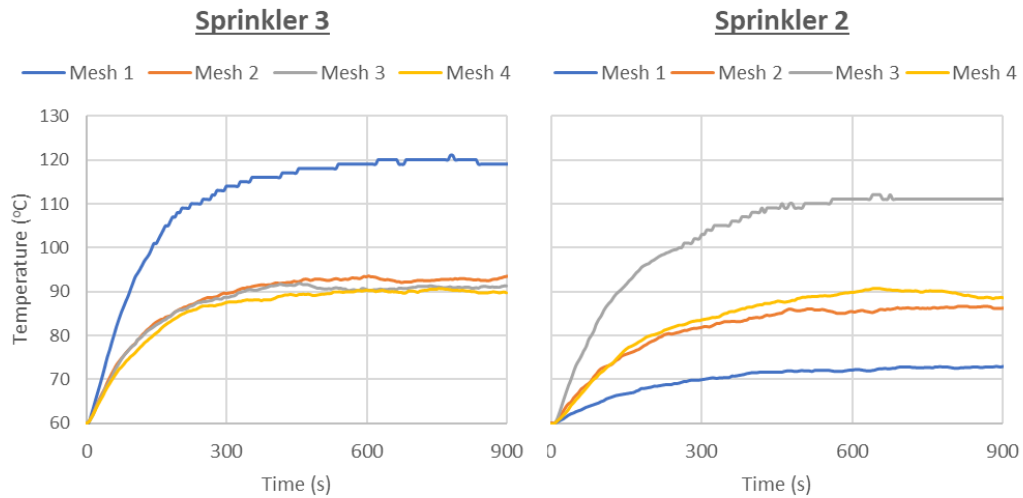


**Figure 12** Sprinkler 3 (left) and 2 (right) temperatures recorded for each mesh set-up

A similar pattern is observed for sprinkler 2 (right hand side of Figure 12), where recorded temperatures are high close to the mesh interface in 'Mesh 3', however, when the interface is moved further away in 'Mesh 4', the recorded temperature is much lower. Note that for 'Mesh 1' and 'Mesh 2', sprinkler 2 temperatures are less reliable due to the low level of mesh refinement.

In conclusion, the results demonstrated that the mesh setup was important. Sufficient resolution should be defined to capture the fire plume and jumps in mesh refinement level should be avoided adjacent to areas of interest.

## Reaction

The selection of appropriate combustion reactions is required to provide a good representation of the fire hazard whilst being conservative in the context of the study type (thermal and/or life safety).

To fully define the combustion reaction in FDS, the composition and stoichiometry of the fuel and products were investigated. It was noted that some data on the cables and reaction yields were provided (cf. Figure 13) however, this was found to be insufficient for fully defining the reaction as the exact fuel and unburnt gas compositions were unknown. Therefore, the sensitivity of the plume, and thus sprinkler temperatures, to the definitions of fuel, products, and stoichiometry needed to be understood.

The cables are PE/PVC cable #900 (7 conductors, 15.9 mm diameter with mass per length of 0.382 kg/m) supplied by U.S. NRC (see appendix). The mass fraction distribution is 55% for the cooper, 27 % for the jacket, 10% for the insulator and 8 % for the filler.

### Characteristics of combustion

Yields of combustion were deduced from the PRF BCM-S2 test results: 0.11 for CO, 1.60 for CO<sub>2</sub>, 0.08 for unburnt gases, 0.03 for HCl and 0.03 for soot. The effective heat of combustion is 24 MJ.kg<sup>-1</sup>. The radiative heat fraction is 0.35. For Benchmark Participants using the FLASH-CAT approach, the bench scale HRR per unit area is 272\* kW.m<sup>-2</sup>.

**Figure 13** Fuel and reaction data provided [2]

The key assumptions applied for the reaction studied are summarised in Table 2. Table 3 details the reactants, products, and stoichiometry of each reaction. The first reaction assumed a standard combustion reaction with pure PVC as the fuel [8], whilst the second reaction used the 'simple chemistry' model in FDS, assuming no presence of chlorine. The PR1, PR2 and PR3 reactions used the information given in Figure 13 with varying assumptions applied to address the unknown unburnt gas composition and to best match the assumed fuel composition.

The cable filler for the analysis was assumed to be polypropylene (PP) [9] the insulator to be Polyethylene (PE), and the jacket to be Polyvinyl chloride (PVC), and using the mass fractions given in Figure 13, the molar ratio of these materials in the fuel is assumed as 1 PP: 1.9 PE: 2.3 PVC.

**Table 2** Key assumptions of the trialled reaction scenarios

| Reaction Scenario | Key Assumptions   |
|-------------------|---|
| <b>PVC</b>        | Fuel is pure PVC (bounding case for % Cl in fuel)<br>All Cl in fuel is converted to HCl<br>Standard combustion stoichiometry and completeness assumed [8] |
| <b>Simple</b>     | Uses FDS 'simple chemistry' model<br>Chlorine presence is neglected<br>PRISME Soot and CO yields from Figure 13 are used                                  |
| <b>PR1</b>        | Yields of C, CO, CO <sub>2</sub> and HCl match data provided in Figure 13<br>Fuel ratio = 1 PP: 1.9 PE: 0.7 PVC   |

| Reaction Scenario | Key Assumptions  |
|-------------------|--|
|                   | Neglects unburnt gases   |
| PR2               | Yields of C, CO, CO <sub>2</sub> and HCl match data provided in Figure 13<br>Fuel ratio = 1 PP: 1.9 PE: 2.3 PVC<br>Uses Cl <sub>2</sub> product as balance to match assumed fuel <sup>10</sup> [10] [11]<br>Neglects unburnt gases |
| PR3               | Yields of C, CO, CO <sub>2</sub> and HCl match data provided in Figure 13<br>Fuel ratio = 1 PP: 1.9 PE: 1.1 PVC<br>Assumes Chlorobenzene as the unburnt gas <sup>11</sup> [10] [11]  |

**Table 3** Stoichiometry of the trialled reaction scenarios

| Reaction Scenario | Reactants                        |                               |                               |                               |                | Products |                 |      |                  |      |                 |                                  |
|-------------------|----------------------------------|-------------------------------|-------------------------------|-------------------------------|----------------|----------|-----------------|------|------------------|------|-----------------|----------------------------------|
|                   | C <sub>2</sub> H <sub>3</sub> Cl | C <sub>2</sub> H <sub>3</sub> | C <sub>3</sub> H <sub>6</sub> | C <sub>2</sub> H <sub>4</sub> | O <sub>2</sub> | CO       | CO <sub>2</sub> | C    | H <sub>2</sub> O | HCl  | Cl <sub>2</sub> | C <sub>6</sub> H <sub>5</sub> Cl |
| PVC               | 1                                | -                             | -                             | -                             | 1.53           | 0.14     | 0.96            | 0.9  | 1                | 1    | -               | -                                |
| Simple            | -                                | 1                             | -                             | -                             | 2.47           | 0.24     | 1.6             | 0.17 | 1.49             | -    | -               | -                                |
| PR1               | 0.03                             | -                             | 0.03                          | 0.08                          | 0.35           | 0.11     | 0.16            | 0.03 | 0.27             | 0.03 | -               | -                                |
| PR2               | 0.07                             | -                             | 0.02                          | 0.05                          | 0.34           | 0.11     | 0.16            | 0.03 | 0.25             | 0.03 | 0.02            | -                                |
| PR3               | 0.11                             | -                             | 0.06                          | 0.18                          | 0.47           | 0.11     | 0.16            | 0.03 | 0.51             | 0.03 | -               | 0.08                             |

The analysis results in Figure 14 showed that variations in the fuel and combustion product ratios have an impact on the predicted sprinkler temperatures.

It was observed that the behaviour of a given reaction on the temperature results was not consistent but differed between the sprinkler locations. However, in contrary to this, for both locations the PVC reaction provided the lowest recorded temperatures. Reaction PR1 gives the highest temperatures for sprinkler 3 and high values for sprinkler 2. The ranking of other reactions in between these two limits is not consistent between the two locations and therefore it is difficult to draw a robust conclusion from this sensitivity assessment.

<sup>10</sup> The key difficulty in matching the assumed fuel composition is the amount of Cl. In most experimental PVC cable fires, less than half of the Cl is released as HCl, implying that much of the original Cl remains in the char [10]. There is no evidence of 'significant' Cl products from PVC fires [11].

<sup>11</sup> Other than CO<sub>2</sub>, C and H<sub>2</sub>O, many toxic species are formed in the combustion of PVC cables, typically dominated by CO, NO<sub>2</sub>, SO<sub>2</sub>, HCN, HCl, benzene, formaldehyde and acrolein [10]. PR3 assumes benzene reacts with Cl to form Chlorobenzene [12] as the unburnt gas, enabling a better balance of Cl with the fuel.

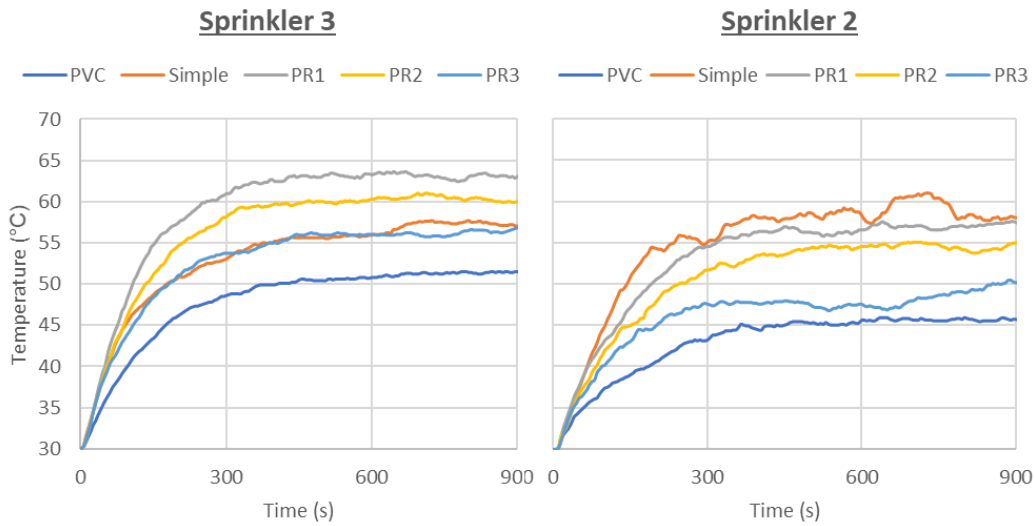


**Figure 14** Sprinkler temperatures recorded during simulation for each reaction scenario

However, based on the results it can be stated that the fuel and product specifications do impact recorded conditions, and thus it is important to define the reaction as accurately as possible. It is noted that the conclusion drawn here is specific to the impact on local fire generated temperatures, and for other scenarios, such as tenability or global fire generated conditions, it may not be applicable.

The PR2 scenario resulted in high temperatures at both sprinklers whilst using the correct proportion of fuel components (PP, PE, and PVC).

### Tray Representation

The cable tray configuration was comprised of two ladder-type trays loaded with PE/PVC cables. The width, height and spacing between the trays as per the real location was replicated in model, however the density of packing of the cables was not known. As noted in the description of uncertainties, the packing density, and its impact on the ability of fire to pass vertically through a stacked tray arrangement, is expected to influence the plume trajectory and temperature. The non-solid porosity of the packed trays can be represented in the model by different blockage areas. On this basis, a sensitivity analysis of two partially closed cable tray representations was developed (cf. Figure 15) and compared to a solid tray obstruction case called 'Single'. Scenario 'Seg1' has 50 % porosity (gaps comprising 50 % of the tray top surface area). Scenario 'Seg2' is less porous, with gaps comprising one third of the tray area. Both segmented tray arrangements were segmented along the length of the tray, rather than across the width.

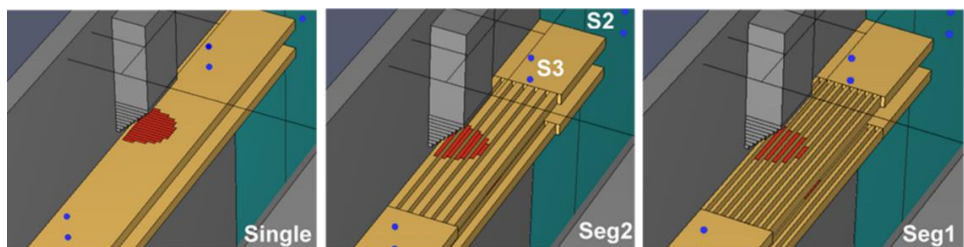


**Figure 15** Model images of cables tray representations tested

To account for the reduced fire vent area and to ensure that the applied HRR is maintained, the specified HRRPUA was proportionately scaled.

Figure 16 illustrates the temperatures recorded by sprinkler 3 and sprinkler 2 during the simulation. The left-hand chart shows how the segmentation causes a significant increase in temperatures at sprinkler 3. This is likely to be attributed to the increased extension of the plume from the lower tray, which passes through the upper tray, causing more heating of the sprinkler. Increased airflow to the lower tray may also facilitate combustion. The right-hand chart in the figure shows reduced temperatures at sprinkler 2 for both segmented tray arrangements. This effect is thought to be due to the reduced lateral spread of the plume underneath the upper tray and a consequential reduction in heat reaching the sprinkler 2 position.

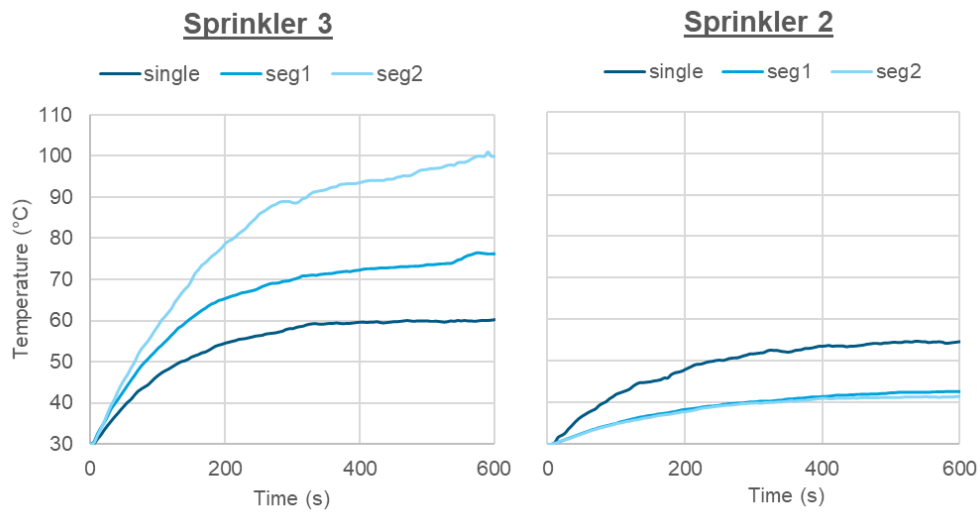


**Figure 16** Sprinkler temperatures recorded during simulation for each tray representation

In conclusion, geometric representation is important at a local level, with representation of cable trays affecting plume trajectory and target temperatures.

### Global Geometry – Height of Openings

The exact height of the five large openings in the model were unknown, and initially assumed to extend the full height of the room. The lack of offset (soffit) from the ceiling enables gases to escape directly from the heater bay without build-up of a hot gas layer and potentially reduces the temperatures at the sprinkler heads. Therefore, a sensitivity analyses was undertaken to determine the impact of including a soffit at different heights on the recorded sprinkler temperatures. Two levels of soffit are studied, 0.4 m and 0.6 m, as shown in Figure 17.

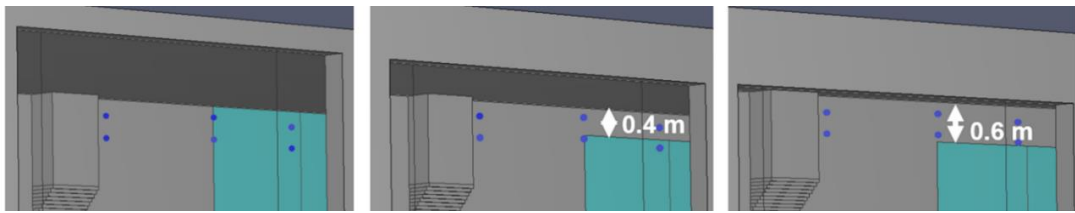


**Figure 18** Opening height scenarios studied, with zero soffit size (left), a 0.4 m soffit (middle) and a 0.6 m soffit (right)

Figure 18 shows the analysis results of the impact introducing a soffit at differing heights on temperatures recorded for all sprinklers. The results indicate that the soffit height has negligible impact on sprinkler 2 and 3 temperatures as they are local to the fire and conditions are dominated by the direct heating from the plume. However, sprinklers 1 and 4 demonstrated an increase in global temperatures in proportion to the increased soffit size, caused by the hot gas layer build-up.

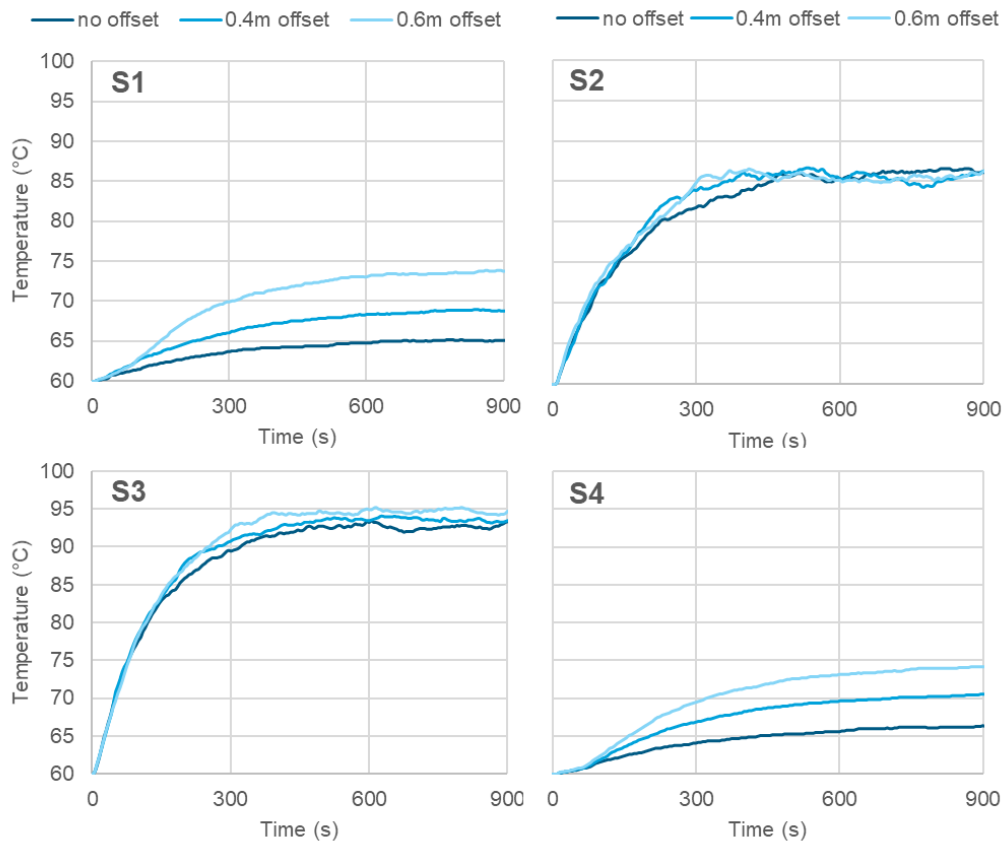


**Figure 18** Sprinkler 1, 2, 3 and 4 temperatures recorded for each offset distance

In conclusion, the geometric representation at a global level may be more or less important depending on whether the target is local to the fire or not.

### Local Geometry - Overhang Position

A representative model geometry is required in order to capture key fire dynamics. Local to the cable trays was an overhanging concrete wall protrusion which could impact the fire plume dynamics. The actual vertical position of the protrusion was not known. How-

ever, the dimensions of the overhang were provided. To understand the impact of the protrusion on the fire dynamics a sensitivity study was undertaken comparing three overhang positions.

The positions considered are illustrated in Figure 19, with the initial height estimate (left), an increased elevation of the overhang (middle) and with the overhang removed (right).

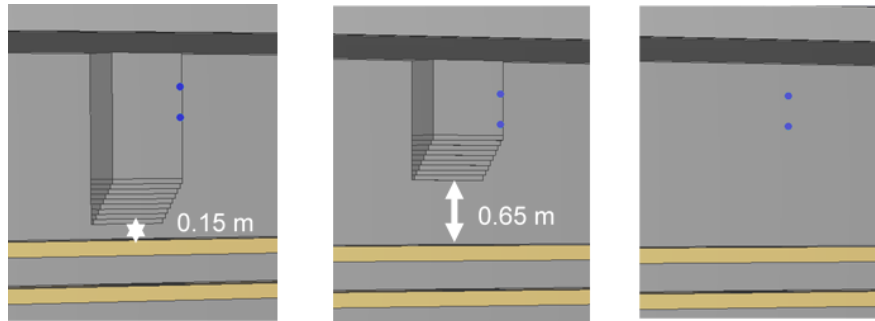


**Figure 19** Overhang scenarios tested

The analysis results showed that increasing the height/removing the overhang increases the temperatures recorded by sprinkler 3, as seen in Figure 20. This is thought to be a) due to reduced heat transfer from the fire plume to the concrete overhang, causing higher temperatures at the sprinkler, and b) the overhang disrupting the plume, increasing its mixing with the surrounding air, cooling it down.

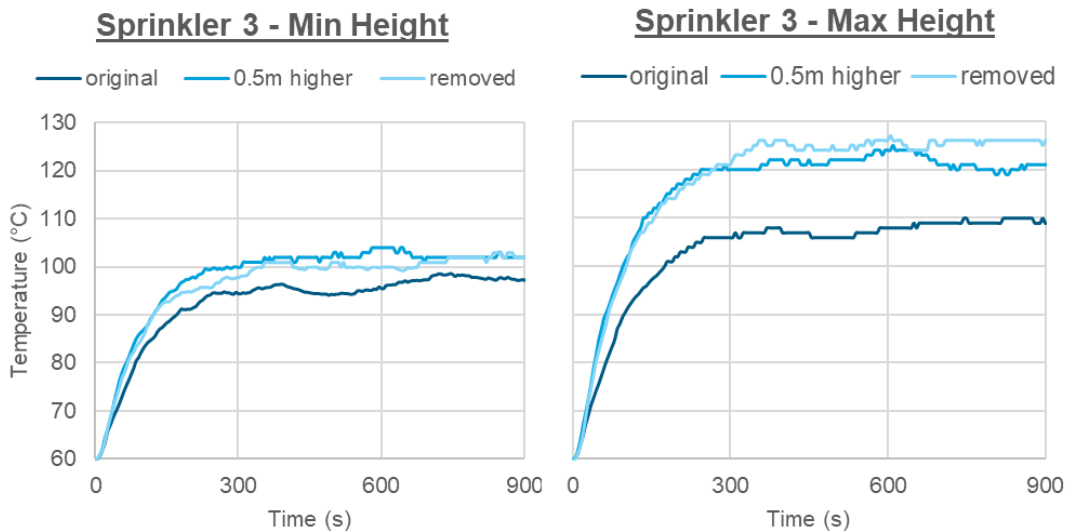


**Figure 20** Sprinkler 3 temperatures at the minimum and maximum placement height

In conclusion, the geometric representation is important at a local level, with representation of local blockages affecting plume trajectory and target temperatures.

### Ambient Temperature

The Benchmark example specification [2] estimated an ambient / initial gas temperature in the compartment of 30 °C. Review of the compartment identified a significant amount of hot pipework, taking account of the steam leak in the heater bay, it was considered likely that the initial temperature could be considerably higher. As a result, a sensitivity study was undertaken to determine the impact of varying the initial ambient temperature

from 30 to 60 °C. These comparisons are shown in Figure 21 at two different HRRPUAs, 250 and 350 kW/m<sup>2</sup>.

Overall, the modelling results indicated that the initial ambient temperature significantly impacts the conditions measured by the sprinkler local to the fire and hence its activation time.

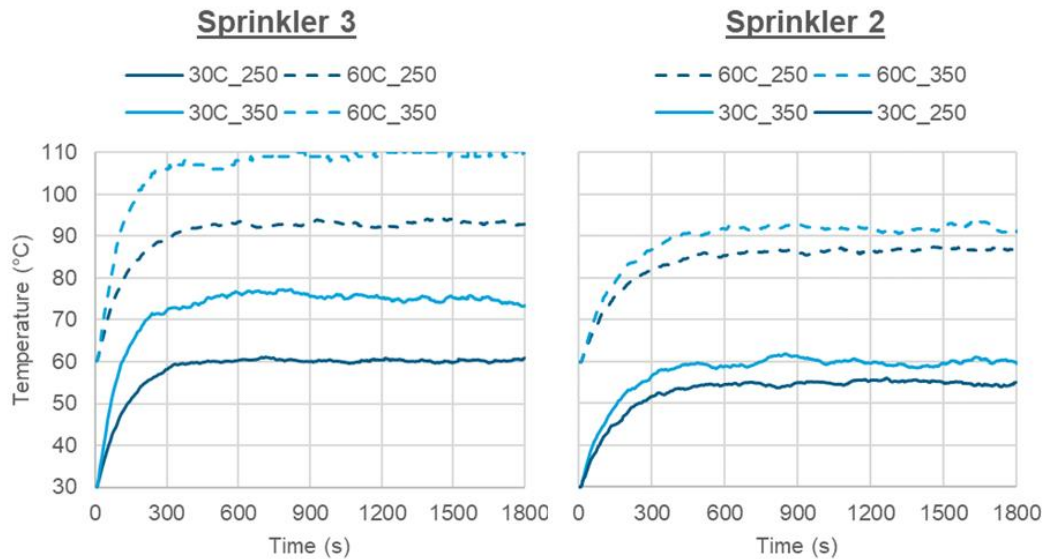


**Figure 21** Sprinkler temperature at a HRRPUA of 250 and 350 kW/m<sup>2</sup> for initial ambient temperatures of 30 and 60 °C

## Fire Definition

The fire definition is based on two parameters, the fire intensity, and the spread rate, each are assessed independently.

### Fire Intensity

The fire intensity (HRRPUA) influences the temperature of a plume and, as identified in the uncertainty description, is considered to be an important parameter in the modelling. Investigations on fire intensity [13] indicate a wide range of fire intensity values based upon material type. The guidance indicates HRRPUA can be broadly split into thermoset- and thermoplastic-type and provides recommended values for each type. The cable type identified in the event is a mixture of materials (including some rubber) but determined by the PBG as being broadly thermoplastic in nature, for which the guidance indicates a HRRPUA of 250 kW/m<sup>2</sup>. However, for the purposes of this analysis it was recognised that there is a large spread of experimental data unpinning the recommended HRRPUA values [13] and, combined with the strong influence of the parameter on the fire conditions, it was therefore considered to be a key sensitivity to be investigated.

The impact of the fire intensity (HRRPUA) on sprinkler temperature and thus activation time is presented in Figure 22 for values of 250, 300 and 350 kW/m<sup>2</sup>.

Figure 22 shows the stabilised temperature of Sprinkler 3 to be proportional to HRRPUA. This is expected as conditions are dominated by local plume-effects. Sprinkler 2 is further away, hence its temperature is indirectly impacted by the plume (and HRRPUA) and is more dominated by global effects.

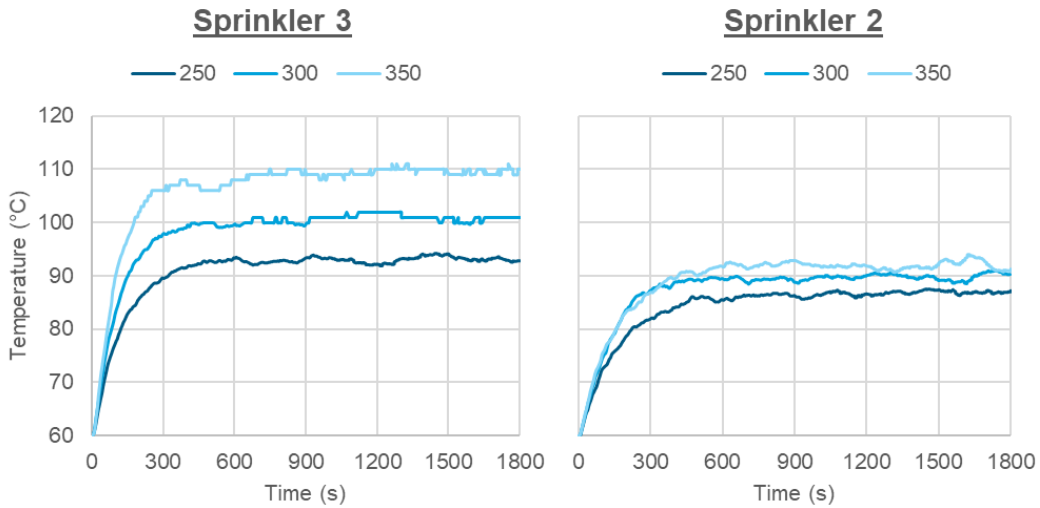


**Figure 22** Sprinkler temperature at a HRRPUAs of 250, 300 and 350 kW/m<sup>2</sup>

In conclusion, the modelling indicates that the fire intensity (HRRPUA) impacts the fire plume temperature which itself impacts the temperatures seen by the sprinklers in close proximity.

### **Fire Spread Rate**

The fire spread rate determines the fire power growth and is important in some scenarios where thermal response times are short.

In previous steps of the PRISME 3 Benchmark Exercises, fire spread rate along and between cable trays were investigated and modelled. A finding from this work was that the cable fire spread rate was well represented by the FLASH-CAT tool [13], albeit with some minor modifications to align with the Benchmark scenario. Due to the arc fault ignition of unknown power and duration, and the downwards spread of fire to the lower tray, it was concluded that the FLASH-CAT tool was not appropriate for this application.

In contrast to all previous sensitivities in which the fire was assumed to be instantaneously at full power, this sensitivity considers the impact of the assumed spread rate on the time taken to reach a stable fire power and target (sprinkler) temperature.

To determine the most appropriate fire spread rate, a sensitivity study was undertaken to fit the known parameters, that is the sprinkler temperature and activation time. Values between 3.2 m/h (thermoplastic) and 1.1 m/h (thermoset) [13] were compared. The outputs of the sensitivity analysis are shown in Figure 23 with the HRR (left) and sprinkler 3 temperature (right) for an instantaneous fire and at spread rates of 3.2, 2.0 and 1.1 m/h (using a HRRPUA of 350 kW/m<sup>2</sup>).

The global HRR, Figure 23 (left), reaches a peak value at a later time as the spread rate is slowed. This effect is reflected in the temperature chart on the right.

The time taken to reach the sprinkler activation is strongly dependent on the spread rate.

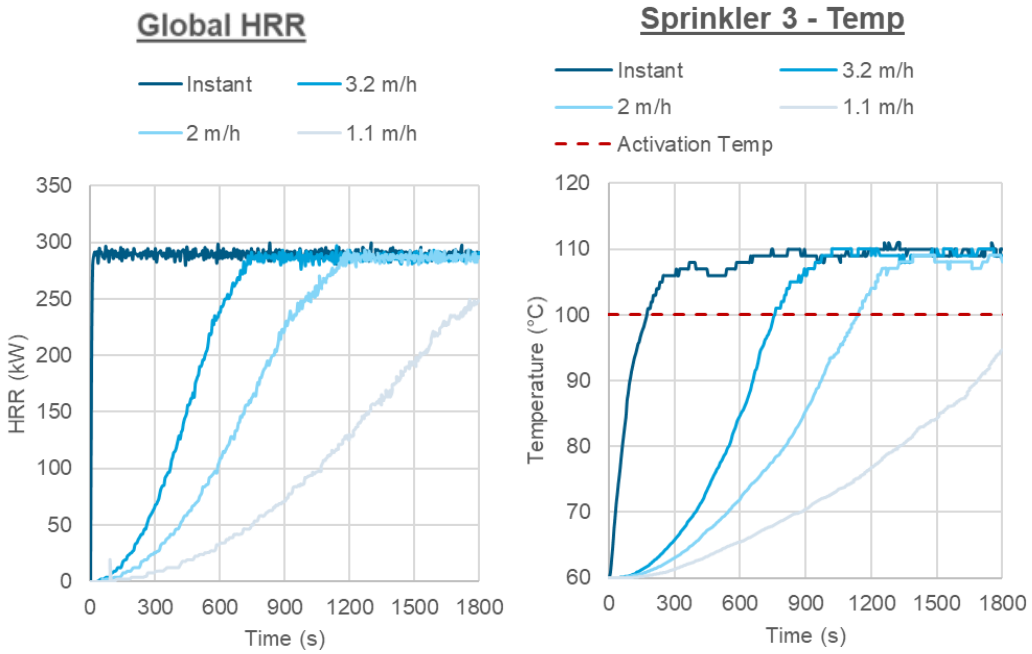


**Figure 23** Global HRR (left) and sprinkler 3 temperature (right) for a 350 kW/m<sup>2</sup> instantaneous fire and using spread at rates of 3.2, 2 and 1.1 m/h

In conclusion, HRRPUA and fire spread rate effectively determine the input HRR curve. This HRR input (through these two parameters) is the most significant input parameter to the fire simulation and has a direct impact on target temperatures.

## BASE CASE

Findings from the sensitivity analyses have been used to set the model variables which are shown in Table 4. Notable changes in the model include setting the initial ambient temperature to 60 °C to account for the steam leak in the heater bay and segmenting the cable trays for greater extension and ventilation of the plume from the lower tray.

It is noted that due to cable packing density, the trays could be represented as solid. If solid trays are used for this scenario, the temperatures observed at sprinkler 3 are predicted to remain below the assumed activation temperature of 100 °C. Therefore, if solid trays are used, a greater HRRPUA value is required (300 kW/m<sup>2</sup> or higher) in order to reach activation temperature. This higher HRRPUA value is within the range of values of thermoplastics detailed in [13] and is therefore a credible alternative approach.

**Table 4** Value of variables in final simulation case

| Variable                            | Initial Value           |
|-------------------------------------|-------------------------|
| Combustion reaction characteristics | Reaction scheme PR2     |
| Tray representation                 | Segmented               |
| Height of openings                  | 6.1 m (height of room)  |
| Overhang position                   | 0.15 m above upper tray |
| Relative humidity                   | 90 %                    |

| Variable            | Initial Value         |
|---------------------|-----------------------|
| Ambient temperature | 60 °C                 |
| Fire HRRPUA         | 250 kW/m <sup>2</sup> |
| Fire spread rate    | 3.2 m/h               |

The base case model was then run using the defined parameters. Figure 24 shows the global HRR and sprinkler 3 temperature resulting from this simulation. The full fire area and thus, maximum HRR are reached at approximately 12.5 minutes. The sprinkler activation temperature is exceeded approximately 12 minutes after ignition. This is less than the 19 minutes estimated in the fire sequence, however, the exact duration of combustion is uncertain due to the unknown extent of smouldering and unignited pyrolysis. Considering the uncertainty in fire characteristics and duration and input data, this case presents a reasonable approximation based on a robust sensitivity analysis of the fire event.

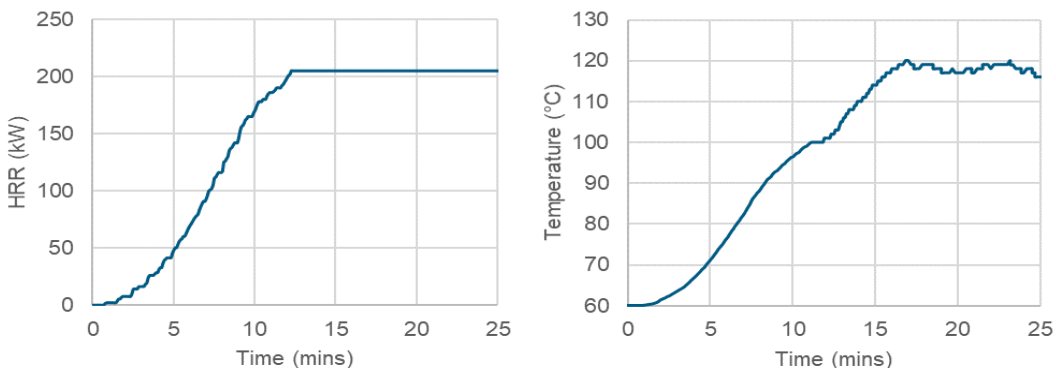


**Figure 24** Global HRR (left) and sprinkler 3 temperature (right) for final simulation case

## COMPARISON TO OTHER MODELLERS

Through the three steps of the PRISME 3 programme, the work of the PRISME PBG has enabled a range of different assessment approaches and tools to be compared. For Step 3 a large proportion of modellers have used FDS or other CFD based fire modelling tools, enabling comparison of results based on modelling choices alone [14].

A large (order of magnitude) variability in the peak heat release was observed between modellers, indicating a lack of consensus on this key input parameter. The growth rate of HRR also varied considerably between PBG contributors, due to differences in assumed fire spread rates, and different assumptions on fire growth mechanisms.

A clear relationship could be seen between the mean room temperature and the heat release rate, with the shape of temperature curves following the HRR curves. Differences also existed due to differing modelling assumptions on the initial / ambient temperatures, with values ranging from 20 to 60 °C. The temperatures recorded at the closest sprinkler head showed a less clear relationship to the HRR due to the indirect heat transfer mechanism. Here the impact of the ambient temperature was observed to be more pronounced and therefore modelling decisions which can influence fire plume dynamics were assumed to have played a significant part.

Therefore, it can be concluded that the large number of variables within a CFD based fire modelling tool has increased potential for modeller decisions to influence the output.

This was observed when comparing the results of the PBG. However, despite these risks, a CFD based fire tool can be considered as a viable option where other tools are unable to capture the fire dynamics. The variability in the results presented here reinforces the need for scenario specific modelling parameter sensitivity assessment and a robust basis for heat release assumptions.

## CONCLUSIONS

This work demonstrates an approach to modelling a real fire event using FDS. Sensitivity analyses have been performed to determine the impact of key variables on simulated conditions, primarily focusing on conditions local to the fire suppression head. The scenarios are relevant to unconfined, non-ventilation-controlled cable tray fires.

With reference to Figure 25, the key variables impacting the simulated sprinkler temperature are as follows:

The growth rate of the sprinkler temperature, and thus the time to activation (moving in direction 'A' in Figure 25) is primarily controlled by changing the specified fire spread rate. Under the modelling assumptions made, a constant spread rate of 2 m/h enabled the matching of the estimated activation time; however, time-dependant behaviour of the fire is uncertain due to unknown pyrolysis effects.

The following variables were found to impact the final sprinkler temperature most significantly (moving in direction 'B' in Figure 25):

- Reaction characteristics – local conditions were sensitive to the specified fuel/product types and stoichiometry; however, the sample size was not large enough to confidently determine correlation.
- Tray representation – segmenting the trays increased the sprinkler temperatures significantly due to increased ventilation and extension of the plume from the lower tray through the upper tray.
- Local geometry – increasing the height/removing the overhang reduces its mixing/cooling effect and the heat it absorbs, thus increasing the local sprinkler temperature recorded.
- Initial ambient temperature – increasing the ambient temperature results in an almost equivalent step change in the final sprinkler temperature local to the fire.
- Fire intensity – increasing the HRRPUA impacts the plume temperatures and increases the final sprinkler temperature.

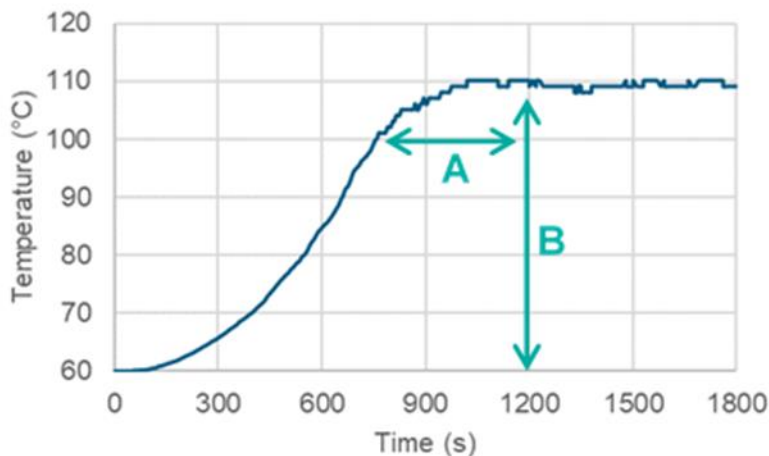


**Figure 25** Reference diagram showing impacts on local sprinkler 3 temperature

A comparison also has been made to the work of other modellers in the PRISME PBG which has demonstrated a large variability in results emphasising the need for scenario specific modelling parameter sensitivity assessment and a robust basis for heat release assumptions.

Overall, this paper has demonstrated the value of sensitivity analysis, for key parameters that should be considered when modelling poorly defined scenarios. This analysis approach can be used in generating a representative base case model and used for further validation activities.

## ACKNOWLEDGEMENTS

The authors would like to thank the UK participants for their contributions in UK industry workshops. The authors would also like to thank IRSN and the PRISME 3 and FIRE Project members for supporting the Benchmark activity.

## REFERENCES

- [1] Organisation for Economic Co-operation and Development (OECD) Nuclear Energy Agency (NEA), Committee on the Safety of Nuclear Installations (CSNI): OECD FIRE Database Version 2017:02, Paris, France, May 2019 (limited to FIRE member countries only).
- [2] Plumecocq, W.: Common OECD/NEA FIRE and PRISME Cable Benchmark Exercise, Specification of Step 3, Presentation at PRISME/FIRE Benchmark Meeting, online meeting, December 2020.
- [3] Plumecocq, W., and S. Bascou: OECD PRISME-3 & FIRE Common Benchmark Exercise, Fire event candidate, Presentation at PRISME/FIRE Benchmark Meeting, Aix-en-Provence, France, April 18, 2018.
- [4] Plumecocq, W., et al.: Investigating A Cable Tray Fire Event in the Frame of An International Benchmark Exercise, in: Röwekamp, M., H.-P. Berg (Eds.): Proceedings of SMiRT 26, 17<sup>th</sup> International Seminar on Fire Safety in Nuclear Power Plants and Installations, GRS-705, ISBN 978-3-949088-96-4, Gesellschaft für Anlagen- und Reaktorsicherheit (GRS) gGmbH, Köln, Germany, November 2022, <https://www.grs.de/publikationen/grs-705>.

- [5] McGrattan, K., and S. Hostikka: Verification and Validation Process of a Fire Model, in: 11<sup>th</sup> International Probabilistic Safety Assessment and Management Conference and the Annual European Safety and Reliability Conference 2012 (PSAM11 ESREL 2012), pp. 3568-3379, ISBN 978-1-62276-436-5, Curran Associates, Inc., Red Hook, NY, USA, 2012,  
<https://www.nist.gov/publications/verification-and-validation-process-fire-model>.
- [6] Forell, B., and J. Spille: Status of information on the Heater Bay Fire from a modelers' perspective, Presentation at the PRISME/FIRE PBG Meeting, Aix-en-Provence, France, November 2019.
- [7] Prétrel, H.: PRISME 3 and FIRE Common Benchmark Exercise - Step 2\_2 – Analysis report, Report IRSN/2020-00839, PRISME-3 n. 40, Institut de Radioprotection et de Sûreté Nucléaire (IRSN), Cadarache, France, 2020.
- [8] McGrattan, K., et al.: Fire Dynamics Simulator User's Guide, NIST Special Publication 1019, National Institute of Standards and Technology (NIST), Gaithersburg, MD, USA, 2022.
- [9] Jiangxi Longtai New Material Co. Ltd.: Cable Filler Material, Taicang City, Jiangsu Province, China, 2021,  
<https://www.polypropylene-twine.com/supplier-109634-cable-filler-material>.
- [10] Andrews, G., O. Aljumaiah, and R. Phylaktou: PVC Cable Fire Toxicity using the Cone Calorimeter, in: Harada, K, et al (Eds.): Fire Science And Technology 2015: The Proceedings of 10<sup>th</sup> Asia-Oceania Symposium on Fire Science and Technology, 2017,  
<https://vdoc.pub/documents/fire-science-and-technology-2015-the-proceedings-of-10th-asia-oceania-symposium-on-fire-science-and-technology-33ji89v2muu0>.
- [11] Bowes, P. C.: Smoke and Toxicity Hazards of Plastics, The Annals of Occupational Hygiene, Volume 17, Issue 2, pp. 143-156, December 1974,  
<https://doi.org/10.1093/annhyg/17.2.143>.
- [12] Clark, J.: Halogenation of Benzene and Methylbenzene, Chemguide, 2016,  
<https://www.chemguide.co.uk/organicprops/arenes/halogenation.html>.
- [13] McGrattan, K., et al.: Cable Heat Release, Ignition, and Spread in Tray Installations During Fire (CHRISTIFIRE) Phase 1: Horizontal Trays, NUREG/CR-7010, Volume 1, prepared for: United States Nuclear Regulatory Commission (U.S. NRC) Office of Nuclear Regulatory Research, Washington, DC, USA, July 2012,  
<https://www.nrc.gov/reading-rm/doc-collections/nuregs/contract/cr7010/v1/index.html>.
- [14] Plumecocq, W., and S. Bascou: Common OECD/NEA FIRE and PRISME Cable Benchmark Exercise, Final Report, Revision 1, Institut de Radioprotection et de Sûreté Nucléaire (IRSN), Cadarache, France, 2022.

# Quality Judgement of Surrogate Models Used for Uncertainty Consideration in Fire Safety CFD Models

Kevin Wothe<sup>1\*</sup>, Florian Köhler<sup>1</sup>, Jan Struve<sup>2</sup>, Ulrich Krause<sup>1</sup>, Ronald Zinke<sup>1</sup>

<sup>1</sup> Otto-von-Guericke University, Institute of Apparatus and Environmental Engineering, Magdeburg, Germany

<sup>2</sup> TÜV NORD EnSys GmbH & Co. KG, Hamburg, Germany

## ABSTRACT

Computational fluid dynamics (CFD) simulations are increasingly used in plant safety for fire simulations and air dispersion modelling. The main reason is the potential higher accuracy by integrating mathematical models which allow an inclusion of observations as realistic as possible. However, one often finds simulations of individual scenarios, typically intermediate or worst-case scenarios, without any discussion of the probabilities of occurrence leading to the selected input parameters.

Parameter studies for uncertainty considerations are possible using Monte Carlo (MCS) or Latin Hypercube sampling (LHS), but usually are not feasible due to the high numerical effort. As an alternative, an algebraic surrogate model, the response surface (RS) based on multivariate polynomials, is used here. To create the RS, CFD simulations must be performed on a grid of specified input parameter values.

A C++ code created for this purpose determines a multivariate polynomial for each cell of the numerical grid which approximately describes the system behaviour depending on the variables included. The corresponding coefficients of the polynomials are determined by square minimization. The number of interpolation points, the polynomial order and the number of coefficients influence the fitting accuracy as well as the fitting effort. In our research project, we want to find an optimal strategy for the highest possible accuracy at low effort.

Within the scope of the research project, the RS is to be used as a surrogate model for CFD simulations for application examples relevant to plant safety. The core aspects are the creation of accurate surrogate models and the performance of error and uncertainty analysis with MCS and LHS as well as the implementation on high performance computing systems (HPC). Therefore, the analysis of variance (ANOVA) is used to assess the significance of development coefficients and polynomial order to optimize the accuracy of the RS here.

## INTRODUCTION

In industry, major incidents are caused by explosions, fires, or releases of hazardous substances, or by mutually dependent events. Therefore, these events must be analysed in order to assess their impact on people and the environment and to be able to take appropriate protective measures. To perform these assessments, experiments as well as theoretical models are used. Experiments offer the possibility to collect data under realistic conditions. However, accident scenarios are very diverse and not all of them can be realized on a statistically representative scale, because changes in input variables and setups required for the investigation are very expensive. Model calculations and theoretical estimations up to the execution of simulations on the computer can therefore

represent a more favourable alternative. Depending on the problem, different types of model calculations can be used. These range from simple algebraic or empirical models to complex simulations. Especially for pollutant dispersion analyses or fire modelling, CFD simulations (computational fluid dynamics) [1] are increasingly used.

In CFD simulations, fluid dynamic partial differential equation systems (Navier-Stokes equations) and numerous other balance and model equations are solved numerically. Thus, spatially and temporally resolved three-dimensional scalar or vector fields, such as concentration or velocity fields, are determined. In most cases, the aim is to achieve the most comprehensive mathematical-physical modelling possible, right down to the sub-model level for minimizing the need to resort to accuracy-limiting approximations. As a result, these models provide the highest potential accuracy, but also very high demands on the quality of the input data. The systems of equations can only be solved numerically, the models are very complex and therefore require a high level of expertise in model development, software operation, and evaluation.

Even though CFD simulations can in principle lead to very detailed results, one must be aware that many input variables are uncertain and can fluctuate within parameter specific distribution functions. Down to the sub-models, numerous model parameters are implemented whose numerical values could realistically fluctuate as well. Literature studies show that numerous CFD simulations are analyses of single scenarios with sharp values and frequently with default values in sub models. A general discussion of the range of different scenarios, in particular a comprehensive error consideration, influence and tolerance analysis, is practically not to be found.

Simple error propagation considerations cannot be carried out for CFD models because the correlation between the input and target variables  $(x_1, \dots, x_m) \rightarrow y$  is not available as a differentiable function. Uncertainty considerations of the input variables are, however, possible by sampling methods such as MCS [2], [3] or LHS [4], [5]. Direct coupling of CFD simulations with the aforementioned sampling methods would require running a simulation for each (randomly chosen) input parameter vector  $(\vec{x}_1, \dots, \vec{x}_n)$ . Even if LHS generally converges faster than MCS, a large number of simulations would still be necessary until the assumed distribution functions of the input variables are sufficiently represented statistically. The effort also increases exponentially with the number of parameters to be considered. Even though individual simulations are usually already carried out on parallel computers, this direct coupling is numerically very complex or even infeasible and can only be carried out in special cases.

An alternative strategy is to try to approximate the correlation  $(x_1, \dots, x_m) \rightarrow y$  by an algebraic surrogate model, here multivariate polynomial systems [6], [7] are used, which is called the Response Surface Method (RSM). If a sufficiently accurate surrogate model exists, it can be coupled directly with the sampling methods because only algebraic operations have to be calculated for each new parameter vector, which can be done in a fraction of the time of a simulation. However, CFD simulations have to be carried out to create the model in order to obtain sufficient support points for the model fitting. If the surrogate model is sufficiently accurate, new parameter combinations can be calculated without the need for direct CFD simulation. In addition to the faster calculation of simulation results, other studies are also possible with the response surfaces. For example, parameter studies, sensitivity analyses and optimisation processes can be carried out.

Since these surrogate models are approximations of the simulation, their accuracy is relevant for the use of this method. With the required accuracy, the effort to determine the RS increases, a compromise between accuracy and effort must therefore be found. For this purpose, ANOVA approaches are examined in order to show application possibilities but also limits of the RSM.

In the scope of this research, a C++ code was created that can generate the RS fully automatically on standard PCs but also on high performance computers. This code can also be used to carry out the simulations for generating grid points as well as further calculations with the RS and has already been applied to industrially relevant CFD simulations [6], [7], [8].

The RSM, the discussion of the accuracy as well as the implementation of the investigations with the C++ code are central points of the current research and will be presented in this paper. In chapter 2, the mathematical basics of the methods used is explained. For this purpose, the RSM is presented in the first paragraph of that chapter, the regression method (least square method) used in the second paragraph, and the ANOVA in the third one. Subsequently, MCS and LHS are briefly outlined. In the third chapter, the C++ code created by the research group and its functionalities are presented. Results from previous projects in connection with the RSM are presented in the fourth chapter before current research approaches are. Finally, some conclusions are given.

## METHODS USED FOR RESPONSE SURFACE MODELLING

### Response Surface Method (RMS)

The RSM aims at modelling the dependency between explanatory variables  $x_i$ ,  $i = 1, \dots, m$  and a response  $y$  representable as  $y \Leftrightarrow (\vec{x})$  or by  $y = f(\vec{x})$ . The method was developed by Box and Wilson [9] for optimizing mainly chemical processes. The approximation makes use of low-order polynomials, which can be justified from a mathematical point of view within the frame of polynomial chaos expansion (PCE). A general representation of such a response surface could be given with:

$$y = \vec{f}(\vec{x}) \cdot \vec{a} + r. \quad (1).$$

Here  $\vec{a} = (a_0, a_1, \dots, a_p)$  is a coefficient vector of  $p + 1$  constant coefficients and  $\vec{f}(\vec{x})$  is a  $(p + 1)$ -dimensional vector field that contains any products of the explanatory variables in each component. With  $r$  a random influence can be modelled, for which usually it is assumed that with  $n$  repetitions of the determination  $(\vec{x}_i \rightarrow y_i)$  the expected value is  $\frac{1}{n} \sum_i r_i \approx 0$ .

For modelling the dependency, typically multivariate models of first or second order are used. An example for a 2<sup>nd</sup> order model is given by:

$$y = a_0 + \sum_{i=1}^n a_i x_i + \sum_{i=1}^n a_{ii} x_i^2 + \sum_{i=1, i \neq j}^n a_{ij} x_i x_j + r. \quad (2).$$

After selecting the variables in the polynomial or a suitable term structure, the coefficients must be determined. For a more general overview on the development and application of this method the reader is referred to [10]. The use of multivariate polynomials can be justified by means of generalized Fourier series expansion of random variables. The distribution properties of the random variables are explicitly taken into account. The expression stochastic response surface model (SRSM) is also used in [11] and [12].

Many quantities in CFD simulations, particularly within the underlying models, are random variables  $X$  from a mathematical point of view. They are formally defined as a measurable function from a probability space to a measure space.

The random variables  $X$  are functions that assign a real number to each result  $\omega$  of the sample space  $\Omega$ :

$$\forall x \in \mathbb{R}: \{\omega \mid X(\omega) \leq x\} \in \Sigma, \quad (3),$$

where  $\Sigma$  is an event space assigned to  $\Omega$ , which is also a  $\sigma$ -algebra on  $\Omega$ . The random variable  $X$  will take the value  $x$  when carrying out a random experiment, which is called a realization.

Since  $Y$  in  $Y = Y(X)$  depends on  $X$ , the realization  $y = f(x)$  will be taken if  $X$  takes the realization  $x$ . If  $Y = Y(X_1, X_2, \dots, X_m)$  is a random variable depending on a vector of  $m$  real random variables  $X_i$ , thus  $Y$  is called a multivariate random variable, and the  $X_i$  marginal distributions. Here, the  $X_i$  must be defined on the same probability space.

If  $f \in L^2$  is considered as a function of a standard normally distributed random variable  $X$  with finite expectation value  $E[f(X)] < \infty$  (now calculated in the probability space with the Lebesgue integral) the following representation can be used as a series:

$$f(X) = \sum_{j=0}^{\infty} f_j H_j(X), \quad \text{with: } f_j = E[f(X), H_j(X)] \quad (4).$$

Although random variables are defined on probability space,  $y = f(x)$  can be expanded into a generalized Fourier series with Hermite polynomials if the random variable  $Y$  has a finite second order moment (finite variance) [13][14]:

$$y = \sum_{j=0}^{\infty} a_j H_j(x), \quad \text{with: } H_j(x) = (-1)^j e^{x^2} \frac{d^j}{dx^j} e^{-x^2}. \quad (5).$$

The index  $j$  indicates the order of the Hermite polynomials. If  $Y = Y(X_1, X_2, \dots, X_m)$  is a random variable which depend on a vector of  $m$  real, normally distributed random variables  $X_i$ , then such an expansion is done by using multivariate Hermite polynomials as polynomial basis. This basis is obtained from the tensor products of the respective univariate basis polynomials:

$$\begin{aligned} y = a_0 \Gamma_0 + \sum_{i=1}^m a_{i1} \Gamma_1(x_{i1}) + \sum_{i_1=1}^m \sum_{i_2=1}^{i_1} a_{i_1, i_2} \Gamma_2(x_{i1}, x_{i2}) \\ + \sum_{i_1=1}^m \sum_{i_2=1}^{i_1} \sum_{i_3=1}^{i_2} a_{i_1, i_2, i_3} \Gamma_3(x_{i1}, x_{i2}, x_{i3}) + \dots. \end{aligned} \quad (6).$$

The first term is a constant, the second contains all terms of the 1<sup>st</sup> order, the third term all multivariate combinations of the variables with the 2<sup>nd</sup> order, identified by the index  $d$  on the expression  $\Gamma_d(x_{i1}, x_{i2}, \dots, x_{im})$ , which is also called polynomial chaos of order  $d$ , and the whole expansion is denoted with polynomial chaos expansion (PCE). The multivariate Hermite polynomials of the order  $d$  for the  $\Gamma_d$  can also be specified (physicist convention) as follows:

$$\Gamma_d(x_{i1}, \dots, x_{id}) = (-1)^d e^{\frac{1}{2}\vec{x}^T \vec{x}} \frac{\partial^d}{\partial x_{i1} \dots \partial x_{id}} e^{-\frac{1}{2}\vec{x}^T \vec{x}}. \quad (7).$$

The expansion coefficients  $a_j$  are to be determined. Furthermore, this polynomial chaos expansion can be generalized if the  $X_1, X_2, \dots, X_m$  are not normally distributed. Then an expansion making use of other orthogonal polynomial systems can be carried out. If one assumes that  $Y$  has a finite second order moment and all  $X_i$  finite moments in any order [15]  $Y$  can be written using orthogonal polynomials  $\{\Psi_j(\mathbf{X}), \mathbf{j} \in \mathbb{N}^m\}$ :

$$Y = \sum_{j \in \mathbb{N}^m} a_j \Psi_j(\mathbf{X}), \quad (8),$$

where  $\mathbf{X}$  is the random vector, and

$$\int_{\mathbb{R}^m} \Psi_j(\mathbf{x}) \Psi_k(\mathbf{x}) f_x(\mathbf{x}) d\mathbf{x} = \delta_{jk}. \quad (9)$$

Here  $\mathbf{j}, \mathbf{k} \in \mathbb{N}^m$  are again multi-indices, which characterizes the order. The element  $j_i \in \mathbf{j}$  thus denotes the order of  $\Psi_j(\mathbf{X})$  in the  $i$ -th variable. The total order  $|\mathbf{j}|$  of  $\Psi_j(\mathbf{X})$  is now  $\sum_i j_i$ .

If the  $m$  random variables are independent of each other, there is again a tensor product representation for  $\Psi_j(\mathbf{X})$ , in which a separate orthogonal polynomial system is used for each individual variable. Thus, also random variables can be developed into polynomials which cannot be converted to standard normal distribution by a simple transformation [16]. An important class of orthogonal polynomials is e.g. the Askey-Wilson [17] polynomial family. In addition to the Hermite polynomials (standard normal distribution), this family also includes the Jakobi polynomials (beta distribution), the Legendre polynomials (uniform distribution), the Laguerre polynomials (gamma distribution), and many others. The distributions given in parentheses are the corresponding density functions in the orthogonality relation of the polynomials. The series expansion is usually terminated at a certain polynomial order to provide a finite set of expansion coefficients. Here, often the order is limited by using [16]:

$$A^{m,d} = \{\mathbf{j} \in \mathbb{N}^m : |\mathbf{j}| \leq d\}, \quad (10),$$

where  $|\mathbf{j}| = \sum_{i=1}^m j_i$  is the total order of  $\Psi_j$  and  $d$  the highest considered order in the polynomial. Then there are  $\binom{m+d}{d}$  coefficients in the polynomial. This scheme will also be used here.

There are different methods for determining the coefficients. In this paper, only sampling points are available for the relationships  $y = f(x_1, x_2, \dots, x_m)$ , such that the coefficients  $a_j$  are being determined using the method of least squares.

## Least Square Techniques

According to the previous section multivariate polynomials have to be fitted to  $n$  sample values within RSM. A common strategy to determine the coefficients are least square methods. Here, the coefficients are determined by minimizing the sum of the squared deviations  $F(a_0, \dots, a_p)$ , which is a function of the  $p + 1$  parameters:

$$F(a_0, \dots, a_p) = \sum_{i=1}^n [f(\vec{x}_i) - \hat{f}(\vec{x}_i)]^2 = \sum_{i=1}^n r_i^2. \quad (11).$$

The necessary condition to be fulfilled is:

$$\nabla F(a_0, \dots, a_p) \stackrel{!}{=} \vec{0}. \quad (12).$$

The derivation of the corresponding system of equations is straight forward but omitted here. It can be shown that with the matrix  $M$  (size  $n \times (p + 1)$ ) defined as:

$$M = \begin{pmatrix} f_0(\vec{x}_1) & f_1(\vec{x}_1) & \dots & f_p(\vec{x}_1) \\ f_0(\vec{x}_2) & f_1(\vec{x}_2) & \dots & f_p(\vec{x}_2) \\ \vdots & \vdots & & \vdots \\ f_0(\vec{x}_n) & f_1(\vec{x}_n) & \dots & f_p(\vec{x}_n) \end{pmatrix} \quad (13),$$

and with:

$$\vec{y}^T = [f(\vec{x}_1), f(\vec{x}_2), \dots, f(\vec{x}_n)] \quad \text{and} \quad \vec{a}^T = [a_0, a_1, \dots, a_p] \quad (14),$$

one finds:

$$M^T M \vec{a} = M^T \vec{y} \quad \Rightarrow \vec{a} = (M^T M)^{-1} M^T \vec{y}. \quad (15).$$

With equation (15), the coefficients can be determined by solving an equation system. Data weighting is also possible by:

$$\vec{a} = (M^T W M)^{-1} M^T W \vec{y}, \quad (16),$$

where  $W$  is a square diagonal matrix of size  $n \times n$ . Here,  $W$  is specified for removing outliers, for modifying the strength of the weighting indirectly proportional to the size of the residual, or for considering the distance between the position of the actual point location and a selected weighting location.

### Analysis of Variance (ANOVA)

In regression problems, one is always confronted with the task of determining or investigating which order the regression polynomial should have and which development coefficients are significant/non-significant. One way of investigating the significance of these coefficients is through ANOVA [18]. This is a group of data analysis procedures based on hypothesis tests. In these procedures, the influence of the variable on the response is described by means of the variance. Consequently, it is possible to draw conclusions about the structures contained in the regression data used and to check the assumptions made in the regression procedure (order, coefficients, etc.).

In the simplest case, the ANOVA corresponds to the generalised t-test. On the other hand, surrogate models of a variable with polynomial chaos expansion were set up in [19], and the coefficient selection of the expansion according to orthogonal polynomials was carried out with a variance analysis. The work shows that ANOVA can be useful to find further conjectures about the original model and optimally insert them into the substitute model. How this can be used for RS in CFD simulations is explained below.

### Monte Carlo and Latin Hypercube Sampling

With both MCS and LHS, random samples are determined according to the distribution properties of the selected variable. For the mathematical background of both methods,

the reader is referred to the literature [2], [3], [4], [5]. The aim is to generate random numbers that statistically represent the underlying distribution function.

With the LHS as well as with the MCS sampling an improvement in the statistical accuracy is achieved when the sample size is increased [20], [21]. However, in case of MCS, usually a very large number of combinations have to be determined for a representative recording of a distribution function, since MCS only converges very slowly. It can be shown that for  $y = f(x)$  the necessary number  $n$  of support points  $x_i$  in order not to exceed a relative error with a given probability is  $\sim \sqrt{1/n}$  [2]. Depending on the required quantiles of the distribution, typically  $n > 10$  to  $n \approx 10^2$  or well above are necessary. Latin hypercube sampling is advantageous here because it converges significantly faster and requires significantly fewer data points for representative sampling. The number actually required depends on the model and cannot be specified as a general rule. In practical applications, LHS is therefore preferable to simple MCS. The C++-code to be discussed below contains both sampling methods.

## C++ CODE

In CFD simulations, scalar or vector fields are output by values for each grid cell or for dedicated calculation nodes [22]. In OpenFOAM [23], the output for each grid cell of the underlying simulation grid is in the form of lists. Therefore, for each grid cell a multivariate polynomial is set up based on the individual simulations carried out, which together form the response surface. The creation of the surrogate model based on OpenFOAM simulations as well as all further calculations with the RS are carried out using a C++ code programmed for this purpose. This code can manage the CFD simulations to be carried out (parameter transfer and simulation start), read in the results of the OpenFOAM simulations and provide the output in a form that can be visualised with ParaView [24]. The code is intended for use on high performance computers (HPCs) but can also be used on PCs under many conventional operating systems. The general workflow of the programme can be seen in Figure 1.

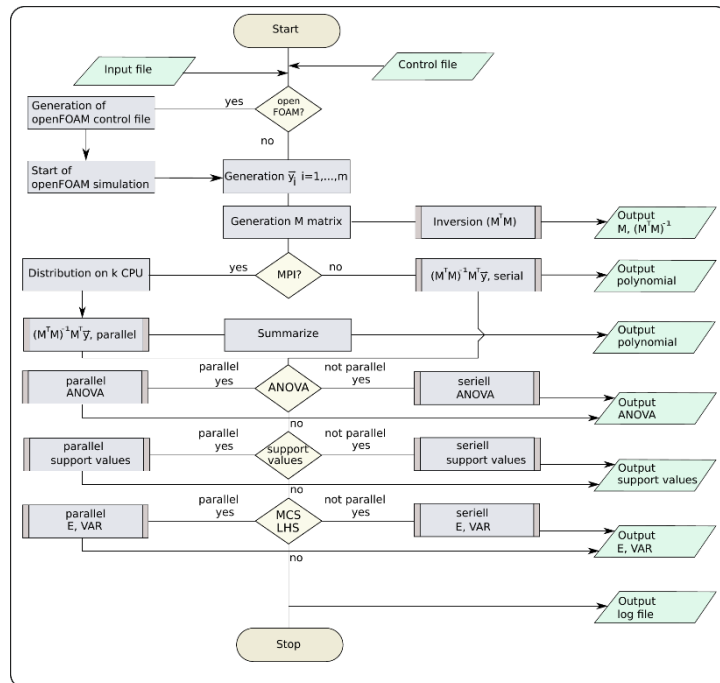


**Figure 1** Schematic representation of the workflow of the C++ code created in the research group [25].

Usually, a simulation folder is created with a prepared OpenFOAM case, and the code creates all other files according to specified parameter vectors, starts the simulations and collects the results. This also makes simple parameter studies easier if no RS is to be created. In addition, even direct application of the sampling methods (MCS or LHS) with the CFD simulation is possible, as long as the necessary resources for the calculations are available in sufficient quantities.

When carrying out the CFD simulations or generating the RS, the user can decide, depending on the circumstances, whether this is to be carried out in parallel or serially and how many processors are to be used for this. The results of the simulations and the RS can then be read directly into the visualisation tool of the simulation programme ParaView [24].

If the CFD simulations have been carried out with any other programme, the results need only be available as a simple text file. The code can also process an input file created from these results, in which first the cell or node coordinates and then the results for each parameter combination considered are entered in column form. Further details on this will be omitted with the note that a comprehensive manual for the procedure and use of the code is included in the package [25].

At the beginning of the calculation of the polynomials, the M-matrix (see equation (13)) is created according to the parameter number and the given polynomial order. This is done only once, regardless of the type of calculation (serial or parallel) since the matrix is identical for all cells of the simulation. Before the coefficients are calculated according to equation (15) and the results are written into an output file, the programme predicts the memory requirement and gives a statement about the feasibility on the computer system used. With the output file for the regression, the code can now calculate further results (interpolations, limited extrapolations in the parameter space) or carry out entire parameter series, ANOVA, MCS or LHS. For detailed information on that, see chapter 4. At the end of each use of the code, a summary of the resources used (time and computer memory) but also of the partial steps carried out (simulation, regression, further value calculations, sampling procedures, etc.) is output (log file, debugging).

Research projects in which this code has been applied [6], [7], [8] are presented below.

## RESULTS AND DISCUSSION

The RSM has already been applied several times to industry-relevant simulations [6], [7], [8]. The results from the completed investigations and projects will be briefly summarized in the following. Subsequently, it will be shown what the current research subject is and why this is essential in the enhancement of the RSM within our research group.

### Applications of the Methodology

With the support of RSM in CFD simulations, gas releases (light gas as well as dense gas) [6], [7], [26] and fire spreading [8] have been investigated within the research group.

The light gas dispersion simulations are focused on VOC emissions from floating roof tanks for the storage of mineral oil products. The aim was to determine concentration fields including conceivable damage scenarios at the tank to estimate the probability of occurrence of a hazardous explosive atmosphere [26]. A comparison of a selected original simulation with Ansys CFX [22] and the RS are presented in Figure 2. It should be noted that the parameter combination of the original simulation was not used to create the RS.

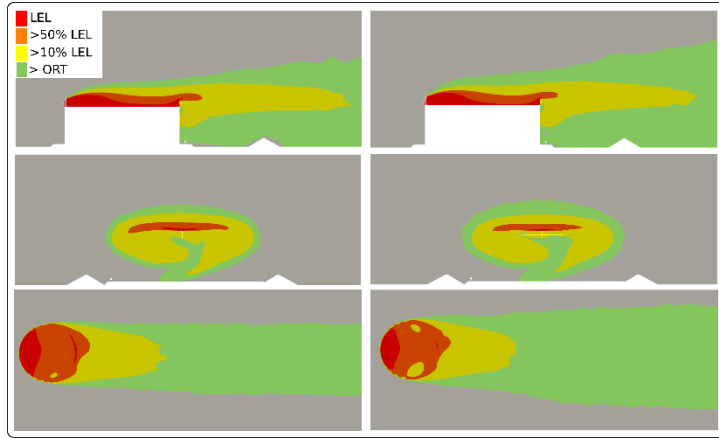


**Figure 2** Comparison of original model (left) and response surface (right) via longitudinal, lateral, and horizontal slices (from top to bottom) of 3D concentration profiles of VOC emissions at a floating roof tank; concentrations of VOCs for the lower explosive limit (LEL, 6000 ppm) and odour recognition threshold (ORT, 6 ppm) were used for colour classification (taken from [6])

It was shown that the RS is a good approximation to the original simulation and can represent three-dimensional fields quite accurately despite the moderate number of grid points used.

The dense gas dispersion simulations were carried out to verify the suitability of a modified turbulence model which is intended to describe dense gas dispersion in the near-ground region as accurately as possible [27]. In [6], these OpenFOAM simulations [23] were used to show how well the surrogate models can capture and reproduce small fluctuations in the input variables. For this purpose, the firmly defined dispersion area XIX according to [28] was used as geometry. Furthermore, the ground roughness  $z_0$ , the wind speed and the source mass flow were selected as variable input parameters.

To analyse the accuracy of the RS with small parameter variations, the polynomials of randomly selected grid cells were evaluated. For this purpose, concentration profiles were generated as a function of ground roughness and wind speed and the RS were directly compared with CFD results generated independently. Figure 3 shows two polynomials at constant ground roughness in comparison with the CFD results. On the one hand, a second-order polynomial with weighted regression (see equation (16)) and a 3<sup>rd</sup> order polynomial are shown. In addition, concentration profiles at other ground roughness's have been added.

The diagram clearly shows that the polynomials reflect the results well. In particular, the data belonging to the adjacent ground roughness can be clearly distinguished from the polynomials. Thus, it could be shown that parameter fluctuations in this order of magnitude can be well resolved with the surrogate model. In these investigations [6], [7], in addition to the comparisons of the substitute model with the CFD simulation, the performance of the C++ code for their creation was also analysed and published for the first time. For example, calculating the polynomials with a core i9 9900K @3.6 GHz CPU required a time of 9 s, whereas the CFDs required a calculation time of about 10 h each. This represents a significant saving in time and resources. For detailed explanations of the performance of the code and the investigations presented, please refer to [6], [7], [27].

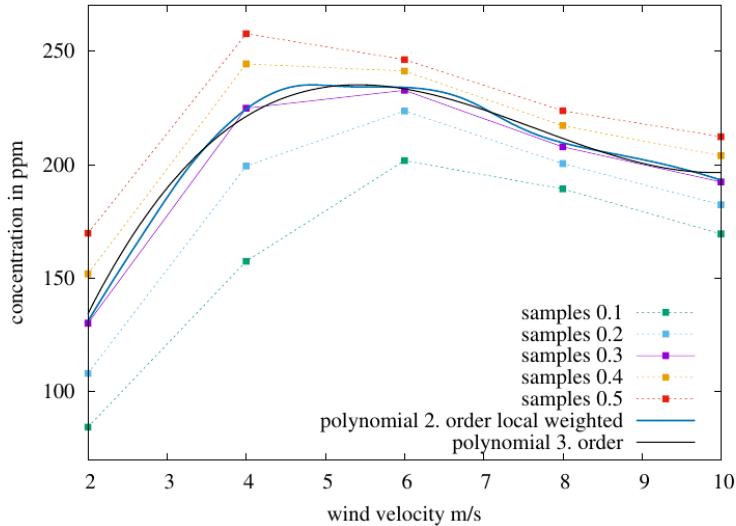


**Figure 3** Illustration of the concentration depending on the wind velocity for a selected cell of the underlying CFD mesh, showing the 2<sup>nd</sup> (local weighted) and 3<sup>rd</sup> order polynomials for  $z_0 = 0.3$  m and, in addition for comparison, CFD data for  $z_0 = 0.1$  m, 0.2 m, 0.4 m, and 0.5 m (dotted curves)

In another project it was shown to what extent the RSM can be applied in the context of fire simulations in complex building structures. This research project (FKZ 1501530) [8] was funded by the former German Federal Ministry of Economy and Energy (BMWi). The main objectives of the project were (i) the simulation of fires in complex building structures and of the subsequent propagation of fire gases, (ii) the consideration of the involved combustibles including the transport of radioactive substances via the gas flow, (iii) a complete tolerance and error analysis with statistical consideration of the distributed input parameters, and (iv) the use of parallel processing on a HPC. The DOOR experiments of the Organization for Economic Co-operation and Development (OECD) Nuclear Energy Agency (NEA) PRISME Project [29] were used as basis for the CFD geometry. In addition, the ambient temperature, the heat release rate, and the air renewal rate were used as variable input parameters for the simulation. Again, a good agreement of the simulation results with the substitute model could be achieved. Figure 4 shows an excerpt of the comparison of the flow fields: the original model (left) compared to the RS with 2<sup>nd</sup> order polynomials (middle) and 2<sup>nd</sup> order polynomials with weighted regression (right). Again, the weighting was indirectly proportional to the residuals (cf. equation (16)). The figure shows the fire compartment of the PRISME experiments used in [8]. The velocity range between  $0 \text{ ms}^{-1}$  and  $4 \text{ ms}^{-1}$  was selected for the colour classification.

It can be seen that the use of second order polynomials is generally a good first approximation. Using weighting, even the positions and size of the eddy structures were well reproduced, which can be seen in the right part of the image compared to the original left. After a good agreement of the RS with the simulation results could be proven, uncertainty considerations were carried out using MC and LHS. For the LHS, 1000 sampling points were calculated, which took  $3 \cdot 10^4$  s on a core i7 4930K @3.4 GHz CPU [8]. A CFD simulation, on the other hand, took several days depending on the parameter combinations.

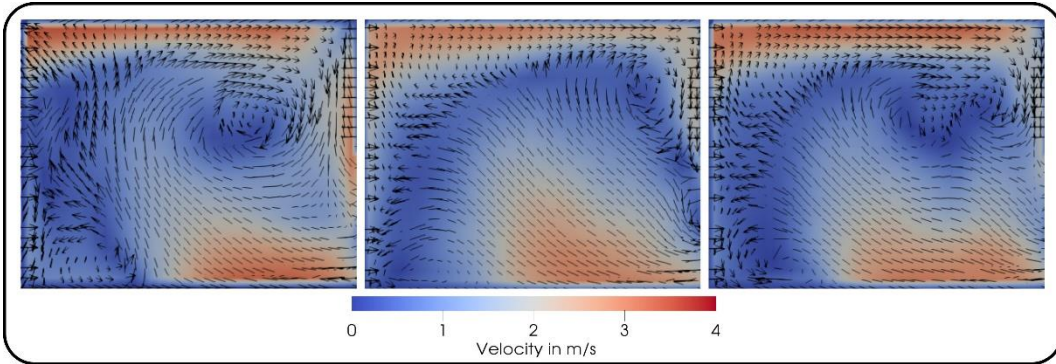


**Figure 4** Comparison of the original model (left) with the response surface (middle: 2<sup>nd</sup> order polynomial and right: 2<sup>nd</sup> order polynomial with local weighting) using a longitudinal cut of the flow field (created with ParaView [24])

In summary, it could be shown that the RSM can generate suitable algebraic surrogate models for CFD simulations, which represent a good approximation of the original. Furthermore, subsequent investigations (uncertainty considerations and interpolations) were carried out using the C++ code of the research group [25]. Due to the algebraic model, these were possible in a fraction of the time it would have taken to calculate this directly with the CFD.

### Investigations on the Accuracy of the RSM

It was shown above in which research projects the RSM, and the C++ code have already been used and what results have been obtained. Qualitative comparisons between the RS and the original simulation were used to evaluate the quality of the model's approximation. This evaluation is important for excluding errors in the process of model creation (incorrect operation, errors in the grid simulations, etc.) but also to provide a justification for the use of the method. This must show why calculations are carried out with the substitute model and not with the original simulation. Thus, a statement about the comparison of effort and benefit of this methodology is always necessary. In order to better compare several surrogate models to each other, but also to further optimise the code and to be able to show the limits of the RSM, quantitative assessment standards for the quality and suitability of the RS are needed. The use of ANOVA is a tool that is the current research subject of the research group as well as an ongoing PhD project and is presented in the following.

First, a simple example from [7] is used to demonstrate the influence of the assumptions made during the regression (polynomial order and structure) on the surrogate model. Furthermore, it is explained how ANOVA can contribute to an optimisation of this model.

For a set of six sampling points, six functional values were determined with the quadratic relation  $y = f(x) = (x - 2)^2$ , to which small, normally distributed errors were added. The value combinations obtained in this way can then be used for the fitting of 1<sup>st</sup> to 5<sup>th</sup> order polynomials (cf. methods shown above). This is shown in Figure 5. For comparison purposes, the sum of the residual squares R for each polynomial is also given.

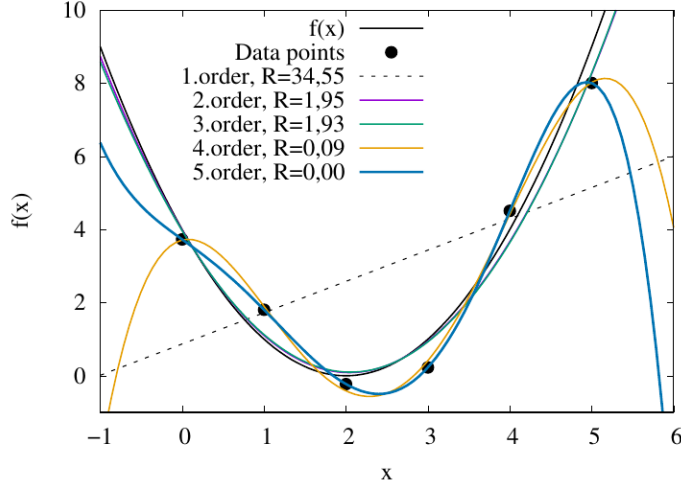


**Figure 5** Illustration of underfitting and overfitting in a regression problem; R being the sum of the magnitudes of the residuals (from [7])

From the figure it is evident that the 1<sup>st</sup> order polynomial does not describe the course of the data points well and the trend of the data points is not correctly reproduced. This is a case of underfitting. As expected, the 2<sup>nd</sup> order polynomial better follows the course of the data points also providing globally good approximations, and therefore seems to be suitable for extrapolations. As the order of the polynomial increases, the sum of the residual squares decreases, and the curves fit the points better. In the case of the 5<sup>th</sup> order polynomial, the residual sum is zero and the curve passes exactly through the data points. However, the polynomial exhibits oscillations that do not correspond to the assumed initial model. This corresponds to an overfitting problem.

If one does not know the underlying relationship  $y = f(x)$ , as is the case with many CFD simulations, and has a limited selection of supporting points because a large number of CFD codes represent a non-profitable expense, the determination of a suitable polynomial is sometimes not obvious. Therefore, for determining the lowest possible order that has sufficient accuracy, the significance of the polynomial and the individual coefficients must be investigated.

A widely used analysis of the significance of the entire polynomial is the so-called F-test [30], [31]. In [19] a modified F-test was used for ANOVA to evaluate the significance of the individual coefficients of a function set up with polynomial chaos expansion. In principle, the test performed here was carried out according to this publication, albeit with different variable definitions due to inconsistencies within the literature source. In order to understand the test procedure, a few definitions should first be given. First,  $R$  is the sum of squares of the residuals:

$$R = \sum_{i=1}^n r_i^2 = \sum_{i=1}^n (y_i - \hat{y}_i)^2. \quad (17)$$

For fitting a polynomial with  $p$  coefficients ( $k = p - 1$  slope coefficients) to  $n$  data points,  $R$  has exactly  $n - p$  degrees of freedom. The entire polynomial has  $p$  degrees of freedom and each term  $y_j, j = 0, \dots, k$  has one degree of freedom. The test statistics are now:

$$F_j = \frac{n-p}{R} \sum_{i=1}^n \hat{y}_{ij}^2, \quad (18),$$

$$F_g = \frac{n-p}{R(k+1)} \sum_{i=1}^n \left( \sum_{j=0}^9 \hat{y}_{ij} \right)^2. \quad (19).$$

For test decision, in equation (18) the  $F_{(1-\alpha)}(1, n-p)$  quantile and in equation (19) the  $F_{(1-\alpha)}(k+1, n-p)$  quantile of the Fischer distribution is used. The value  $\alpha = 0.05$  is often used as the significance level for the decision for or against the null hypothesis. The hypotheses are as follows:

- $H_0$ : All explanatory variables have no influence on the dependent variable, thus the associated coefficients from  $F_j$  and  $F_g$  are zero.
- $H_1$ : At least one variable is significant.

If the values calculated according to equations (18) or (19) for  $F_j$  or  $F_g$  at a given significance level exceeding the critical value of the  $F_{(1-\alpha)}(1, n-p)$  or the  $F_{(1-\alpha)}(k+1, n-p)$  quantile of the Fischer distribution the null hypothesis is rejected in favour of the alternative hypothesis.

Based on this calculation procedure, the ANOVA will be implemented in the C++ code for examining selected parts of the RS or the entire RS. Once the RS has been set up according to the user input, the ANOVA will be carried out according to the formulas and decision criteria shown above. If the ANOVA is applied to the RS the results are statistically analysed to see how the significance of the coefficients is distributed. Basically, a differentiation is made between significant and non-significant coefficients. However, this classification cannot only be determined based on a sharply defined limit, but it must also be possible to consider the deviations from the limit value in the significance decision. How this is integrated into the process is only one challenge within the research project.

The results of the ANOVA should then be used to evaluate the influences of the input parameters and thus to better approximate the functional relationship within the simulation. If coefficients are determined to be non-significant this can be considered in a new regression. In this way, the coefficients can be omitted, and the structure of the polynomials can be adjusted. This can significantly reduce the effort required for calculations with the polynomials in parameter studies or sampling procedures. Furthermore, an adjustment of the order can take place at the same time without the potential need for a higher number of coefficients. This can further reduce the deviations between the original and the replacement model and thus lead to more accurate models.

The adaptation and implementation of ANOVA and other methods for optimising and analysing the accuracy of RSM are, however, only partial steps within the research project of the working group. Finally, by applying these methods, the limits of the RSM can be identified and investigated. This should enable the analysts to give recommendations for dealing with the RSM and use these to expand the C++ code.

## SUMMARY AND CONCLUSIONS

In this paper, the RSM and its application to CFD simulations have been presented. First, the mathematical basics of the methodology and the regression methods applied have been discussed. In a second step it has been shown how OpenFOAM-based CFD

simulations can be started and the RSM and further calculations with the substitute models can be carried out fully automatically with applying a C++ code [25]. Afterwards the results from already completed research projects [6], [7], [8], in which the RSM and the C++ code have been applied, have been briefly summarised. It could be shown that the RS approximate the results of the original models quite well in the investigations.

Moreover, with the support by surrogate models, uncertainty considerations were possible for the analysis of input parameter variations in the CFD simulations by means of MCS and LHS. It was also possible to show how effectively the C++ code works. Finally, a current topic of the research group has been presented. An explanation has been given why accuracy considerations of the surrogate models are important in the regression process and how these can be carried out by means of an adapted ANOVA procedure. For this purpose, the basic mathematical equations have been presented and an approach for applying them in the C++ code was given. Last not least, the need for further research, especially in the implementation of the methodology in the code but also in the subsequent investigations of the RS to analyse application limits of this methodology was pointed out.

## REFERENCES

- [1] Shen, R., et al.: Recent application of Computational Fluid Dynamics (CFD) in process safety and loss prevention: A review, *Journal of Loss Prevention in the Process Industries* 67, p. 104252, ISSN 095042302020, <http://dx.doi.org/10.1016/j.jlp.2020.104252>.
- [2] Sobol, I. M.: *Die Monte-Carlo-Methode*, Deutscher Verlag der Wissenschaften, Berlin, Germany, 1991 (in German).
- [3] Müller-Gronbach, T., E. Novak, and K. Ritter: *Monte Carlo-Algorithmen*, ISBN 978-3-540-89140-6, Springer Verlag, Berlin Heidelberg, Germany 2012 (in German), <http://dx.doi.org/10.1007/978-3-540-89141-3>.
- [4] McKay, M. D., R. J. Beckman, and W. J. Conover: Comparison of Three Methods for Selecting Values of Input Variables in the Analysis of Output from a Computer Code, *Technometrics* 21 No. 2, ISSN 0040-1706, pp 239-245, 1979, <http://dx.doi.org/10.1080/00401706.1979.10489755>.
- [5] Iman, R. L., J. L. Helton, an J. E. Campbell: An Approach to Sensitivity Analysis of Computer Models: Part I—Introduction, Input Variable Selection and Preliminary Variable Assessment, *Journal of Quality Technology* 13, No. 3, pp. 174-183, 1981, <http://dx.doi.org/10.1080/00224065.1981.11978748>.
- [6] Zinke, R., et al.: Uncertainty consideration in CFD-models via response surface modelling: application on realistic dense and light gas dispersion simulations, *Journal of Loss Prevention in the Process Industries* 75, ISSN 0950-4230, 2022, <http://dx.doi.org/https://doi.org/10.1016/j.jlp.2021.104710>.
- [7] Zinke, R.: *Unsicherheitsbetrachtungen und Fehlerfortpflanzung in quantitativen Risikoanalysen*, Habilitationsschrift, Otto-von-Guericke Universität, Magdeburg, Germany, 2022 (in German), <http://nbn-resolving.de/urn/resolver.pl?urn=urn:nbn:de:gbv:ma9:1-1981185920-900867>.
- [8] Zinke, R., and F. Köhler: *Modellierung von Brandszenarien in komplexen Gebäudestrukturen*, Reaktorsicherheitsforschung - Vorhaben-Nr.: 1501530, Otto-von-Guericke Universität, Magdeburg, Germany, 2021 (in German).

- [9] Box, G. E. P., and K. B. Wilson: On the Experimental Attainment of Optimum Conditions, *Journal of the Royal Statistical Society: Series B (Methodological)* 13, No. 1, pp. 1-38, 1995, <https://doi.org/10.1111/j.2517-6161.1951.tb00067.x>.
- [10] Khuri, A. I., and S. Mukhopadhyay: Response surface methodology, *Wiley Interdisciplinary Reviews: Computational Statistics* 2, No. 2, ISSN 1939-5108, pp. 128-149, 2010, <http://dx.doi.org/10.1002/wics.73>.
- [11] Isukapalli, S. S., A. Roy, and P. G. Georgopoulos: Stochastic Response Surface Methods (SRSMs) for Uncertainty Propagation: Application to Environmental and Biological Systems, *Risk Analysis* 18, No. 3, p. 12, 1998, <http://dx.doi.org/10.1111/j.1539-6924.1998.tb01301.x>.
- [12] Chutia, R., S. Mahanta, and D. Datta: Uncertainty modelling of atmospheric dispersion by stochastic response surface method under aleatory and epistemic uncertainties, *Sadhana* 39, p. 18, 2014, <http://dx.doi.org/10.1007/s12046-013-0212-7>.
- [13] Ghanem, R. G., and P. D. Spanos: Spectral techniques for Stochastic Finite Elements, *Archives of Computational Methods in Engineering* 4, No. 1, pp. 63-100, 1997, <https://doi.org/10.1007/BF02818931>.
- [14] Cameron, R. H., and W. T. Martin: The Orthogonal Development of Non-Linear Functionals in Series of Fourier-Hermite Functionals, *The Annals of Mathematics* 48, No. 2, pp. 385-392, 1947, <https://doi.org/10.2307/1969178>.
- [15] Ernst, O. G.; et al.: On the convergence of generalized polynomial chaos expansion, *ESAIM: M2AN* 46 (2012), No. 2, pp. 317-339, 2012, <http://dx.doi.org/10.1051/m2an/2011045>.
- [16] Xiu, D., A. Roy, G. E. Karniadakis: The Wiener-Askey Polynomial Chaos for Stochastic Differential Equations, *SIAM Journal on Scientific Computing* 24, No. 2, p. 25. 2002, <http://dx.doi.org/10.1137/S1064827501387826>.
- [17] Askey, R., and J. Wilson: Some basic hypergeometric orthogonal polynomials that generalize Jacobi polynomials, *Memoirs of the American Mathematical Society* 54, 1985, <https://dx.doi.org/10.1090/memo/0319>.
- [18] Dormann, C. F.: *Parametrische Statistik: Verteilungen, maximum likelihood und GLM in R*, Springer Spektrum (Statistik und ihre Anwendungen), ISBN 978-3-642-34785-6, Berlin, Germany, 2013.
- [19] Choi, S.-K., et al.: Polynomial Chaos Expansion with Latin Hypercube Sampling for Estimating Response Variability, *AIAA Journal* 42, No. 6, pp. 1191-1198, 2004, <http://dx.doi.org/10.2514/1.2220>.
- [20] Saltelli, A., K. Chan, and E. M. Scott: *Sensitivity Analysis* (Wiley Series in Probability and Statistics), Wiley, 2009, ISBN 978-0-470-74382-9, <https://www.wiley.com/en-us/Sensitivity+Analysis-p-9780470743829>.
- [21] Helton, J. C., and F. J. Davis: Sampling-Based Methods for Uncertainty and Sensitivity Analysis, 22, No. 3, p. 31, 2002, <http://dx.doi.org/10.1111/0272-4332.00041>.
- [22] ANSYS Inc. Academic Research, Release 17.2, <https://www.ansys.com>, last access September 24, 2022.
- [23] OpenFOAM Ltd.: OpenFOAM, <https://www.openfoam.com>, last access September 24, 2022.

- [24] Ahrens, James, Geveci, Berk, Law, Charles, ParaView: An End-User Tool for Large Data Visualization, *Visualization Handbook*, Elsevier, 2005, ISBN-13: 978-0123875822, <https://www.paraview.org/publications/>.
- [25] Zinke, R., et al.: C++ code for the creation of multipolynomial surrogate models for CFD simulations (unpublished working material), Otto-von-Guericke Universität, Magdeburg, Germany, 2022.
- [26] Zinke, R., and F. Köhler: Berufsgenossenschaft Rohstoffe und chemische Industrie (Hrsg.): Emissionen leichtflüchtiger Kohlenwasserstoffe aus Schwimmdachtanks und deren lokale Ausbreitung: Betrachtungen zum bestimmungsgemäßen Betrieb und Schadensfall, Magdeburg, Germany, 2019 (in German).
- [27] Schalau, S., A. Habib, and S. Michel: Atmospheric Wind Field Modelling with Open-FOAM for Near-Ground Gas Dispersion, *Atmosphere* 12, No. 8, p. 933, 2021, <http://dx.doi.org/10.3390/atmos12080933>.
- [28] Verein Deutscher Ingenieure (VDI) e.V. / Deutsches Institut für Normung (DIN) - Kommission Reinhaltung der Luft (KRdL) - Normenausschuss: VDI 3783, Blatt 2:1990-07: Environmental meteorology; dispersion of heavy gas emissions by accidental releases, safety study, Düsseldorf, Germany, 1990.
- [29] Organization for Economic Co-operation and Development (OECD) Nuclear Energy Agency (NEA) Committee on the Safety of Nuclear Installations (CSNI): OECD/NEA PRISME Project Application Report, NEA/CSNI/R(2012)14, Paris, France, July 2012, [https://www.oecd.org/officialdocuments/publicdisplaydocumentpdf/?cote=NEA/CSNI/R\(2012\)14&docLanguage=En](https://www.oecd.org/officialdocuments/publicdisplaydocumentpdf/?cote=NEA/CSNI/R(2012)14&docLanguage=En).
- [30] Hartung, J., B. Elpelt, and K.-H. Klösener: Statistik: Lehr- und Handbuch der angewandten Statistik, (mit zahlreichen durchgerechneten Beispielen) 15. überarbeitet und wesentlich erweiterte Auflage, ISBN 978-3486590289, Oldenbourg, München, Germany, 2009 (in German).
- [31] Fahrmeir, L.: Regression: models, methods and applications, ISBN 978-3-642-34332-2, Springer Science and Business Media, 2013, <https://doi.org/10.1007/978-3-642-34333-9>.

# Modelling of Fire Scenarios in Complex Building Structures: A Project Presentation

Florian Köhler<sup>1\*</sup>, Kevin Wothe<sup>1</sup>, Jan Struve<sup>2</sup>, Ulrich Krause<sup>1</sup>, Ronald Zinke<sup>1</sup>

<sup>1</sup> Otto-von-Guericke University, Institute of Apparatus and Environmental Engineering,  
Magdeburg, Germany

<sup>2</sup> TÜV NORD EnSys GmbH & Co. KG, Hamburg, Germany

## ABSTRACT

Fire events can severely endanger private, public, or industrial infrastructure. Architectural and organisational measures, sometimes prescribed by law, should take account of relevant scenarios analysed in advance. The legal requirements for adequate fire safety usually include the use of the building and its purpose via assignment of a building class. Depending on the latter, special requirements for proving adequate fire safety, must be considered.

Fires in nuclear facilities are fire events in special building structures. Frequently found characteristics are a lack of windows, active ventilation features, special access and escape routes, and safety concepts including the risk associated with radioactive materials involved. The software or the mathematical/physical level with which a conceivable fire scenario has to be modelled in advance, is usually not specified. However, proof must be provided that legally prescribed protection goals are met. Due to a general desire for higher accuracy, there is a transition from simpler models towards potentially more accurate CFD (computational fluid dynamics) simulations.

CFD simulations are predominantly only simulations of individual scenarios, often without a statement regarding the likelihood of occurrence. A general examination of the range of different scenarios, a comprehensive error or tolerance analysis, is numerically very complex and often left out. The number of necessary simulations increases rapidly, if uncertainties are considered, e.g., via sampling algorithms such as Latin Hypercube (LHS), or Monte Carlo sampling (MCS). Therefore, more efficient methodologies are required.

A possible strategy was investigated within a research project MBKG, funded by the German Federal Ministry for Economic Affairs and Climate Action (BMWK), formerly the Federal Ministry for Economics and Energy (BMWi).

The scope of the project was to conduct simulations of fires in complex building structures including a complete tolerance and error analysis. For this purpose, a strategy was developed to include uncertainties via a suitable definition of a Response Surface (RS) and its determination with high performance computing systems (HPC). CFD fire simulations were carried out to demonstrate the procedure. The chosen geometry is based on the DIVA facility which was used by the French Institut de Radioprotection et de Sûreté Nucléaire (IRSN) for investigations within the Organization for Economic Co-operation and Development (OECD) Nuclear Energy Agency (NEA) experimental fire research project PRISME (French: *Propagation d'un incendie pour des scenarios multilocaux élémentaires*).

The aim of this paper is to present the MBKG project and to show how the Response Surface can be determined and used for uncertainty considerations.

## INTRODUCTION

Fires in nuclear facilities can lead to both impairments and failures of structures, systems, and components (SSCs) important to safety as well as to releases of radioactive substances. The latter is particularly relevant during decommissioning and dismantling of nuclear facilities, since in this context, radioactive materials are increasingly handled, and special fire risks can arise. Various models of different complexity are available for investigating the effects of plant internal fires, e.g. in the frame of safety analyses.

The current state of the art in fire modelling is the use of algebraical (or empirical, see further below) models, zone models, or CFD codes. Empirical and zone models represent the fire event in a greatly simplified manner. They are comparatively easy to use but cannot describe the dynamics of the fire process and only have a limited spatial resolution. Moreover, zone models also depict the fire sequence in a very simplified manner and assume the homogeneity of physical variables within the zones such that local dependencies of the target quantities are not recorded. On the other hand, CFD simulations are potentially the most accurate ones due to the inclusion of all relevant influencing variables, if necessary, in an explicitly location and time dependent manner and due to the fact that global approximations are avoided as far as possible [1].

However, the higher accuracy is only beneficial if the sometimes difficult modelling is performed correctly and if the required input parameters are known or can be determined with sufficient accuracy. The time required for the numerical simulations is in the range of hours to days on parallel computers for problems of practical relevance. In the context of safety related considerations, a general issue is that many simulations published are investigations of scenarios with a single set of parameters. A comprehensive error consideration as well as an influence and tolerance analysis are practically not found. Solution strategies to mitigate this problem have been analysed in the frame of the research project MBKG (FKZ 1501530) [2], funded by the former German Federal Ministry for Economy and Energy (BMWi).

The main focus of this paper is on how to include uncertainties and parameter variations in CFD simulations of fire induced flows of smoke gases within building structures of nuclear facilities. For this purpose, the paper is organised as follows: A brief overview of fire models currently applied is given in the second section, with the focus on CFD simulations and the associated sources of uncertainties.

It is shown that considerations of uncertain parameters within CFD simulations are usually not possible if uncertainties within input data are considered by taking probability distributions into account, e.g., via sampling algorithms as LHS or MCS. An alternative strategy is the application of surrogate modelling, here the so-called Response Surface Method (RSM). The basic principle of the RSM and how it is used in this context is also covered below.

The third section shows the application for fire scenarios in the DIVA facility investigated in the frame of the OECD/NEA PRISME Project [3]. This includes a description of the model geometry and the selected simulation conditions. The uncertain parameters for determining the Response Surface are also specified there. The simulation results are compared to those from the Response Surface and important insights are discussed and conclusions drawn. Finally, the results of the project are summarized.

## METHODS FOR FIRE AND SURROGATE MODELLING

### Fire Modelling

In Germany, requirements for fire protection of nuclear facilities are provided in detail in the Nuclear Standards Commission's fire protection standards KTA 2101, Part 1 to 3 [4].

However, explicit requirements leading to an obligation for the use of CFD simulations regarding fire protection issues within nuclear facilities cannot be derived from this. The model is therefore to be selected based on the question in each individual case. An overview of models suitable for describing fires in nuclear facilities is given in [5]. In this guideline, selected computer programs and computerised implementations of the various model classes were validated using specific benchmark exercises and examined with respect to the corresponding areas of application. The result shows that CFD simulations always offer an advantage over the simpler models in case of impact assessments in complex geometries, i.e., geometries deviating from a rectangular geometry as well as for investigations of local or time-dependent variables, or if mechanical ventilation conditions must be taken into account. In the following, major model groups, their requirements and limitations are briefly discussed.

### ***Empirical or Simple Algebraic Models***

Empirical models are usually based on interrelations of selected physical quantities but derived without a deep insight into the functional or causal behaviour of the system. The specification of numerical values for input variables is typical for the application of empirical models in order to calculate values for output variables. The underlying system can still be viewed as a black box. The model equations, often derived by dimensional analysis and subsequent experimental determinations of constants or functions of dimensionless combinations of the variables involved, are usually easy to handle but can only be used within narrow ranges of validity. Algebraic models are those in which only simple arithmetic operations occur, e.g. no ordinary or partial differential operations. Next, unlike the empirical models, these can be the result of a detailed systems analysis. However, both have in common that they are mostly easy to use. Examples are equations for flame heights, heat radiation and smoke gas mass flows as a function of fire intensity or geometric factors [6], [7]. Sometimes these approaches are included as sub-models in more complex descriptions as well as within sub-models of CFD-simulations as, e.g., radiation models, chemical models, and others [8].

### ***Zone Models***

Hot smoke gases released by a fire within rooms can form a characteristic layer of hot gas under the ceiling. Cold gases, on the other hand, remain close to the ground. The amount of hot gas and its temperature is determined by so-called plume models, which have been developed based on empirical data. There are various plume models, whereby the specific model selection depends on the area of application [6], [7]. The aim of the zone models is to determine the characteristics (e.g., temperature, height, composition) of the different layers and their properties for different fire phases, taking emissivity, energy exchange with the environment, or pressure distributions into account. Within the individual layers (zones); however, a homogeneity of the descriptive variables is predominantly assumed. From a mathematical point of view, conservation equations for mass and energy are set up and solved numerically [6], [7]. Zone models are sufficiently accurate for numerous applications but cannot be used if the flow has to be described precisely and the assumption of homogeneity within the zones is not plausible or even inhomogeneities are to be explicitly determined as a function of location and time.

### ***CFD-Simulations***

A third group of modelling approaches for fire scenarios are CFD simulations [8]. Model equations used are the Navier-Stokes equations for the fluid flow, but, in addition also all physical and chemical processes or phenomena considered to be relevant after devel-

oping a suitable mathematical model. For fire simulations, models for describing the flow, chemical reactions (combustion models), radiation, buoyancy effects, particle transport, thermophysical properties and pyrolysis are important.

For the description of the flow, it is practically always necessary to explicitly model the turbulence, because otherwise the requirements for local resolution by capturing all vortex structures would lead to numerically unmanageable simulations. By capturing all relevant influencing variables, if necessary, in an explicitly location- and time-dependent form, and by avoiding global approximations as far as possible, CFD simulations are potentially most accurate. However, the higher accuracy can only be profited from if the sometimes difficult modelling is correctly performed (avoiding partly non-trivial application errors, observing best practice guidelines) and the required input parameters are known or can be determined with sufficient accuracy. The time required for the numerical simulations is in the range of hours to days on parallel computers for problems relevant to practice.

### ***Uncertainties in CFD-Simulations***

A CFD simulation includes in addition to the actual simulation also pre- and post-processing. Based on a problem to be analytical resolved, relevant physical parameters, structural or spatial conditions must first be determined. This is followed by geometry and grid definitions as well as by the definition of the initial and boundary conditions within pre-processing. The simulation is carried out applying a suitable software. For this purpose, mathematical methods must be selected for the solution of the assigned discretised system of equations, right up to the control of time and spatial increments, the definition of convergence criteria and the output values. The simulation results are evaluated as part of post-processing. The work steps listed so far contain their own sources of errors or uncertainties, e.g., modelling errors, unfavourable turbulence sub-models, discretisation errors, and others.

For more information here, reference is made to the literature [1], [9], [10]. In this work, only uncertainties in the model parameters are to be considered. In this context, it is assumed that there is a relationship  $y = f(x_1, \dots, x_n)$  between an interesting target variable  $y$  and one or more explanatory variables  $x_1, \dots, x_n$ . If this relationship (function) is known and differentiable error propagation such as e.g. the total differential can be applied.

Such a functional relationship does not exist for CFD simulations. In [11], [12], [13], two groups are distinguished for a more detailed description of the uncertainties: non-probabilistic methods and probabilistic methods. Non-probabilistic methods in turn have two subgroups. First, by specifying an interval and second, by specifying a membership function, while probabilistic methods are based on specifying probability density functions. The latter is always assumed here. Such a probability density function for modelling parameter uncertainty can be included using MCS or LHS by generating a sufficient number of parameter sets to reproduce the distribution properties. However, this usually requires a high number of CFD simulations and thus can be unfeasible due to the numerical effort. An alternative strategy was used in [14], [15], [16]. The input parameters within the uncertainty analysis were rasterised in the parameter space. A CFD simulation was carried out for each combination so that a sufficient number of support points was determined to create a surrogate model, in the following denoted as response surface (see next section). The response surface is formed by multivariate polynomials. The number of variables depends on the number of input parameters to be examined, with the exception of the spatial coordinates (cell or node coordinates for the CFD simulation). Thus, the response surface consists of as many polynomials of a predetermined order as there are cells in the CFD grid.

In addition to previously published work, it was shown in [16] how three-dimensional flow fields can be generated in this way for realistic dense and light gas emissions. Furthermore, it was shown how the results can be visualised with freely available software packages (ParaView, [17]) already included in OpenFOAM [18].

### Response Surface Method

The RSM was developed by Box and Wilson [19] for optimising chemical processes (see also [20] for a general overview). The aim of RSM is modelling the dependency between explanatory variables  $x_i, i = 1, \dots, m$  and a response  $y$  representable as  $y \Leftrightarrow (\vec{x})$  or by  $y = f(\vec{x})$ . This dependency can be approximated using low-order polynomials:

$$y = \vec{f}(\vec{x}) \cdot \vec{a} + r \quad (1)$$

Here  $\vec{a} = (a_0, a_1, \dots, a_p)$  is a coefficient vector made up of  $p + 1$  constant coefficients and  $\vec{f}(\vec{x})$  is a  $(p + 1)$ -dimensional vector field that can consist of any products of the explanatory variables in each component. With  $r$  a random influence can be modeled, which one usually assumes that with  $n$  repetition of the determination  $(\vec{x}_i \rightarrow y_i)$  the expectation value  $\frac{1}{n} \sum_i r_i \approx 0$ .

For modelling the dependency, usually the multivariate models of low order are used. After selecting the variables in the polynomial or a suitable term structure, the coefficients have to be determined. For a more general overview of the development and application of this method, the reader is referred to [21]. The use of multivariate polynomials can be justified mathematically by means of generalised Fourier series expansion (Polynomial Chaos Expansion (PCE)) of random variables. Here, the distribution properties of the random variables can be explicitly considered. In [12] and [13], the extended expression Stochastic Response Surface Models (SRSM) are used in these cases.

The PCE represents an extension of the Fourier series expansion of square-integrable functions  $f \in L^2$  on random variables that are formally defined on probability spaces. For normally distributed random variables, it can be shown that an expansion in Hermite polynomials can be carried out because the Hermite polynomials satisfy an orthogonality relation regarding the density function of the normal distribution. An important class of orthogonal polynomials are summarised in the so-called Askey-Wilson [22] polynomial family. In addition to the Hermite polynomials (standard normal distribution), this family also includes the Jacobi polynomials (beta distribution), which contain the Legendre polynomials as a special case (uniform distribution), the Laguerre polynomials (gamma distribution) and others. In [23], PCE were shown for a subset of the Askey-Wilson polynomial family, which also affects the ones listed here. The distribution given in brackets is the corresponding density function in the orthogonality relation of the polynomials. For the purposes of this work, however, the special structure of the polynomials does not have to be considered explicitly. In practical applications, the series expansion is usually terminated at a certain polynomial order to have a finite set of expansion coefficients. In this paper, only sampling points are available for the relationships  $y = f(x_1, x_2, \dots, x_n)$ , such that the coefficients  $a_j$  are going to be determined using the method of least squares. For further details on the justification for the development of PCE and for more detailed explanations, see [2]. A detailed mathematical description of the PCE can be found e.g. in [24] and [25].

## Least Square Techniques

In the previous section, it was shown that multivariate polynomials have to be fitted to  $n$  sample values within RSM. A simple and widely used option are least square methods in which the coefficients are determined in such a way that the sum of the squared deviations, calculated with a multivariate polynomial, is minimal. The sum of the squared deviations  $F(a_0, \dots, a_p)$  is a function of the  $p + 1$  parameters:

$$F(a_0, \dots, a_p) = \sum_{i=1}^m [f(\vec{x}_i) - \hat{f}(\vec{x}_i)]^2 = \sum_{i=1}^m r_i^2 \quad (2)$$

The necessary condition for minimising the sum of the squared deviations is:

$$\nabla F(a_0, \dots, a_p) = \vec{0} \quad (3)$$

The straight-forward derivation of the corresponding system of equations is omitted here. It can be shown that with the matrix  $M$  (size  $m \times (p + 1)$ ):

$$M = \begin{pmatrix} f_0(\vec{x}_1) & f_1(\vec{x}_1) & \dots & f_p(\vec{x}_1) \\ f_0(\vec{x}_2) & f_1(\vec{x}_2) & \dots & f_p(\vec{x}_2) \\ \vdots & \vdots & & \vdots \\ f_0(\vec{x}_m) & f_1(\vec{x}_m) & \dots & f_p(\vec{x}_m) \end{pmatrix} \quad (4)$$

and with:

$$\vec{y}^T = [f(\vec{x}_1), f(\vec{x}_2), \dots, f(\vec{x}_m)], \quad \vec{a}^T = [a_0, a_1, \dots, a_p], \quad (5)$$

the following equation is derived:

$$M^T M \vec{a} = M^T \vec{y} \Rightarrow \vec{a} = (M^T M)^{-1} M^T \vec{y} \quad (6)$$

With (6) the coefficients can be determined by solving an equation system. The data can also be weighted to remove outliers, to weight according to the size of the residual or depending on the location (moving least square):

$$\vec{a} = (M^T W M)^{-1} M^T W \vec{y}, \quad (7)$$

where  $W$  is a square diagonal matrix of size  $m \times m$ . The special case without weighting is still included in (7) if the identity matrix is chosen for  $W$ .

## Monte Carlo and Latin Hypercube Sampling

With MCS, random samples are determined according to the distribution properties of the selected variable. A characteristic property of the determination process is its memory lessness, which means that the  $n + 1$ -th value of the sample is independent of the  $n$  previously determined ones. In case MCS is coupled directly with CFD simulations, usually a very large number of combinations must be considered, since MCS only converges very slowly. It can be shown that for  $y = f(x)$  the necessary number  $n$  of support points  $x_i$  in order not to exceed a relative error with a given probability is  $\sim \sqrt{1/n}$  [26]. For a representative recording of a distribution function, thus very large sample

sizes are necessary. Concrete numbers depend on the required quantiles of the distribution but  $n > 10$  to  $n \approx 10^2$  or well above are common. The basic idea of LHS is to determine a representative sample as well, but with a significant smaller sample size. A Latin Square [27], [28] is a regular division of a square into  $n$  rows and  $n$  columns, each field is assigned one of  $n$  different values. Each value appears exactly once in each row and column. A Latin Hypercube is the generalisation of the Latin Square to any dimensions  $d \geq 2$ .

Both with LHS and MCS, an improvement in the statistical accuracy is achieved when the sample size is increased [29], [30]. However, LHS is advantageous because it converges significantly faster and requires significantly fewer data points for representative sampling. The number of samples required depends on the model and cannot be specified as a general rule. In practical applications, LHS is therefore preferable to MCS. For the determination of the parameter sets, the corresponding probability density functions  $f_i(x)$  of all variables  $x_i$  is divided in  $m$  intervals of equal probability. This allows the generation of  $m$  random support values. From these  $m$  support values for each variable  $x_i$  exactly one is taken at random. As a result, the distribution density function  $f_i(x_i)$  of  $x_i$  is represented by  $m$  samples.

To generate the parameter sets  $\vec{x}_j = (x_{1,j}, x_{2,j}, \dots, x_{n,j})$ ,  $j = 1, \dots, m$  the lists obtained are randomly combined, so that there is exactly one representative from each of the  $m$  sample sets in each parameter set (which results in the Latin Hypercube). In this work, it was assumed that the variables are always uncorrelated.

## APPLICATION TO THE DIVA FACILITY

One of the geometries examined in our research was the DIVA facility used for the OECD/NEA PRISME Project [3]. This geometry has essential characteristics of a nuclear facility as mechanical ventilation and several connected rooms without windows. Furthermore, the DIVA facility of IRSN is a facility for fire experiments for which fire modelling is a typical CFD application area. For example, plume models cannot determine the spatial distribution within the geometry, and for zone models, the basic assumption of sufficient stratification is violated by the active ventilation. Particular air flows, such as flows around built-in components or a visualisation of the flow field, can also not be simulated by zone models.

As part of the project presented, the CFD fire simulations were carried out with the software packages OpenFOAM [18] (open source) and Ansys CFX [31] (commercial). Both codes provided comparable results and subsequent visualisations of temperature and velocity fields.

In this paper, some of the results determined with OpenFOAM are presented. The aim is to provide an impression of the RSM and its additional possibilities. In many cases, a direct coupling of CFD simulations and probabilistic methods for uncertainty analysis cannot be implemented due to the high numerical effort. The number of individual simulations required for each parameter combination would lead to very high computing times even on HPC systems or is simply not feasible. However, the algebraic substitute models determined with the RSM can enable this coupling. The polynomials of the Response Surface, which were derived from a manageable set of CFD simulations (interpolation points), can be coupled directly with the sampling process. Despite the very high number of these polynomials, parameter calculations can be carried out very quickly and can also be ideally parallelised on HPC systems. The procedure used for this is shown using the case study of the DIVA facility from the OECD/NEA PRISME Project [3].

In the first part of this section, the considered geometry and the generated numerical grid are described. Next, the simulation model as well as the implementation in OpenFOAM

[18] is described in more detail. This includes the solver, fire simulation specific sub-models and the initial and boundary conditions selected. Finally, the creation of the Response Surface is described. For this purpose, physical variables were selected which obviously influence the fire sequence and can be regarded as unsafe parameters. Distribution functions were defined to consider the fluctuations in these parameters, which are not unrealistic but should only be used here to illustrate the principle. It should be noted that radioactivity was not considered for the examples given here. It is intuitively clear that the quantities or fields describing the dispersion or submersion could be included in the same way. This will be shown in future work.

## Model Geometry

In this study, different geometry designs were considered, whereby the example chosen here refers to the geometry design in the PRISME DOOR tests with three mechanically-ventilated rooms connected by doors. The experimental setup is shown in the upper part of Figure 1.

The lower part shows a cut through the CAD model (left) and illustrates the structured mesh generated from it (right). Here, an edge length of 0.10 m was selected. The structural properties have a significant effect on the precision of the calculation and can cause numerical artefacts. Thus, the model suitability must be demonstrated separately [32], [33], [34]. For example, the interior angles of the cells must not be less than 20° or larger than 160°, the size ratio between two adjacent cells must not exceed a factor of 2, and the ratio of the edges of a cell must be less than 10 to 50 [32], [34].

One of the most important properties is a sufficient resolution of the geometry through the grid, in order to depict all relevant processes and the parameters associated with them. Conducting a grid sensitivity study has proven to be best practice [33], [34]. Here, a relatively coarse grid is continuously refined until the results, e.g. for the temperature distribution, no longer change significantly with increasing refinement. For the grid study shown in Figure 2, the edge length of the cubes was varied from 0.05 m to 0.25 m. To discuss the geometric influences, the temperature distribution at a selected location in the geometry was considered here as a representative. It can be seen that the precision of the simulation (spatial resolution) increases with each level of refinement, as expected. With increasing grid resolution, details such as vortex structures at edges become more pronounced, but also important assessments of the basic temperature distribution. However, these differences are not relevant for the comparisons to be carried out in this research project. Therefore, the Response Surface is created on the grid with an average for the cubes. Some properties of the grid such as grid size edge length of the cubes of 0.10 m. Here, the simulation results are not too detailed but can still be determined with little numerical effort. The temperature distributions given for the 0.05 m and 0.07 m grids do not show any new details or relevant differences regarding a possible discussion of the results.

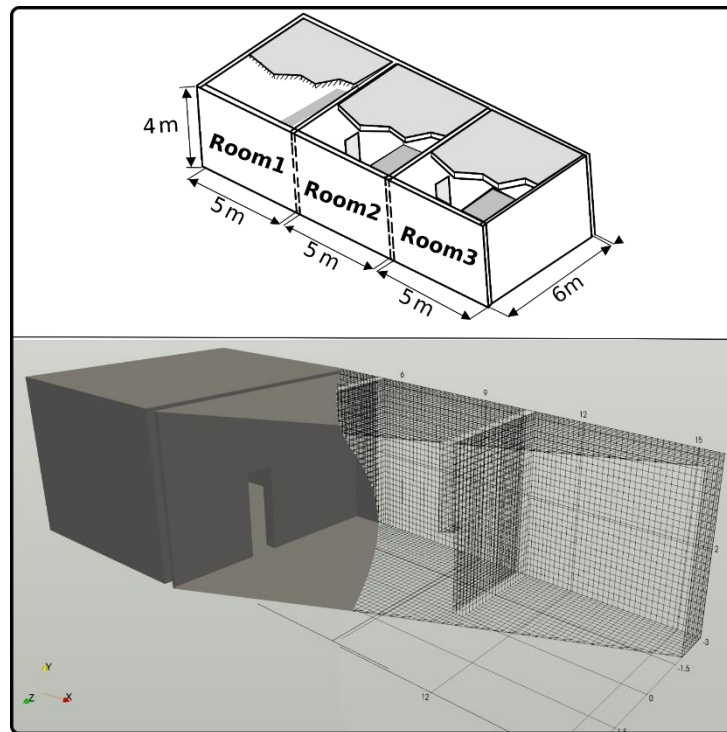


**Figure 1** Illustration of the DIVA facility (based on [3], upper figure), below: representation of the geometry (CAD model) and the structured CFD grid with 0.10 m edge length

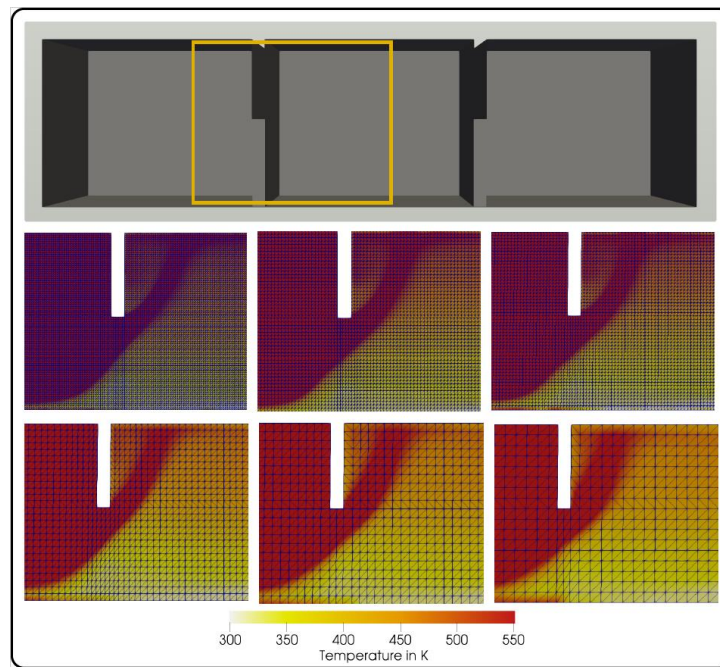


**Figure 2** Overview of the temperature distribution within the grid study (created with ParaView); the (average) edge length of the mesh is (from top left to bottom right) 0.05 m, 0.07 m, 0.10 m, 0.15 m, 0.20 m, and 0.25 m

## Description of CFD Codes

Within the project, the CFD fire simulations were carried out with the software packages OpenFOAM [18] and Ansys CFX [31]. OpenFOAM is freely available open-source software, while Ansys CFX is a commercial software package that requires the purchase of appropriate licenses to be used. Both software packages correspond to the state of the art in science and technology in terms of the applications that can be modelled. OpenFOAM was used for the examples presented in this paper because this program can be used without a license and with any number of CPUs on HPC at the same time. A fully automatic use of the method described here implies a parallel start of numerous CFD simulations, which are not possible otherwise. The software package contains the solver for FireFoam, which is especially designed for fire simulations, turbulent diffusion flames with reacting particle clouds, and pyrolysis processes [8]. It describes the heat convection and smoke propagation in fires as an incompressible flow and can be used not only for questions of thermo- and fluid dynamics but also for the analysis of multi-phase problems [35].

The combustion model takes into account various thermophysical and thermochemical properties of the reacting substances such as combustion enthalpies, substances, and substance properties. Moreover, it includes chemical reactions, transport, and turbulence properties of the flow in which the reaction takes place. Here, the eddy dissipation model was used, in which the reaction speed is limited by the turbulent mixture of fuel and air and the time required for this. This assumption is based on the fact that the time scale for the mixing of fuel and air in the turbulent diffusion flames considered in this study is many times larger than the time scale of the chemical reaction. The turbulent flow was described using the SST (Shear Stress Transport) turbulence model, which is a combination of a  $k - \omega$  model in cells close to the wall and a  $k - \epsilon$  model in cells further away from the walls. Heat is generally transferred by thermal conduction, thermal flow, and thermal radiation. Here, only the thermal flow and thermal radiation were taken into account. A description of the radiative transport through a medium can be given with the radiative transport equation (integro-differential equation), which is difficult to solve. Approximations are possible using the Discrete Ordinate Method (DOM), which was also used in OpenFOAM here. The radiative transfer equation for  $n$  directions in the medium is thus solved, but without accounting for scattering. Through the directional discretisation, the scattering integral of the radiative transport becomes a sum over the angles considered, which is the reason for the simplification [8].

## Boundary Conditions and Consideration of Uncertain Parameters

In addition to the geometry of the PRISME DOOR tests, the report [3] also published structural properties, test descriptions and measurement data. The walls (concrete) can be considered as hydraulically smooth surfaces and therefore be modelled by no-slip boundary conditions.

The power of the fire is defined by the heat release rate (HRR). For this purpose, a mass flow inlet was defined through which fuel (methane) flows in continuously. The air inlets were defined as volume sources. The air flows in through the ventilation opening at ambient temperature. The volume flows used were set according to the test series considered from [3]. The properties of an opening were assigned to the exhaust air outflow areas, through which the smoke gases can escape without counter-pressure. At the start of the simulation there is only air in the domain. The air as well as all components are at ambient temperature. The evaluation of the test data in [3] showed that the HRR can vary significantly despite identical test conditions. Even with specific fire protection designs the HRR can often not be determined exactly, since for example different fuels, fire loads and distributions of the fire loads are possible. Various ventilation volume flows

were also examined, as these can also vary greatly in practice depending on how the rooms are used. Therefore, the variables ambient temperature  $T$ , HRR  $\dot{q}$  and the air exchange rate  $\dot{V}$  were included here as examples of uncertain parameters.

## RESULTS AND DISCUSSION

For the generation of the Response Surface, 45 parameter combinations were taken into account and 416 916 polynomials were adjusted. The combinations result from the following interpolation points of the three parameters considered:

$$\begin{aligned} T &= \{273, 288, 303\} \text{ K} \\ \dot{q} &= \{0.5, 1.0, 1.5, 2.0, 3.0\} \text{ MW} \\ \dot{V} &= \{335, 670, 1005\} \text{ m}^3 \text{h}^{-1} \end{aligned} \quad (8)$$

For a comparison, 2<sup>nd</sup> order polynomials, with and without local weighting, were adjusted. The simulation time was specified to 600 s to ensure stationary behaviour. The comparison between the original model and the Response Surface is made with visualisations on a section through the x-y plane  $T = 288 \text{ K}$ ,  $\dot{q} = 2 \text{ MW}$  and  $\dot{V} = 670 \text{ m}^3 \text{h}^{-1}$  were chosen as the parameter combination. The resulting spatial temperature distribution is shown in Figure 3.

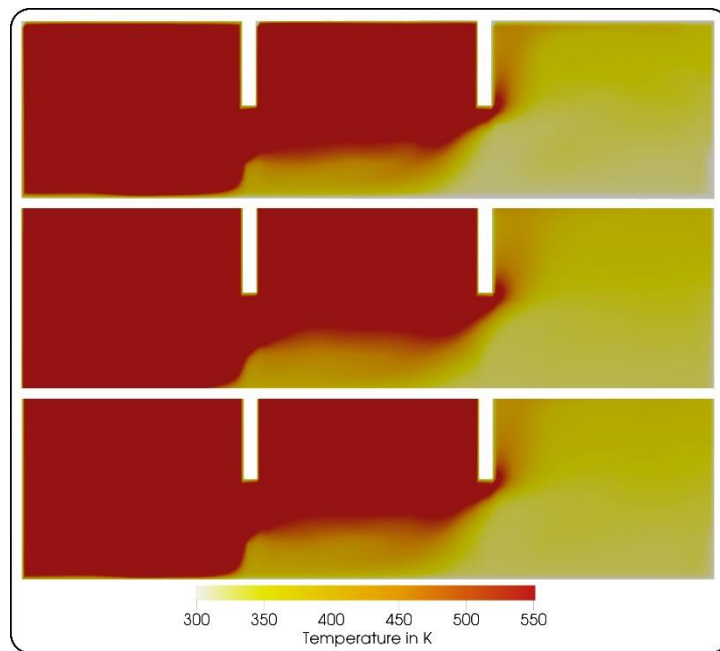


**Figure 3** Comparison of the CFD result (top) with the Response Surface (middle: 2<sup>nd</sup> order polynomial and bottom: 2<sup>nd</sup> order polynomial with local weighting) using a longitudinal cut of the spatial temperature distribution; the range between 300 K and 550 K was chosen for the colour classification

It can be seen that there are only small differences between the original model and the Response Surface. Even between the polynomials with and without local weighting, only small deviations can be seen. The flow field after a fire time of 600 s is also shown in Figure 4 by a longitudinal cut through the fire rooms. In order to create the Response Surface, each directional component of the velocity field was adjusted separately, and the components were reassembled into a vector field for the representation. For this

purpose, a C++-code was created for an automatic generation of an output file that can be visualised directly with ParaView. In addition to the velocity distribution, the vectors are explicitly visualised in Figure 4.

Here, a high degree of agreement can also be found. However, the polynomials with local weighting map the velocity vectors somewhat better. In general, the illustrated fields using the original and substitute models agree very well and there are no deviations relevant to the assessment of fire events. Even when comparing the temperature values in a cell (or in Ansys CFX at a calculation node), there is a similar agreement.

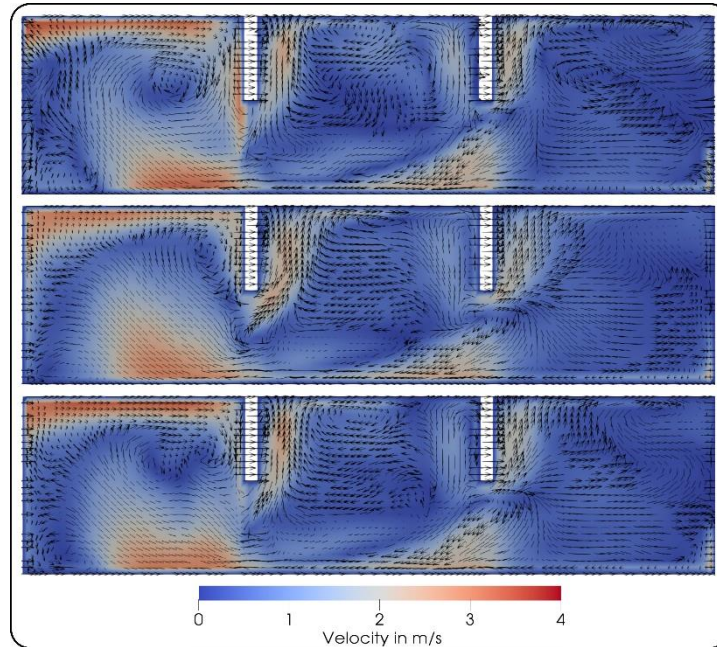


**Figure 4** Comparison of the original model (top) with the Response Surface (middle: 2<sup>nd</sup> order polynomial and bottom: 2<sup>nd</sup> order polynomial with local weighting) using a longitudinal cut of the flow field; the range between 0 ms<sup>-1</sup> and 4 ms<sup>-1</sup> was selected for the colour classification

Figure 5 shows the temperature as a variable dependent on the HRR (the other variables were kept constant). One observation is that the 2<sup>nd</sup> order polynomials with local weighting interpolate noticeably better for the detailed consideration of a calculation node.

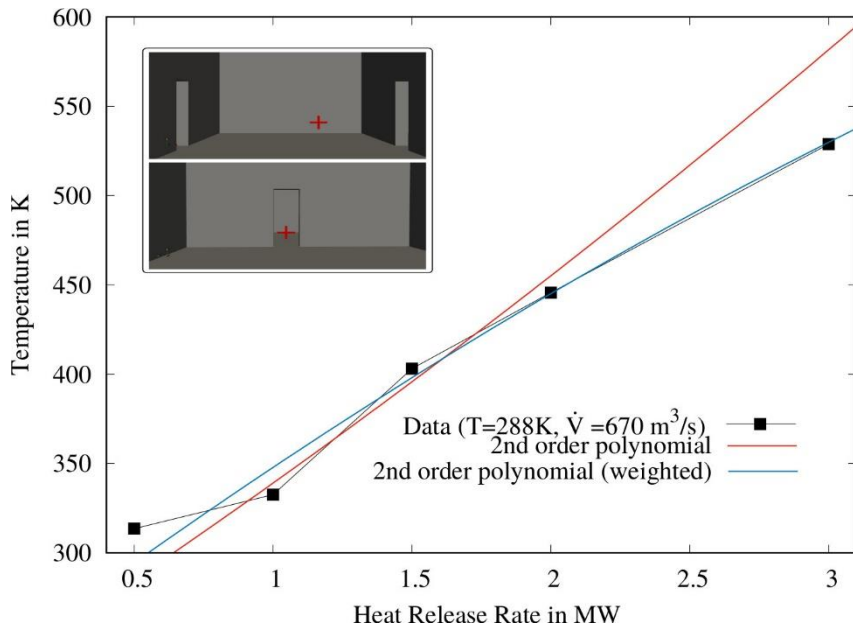


**Figure 5** Illustration of the temperature depending on the HRR for a selected cell (inset figure: red cross) using polynomials of the 2<sup>nd</sup> order (with and without local weighting)

It can be stated that the quality of the fit is similar for all cells, such that the Response Surface can be regarded as a good (2<sup>nd</sup> order polynomials) or very good (2<sup>nd</sup> order polynomials with local weighting) surrogate model. Next, to include parameter uncertainties, the Response Surface is used together with sampling methods. For this purpose, the MCS and LHS were coupled with the locally weighted 2<sup>nd</sup> order polynomials. The input parameters were varied according to the specified density functions (see further below) until the expectation values and variances of the target variable are sufficiently stable (two significant digits). For the demonstration of the methodology  $\dot{q} \sim N(2; 0.25)$ ,  $\dot{V} \sim U[303; 1005]$  and  $T_R \sim U[273; 303]$  were assumed.

Figure 6 shows the temperature distribution for the expectation value and additionally  $\pm$  one standard deviation. About 10,000 (MCS) or 1,000 (LHS) samples were required to meet the termination condition. In comparison, the differences due to the inclusion of the uncertainties assumed here are much higher than the deviation between the original and surrogate model. This shows that the methodology can be suitable for including the influence of tolerances and fluctuations in the input variables. Furthermore, it could be demonstrated that such probabilistic investigations have high potential to design fire protection provisions based on probability in the future and to transfer the design process itself to a performance-based design.

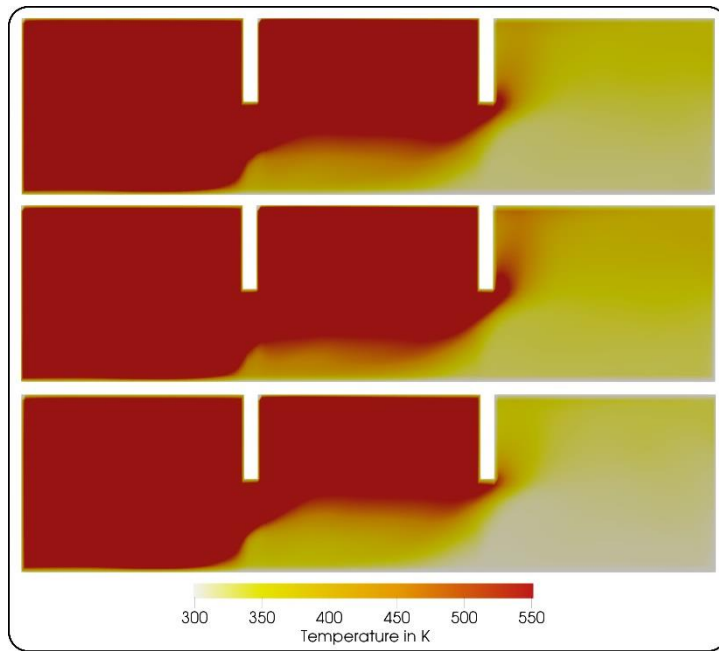


**Figure 6** Illustration of the temperature distribution for the expectation value (top) and for the influence of the fluctuations (middle, bottom,  $\pm$  one standard deviation) using a longitudinal cut through the fire rooms

## SUMMARY

In this work, the research project MBKG, funded by the former German Federal Ministry for Economics and Energy (BMWi) has been presented, in which fire simulations in complex building structures and the consideration of uncertain input parameters of the simulations were examined. This paper has provided an overview of empirical approaches, zone models and CFD-simulations, as well as the advantages of CFD over the other approaches were given. In order to benefit from the potentially higher accuracy, uncertainties and parameter fluctuations of the input parameters need to be considered. Simple error propagation calculations, as are possible for empirical models, but cannot simply be transferred to CFD simulations. Within the Response Surface Method presented here, a simpler algebraic surrogate model has been determined. This opens up a possibility for extensive parameter studies and the coupling of CFD fire simulations with probabilistic fire risk assessment methods.

The geometry and boundary conditions of the example shown as well as the quality of the mesh, the generation of the CFD model applied, and possible uncertainties of the input parameters were discussed. The complete procedure was shown using an example. First, Response Surfaces were generated from 45 parameter combinations. Spatial fields determined via the Response Surfaces as the temperatures and flow velocities were compared to the results of CFD simulations with the same boundary conditions. The calculated distributions of the Response Surfaces agreed very well with the CFD results. Subsequently, by coupling the Response Surface with sampling methods, an uncertainty analysis for the fire simulations was carried out depending on the fluctuating parameters. Here, the influence of uncertain input parameters on the calculation result could be shown by the standard deviation from the expected value. The necessary procedure was automated in the C++ code, which is also suitable for parallel use on HPC systems, so that extensive parameter studies or uncertainty and tolerance analyses are also possible.

## ACKNOWLEDGEMENTS

This work has been funded by the former German Federal Ministry for Economy and Energy (BMWi).

## REFERENCES

- [1] Franke, J., et al.: Best Practice Guideline for the CFD Simulation of Flows in the Urban Environment, COST Action 732 Quality Assurance and Improvement of Microscale Meteorological Models, Meteorological Institute University of Hamburg, Hamburg, Germany, 2007.
- [2] Zinke, R., and F. Köhler: Modellierung von Brandszenarien in komplexen Gebäudestrukturen, Reaktorsicherheitsforschung – Vorhaben-Nr.: 1501530, Otto-von-Guericke Universität, Magdeburg, Germany, 2021 (in German).
- [3] Organisation for Economic Co-operation and Development (OECD) Nuclear Energy Agency (NEA) Committee on the Safety of Nuclear Installations (CSNI): OECD/NEA PRISME OECD/NEA PRISME Project Application Report, NEA/CSNI/R (2012)14, Paris, France, July 2012, [https://www.oecd.org/officialdocuments/publicdisplaydocumentpdf/?cote=NEA/CSNI/R\(2012\)14&docLanguage=En](https://www.oecd.org/officialdocuments/publicdisplaydocumentpdf/?cote=NEA/CSNI/R(2012)14&docLanguage=En).
- [4] Nuclear Safety Standards Commission (KTA, German for Kerntechnischer Ausschuss): KTA 2101.1-3 (2015-11) Fire Protection in Nuclear Power Plants, Part 1 to 3, November 2015, [http://www.kta-gs.de/e/standards/2100/2101\\_1\\_engl\\_2015\\_11.pdf](http://www.kta-gs.de/e/standards/2100/2101_1_engl_2015_11.pdf). [http://www.kta-gs.de/e/standards/2100/2101\\_2\\_engl\\_2015\\_11.pdf](http://www.kta-gs.de/e/standards/2100/2101_2_engl_2015_11.pdf). [http://www.kta-gs.de/e/standards/2100/2101\\_3\\_engl\\_2015\\_11.pdf](http://www.kta-gs.de/e/standards/2100/2101_3_engl_2015_11.pdf).
- [5] United States Nuclear Regulatory Commission (U.S. NRC) Office of Nuclear Regulatory Research: Nuclear Power Plant Fire Modeling Analysis Guidelines (NPP FIRE MAG), Final Report, NUREG-1934 and EPRI 1023259, Washington, DC, USA, November 2012, <https://www.nrc.gov/docs/ML1231/ML12314A165.pdf>.
- [6] Häupl, P., et al.: Lehrbuch der Bauphysik, 7. Auflage, Springer Fachmedien Wiesbaden, Germany, 2013 (in German), <https://doi.org/10.1007/978-3-8348-2101-0>.
- [7] Schneider, U.: Ingenieurmethoden im Brandschutz, 2. Auflage, ISBN 978-3-846-20346-0, Reguvis Fachmedien GmbH, Köln, Germany, 2009 (in German).
- [8] OpenFOAM Ltd.: API Guide v 2112, The open source CFD toolbox, <https://www.openfoam.com/documentation/guides/latest/api/>.
- [9] Laurien, E., and H. Oertel Jr.: Numerische Strömungsmechanik. Springer-Verlag Berlin Heidelberg, Germany, 2013 (in German), <https://doi.org/10.1007/978-3-658-03145-9>.
- [10] Freitas, C. J.: The issue of numerical uncertainty, in: Applied Mathematical Modelling 26, No. 2, pp. 237-248, 2002, [https://doi.org/10.1016/S0307-904X\(01\)00058-0](https://doi.org/10.1016/S0307-904X(01)00058-0).
- [11] Faragher, J.: Probabilistic Methods for the Quantification of Uncertainty and Error in Fluid Dynamics Simulation, DSDO-TR-1633, Australian Government, Department of Defence, Defence Science and Technology Organization, Sydney, Australia, 2004.

- [12] Chutia, R., S. Mahanta, and D. Datta: Uncertainty modelling of atmospheric dispersion by stochastic response surface method under aleatory and epistemic uncertainties, *Sadhana* 39, pp. 467-485, 2014, <https://doi.org/10.1007/s12046-013-0212-7>.
- [13] Isukapalli, S. S., A. Roy, and P. G. Georgopoulos: Stochastic Response Surface Methods (SRSMs) for Uncertainty Propagation: Application to Environmental and Biological Systems, *Risk Analysis* 18, No. 3, pp. 351-363, 1998, <https://doi.org/10.1111/j.1539-6924.1998.tb01301.x>.
- [14] Van Weyenberge, B., et al.: Response surface modelling in quantitative risk analysis for life safety in case of fire, *Fire Safety Journal* 91, pp. 1007-1015, 2017, <https://doi.org/10.1016/j.firesaf.2017.03.020>.
- [15] Choi, S.-K., et al.: Polynomial Chaos Expansion with Latin Hypercube Sampling for Estimating Response Variability, *AIAA Journal* 42, No. 6, pp. 1191-1198, 2004, <https://doi.org/10.2514/1.2220>
- [16] Zinke, R., et al.: Uncertainty consideration in CFD-models via response surface modelling: application on realistic dense and light gas dispersion simulations, *Journal of Loss Prevention in the Process Industries* 75, 2022, <https://doi.org/10.1016/j.jlp.2021.104710>.
- [17] Ahrens, James, Geveci, Berk, Law, Charles, ParaView: An End-User Tool for Large Data Visualization, *Visualization Handbook*, ISBN 13: 978-0123875822, Elsevier, 2005, <https://www.paraview.org/publications/>.
- [18] OpenFOAM Ltd.: OpenFOAM. <https://www.openfoam.com>, last access September 24, 2022.
- [19] Box, G. E. P., and K. B. Wilson: On the Experimental Attainment of Optimum Conditions, *Journal of the Royal Statistical Society: Series B (Methodological)* 13, No. 1, 1–38, 1995, <https://doi.org/10.1111/j.2517-6161.1951.tb00067.x>.
- [20] Myers, R. H., D. C. Montgomery, and C. M. Anderson-Cook: Response Surface Methodology: Process and Product Optimization Using Designed Experiments, ISBN: 978-1-118-91601-8, Wiley, 2016, <https://www.wiley.com/en-us/Response+Surface+Methodology:+Process+and+Product+Optimization+Using+Designed+Experiments,+4th+Edition-p-9781118916018#download-product-flyer>.
- [21] Khuri, A. I., and S. Mukhopadhyay: Response surface methodology, In: *Wiley Interdisciplinary Reviews: Computational Statistics* 2, No. 2, pp. 128-149, 2010, <http://dx.doi.org/10.1002/wics.73>.
- [22] Askey, R., and J. Wilson: Some basic hypergeometric orthogonal polynomials that generalize Jacobi polynomials, *Memoirs of the American Mathematical Society* 54, 1985, <https://dx.doi.org/10.1090/memo/0319>.
- [23] Xiu, D., A. Roy, and G. E. Karniadakis: The Winer-Askey Polynomial Chaos for Stochastic Differential Equations, *SIAM Journal on Scientific Computing* 24, No. 2, pp. 619-644, 2002, <https://doi.org/10.1137/S1064827501387826>.
- [24] Mugler, A.: Verallgemeinertes Polynomielles Chaos zur Lösung stationärer Diffusionsprobleme mit zufälligen Koeffizienten, Brandenburgische Technische Universität Cottbus, Cottbus, Germany, 2013 (in German).
- [25] Ernst, O. G., et al.: On the convergence of generalized polynomial chaos expansion, *ESAIM: M2AN* 46, No. 2, pp. 317-339, 2012, <https://doi.org/10.1051/m2an/2011045>.

- [26] Sobol, I. M.: Die Monte-Carlo-Methode, 4. Auflage, Deutscher Verlag der Wissenschaften, Berlin, Germany, 1991 (in German).
- [27] McKay, M. D., R. J. Beckman, and W. J. Conover.: Comparison of Three Methods for Selecting Values of Input Variables in the Analysis of Output from a Computer Code, *Technometrics* 21, No. 2, pp. 239-245, 1979, <https://doi.org/10.1080/00401706.1979.10489755>.
- [28] Iman, R. L., J. C. Helton, and J. E. Campbell: An Approach to Sensitivity Analysis of Computer Models: Part I—Introduction, Input Variable Selection and Preliminary Variable Assessment, *Journal of Quality Technology* 13, No. 3, p. 9, 1981, <https://doi.org/10.1080/00224065.1981.11978748>.
- [29] Saltelli, A., K. Chan, and E. M. Scott: Sensitivity Analysis (Wiley Series in Probability and Statistics), ISBN 978-0-470-74382-9, Wiley, 2009, <https://www.wiley.com/en-us/Sensitivity+Analysis-p-9780470743829>.
- [30] Helton, J. C., and F. C. Davis: Illustration of Sampling-Based Methods for Uncertainty and Sensitivity Analysis, Wiley, 2002, <https://doi.org/10.1111/0272-4332.00041>
- [31] ANSYS Inc.: Academic Research, Release 17.2, <https://www.ansys.com>, last access September 24, 2022.
- [32] Verein Deutscher Ingenieure (VDI): Ingenieurverfahren zur Bemessung der Rauchableitung aus Gebäuden VDI 6019, Blatt 1 und 2, 2006 (in German), <https://www.vdi.de>.
- [33] Hurley, M. (Ed.): Society of Fire Protection Engineers (SFPE) Handbook of Fire Protection Engineering, 5<sup>rd</sup> Ed., ISBN 978-1-4939-2564-3, National Fire Protection Association (NFPA), Quincy, MA, USA; 2016:
- [34] Organisation for Economic Co-operation and Development (OECD) Nuclear Energy Agency (NEA) Committee on the Safety of Nuclear Installations (CSNI): Best Practice Guidelines for the Use of CFD in Nuclear Reactor Safety Application Revision, NEA/CSNI/R(2014)11, Paris France February 2015, [https://www.oecd-nea.org/jcms/pl\\_19548/best-practice-guidelines-for-the-use-of-cfd-in-nuclear-reactor-safety-applications-revision?details=true](https://www.oecd-nea.org/jcms/pl_19548/best-practice-guidelines-for-the-use-of-cfd-in-nuclear-reactor-safety-applications-revision?details=true).
- [35] Husted, B. P., et al.: Verification, validation and evaluation of FireFOAM as a tool for performance design, (TVBB; No. 3176), (Brandforsk rapport; Vol. 2017, No. 2), Lund University, Department of Fire Safety Engineering, Lund, Sweden, 2017, <https://portal.research.lu.se/en/publications/verification-validation-and-evaluation-of-firefoam-as-a-tool-for->.

# **Implementation and Further Development of An Assessment Tool for Fire Analysis in Confined and Mechanically Ventilated Compartments Using A Well-Stirred Reactor Approach**

Frederick Bonte<sup>1\*</sup>, Laurens Van Eykeren<sup>2</sup>

<sup>1</sup> Flex-A bv, Aalter, Belgium

<sup>2</sup> Independent Contractor with Flex-A bv

## **ABSTRACT**

In order to bring proper design directions or deliver overall preliminary safety evaluations in the frame of fire hazard analysis during licensing purposes of nuclear facilities, Flex-A has developed a fire model named FORCED (*FireModel well-stirred meChanically vEntilateD*). It is a well-stirred reactor approach single-zone model based on the work of Tarek Beji and Bart Merci [1].

The FORCED model can be used as a screening and predesign tool to determine the design scenarios in terms of heat release rate (HRR) for fire scenarios in confined and mechanically ventilated compartments. As output, the model provides the temperature, oxygen concentration, and pressure within the rooms or hot cells. Additionally, the leak rate of potentially contaminated smoky air escaping through leaks or evacuated through branch elements from the enclosure can be monitored.

The basic well-stirred model is extended for convenience with the ability to add leakages, control multiple branches with dampers, a module to monitor last filtration level heat attack within the ventilation systems for nuclear installations by additional cold air mixing, and other dedicated features.

This paper provides an understanding of the overall modelling and the burning model. It additionally provides insights in a first validation campaign which is undertaken on the model based on the Organisation for Economic Co-operation and Development (OECD) Nuclear Energy Agency (NEA), Committee on the Safety of Nuclear Installations (CSNI) PRISME (French acronym for Fire Propagation in Elementary Multi-room Scenarios) SOURCE testing [2] and even so the functional verification of the Python based code [3] that is based on unit testing as well as integration testing.

Based on the verification and validation (V&V) campaign, it can be concluded that the FORCED model is suited for a closed room or cell with forced ventilation flows where fast filling of the room by smoke is to be expected due to smoke layer depth or turbulences by the ventilation. Modelling of the ventilation boundary conditions could be improved to provide better pressure estimates, although the current modelling is acceptable as a fire safety engineering tool for its intended purpose.

## TERMINOLOGY AND ABBREVIATIONS

|                |  |                |                                  |                             |   |
|----------------|--|----------------|----------------------------------|-----------------------------|---|
| A              | section or area [m <sup>2</sup> ]                                  | L <sub>v</sub> | heat of vaporization of the fuel | T                           | temperature [K]                                   |
| a              | ambient  | M              | model (prediction)               | V                           | volume [m <sup>3</sup> ]                          |
| C <sub>p</sub> | specific heat [J/kg/K]   | m              | mass [kg]                        | ̇V                          | volume flow [m <sup>3</sup> /s]                   |
| D              | diameter [m]   | ̇m             | mass flow rate [kg/s]            | w                           | Wall  |
| E              | experiment (measurement)   | MLR            | mass loss rate                   | Y                           | mass fraction [kg/kg]                             |
| ex             | exhaust (flow-out)   | N              | number of data points            | γ                           | isentropic coefficient of gas                     |
| F              | configuration factor   | NED            | normalized Euclidean distance    | ΔH <sub>c</sub>             | heat of combustion [J/kg]                         |
| f <sub>i</sub> | filter i   | P              | pressure [Pa]                    | ΔH <sub>O<sub>2</sub></sub> | heat of combustion per unit of oxygen mass [J/kg] |
| h              | Heat transfer coefficient [W/m <sup>2</sup> /°C]                   | p              | [subscript] prediction           | ε                           | local error                                       |
| i              | counting number i  | Q <sub>m</sub> | mass flow rate [kg/s]            | μ                           | mean  |
| in             | inlet (flow-in)  | ̇Q             | heat flow rate (kW)              | ρ                           | density [kg/m <sup>3</sup> ]                      |
| k              | conductivity [W/m/°C]  | R              | resistance value                 | σ                           | Stefan-Boltzmann constant                         |
| K              | extinction coefficient x mean beam length (Babrauskas' correction) | t              | time [s]                         | X                           | combustion efficiency                             |
| L              | length   | t              | (subscript) time points          | "                           | per unit of surface [1/m <sup>2</sup> ]           |

## INTRODUCTION

For a nuclear installation, an analysis establishing compliance with the safety criteria and limits for the radiological impact, with information of a description of the margins, should be performed and kept up to date. In order to keep the radiological impact for both workers and public below the legal limits, several safety provisions are taken. For nuclear installations, confinement is an important provision and is often considered a safety function. The containment methods, i.e., the means to achieve the safety function confinement, could however be endangered by an installation internal fire event. Of particular importance is that a fire can endanger the arrangements, both static barriers and dynamic systems consisting of a specific ventilation system and appropriate air-cleaning devices, that are in place to separate environments inside and outside a cell or room.

Nuclear industry has invested to a large extent in understanding the phenomena of fire in well-confined and mechanically ventilated cells in the last decades. Therefore, a tremendous advancement in knowledge has been gained [2]. A fire in a confined environment is quite different due to the absence of 'regular' openings. It is the leakage and pressure effects, the latter due to both fire and mechanical ventilation, that determines the inflow into and outflow out of an enclosure, and thus finally determines the amount of oxygen available in the cell for burning. One of the most important elements in any fire

assessment is the amount of heat that can be generated over time. This energy that drives the dynamics, and can potentially endanger the containment provisions in place, is generated by burning an amount of fuel mass that is consumed per unit of time during a combustion process.

It is known that this burning rate is substantially affected by the dynamic interaction between the fuel mass loss rate (MLR) and the rate of air supplied by mechanical ventilation. The fuel MLR is controlled by (i) the amount of oxygen available in the room (i.e., vitiation oxygen effect) and (ii) the thermal enhancement via radiative feedback from the hot gas to the fuel surface. The steady-state burning rate is determined by the 'interplay' and balance between the limiting effect of oxygen vitiation and the enhancing effect of radiative feedback.

It is thus evident that the outcome of fire analysis could strongly depend on the setup of the mechanical ventilation. During basic design of a facility however, details of the ventilation systems or other containment mechanisms are often still unknown or not worked out in detail. In order to provide proper design directions or overall preliminary safety evaluations for licensing purposes, providing input in a timely manner can be problematic when evaluations are done with time consuming CFD (computational fluid dynamics) packages. Moreover, as often details are needed or lots of assumptions need to be made, it can be burdensome even for use of well-known software packages, sometimes not completely fit for purpose, i.e., the simulation of fire in a well-confined and mechanically ventilated cell.

## NUMERICAL MODELLING

### Well-Stirred Reactor Model

The theoretical well-stirred reactor model is based on a macroscopic description of the gas phase within the compartment considered as homogeneous [4] and the solution of three conservation equations for mass, oxygen, and energy. It is used to study the overall behaviour of room fires and was previously applied to the mechanically ventilated case to provide insights in the quasi steady-state MLR [1], [5].

The conservation of mass is expressed as

$$V \frac{d\rho}{dt} = \dot{m}_{fuel} A_{fuel} + \rho_{in} \dot{V}_{in} - \rho_{ex} \dot{V}_{ex}.$$

The exhaust gas density is taken as gas density within the room (i.e.,  $\rho_{in} = \rho_a$  and  $\rho_{ex} = \rho$ ). For reverse flow due to overpressure where the inlet fan acts as an exhaust the inlet density becomes equal to the gas density as for an exhaust fan (i.e.,  $\rho_{in} = \rho$ ). Likewise, for the under pressure situation, the density at the exhaust becomes the ambient density (i.e.,  $\rho_{ex} = \rho_a$ ). The gas temperature is calculated through the ideal gas equation  $T = 353 / \rho$ .

The conservation of oxygen is written as

$$V \frac{d(\rho Y_{O2})}{dt} = \dot{m}_{in} Y_{O2,in} - \dot{m}_{ex} Y_{O2,ex} - \frac{\dot{Q}_{fuel}}{\Delta H_{O2}}.$$

As for the density,  $Y_{O2}$  taken depends on the flow direction of the inlet and exhaust. For both density and oxygen mass fractions, this sudden transition modelled is believed not to alter the results significantly, especially not for the steady-state stage.

The conservation of energy is expressed as

$$\frac{V}{\gamma-1} \frac{dP}{dt} = C_p \dot{m}_{in} T_{in} - C_p \dot{m}_{ex} T_{ex} + C_p \dot{m}_{fuel} T_{vaporization} + \dot{Q}_{fuel} - \dot{Q}_{wall\_boundaries}.$$

The heat loss to the boundaries is expressed as a series of natural convection (from the gas to walls, ceiling, and floor) and conduction (through the solid boundaries):

$$\dot{Q}_{wall\_boundaries} = (h_c^{-1} + h_k^{-1})^{-1} A_w (T - T_a).$$

As the thermally thick assumption is likely to be true for a hot cell or room in a nuclear facility, the heat transfer coefficient becomes  $h_k = (\frac{k_w \rho_w c_{p,w}}{t})^{1/2}$ .

## Fuel Response Model

The fuel MLR per unit area is implemented as

$$\dot{m}''_{fuel} = \dot{m}''_{fuel,open} \left( 2.1 \frac{Y_{O2}}{Y_{O2,open}} - 1.1 \right) + \frac{F\sigma\varepsilon(T^4 - T_v^4)}{L_v},$$

while assuming a fuel surface absorptivity equal to unity. The first term on the right side expresses the oxygen effect on the fuel MLR (i.e., linear decrease) in vitiated conditions as proposed by Peatross and Beyler [6]. The second term on the right side of the equation expresses the effect of thermal radiative feedback on the vaporization of a liquid pool as proposed in [7]. The user interface allows to turn on or off one or another term by a simple true or false statement.

The steady-state MLR in free-burning conditions,  $\dot{m}''_{fuel,open}$ , can be a user defined input over time, constant, or defined by the Babrauskas estimation [8], including the correction for the diameter  $\dot{m}''_{fuel,open}(1 - \exp(-KD))$ . In order to capture the fire growing phase, the user is offered a t-squared model as per NFPA 72 [9] or NFPA 92B [10].

For the overall MLR of a pool fire, the dimensionless fuel MLR is also implemented as proposed by Prétrel and Le Saux [11], [12]. The latter model, named  $\dot{m}_{OECD}$  further, introduces more phases of a developing fire, i.e., the propagation phase (t-squared) followed by a phase of slower growth, the third corresponds to a continuous increase with a changing second derivative and finally the last phase representing the steady-state. By comparison of the relationships with experimental results, a single set of parameters could be set indicating that the fuel MLR behaviour does display a generic behaviour regardless of the surface area of the pool.

Apart from the extinction criteria by lack of oxygen linked to the use of the Peatross and Beyler equation [6], the fuel mass within the model is tracked. In consequence, the user interface permits to trigger extinction due to the lack of fuel (i.e.,  $m_{fuel} = 0$ ) and extinction on a MLR criterion (i.e.,  $\dot{m}''_{fuel} < \dot{m}''_{ref}$ ) with  $\dot{m}''_{ref}$  the critical pyrolysis rate of liquids or solid fuels as per literature.

Finally, the heat release rate is calculated as  $\dot{Q}_{fuel} = \chi \dot{m}''_{fuel} \Delta H_c$ .

A comprehensive overview of the fuel response (or burning) model is depicted in Figure 1 and is represented as the block “burning model” in the algorithmic structure (cf. Figure 2).

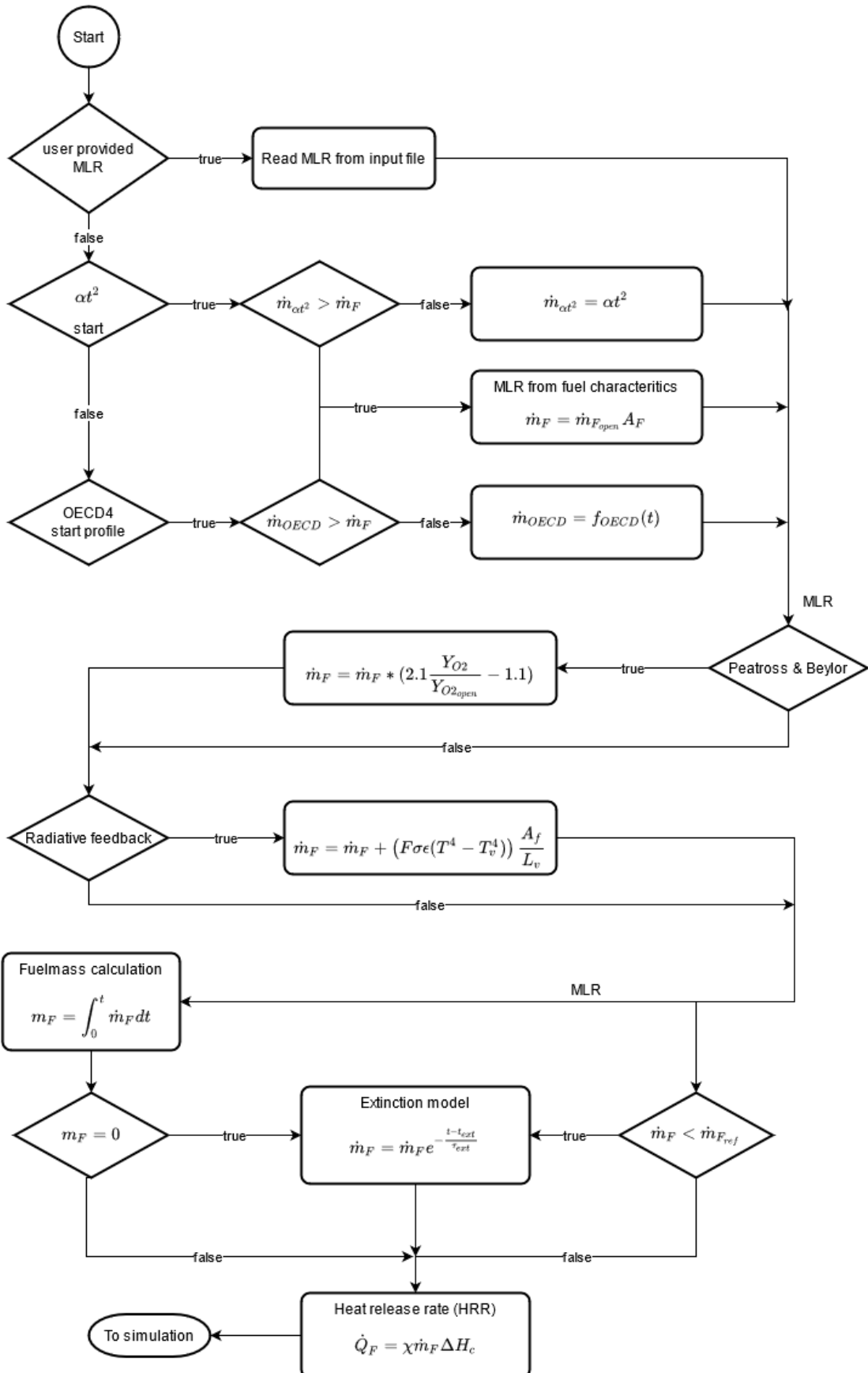


**Figure 1** Comprehensive overview of the fuel response (or burning) model

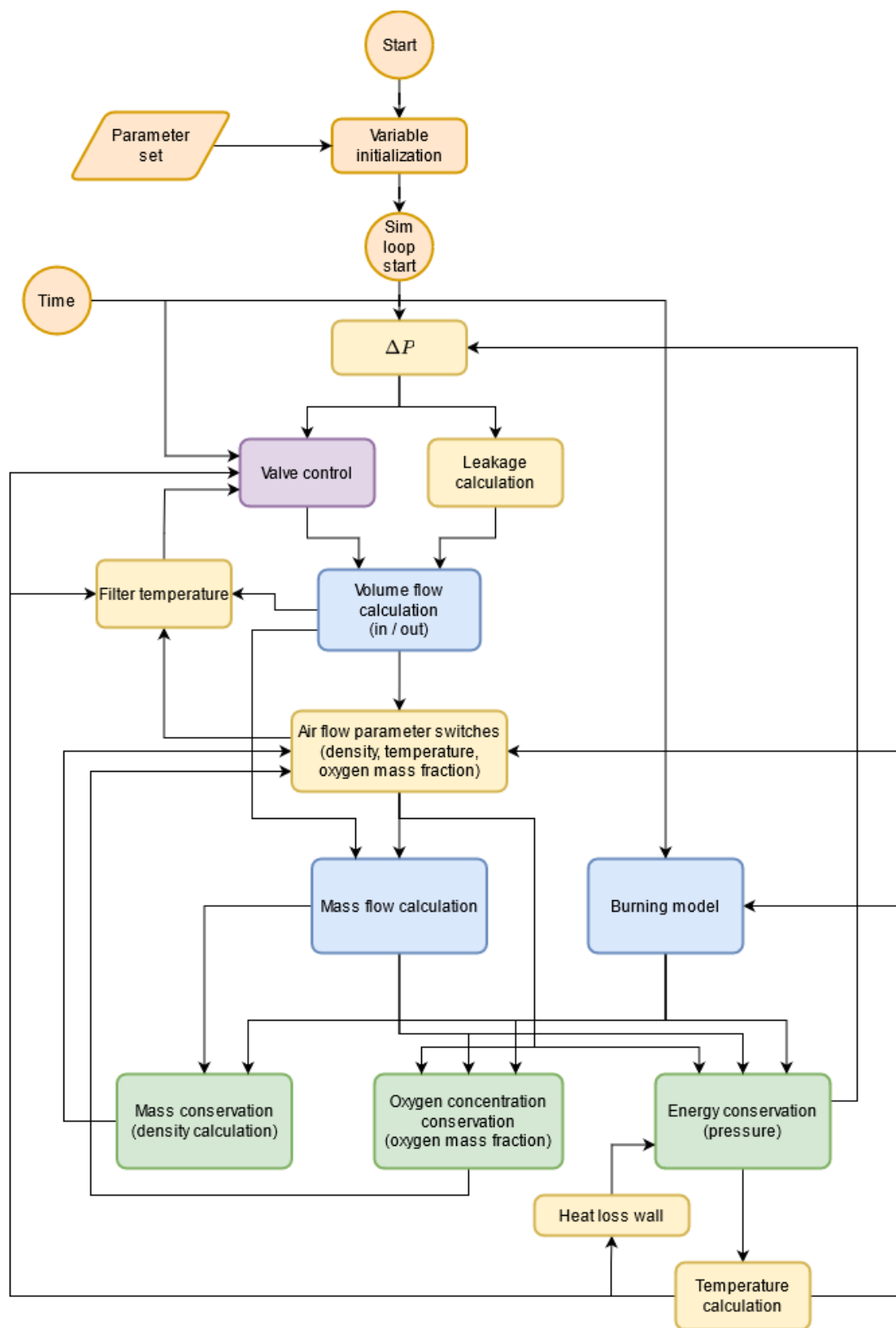


**Figure 2** FORCED model overview

## Mechanical Ventilation Sub-Models

The setup of mechanical ventilation is done by reducing the complex network to  $i$  quadratic in- and exhaust fan driven ducts whereby the volume flow of each branch  $i$  is expressed as quadratic curves [13] per equation

$$\dot{V} = \dot{V}_0 \operatorname{sign}(\Delta p_{max,i} - \Delta p) \sqrt{\frac{|\Delta p - \Delta p_{max,i}|}{\Delta p_{max,i}}}.$$

Additionally, one can add flow through single ducts and leakages, e.g., for cases with passive air transfer between the environment and the enclosure. The user can introduce  $i$  single ducts or pipes, which can be combined with the fans. The pipes are modelled with the generalised Bernoulli equation which accounts for the effect of branch length  $L$  on the mechanical inertia:

$$\frac{L}{A} \frac{dQ_m}{dt} = P_{total,1} - P_{total,2} + \rho g(z_1 - z_2) + f.$$

The function  $f$  is the characteristic function and depends on the branch type (laminar, turbulent, mixed, filter, check valve, under or overpressure valve, door, etc), but can be generalized as

$$f = -\operatorname{sgn}(Q_m)R(in, out, closed) \frac{|Q_m|^\alpha}{\rho^\beta}.$$

Parameters can be user specified for each pipe  $i$ .

Rooms are not always airtight, and some egress or ingress of air can exist during a fire event, which also can significantly influence the pressure [14]. The volume flow through small gaps, cracks and other or leak area  $A_L$  can be added in the user interface and is expressed by

$$\dot{V}_{leak} = A_L \operatorname{sign}(\Delta p) \sqrt{2 \frac{|\Delta p|}{\rho_a}} \text{ and } A_L = A_{L,ref} \left( \frac{\Delta p}{\Delta p_{ref}} \right)^{n-0.5}$$

and  $n = 1$  for long thin cracks while 0.5 for perfect rounds. The volume flow and thus the airtightness of the setup can be measured using a blower door test (cf. ASTM E 779 [15]) both ducts being closed with an airtight metal cap.

The user is also offered valve control features. Indeed, each element  $i$  can be equipped with a closure device, provided the leakage percentage or  $R$  when closed. Even so controls (switches) are foreseen: temperature threshold (room or filter), activation time and dependency on other closure devices.

An additional option is the possibility to define an entrainment air flow (with properties equal to the ambient condition) for each defined exhaust fan. This allows for the calculation of the exhaust temperature  $T_{f_i}$  that is affecting the related last filtration level  $i$  (the “filter temperature” block in Figure 2) downstream, and is implemented using the following equation

$$T_{f_i} = \frac{(T_{ex_i} m_{ex_i} + T_a m_{ent_i})}{m_{ex_i} + m_{ent_i}} = \frac{(T_{ex_i} V_{ex_i} \rho_{ex_i} + T_a V_{ent_i} \rho_{ent_i})}{V_{ex_i} \rho_{ex_i} + V_{ent_i} \rho_{ent_i}}.$$

A possible refinement for the future is the implementation of an evaluation of the clogging of the filters.

## Algorithmic Structure

Figure 2 shows the algorithmic structure of the code. The procedure solves the three conservation equations and sub-models. The connection between the sub-models and the conservation equations is indicated.

In essence, the simulation starts from a variable initialization, which is based on the configuration file that is read in (see next section). Based on the pressure difference over the inlet and exhaust ducts (with or without fans and valves), the volume flow in and out of the room is calculated. For this, also the valve control is evaluated based on the time and temperatures, dependent on the control configuration of the related valves.

Next, based on the direction of the airflows, the properties (density, temperatures, oxygen fraction, etc.) are calculated, which are used for calculating the mass airflows. Together with the output of the fuel response model, the three main equations of the model can be calculated, i.e., conservation of mass, oxygen mass fraction calculation, and the conservation of energy. Once these derivatives are calculated, an Euler integration is performed. As a last calculation, the temperature in the room is calculated, and can then be used in next timestep.

From a pure simulation technology perspective, the only parameter that can be configured is the time step. This is part of the configuration input file and is defined by the user. Dependent on the dynamics of the fire, the user can (iteratively) choose this time step to achieve a stable simulation, while performing the trade-off with the required time to execute the simulation. For now, a fixed timestep is used throughout the simulation time. In future versions, for further optimizing the simulation time and increase the numerical stability, a variable timestep could be implemented in combination with more advanced solvers, to account for more dynamic periods in the simulation, especially at flow reversal in the ventilation branches.

## Tooling for Engineering Purposes

All the simulation code as well as the configuration of the simulations is implemented in Python 3.8 [3]. The main reason for this choice is the combination of an environment that is open source and provides features for optimizing the running time of the simulation and for distributing the software.

First, once implemented, it becomes very efficient to run multiple simulations in parallel with only a few extra lines of code, allowing the evaluation of hundreds to thousands of simulations in a limited time, taking advantage of desktop computing power.

Second, with only a few lines of the code, the simulation software can be packaged into a standalone executable. The main advantage of this is to be able to guarantee traceability, as once compiled, you can refer to the exact version that was used. In addition, the compiled version can be shared with third parties that can run the simulations on themselves to verify the results.

The setup of the simulations to be performed is done through an MS EXCEL® template spreadsheet. This spreadsheet is the interface that enables the user to configure all aspects of the simulation. It starts with the definition of the experiments to simulate (multiple simulations can run in parallel), the definition of the room, the fuels, the fans and ducts, the control on the valves. Lastly, there are the options to run in parallel (or not) and to output the plots (or not).

This configuration MS EXCEL® is then to be provided as in input to the simulation code. The program will generate the results and provide these in the form of standard graphs with the major variables (temperature, pressures, oxygen fractions, heat release rate, etc.), and time sequences of these variables in .csv files.

The overall algorithmic structure of this tooling program is depicted in Figure 3.

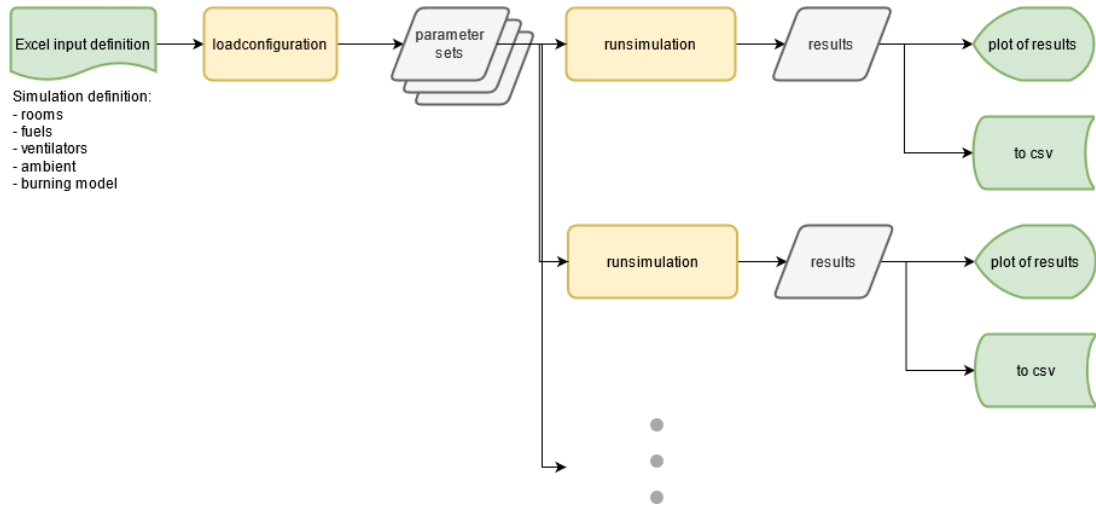


**Figure 3** Tooling program for user interface (MS EXCEL®) with multiple simulations runs

## MODEL VERIFICATION

Several measures are taken to assure the correct functioning of the code.

First, the version control of all the code is performed using git. This allows full traceability of the developed code. In combination with specific releases that are tagged, this approach allows to recreate past results in an exact way. Every tagged version is compiled into a standalone executable, and these are used for performing the simulations for customer projects. This workflow ensures the traceability.

Secondly, only a limited number of public libraries are used, to limit the exposure to external bugs and to keep the implementation as lean as possible. The public python libraries used are numpy, pandas, openpyxl (for reading the configuration MS EXCEL® file) and matplotlib (for the visualization of the results). These libraries are very widely used and well documented.

A third layer to ensure the correct functionality is to split the simulation into separate functions. Although not all functionality is already implemented as functions, the ones that are can be tested individually using a unit testing framework. This testing including the assertion of the essential outcomes of the functions can be run automatically, resulting in a report. The functions that are tested this way in the current version of the software are: the calculation of the airflow speed, the valve dependencies on each other, the MLR burning start model, and some other supporting functions. The results of these tests are represented in a report, together with some visualizations. An example of such a test report is shown in Figure 4, while an example of a typical parameter sweeps to the test function is shown in Figure 5.

| : 11 total, 11 passed             |   |
|-----------------------------------|---|
|                                   | 553 ms  |
|                                   | <a href="#">Collapse</a>   <a href="#">Expand</a> |
| <b>unittestsBurnExp</b>           | 553 ms  |
| <b>BurnExpUnitTestFunctions</b>   |   |
| <b>test_calctemperature</b>       | passed 0 ms                                       |
| <b>test_calcvdot_maxdeltap</b>    | passed 0 ms                                       |
| <b>test_calcvdot_negativeflow</b> | passed 0 ms                                       |
| <b>test_calcvdot_positiveflow</b> | passed 0 ms                                       |
| <b>test_calcvdot_zeropressure</b> | passed 0 ms                                       |
| <b>test_oecd4model</b>            | passed 3 ms                                       |
| <b>test_smoothfunction</b>        | passed 1 ms                                       |
| <b>test_ventdependencies</b>      | passed 0 ms                                       |
| <b>test_calcvdot_graph</b>        | passed 372 ms                                     |
| <b>test_oecd4mlrmodel_graph</b>   | passed 110 ms                                     |
| <b>test_smoothfunction_graph</b>  | passed 67 ms                                      |

**Figure 4** Example of a test report for the unit testing, in which the separate functions are tested before being used in the simulation

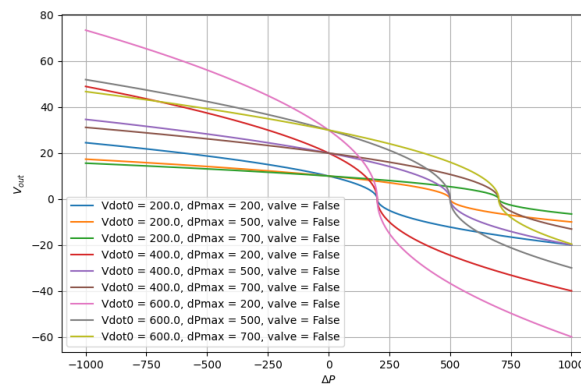


**Figure 5** Example of a parameter sweep over the calculation of the air flow over the fan

A last verification layer is the testing of different scenarios using the full code and performing the qualitative assessment of the physical behaviour. For this purpose, a specific input configuration is created defining these scenarios. The simulations are run subsequently, and the results are assessed through the visualization. This approach is taken, as for some of the functionalities the interactions between the different physical phenomena are essential. This is what typically is referred to as integration testing.

Typical tests that are performed this way are:

- Fuel combustion without any ventilation, which should result in a pressure increase and a decrease in the oxygen mass fraction;
- Dynamically closing the outward (or inward) airflow during simulation without a burning fuel, which should result in a pressure increase (or decrease);
- Triggering of the extinction model when the MLR is below the set threshold, or when the fuel mass is completely burnt;
- The effect of Peytross and Beyler on the radiative feedback;
- The control of the valves based on time, temperature, and dependencies on each other.

An example of such a test for the negative room pressure when closing the inward flow is shown in Figure 6. An example for the valve dependencies is shown in Figure 7.

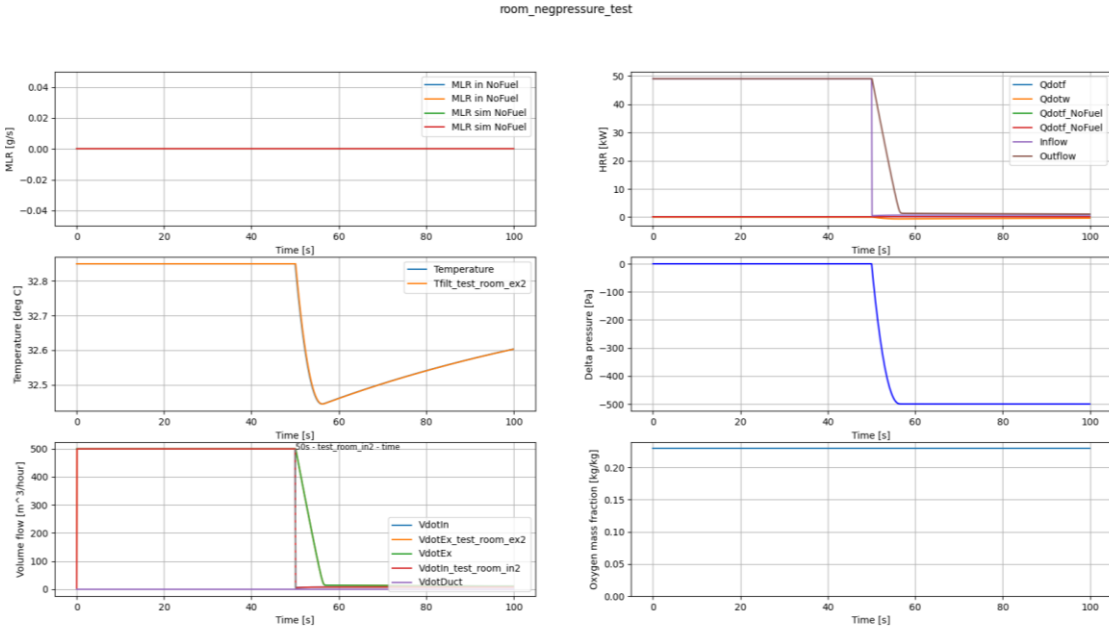


**Figure 6** Results of the test to close the valve at the inflow of air, with the result of a decrease in pressure

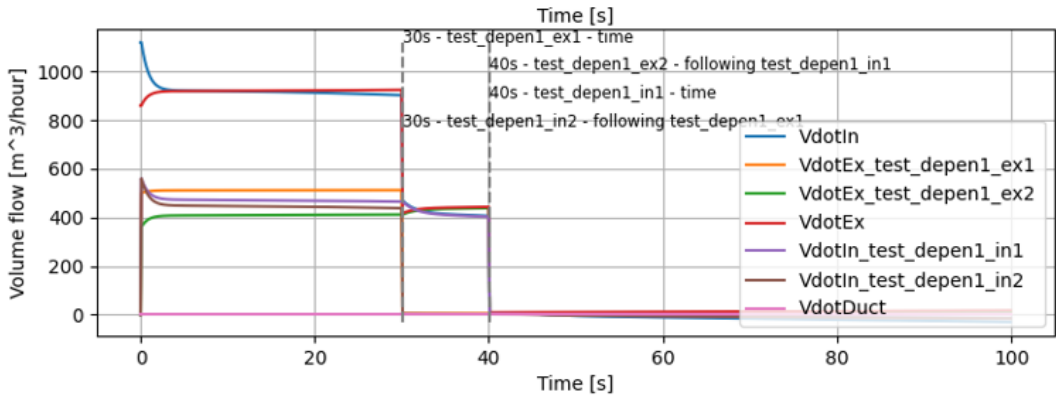


**Figure 7** Example of testing the valve dependencies

Towards the future, a further decomposition into separate functions will be performed, to ease the process of verifying the code base and to increase the modularity to enable further development.

## MODEL VALIDATION

### Validation Method

As first part of the validation, it is decided to impose the fuel MLR as measured in the experiments. Because for engineering purposes often no experimental data is available for each situation, the fuel response model is of outmost importance. Based on the simulations conducted earlier by the author [16], it was decided to introduce the oxygen model proposed by Peatross and Beyler [6] and not to repeat model response testing on the fuel MLR as per free atmosphere experiments. Indeed, for most engineering purposes, such experiments are not available, and the free burning fuel MLR is also modelled

(Babrauskas' estimation, the t-squared model, the dimensionless fuel MLR estimation, etc.) and is consequently taken into account when deriving uncertainty metrics.

In order to cover the full extent of ventilation conditions given by the variation of ventilation flow rates, validation is done for both low ( $1.5 \text{ h}^{-1}$ ) and high ( $8.4 \text{ h}^{-1}$ ) air renewal rates. In all cases the initial air intake and extraction flow rates are equal.

## Evaluation Method and Criteria

To evaluate quantities predicted by numerical methods for fire safety engineering, both local metrics – comparing single points – and global metrics – comparing the entire course of two time series are used. Based on [17], it has been decided to report the normalized Euclidean distance (NED or standardized L2 norm) as global metric instead of the global error and cosine of the normalized inner product as previously reported [16] by the author of the paper at hand.

For the single-point comparison using peak value, the normalized relative difference, called Local Error, describes the relative difference of model peak and experimental peak, and is given by

$$\epsilon = \frac{(M_p - M_a) - (E_p - E_a)}{(E_p - E_a)}.$$

Note that  $\epsilon$  has neither an upper nor a lower bound and yields the value 0 as an optimal result, in terms of an exact congruence of the extreme values in experiment and simulation.

In order to obtain an overall comparison of two curves, the single-point comparison is extended to multiple points. Each of these curves is therefore represented as a multidimensional vector, with each point in time defining an additional dimension. The NED (normalized Euclidean distance) reported is defined as

$$NED = \sqrt{\frac{\sum_{t=1}^N (\Delta M_t - \Delta E_t)^2}{\sum_{t=1}^N (\Delta E_t)^2}},$$

which encompasses normalization with respect to measurements.

Both the Local Error and the NED deviation between model simulation and experimental measurement are calculated for each relevant sensor, and the ( $\epsilon$ , NED) results of the different sensors are depicted as points in a two-dimensional scatterplot. Both metrics are evaluated from  $t = 0$  until the end of steady state, i.e., before the occurrences of instabilities prior to extinction.

Comparing  $\epsilon$  and NED, first note that  $\epsilon$  has neither an upper nor a lower bound and yields the value 0 as an optimal result, in terms of an exact congruence of the extreme values in experiment and simulation. The value - 1 describes a significant limit. For values lower than - 1, the signs of the extrema of the experiment and simulation are different, and a detailed analysis of the time series is advisable. The value 0 describes the optimal result.

In order to decide whether the model is suitable for the experiment at hand, it is incorporated confidence regions for  $\epsilon$  and NED in the validation process as per [17] (95 % confidence ranges for both quantities). The 95 % confidence interval is approximated by

$[- U\epsilon, + U\epsilon]$ , where  $U\epsilon = \sqrt{\tilde{U}_E^2 + \tilde{U}_M^2}$ . Here,  $\tilde{U}_E$  denotes a measure of relative experimental (measurement) uncertainty and  $\tilde{U}_M$  denotes a measure of relative numerical (model input) uncertainty [18]. For the present study the relative uncertainties  $\tilde{U}_E = 2\tilde{u}_E$  are taken from [19] and [20] and are shown with  $\tilde{U}_M = 2\tilde{u}_M$  in Table 1.

**Table 1** Experimental and model relative uncertainties

| Quantity                         | $\tilde{U}_E$ | $\tilde{U}_M$ |
|----------------------------------|---------------|---------------|
| Temperature (HGL)                | 0.1           | 0.1           |
| Room pressure                    | 0.3           | 0.42          |
| Gas concentration O <sub>2</sub> | 0.02          | 0.08          |
| Air flow rate                    | 0.16          | 0.15          |
| HRR (and MLR)                    | 0.14          | 0.2           |

In line with the  $\epsilon$  approach, an approximation for the variance of NED is

$$\widehat{Var}(NED) = \frac{(\sum_{t=1}^N \Delta E_t)^2}{\sum_{t=2}^N \Delta E_t \Delta E_{t-1}} \frac{\tilde{u}_M^2 + \tilde{u}_E^2}{N}.$$

As the NED values are always positive, the accuracy of numerical predictions concerning the NED criteria is given with the confidence interval  $[0, + U_{NED}]$  with  $U_{NED} = 2 \widehat{Var}(NED)^{1/2}$ .

## Experimental Data

Fire experiments have been performed in the context of the OECD/NEA PRISME Project in the IRSN DIVA facility, located at the Cadarache site in France [2]. The DIVA facility is included in the JUPITER facility, which has a free volume of 2630 m<sup>3</sup>. Within, a 120 m<sup>3</sup> well-confined and mechanically ventilated room is used as the fire room. It consists of a 30 cm thick reinforced concrete structure and equipment is sized to withstand a gas pressure range from - 100 hPa to 520 hPa. The doors are made of steel and are leak tight. A pool fire is placed at the floor level. More details of the ventilation and other systems are provided in [16].

All eight OECD/NEA PRISME SOURCE tests [2] served for the validation case for which the test grid is depicted in Table 2. The geometrical configuration considered in this validation work is shown in Figure 8. The ventilation system consists basically of an inlet fan and an exhaust fan that releases smoke to the atmosphere (ambient conditions).

**Table 2** OECD/NEA PRISME SOURCE test grid

| Test Name | $A_{fuel}$ [m <sup>2</sup> ] | Air Renewal Rate                                | $m_{fuel}$ [kg] | Position Intake | $\dot{V}_0$ [m <sup>3</sup> /s] | $\Delta p_{max,in}$ [Pa] | $\Delta p_{max,ex}$ [Pa] |
|-----------|------------------------------|---|-----------------|-----------------|---------------------------------|--------------------------|--------------------------|
| PRS-SI-D1 | 0.4                          | 4.7 h <sup>-1</sup><br>(560 m <sup>3</sup> /h)  | 14.6            | High            | 0.156                           | 254                      | 695                      |
| PRS-SI-D2 | 0.4                          | 8.4 h <sup>-1</sup><br>(1020 m <sup>3</sup> /h) | 15.7            | High            | 0.283                           | 338                      | 567                      |
| PRS-SI-D3 | 0.4                          | 1.5 h <sup>-1</sup><br>(180 m <sup>3</sup> /h)  | 15.9            | High            | 0.058                           | 204                      | 778                      |
| PRS-SI-D4 | 0.4                          | 4.7 h <sup>-1</sup><br>(575 m <sup>3</sup> /h)  | 15.7            | High            | 0.160                           | 325                      | 80                       |

| Test Name  | $A_{fuel}$ [m <sup>2</sup> ] | Air Renewal Rate                                | $m_{fuel}$ [kg] | Position Intake | $\dot{V}_0$ [m <sup>3</sup> /s] | $\Delta p_{max,in}$ [Pa] | $\Delta p_{max,ex}$ [Pa] |
|------------|------------------------------|---|-----------------|-----------------|---------------------------------|--------------------------|--------------------------|
| PRS-SI-D5  | 0.2                          | $4.6 \text{ h}^{-1}$<br>(555 m <sup>3</sup> /h) | 7.17            | High            | 0.154                           | 322                      | 685                      |
| PRS-SI-D5a | 0.2                          | $1.6 \text{ h}^{-1}$<br>(190 m <sup>3</sup> /h) | 7.8             | High            | 0.053                           | 236                      | 783                      |
| PRS-SI-D6  | 0.4                          | $4.7 \text{ h}^{-1}$<br>(560 m <sup>3</sup> /h) | 15.9            | Low             | 0.156                           | 324                      | 574                      |
| PRS-SI-D6a | 0.4                          | $1.7 \text{ h}^{-1}$<br>(200 m <sup>3</sup> /h) | 15.8            | Low             | 0.056                           | 128                      | 193                      |

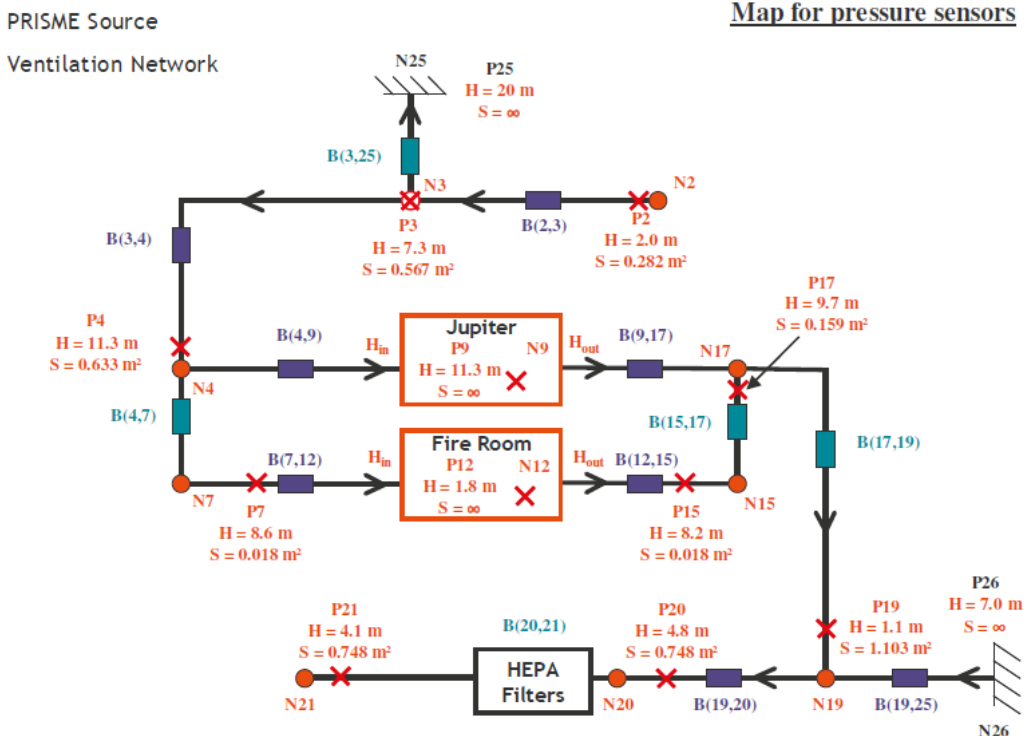
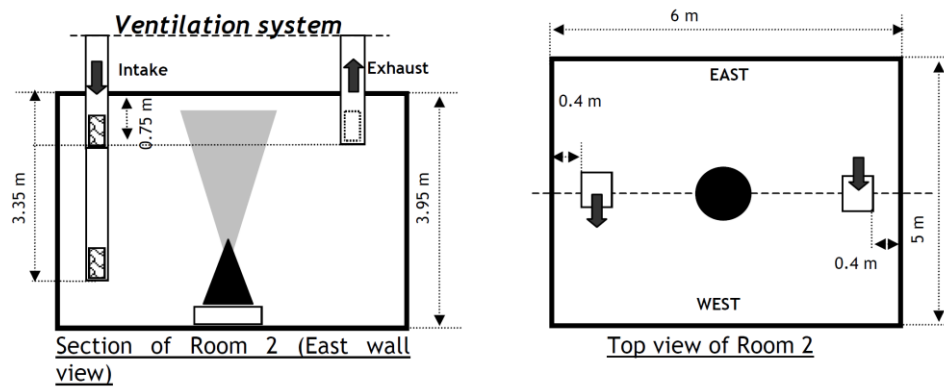


**Figure 8** Geometrical configuration considered for the FORCED validation work

### Setup of the Numerical Simulations

The parameters specified the FORCED model for validation purposes are depicted in Table 3.

In order to setup the boundary conditions for the fire room, the following simplifications are considered: no regulation is acting due to the pressure conditions generated during fire and can thus be ignored; it is assumed that the pressure upstream of the inlet collector from which the room is supplied is constant, likewise for the pressure on the collector in front of the last exhaust filters from all other rooms and extraction. Indeed, for the latter the change in flow of one single duct (the room inlet for supply or the room or cell extraction) will not significantly change the flow in the collector thus neither the pressure.

**Table 3** Specified parameters in FORCED

| Compartment Parameters |                       | Fluid Parameters |                         | T <sub>v</sub>                | 461 K                  | h <sub>c</sub>   | 25 W/m <sup>2</sup> .K<br>(start)                          |
|------------------------|-----------------------|------------------|-------------------------|-------------------------------|------------------------|------------------|--|
| Length                 | 6 m                   | ρ <sub>a</sub>   | 1.154 kg/m <sup>2</sup> | ṁ <sup>"</sup> <sub>ref</sub> | 4 g/m <sup>2</sup> .s  |                  | 12 W/m <sup>2</sup> .K<br>(steady state)                   |
| Width                  | 5 m                   | T <sub>a</sub>   | 306 K                   | K                             | 1.8                    | c <sub>p,w</sub> | 736 J/(kg.K)   |
| Height                 | 4 m                   | c <sub>p</sub>   | 1000 J/kg.K             | A                             | 11.72 W/s <sup>2</sup> | ρ <sub>w</sub>   | 2430 kg/m <sup>3</sup>                                     |
| A <sub>L,ref</sub>     | 0.0001 m <sup>2</sup> | Fuel Parameters  |                         | ΔH <sub>O2</sub>              | 13 100 kJ/kg           | γ                | 1.4  |
| n                      | 1                     | L <sub>v</sub>   | 361 kJ/kg               | Heat Transfer Parameters      |                        | σ                | 5.67 x 10 <sup>-8</sup><br>W/m <sup>2</sup> K <sup>4</sup> |
| Δp <sub>ref</sub>      | 100 Pa                | ΔH <sub>c</sub>  | 39 993 kJ/kg            | k <sub>w</sub>                | 1.5 W/(m.K)            | X                | 1  |

Values for relative static pressures (cf. Figure 8: P4, P17, P12) and air flow rates (see Figure 8: fire room H<sub>in</sub> = H<sub>out</sub>) are taken as measured before ignition (steady state). Total pressures are first calculated with the well-known simplified conservation of energy along a streamline (Bernouilli). The stall pressure Δp<sub>max,i</sub> is set at the point where the volume flow becomes 0, i.e., when the total pressure difference between the fire room and collector equals 0. The corresponding numerical values are depicted in Table 2. The above assumptions are defendable in order to set the FORCED model via the virtual quadratic fan curves. Even so, it has been concluded in [1] that the stall pressure setting reveals no significant impact on the steady-state heat release values.

For illustrative purposes, the output plot result for the PRS-SI-D1 simulations is provided (cf. Figure 9) for the three MLR input variants, i.e., the measured MLR (REAL), the model proposed by Prétrel and Le Saux (ṁ<sub>OEC</sub>) and the Babrauskas with t<sup>2</sup> start (alpha TT).

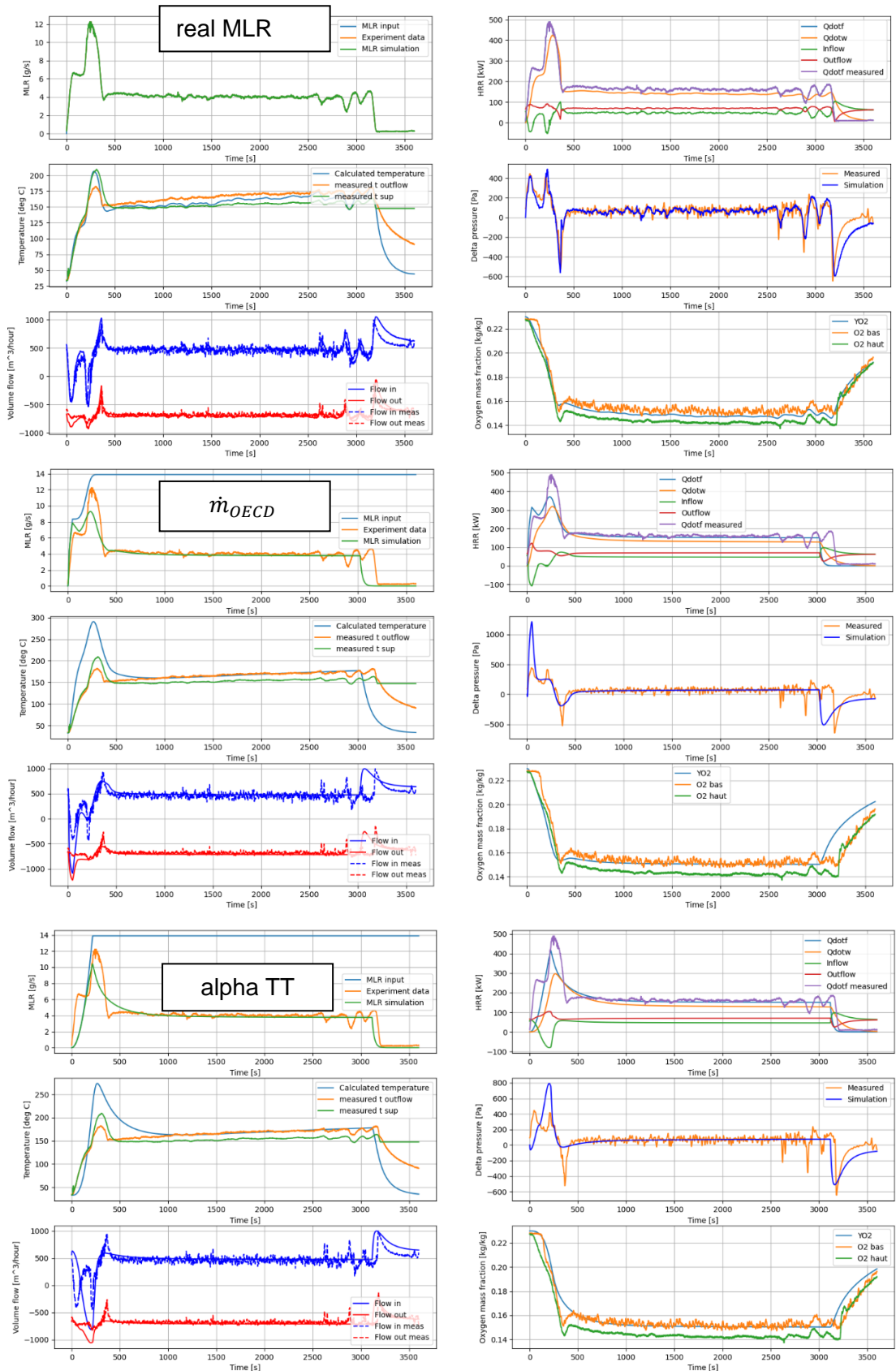


**Figure 9** FORCED PRS-SI-D1 plotted simulation results

## Evaluation of the Numerical Simulations

The simulations with the FORCED model of the experimental data are subsequently contrasted with the data measured during the test and analysed by application of the evaluation method and criteria as described earlier.  $U_{NED}$  and  $U_e$  which represents the 95 % confidence ranges for both quantities are shown with red and green bands respectively.

Figure 10 below summarizes the results concerning the validation study of the FORCED model for the quantities MLR, HRR,  $O_2$ , pressure, temperature flow-in and flow-out for all OECD/NEA PRISME SOURCE fire tests.

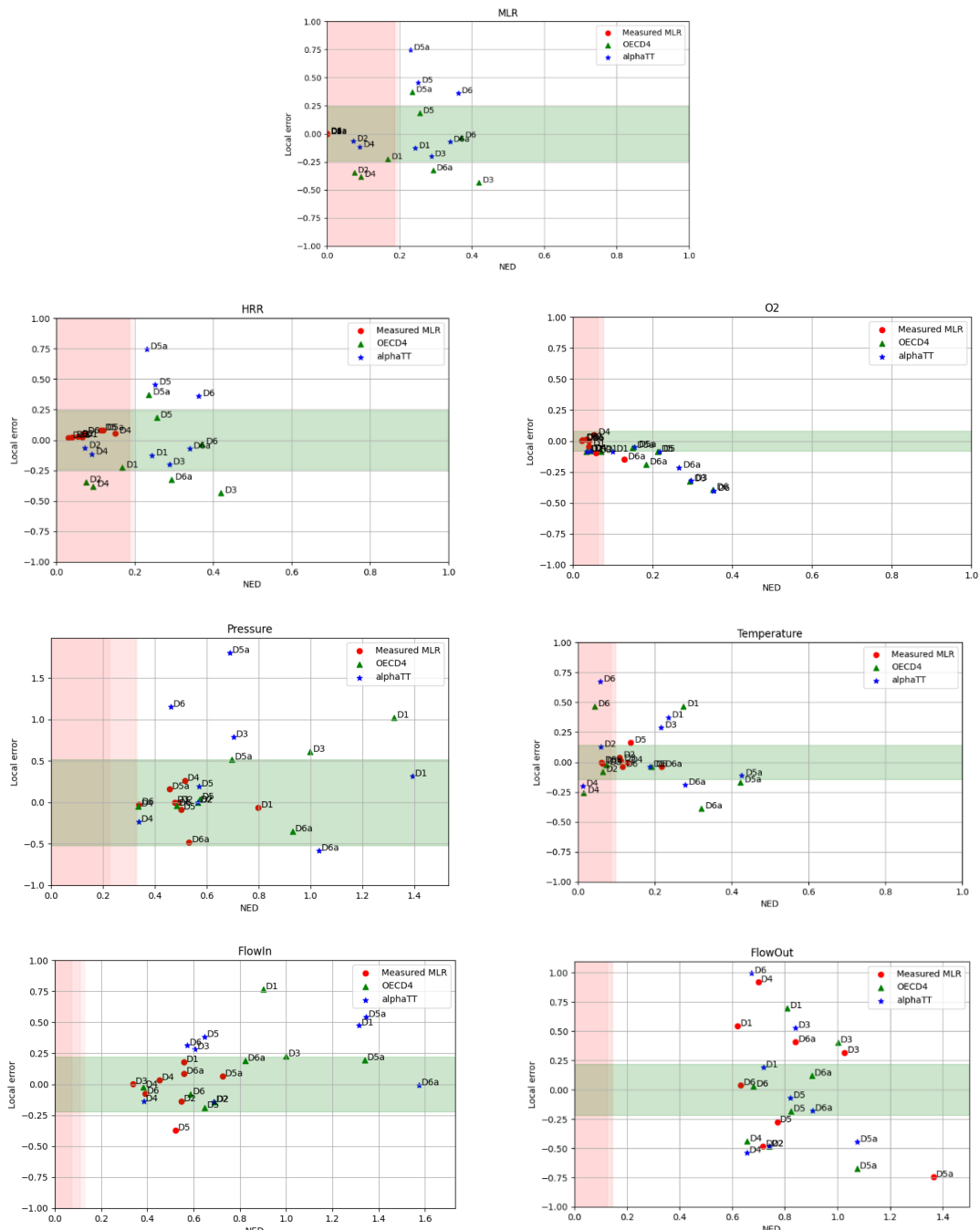


**Figure 10** Validation study of the FORCED model on all PRISME SOURCE tests

In this sense Figure 10 is rather compact but yet an informative presentation of the model evaluation. It can be summarized as follows:

- For all sensors (points) in this graphic lying in the intersection of the green and red area, model and experiment fit well with respect to both criteria NED and Local Error. For Local Error or NED values, which lie within these intervals, it is assumed that there were no irregularities in the experimental execution or in the FORCED simulation model.
- For all sensors (points) in this graphic lying within the green but outside the red area, model and experiment fit well with respect to their Local Error values but differ significantly with respect to their overall structure (and vice versa for points within the red but outside the green area).
- If the sensor points are located in the white area, there are doubts on the validity of the model.
- For sensors behaving as described in the latter two bullet points, a deeper analysis is advisable, e.g., using the actual plots of modelled and measured results (as per Figure 9).

Additionally, for statistical evaluation, the mean ( $\mu$ ) for the Local Error and the NED have been computed for all data and for individual sensors. For each group of the MLR model, the mean ( $\epsilon$ , NED) values for each sensor group are illustrated in Figure 11. The figure also contains horizontal and vertical whiskers for each sensor group. The horizontal whiskers of length  $U_{NED}$  are used in a one-sided manner (to the left) since all NED values are larger than the optimal value zero by construction of this quantity. If these whiskers cross the ordinate, the model fits the data well (on average) for the corresponding sensor class in terms of NED value. Since Local Error values of sensors can be smaller or larger than the optimal value zero, we use two-sided whiskers of length  $U\epsilon$  here. If they cross the abscissa, the model fits the data well (on average) for the corresponding sensor class in terms of  $\epsilon$  value.

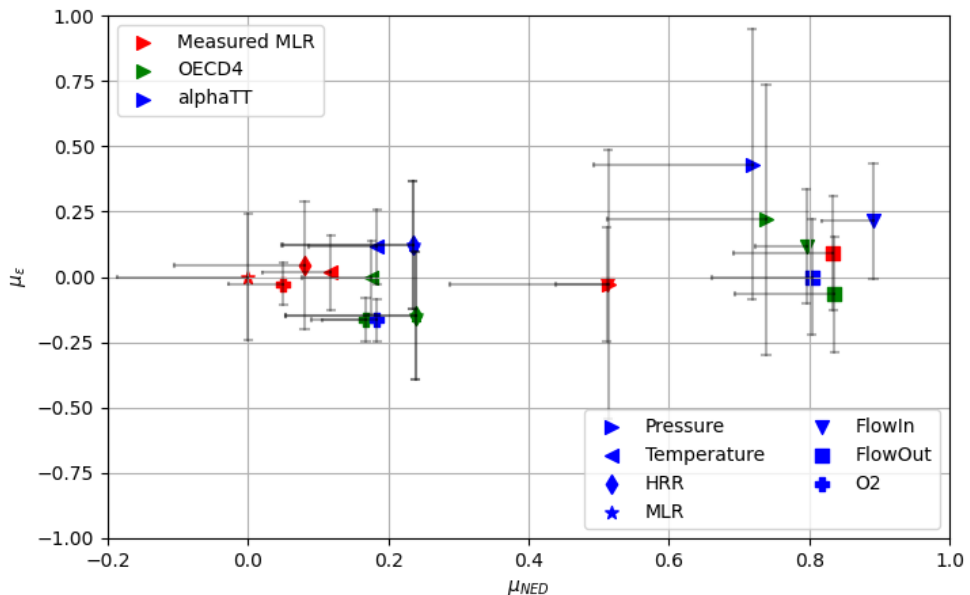


**Figure 11** Mean values  $\mu$  of Local Error and NED for relevant sensor groups

The results illustrated in Figure 11 are summarized in the following:

- The forecast capability of the FORCED model is best for HRR, O<sub>2</sub> and temperature.
- The use of at<sup>2</sup>/Babrauskas' or the  $\dot{m}_{OECD}$  (Prétrel and Le Saux) MLR model provides similar results for the MLR and HRR predictions, nevertheless the  $\dot{m}_{OECD}$  model results in an underestimation of the HRR while inverse for the at<sup>2</sup>/Babrauskas model.
- With both MLR models, the Local Errors are positive for temperature and pressure, indicating those values are over-estimated in the whole. The best estimate for both parameters is with the  $\dot{m}_{OECD}$  model.
- The Local Errors for O<sub>2</sub> are slightly negative in all cases, indicating an under-estimation of the O<sub>2</sub> levels.
- Considering the whiskers, the above statements could not be 95 % guaranteed. However, a sensitivity analysis could be performed to set (conservative) input parameters in order to demonstrate a quantify of concern (e.g., temperature, pressure) is with a degree of certainty over- or under-estimated.
- Mean NED for pressure, flow-in and flow-out have larger values than for other sensor groups. It has been noticed both pressure and flow experimental measurements have considerable experimental fluctuations (quite high frequency). Applying a Savitzky-Golay smoothing filter on the experimental data improves the NED slightly, nevertheless the NED values stay quite high, even for the measured MLR model. For example the D1 NED for pressure modelled with the measured MLR is still out of the validity range (cf. Figure 10), while the plot in Figure 9 would generally be accepted within the fire safety community as quite a success. Some deeper investigation already revealed that, despite the whiskers that account for the large uncertainty in the experimental data, the NED as a metric is very sensitive to rather small changes in near-zero denominator values, leading to higher NED values for pressure in this case. On the other hand, it is an indication that the next step could be to improve the FORCED predictive capacity by adding more complexity to the quadratic in- and exhaust fan driven duct boundary condition in order to better capture the aeraulic behaviour.

## CONCLUSIONS

The Python based code Flex-A FORCED, a well-stirred reactor approach single-zone model based on [1] is intended to be used as screening and predesign tool to determine the design scenarios in terms of HRR for scenarios in confined and mechanically ventilated compartments as found often within nuclear facility. As output, the model provides temperature, oxygen concentration and pressure within the cell or rooms as .csv file and associated automatically generated plots.

For convenience and to be able to add leakages, control multiple branches with dampers and check filter temperatures, dedicated features were added to the basic well-stirred model. Next to this, basic tooling for fast, efficient, and consistent engineering analysis has been created.

Furthermore, verification and validation (V&V) is performed. Validation of the model is conducted through comparison based on both local error and the normalized Euclidean distance between the model results and the experimental ones, the latter conducted in the frame of the OECD/NEA PRISME Project. Several verification measures are taken to assure the correct functioning of the code. First, the version control of all the code is performed using git. Secondly, only a limited number of public libraries are used, to limit the exposure to external bugs and to keep the implementation as lean as possible. A third layer ensures the correct functionality by splitting the simulation into separate tested

functions. A last verification layer consists of checking the essential interaction between the different physical phenomena by specifying different input scenarios and assess the results through the visualisation using the full code and performing the qualitative assessment of the physical behaviour.

The V&V has demonstrated the model is suited for fire modelling within closed enclosures with forced ventilation flows both at low ( $1.5 \text{ h}^{-1}$ ) and high ( $8.4 \text{ h}^{-1}$ ) air renewal rates were fast filling of the room by smoke is to be expected due to smoke layer depth or turbulences by the ventilation as often observed within nuclear facilities.

## ACKNOWLEDGMENTS

The activities as described in this paper were possible through the confidence given to Flex-A by the Belgian Nuclear Research Centre SCK-CEN in order to deliver a suitable method to justify the design against internal fire hazards for a highly active hot cell facility. Moreover, Flex-A wants to thank Tarek Beji of the Department of Structural Engineering and Building Materials of the Ghent University to listen to our questions, to answer them and make us understand some details about the research published in [1].

## REFERENCES

- [1] Beji, T., and B. Merci: Assessment of the Burning Rate of Liquid Fuels in Confined and Mechanically Ventilated Compartments Using a Well-Stirred Reactor Approach, *Fire Technology* 52, pp.469–488, 2016, <http://dx.doi.org/10.1007/s10694-014-0418-1>.
- [2] Audouin, L., et al.: OECD PRISME Project: Fires in confined and ventilated nuclear-type multi-compartments - Overview and main experimental results, *Fire Safety Journal* 62, 2013, pp. 80-101, <https://doi/10.1016/j.firesaf.2013.07.008>.
- [3] Python Software Foundation: Python, version 3.8.1.3, March 2022, <https://www.python.org/downloads/release/python-3814/>.
- [4] Quintiere, J. G.: *Fundamentals of Fire Phenomena*, ISBN 9780470091159, John Wiley & Sons, United Kingdom, March 2006, <https://doi.org/10.1002/0470091150>.
- [5] Melis, S., and L. Audouin: Effects of ventilation on the heat release rate in mechanically-ventilated compartment fires, *Fire Safety Science*, pp. 931-942, 2008, [https://publications.iafss.org/publications/fss/9/931/view/fss\\_9-931.pdf](https://publications.iafss.org/publications/fss/9/931/view/fss_9-931.pdf).
- [6] Peatross, M. J., and C. L. Beyler: Ventilation effects on compartment fire characterization, *Fire Safety Science*, 1997, <https://doi.org/10.3801/IAFSS.FSS.5-403>.
- [7] Utiskul, Y., et al.: Compartment fire phenomena under limited ventilation, *Fire Safety Journal* 40, pp. 367-390, 2005, <https://doi.org/10.1016/j.firesaf.2005.02.002>.
- [8] Babrauskas, V.: Estimating large pool fire burning rates, *Fire Technology* 19, pp. 251-261, 1983.
- [9] National Fire Protection Association (NFPA): NFPA 72, National Fire Alarm Code, 1999 Edition, Quincy, MA, USA, January 1999.
- [10] National Fire Protection Association (NFPA): NFPA 92B, Guide for Smoke Management Systems in Malls, Atria, and Large Areas, 2000 Edition, Quincy, MA, USA, 2000.

- [11] Le Saux, W., et al.: Experimental Study of the Fire Mass Loss Rate in Confined and Mechanically Ventilated Multi-Room Scenarios, *Fire Safety Science*, 2009, <https://dx.doi.org/10.3801/IAFSS.FSS.9-943>.
- [12] Prétrel, H., et al.: Experimental Study of the Burning Behaviour of Pool Fires in Confined and Ventilated Compartments, in: *Proceedings of Post-Conference Seminar III of the 18<sup>th</sup> International Conference on Structural Mechanics in Reactor Technology (SMiRT 18) 9<sup>th</sup> International Seminar on Fire Safety in Nuclear Power Plants and Installations*, August 22-24, 2005 - Hosted by IAEA, Vienna, Austria, 2005.
- [13] Beji, T., F. Bonte, and B. Merci: Numerical Simulations of a Mechanically-Ventilated Multi-Compartment Fire, *Fire Safety Science*, 2014, <https://doi.org/10.3801/IAFSS.FSS.11-499>.
- [14] Wahlqvist, J., and P. van Hees: Validation of FDS for Large-Scale Well-Confined Mechanically Ventilated Fires Scenarios with Emphasis on Predicting Ventilation System Behavior, *Fire Safety Journal* 62, pp. 102-114, 2013, <https://doi.org/10.1016/j.firesaf.2013.07.007>.
- [15] American Society for Testing and Materials (ASTM): *ASTM E 779, Standard Test Method for Determining Air Leakage Rate by Fan Pressurization*, 2001 Edition, West Conshohocken, PA, USA, 2001.
- [16] Bonte, F., et al.: Computer simulations to study interaction between burning rates and pressure variations in confined enclosures, *Fire Safety Journal* 62, pp.125-143, 2013, <https://doi.org/10.1016/j.firesaf.2013.01.030>.
- [17] Riese, O., et al.: Evaluation of Fire Models by Using Local and Global Metrics and Experimental Uncertainty Estimates: Application to OECD/NEA PRISME DOOR Tests, *Fire Technology*, 2022, <https://doi.org/10.1007/s10694-022-01276-5>.
- [18] Salley, M. H., and R. Kassawara: Verification and Validation of Selected Fire Models for Nuclear Power Plant Applications: Experimental Uncertainty, NUREG-1824, Volume 2, and EPRI 1011999, Final Report, prepared for: United States Nuclear Regulatory Commission (U.S. NRC) Office of Nuclear Regulatory Research (RES), Washington, DC, USA, May 2007, <https://www.nrc.gov/docs/ML0717/ML071730305.pdf>.
- [19] Prétrel, H., L. Bouaza, and S. Suard: Multi-scale analysis of under-ventilated combustion regime in case of fire event in a confined and mechanically ventilated compartment, *International Symposium of Fire Safety, IAFSS*, Waterloo, ONT, Canada, April 2021, <https://doi.org/10.1016/j.firesaf.2020.103069>.
- [20] Audouin, L., et.al.: Quantifying differences between computational results and measurements in the case of a large-scale well-confined fire scenario, *Nuclear Engineering and Design* 241, 2011, <https://doi.org/10.1016/j.nucengdes.2010.10.027>.

### **3.6 Session on Operating Experience**

The last session of the seminar, chaired again by Marina Röwekamp, was mainly devoted to the more recent operating experience regarding fires and fire protection issues in nuclear installations.

Three presentations were given. The first one was a presentation from the Sellafield nuclear site in the United Kingdom on fires recently occurred, their investigation, and the lessons learned from these.

A curious fire, which had occurred during steam generator cutting in a NPP under decommissioning igniting a non-negligible amount of fire-retardant coating materials was presented from Germany.

Last not least, a present activity on categorising release fractions of radioactive waste packages in case of fires were presented.

The seminar contributions of the last session are provided hereafter.

# Sellafield Ltd. Recent Fires and Learning

Alexa Seward

Sellafield Ltd., Seascale, Cumbria, CA20 1PG, United Kingdom

## ABSTRACT

We are continuously striving to improve conventional and nuclear safety at Sellafield. One key focus is fire safety, and one way to do this is by learning from events that have happened to ensure they do not happen again. This presentation will focus on a recent fire that occurred in a building on the Sellafield nuclear site causing significant fire and smoke damage. This had resultant cost and operational implications.

This report highlights the main factors leading to the fire and its consequences. It will focus on the investigations and root cause analysis that followed. For example, a notable part of the fire investigation was a heat transfer analysis using numerical methods to assess the cause of the fire. The methodology and how it was adapted will be discussed, along with the results gained and how they were used.

It will also consider the relevant learning, including how each shortfall and recommendation from the investigation has been addressed in a site improvement plan. In particular, the fire investigation identified improvements in guidance on the appropriate type of fire safe scaffolding to use. In the report we cover the new scaffolding policy that has been created, including the background research work that went into it, the stakeholders who were consulted and the improvements to fire safety that will result.

## INTRODUCTION

In October of 2021, a fire occurred in a Magnox Reprocessing Ancillary building. It was found that the fire started within a plastic light diffuser in a thermal denitration (TDN) cell however, the cause of ignition could not be identified. It was initially assumed that an electrical fault within the light itself caused ignition, but it was later found that there had been a fault within the pre-heater nearest to the plastic light diffuser and that it had been at an elevated temperature. An investigation was held to investigate the fire and identify what the most likely cause of ignition was. A heat transfer analysis was carried out on the pre-heater and the surrounding lagging to determine whether it could have caused the plastic light diffuser to reach its critical heat flux. This report will discuss the heat transfer analysis and its conclusions, as well as the learnings from the investigation.

A significant bit of learning that was taken from the investigation was an immediate change to the Scaffolding policy and a hierarchy for scaffold boards, to define the 'Relevant Good Practice' (RGP) for scaffolding boards and accompanying accessories. This report will demonstrate the underpinning research and evidence that fed into the policy, what relevant stakeholders were consulted, and the fire safety improvements expected.

## BACKGROUND

Sellafield is a part of the Nuclear Decommissioning Authority (NDA) in the United Kingdom and deals with the legacy nuclear waste and spent fuel. The Sellafield site as we know it today started in 1947 as a new atomic energy site known as "Windscale". The

site has been home to two pile reactors – plutonium producing atomic reactors, Calder Hall – the world's first commercial nuclear power plant (NPP), and the Windscale Advanced Gas Reactor (AGR). In 1964 the Magnox reprocessing plant opened, recycling Magnox fuel. Sellafield is now responsible for taking the waste out of the buildings on site and dealing with legacy nuclear waste, storing spent fuel, and repackaging the country's stockpile of nuclear material.

Magnox fuel reprocessing spanned across multiple buildings, including one which completed the finishing and evaporation processes. This building can be divided into three parts: evaporation, nitric acid recovery, and thermal denitration. The fire took place in the thermal denitration part, in the TDN cell. In the TDN cell pre-heated Uranyl Dioxide is oxidised with compressed air to make Uranyl Trioxide, this is done in a fluidised bed which operates at around 500 °C. The environment of the cell is warm, approximately 40 °C, and dry.

## FIRE INVESTIGATION [1]

An abnormal temperature of 800 °C was first recorded in the pre-heater at 23:45 h and 45 minutes later the fire alarm went off. The pre-heater was turned on at approximately 23:15 h, starting at a temperature of 30 °C. It reached a temperature of 800 °C at approximately 23:45 h. The cell in which the fire took place, is usually at an ambient temperature of approximately 40 °C. Using this information and the model shown in Figure 1, a heat transfer analysis was performed to determine whether the heat flux produced by the abnormally high temperature in the pre-heater could have caused autoignition of the plastic light diffuser.

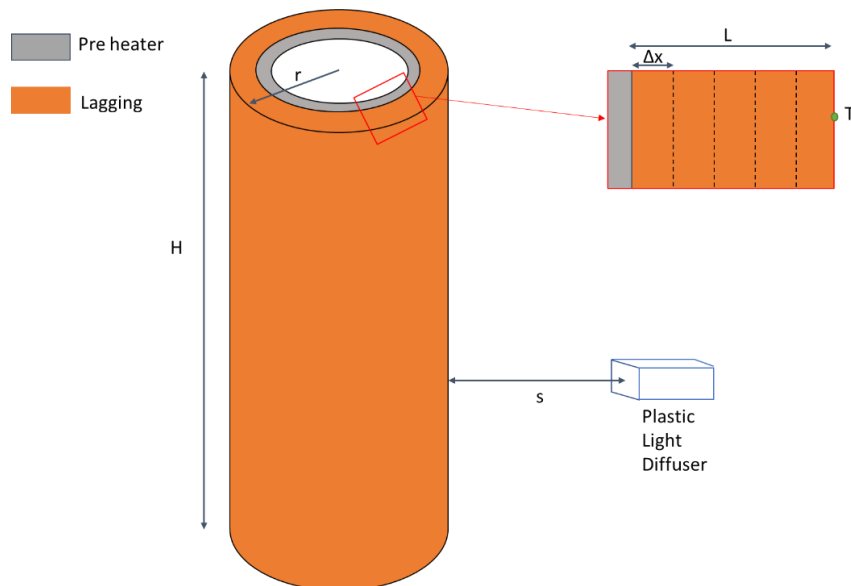


**Figure 1** Heat transfer model and parameters of the pre-heater system

The methodology used was Numerical methods, as described in D. Drysdale, An Introduction to Fire Dynamics [2]. The assessment used numerical methods to predict the change in temperature across the radius of the lagging over the defined amount of time. To calculate the temperature profile across the lagging, it was broken down into strips that were 0.02 m wide. As the lagging had a thickness of 0.10 m it was broken down into five strips in total. The temperature was calculated at each interface between the strips, this is shown in more detail in Figure 2.

The effects of heat transfer via conduction through the wall of the pre-heater itself were ignored as it was assumed that the temperature throughout the radius of the pre-heater was constant and thus the measured temperature of the pre-heater was equal to that of the inner edge of the lagging.

The heat transfer was modelled for a lower and upper limit temperature of the pre-heater of 800 °C and 1200 °C. The value of 800 °C was used as it was the last measurable temperature within the pre-heater to be taken before the temperature got too high to provide accurate readings. The lagging was reported as remaining intact after the fire and thus was assumed to not have melted. Therefore, the maximum temperature that the pre-heater could have reached was the melting temperature of the lagging, which is reported as over 1000 °C [3]. For the sake of conservatism, the maximum temperature has been taken as 1200 °C.

The temperature profile of the lagging was modelled by assuming a steady rise in the temperature of the pre-heater from 30 °C to 800 °C and 1200 °C over a period of 30 minutes. The temperature profile of the lagging was then modelled for a further period of 45 minutes at 800 °C and 1200 °C. This was done assuming a constant ambient temperature in the room at 40 °C. This model was then repeated where the ambient temperature was instead assumed to be equal to the temperature of the outer edge of the lagging.

To provide a further bounding case, the temperature profile of the lagging was also modelled where the temperature of the pre-heater rose from 350 °C to 800 °C and 1200 °C in a period of 30 minutes, and then modelled for a further 45 minutes at 800 °C and 1200 °C. This was done where it was assumed the ambient temperature was 40 °C and where it was assumed the ambient temperature was equal to the temperature of the outer edge of the lagging.

The lagging was Rockwool ProRox PS 971, which is a high-density stone wool. All Rockwool® insulation products have a Euroclass A1 non-combustible rating in accordance with BS EN 13501-1 Reaction to Fire classification [4]; however, the individual Rockwool® products do not have a fire rating on their own and are always tested as part of a system [5]. Having an A1 non-combustible rating with BS EN 13501-1, means that the materials tested obtain a certain classification for the reaction to fire tests BS EN ISO 1182 and EN ISO 1716 for non-combustibility and determination of the gross heat of combustion, respectively [6], [7]. The material properties of Rockwool® ProRox PS 971 were found from the data sheet provided by Rockwool [8] and the Ignition Handbook [9].

The plastic light diffuser, that was assumed to be the ignition point of the fire, was made of Polycarbonate. Polycarbonate has a good heat resistance and is an inherently flame-retardant material which tends to burn slower than other hydrocarbon plastics as it contains oxygen molecules which do not burn [10]. Polycarbonate is very hard to ignite and will stop burning when the supporting flame is removed but it will melt as it burns [10].

## Heat Transfer Assessment

Numerical methods were used to predict the temperature profile by splitting it into thin strips, where the temperature is assumed constant across the strip. The interface between each strip or between the internal/external compartment and strip is called a node. The temperature at each node is calculated using the temperatures calculated at the previous time step ( $\Delta t$ ). This process continues until the total time is reached. A diagram showing the parameters used in numerical methods can be seen in Figure 2.

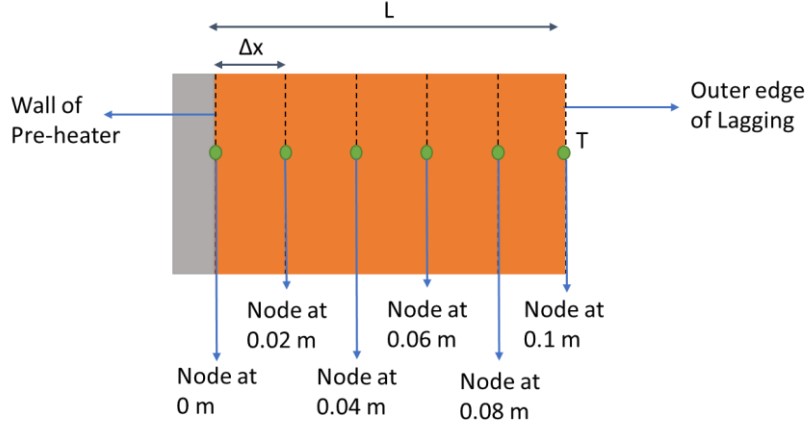


**Figure 2** Diagram showing numerical methods parameters on the pre-heater system

For this method the time step and change in thickness were chosen such that [2]:

$$\frac{\alpha \Delta t}{(\Delta x)^2} < 0.5 \quad (1),$$

where:

$\alpha$  = thermal diffusivity [ $\text{m}^2/\text{s}$ ],

$\Delta t$  = time step [s],

$\Delta x$  = change in thickness [m].

The time step used was 15 s and the change in thickness was 0.02 m.

The thermal diffusivity was calculated using the relationship with thermal conductivity, density, and specific heat capacity [2]:

$$\alpha = \frac{k}{\rho C} \quad (2),$$

where:

$k$  = thermal conductivity [ $\text{W/mK}$ ] = 0.04  $\text{W/mK}$ ,

$\rho$  = density [ $\text{kg/m}^3$ ] = 140  $\text{kg/m}^3$ ,

$C$  = specific heat capacity [ $\text{J/kgK}$ ] = 920  $\text{J/kgK}$ ,

The thermal diffusivity was calculated as  $3.1 \times 10^{-7} \text{ m}^2/\text{s}$ .

It was assumed that the strip adjacent to the internal compartment (the pre-heater) was equal to the temperature of the pre-heater itself. Equation (1) and equation (2) were used to calculate the temperatures at each node [2]:

$$T_P^{n+1} = T_P^n + \frac{k \Delta t}{\rho C (\Delta x)^2} (T_H - 2T_P^n + T_C) \quad (3),$$

$$T_P^{n+1} = T_P^n + \frac{h \Delta t}{\rho C (\Delta x)} (T_a - T_P^n) + \frac{k \Delta t}{\rho C (\Delta x)^2} (T_H - T_P^n) \quad (4),$$

where:

$T_P^{n+1}$  = temperature of node at time  $t + \Delta t$  [ $^\circ\text{C}$ ],

$T_P^n$  = temperature of node at time  $t$  [ $^\circ\text{C}$ ],

$T_H$  = temperature of the previous node towards the hot side [ $^\circ\text{C}$ ],

$T_C$  = temperature of the previous node towards the cold side [ $^\circ\text{C}$ ],

$T_a$  = ambient room temperature [°C],

$h$  = convection coefficient [W/m<sup>2</sup>K] = 5 W/m<sup>2</sup>K (cold side) = 50 W/m<sup>2</sup>K (hot side) [2].

Equation (1) was used for the strips which were not at either edge of the lagging, thus were only affected by conduction. Equation (2) was used for the strip which was adjacent to the external compartment (the surrounding air).

The temperature profiles are included in full in Appendix A and B. The maximum temperatures for the outer edge of the lagging were in the range of 62 – 359 °C. The temperature of the outer edge of the lagging (the strip adjacent to the external compartment) was used to find the radiative heat flux emitted from the lagging [2].

$$\dot{q}_e'' = \varepsilon \sigma T^4 \quad (5),$$

where:

$\dot{q}_e''$  = radiative heat flux from the lagging [kW/m<sup>2</sup>],

$\varepsilon$  = emissivity = 1 (assumed for conservatism),

$\sigma$  = Stefan-Boltzmann constant = 5.67 x 10<sup>-8</sup> W/m<sup>2</sup>K<sup>4</sup>,

$T$  = temperature of outer edge of lagging [°C].

The radiative heat flux emitted from the lagging was calculated as 0.71 – 11.29 kW/m<sup>2</sup>.

The amount of the radiative heat flux received by the plastic light diffuser was calculated using a radiation configuration factor [11]:

$$X = \frac{W}{s}$$

$$Y = \frac{H}{s}$$

$$F_{1 \rightarrow 2} = \frac{1}{2\pi} \left( \frac{X}{\sqrt{1+X^2}} \tan^{-1} \frac{Y}{\sqrt{1+X^2}} + \frac{Y}{\sqrt{1+Y^2}} \tan^{-1} \frac{X}{\sqrt{1+Y^2}} \right)$$

where:

$W$  =  $2\pi r$  = width of the emitter (lagging) = 1.4 m,

$H$  = height of the emitter (lagging),

$s$  = distance between emitter and receiver (pre-heater and light diffuser) = 0.5 m,

$F_{1 \rightarrow 2}$  = configuration factor.

The configuration factor was calculated as 0.78.

The heat flux that was received by the plastic light diffuser was then proportionately calculated from the radiative heat flux emitted by the lagging, using the configuration factor [2].

$$\dot{q}_T'' = F_{1 \rightarrow 2} \dot{q}_e'' \quad (6),$$

where:

$\dot{q}_T''$  = radiative heat flux received by target [kW/m<sup>2</sup>].

The radiative heat flux received by the plastic light diffuser was calculated as 0.55 – 8.8 kW/m<sup>2</sup>.

The radiative heat flux received by the plastic light diffuser was measured against a critical heat flux (CHF) of ignition for the material of the plastic light diffuser, Polycarbonate, found in the SFPE Handbook of Fire Protection Engineering as 15 kW/m<sup>2</sup> [11]. If the radiative heat flux received by the target (plastic light diffuser) is above the critical heat

flux, then there is a possibility of ignition. The time to ignition ( $t_{ig}$ ) could then be found using the following equation [9]:

$$\sqrt{\frac{1}{t_{ig}}} = \frac{(\dot{q}_T'' - CHF)}{TPR} \quad (7),$$

where TPR is the thermal response parameter [ $\text{kW}\text{s}^{1/2}/\text{m}^2$ ] which is given in the Society of Fire Protection Engineering (SFPE) Handbook of Fire Protection as  $331 \text{ kW}\text{s}^{1/2}/\text{m}^2$  for Polycarbonate [11].

The calculated range of radiative heat flux received by the plastic light diffuser was well below the critical heat flux for ignition of Polycarbonate and therefore, it is unlikely that the pre-heater could have caused ignition of the plastic Polycarbonate light diffuser.

## Investigation Results

Heat transfer assessments were performed at both  $800^\circ\text{C}$  and  $1200^\circ\text{C}$  on the lagging surrounding the pre-heater. As can be seen in Figure 3, none of these assessments show that the temperature of the outer edge of the lagging caused a sufficient radiative heat flux to be received by the plastic light diffuser, so much that it was over the critical heat flux for ignition of Polycarbonate. In summary, the radiative heat flux produced by the pre-heater at an elevated temperature is not enough to surpass the critical heat flux for ignition for Polycarbonate.

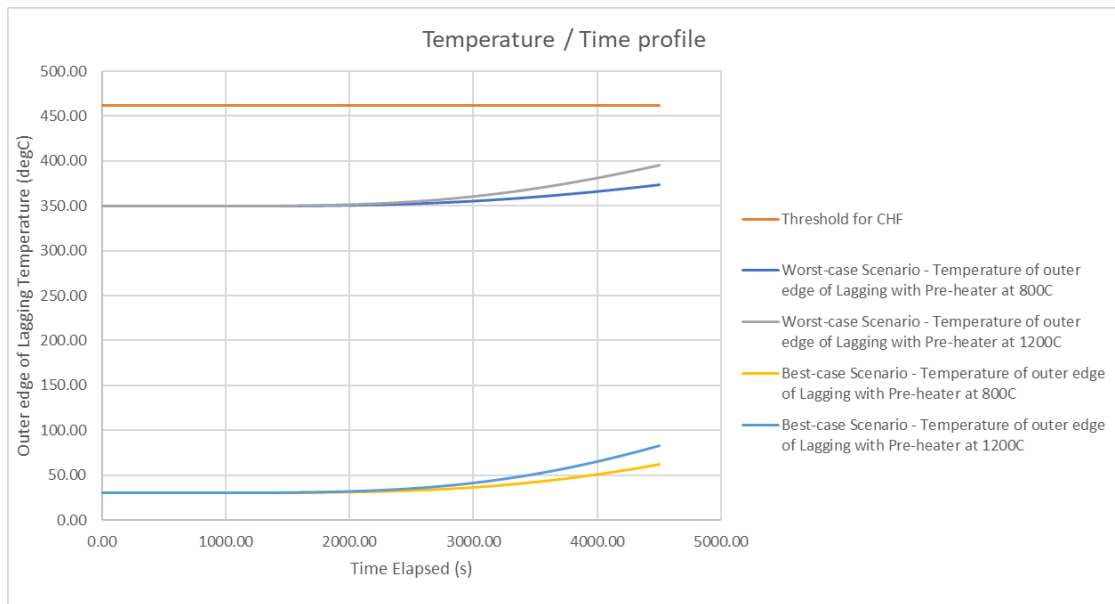


**Figure 3** Graph showing the temperature profile of the outer edge of the lagging using the upper and lower limits of the pre-heater temperature

The worst-case scenario was found through the assumption that the lagging was initially at a temperature of  $350^\circ\text{C}$  and the ambient temperature was equal to that of the outer edge of the lagging. For these cases, the radiation heat flux received by the Polycarbonate light diffuser was  $7.73 \text{ kW/m}^2$  and  $8.80 \text{ kW/m}^2$ , respectively. The best-case scenario was found through the assumption that the lagging was initially at a temperature of  $30^\circ\text{C}$  and the ambient temperature was equal to that of the outer edge of the lagging. This gave temperatures of  $62^\circ\text{C}$  and  $83^\circ\text{C}$  for the  $800^\circ\text{C}$  and  $1200^\circ\text{C}$  cases, respectively. For these cases, the radiation heat flux received by the Polycarbonate light diffuser was  $0.55 \text{ kW/m}^2$  and  $0.71 \text{ kW/m}^2$ , respectively.

As it was reported that the pre-heater was initially off and thus at a temperature of 30 °C at time zero, it could be assumed that the worst case is unlikely to be accurate to what occurred. However, it acts as a reassurance that even in the worst-case scenario, the critical heat flux of Polycarbonate was not reached.

The other combustible components on the light fitting had a critical heat flux for ignition approximately equal to or more than that of Polycarbonate. For example, the Polyvinyl Chloride (PVC) used in the caps of the trunkings had a critical heat flux for ignition of 17 kW/m<sup>2</sup> and the PVC power cables had a critical heat flux of ignition of between 13 – 25 kW/m<sup>2</sup> [11]. The cables; however, would have been contained within a stainless-steel trunking and thus had a high level of protection. As these components were relatively close to the Polycarbonate diffuser, it can be assumed that the diffuser was the worst-case material nearby and the most likely one to ignite.

The low heat flux emitted from the outer edge of the lagging is likely due to the Rockwool® insulation used in the cell having a very high density and a very low thermal conductivity, which in combination means that the insulation is very good at absorbing the heat produced by the pre-heater, even at elevated temperatures.

Whilst various assumptions were made throughout the assessment to model the heat transfer, the difference between the radiative heat flux received by the plastic light diffuser and the critical heat flux of ignition of Polycarbonate is large enough to suggest that assumptions made have not impacted the integrity of the results.

## **LEARNING FROM EXPERIENCE [12]**

One of the main aspects of the fire where learning was taken was the contribution of the combustible plastic scaffold boards in the area, that added to the overall fire load.

The main reason metal boards were not used in the area was the chemical challenge. Nitric acid at the concentrations used in the area in contact with the metal boards would produce NO<sub>x</sub> gases which challenge the safety of man entry. Plastic composite boards were therefore used in this case. Timber boards are avoided in radiologically classified areas as they can absorb any material spilled in the area and therefore cannot be cleaned for reuse and become a waste. They also have the potential to splinter and become a source of contamination which could result in injection of material hazardous to any doer in the area or for scaffolders constructing the platforms.

A guide was created to help with the decision of what scaffolding is appropriate to use in the different areas on and offsite both active and non-active areas. It includes flowsheets for construction and non-construction sites, that instruct what the appropriate scaffold board is for the specific area for which they are to be used. The guide also details the other accessories used in scaffolding and what fire standards they need to meet to be used on and offsite. Further details of the British Standards, British Standard European Norms, fire tests, and industry standards were provided in the appendices along with examples of fires involving scaffold boards and the accompanying accessories.

The first choice for materials on a nuclear site is always non-combustible; however, where these are unavailable or not reasonably practicable then a fire retardant (FR) material is acceptable provided the approach is justified and documented depending on the context and consequences of use. With regards to scaffold boards this means that metal boards are the first choice, followed by FR timber boards, and finally FR composite boards.

For non-radiologically classified areas it is acceptable to use FR timber boards. If they are to be used inside, they must be FR rated. If they are to be used outside and it can be justified that there is a very low fire risk, then it may be acceptable to use non-FR

rated boards. However, this would be deviating from RGP, and so would have to be fully justified and should be done at the discretion of the fire assessor for each individual facility or operation. If there is hot work in the area or the scaffolding is in close proximity to an existing building metal boards should be used.

For radiologically classified areas metal boards are the preferred scaffold boards to be used. However, where there are instances where it would be unsuitable to use metal boards, such as where there are chemical challenges present, FR composite boards should be used. This is true for use both inside and outside.

A visual representation of this guidance can be seen in Figure 4, which is a flowsheet designed to determine what type of scaffold board is most suitable for a given area.

Where possible, the cutting of boards should be avoided. If it is not avoidable then, it should be ensured that any fire retardance is not affected by the cutting. Any relevant marking should also be kept clear on both the original board and the cut section to help clearly identify its fire performance.

For use on any Sellafield facility any scaffold sheeting, building paper or netting used must comply with Loss Prevention Scheme (LPS) 1207 (temporary internal coverings) [13] or LPS 1215 (external coverings) [14]. This will be demonstrated by an accompanying Loss Prevention Council Board (LPCB) marking on the product. To check whether the product is LPCB approved, it can be searched for on RedBook Live: Home [15].

For use on any Sellafield facility, the RGP would be for any accessories (end caps, armadillos, base plates) to be metal or where unavailable, to be non-combustible. Having looked and reviewed the market such items do not exist and so to comply with this, products would have to be specifically manufactured which is not reasonably practicable. The named plastic accessories present a minimal fire load, and there are other safety factors to consider regarding their use. Their ignitability is reduced as they are a dispersed fire load when in use on scaffolding. The danger would come from the bulk storage of the excess plastic accessories in combustible bags, as they would present a much more concentrated fire load. As such these materials should be stored safely within non-combustible/fire resisting containers where these are to be stored in nuclear facilities.

Brick guards are required when working at height, the preferred types of brick guards are made of metal.

## **JUSTIFICATION**

The guidance presented was mirroring or comparable to the standard guidance given in the industry, provided by members of the NIFSCC (Nuclear Industry Fire Safety Co-ordinating Committee). The guidance followed British, European, and international guidance; IAEA Safety Standards Series No. NS-G-1.7 now superseded by No. SSG-64 [16], Sellafield Ltd. Engineering Design Safety Principles [17], and the ONR Safety Assessment Principles [18].

Where compromises have been made in favour of minimising the fire risk as opposed to other risks (radiological, conventional etc.), this has been done where these risks can be controlled and managed, whereas the consequences of a fire would have been much harder to control and contain. For example, even though from a waste perspective, composite boards are preferred over flame retardant timber boards in radiologically classified areas, they present a much higher fire risk. Sellafield already deals with contaminated materials and have defined processes to deal with this, but it is much harder to deal with a fire and its waste products involving scaffolding in radiologically classified areas.

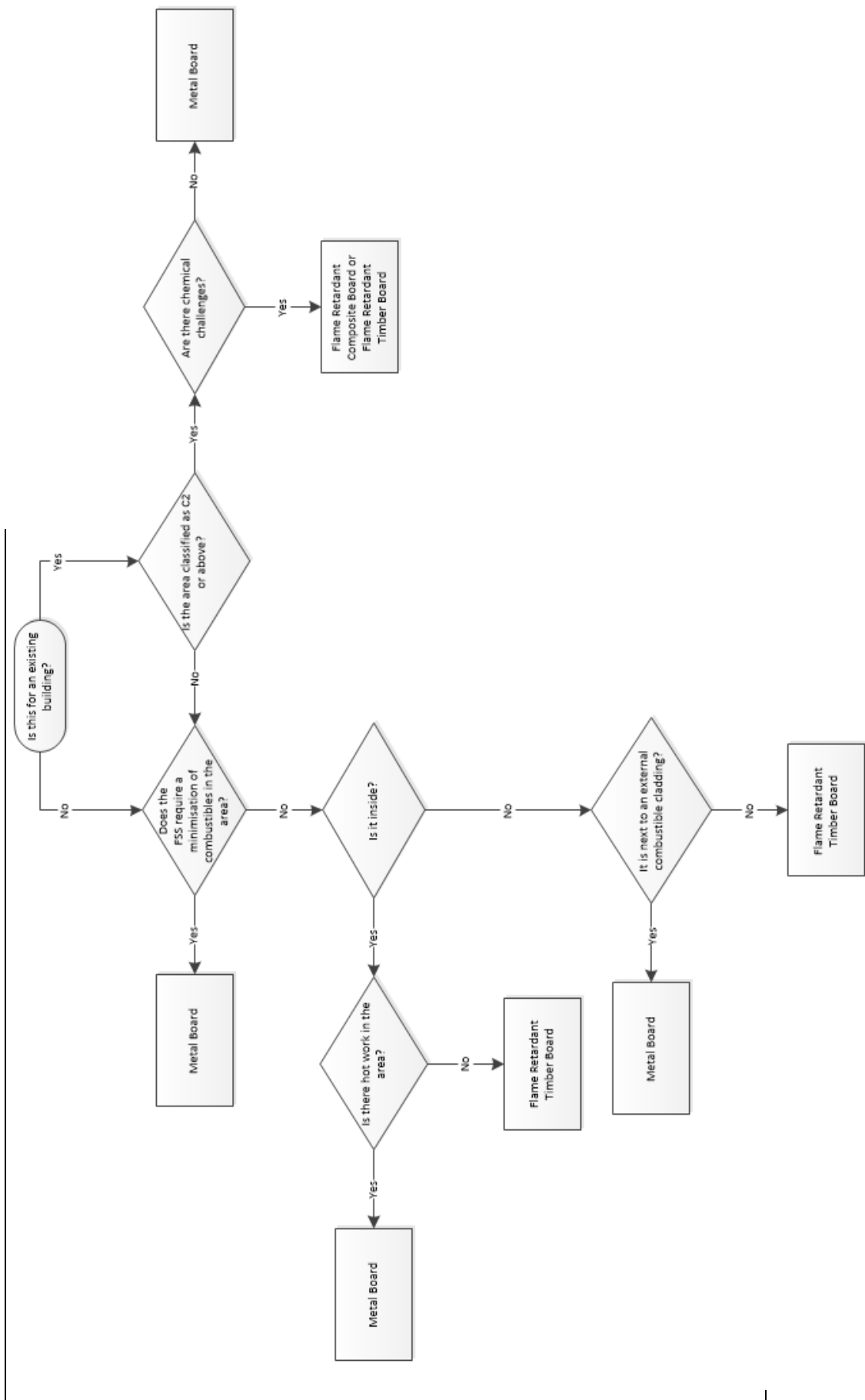


Figure 4

Decision flowsheet for scaffolding boards

## CONCLUSIONS

The conclusion from the fire investigation was that the elevated temperatures in the pre-heater was not the cause of the fire as it did not emit a high enough heat flux to reach the critical heat flux of the plastic light diffuser and cause autoignition. Whilst the exact cause could not be determined, it was assumed to be due to an electrical fault. This conclusion was drawn from past experience and the ignition point of the fire. However, the fire itself did result in a reflection of the policies on Sellafield site relating to fire safety particularly those involving scaffolding. Following industry standards and both British, European and international guidance, a non-combustible approach was used.

## REFERENCES

- [1] Seward, A.: Sellafield Note For the Record – Assessment of Heat Transfer from the Pre-heater, Sellafield Ltd., Seascale, Cumbria, United Kingdom, December 2021.
- [2] Drysdale, D.: An Introduction to Fire Dynamics, Second Edition, John Wiley & Sons, Ltd, Chichester, United Kingdom, 1998.
- [3] Rockwool: Technical Insulation, Safe Use Instruction Sheet - ProRox & SeaRox products, Version 16.30 2021, [https://rti.rockwool.com/siteassets/marine--offshore/certificates/safe-use-instructions-sheet/rw-ti\\_certificate\\_safe\\_use\\_instruction\\_sheet.pdf](https://rti.rockwool.com/siteassets/marine--offshore/certificates/safe-use-instructions-sheet/rw-ti_certificate_safe_use_instruction_sheet.pdf).
- [4] British Standards Institute (BSI): BS EN 13501-1:2018, Fire classification of construction products and building elements,. Part 1: Classification using data from reaction to fire tests, BSI Standards Limited, London, United Kingdom, 2019.
- [5] Rockwool: Frequently Asked Questions, <https://www.rockwool.com/uk/advice-and-inspiration/faqs/#performance>, [Accessed 6 December 2021].
- [6] British Standards Institute (BSI): BS EN ISO 1182:2020, Reaction to fire tests for products - Non-combustibility test, BSI Standards Limited, London, United Kingdom, 2020.
- [7] British Standards Institute (BSI): BS EN ISO 1716:2018, Reaction to fire tests for products - Determination of the gross heat of combustion (calorific value), BSI Standards Limited, London, United Kingdom, 2018.
- [8] Rockwool: Technical Insulation ProRox Ps 971 Data Sheet, United Kingdom, 2018, <https://rti.rockwool.com/uk/products/industrial/prorox-ps-971-uk/>.
- [9] Babrauskas, V.: Ignition Handbook, pp. 880-881, ISBN-10: 0-9728111-4-1, Fire Science Publishers, Issaquah, WA, USA, 2003.
- [10] Fire, F. L.: Combustibility of plastics, ISBN 0-442-23801-0, Van Nostrand Reinhold, New York, NY, USA, 1991.
- [11] DiNenno, P. J. (Ed.): Society of Fire Protection Engineers (SFPE) Handbook of Fire Protection Engineering, 3<sup>rd</sup> Ed., ISBN 978-0877654513, National Fire Protection Association (NFPA), Quincy, MA, USA; 2002.
- [12] Seward, A.: Scaffolding Systems Fire Performance Requirements Relevant Good Practice (RGP), Sellafield Ltd., Seascale, Cumbria, United Kingdom, May 2022.

- [13] Loss Prevention Certification Board (LPCB): Loss Prevention Standard (LPS) LPS 1207: Issue 3.1, Fire requirements for the LPC approval and listing of protective covering materials for use in the interior of buildings, July 2014, <https://www.redbooklive.com/download/pdf/LPS1207.pdf>.
- [14] Loss Prevention Certification Board (LPCB): Loss Prevention Standard (LPS) LPS 1215: Issue 4.1, Requirements for the LPCB Approval and Listing for Fire Performance of Containment Net and Sheet Materials for External Use on Construction Sites, 2014, <https://www.redbooklive.com/download/pdf/LPS-1215.pdf>.
- [15] RedBook Live: Search for approved products and services, <https://www.redbooklive.com/search/index.jsp> [Accessed 23 February 2022].
- [16] International Atomic Energy Agency (IAEA): Protection against Internal Fires and Explosions in the Design of Nuclear Power Plants, Safety Guide No. NS-G-1.7, Vienna, Austria, 2004, [https://www-pub.iaea.org/MTCD/Publications/PDF/Pub1186\\_web.pdf](https://www-pub.iaea.org/MTCD/Publications/PDF/Pub1186_web.pdf).
- [17] Sellafield Ltd.: SLM 1.02.06, Engineering Design Safety Principles Manual, Issue 3, Sellafield Ltd., Seascale, Cumbria, United Kingdom, September 2019.
- [18] Office for Nuclear Regulation (ONR): Safety Assessment Principles for Nuclear Facilities, 2014 Edition, Revision 1, January 2020, <http://www.onr.org.uk/saps/>.

# Small Fire Event During Dismantling of a Steam Generator

Andreas Artz<sup>1\*</sup>, Katrin Borowski<sup>2</sup>

<sup>1</sup> RWE Nuclear GmbH, Rückbauanlage Biblis, Biblis; Germany

<sup>2</sup> RWE Nuclear GmbH, Essen, Germany

## ABSTRACT

The steam generators (SGs) are dismantled in the installation position in the nuclear fuel-free dismantling facility of the Biblis nuclear power plant under decommissioning. A small fire occurred during the cold cutting process at a steam generator on 17 February 2022.

The paper describes the cutting process used and the hazard assessment performed in advance. The cause of the fire is analysed and verified by laboratory tests. The consequences of the fire and measures to repair the damage are presented.

Effective preventive measures could be derived based on the reconstructed cause of the fire.

## INTRODUCTION

The Biblis nuclear power plant (NPP) units lost their authorisation for power operation as a result of the nuclear Accidents of Fukushima in 2011. The Biblis NPP under decommissioning is meanwhile a dismantling facility free from nuclear fuel since 2017.

There were four steam generators in both NPP units A and B in accordance with the redundancy concept in power operation. The hot steam of the primary circuit ran in a closed circuit through each of the steam generators that supplied the steam for the turbines in the secondary circuit. The steam generators were part of the full system decontamination of the primary circuit after termination of power operation. The radioactivity could thus be reduced by a factor of about 10. The approximately 20 m high steam generators, each weighing approx. 300 t, are being successively dismantled in the installation position into parts with a height of less than 2 m [1].

The following Figure 1 shows the location of the steam generators in the dismantling facility as well as schematically the enclosure, projecting edges and other systems that are dismantled together with the steam generator and the dismantling equipment.

In the course of dismantling activities on one of the four steam generators in Biblis, unit A, a small fire occurred on 17 February 2022 [2].

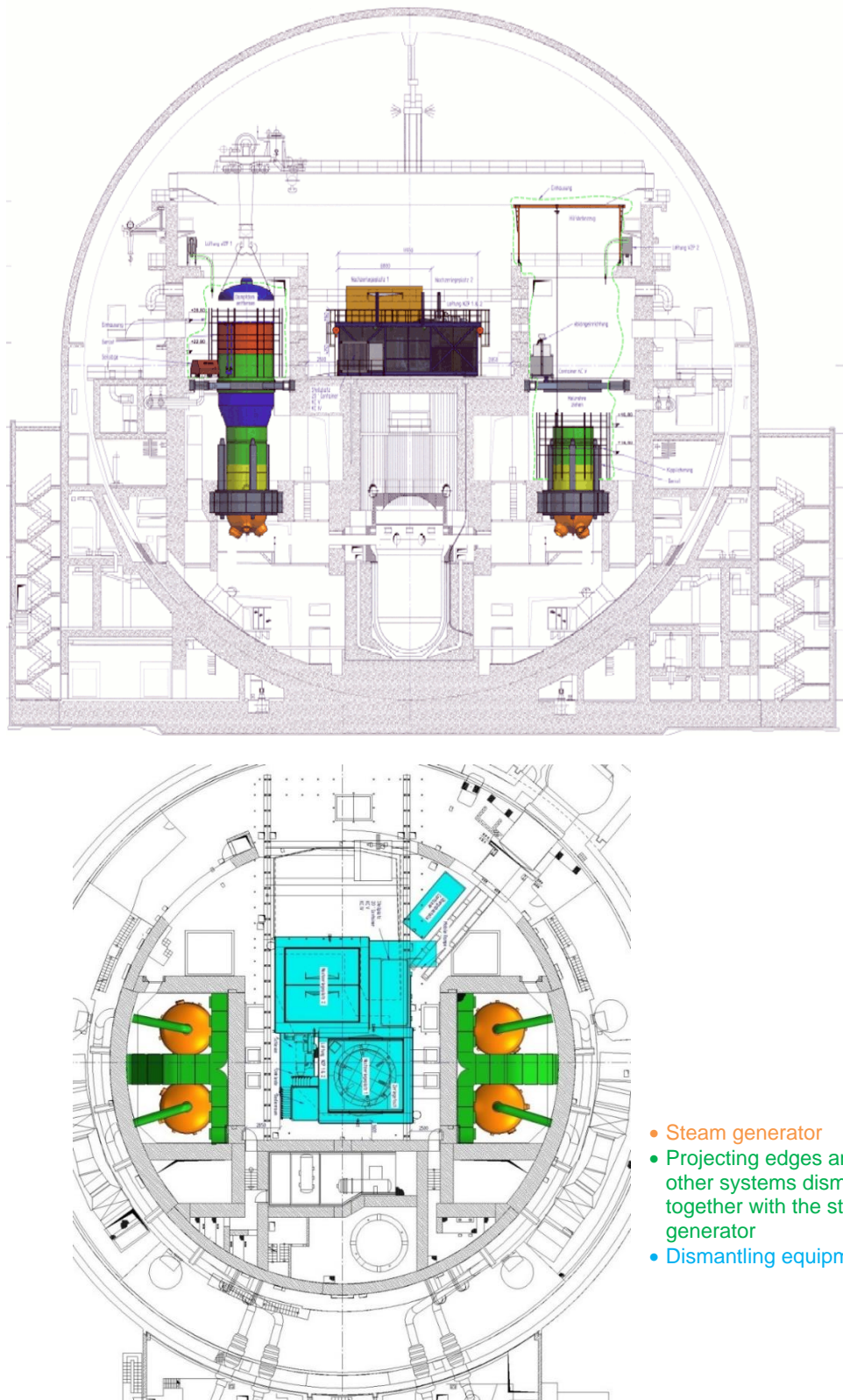


**Figure 1** Location of the steam generators and systems and equipment affected by their dismantling

## DISMANTLING DESCRIPTION

The steam generators are primarily dismantled with an electrically operated wire saw.

Dismantling segments for further processing or final storage of the resulting waste are produced by dry cutting (cold cutting process) using a diamond wire. The basic equipment of the wire saw includes the drive unit with a wire store, a control panel, a pneumatic compressor as well as the deflection pulleys necessary for guiding the wire. The saw is operated at the control panel outside the hazardous zone by trained and experienced personnel when dismantling the steam generator. The wire guide is also monitored in real time by means of video cameras as shown in Figure 2.



**Figure 2** Monitoring station with control panel and monitor outside the hazardous zone

Dry cutting with the diamond wire produces fine metal dust. The sawing area is enclosed as shown in Figure 3. The enclosure comprises a frame of (non-combustible) scaffolding material and films of class B1 building material in accordance with DIN 4102 [3] that are taped at the joints with tissue adhesive tape (combustible). A recirculating air filtration system (1500 m<sup>3</sup>/h, filter class HI3/HI4) is connected to the enclosure for targeted air routing.

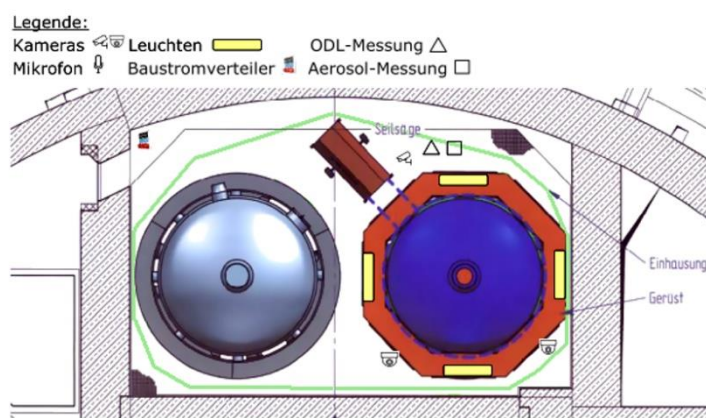


**Figure 3** Schematic representation of the pre-cutting station

All fire detectors in the sawing area are deactivated because of the fine dust produced during sawing. The wire heats up to approx. 70 – 80 °C during cutting. This classifies this cutting technique as a cold cutting process.

75 wire saw cuts have been made on all four steam generators in the installation position within one year since February 2021. Approximately 3000 m of sawing wire were used in the process. There were no abnormalities regarding inadmissible heat development due to dismantling by means of a wire saw until the small fire occurred during these activities.

## DESCRIPTION OF THE ACTIVITIES PRECEDING THE SMALL FIRE EVENT

Course 4 of the tube lane, including the guide shell, was cut off at steam generator III using a wire saw vertical cut on Thursday, 17 February 2022. Multiple sheets, some grids, and individual tubes are cut through in this process. The sawing wire is subject to higher stress, wears out more quickly, and wire breaks occur frequently due to the inhomogeneous cutting geometry. The cut (marked in yellow in Figure 4) was already 95 % complete. The wire broke at about 15:30 h. The work was interrupted due to a break at around 15:40 h.



**Figure 1** Wire saw cuts through the steam generator

## TIME SEQUENCE OF THE SMALL FIRE EVENT

At 16:38 h, the control room received a phone call reporting 'smoke in the controlled area'. An escape alarm was immediately triggered for the controlled area. There were three persons in the controlled area who left it swiftly and in an orderly manner at that time. In parallel to the escape alarm, an alarm was triggered for the plant fire brigade.

The fire self-extinguished, the plant fire brigade confirmed 'fire out' at 16:55 h.

A film surface of approx. 30 m<sup>2</sup> burned and released soot particles to the atmosphere. The containment was locked. The filters of the exhaust air systems were changed three times within 24 hours.

## DAMAGE DESCRIPTION AND ROOT CAUSE ANALYSIS

The small fire site was visited for root cause analysis on Friday, 18 February 2022. The area contaminated by the smouldering fire was located at the level + 6 m (see Figure 5 and Figure 6 below) between two rooms that are not separated in terms of fire protection.

The area was enclosed with B1 film due to the activities. The floor (level + 6 m) comprises a steel platform with gratings, which were also covered with B1 film and partly with steel plates. The small fire affected a film area of approx. 30 m<sup>2</sup>. Most of the film smouldered. Only a small part of it really burned. Contamination was visible on mineral and metallic surfaces as well as on scaffolding materials.

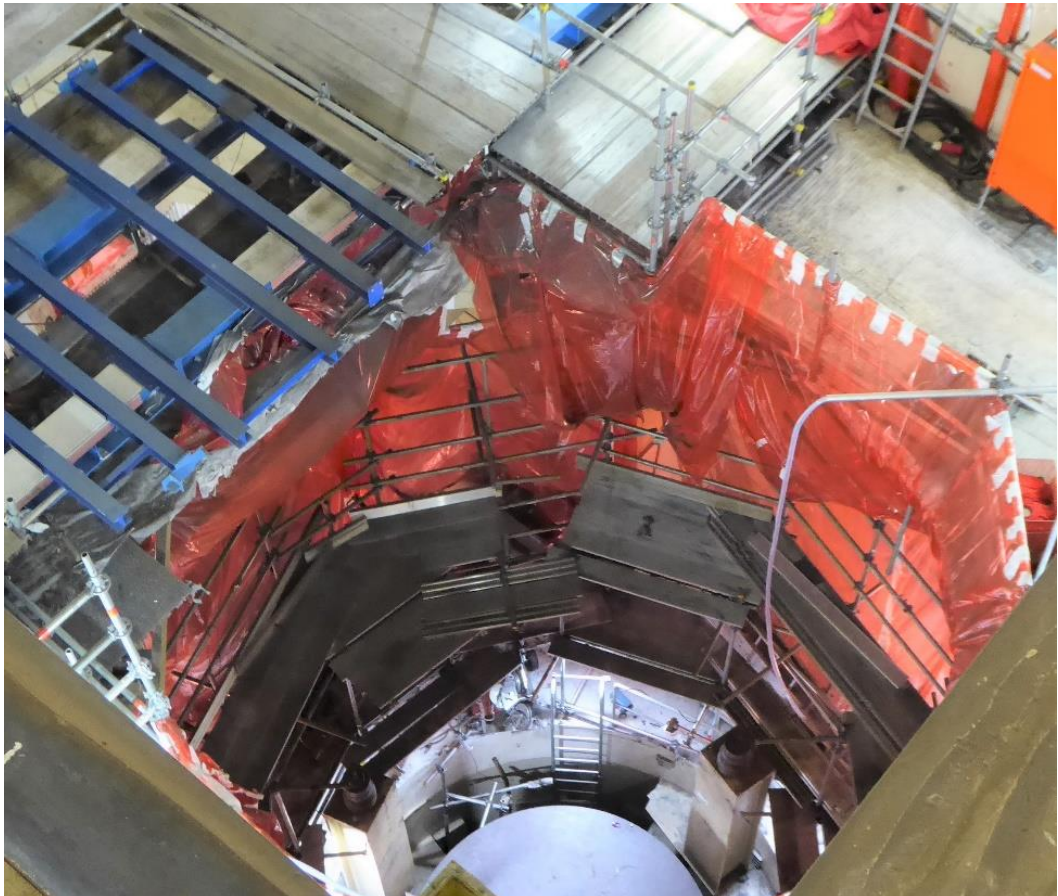


**Figure 5** View from the level + 30.5 m on the steam generator dismantling

There were large areas of potentially radioactively contaminated metal chips in the area of the construction site due to the wire sawing work performed until the fire event occurred. There were also some cable trays exposed and loose, partly smouldered cables in the fire area. The visible contamination was caused both by the flue gas that had spread to the areas above and to the side and by the fire debris dripping onto the gratings.



**Figure 6** View of the fire scene from + 6 m to + 9 m and on burned film enclosure in the entrance area

The following conclusions can be drawn based on the fire description (self-extinguishing smouldering fire) and the damage pattern since there are no direct observations of the fire event sequence:

- approx. 5 kg burned/smouldered plastic (1 kg red and 4 kg white film);
- relatively severe soot development due to the fire-retardant effect of B1 films;
- moderate fire – as there is no large-scale peeling or spalling on mineral surfaces ( $T < 400^{\circ}\text{C}$ );
- local temperature at the source of the fire  $> 400^{\circ}\text{C}$  (ignition temperature of the polyamide film);
- no static impairments of the building structures.

No radionuclides were released as result of the fire.

### Ignition Source

Only the wire sawing activities can be considered as the trigger (ignition source) of the smouldering fire due to the local and temporal connections. No other work was performed at the time. Furthermore, other heat sources (e.g., halogen spotlights) and electrically defective tools or short circuits can be excluded as causes.

The tube lane including the guide shell was cut vertically and the cut was already 95 % complete when a wire break occurred at around 15:30 h. Immediately before this, a heated spacer section of about 10 cm length had also been sawed off in the area of the wire exit. Figure 7 shows the spacer section and the wire exit on the other site.

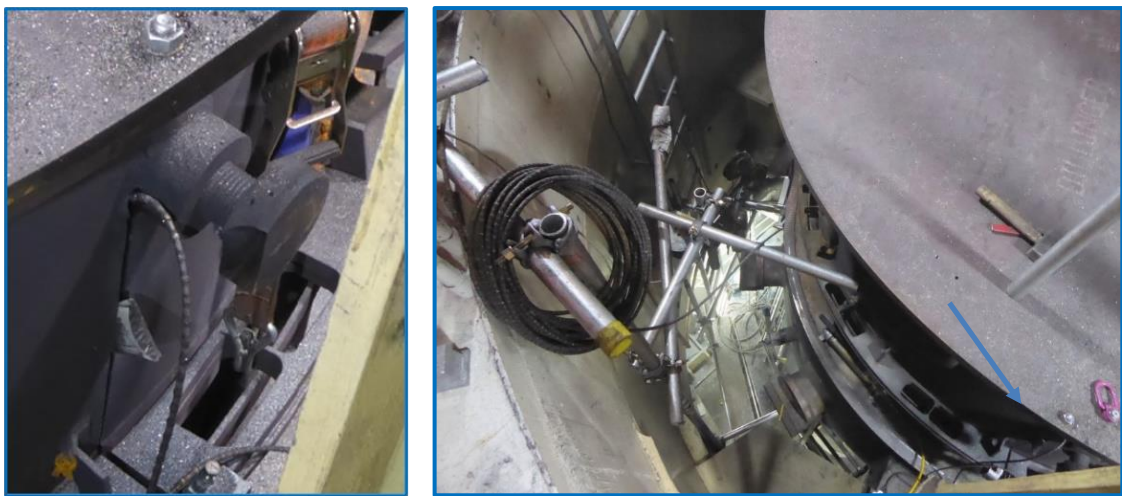


**Figure 7** Detached spacer section at + 11 m level and wire exit on the other side

The section dropped by about 5 m (as shown in Figure 8) and was stopped by the film enclosure that separated the work area. The section gave off its heat energy absorbed by the saw cut and thus caused ignition.

The work was interrupted due to a break at around 15:40 h. Up to this time, the staff had not noticed any smell of fire or smoke at the level + 12 m (monitoring position).

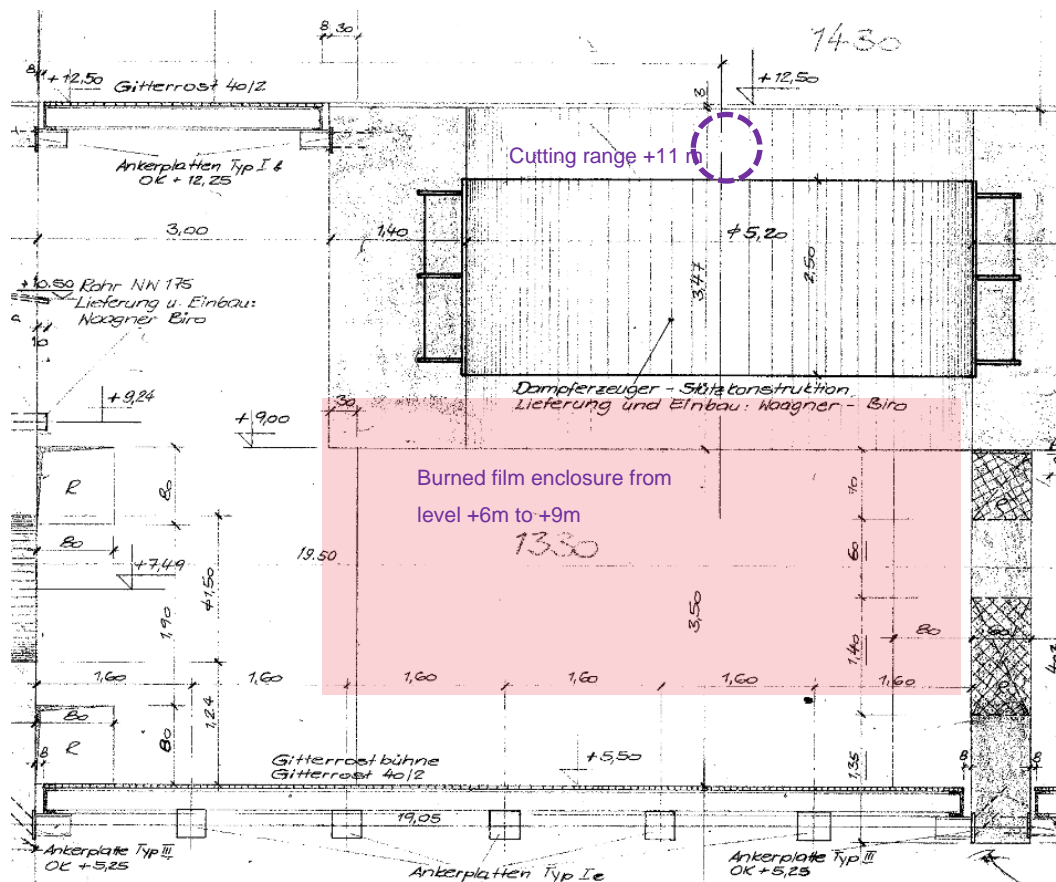


**Figure 8** Detached spacer section dropping to the + 6 m level and triggering a smouldering fire of the film there

## Cutting Tests – Determination of Maximum Temperatures

Cutting tests were performed with the wire saw on 25 May 2022. The purpose of the tests was generating the highest possible temperatures on the material being cut in order to verify the ignition source (spacer section) of the small fire of 17 February 2022 and to derive further measures if necessary.



**Figure 9** Test setup (top) and on a spacer 50 % cut with new wire (bottom left) and 90 % cut with depleted wire (bottom right)

The tests were conducted with a new and a nearly depleted saw wire at an ambient temperature of 25 °C. The specified test setup (cf. Figure 9), in particular the attachment of the compact spacer by means of threaded rods, ensures that during the sawing pro-

cess the thermal energy generated by friction remains in the spacer and is only insignificantly dissipated into the solid steel structure support (SG II dome).

All cuts were made with approximately the same cutting power of the wire saw (wire speed: 7.1 m/s, current: 30 A, wire tension/pressure: 1.8 – 2.2 bar). The temperatures of the saw wire, the spacer, and of the smaller section were measured at half (approx. 50 %) of the cut and briefly before the end of the cut (approx. 90 %) in both cutting tests. Table 1 provides the measured temperatures.

**Table 1** Temperatures during cutting tests

| Saw Wire | Cutting Depth | Cutting Time | Wire Temperature | Spacer Temperature | Section Temperature |
|----------|---------------|--------------|------------------|--------------------|---------------------|
| New      | 50 %          | 5 min        | 62 °C            | 150 °C             | 310 °C              |
| New      | 90 %          | 5 min        | 60 °C            | 220 °C             | 390 °C              |
| used-up  | 50 %          | 6 min        | 72 °C            | 200 °C             | 420 °C              |
| used-up  | 90 %          | 7 min        | 82 °C            | 420 °C             | 990 °C              |

The measured values show that the cutting time increases slightly with increasing wear of the saw wire. Accordingly, more friction is generated and converted into heat energy due to the associated decrease in the cutting performance. This is evident at all three temperature measuring points (wire, spacer, and section). The spacer, which had not yet cooled down to room temperature, additionally influenced the measured temperatures with the depleted wire. There were only about 45 min between the two cutting attempts (change to depleted wire). The temperature of the spacer before the start of the second cutting test was not measured.

Very high temperatures were measured due to the specified experimental setup with a large cut surface (approx. 40 mm x 120 mm = 4800 mm<sup>2</sup>) and a very low mass (approx. 5 kg) of the spacer. The extremely unfavourable ratio of cutting time to cut surface and mass of the experimental setup is not transferable to the actual conditions of the steam generator dismantling work.

Verification of the spacer section as the trigger (ignition source) of the small fire of 17 February 2022 has been completed with the measured temperatures of the cutting tests.

## CONSEQUENTIAL ACTIVITIES AND MEASURES TO REPAIR THE DAMAGE

Figure 10 shows fire residues on the ceiling (a), wall (b) and floor (c) area.



**Figure 10** Fire residues on the ceiling (a), wall (b) and floor (c) area

The following steps were taken to repair the damage with the participation of the radiation protection department, the fire protection officer, the hazardous substances officer, the occupational safety department, and the head of the 'SG dismantling' project after clarifying the cause of the fire, in particular after identification of the ignition source:

- Consultation with experts on the topic of fire residues and possible pollutants;
- Sampling of fire residues by experts for analysis;
- Inspection date setting for fire damage restoration with specialist companies for environmental technologies and radiation protection;
- Brief report and test report 'Fire residues/pollutants' by the experts for hazardous substances;
- Resumption of wire sawing work on SG IV with additional measure: Cyclical thermal inspection of wire exit incl. documentation;
- Start of fire restoration (phase 1);
- Completion of dismantling and packaging activities on the SG III guide shell;
- Start of fire restoration (phase 2);
- Cutting test – determination of maximum temperatures on the cut material;
- Completion of fire restoration with sampling for analysis of possible pollutant residues (preserving evidence).

A total of 100 person-hours were needed for fire restoration in the controlled area. The resulting collective dose was 0.1 mSv.

## **DERIVATION OF PREVENTIVE MEASURES**

Additional measures or adaptation of the working method were discussed with the parties involved before resuming the wire sawing work (metal, dry cutting). The goal of this process was to ensure that no unacceptably high temperatures occur at the cut material. On the one hand, this is a question of avoiding a potential ignition source (fire hazard), and on the other hand, one of complying with the criteria of the cold cutting process.

The measures identified in relation to the 'SG dismantling' project were:

- Cutting outside the area of small cuttings or prior removal of the small cuttings in the area of the saw wire to ensure the distribution or dissipation of the heat energy introduced by the wire;
- Cyclic thermal inspection of the cut material (wire exit) during cut control, before breaks, and at the end of work, incl. documentation;
- Establishing a fire watch for measurements  $> 100^{\circ}\text{C}$  (up to temperature  $< 100^{\circ}\text{C}$ ).

Wire sawing on the SG IV within the 'SG dismantling' project was resumed with implementation of the abovementioned measures on 7 March 2022. Maximum temperatures of  $95^{\circ}\text{C}$  have been measured on the cut material for eight different wire saw cuts to date since then.

## CONCLUSIONS

A small (smouldering) fire broke out despite the selected cold cutting process during steam generator dismantling.

It was caused by a disconnected spacer piece, which had heated up considerably due to the cutting process. Cutting of smaller steel segments is not planned but may occur. Subsequent presence of the strongly heated part on the film (B1), which is classified as non-combustible but fixed with adhesive tape – which lacks this classification – caused the small fire.

The fire self-extinguished.

The precautions taken against fires, such as the use of non-combustible covers, prevented significant effects.

The following preventive measures

1. cutting outside the area of small cuttings,
2. cyclic thermal inspection of the cut material, and
3. establishing a fire watch, if necessary,

were implemented in the 'SG dismantling' project since resumption of wire sawing work. These are suitable in terms of their nature and scope and assessed as effective by the further wire sawing performed.

Based on the temperatures measured in the two cutting tests, it is generally recommended to set temperature limits on the material to be cut that are appropriate for dry cutting wire sawing work and to perform a cyclical thermal check.

## REFERENCES

- [1] RWE Nuclear GmbH: Abbau der Dampferzeuger Block A, Abbaumaßnahmeverfahren A608/17, Maßnahmenbeschreibung, Biblis, Germany, 13 January 2021 (in German).
- [2] RWE Nuclear GmbH: DE III – Kleinbrandereignis an einer schwer entflammbaren Folieneinhausung (B1), Arbeitsbericht, PNB-A/2022/003-0, Biblis, 20 June 2022 (in German).
- [3] Deutsches Institut für Normung (DIN) e.V.: DIN 4102: 1998-05, Brandverhalten von Baustoffen und Bauteilen – Teil 1: Baustoffe; Begriffe, Anforderungen und Prüfungen (Englisch: Fire behaviour of building materials and building components – Part 1: Building materials; concepts, requirements and tests), Berlin, Germany, May 1998,  
<https://www.din.de/de/meta/suche/62730!search?query=Din+4102&submit-btn=Submit>.

# Release Fractions of Radioactive Waste Packages in Case of Fire

Burkhard Forell\*, Cornelia Richter

Gesellschaft für Anlagen- und Reaktorsicherheit gGmbH, Köln; Germany

## ABSTRACT

This paper gives an overview on the German approach to assess radioactive releases from accidents involving radioactive waste packages as performed and continuously refined for the German repository named "Konrad" for low and intermediate level radioactive waste. The approach considers various mechanical and thermal impacts by nine different impact classes. As the waste packages have been binned in eight different groups, 72 combinations of impact class and waste package group have been studied, for which the release fractions of four different types of radionuclides have been conservatively estimated. The release fractions are presented separately for the respirable aerosol fraction of aerodynamic equivalent diameter  $AED < 10 \mu\text{m}$  and the larger diameter fraction of  $10 \mu\text{m} < AED < 100 \mu\text{m}$ .

## INTRODUCTION

In the following, an overview is given on the German approach to assess radioactive releases from accidents involving radioactive waste packages like as performed for the German Konrad repository for low and intermediate level radioactive waste. The approach was first applied already 1991 [1]. Later, the approach was enhanced and extended to take into account newer experimental data and to reduce the level of conservativity [2] to [5].

Radioactive waste of low and medium activity levels is stored and transported in classified containers called waste packages. Within the Konrad safety studies certain accidental scenarios have been considered regarding storage and transport of such packages. These accidents consist of a mechanical impact that may be combined with a thermal load from a fire scenario. For the combination of different mechanical and thermal impacts discrete *impact classes* (German: Belastungsklassen, BK) were defined.

Depending on the container type and the characteristics (including conditioning) of the radioactive waste, the waste packages are categorized by different *waste package groups* (German: Abfallgebindegruppe, AGG). For each combination of a given AGG exposed to a certain impact according to an impact class BK, the following release fractions were defined for different types of radionuclides:

- Tritium H-3,
- C-14,
- halogens and their compounds, and
- other radioactive aerosols.

A release fraction is the relative proportion of a particular radioactive inventory released from a given waste package during an accident. Going back on experimental results, for fire related releases the aerosols released are always assumed to have an aerodynamic

equivalent diameter less than 10 µm, whereas for releases from a mechanical impact also larger diameters up to 100 µm are assumed.

## IMPACT CLASSES

The mechanical and thermal loads were subdivided into so-called impact classes. A distinction is made between the following three different thermal loads:

- no fire,
- a fully enveloping fire with a temperature of 800 °C lasting 30 min, and
- a fully enveloping fire with a temperature of 800 °C lasting 60 min.

The temperature of the thermal load rises from 30 °C to 800 °C within 5 min and decreases immediately to 30 °C after the defined time of 30 / 60 min.

For the mechanical loads, the impact of a waste package on an inelastic obstacle is considered. A distinction is made between three different loads, each of which is given by a maximum impact velocity. The decisive factor for the mechanical load is the specific mechanical energy input, i. e. the mechanical energy that is available per waste package mass for the deformation and destruction of the container.

The mechanical loads are

- a velocity of 35 km/h (drop height 4.8 m, specific mechanical energy input of 47.3 J/kg),
- a velocity of 80 km/h (drop height 25.2 m, specific mechanical energy input 246.9 J/kg), and
- a velocity of 110 km/h (drop height 47.6 m, specific mechanical energy input 466.8 J/kg).

Higher impact velocities are not considered in the transport studies, as it can be assumed that freight trains or trucks do not travel faster.

The combination of three thermal and three mechanical loads leads to a total of nine impact classes which are displayed in Table 1.

**Table 1** Overview of the nine different impact classes BK 1 to BK 9

| Mechanical Impacts      |                     |  | Thermal Impacts |             |             |
|-------------------------|---------------------|--|-----------------|-------------|-------------|
| Maximum Impact Velocity | Maximum Drop Height | Maximum Specific Mechanical Energy Input | No Fire         | 30 min Fire | 60 min Fire |
| 35 km/h (9.7 m/s)       | 4.8 m               | 47.3 J/kg                                | BK 1            | BK 2        | BK 3        |
| 80 km/h (22.2 m/s)      | 25.2 m              | 246.9 J/kg                               | BK 4            | BK 5        | BK 6        |
| 110 km/h (30.6 m/s)     | 47.6 m              | 466.9 J/kg                               | BK 7            | BK 8        | BK 9        |

## WASTE PACKAGE GROUPS

Eight different waste package groups were defined as of 2009 [3]. The groups are given in Table 2. The assignment depends on the characteristics of the waste (from non-fixed combustible waste, over compacted and cemented waste to metal waste) and the characteristics of the containers (e. g. steel plate containers or more stable concrete containers or even cast iron containers).

**Table 2** Waste package groups (AGGs) according to the 2009 definition [3]

| AGG | Definition  |
|-----|---|
| 1   | Combustible, non-fixed waste in steel plate containers  |
| 2   | Non-fixed and non-compactable metal and non-metal waste (including evaporator concentrate) in steel plate containers or concrete containers |
| 3   | Metal waste in steel plate container or concrete containers   |
| 4   | Compactable waste in steel plate containers or concrete containers  |
| 5   | Cemented waste in steel plate containers  |
| 6   | Combustible, non-fixed waste in concrete containers   |
| 7   | Cemented waste in concrete containers   |
| 8   | Waste in cast iron containers   |

For a container that is assigned to a certain AGG it is expected that its behaviour in case of an accident of a certain BK and therefore the release of radionuclides can be estimated conservatively by applying the release fractions approach introduced in the Konrad safety studies.

## RELEASE MECHANISMS

### Mechanical Impact

After a mechanical impact the release depends on the potential damage of the protective casing of the container and on how the content may be dispersed inside the container.

For example, in the event of a low mechanical impact (BK 1, cf. Table 1) for the concrete containers (AGG 5 and AGG 6) as well as for the cast iron containers (AGG 8) the release fraction is zero for all radionuclides, because it is assumed that containers will be sufficiently intact after the impact.

For the medium mechanical impact (BK 4, cf. Table 1) only the cast iron containers (AGG 8) are assumed to maintain an intact casing.

Regarding the radioactive content of the containers, it is distinguished between

- non-fixed waste (AGG 1 and AGG 2 as well as AGG 8),
- partly non-fixed waste, such as metal waste (AGG 3) or compactable waste (AGG 4) where a non-fixed fraction of the radioactivity of 1 % is assumed [4], or
- cemented waste (AGG 5 and AGG 7).

The non-fixed fraction of AGG 3 and AGG 4 is treated like that of AGG 1 and AGG 2; therefore, two models were developed for mechanically induced releases, one considering non-fixed and the other considering cemented waste.

The model for non-fixed waste is based on a conservative powder-model. In the empirical relation for the respirable ( $0 \mu\text{m} < \text{AED} < 10 \mu\text{m}$ ) aerosol fraction

- it increases linearly with the drop height (potential energy),
- it scales with the container volume about  $V^{2/3}$ , and
- the release fraction of aerosols with an aerodynamic equivalent diameter (AED) of  $10 \mu\text{m} < \text{AED} < 100 \mu\text{m}$  is about two times the respirable aerosol fraction.

The effect of the steel plate containers to retain the releases is assumed to be similar for non-fixed and for cemented wastes [4] with a retention factor of

- $r_{\text{steel-plate}} = 0.1$  for BK 1 to BK 3,
- $r_{\text{steel-plate}} = 0.3$  for BK 4 to BK 6, and
- $r_{\text{steel-plate}} = 1.0$  for BK 7 to BK 9.

For cemented waste in concrete containers, it is assumed that the containers do not break due to a low mechanical impact, while for a medium or high mechanical impact the release fraction will only be half of the fraction for the steel plate container.

The release fraction of cemented waste modelled also scales with the drop height (potential energy), but the volume is considered by a proportionality of  $V^{0.43}$ . The release fraction of aerosols with an aerodynamic equivalent diameter (AED) of  $10 \mu\text{m} < \text{AED} < 100 \mu\text{m}$  is about nine times the respirable aerosol fraction.

### **Thermal Impact**

Four mechanisms are considered occurring during thermal impact and leading to releases. Depending on the waste characteristics, the container type, the additional mechanical impact, and the intensity/duration of the thermal load, the following mechanisms may be relevant for the releases to a certain extent:

- pyrolysis of the waste product,
- combustion of the waste product,
- vaporization of water in the waste product, including entrainment of other radionuclides into water vapour, and
- sublimation or vaporization of radioactive substances in the waste products.

The pyrolysis of the waste products will occur for combustible waste in case of a thermal impact while the protective casing of the container is still closed. The endothermic pyrolysis process is considered for those fractions of the waste that are heated up to more than 300 °C.

The combustion of the waste products will occur for combustible waste in case of a thermal impact when the protective casing of the container is damaged, or the lid of the containers is opened so that air can enter the waste. There is no internal threshold temperature for the combustion to start.

The vaporization of water is relevant for cemented waste because it contains a relevant amount of water. The vaporization of water leads to the entrainment of certain radionuclides into the vapour flow which will also be released. The vaporization is assumed for waste fractions that are heated up to more than 100 °C.

The process of sublimation and vaporisation of radioactive substances other than water concerns halogens and their compounds, for which a conservative threshold temperature of 40 °C is assumed.

### **RELEASE FRACTION TABLES FOR DIFFERENT WASTE PACKAGE GROUPS**

In the following, the release fractions for different waste package groups AGG 1 to AGG 8 are presented for the different impact classes BK 1 to BK 9 in the corresponding Table 3 to Table 10.

**Table 3** Release fractions for AGG 1 [5]

| AGG 1: Combustible non-fixed waste in steel plate containers |                      |                                      |                      |                                      |                      |                                      |                                      |
|--|----------------------|--------------------------------------|----------------------|--------------------------------------|----------------------|--------------------------------------|--------------------------------------|
| BK   | Other Nuclides       |                                      |                      | H-3                                  |                      | C-14                                 | Halogens                             |
|  | 0 - 10 $\mu\text{m}$ | 10 $\mu\text{m}$ - 100 $\mu\text{m}$ | 0 - 10 $\mu\text{m}$ | 10 $\mu\text{m}$ - 100 $\mu\text{m}$ | 0 - 10 $\mu\text{m}$ | 10 $\mu\text{m}$ - 100 $\mu\text{m}$ | 10 $\mu\text{m}$ - 100 $\mu\text{m}$ |
| 1  | 5.0 E-06             | 1.0 E-05                             | 5.0 E-06             | 1.0 E-05                             | 5.0 E-06             | 1.0 E-05                             | 5.0 E-06                             |
| 2  | 1.0 E-01             | 1.0 E-05                             | 1                    | 0                                    | 1                    | 0                                    | 1                                    |
| 3  | 1.0 E-01             | 1.0 E-05                             | 1                    | 0                                    | 1                    | 0                                    | 1                                    |
| 4  | 5.0 E-05             | 1.0 E-04                             | 5.0 E-05             | 1.0 E-04                             | 5.0 E-05             | 1.0 E-04                             | 5.0 E-05                             |
| 5  | 1.0 E-01             | 1.0 E-04                             | 1                    | 0                                    | 1                    | 0                                    | 1                                    |
| 6  | 1.0 E-01             | 1.0 E-04                             | 1                    | 0                                    | 1                    | 0                                    | 1                                    |
| 7  | 3.0 E-04             | 6.0 E-04                             | 3.0 E-04             | 6.00 E-04                            | 3.0 E-04             | 6.0 E-04                             | 3.0 E-04                             |
| 8  | 1.0 E-01             | 6.0 E-04                             | 1                    | 0                                    | 1                    | 0                                    | 1                                    |
| 9  | 1.0 E-01             | 6.0 E-04                             | 1                    | 0                                    | 1                    | 0                                    | 1                                    |

**Table 4** Release fractions for AGG 2 [5]

**AGG 2: Non-fixed and non-compactable metal and non-metal waste (including evaporator concentrate) in steel plate containers or concrete containers**

| <b>BK</b> | <b>Other Nuclides</b>           |   |                                 | <b>H-3</b>  |                                 |   | <b>C-14</b>                     |   |                                 | <b>Halogens</b>                                     |                                 |   |
|-----------|---------------------------------|---|---------------------------------|---|---------------------------------|---|---------------------------------|---|---------------------------------|---|---------------------------------|---|
|           | <b>0 - 10 <math>\mu</math>m</b> | <b>10 <math>\mu</math>m - 100 <math>\mu</math>m</b> | <b>0 - 10 <math>\mu</math>m</b> | <b>10 <math>\mu</math>m - 100 <math>\mu</math>m</b> | <b>0 - 10 <math>\mu</math>m</b> | <b>10 <math>\mu</math>m - 100 <math>\mu</math>m</b> | <b>0 - 10 <math>\mu</math>m</b> | <b>10 <math>\mu</math>m - 100 <math>\mu</math>m</b> | <b>0 - 10 <math>\mu</math>m</b> | <b>10 <math>\mu</math>m - 100 <math>\mu</math>m</b> | <b>0 - 10 <math>\mu</math>m</b> | <b>10 <math>\mu</math>m - 100 <math>\mu</math>m</b> |
| 1         | 5.0 E-06                        | 1.0 E-05  |
| 2         | 1.2 E-03                        | 1.0 E-05  | 1                               | 0   | 1                               | 0   | 0                               | 0   | 1                               | 0   | 0                               | 0   |
| 3         | 5.0 E-03                        | 1.0 E-05  | 1                               | 0   | 1                               | 0   | 0                               | 0   | 1                               | 0   | 0                               | 0   |
| 4         | 5.0 E-05                        | 1.0 E-04  |
| 5         | 5.0 E-03                        | 1.0 E-04  | 1                               | 0   | 1                               | 0   | 1                               | 0   | 1                               | 0   | 0                               | 0   |
| 6         | 5.0 E-03                        | 1.0 E-04  | 1                               | 0   | 1                               | 0   | 1                               | 0   | 1                               | 0   | 0                               | 0   |
| 7         | 3.0 E-04                        | 6.0 E-04  |
| 8         | 5.0 E-03                        | 6.0 E-04  | 1                               | 0   | 1                               | 0   | 0                               | 0   | 1                               | 0   | 0                               | 0   |
| 9         | 5.0 E-03                        | 6.0 E-04  | 1                               | 0   | 1                               | 0   | 1                               | 0   | 1                               | 0   | 1                               | 0   |

**Table 5** Release fractions for AGG 3 [5]

| AGG 3: Metal waste in steel plate container or concrete containers |                      |                                    |                      |                                    |                      |          |          |
|--|----------------------|------------------------------------|----------------------|------------------------------------|----------------------|----------|----------|
| BK   | Other Nuclides       |                                    |                      | H-3                                |                      | C-14     | Halogens |
|  | 0 - 10 $\mu\text{m}$ | 10 $\mu\text{m} - 100 \mu\text{m}$ | 0 - 10 $\mu\text{m}$ | 10 $\mu\text{m} - 100 \mu\text{m}$ | 0 - 10 $\mu\text{m}$ |          |          |
| 1  | 5.0 E-08             | 1.0 E-07                           | 5.0 E-08             | 1.0 E-07                           | 5.0 E-08             | 1.0 E-07 | 5.0 E-08 |
| 2  | 2.0 E-04             | 1.0 E-07                           | 1                    | 0                                  | 1                    | 0        | 1        |
| 3  | 4.0 E-03             | 1.0 E-07                           | 1                    | 0                                  | 1                    | 0        | 0        |
| 4  | 5.0 E-07             | 1.0 E-06                           | 5.0 E-07             | 1.0 E-06                           | 5.0 E-07             | 1.0 E-06 | 5.0 E-07 |
| 5  | 2.0 E-04             | 1.0 E-06                           | 1                    | 0                                  | 1                    | 0        | 1        |
| 6  | 4.0 E-03             | 1.0 E-06                           | 1                    | 0                                  | 1                    | 0        | 1        |
| 7  | 3.0 E-06             | 6.0 E-06                           | 3.0 E-06             | 6.0 E-06                           | 3.0 E-06             | 6.0 E-06 | 3.0 E-06 |
| 8  | 2.0 E-04             | 6.0 E-06                           | 1                    | 0                                  | 1                    | 0        | 1        |
| 9  | 4.0 E-03             | 6.0 E-06                           | 1                    | 0                                  | 1                    | 0        | 1        |

**Table 6** Release fractions for AGG 4 [5]

| AGG 4: Compactable waste in steel plate containers or concrete containers |                      |                                      |                      |                                      |                      |                                      |                      |
|---|----------------------|--------------------------------------|----------------------|--------------------------------------|----------------------|--------------------------------------|----------------------|
| BK  | Other Nuclides       |                                      |                      | H-3                                  |                      | C-14                                 | Halogens             |
|   | 0 - 10 $\mu\text{m}$ | 10 $\mu\text{m}$ - 100 $\mu\text{m}$ | 0 - 10 $\mu\text{m}$ | 10 $\mu\text{m}$ - 100 $\mu\text{m}$ | 0 - 10 $\mu\text{m}$ | 10 $\mu\text{m}$ - 100 $\mu\text{m}$ | 0 - 10 $\mu\text{m}$ |
| 1   | 5.0 E-08             | 1.0 E-07                             | 5.0 E-08             | 1.0 E-07                             | 5.0 E-08             | 1.0 E-07                             | 5.0 E-08             |
| 2   | 4.0 E-04             | 1.0 E-07                             | 1                    | 0                                    | 1                    | 0                                    | 1                    |
| 3   | 1.6 E-03             | 1.0 E-07                             | 1                    | 0                                    | 1                    | 0                                    | 0                    |
| 4   | 5.0 E-07             | 1.0 E-06                             | 5.0 E-07             | 1.0 E-06                             | 5.0 E-07             | 1.0 E-06                             | 5.0 E-07             |
| 5   | 4.0 E-04             | 1.0 E-06                             | 1                    | 0                                    | 1                    | 0                                    | 1                    |
| 6   | 1.6 E-03             | 1.0 E-06                             | 1                    | 0                                    | 1                    | 0                                    | 1                    |
| 7   | 3.0 E-06             | 6.0 E-06                             | 3.0 E-06             | 6.0 E-06                             | 3.0 E-06             | 6.0 E-06                             | 3.0 E-06             |
| 8   | 4.0 E-04             | 6.0 E-06                             | 1                    | 0                                    | 1                    | 0                                    | 1                    |
| 9   | 1.6 E-03             | 6.0 E-06                             | 1                    | 0                                    | 1                    | 0                                    | 1                    |

**Table 7** Release fractions for AGG 5 [5]

| AGG 5: Cemented waste in steel plate containers |                      |                                    |                      |                                    |                      |                                    |                      |
|---|----------------------|------------------------------------|----------------------|------------------------------------|----------------------|------------------------------------|----------------------|
| BK  | Other Nuclides       |                                    |                      | H-3                                |                      | C-14                               | Halogens             |
|   | 0 - 10 $\mu\text{m}$ | 10 $\mu\text{m} - 100 \mu\text{m}$ | 0 - 10 $\mu\text{m}$ | 10 $\mu\text{m} - 100 \mu\text{m}$ | 0 - 10 $\mu\text{m}$ | 10 $\mu\text{m} - 100 \mu\text{m}$ | 0 - 10 $\mu\text{m}$ |
| 1   | 3.0 E-08             | 2.7 E-07                           | 3.0 E-08             | 2.7 E-07                           | 3.0 E-08             | 2.7 E-07                           | 3.0 E-08             |
| 2   | 2.6 E-04             | 2.7 E-07                           | 6.0 E-02             | 2.7 E-07                           | 2.6 E-04             | 2.7 E-07                           | 5.0 E-01             |
| 3   | 5.0 E-04             | 2.7 E-07                           | 5.0 E-01             | 2.7 E-07                           | 5.0 E-04             | 2.7 E-07                           | 1                    |
| 4   | 4.0 E-07             | 3.6 E-06                           | 4.0 E-07             | 3.6 E-06                           | 4.0 E-07             | 3.6 E-06                           | 4.0 E-07             |
| 5   | 2.8 E-03             | 3.6 E-06                           | 5.0 E-01             | 3.6 E-06                           | 2.8 E-03             | 3.6 E-06                           | 1                    |
| 6   | 2.8 E-03             | 3.6 E-06                           | 5.0 E-01             | 3.6 E-06                           | 2.8 E-03             | 3.6 E-06                           | 1                    |
| 7   | 3.0 E-06             | 2.7 E-05                           | 3.0 E-06             | 2.7 E-05                           | 3.0 E-06             | 2.7 E-05                           | 3.0 E-06             |
| 8   | 2.8 E-03             | 2.7 E-05                           | 5.0 E-01             | 2.7 E-05                           | 2.8 E-03             | 2.7 E-05                           | 1                    |
| 9   | 2.8 E-03             | 2.7 E-05                           | 5.0 E-01             | 2.7 E-05                           | 2.8 E-03             | 2.7 E-05                           | 1                    |

**Table 8** Release fractions for AGG 6 [5]

| AGG 6: Combustible, un-fixed waste in concrete containers |                      |                                    |                      |                                    |                      |                                    | Halogens             |          |
|---|----------------------|------------------------------------|----------------------|------------------------------------|----------------------|------------------------------------|----------------------|----------|
| BK  | Other Nuclides       |                                    |                      | H-3                                |                      | C-14                               |                      | Halogens |
|   | 0 - 10 $\mu\text{m}$ | 10 $\mu\text{m} - 100 \mu\text{m}$ | 0 - 10 $\mu\text{m}$ | 10 $\mu\text{m} - 100 \mu\text{m}$ | 0 - 10 $\mu\text{m}$ | 10 $\mu\text{m} - 100 \mu\text{m}$ | 0 - 10 $\mu\text{m}$ |          |
| 1   | 0                    | 0                                  | 0                    | 0                                  | 0                    | 0                                  | 0                    | 0        |
| 2   | 0                    | 0                                  | 0                    | 0                                  | 0                    | 0                                  | 0                    | 0        |
| 3   | 0                    | 0                                  | 0                    | 0                                  | 0                    | 0                                  | 5.0 E-01             | 0        |
| 4   | 2.5 E-05             | 5.0 E-05                           | 2.5 E-05             | 5.0 E-05                           | 2.5 E-05             | 5.0 E-05                           | 2.5 E-05             | 5.0 E-05 |
| 5   | 0.1                  | 5.0 E-05                           | 1                    | 0                                  | 1                    | 0                                  | 1                    | 0        |
| 6   | 0.1                  | 5.0 E-05                           | 1                    | 0                                  | 1                    | 0                                  | 1                    | 0        |
| 7   | 1.5 E-04             | 3.0 E-04                           | 1.5 E-04             | 3.0 E-04                           | 1.5 E-04             | 3.0 E-04                           | 1.5 E-04             | 3.0 E-04 |
| 8   | 0.1                  | 3.0 E-04                           | 1                    | 0                                  | 1                    | 0                                  | 1                    | 0        |
| 9   | 0.1                  | 3.0 E-04                           | 1                    | 0                                  | 1                    | 0                                  | 1                    | 0        |

**Table 9** Release fractions for AGG 7 [5]

| AGG 7: Cemented waste in concrete containers |                      |                                    |                      |                                    |                      |                                    | Halogens             |          |
|--|----------------------|------------------------------------|----------------------|------------------------------------|----------------------|------------------------------------|----------------------|----------|
| BK   | Other Nuclides       |                                    |                      | H-3                                |                      | C-14                               |                      | Halogens |
|  | 0 - 10 $\mu\text{m}$ | 10 $\mu\text{m} - 100 \mu\text{m}$ | 0 - 10 $\mu\text{m}$ | 10 $\mu\text{m} - 100 \mu\text{m}$ | 0 - 10 $\mu\text{m}$ | 10 $\mu\text{m} - 100 \mu\text{m}$ | 0 - 10 $\mu\text{m}$ |          |
| 1  | 0                    | 0                                  | 0                    | 0                                  | 0                    | 0                                  | 0                    | 0        |
| 2  | 0                    | 0                                  | 0                    | 0                                  | 0                    | 0                                  | 0                    | 0        |
| 3  | 0                    | 0                                  | 0                    | 0                                  | 0                    | 0                                  | 5.0 E-01             | 0        |
| 4  | 2.0 E-07             | 1.8 E-06                           | 2.0 E-07             | 1.8 E-06                           | 2.0 E-07             | 1.8 E-06                           | 2.0 E-07             | 1.8 E-06 |
| 5  | 1.4 E-03             | 1.8 E-06                           | 2.5 E-01             | 1.8 E-06                           | 1.4 E-03             | 1.8 E-06                           | 5.0 E-01             | 1.8 E-06 |
| 6  | 1.4 E-03             | 1.8 E-06                           | 2.5 E-01             | 1.8 E-06                           | 1.4 E-03             | 1.8 E-06                           | 5.0 E-01             | 1.8 E-06 |
| 7  | 1.5 E-06             | 1.4 E-05                           | 1.5 E-06             | 1.4 E-05                           | 1.5 E-06             | 1.4 E-05                           | 1.5 E-06             | 1.4 E-05 |
| 8  | 1.4 E-03             | 1.4 E-05                           | 2.5. E-01            | 1.4 E-05                           | 1.4 E-03             | 1.4 E-05                           | 5.0 E-01             | 1.4 E-05 |
| 9  | 1.4 E-03             | 1.4 E-05                           | 2.5. E-01            | 1.4 E-05                           | 1.4 E-03             | 1.4 E-05                           | 5.0 E-01             | 1.4 E-05 |

**Table 10** Release fractions for AGG 8 [5]

| <b>AGG 8: Waste in cast iron containers</b> |  |  |  |  |  |  |                 |
|---|--|--|--|--|--|--|-----------------|
| <b>BK</b>                                   | <b>Other Nuclides</b>                  |  | <b>H-3</b>                             |  | <b>C-14</b>                            |  | <b>Halogens</b> |
|   | <b>0 - 10 <math>\mu\text{m}</math></b> | <b>10 <math>\mu\text{m} - 100 \mu\text{m}</math></b> | <b>0 - 10 <math>\mu\text{m}</math></b> | <b>10 <math>\mu\text{m} - 100 \mu\text{m}</math></b> | <b>0 - 10 <math>\mu\text{m}</math></b> | <b>10 <math>\mu\text{m} - 100 \mu\text{m}</math></b> |                 |
| 1   | 0                                      | 0  | 0                                      | 0  | 0                                      | 0  | 0               |
| 2   | 1.1 E-07                               | 0  | 7.3 E-07                               | 0  | 1.6 E-04                               | 0  | 1.6 E-04        |
| 3   | 2.0 E-05                               | 0  | 4.0 E-03                               | 0  | 6.0 E-03                               | 0  | 4.0 E-02        |
| 4   | 0                                      | 0  | 0                                      | 0  | 0                                      | 0  | 0               |
| 5   | 1.1 E-07                               | 0  | 7.3 E-07                               | 0  | 1.6 E-04                               | 0  | 1.6 E-04        |
| 6   | 2.0 E-05                               | 0  | 4.0 E-03                               | 0  | 6.0 E-03                               | 0  | 4.0 E-02        |
| 7   | 3.0 E-08                               | 0  | 3.0 E-08                               | 0  | 3.0 E-08                               | 0  | 3.0 E-08        |
| 8   | 2.6 E-04                               | 0  | 6.0 E-02                               | 0  | 5.0 E-01                               | 0  | 5.0 E-01        |
| 9   | 4.0 E-03                               | 0  | 5.0 E-01                               | 0  | 1                                      | 0  | 1               |

## CONCLUSIONS

The methodology developed and continuously refined for the German Konrad repository for low and intermediate level radioactive waste allows for the consideration of various mechanical and thermal impacts in nine different combinations. As the waste packages have been binned in eight different groups, 72 combinations of impact classes (BK) and waste package groups (AGG) have been studied, for which the release fractions of four different types of radionuclides were estimated in a conservative manner. The release fractions are presented separately for the respirable aerosol fraction of  $AED < 10 \mu\text{m}$  and the larger diameter fraction of  $10 \mu\text{m} < AED < 100 \mu\text{m}$ . The presented tables represent release fractions as they were finalized in a project [5] ending in the year 2017. In a currently ongoing research and development project the calculation methods for the release fractions are reviewed and further adapted.

## ACKNOWLEDGEMENTS

The authors are grateful for the support provided by the German Federal Ministry for the Environment, Nature Conservation, Nuclear Safety and Consumer Protection (Bundesministerium für Umwelt, Naturschutz, nukleare Sicherheit und Verbraucherschutz, BMUV) for having funded the underlying projects.

## REFERENCES

- [1] Gründler, D., and G. Philip: Freisetzung aus radioaktiven Abfallgebinden bei mechanischen und thermischen Belastungen, Annex IV of: Schwarz, G., et al.: Transportstudie Konrad: Sicherheitsanalyse des Transports radioaktiver Abfälle zum Endlager Konrad, (Ergänzungsband), GRS-A-1755/II, Gesellschaft für Anlagen- und Reaktorsicherheit (GRS) mbH, Köln, Germany, June 1991 (limited distribution, in German).
- [2] Lange, F., et al.: Transport Accident Release Modelling and Release Fractions, Annex Section B of: Lange, F., et al.: Assessment, Evaluation and further Development of the Safe Transport of Radioactive Material. Final Report of the Research Project SR 2479 (Working Area 4): Methods and Tools Applied for Radioactive Material Transport Risk Analysis Purposes. GRS-A-3378/IV, Gesellschaft für Anlagen- und Reaktorsicherheit (GRS) mbH, Köln, Germany, June 2007 (limited distribution).
- [3] Sentuc, F.-N., et al.: Transportstudie Konrad 2009, Sicherheitsanalyse zur Beförderung radioaktiver Abfälle zum Endlager Konrad, Gesellschaft für Anlagen- und Reaktorsicherheit (GRS) mbH, GRS-256, 190 S., ISBN 978-3-939355-31-1: Köln, Germany, December 2009, with corrigendum April 2010, <https://www.grs.de/sites/default/files/publications/GRS-256%2520-%2520Corr.pdf> (in German).
- [4] Brücher, W., et al.: Vertiefung und Ergänzung ausgewählter Aspekte der Abfalltransportrisikoanalyse für die Standortregion der Schachtanlage Konrad, GRS-A-3684, Gesellschaft für Anlagen- und Reaktorsicherheit (GRS) mbH, Köln, Germany, February 2013, <https://www.grs.de/de/aktuelles/publikationen/grs-3684-vertiefung-und-ergaenzung-ausgewaehler-aspekte-der> (in German).
- [5] Richter, C., B. Forell, and F.-N. Sentuc: Überprüfung des unfallbedingten Freisetzungsvorhaltes bei der Beförderung radioaktiver Stoffe, GRS-482, Gesellschaft für Anlagen- und Reaktorsicherheit (GRS) gGmbH, Köln, Germany, October 2017, <https://www.grs.de/sites/default/files/publications/grs-482.pdf> (in German).

The seminar itself ended with a very short panel discussion initiated by the session chairs summarizing the highlights of their sessions.



## 4 Seminar Conclusions and Outlook

The 17<sup>th</sup> International Seminar on ‘Fire Safety in Nuclear Power Plants and Installations’ clearly demonstrated the continuously ongoing progress in nuclear fire safety on a national as well as international level by all parties involved – licensees and operators of nuclear installations, regulators, and experts from technical support organisations, but also from manufacturers of fire protection features for nuclear facilities and other scientists involved.

The seminar sessions covered the following major topics:

- Developments and improvements in regulations,
- Self-assessment of fire safety,
- Advancements in deterministic and probabilistic fire safety analyses, including recent results from experimental investigations and research, analytical methods and tools for different purposes,
- Specific challenges, such as HEAF, and
- Lessons learned from fire safety related operating experience.

The presentations given in the frame of this seminar provided a non-negligible added value to the state-of-the-art in nuclear fire safety highlighting recent developments and improvements, but also presenting still unsolved issues and challenges in this area in an open manner.

The following conclusions have been drawn from the seminar sessions and the final panel discussion:

Remarkable progress has been achieved with respect to fire safety in nuclear installations and its assessment. And this trend observed already in seminars of this series before, is ongoing. This progress is also reflected in the most recent nuclear regulations, standards, and guidance documents, particularly from international organisations such as the International Atomic Energy Agency (IAEA) or the Western European Nuclear Regulators Association (WENRA), but also in the national context of different countries with nuclear installations.

The seminar has clearly indicated that a specific focus of fire safety at nuclear reactor facilities in countries with existing nuclear power stations close to the end of their commercial lifetime is on the post-commercial safe shutdown and decommissioning phases, but also on fires during nuclear waste treatment, transport, and storage.

For countries continuing or starting to operate nuclear reactors either enhanced Gen. III ones or even more advanced and very different Gen. IV type reactors, such as small modular reactors (SMRs) or other advanced nuclear technologies (ANTs), fire protection remains an issue which may present new challenges.

The seminar presentations on recent, partly ongoing activities have clearly demonstrated that new insights regarding nuclear fire protection, including fire safety analyses but also the different fire protection concepts and their implementation in the different types of nuclear facilities are to be expected in the near-term.

Regarding the risk significant topic of high energy arcing faults (HEAF) with the potential of ensuing fires the respective seminar presentations and discussions have confirmed that HEAF in high voltage electrical devices such as electrical breakers in cabinets, bus ducts etc. may result in a severe event sequence resulting from the HEAF with its two distinct phases, (i) the extremely short and rapid release of electrical energy, which may impair or damage items important to safety and (ii) the HEAF induced ensuing fire. The results from HEAF experiments in Japan and the United States but also those conducted internationally within an international research project of the OECD Nuclear Agency (NEA) have provided important lessons learned. The risk profiles of NPPs in the United States have additionally shown that fires at electrical cabinets and other electrical components with the potential of HEAF are non-negligible contributors to the overall plant risk. This insight was also supported by results from the Fire PSA of U.S. NPPs. Meanwhile, a first approach to calculate the HEAF zone of influence (ZOI) has been developed and may serve as a means to analyze HEAF fire events more reliably events in the future.

New standards are already being enforced in Japan and the United States regarding HEAF fire prevention. However, a consensus by experts on an international basis is still needed how HEAF fire events can be mitigated and their consequences limited to as low as reasonably practical (ALARP).

Recent experimental research and fire modelling activities carried out in an international framework, including the joint cable fire benchmark of the OECD/NEA projects FIRE and PRISME 3 have demonstrated that knowledge gaps remain requiring further investigations, particularly of fires at electrical components. To close at least some of these gaps further research on cable fires is intended. Cables representing a major fire source within nuclear installations due to their non-negligible fire load but also acting as an ignition source because of technical malfunction need to be investigated regarding the influence of the cable length on the fire propagation and of cable ageing under real conditions on the overall fire behaviour

Last but not least, more recent operating experience from nuclear power plants has identified new types of fire events during decommissioning activities which may occur more frequently in the future when there will be more power reactors under decommissioning. The observations from recent fire events have indicated the need to adapt the existing nuclear fire protection for reactors to these phases.

The participants from Europe, Asia and North America representing all the different parties involved in nuclear fire safety emphasized the benefits from the information exchange and the expert discussions in this seminar being shared within the nuclear fire experts' community. They strongly expressed their wish of continuing this series of fire safety seminars on a regular basis in time intervals of approximately two years. The next, 18<sup>th</sup> seminar of this series is therefore planned to be conducted in late summer 2024 in France as another Post-conference Seminar of the 27<sup>th</sup> 'International Conference on Structural Mechanics in Reactor Technology' (SMiRT 27), which will take place in Yokohama, Japan in March 2024 (cf. <https://www.smirt27.org/>).

**Gesellschaft für Anlagen-  
und Reaktorsicherheit  
(GRS) gGmbH**

Schwertnergasse 1  
**50667 Köln**  
Telefon +49 221 2068-0  
Telefax +49 221 2068-888

Boltzmannstraße 14  
**85748 Garching b. München**  
Telefon +49 89 32004-0  
Telefax +49 89 32004-300

Kurfürstendamm 200  
**10719 Berlin**  
Telefon +49 30 88589-0  
Telefax +49 30 88589-111

Theodor-Heuss-Straße 4  
**38122 Braunschweig**  
Telefon +49 531 8012-0  
Telefax +49 531 8012-200

[www.grs.de](http://www.grs.de)